

# Monday Morning, May 12, 2025

## Plenary Lecture

### Room Town & Country A - Session PL-MoM

## Plenary Lecture

Moderator: Dr. Peter Kelly, Manchester Metropolitan University, UK

8:00am PL-MoM-1 Welcome and Opening Remarks,

8:20am PL-MoM-2 ICMCTF Plenary Lecture: Past, Present and Future of All Solid State Batteries – Challenges and Opportunities, *Shirley Meng* [[shirleymeng@uchicago.edu](mailto:shirleymeng@uchicago.edu)], Argonne National Lab, The University of Chicago, USA

### INVITED

Compared with their liquid-electrolyte analogues, Solid state electrolytes SSEs have drawn increased attention as they promote battery safety, exhibit a wide operational temperature window, and improve energy density by enabling Li metal as anode materials for next-generation lithium-ion batteries. Despite suitable mechanical properties to prevent Li dendrite penetration, relatively wide electrochemical stability windows, comparable ionic conductivities, and intrinsic safety, most SSEs are found to be thermodynamically unstable against Li metal, where SSE decomposition produces a complex interphase, analogous to the SEI formed in liquid electrolyte systems. An ideal passivation layer should consist of ionically conductive but electronically insulating components to prevent the SSE from being further reduced. The past four decades have witnessed intensive research efforts on the chemistry, structure, and morphology of the solid electrolyte interphase (SEI) in Li-metal and Li-ion batteries (LIBs) using liquid or polymer electrolytes, since the SEI is considered to predominantly influence the performance, safety and cycle life of batteries. All-solid-state batteries (ASSBs) have been promoted as a highly promising energy storage technology due to the prospects of improved safety and a wider operating temperature range compared to their conventional liquid electrolyte-based counterparts. While solid electrolytes with ionic conductivities comparable to liquid electrolytes have been discovered, fabricating solid-state full cells with high areal capacities that can cycle at reasonable current densities remains a principal challenge. Silicon anode offers a possibility to overcome the challenges that lithium metal anode faces. In this talk, we will highlight solutions to these existing challenges and several directions for future work are proposed.

# Monday Morning, May 12, 2025

## Advanced Characterization, Modelling and Data Science for Coatings and Thin Films

### Room Town & Country C - Session CM4-1-MoM

## Simulations, Machine Learning and Data Science for Materials Design and Discovery I

Moderators: Dr. Ferenc Tasnadi, Linköping University, Sweden, Dr. Davide G. Sangiovanni, Linköping University, Sweden

### 10:00am CM4-1-MoM-1 Crystal Symmetry Determination in Electron Diffraction Using Machine Learning, Kevin Kaufmann [kevin.kaufmann@oerlikon.com], Oerlikon Metco, USA INVITED

The recent adoption by the general public of artificial intelligence (AI) tools such as ChatGPT has reinvigorated research into AI applied to material science. Deep learning, a subset of AI, allows computer systems to autonomously learn patterns in data and construct efficient decision rules for tasks including classification, regression, or segmentation. In material analysis, these tools have primarily been applied to techniques requiring analysis of data collected in the form of images. Electron backscatter diffraction (EBSD) is one such technique benefitting from these recent efforts to improve material analysis by leveraging deep neural networks. Within the last decade, advancements in EBSD equipment have enabled the capture of high-definition diffraction patterns at rates exceeding 3,000 Hz. This creates significant opportunities for increasing the amount of information that can be ascertained from a sample, as well as opens the door for training data intensive deep neural networks.

Deep neural network-based classification of the diffraction patterns is motivated by Hough-based EBSD's susceptibility to structural misclassification; a failure mode that modern EBSD can encounter even when the researcher has complete knowledge of the sample prior to beginning analysis. While several methods to improve phase-differentiation have been proposed, each still requires pre-selection of phases and additional data (e.g. chemistry or simulated diffraction patterns) to be available. In contrast, deep neural network-based methods have demonstrated effective phase differentiation and identification of phases to the space group level without the need for further information. The deep learning approach to EBSD diffraction pattern analysis is capable of these more advanced analyses because it uses all information in the image when assessing a diffraction pattern, whereas traditional Hough-based EBSD pattern analysis discards a significant amount of information.

To promote adoption of AI tools, it must be determined if and when it is prone to error. To test the ideal operating conditions, the deep neural network model is trained using diffraction patterns captured with a fixed geometry and SEM settings, and a parametric study is performed to develop an understanding of model performance as several of the most common EBSD operating conditions are varied. Each time one parameter is varied, the diffraction patterns are re-collected, and the CNN used to reassess the space group identification. Ultimately, the model is found to retain a high classification accuracy even with significant changes to the diffraction conditions.

### 10:40am CM4-1-MoM-3 Perturbation Analysis and Solutions to the One-Dimensional Cahn-Hilliard Equation in Thin Films, Rahul Basu [raulbasu@gmail.com], 71 Nagavarpalyam, India

This paper presents an analytical investigation of phase separation dynamics in thin films using the one-dimensional Cahn-Hilliard equation. The main focus is on the development of perturbation solutions for Greens functions under various boundary conditions, specifically periodic, Neumann, and Dirichlet. The derived solutions provide insight into the behavior of concentration profiles, essential for understanding the phase separation process in technologically relevant thin film materials.

Thin films are widely used in various technological applications, including microelectronics and energy storage. The phase separation within these films is critical to their performance and properties. The one-dimensional Cahn-Hilliard equation serves as a fundamental model for studying the evolution of concentration profiles during phase separation. This paper aims to explore the dynamics of phase separation under different boundary conditions by deriving similarity transform and perturbation solutions to the Cahn-Hilliard equation.

Starting with the 1D Cahn Hilliard equations, Perturbation expansions are applied to the Green function solution and then evaluated for various boundary conditions. Alloys evaluated were Cu-Ni and Pd-Si.

Results showed differences for the different Boundary conditions and material parameters involved. The small perturbation parameter is chosen to be  $k$  the interface parameter. in the CH equation.

The results are hoped to be useful in designing surface thin films, using inputs like thermal diffusivity  $M$  and the interface parameter appearing in the CH equation.

### 11:00am CM4-1-MoM-4 Predicting Segregation Behaviour in Polycrystalline Materials: A Case Study of P in Fe, Amin Reiners-Sakic, Christoph Dösinger, Alexander Reichmann, Ronald Schnitzer, Lorenz Romaner, David Holec [david.holec@unileoben.ac.at], Montanuniversität Leoben, Austria

The segregation of solutes to grain boundaries has a significant impact on material behaviour, particularly with regard to its mechanical properties and microstructural evolution. Computational tools have previously been employed to investigate this phenomenon, although the majority of studies are limited to coincidence site lattice (CSL) symmetrical boundaries. A methodology incorporating geometries associated with general grain boundaries, as observed in polycrystals, has recently been employed to investigate the substitutional segregation of phosphorus in iron. In this study, we further develop this approach to include interstitial sites. The model of polycrystalline bcc Fe comprises approximately  $7 \times 10^5$  atoms distributed across 12 grains of  $\sim 8 \text{ nm}^3$  total volume. Of these, approximately  $1 \times 10^5$  are substitutional segregation sites. In addition, approximately 1.2 million interstitial sites have been identified. The full segregation spectra for all of the aforementioned sites have been investigated using interatomic potentials in conjunction with state-of-the-art machine-learning techniques. The results demonstrate that phosphorus segregates to both site types, with a lower mean segregation energy for substitutional sites in comparison to interstitial sites. However, due to the higher number of interstitial sites, the total number of sites with comparable segregation energies to substitutional sites is significantly greater. By incorporating both segregation distributions, we can accurately predict P enrichment at different concentrations and temperatures, in agreement with experimental data. To validate this approach, we applied it also to Ni and H, showing that Ni segregates, albeit moderately, only to substitutional sites, while H segregates exclusively to interstitial sites, in line with existing literature.

### 11:20am CM4-1-MoM-5 Tunable Interface Stress in Cu/W Nanomultilayers, Yang Hu [yang.hu@empa.ch], Giacomo Lorenzin, Jeyun Yeom, Empa, Swiss Federal Laboratories for Materials Science and Technology, Switzerland; Manura Liyanage, William A. Curtin, EPFL, Switzerland; Lars P.H. Jeurgens, Jolanta Janczak-Rusch, Claudia Cancellieri, Vladyslav Turlo, Empa, Swiss Federal Laboratories for Materials Science and Technology, Switzerland

Controlling the intrinsic stresses developed during the growth of nanomultilayers (NMLs) is critical for their performance and applications. In Cu/W NMLs, a transition from positive to negative interface stresses has been observed under varying film deposition conditions, yet the underlying mechanisms driving this transition remain unresolved. The sign of experimentally measured interface stress has long been debated, highlighting the complexity of interface phenomena in NMLs. To address this, we employed atomistic simulations using a state-of-the-art neural network potential to uncover the strong influence of intermixing and metastable phase formation at Cu/W interfaces on interface stress. These simulations provide a direct link between interface chemistry and stress, a connection that is challenging to establish experimentally due to the difficulty of characterizing interfacial structures and compositions at atomic resolution for the Cu/W system. The insights gained from this work offer a deeper understanding of the interplay between interface structure, stress, and deposition conditions, paving the way for the rational design of NML coatings with tunable stress states. This approach enables the optimization of the thermomechanical stability and multifunctional properties of NMLs, advancing their applications in fields such as flexible electronics, energy storage, and protective coatings. Our findings also underscore the power of advanced computational methods in guiding materials design and addressing long-standing challenges in interface engineering.

# Monday Morning, May 12, 2025

11:40am **CM4-1-MoM-6 Understanding the Effects of Underlayer Materials on Electron Beam Resists Through the Use of Monte Carlo Simulations and the Development of a New Simulation Tool**, *David Castillo Lozada [dcastil2@caltech.edu]*, *Toby Thomassen, Scott Lewis, Axel Scherer, Guy De Rose*, California Institute of Technology, USA; *Luisa Bozano, Kevin Gu*, Applied Materials, USA

The ability to write structures at the nanoscale using lithography underpins all modern society. The electronic devices we take for granted contain integrated circuits, the key component being the field-effect transistors (FETs). They have reduced in size by a factor of two every two years for over fifty years, following "Moore's Law". This size reduction is dependent on the continuous development of materials and techniques that produce better line resolution. The technical program aimed to apply a simulation tool called Excalibur to materials and processing problems critical to Applied Materials Inc. The Excalibur simulation suite can model the behavior of electrons and ions in the range of 100 keV to 3.6 eV. This software allows rapid prototyping of the next-generation resists for electron beam lithography (EBL) and ion beam lithography (IBL) for the semiconductor industry. Although Excalibur currently does not simulate extreme ultraviolet (EUV) radiation, we propose that it can provide a first-order analysis and prediction of EUV based on e-beam behavior. This project provides evidence that such prediction can be well modeled using the Excalibur tool. We also provide an alternative simulation, which we call Merlin, that aims to be more accurate and faster than its predecessor.

## Functional Thin Films and Surfaces

### Room Palm 5-6 - Session MB2-1-MoM

#### Thin Films for Electronic Devices I

**Moderators:** *Dr. Jiri Houska*, University of West Bohemia, Czechia, *Spyros Kassavetis*, Aristotle University of Thessaloniki, Greece

10:40am **MB2-1-MoM-3 Impact of Zn Alloying to CsZn<sub>x</sub>Pb<sub>1-x</sub> Perovskite Conversion Efficiency of Solar Cells**, *Abdul Mannan Majeed [mannan.majeed@ff.vu.lt]*, Vilnius University, Lithuania

High-quality perovskite films are essential for developing efficient planar perovskite solar cells (PSCs). However, as-prepared perovskite films typically exhibit low crystallinity and high trap densities, leading to degraded performance in PSCs. Moreover, the challenge of creating low-toxicity, high-performance mixed Zn/Pb halide perovskite solar cells at a reduced cost remains a significant hurdle. To address this, zinc (Zn) was introduced as a cation substitute for the toxic lead (Pb) in the CsZn<sub>x</sub>Pb<sub>1-x</sub> perovskite compound, leveraging its non-toxic nature, oxidation resistance, and earth abundance. This study investigates the structural and photovoltaic properties of Zn-alloyed Pb/Zn hybrid perovskite solar cells (PSCs). The results demonstrate that a 50% Zn-alloyed perovskite significantly enhances crystal quality, surface coverage, and grain size while reducing non-radiative recombination by increasing carrier lifetime. These improvements lead to a notable boost in photovoltaic performance. Specifically, the CsZn<sub>0.5</sub>Pb<sub>0.5</sub> compound achieved a power conversion efficiency (PCE) of 10.3%, with a fill factor (FF) of 53%, demonstrating the highest performance with minimal Pb content. Additionally, the device exhibited a V<sub>oc</sub> of 0.99 V and an I<sub>sc</sub> of 18.7 mA/cm<sup>2</sup>. The performance of the CsZn<sub>0.5</sub>Pb<sub>0.5</sub> solar cell was found to vary with light intensity, showing changes in short-circuit current and open-circuit voltage. These findings open new avenues for further research into lead-reduced hybrid perovskite solar cells and offer valuable insights into the mechanisms underlying PCE degradation in practical devices, thereby contributing to the advancement of perovskite solar cell technology.

11:00am **MB2-1-MoM-4 Experimental Investigation of Thermal Conductivity During Aging of Nanoporous Sintered Silver Joints**, *Yann Billaud, Anas Sghuri, Didier Saury, Xavier Milhet [xavier.milhet@ensma.fr]*, Institut Pprime - CNRS - ENSMA - Université de Poitiers, France

Silver (Ag) paste sintering is used as a die-bonding technology for the next generation of power electronic modules as Ag offers a high melting temperature as well as excellent thermal and electrical conductivities. Ag paste sintering is performed using specific conditions depending on the type of paste and the users' specifications (temperature, time, pressure), ending up in a porous joint. As a result, the properties of those joints are heavily influenced by their densities (i.e. porosity). Despite the numerous studies reported in the literature, the relationship between the density of the joint and its thermal conductivity remains an issue since access to the density of an embedded thin joint is very challenging. Furthermore, little is known on the evolution of the thermal conductivity in operating conditions. In this study, these issues were investigated by developing self-standing

Monday Morning, May 12, 2025

specimens with microstructures representative of those of real joints. In order to study a wide range of porosity, sintering was performed using a single time/temperature under various pressures. The thermal conductivity was measured using 3D flash method, consisting in applying a short non-uniform laser excitation on the surface of the sample, leading to three-dimensional heat transfer. The relationship between porosity and thermal conductivity is established for the as-sintered state and after aging up to 500h at temperatures ranging from 150 °C to 350 °C and is compared to existing models. The evolution of the thermal properties during thermal aging is discussed considering both the elaboration conditions and the microstructure evolution.

11:20am **MB2-1-MoM-5 Patterned Silver Nanowire Network for CdSe/CdZnS/ZnS Green Quantum Dot Light-Emitting Diodes**, *Chia-Yu Lin, Tzu-Hsu Wen, Chun-Yuan Huang [cyhuang2004@gm.ntu.edu.tw]*, National Taitung University, Taiwan

Silver nanowire (AgNW) network possesses excellent conductivity and flexibility, making it an ideal material for electrodes of flexible optoelectronic devices. However, their high surface roughness can negatively impact device performance. To address this issue, the roughness of the patterned AgNW network electrode was reduced using a transparent photopolymer. To fabricate the patterned AgNW films, firstly, the polydimethylsiloxane (PDMS) substrates with proper size (18×18 mm<sup>2</sup>) were covered with the stainless-steel shadow mask and then treated with UV ozone for 30 minutes. A 2 wt % AgNWs-ethanol solution was spin-coated, annealed, and then covered with UV-curable polyurethane (Norland Optical Adhesive 63, Edmund Optics). After UV curing, the composite of AgNW/polyurethane was then peeled off from the PDMS, allowing the AgNWs/polyurethane composite conductive film to adhere to the poly(ethylene terephthalate)(PET) substrate. Accordingly, with high transparency of 77% and low sheet resistance of 7~9 Ω/sq, the patterned AgNW network embedded in the polyurethane matrix was obtained for the subsequent fabrication of quantum dot light-emitting diodes (QLEDs). The electrode was applied as the anode in green CdSe/CdZnS/ZnS QLEDs. With the device structure of AgNW network/PEDOT:PSS/TFB/QD/MgZnO/Al, the QLED emitting pure green light centered at 536 nm resulted in a turn-on voltage of 2.4 V, a maximum brightness of 72,922 cd/m<sup>2</sup>, and a current efficiency of 27.8 cd/A.

11:40am **MB2-1-MoM-6 Effects of Room Temperature Sputtered Nano-Interfaced WxMo<sub>y</sub>O<sub>3</sub> Nanograins on Highly Responsive NO Sensing**, *Somdatta Singh [somdatta@ic.iitr.ac.in]*, Indian Institute of Technology Roorkee, India; *Ravikant Adalati*, University of Mons, Belgium, India; *Prachi Gurawal, Raman Devi*, Indian Institute of Technology Roorkee, India; *Gaurav Malik*, Jeonbuk National University, Republic of Korea, India; *Davinder Kaur, Ramesh Chandra*, Indian Institute of Technology Roorkee, India

This work demonstrates a heterostructure of monoclinic molybdenum trioxide (n-MoO<sub>3</sub>) and tungsten trioxide (n-WO<sub>3</sub>) with nano-interfaced (n-i@WxMo<sub>y</sub>O<sub>3</sub>) based NO gas sensing material. The nanocrystalline n-i@W<sub>x</sub>Mo<sub>y</sub>O<sub>3</sub> thin film was coated using a single-step magnetron sputtering technique on an n-type (100) silicon substrate. Within the temperature range of approximately ambient temperature (50°C) to 350°C, this sensing material, W<sub>x</sub>Mo<sub>y</sub>O<sub>3</sub> (where x = 0.71 and y = 0.29), detects NO gas and investigates the impact of crystal structure and nanointerfaces on sensing performance. A heterostructure composed of several materials can enhance the interaction between the gas molecules and the sensor surface by producing interfaces that promote charge transfer. With a response/recovery time of around 300 seconds/125 seconds at 300°C, the n-i@W<sub>x</sub>Mo<sub>y</sub>O<sub>3</sub> has a low limit of detection (DL) of about 39 ppb and an excellent sensor response (SR = R<sub>g</sub>/R<sub>a</sub>) of about 44.15 for 50 ppm NO gas. Even at 50°C, the enhanced sensitivity of the sensing material with the nanointerface shows a strong affinity for NO molecules. It provides around 1.03 SR with response/recovery times of 53 and 71 seconds, respectively. The robustness of the n-i@W<sub>x</sub>Mo<sub>y</sub>O<sub>3</sub> thin film sensor was established by its excellent selectivity (SR = ~44.15) and long-term stability (60 days) towards 50 ppm NO at 300°C. The remarkable sensing properties of MoO<sub>3</sub> functionalized WO<sub>3</sub> nanograins indicate an exciting potential for NO gas sensors that operate close to ambient temperature (50°C).

12:00pm **MB2-1-MoM-7 Study on the Effect of Different Oxygen Flow Rates on Vanadium-Doped Zinc Oxide Thin Film Piezoelectric Pressure Sensors**, *CHENG HAN HSU [e204242271@gmail.com]*, National Cheng Kung University (NCKU), Taiwan

The piezoelectric effect is a phenomenon where certain materials generate an electric charge when subjected to mechanical stress. This property is

widely utilized in sensors, and energy-harvesting devices because it converts mechanical energy into electrical energy. ZnO is a promising material for energy-harvesting devices due to its piezoelectric and semiconductor properties, along with good biocompatibility and low environmental impact. However, its relatively low piezoelectric coefficient (12.4 pC/N) limits its potential in these applications. To enhance the piezoelectric coefficient, vanadium was doped into ZnO thin films. Vanadium ions have a higher valence than zinc ions, which improves electric polarization and increases the piezoelectric coefficient. Additionally,  $V^{5+}$  ions, having a higher positive charge than  $V^{3+}$  ions, create stronger polarity, further boosting the piezoelectric properties. By adjusting the oxygen flow rate during the sputtering process, the  $V^{5+}$  content in the films is increased, enhancing the piezoelectric coefficient. In this study, we utilized an RF sputtering system with varying oxygen flow rates to prepare vanadium-doped zinc oxide thin films, which were then used to fabricate piezoelectric pressure sensor devices. The results show that as the oxygen flow rate increases, the grain shape of the thin films changes, and the grain size decreases. SEM reveal significant changes in the grain structure. XRD shows that the intensity of the 002 peak weakens as the oxygen flow rate increases, indicating structural changes in the thin films. XPS reveals that the content of pentavalent vanadium increases with higher oxygen flow rates, but decreases after reaching a critical value, which correlates with the trend observed in piezoelectric coefficient measurements. Further analysis of the O1s XPS shows that the lattice oxygen content in the films is higher than the surface adsorbed oxygen, with the lowest number of oxygen vacancies at a certain oxygen flow rate, which then increases as the oxygen flow rate rises. UV-visible spectra indicate that, due to the Burstein-Moss effect, the energy band structure of the thin films initially decreases and then increases with increasing oxygen flow rates. Finally, piezoelectric pressure sensors were fabricated from these thin films, and the stress sensitivity at different oxygen flow rates was measured. This study provides a comprehensive investigation of the structural, optical, piezoelectric properties of V-doped zinc oxide thin films at varying oxygen flow rates and explores their application as piezoelectric pressure sensors. The findings offer insights for optimizing thin film performance in piezoelectric sensing devices.

## Surface Engineering of Biomaterials, Medical Devices and Regenerative Materials

### Room Palm 1-2 - Session MD1-1-MoM

#### Development and Characterization of Bioactive Surfaces/Coatings I

**Moderators:** Dr. Mathew T. Mathew, University of Illinois College of Medicine at Rockford and Rush University Medical Center, USA, Dr. Sandra E. Rodil, Universidad Nacional Autónoma de México

10:00am **MD1-1-MoM-1 Hybrid Ceramic Coating with Enhanced Corrosion Resistance for Magnesium-Based Biodegradable Implants**, **Abdelrahman Amin** [xml111@mocs.utc.edu], Diya Patel, University of Tennessee at Chattanooga, USA; Bryce Williams, Thomas McGehee, Alyssandra Navarro, Mostafa Elsaadany, University of Arkansas, USA; Hamdy Ibrahim, University of Tennessee at Chattanooga, USA; Merna Abd Rabo, The University of Tennessee at Chattanooga, USA

Biodegradable implants, recognized for their unique mechanical properties and compatibility with human bone, have become essential in various biomedical applications. Magnesium, a key material in such implants, is notable for its favorable biodegradability within the human body. However, one limitation of magnesium is its tendency to degrade too quickly, leading to a loss of mechanical integrity before bone healing is complete. This rapid degradation can undermine the implant's effectiveness, driving efforts to manage magnesium's high corrosion rate through various approaches. Among these, the development of protective coatings on magnesium alloys has shown significant promise. Such coatings provide a temporary protective layer, thereby slowing down the corrosion process and extending the implant's functionality. Hybrid coatings, particularly those combining Plasma Electrolytic Oxidation (PEO) with sol-gel techniques, have improved the ability to control and adjust corrosion rates while incorporating bioactive agents like hydroxyapatite (HA) nanoparticles. These nanoparticles contribute to enhanced bioactivity and osteoconductivity, further supporting bone healing. In this study, the primary objective is to explore how altering the key parameters of Sol-gel coating affects the corrosion resistance of a magnesium alloy substrate that has been pre-coated with a PEO layer. Specifically, the combined impact of varying HA

concentration within the Sol-gel solution, dip time, and the number of layers deposited are examined. The findings of this work establish the relationship between the sol-gel coating process parameters and the corrosion properties of the developed hybrid coating leading to a better understanding of their effect on developing magnesium-based implants with superior properties.

10:20am **MD1-1-MoM-2 Functional Coatings by Low Vacuum Plasma for the Innovation in Regenerative and Reparative Medicine**, **Pascale Chevallier**, Carlo Paternoster, Francesco Copes, Laval University, Canada; **Andranik Sarkissian**, Plasmionics Inc., Canada; **Diego Mantovani** [diego.mantovani@gmn.ulaval.ca], Laval University, Canada **INVITED**

Over the last 50 years, biomaterials, prostheses and implants saved and prolonged the life of millions of humans around the globe. Today, nanobiotechnology, nanomaterials and surface modifications provide a new insight to the current problem of biomaterial complications, and even allows us to envisage strategies for the organ shortage. In this talk, creative strategies for modifying and engineering the surface and the interface of biomaterials, including metals, polymers from natural and synthetic sources, will be discussed. The unique potential of low-pressure low-temperature plasma surface modification will be detailed with the overall aim to envisage today how far innovation can bring tomorrow solutions for reparative and regenerative medicine. Applications for health will be emphasized, including biologically active-based, biomimetic, low-fouling, bactericidal, and antiviral coatings.

#### References

1. M. Shekargoftar, S. Ravanbakhsh, V. Sales de Oliveira, J. Buhagiar, N. Brodusch, S. Bessette, C. Paternoster, F. Witte, A. Sarkissian, R. Gauvin, D. Mantovani. Effects of Plasma Surface Modification of Mg-2Y-2Zn-1Mn for Biomedical Applications [https://www.sciencedirect.com/science/article/pii/S2589152924002825], *Materialia*, 102285, 2024.
2. S.H. Um, J. Lee, M. Chae, C. Paternoster, F. Copes, P. Chevallier, D.H. Lee, S.W. Hwang, Y.C. Kim, H.S. Han, K.S. Lee, D. Mantovani, H. Jeon. Biomedical Device Surface Treatment by Laser-Driven Hydroxyapatite Penetration-Synthesis Technique for Gapless PEEK-to-Bone Integration [https://onlinelibrary.wiley.com/doi/abs/10.1002/adhm.202401260]. *Adv Healthcare Mater*, 13, 26, 2401260, 2024.
3. M.E. Lombardo, V. Mariscotti, P. Chevallier, F. Copes, F. Boccafoschi, A. Sarkissian, D. Mantovani. Effects of cold plasma treatment on the biological performances of decellularized bovine pericardium extracellular matrix-based films for biomedical applications [https://www.explorationpub.com/Journals/ebmx/Article/10137]. *Exploration of BioMat-X*, 1, 2, 84-99, 2024.
4. L. Bonilla-Gameros, P. Chevallier, X. Delvaux, L.A. Yáñez-Hernández, L. Houssiau, X. Minne, V.P. Houde, A. Sarkissian, D. Mantovani. *Nanomaterials*, 14, 7, 609, 2024.
5. L. Marin de Andrade, C. Paternoster, P. Chevallier, S. Gambaro, P. Mengucci, D. Mantovani. *Bioactive Materials*, 11, 166, 2022.

11:00am **MD1-1-MoM-4 10-h2da Coating on Polyvinyl Chloride Catheter Biomaterials for Prevention of Candida-Associated Urinary Tract Infections**, **Jermiah Tate** [jdtate3@memphis.edu], Joel Bumgardner, Tomoko Fujiwara, J. Amber Jennings, University of Memphis, USA

Urinary catheters made of polyvinyl chloride (PVC) are susceptible to microbial biofilm formation. 10-hydroxy-2-decenoic acid (10-H2DA) is a dispersal signaling molecule known to inhibit biofilm and planktonic growth of microorganisms. This study hypothesized that coating PVC with 10-H2DA would inhibit planktonic and biofilm-associated *Candida albicans*. Interactions of the PVC and 10-H2DA molecules were analyzed using Video Contact Angle (VCA), Fourier Transform Infrared (FTIR), and High-Performance Liquid Chromatography (HPLC). Successful coating of PVC with 10-H2DA was demonstrated through a lowered contact angle. The control group displayed an average contact angle of 107° with a p value <0.0001 of significance compared to the following groups: 10mg/ml (65.8°), 15mg/ml (80.7°), and 20 mg/ml (55.8°). FTIR peaks appeared in regions indicative of the 10-H2DA on the surface of PVC. Elution data displays a burst release of 50% 10-H2DA within 3-6-hours. After 48 hours of incubation, over 60% of planktonic *C. albicans* growth was inhibited (p<0.0001) in the environment of PVC coated with 10-H2DA compared to uncoated PVC. There were no significant reductions of biofilm. Immersing PVC in 10-H2DA showed short-term surface activity, attributed to the short timeframe of release of 10-H2DA. Further investigations will explore anti-biofilm properties of 10-H2DA on the PVC surface against other common microorganisms responsible for

# Monday Morning, May 12, 2025

biofilm development on urinary catheters and chemical conjugation for longer term release.

11:20am **MD1-1-MoM-5 Hydrogen-Treated Orthopedic Implants : A Novel Approach to Enhance Biocompatibility and Mitigate Inflammation, Ren-Jei Chung [rjchung@mail.ntut.edu.tw]**, National Taipei University of Technology, Taiwan

INVITED

The surface modification of cobalt-chromium-molybdenum (CoCrMo) alloy to create hydrogenated CoCrMo (H-CoCrMo) surfaces has shown promise as an anti-inflammatory orthopedic implant. Utilizing the electrochemical cathodic hydrogen-charging method, the CoCrMo alloy surface was hydrogenated, resulting in improved biocompatibility, reduced free radicals, and an anti-inflammatory response. *In vitro* studies demonstrated enhanced hydrophilicity and the deposition of hydroxyapatite. The cell study result revealed a suppression of osteosarcoma cell activity. Finally, the *in vivo* test suggested a promotion of new bone formation and a reduced inflammatory response. The diffusion of hydrogen to a depth of approximately  $106 \pm 27$  nm on the surface facilitated these effects. The findings suggest that electrochemical hydrogen charging can effectively modify CoCrMo surfaces, offering a potential solution for improving orthopedic implant outcomes through anti-inflammatory mechanisms.

## Plasma and Vapor Deposition Processes

### Room Town & Country A - Session PP1-1-MoM

#### PVD Coatings and Technologies I

**Moderators: Dr. Qi Yang**, National Research Council of Canada, **Dr. Christian Kalscheuer**, IOT, RWTH Aachen, Germany

10:00am **PP1-1-MoM-1 Complementary Cutting-Edge Plasma Monitoring Techniques for Process Development, Production Control and Machine Learning (ML), Thomas Schütte [schuette@plasus.de]**, Jan-Peter Urbach, Peter Neiß, Marius Radloff, Hokuto Kikuchi, PLASUS GmbH, Germany

INVITED

As specifications in the thin film industry become more and more demanding, high production yields and cost effective production becomes a major factor in this competitive market. Increasing demands for better specifications and lower scrap rates drive the demand for efficient process control systems.

In addition, data analysis using artificial intelligence (AI) and machine learning (ML) technologies has made tremendous progress in recent years, sparking interest in using these methods for the diagnostics and control of plasma applications. To utilize this capability, a large number of data sets from complementary process diagnostics methods are required.

This presentation will highlight the opportunities and advantages of utilizing the latest developments in real-time in-situ data acquisition of different diagnostic techniques in a single system: Spectroscopic plasma process monitoring acquires data from the actual process plasma whereas in-situ broadband photometric measurements gather properties of the growing coating such as film thickness or color values. In addition, time-resolved electrical measurements of generator power, voltage and current provide valuable electrical process information especially in pulsed plasma applications.

Selected plasma applications are used to illustrate how process variations influence the results of the different measurement techniques. Consequently, by combining different methods and analyzing the complementary data in real-time, interdependencies between process and product properties become visible and can be used to achieve more accurate and reliable process control. At the same time the collected data can be fed into the analysis using AI and ML techniques to improve product quality and long-term production stability.

Real-time process control examples combining different diagnostic methods will be presented and first approaches to the application of ML methods will be illustrated using various coating applications from industry and R&D, such as metallic and reactive sputtering, HIPIMS and PECVD processes for tribological, optical and glass coating processes.

10:40am **PP1-1-MoM-3 Plasma Diagnostics and Thin Film Synthesis Using an Industrial-Sized DC Vacuum Arc Source with Magnetic Steering and a TaB<sub>2</sub> Cathode, Igor Zhirkov [igor.zhirkov@liu.se]**, Andrejs Petruhins, Ali Saffar Shamshirgar, Materials Design Division, Linköping University, Sweden; Philipp Immich, IHI Hauzer Techno Coating B.V., Netherlands; Szilard Kolozsvári, Peter Polcik, PLANSEE Composite Materials GmbH., Germany; Johanna Rosen, Materials Design Division, Linköping University, Sweden

Due to physical and chemical characteristics of transition metal borides, thin films thereof are gaining increasing attention as protective hard coatings. Most publications in this area focus on TiB<sub>2</sub>, synthesized through various physical vapor deposition (PVD) techniques. Tantalum diboride, TaB<sub>2</sub>, is characterized by a hardness comparable to TiB<sub>2</sub>, but with an elastic modulus  $\sim 2$  times lower. It results in a combination of high strength and high resistance to elastic and plastic deformation, for potential use in protective coating industry. However, there are no reports on deposition of TaB<sub>2</sub> coatings with DC vacuum arc, a process commonly used in industry, in particular with magnetic steering. In this work, we present analysis of the process (cathode weight loss, film deposition rate), plasma composition, and the (micro-) structure and composition of the cathode as well as of films, using a Hidden EQP mass-energy analyzer, SEM, XRD, and XPS. The study is performed using an industrial scale arc plasma source, Hauzer CARC+, which utilizes plane cathodes of 100 mm in diameter. The TaB<sub>2</sub> cathodes were provided by PLANSEE Composite Materials GmbH. The magnetic arc steering system, based on variation of magnitude of electrical current flowing through the solenoid placed behind the cathode, allows tuning of the strength of the magnetic field at the center point of the cathode surface in the range  $\pm 8$  mT (different polarity). The steering system is found to improve the stability of the arcing process and result in more smooth erosion of the cathode surface. Plasma analysis performed at base pressure ( $10^{-5}$  Torr) shows peak ion energies consistent with the velocity rule, around 140 and 10 eV for Ta and B, respectively. The ion energies, the ion charge states, and the plasma ion compositions were found to be strongly affected by the operating pressure, with a plasma ion composition showing a lower B content ( $\sim 60\%$  Ta and  $\sim 40\%$  B at base pressure) compared to the cathode stoichiometry. Even lower B ion signals were recorded at higher pressures. The plasma properties were correlated to the deposited thin films, their composition and structure. The lack of B within the deposited films was found to be less pronounced than for the plasma ions. Altogether, the results show that DC vacuum arc can be used for TaB<sub>2</sub> depositions with stability provided by the magnetic steering.

11:00am **PP1-1-MoM-4 Novel Approach in Cathodic Arc Evaporation Enabling Precise Control Over Energy of Deposited Ions in Industrial Conditions, Martin Učík [m.ucik@platit.com]**, Masaryk University, Czechia

#### Introduction

Commonly, in cathodic arc evaporation (CAE), where multiple elements are contained in a coating, materials of several targets are simultaneously evaporated. This evaporated material, being near-complete ionization due to the exceedingly high power densities in cathode spots with significant number or even predominance of multiply charged ions (2+, 3+, etc.), is condensed onto the substrate under applied bias which is constant. Therefore, often the currents and the substrate bias need to be optimized in order to avoid undesirable effects such as delivering excessive energy to the growing coating.

With a new approach of pulsed arc and synchronized bias relative to the arc pulses, we are now able to select which evaporated material is accelerated towards the substrate at what applied voltage, therefore controlling the delivered energy or, in other words, having a mechanism to regulate the energy of impacting ions.

#### Methods

Here, we choose one of the most widely studied coatings – AlCrN – to investigate the effect of synchronized bias. On two single element targets (Al, Cr), both arcs are simultaneously periodically pulsed and a substrate bias (from 30V up to 240V) is either constant or also pulsed in respect to the arc pulses (e.g. by Al pulse, we mean that arc current of Al cathode is at its maximum level). This offers us three basic modes we have focused on: (i) with a constant substrate bias, (ii) with bias applied during the Al pulse and leaving the substrate at a floating potential during Cr pulse and (iii) vice-versa applying the bias only during Cr pulse.

#### Results

By simply choosing the mode other than (i), we can change the coating microstructure, thus the properties – e.g., grain size, lattice orientation,

# Monday Morning, May 12, 2025

residual stress, etc. We also investigated the effect of synchronized bias in a cutting test, where we observed an influence of a mode choice on cutting edge wear.

## Conclusion

In summary, this study shows new possibilities of cathodic arc evaporation enabling to fine-tune coating microstructure to obtain desired properties and further more cutting performance.

to be submitted to Technical Symposium PP Plasma and Vapor Deposition Processes, and section PP1 PVD Coatings and Technologies (oral contribution)

11:20am **PP1-1-MoM-5 Industrial-Scale PVD Deposition of Aluminium Oxide**, *Ivan Kolev [ikolev@hauzer.nl]*, IHI Hauzer Techno Coating B.V., Netherlands; *Philipp Immich, Daniel Barnholt, Julia Janowitz, Louis Tegelaers*, IHI Hauzer Techno Coating B.V., Netherlands; *Rolf Schäfer*, Robeko GmbH & Co. KG, Germany; *Tobias Radny*, Robeko GmbH & Co., KG, Germany

Aluminium oxide ( $Al_2O_3$ ) is a well-known material with versatile properties, such as high hardness, electrical insulation, chemical inertness, and thermal stability. These properties make alumina also a desired thin film in various industrial applications. Its hardness and thermal stability are very beneficial for coatings on inserts. Other emerging application field is the sensor coatings, where the need of highly insulating films makes aluminium oxide a primary choice. Its optical transparency in combination with high hardness and chemical resistance find application in protective coatings.

Despite these multiple applications, efficient industrial-scale deposition of alumina thin films still has its challenges. RF sputtering from compound targets can produce stoichiometric high-quality coatings. However, its notoriously low deposition rate makes it unsuitable for large-scale mass production. Dual magnetron sputtering (DMS), from the other hand, can provide industrially meaningful deposition rates from metallic targets and successfully to circumvent the problem with the disappearing anode. However, it requires a very fast and solid regulation, allowing for long-term stable operation at narrow operating range. Special attention needs to be paid for arc handling on the target and substrate and its influence on the regulating algorithm.

In this talk, the contemporary state of the art for industrial DMS deposition of aluminium oxide for tool and sensor application is presented. Different ways of regulating are discussed and compared. The properties of low- and high-temperature deposited alumina films are reported. Future technology improvements are also discussed.

11:40am **PP1-1-MoM-6 Control of Microstructure and Phase of Sputter-Deposited Tantalum Thin Films for Inkjet Device Applications**, *Brittney Burant [brittney.burant@hp.com]*, HP Inc, USA

Tantalum (Ta) has long been used in thermal inkjet devices and plays a crucial role in the ink ejection cycle. It forms the bubble nucleation surface that transfers heat from the resistor to the ink, and also acts as a cavitation barrier that mechanically and chemically protects the resistor from damage during bubble collapse. Ta has a bulk stable  $\alpha$ -phase with BCC structure, however, the metastable  $\beta$ -phase has historically been used in inkjet devices. Microstructure and phase control of the thin film is important for promoting cohesive bubble nucleation during ink firing cycles and ensuring the device functions reliably through its lifetime.

When pursuing new product architectures with reduced die separation ratios, it was found that sputter-deposited Ta films began to exhibit mixed phases, compromising the integrity of the cavitation barrier. Much research has been done to characterize the phase selection of Ta, however not much is understood about the underlying mechanisms of  $\beta$ -phase initiation and many studies report contradictory process parameters for phase selection. Through our work, we were able to demonstrate that substrate pre-treatment was promoting mixed phase formation during deposition, independent of other deposition parameters. We further aim to show that both substrate roughening and native oxide of the passivation surface plays a key role in initiating  $\beta$ -phase film growth on the substrate, by modifying the pre-sputter etch conditions and characterizing the surface and subsequent Ta phase.

12:00pm **PP1-1-MoM-7 Dc Magnetron Sputtering Yield Amplification of C, Si, and Ge Doped with W, Cu, Ta, or Mo**, *Julio Cruz [julio@ens.cnyun.unam.mx]*, Instituto de Investigaciones en Materiales, Universidad Nacional Autónoma de México; *Rebecca Giffard*, Universidad de Guadalajara, Mexico; *Stephen Muhl, Marco Martínez*, Instituto de Investigaciones en Materiales, Universidad Nacional Autónoma de México; *Roberto Sanginés, Roberto Machorro*, Centro de Nanociencias y Nanotecnología, Universidad Nacional Autónoma de México; *Efraín Chávez*, Instituto de Física, Universidad Nacional Autónoma de México

S. Berg in 1991 discovered the phenomenon called Sputtering Yield Amplification, SYA. The phenomenon is related to doping a sputtering target with atoms of different atomic mass than the target material. Such doping changes the collision cascade on the surface of the target, consequently increasing the number of ejected atoms from the target. In this work, we present a way of generating SYA of C and Si with two different types of co-sputtering experiments, in both by adding the doping element as small pieces on the surface racetrack. First, we increased the amount of W on C, Ge, and Si targets. Second, we increased the working gas pressure, i.e., the number of collisions in the gas phase, using a Si target and doping it with Cu, Mo, and Ta. Then we studied the number of dopant atoms returning to the target racetrack surface and its spatial distribution. To determine their effect on the cascade of collisions and, consequently, the change in the target sputtering yield. With the Perfilometry and Rutherford Backscattering Spectrometry techniques, we measure the thickness of the deposited films and the total number of atoms deposited on the substrate. With Optical Emission Spectroscopy we analyze the intensity of the emission lines of neutral and ionized species in the sputtering plasma. Furthermore, with SIMTRA code we theoretically estimated the spatial distribution of atoms that were redeposited on the target. The results showed Si and C SYA doped with W. Somewhat similar results have been reported earlier. Furthermore, significant Si SYA doped with Cu, Mo, and Ta. These results may be interesting for materials that have both lower sputtering yield and important applications in the thin films industry.

## Topical Symposium on Sustainable Surface Engineering Room Town & Country B - Session TS1-1-MoM

### Coatings for Batteries and Hydrogen Applications I

**Moderators:** *Dr. Martin Welters*, KCS Europe GmbH, Germany, *Prof. Chen-Hao Wang*, National Taiwan University of Science and Technology, Taiwan, *Prof. Fan-Bean Wu*, National United University, Taiwan

10:00am **TS1-1-MoM-1 Coating Innovations for Green Energy: Enabling Hydrogen Technologies**, *Mehmet Öte [oetehm@schaeffler.com]*, Schaeffler Technologies AG & Co. KG, Germany **INVITED**

In light of urgent climate challenges, the transition from fossil fuels to green energy sources necessitates significant advancements in hydrogen technologies. This keynote presentation will emphasize the crucial role of innovative coatings across all components of electrolyzers and fuel cells, including bipolar plate coatings, transport layer coatings, and catalyst-coated membranes. We will provide a comprehensive review of the evolving requirements for these coatings, assessing their impact on both performance and sustainability.

Key focus areas will include advancements in anti-corrosion and electrically conductive coatings designed to enhance the efficiency and lifespan of components within hydrogen systems. These innovations not only achieve exceptional electrical conductivity and corrosion resistance but also play a pivotal role in significantly reducing the CO<sub>2</sub> footprint of critical components. Ultimately, this talk aims to contribute to the ongoing discourse in the energy sector, demonstrating how advanced materials and coatings can facilitate the widespread adoption of hydrogen as a clean energy carrier.

10:40am **TS1-1-MoM-3 Intermediate-Temperature Proton-Conducting Solid Oxide Fuel Cells and Electrolyzers for Clean Energy**, *Sheng-Wei Lee [swlee@ncu.edu.tw]*, Chung-Jen Tseng, Szu-Yuan Chen, National Central University, Taiwan **INVITED**

The solid oxide cells (SOCs), which can operate in fuel cell or electrolyzer mode, is a promising technology to store electrical energy as chemical energy and to reconvert it into electricity upon demand. In recent years, extensive efforts have been devoted to developing proton-conducting SOC (P-SOCs) that operate in the low-to-intermediate temperature range (400-800 °C). Compared to the conventional oxygen ion-conducting SOC (O-

SOCs) that require high operating temperature (800- 1000 °C), this scheme enables more reliable sealing, use of cheaper materials for interconnect, and a better control of electrode/electrolyte interactions, thus prolonging the operational lifetime of SOC.

In this presentation, a variety of nanostructured electrode for P-SOCs is demonstrated via nano-engineering and have demonstrated their excellent cell performance. For example, we present a nanofiber-derived functional anode and cathode for proton-conducting SOFCs. The significantly lower polarization resistance elements indicate that the nano-fibrous electrode has superior catalytic activity for HOR and ORR. We also use PS nanospheres as pore former to fabricate an LSCF cathode with graded porosity, thus greatly improving the cell performance. In addition, we employ spin-coating technique and pulsed laser deposition (PLD) with doping strategy to fabricate thin-film electrolyte for P-SOCs. A bulk heterojunction GCCCO-BCZY layer with a domain width of ~5 nm by PLD via spontaneous phase separation is demonstrated as an electrolyte/cathode interlayer, which effectively increases the interfacial area between the two distinct phases and facilitates proton transport across the interface. Finally, we also discuss the SOC performance when fed with a variety of fuels and in the electrolysis mode.

11:20am **TS1-1-MoM-5 Development of Anode Electrodes for Water Electrolysis by Electroplating**, *Pei-Chi Lin, Chieh-Fu Huang, Yong-Song Chen [imeysc@ccu.edu.tw]*, National Chung Cheng University, Taiwan **INVITED**

Anion exchange membrane water electrolysis (AEMWE) has drawn much attention recently as a sustainable and cost-effective method for hydrogen production. Unlike proton exchange membrane water electrolysis, AEMWE employs non-precious metal as catalysts, which can significantly reduce material costs. However, it remains challenging to develop efficient and durable anode electrodes that can withstand alkaline environments while maintaining high performance in the oxygen evolution reaction (OER). In this study, stainless steel paper (SSP) is employed as the porous transport layer (PTL) of the anode in AEMWE. The effects of various surface modifications on SSP are investigated to assess their impact on electrochemical performance, including heat treatment, acid treatment, and electroplating.

Surface morphology, Brunauer–Emmett–Teller (BET) surface area, and current-voltage (I-V) characteristics are analyzed across treatments to evaluate their impact on catalytic activity. Results indicate that electroplating nickel (Ni) onto acid-treated SSP significantly enhances anode performance, achieving over a 10% increase in efficiency compared to untreated SSP. This enhancement is attributed to the increased specific surface area provided by acid treatment, combined with the catalytic benefits of Ni from electroplating. BET analysis supports that acid treatment creates a rough surface on the SSP fibers, thereby increasing active surface area. Additionally, I-V curves demonstrate that Ni-electroplated, acid-treated SSP exhibits lower overpotentials and higher current densities. This approach utilizes low-cost, commercially available stainless steel, supporting the potential for mass production and enhancing the economic feasibility of AEMWE in hydrogen production applications.

12:00pm **TS1-1-MoM-7 Development of Three-Dimensional Lithium Metal Composite Electrode with Lithiophilic ALD Coating**, *Yu-Lun Cheng, Chih-Liang Wang [wangcl@mx.nthu.edu.tw]*, National Tsing Hua University, Taiwan

Lithium (Li) metal is widely regarded as an ideal anode material for lithium-ion batteries thanks to its high theoretical capacity (3860 mAh/g) and low electrochemical potential (-3.04 V vs. standard hydrogen electrode). However, practical use is limited by challenges such as lithium dendrite growth, volume expansion, and dead lithium, which degrade performance. This study addresses these issues by applying atomic layer deposition (ALD) of zinc oxide (ZnO) onto electrospun carbon nanofibers (CNFs) to create a high-performance, three-dimensional (3D) lithium metal composite anode. Polyacrylonitrile (PAN) was first electrospun to form the CNF framework. The lithiophilic properties of CNFs were systematically explored by adjusting the number of ALD ZnO cycles. The 3D lithium metal composite anodes were then produced by infusing molten lithium into the ZnO-coated CNFs. These composite electrodes showed excellent electrochemical performance, including low overpotential and extended cycle life in symmetric cell tests. In full-cell tests with LiFePO<sub>4</sub>, the 3D Li composite anode delivered higher capacity than traditional Li metal foil. Overall, the combination of electrospinning and ALD techniques demonstrates substantial potential in creating 3D lithium metal composite electrodes, offering improved lithium diffusion, current distribution, battery stability, cycle life, and rate performance.

# Monday Afternoon, May 12, 2025

## Keynote Lectures

### Room Town & Country A - Session KYL-MoKYL

#### Keynote Lecture I

**Moderator: Dr. Ivan G. Petrov**, University of Illinois at Urbana-Champaign, USA

1:00pm **KYL-MoKYL-1 Bill Sproul Award and Honorary ICMCTF Lecture: Robust Plasmonically-Active Nanoscale Multilayer TiN/NbN Coatings**, Arunprabhu Sugumaran Arunachalam Sugumaran, Sheffield Hallam University, United Kingdom; Ryan Bower, Ming Fu, Imperial College London, UK; David Owen, Papken Eh. Hovsepian, Sheffield Hallam University, UK; Peter K. Petrov, Rupert Oulton, Imperial College London, UK; **Arutiun P. Ehasarian [A.EHASARIAN@SHU.AC.UK]<sup>1</sup>**, Sheffield Hallam University, UK

#### INVITED

Plasmonic catalysis enabled by visible light is vital to enhancing the activity of surfaces in promoting a broad range of chemical reactions including water splitting and associated production of bioactive reactive oxygen species. However standard catalysts that rely on nanoparticles are not sufficiently robust for deployment in the environment. Transition metal nitrides are promising candidates whose function is highly dependent on their purity and structure. High-Power Impulse Magnetron Sputtering has been deployed to tailor the texture and morphology of nanoscale multilayer TiN / NbN coatings and evaluate the effect of their plasmonic activity. Plasma characterisation show a significant fractions of dissociated nitrogen and double-charged metal ions in both TiN and NbN deposition conditions. Time-resolved ion energy distribution functions obtained from energy-resolved mass spectroscopy indicate that 30% of dissociated nitrogen possesses a high-energy tail and originates from sputtering from the target surface alongside Ti and Nb thereby increasing adatom mobility and intergranular density and promoting a strong (200) fibre texture as observed in pole figures. Nevertheless oxidation of the surface detected through XPS deteriorated the plasmonic performance of the films as observed through ellipsometry. Pump-probe laser measurements showed significant increases in the lifetime of active electron species in the films due to trapping of hot carriers in oxygen vacancies such as Nb<sup>3+</sup> and Ti<sup>3+</sup>, with Nb being more sensitive due to a higher enthalpy of its oxide. Nanoscale multilayer films deposited with small bi-layer thickness of 1.7 nm exhibited strong intermixing between the TiN and NbN layers which led to small grain size observed by AFM and longer hot carrier lifetime. Bilayer thickness of 2.4 and 3.5 nm led to doubling of the grain size and shorter hot carrier lifetimes. A graded structure, starting from a bilayer thickness of 2.4 and reducing to 1.7 nm exhibited a large grain size and increased hardness and toughness as determined from nanoindentation. Ellipsometric measurements of the real component of the dielectric permittivity confirmed an excellent plasmonic activity. The effects of carrier lifetime on photocatalytic activity are discussed. The results pave the way to using nanoscale multilayer coatings for catalysis.

---

<sup>1</sup> Bill Sproul Awardee



# Monday Afternoon, May 12, 2025

## Advanced Characterization, Modelling and Data Science for Coatings and Thin Films

### Room Town & Country C - Session CM4-2-MoA

## Simulations, Machine Learning and Data Science for Materials Design and Discovery II

Moderators: Dr. Davide G. Sangiovanni, Linköping University, Sweden, Dr. Ferenc Tasnadi, Linköping University, Sweden

1:40pm **CM4-2-MoA-1 Computational Approach to Probing Hydrogen in Atomic Layer-Deposited Barrier Coatings**, Vladyslav Turlo [[vladyslav.turlo@empa.ch](mailto:vladyslav.turlo@empa.ch)], Empa, Swiss Federal Laboratories for Materials Science and Technology, Switzerland

INVITED

The energy transition of our society requires an improved fundamental understanding of the chemical interaction of H with oxide materials, such as oxide membranes for H-purification, oxides for photocatalytic water splitting, and passivated oxides on steel. In particular, the effect of H impurities on the barrier properties of oxide layers grown by Atomic Layer Deposition (ALD) is of great scientific and technological interest, since hydrogen permeation barriers fabricated by ALD are broadly applied to address specific challenges for transport, handling, and storage of H, as well as for electronics, catalysis and gas sensing. However, resolving tiny changes in local chemical bonding states and structure of e.g. amorphous alumina oxides, as induced by H impurities originating from the ALD deposition process, still poses huge challenges for modern analytical tools up to date.

Here, the effect of hydrogen on the local chemical bonding states and structures of amorphous ALD alumina films is disclosed by predicting Auger parameter shifts, as measured by XPS/HAXPES, using a combination of atomistic and electrostatic modeling. First of all, it is demonstrated that a conventional melt quenching simulation procedure is not applicable for generating representative amorphous oxide structures with different H contents and densities, as observed in the experiment. Instead, a novel approach is proposed for simulating amorphous H-containing oxide structures by annealing reconstructed, highly defective crystalline hydroxide structures using a universal machine learning interatomic potential. As such, excellent agreement between the density, structure, and H-content was obtained between theory and experiment. Moreover, measured Auger parameter shifts for Al as a function of the H-content were accurately predicted by assuming all H atoms to be present in the form of hydroxyl ligands in the randomly interconnected 4-fold, 5-fold, and 6-fold nearest-coordination spheres of Al (by O). Combined atomistic and electrostatic modeling shows in detail how measured Auger shifts depend on the complex correlations between local coordination, bond lengths, bond angles, and ligand type(s) around the core-ionized atom, which equally applies to amorphous and crystalline compounds.

This work enables the computational design of new barrier coatings for hydrogen economy, providing a comprehensive computational characterization framework able to interpret even the tiniest Auger parameter chemical shifts obtained from experimental XPS/HAXPES techniques.

2:20pm **CM4-2-MoA-3 Conditions for the Preparation of Maximum-Quality Crystalline ZnO by Molecular Dynamics Simulations of the Atom-by-Atom Film Growth**, Jiri Houska [[jhouaska@kfy.zcu.cz](mailto:jhouaska@kfy.zcu.cz)], Kamila Hantova, University of West Bohemia, Czechia

Crystalline zinc oxide thin films are important due to a combination of optical transparency, electrical conductivity and piezoelectric and pyroelectric properties. These functional properties largely depend on perfection of the crystalline structure. Reproducing the growth of thin films by molecular-dynamics (MD) simulations is very useful for the disentanglement of processes and phenomena which take place in parallel in the experiment and can yield a lot of atomic-scale information which is difficult to access experimentally. After introducing MD simulations in general, classical MD based on a reactive force field is used to study the atom-by-atom growth of ZnO<sub>x</sub> films on a crystalline template. The effect of kinetic energy of fast atoms ( $E_{fast}$ ) and fraction of fast atoms ( $f_{fast}$ ) at varied elemental ratio ( $x = [O]/[Zn]$ ) is analyzed in a wide range. Following the visual inspection, the crystallinity is quantified in terms of network ring statistics.

Simulations with fixed  $f_{fast} = 100\%$  revealed that the highest crystal quality was obtained at  $x = 1.03$  (not at the intuitive ratio  $x = 1.00$ ) and  $E_{fast} = 3-12$  eV with a maximum at  $E_{fast} = 10$  eV. When only a low  $E_{fast} = 1$  eV is available, even higher  $x = 1.10$  leads to the relatively best results. Simulations with varied  $f_{fast}$  and fixed  $E_{fast} = 10$  eV revealed that the crystallinity at  $f_{fast} \geq 50\%$

is saturated. The ratio  $x = 1.03$  is optimum at all these  $f_{fast}$  values and it is followed by  $x = 1.05$  which also leads to higher crystal quality than  $x = 1.00$ . However, the ratio  $x = 1.10$  is for the present energy distribution functions too high, not only in terms of growth rate which decreases with increasing  $x$ , but also in terms of crystal quality.

First, the results provide a quantitative insight into the role of individual deposition parameters. Second, the results explain available experimental data (for example, the dependence of the mobility of free charge carriers on the pulse-averaged target power density expresses the same character as the dependence of network ring statistics on  $E_{fast}$ ). Third, the results facilitate a further improvement of the film properties. For example, it is important that the recommended  $E_{fast}$  is comparable to achievable positions of maxima of energy distribution functions during reactive HiPIMS.

2:40pm **CM4-2-MoA-4 Effect of the Presence of Oxygen on Hydrogen Adsorption on BCC Fe Surface: A Density Functional Theory Study Combined with Molecular Dynamics Simulations**, Zixiong Wei, Fei Shuang, Poulumi Dey [[p.dey@tudelft.nl](mailto:p.dey@tudelft.nl)], Delft University of Technology, Netherlands

Hydrogen is one of the most promising candidates for the replacement of current carbon-based energy sources. It is one of the most potential candidates of sustainable energy produced in an eco-friendly manner. However, the use of hydrogen as an energy source is severely restricted by its damaging effect on mechanical properties of materials widely known as Hydrogen Embrittlement (HE). It is, thus, urgently needed to develop new HE resistant alloys or re-design the existing alloys for safe and efficient hydrogen storage and transportation. In this regard, Density Functional Theory (DFT) based approach is particularly important for obtaining atomistic insights into hydrogen interaction with surfaces to ensure less uptake of hydrogen by the material e.g. steels. Within this study, DFT is employed to obtain atomistic insights into hydrogen adsorption on different surfaces of bcc-Fe in the presence of oxygen. At the initial stage, we investigate the adsorption of oxygen on different surfaces of bcc-Fe using DFT following which we study the adsorption of hydrogen on Fe surface in the presence of the oxygen. At the next stage, we employed Molecular Dynamics (MD) simulations to study hydrogen diffusion into the bulk of bcc Fe from the surface in the presence of oxygen atoms on the surface. Our combined DFT-MD study thus offers atomistic insights into how surface oxygen atoms influence hydrogen intake into bcc Fe.

3:00pm **CM4-2-MoA-5 Machine Learning Prediction of Work Functions for No, No<sub>2</sub>, Co, Co<sub>2</sub>, and H<sub>2</sub>S Gas Molecules Adsorbed on ZnGa<sub>2</sub>O<sub>4</sub>(111) Surfaces**, Po-Liang Liu [[pliu@dragon.nchu.edu.tw](mailto:pliu@dragon.nchu.edu.tw)], Hsiang-Yu Hsieh, Chao-Cheng Shen, National Chung Hsing University, Taiwan

Zinc gallium oxide is a metal oxide gas sensing layer with exceptional thermal and chemical stability, capable of detecting gases such as NO, NO<sub>2</sub>, CO, CO<sub>2</sub>, and H<sub>2</sub>S. The work function of Zinc gallium oxide can be assessed through first-principles calculations based on Density Functional Theory, which allows for the prediction of the sensor's sensitivity. Although Density Functional Theory provides accurate computational results, its high computational cost and time requirements limit its applicability for large-scale surface screening. This study used a database based on a density functional theory-based zinc gallium oxide sensor model. We developed an automated workflow using Python programming to extract crystal structure features as input for the machine learning model. The processed and filtered input features were employed to predict the work function of the sensor model, achieving a mean absolute percentage error below 6% in the prediction results. This study presents a trained machine-learning model interface that allows users to input crystal structure files for the rapid and accurate evaluation of the work function of Zinc gallium oxide sensors.

3:20pm **CM4-2-MoA-6 ML-Assisted Atomistic Modeling of Transition Metal Diborides: Mechanical Response and Phase-Dependent Phenomena**, Shuyao Lin [[shuyao.lin@tuwien.ac.at](mailto:shuyao.lin@tuwien.ac.at)], TU Wien, Institute of Materials Science and Technology, Austria; Davide Sangiovanni, Lars Hultman, Linköping Univ., IFM, Thin Film Physics Div., Sweden; Paul Mayrhofer, Nikola Koutna, TU Wien, Institute of Materials Science and Technology, Austria

Transition metal diborides (TMB<sub>2</sub>) represent materials with ultra-high hardness and melting points but limited resistance to crack propagation. Understanding the thermodynamic stability of typical TMB<sub>2</sub> polymorph structures ( $\alpha$ ,  $\omega$ , and  $\gamma$ ) at finite temperatures as well as the phase-dependence of mechanical and fracture properties has been challenging due to non-trivial synthesis and structural similarity of the phase polymorphs, complicating their detection. This work presents uniform shear and tensile strain simulations of defect-free Group IV-VII TMB<sub>2</sub>

# Monday Afternoon, May 12, 2025

ceramics using *ab initio* molecular dynamics as well as molecular dynamics powered by machine-learning interatomic potentials (MLIP), trained in the moment tensor potential framework. Studied materials include TiB<sub>2</sub> (Group IV), TaB<sub>2</sub> (Group V), WB<sub>2</sub> (Group VI), and ReB<sub>2</sub> (Group VII), covering the  $\alpha$ ,  $\omega$ , and  $\gamma$  polymorphs. Among our main results is a robust workflow for training transferable MLIPs. These MLIPs are suitable for atomic-to-nanoscale MD simulations, allowing to understand deformation and fracture mechanisms of each TiB<sub>2</sub>, and extending the insights into phase transformation mechanisms under shear deformation. By demonstrating the outstanding mechanical performance of TiB<sub>2</sub>s in extreme environments, our predictions clearly underpin their huge application potential in protective coatings and high-temperature engineering. To deepen our understanding of fracture behavior, we additionally perform Mode-I fracture simulations allowing to quantitatively assess fracture toughness ( $K_{Ic}$ ) using pre-cracked models. The results are discussed in light of relevant experimental data, including high-resolution transmission electron microscopy analysis of nanoindentation experiments on TiB<sub>2</sub> thin films.

4:00pm **CM4-2-MoA-8 Computational Modeling of Nanoelectronics and Emerging Materials**, *Chao-Cheng Kaun [kauncc@gate.sinica.edu.tw]*, Academia Sinica, Taiwan **INVITED**

Using first-principles calculations, we investigate electronic transport through carbon-, oxide- and transition metal dichalcogenide (TMD)-based nanojunctions for nanoelectronic applications. Effects of biasing, defecting, contacting and quantum interfering are addressed. We study noncollinear interlayer exchange coupling in magnetic trilayers for spintronic application. Effects of spacing are uncovered. We also study the efficiencies of hybrid-protected perovskite quantum dot films for LED backlighting and hydrogen evolution reaction in oxides for sustainable-energy applications. Effects of polymer-adsorbing and material-configuring are highlighted. Moreover, we explore the plasmonic properties of complex transition metal nitrides for photonic applications.

## Surface Engineering - Applied Research and Industrial Applications

### Room Town & Country D - Session IA2-1-MoA

#### Surface Modification of Components in Automotive, Aerospace and Manufacturing Applications I

**Moderators:** Dr. Satish Dixit, Plasma Technology Inc., USA, Masaki Okude, Mitsubishi Materials Corporation, Japan, Dr. Jan-Ole Achenbach, KCS Europe GmbH, Germany

1:40pm **IA2-1-MoA-1 Laser Surface Remelting Induced Reaction Sintering of Nickel and Titanium Powders**, *Milton Lima [miltonsflima@gmail.com]*, Institute for Advanced Studies, Brazil; *Alana Brito*, Technological Institute of Aeronautics, Brazil; *Felipe Costa*, BRENG Co., Brazil; *Rafael Siqueira*, Technological Institute of Aeronautics, Brazil; *Sheila Carvalho*, Federal University of Espirito Santo, Brazil

There is currently an interest in the synthesis and applications of mnemonic structure materials for various applications, such as biomedical, aerospace, automotive, and robotics. Shape memory alloys (SMAs) are metallic materials that can return to their initial state after being subjected to deformation as a result of increased temperature, increased pressure, or other stress conditions. These materials have been used in thermoelastic actuators in space applications, such as antenna supports and solar panel deployments, and can impact the manufacture of polymorphic aircraft engines and fuselages. SMAs, such as Nitinol (equimolar alloy of Ni and Ti), are difficult to fabricate, and the powder metallurgy route, whether classical or using laser powder bed fusion (L-PBF), has been constantly improved to meet new application niches. This study proposes reactive sintering of samples with equiatomic compositions of Ni and Ti to form Nitinol using laser surface remelting. Elementary powders were inserted into a high-energy ball mill to fabricate mechanically alloyed Ni-Ti powders, which were subsequently pressed in the form of discs (20 mm diameter, 5 mm thickness). An experimental arrangement with a vacuum chamber and fiber laser beam manipulation was developed to induce sufficient heat for the reaction of elementary powders. Spiral scanning of the fiber laser beam produced surface remelting that ignited the pressed powder mixture. Macro- and microstructural analyses, the crystalline structure, and the composition of the sample surface remelted with a beam power ranging from 10 to 46 W were performed. In this power range, the sintering time was varied between 55 and 295 s when the laser power was varied from 46

W to 10 W. Although the presence of intermetallic phases was approximately the same, the microstructure in the laser-surface-remelted region was more homogeneous than that in the sintered volume. At the end of sintering, tablets were obtained with an apparent density of 61%–67% and a large number of intermetallic phases, such as NiTi<sub>2</sub>, Ni<sub>3</sub>Ti, and Ni<sub>4</sub>Ti<sub>3</sub>, together with unreacted elemental powders (Ni and Ti). The samples prepared in air also presented these phases in addition to TiO<sub>2</sub> and NiTi. The air-processed samples presented an equimolar Nitinol phase, as observed by X-ray diffractometry. According to mass spectrometry analyses of secondary ions, the presence of air oxidized the surface of the grains, which reacted at shorter distances and generated the Nitinol phase.

2:00pm **IA2-1-MoA-2 A Comparative Study on the Formation of Micro-Arc Oxidation Coatings on AZ31 and AC84 Magnesium Alloys**, *Chi-Hua Chiu [chiuhua90@gmail.com]*, *Shih-Yen Huang*, *Yueh-Lien Lee*, *Yu-Ren Chu*, National Taiwan University, Taiwan

Magnesium-aluminum-calcium (Mg–Al–Ca) alloys have attracted significant attention due to their excellent strength-to-weight ratio, good castability, and potential for flame retardancy, owing to the presence of calcium and aluminum. However, the applications of these alloys are limited by their poor corrosion resistance. Micro-arc oxidation (MAO) is one of the most common techniques for corrosion protection of magnesium alloys; however, the formation mechanism of MAO coatings is extremely complex and influenced by numerous process parameters, including the substrate effect. In this study, the mechanism of MAO coating formation on the AZ31 and dual-phase AC84 (Mg–8Al–4Ca) alloys was comparatively examined. The preliminary results reveal that, during MAO treatment at a constant anodizing voltage of 150V, unreacted Al<sub>2</sub>Ca secondary phases were observed in the micro-arc oxidation coatings of AC84 magnesium alloys, causing non-uniform surface structures and thicknesses, which led to poor corrosion resistance compared to the MAO coating formed on AZ31. Conversely, AC84 exhibited better corrosion resistance than AZ31 when the voltage was increased to 250V. Further increasing the voltage to 300V resulted in the involvement of secondary phases in the reaction, leading to more uniform microstructures and chemical compositions of the coatings on both alloys. These findings suggest that the anodizing voltage plays a crucial role in the reaction behavior of secondary phases and the properties of the MAO coatings.

2:20pm **IA2-1-MoA-3 Ultra-High Vacuum Test System for Quantitative Determination of Hydrogen Permeability of Various Ceramic Coatings on Stainless Steel**, *Ewa Rennebro [ewa.ronnebro@pnnl.gov]*, Pacific Northwest National Laboratory, USA **INVITED**

We will discuss a recently built state-of-the-art ultra-high-vacuum (UHV) test system with high accuracy and precision to quantify hydrogen uptake, solubility and diffusion in various materials. The design was developed by Pacific Northwest National Laboratory (PNNL) in collaboration with Vacuum Technology Inc (VTI). This automated UHV system can be used for several studies of hydrogen-metal interactions including absorption/desorption kinetics, thermodynamics, isotherms, plateau pressures, isotope studies, gaseous impurity identification and permeation rate. We will present recent permeation rate data of ceramic coatings to reduce permeation through stainless steel.

3:00pm **IA2-1-MoA-5 HIPIMS – Fascinating Technology to Make Next Steps in Tool, Decorative and Functional Applications**, *Philipp Immich [pimmich@hauzer.nl]*, *Ivan Kolev*, *Andreas Fuchs*, *Daniel Barnholt*, *Julia Janowitz*, *Louis Tegelaers*, *Huub Vercoulen*, *Chinmay Trivedi*, *Geert-Jan Fransen*, IHI Hauzer Techno Coating B.V., Netherlands; *Holger Hoche*, *Thomas Ulrich*, TU Darmstadt, Germany; *Peter Polcik*, Plansee Composite Materials GmbH, Australia

The PVD (Physical Vapor Deposition) market is rapidly expanding into new application fields. To achieve these new applications, various PVD coating techniques are employed, with HIPIMS (High Power Impulse Magnetron Sputtering) being one of the most fascinating since its discovery. Over the past 25 years, numerous advancements have been made in latest Generation 3 - HIPIMS power supply technology, including modifications in bipolar mode, pulse shape, pulse length, pulse trains, and higher frequencies. Synchronization of cathodes and HIPIMS-based bias has also led to innovative PVD coating solutions.

Beyond the well-known performance improvements in HIPIMS-coated cutting tools, HIPIMS has demonstrated its potential for various other applications. We will showcase the ability to create different colors using HIPIMS technology and highlight its advantages for decorative applications on 3D products. For components, HIPIMS is an excellent tool for enhancing the wear and corrosion resistance of existing material systems. We will also

# Monday Afternoon, May 12, 2025

present the latest coating development for cutting tools. Our presentation will illustrate how combining HIPIMS with new material systems can further expand and enhance potential application areas.

Decorative, tool and tribological markets are driven by production costs, making coating volume and size crucial factors. To meet these demands, we have scaled up our HIPIMS developments to deposit coatings on our largest industrial platforms, e.g. the Flexicoat 1500 to address market needs.

We will also provide an outlook on future developments and what can be expected next in the PVD market.

**3:20pm IA2-1-MoA-6 Inorganic Sputtered Coatings to Reduce Snow Friction for Cross-Country Skiing, Pauline Lefebvre [pauline.lefebvre@grenoble-inp.fr]**, SIMAP, Grenoble-INP, CNRS, France; Fabian Wolfspurger, WSL Institute for Snow and Avalanche Research SLF, Switzerland; Jean Herody, FFS, France; Matthias Jaggi, WSL Institute for Snow and Avalanche Research SLF, Switzerland; Arnaud Mantoux, SIMAP, CNRS, University Grenoble Alpes, France; Nicolas Coulmy, FFS, France; Pascal Hagemmuller, Centre d'Etudes de la Neige, CNRM, Météo-France; Elisabeth Blanquet, SIMAP, Grenoble-INP, CNRS, France

In cross-country skiing, reducing the friction coefficient between the skis and snow is essential for sportive performance [1]. Fluorinated waxes, i.e. containing perfluoroalkyl (PFA) are known for their hydrophobic properties and were remarkably efficient in wet snow conditions. However, the International Ski and Snowboard Federation (FIS) has banned fluorinated wax since winter 2023/2024 -for health and environmental reasons [2]. Since then, no alternative with equivalent performance has been found. This project aims to develop hard and hydrophobic coatings based on titanium nitride (TiN), aluminum nitride (AlN) and alumina (Al<sub>2</sub>O<sub>3</sub>) materials directly deposited on ski bases and UHMW polyethylene. The role of coating surface properties and structure in friction is investigated

Thin films were deposited using DC and RF magnetron sputtering. The surface (contact angle, roughness, chemical composition), mechanical and thermal properties of the coatings were investigated. Friction coefficient of coated samples was evaluated on snow with a linear tribometer (speed: 0.1 m/s, displacement: 130 mm, contact pressure: 50 kPa). The tribo-system is therefore a 10cm-long coated ski sliding on controlled man-made snow in a cold-room at 0°C and dry air. Snow with different liquid water content were used for the tests.

Results are encouraging as deposition on ski base is feasible at ambient temperature with adhesive and dense coatings. Coating thicknesses were evaluated by scanning electronic microscopy between 50 and 200 nm depending on process parameters. Chemical analysis with XPS indicates nitride films contain a relative high amount of carbon and oxygen. Coatings, selected for their hydrophobicity and structural properties, were investigated in gliding tests. AlN and Al<sub>2</sub>O<sub>3</sub>-based coatings presented very high friction coefficient (0.2-0.3). TiN-based coating had the lower friction coefficient with a value of 0.11 on very wet snow, whereas a ski waxed with PFA friction coefficient was measured at 0.072.

To sum up, deposition of sputtered coatings was realized with success and may be a promising technique for preparing competition skis. For winter sport application, titanium nitride seems to be the most promising: it is indeed known for better mechanical properties [3] and lower thermal conductivity [4] which will be further investigated.

## References:

- [1] Moxnes, J. F. et al, J Sports Med, 4, 127-139 (2013).
- [2] Freberg, B. I. et al, Environ Sc & Techno, 44, 7723-7728 (2010).
- [3] Glocker, D. A. et al, Bristol, UK: Inst of Phys (1995).
- [4] Moraes V. et al, J Appl Phys, 119, 225304 (2016).

**4:00pm IA2-1-MoA-8 Influence of Corrosion on Wear and Brake Particle Emissions of Alumina-Coated and Uncoated Cast Iron Brake Discs, Ran Cai [cai12r@uwindsor.ca]**, Xueyuan Nie, University of Windsor, Canada; Yezhe Lyu Lyu, Jens Wahlström, Lund University, Sweden

Hard coatings can be applied to cast iron brake discs to enhance wear and corrosion resistance and reduce brake particle emissions. This study investigated the influence of corrosion on brake particle emissions from cast iron discs through comparison of plasma electrolytic aluminized (PEA)-coated and uncoated surfaces. Six discs were subjected to corrosion in raining-snowy conditions for 24, 48, and 72 hours before undergoing tribological testing using a pin-on-disc tribotester combined with an airborne particle emission measurement system. The counterpart pins were machined from a commercially available low-steel (LS) brake pad. Data of particle concentration, size distribution, and total wear (disc and pad) were

collected, while wear tracks, friction transfer layers and worn pad surfaces were analyzed using scanning electron microscopy (SEM) and energy dispersive X-ray spectroscopy (EDX). The results showed that the degree of corrosion of the uncoated disc increased with time, while the coated discs didn't show any corrosion sign. The corrosion products on the uncoated discs can be cleaned during the early stage of the tribotests where the particle emission was much higher than the later stage. The PEA coating effectively mitigated the effects of corrosion, resulting in significantly lower wear and brake particle emissions compared to uncoated discs. These findings demonstrate the potential of PEA coatings to reduce wear and emissions under winter conditions, offering benefits for environmental sustainability and public health.

**4:20pm IA2-1-MoA-9 The Effect of Mg Addition on the Corrosion Resistance of Two-Step Galvanizing Zn-5Al Coating, Huan-Chang Liang [hcliang@niu.edu.tw]**, Department of Mechanical and Electro-Mechanical Engineering, National I-Lan University, Taiwan; Yen-Kai Chen, Chaur-Jeng Wang, Department of Mechanical Engineering, National Taiwan University of Science and Technology, Taiwan

The atmospheric corrosive substances like Cl<sup>-</sup> ions or SO<sub>3</sub><sup>2-</sup> ions make it easier for soluble zinc salts to form. Consequently, the introduction of more magnesium into the Zn-Al alloy bath enhances the formation of basic zinc salts that are susceptible to environmental corrosion. Zinc-aluminum carbonate hydroxide and aluminum-magnesium carbonate hydroxide are particularly notable corrosion products because of their stable and compact characteristics. Local acidity influences the rate of transformation of zinc hydroxide from zinc oxide, while the formation of Mg(OH)<sub>2</sub> mitigates the surface reduction of the galvanizing coating.

Although the Zn-5Al-2Mg coating is effectively produced using the continuous galvanizing process, the maximum coating thickness achieved is 20 μm. Numerous studies present their experimental findings about batch galvanizing zinc alloys. The coating structure is nonuniform, with an enrichment of iron content resulting from the elevated operating temperature, which inhibits the formation of a dense and continuous layer of corrosion products. Consequently, two-step batch galvanizing is utilized to provide a zinc alloy coating of adequate thickness. The initial process involves immersing samples in pure zinc, followed by immersion in zinc alloy. The coating's microstructure consists of an outer layer formed from zinc alloy and internal layers including an iron-aluminum intermetallic compound combined with a eutectic phase.

This study aims to examine the microstructure of two-step batch galvanizing Zn-5Al and Zn-5Al-2Mg coatings on low-carbon steel. The samples are produced by batch galvanizing pure zinc for 10 minutes, followed by batch galvanizing zinc alloy for 2.5 minutes. The corrosion resistance performance of both samples is evaluated by interfacial polarization and impedance matching. The microstructure of two-step galvanizing Zn-5Al and Zn-5Al-Mg consists of four distinct layered structures: a binary (Zn-Al) or ternary (Zn-Al-Mg) eutectic phase layer, a branch-like FeAl<sub>3</sub> phase layer, a dense FeAl<sub>3</sub> phase layer, and an internal eutectic phase layer. As the zinc content in the coating layer increases, there is a corresponding decrease in the charge transfer impedance (R<sub>ct</sub>). This behavior is ascribed to the area fraction of the FeAl<sub>3</sub> phase in conjunction with the eutectic phase. The addition of magnesium into the zinc alloy bath enhances the R<sub>ct</sub> of the entire coating layer. The advantageous effect arises from the disparity in corrosion potential between magnesium and zinc. Magnesium functions as a sacrificial anode for the Zn-rich phase, hence enhancing the effectiveness of cathodic protection.

## Functional Thin Films and Surfaces

### Room Palm 5-6 - Session MB2-2-MoA

#### Thin Films for Electronic Devices II

**Moderators: Spyros Kassavetis**, Aristotle University of Thessaloniki, Greece, **Dr. Tomas Kubart**, Angstrom, Switzerland

**2:00pm MB2-2-MoA-2 "Flexible Electronics" Sustainability — Challenges and Opportunities: a Materials Science View, Natalie Stigelin [natalie.stigelin@mse.gatech.edu]**, Georgia Institute of Technology, USA  
**INVITED**

In recent years, immense efforts in the flexible electronics field have led to unprecedented progress and to devices of ever increasing performance. Despite these advances, new opportunities are sought in order to widen the applications of flexible electronics technologies, expand their

# Monday Afternoon, May 12, 2025

functionalities and features, with an increasing view on delivering sustainable solutions. We discuss here opportunities the use of multicomponent systems for, e.g., increasing the mechanical flexibility and stability of organic electronic products, or introducing other features such as self-encapsulation and faster mixed ion-electron transport. One specific strategy is based on blending polymeric *insulators* with organic semiconductors; which has led to a desired improvement of the mechanical properties of organic devices, producing in certain scenarios robust and stable architectures. Here we discuss the working principle of semiconductor:insulator blends, examining the different approaches that have recently been reported in literature. We illustrate how organic field-effect transistors (OFETs) and organic solar cells (OPVs) can be fabricated with such systems without detrimental effects on the resulting device characteristics even at high contents of the insulator. Furthermore, we review how blending can assist in the fabrication of more reliable and versatile organic electrochemical transistors (OECT)s.

**2:40pm MB2-2-MoA-4 Polycarbonate Transfer Techniques for the Fabrication of MoS<sub>2</sub> Based Field Effect Transistors**, *Chih-Hao Chiang, Ruo-Yao Wang [tsubasaja@gmail.com], Meng-Lin Tsai*, National Taiwan University of Science and Technology, Taiwan

In recent years, transition metal dichalcogenides (TMDs) have received significant attention due to their immense potential to extend Moore's Law, positioning them as promising semiconductor materials for next-generation electronic devices. The challenges of large-scale production and commercialization of TMDs remain key challenges for future development in practical applications. In the fabrication of TMD-based semiconductor devices, the interface between metal electrodes and TMD layers is critical. Traditional metal electrode deposition techniques facilitate the diffusion of metals in the TMD, potentially reducing the device performance or preventing proper operation. In this study, the metal electrode transfer technique using polycarbonate has been developed to significantly reduce such damage, ensuring the reliable operation of semiconductor devices. Gold electrodes initially deposited on silicon or SiO<sub>2</sub>/Si substrates via metal mask (channel length of 20 μm) and photolithography (channel lengths of 8 μm for photodetectors and 3 μm for field-effect transistors, FETs) have been successfully onto chemical vapor deposition (CVD)-grown MoS<sub>2</sub> nanosheets. The as-fabricated field effect transistors (FETs) have been characterized to exhibit switching current ratios of approximately 10<sup>4</sup>.

**3:00pm MB2-2-MoA-5 Advancing Piezo-Gated Transistor Performance by Bilayer of V-doped ZnO and Mesoporous PVDF-TrFE**, *YU ZHEN ZHANG [h56124650@gs.ncku.edu.tw]*, National Cheng Kung University (NCKU), Taiwan

In recent years, technology has rapidly advanced, enabling the development of flexible wearable electronics with great potential for applications such as nanogenerators and pressure sensors. Among flexible materials, β-phase PVDF-TrFE, which exhibits piezoelectric properties ( $d_{33}=30\text{--}40\text{pC/N}$ ), stands out as a promising composite. This polymer has a semicrystalline structure and displays excellent piezoelectric and ferroelectric properties while maintaining flexibility. However, VZO ( $d_{33}=12\text{--}22\text{pC/N}$ ) is also a piezoelectric material, and we aim to improve the device output by depositing it on PVDF-TrFE.

In this study, we aimed to enhance the flexibility and piezoelectric performance of PVDF-TrFE by blending it with zinc oxide nanoparticles and subjecting the mixture to thermal annealing at 120°C. We then applied 11,000 V through corona poling to align the dipole directions within the composite, followed by etching the ZnO to create a porous structure. Additionally, we used radio frequency magnetron co-sputtering that uses ZnO and V<sub>2</sub>O<sub>5</sub> as targets to deposit VZO thin film on both sides of the PVDF-TrFE to serve as conduction pathways. Finally, we deposited two Au electrodes to make a piezoelectric gate transistor device.

In the XRD analysis, we examined unpoled and corona-poled samples. The XRD patterns of the unpoled sample showed two peaks corresponding to the α phase which has negatively affects the piezoelectric properties. After poling, the pattern of the poled sample confirmed that the β phase completely dominates the PVDF-TrFE.

We investigated the current output of the piezoelectric gate transistor under various mechanical stresses at a 1V bias and 1Hz frequency. Devices with different dipole orientations exhibited opposite behaviors. Applying mechanical stress to the positively polarized surface generated negative charges at the VZO and PVDF-TrFE interface, creating a depletion region in the top surface channel and reducing current. Conversely, this led to an accumulation region, enhancing current. By applying a piezoelectric field to the gate, we could adjust the semiconductor channel's resistance and

control current flow. This technique significantly advances the piezoelectric gate transistor device, paving the way for advanced applications in flexible and wearable electronics and sensing technologies.

**3:20pm MB2-2-MoA-6 Enhanced Synaptic Characteristics Under Applied Magnetic Field in V<sub>2</sub>O<sub>5</sub>/NiMnIn Based Switching Device for Neuromorphic Computing**, *Kumar Kaushlendra [kumar\_k@ph.iitr.ac.in]*, Indian Institute of Technology Roorkee, India; *Davinder Kaur*, Indian Institute of Technology Roorkee, India

The present study reports a memory structure Al/V<sub>2</sub>O<sub>5</sub>/NiMnIn on a flexible stainless-steel (SS) substrate for neuromorphic applications. The fabricated device exhibits gradual SET and RESET switching characteristics with an OFF/ON resistance ratio of ~100, good consistency of 4500, and excellent data retention capability up to 3000 s. The current-voltage (I-V) study supports an Ohmic conduction mechanism in the low resistance state (LRS). In contrast, the trap-controlled modified space charge conduction mechanism demonstrated the high resistance state (HRS). The resistance versus temperature measurement (R-T) in the LRS and HRS of the device signifies that oxygen vacancies form the conduction filament. We further analyze the synaptic functioning by applying identical consecutive voltage pulses, and the device's conductance change has been observed. These characteristics show a good representation of the biological memory synapse in terms of the artificial memory device. Long-term potentiation (LTP) and long-term depression (LTD) show nonlinear and asymmetry behavior, which is substantial for neuromorphic applications. A considerable shift in LTP and LTD was detected by applying external temperature and magnetic field. This is explained via temperature and magnetic field strain in the functional NiMnIn bottom electrode of the fabricated device. The mechanical flexibility of the memory structure was tested by exploring the switching characteristics with various bending angles and bending cycles. Therefore, the present study offers new avenues for flexible devices with high data storage capability for futuristic neuromorphic applications.

**4:00pm MB2-2-MoA-8 Fabrication and Characterization of Iron Titanate Thin Films as a Potential Tunnel Barrier for Magnetic Tunnel Junction (MTJ's)**, *Adnan Kareem [adnankareem94@gmail.com]*, Jozef Stefan Institute, Slovenia, Pakistan

Spintronics addresses rising power dissipation in electronic circuits by offering advantages such as 0% standby leakage, low power consumption, unlimited durability, non-volatility, and compatibility with CMOS technology [1]. In this research work focuses on magnetic tunnel junctions (MTJs) in spintronics, investigating the barrier layer for efficient electron spin transfer, crucial for Magnetic Random Access Memory (MRAM). Iron titanate thin films have attracted research interest due to their potential applications in spintronic devices [2]. An application-oriented electrodeposition technique was used to prepare iron titanate thin films with varying electrolyte molarities [1,2]. XRD results reveals the amorphous behavior of As-deposited thin films. Magnetic field (MF) annealing improved the structural and magnetic properties, the Fe<sub>2</sub>TiO<sub>4</sub> phase was observed, confirming a spinel structure with increased crystallite size and strengthened phase as molarity increased. Magnetic analysis using a vibrating sample magnetometer (VSM) showed soft ferromagnetic behavior in annealed thin films, while the as deposited thin films show para-ferromagnetic mixed behavior. As-deposited films had lower saturation magnetization compared to annealed films.

In conclusion, Fe<sub>2</sub>TiO<sub>4</sub> thin films fabricated via electrodeposition demonstrate significant potential for future spintronic devices specifically in the advancements of MRAM technology.

References:

- Moore. G.E., (2002). Handbook of thin-film Deposition processes & techniques. In: Seshen. K., 2nd edition. Noyes publication/ William Andrew, Inc.
- Omari, L.H., Hajji, L., Haddad, M., Lamhasni, T. and Jama, C., (2019). Synthesis, Structural, Optical and electrical properties of La-modified Lead Iron Titanate Ceramics for NTCR thermo-resistance-based sensors. Materials chemistry and Physics, 233, pp.60-67

**4:20pm MB2-2-MoA-9 Fabrication of IZO/IGZO-Based Vertical Thin-Film Transistor and Its Integration with OLEDs for High-Density Display**, *Nahyun Kim [knhangle0215@naver.com]*, *Seok Hee Hong, Jun Hyeok Lee, Ho Jin Lee, Tae Geun Kim*, Korea University, Republic of Korea

The rising demand for next-generation applications, such as augmented reality (AR), virtual reality (VR), and wearable devices, has made ultra-high-resolution displays with pixel densities reaching thousands of pixels per

# Monday Afternoon, May 12, 2025

inch (PPI) essential. Achieving such high resolutions requires innovative driving circuits and advanced structures for the driving units. Conventional planar thin-film transistors (TFTs) face significant challenges at nanoscale channel lengths, including short-channel effects and threshold voltage ( $V_{th}$ ) instability, which reduce reliability and performance [1]. Therefore, planar TFTs are inadequate as drivers for high-resolution displays, positioning vertical channel TFTs (VTFTs) as a promising alternative [2]. Conventional VTFTs feature spacers between the top and bottom electrodes, with a channel layer formed along the spacer sidewalls. However, sidewall interface conditions can result in unstable channel characteristics and lower carrier mobility compared to planar TFTs [3],[4].

Herein, we propose a novel VTFT architecture utilizing a dual-layer metal oxide channel structure, as depicted in Figure 1(a). To further enhance integration, the top electrode of the VTFT is employed as the reflective electrode in OLED devices, enabling a VTFT-based top-emitting OLED integration. We address channel stability by implementing an  $HfO_x$ -based dual-layer oxide spacer, which generates a quasi-2D electron gas at the oxide interfaces with high electron density, as shown in Figure 1(b). This concentrated electron layer facilitates main channel formation at the interface while optimizing the dual-layer thickness maximizes carrier mobility along the channel path. Additionally, pulsed Joule heating enables localized activation of the active layer without external thermal processing, allowing low-temperature processing by avoiding direct substrate heating. This supports flexible display applications compatible with various substrate materials. Experimental results indicate high performance with a mobility of  $16.34 \text{ cm}^2/\text{Vs}$ ,  $V_{th}$  of 0.2 V, subthreshold swing of 0.4 V/dec, and an on/off ratio exceeding  $10^5$  (Figure 1(c)).

Finally, based on these results, we propose an integrated VTFT/OLED structure, realizing a high-integration display component. The integrated VTFT/OLED solution not only offers superior mobility and stability but also supports low-temperature processing for diverse substrates, contributing significantly to advancements in next-generation display technologies. This approach shows substantial potential for applications in AR/VR, wearable devices, and high-resolution monitors, advancing new possibilities in display technology.

## Surface Engineering of Biomaterials, Medical Devices and Regenerative Materials

### Room Palm 1-2 - Session MD1-2-MoA

#### Development and Characterization of Bioactive Surfaces/Coatings II

**Moderators:** Dr. Hamdy Ibrahim, University of Tennessee at Chattanooga, USA, Dr. Sandra E. Rodil, Universidad Nacional Autónoma de México

1:40pm **MD1-2-MoA-1 Surface Characteristics of Magnesium-Based Nanocomposite for Enhanced Biomedical Implants, Merna Abrabro [jgs684@mocs.utc.edu], Tooba Tanveer, Abdelrahman Amin, Diya Patel, University of Tennessee at Chattanooga, USA; Thomas McGehee, Mostafa Elsaadany, University of Arkansas, USA; Hamdy Ibrahim, University of Tennessee at Chattanooga, USA**

Magnesium (Mg) possesses unique properties that make it a promising candidate for various biomedical applications. That includes biodegradability and an elastic modulus that is closer to that of the human bone compared to titanium and stainless-steel implants, significantly reducing the risk of stress shielding. However, the use of magnesium in biomedical implants has been limited by its high chemical reactivity and limited strength. Therefore, a significant amount of research has been focused on enhancing the strength and corrosion characteristics of Mg-based biomedical implants by developing nanocomposites through novel fabrication methods. This study focuses on investigating the surface properties of novel Mg-based nanocomposites containing boron nitride and silicon carbide nanoparticles. The examination includes testing the morphology, corrosion characteristics, microhardness, wettability, and in-vitro cytotoxicity of the prepared surfaces. In this work, a novel acoustic powder mixing technique, combined with powder metallurgy, is utilized to prepare the Mg-based nanocomposite samples. The findings of this work provide a good understanding of the effect of the process parameters on the corrosion characteristics of these novel materials, which could pave the way for the manufacturing of Mg-based implants with superior properties, contributing to advanced applications in the biomedical field.

2:00pm **MD1-2-MoA-2 Carbide Derived Carbon Conversion Coatings for Tribological Applications, Mike McNallan [mcnallan@uic.edu], University of Illinois - Chicago, USA**

**INVITED**

Carbide Derived Carbon (CDC) is a unique structure of carbon that is produced by extraction of the metal component from a ceramic carbide. When the conversion is carried out at a temperature below 1200 degrees Celsius, the result is a disordered graphitic structure with largely  $sp^2$  bonding. This is because there is not sufficient thermal energy under these conditions for the carbon to relax fully from the ceramic structure to the equilibrium graphitic state.

Carbide Derived Carbon (CDC) has a slick, hydrophobic surface and a low coefficient of friction when paired with most other materials. Because it is grown into a ceramic surface, rather than deposited onto the surface by a CVD or PVD process, CDC coatings can be applied with minimal dimensional changes and are resistant to spallation in comparison to other tribological coatings. CDC coatings have been applied to SiC and WC ceramics by exposure to chlorine gas at temperatures in the range of 800 to 1000 degrees Celsius. In this temperature range, the metal species form volatile chlorides, while the carbon is left behind as a solid.

Tribocorrosion, in which synergistic degradation by corrosion and wear is a particular concern for orthopedic implants such as artificial joints. The Ti-6Al-4V alloy is popular for this application, and carbide ceramics are not favored for this application because of their inherent brittleness. Titanium is a strong carbide former, so titanium carbide surface layers can be formed on titanium alloys by a carburization treatment in a packed bed of carbon. Subsequently, a layer of carbide derived carbon (CDC) can be formed on the surface of the titanium carbide layer by chlorination or by an anodic electrolysis treatment in molten chloride salt. The formation of CDC can be verified by Raman spectroscopy and the improvement of tribocorrosion resistance can be verified by tribocorrosion testing at the free corrosion potential. The results demonstrate a dramatic decrease in corrosion when a CDC layer is present during mechanical sliding.

2:40pm **MD1-2-MoA-4 Nano-Mechanical Characterization of Sol-Gel Nanocoatings in the Context of Antibacterial/Antiviral Advanced High-Traffic Surfaces, Iilaria Favuzzi [ilaria.favuzzi@uniroma3.it], Edoardo Rossi, Università degli studi Roma Tre, Italy; Angelo Meduri, Mario Tului, RINA-CSM, Italy; Marco Sebastiani, Univeristà degli studi Roma Tre, Italy**

The global pandemic caused by the SARS-CoV-2 virus has prompted a re-evaluation of surface hygiene practices, leading to an increased focus on the use of antimicrobial coatings. Sol-gel methodologies, known for their durability and cost-effectiveness, have emerged as a leading technology. MIRIA European project aims to advance sol-gel technologies, utilising nanoparticles such as silver or copper to enhance safety in a variety of public environments (e.g. hospitals, public transportation) and contribute to infectious disease management strategies.

In this work, antimicrobial thin films were deposited via dip coating on glass substrates starting from silicon-based hybrid organic-inorganic sol-gel formulations. The formulations differed in terms of the organosilicon additives and the presence of nanoparticles. A nanomechanical integrated protocol was applied to assess mechanical properties, adhesion and wear durability, by using three primary testing methodologies: nanoindentation, scratch, and wear testing. Nanoindentation was conducted using a KLA G200 Nanoindenter in CSM mode to extract the elastic modulus and hardness of the films, with appropriate models employed to correct for substrate influences. Subsequently, abrasive wear tests were conducted in accordance with the UNI-EN1071-6 standard, while scratch resistance was evaluated using the same nanoindenter, configured for nano-scratch testing with a rounded cone tip and lateral force measurement. Moreover, the antibacterial efficacy against *Staphylococcus aureus* and the antiviral efficacy against the MO10.5 virus were evaluated.

Two data-based interpretation models were employed to extract intrinsic hardness and modulus of the films from nanoindentation data. An increase in stiffness was observed in the nanoparticle-filled formulations. This is associated with improved adhesion (scratch critical loads), as an increase in modulus results in the maximum contact shear stress occurring at higher depths, thereby causing later chipping during scratch. The wear performance of the coatings was evaluated through abrasive wear tests, which demonstrated that all coatings enhanced wear resistance compared to the uncoated glass substrate. The coatings containing copper oxide nanoparticles demonstrated the highest resistance and were the most effective in terms of antimicrobial performance, achieving a 3log (99.9%) reduction in microbial count after a 24-hour contact period.

# Monday Afternoon, May 12, 2025

Finally, a critical evaluation on the potential industrial scale-up of the proposed coating solutions is presented.

4:00pm **MD1-2-MoA-8 Noble Nanoparticles Arrays Coating for Electrochemical (EC) and Surface-Enhanced Raman Spectroscopy (SERS) Biosensors**, *Ting-Yu Liu [tyliu@mail.mcut.edu.tw]*, Ming Chi University of Technology, Taiwan **INVITED**

We have demonstrate a facile and low-cost preparation process to fabricate the laser scribed graphene (LSG)-based electrochemistry (EC) and surface-enhanced Raman spectroscopy (SERS) substrate for bio and environmental detection. LSG substrate was fabricated via laser scribed and deposited the Au nanoparticles on the LSG by thermal evaporation or electrochemical deposition. 3D porous microstructure of LSG can improve the SERS signal of Au@LSG substrate, and further fine-tune the thickness of Au nanoparticles (5-25 nm) to optimize the EC-SERS enhancement. The developed sensor demonstrates exceptional performance in detecting uremic toxins. The results show that 20 nm of Au nanoparticles coated on LSG substrate obtains the highest SERS enhancement effects, and successfully detects the dye molecules (rhodamine 6G, R6G) and uremic toxins (urea, uric acid and creatinine). The EC-SERS signals of R6G would enhance 17 times at the potential of -1.3 V, compared to SERS signals without applying an electric field. Moreover, the urea also displays 4 times higher at the potential of -0.2 V. Furthermore, it achieves remarkably low detection limits ( $10^{-3}$  M for creatinine/uric acid,  $10^{-4}$  M for urea) and offers distinct, concentration-dependent responses for different toxins in cyclic voltammetry (CV) measurements. The detecting molecules could be selected to enhance SERS signals by different voltages, showing the capability of selectively detecting biomolecules, bacteria, and virus, which can solve the problem of complex sample pretreatment.

## Plasma and Vapor Deposition Processes

### Room Town & Country A - Session PP1-2-MoA

#### PVD Coatings and Technologies II

**Moderators: Dr. Christian Kalscheuer**, IOT, RWTH Aachen, Germany, **Dr. Qi Yang**, National Research Council of Canada

1:40pm **PP1-2-MoA-1 From PVD to CVD to ALD - Changes in Demand for Semiconductor Interconnect Metals**, *Estrelita (Lita) Shon-Roy [lshonroy@techcet.com]*, TECHCET, USA

PVD Technology has been used for more than 50 years as a method to deposit interconnect metal in semiconductor device technology, however this has changed dramatically as device technology has driven chip manufacturing processes toward CVD and now ALD technology. Lita Shon-Roy will present the current and future outlook on metallization used for semiconductor device production and the key technical and market drivers behind the increasing use of CVD and ALD technology for chip process development. As an expert in materials markets and trends, Shon-Roy will discuss market drivers alongside technical challenges leading to the development of new/different metal precursor materials.

2:00pm **PP1-2-MoA-2 Material-Dependent Loss in Deposition Rate of High Power Impulse Magnetron Sputtering Discharges**, *Martin Rudolph [martin.rudolph@iom-leipzig.de]*, Leibniz Inst. of Surface Eng. (IOM), Germany; *Kateryna Barynova*, University of Iceland; *Nils Brenning*, KTH Stockholm, Sweden; *Swetha S. Babu*, University of Iceland; *Joel Fischer*, *Daniel Lundin*, Linköping University, Sweden; *Michael A. Raadu*, KTH Stockholm, Sweden; *Jon Tomas Gudmundsson*, University of Iceland, Sweden

High power impulse magnetron sputtering is an ionized physical vapor deposition technique in which the sputtered metal flux from the target is partially ionized. This enhances film properties like density and adhesion. At the same time, some of the produced metal ions are back-attracted to the target and therefore lost from the deposition process. We show that this loss in deposition rate is largely dependent on the sputter yield of the target material. Here, two extremes can be distinguished: 1) Discharges with low sputter yield targets are dominated by argon, and 2) discharges with high sputter yield targets are metal-rich. In the first case, the electron temperature must be significantly higher to enable sufficient ionization of predominantly the working gas to generate the experimentally observed high discharge currents. In those discharges we find strong electron energization by Ohmic heating in the ionization region extending beyond the cathode sheath. In the second case, we find that Ohmic heating is considerably weaker compared to the low sputter yield discharges. At the same time, frequent collisions with metal atom cool the electron

population, which leads to a decrease in electron temperature. By examining a range of different target materials using the Ionization Region Model (IRM) we find a consistent trend of decreasing back-attraction probability and electron temperature as the sputter yield of the target material increases. A lower electron temperature increases the mean free path of ionization of sputtered species, shifting the average location of ionization away from the target. The much weaker electric fields at those locations compared to the target vicinity, ultimately facilitates ion escape toward the substrate, which thus explains the observed reduction in back-attraction.

2:20pm **PP1-2-MoA-3 Effect of Acetylene Gas Flow Rates on Target Poisoning, Phase Composition, Microstructure, Mechanical Properties and Corrosion Resistance of AlCrNbSiTiC High Entropy Alloy Carbide Thin Films**, *Hsiang Yu Tsai*, *Yung Chin Yang*, National Taipei University of Technology, Taiwan; *Chia Lin Li*, Ming Chi University of Technology, Taiwan; *Bih Show Lou*, Chang Gung University, Taiwan; *Jyh Wei Lee [jeflee@mail.mcut.edu.tw]*, Ming Chi University of Technology, Taiwan

High entropy alloy carbide (HEAC) differs from conventional carbides, which are typically composed of one or two metallic elements. HEAC demonstrates remarkable properties, including an extremely high melting point, enhanced hardness, and superior wear resistance. In this study, AlCrNbSiTiC HEAC thin films with varying carbon contents were deposited using a superimposed high power impulse magnetron sputtering (HiPIMS) and medium-frequency (MF) sputtering technique by a plasma emission monitoring (PEM) feedback control system. The optical emission signal of Cr element was monitored under different argon/acetylene gas flow ratios and the target poisoning effect was studied by the PEM system. The cross-sectional morphology, chemical compositions, and crystal structure of the films were characterized using field emission scanning electron microscopy (FE-SEM), FE-electron probe microanalyzer (FE-EPMA), and X-ray diffraction (XRD), respectively. The mechanical properties of the HEAC thin films, including hardness, elastic modulus, adhesion, and wear resistance, were evaluated using nanoindentation, scratch testing, and pin-on-disk wear testing. The corrosion resistance of HEAC films in the 0.5M sulfuric acid aqueous solution was explored. This study systematically investigated the influence of target poisoning ratios and carbon content on the phase composition, microstructure, mechanical properties, and corrosion resistance of AlCrNbSiTiC HEAC thin films. Potential applications of these HEACs films were also proposed in this work.

2:40pm **PP1-2-MoA-4 Duplex Coating Process by Plasma Enhanced Magnetron Sputtering**, *Jianliang Lin [jlin@swri.org]*, Southwest Research Institute, USA

Metallic substrates can be treated by a combination of nitriding and subsequent deposition of a physical vapor deposition (PVD) coating to improve coating adhesion, wear/abrasion resistance, and corrosion resistance. The combination of the two processes is known as duplex treatment. In general, conventional nitriding treatment and PVD coating deposition are typically performed as two separate processes in distinct facilities and environments. Consequently, the lead time and production cost are not optimized. We present a duplex coating process by integrating plasma nitriding and magnetron sputtering using hot filament assisted and plasma enhanced magnetron sputtering (PEMS) within the same facility. In the process, a global nitrogen plasma is generated by impact ionization from electrons emitted from the hot filaments and attracted towards the substrate surface for nitriding. In this study, the effects of the PEMS process on the structure and properties of the nitrided stainless steel have been studied. The PEMS treated stainless steel exhibited greatly improved surface hardness, wear resistance, and hydrophobicity in oil formula. In addition, duplex TiSiCN and DLC coatings deposited using the integrated process showed improved mechanical properties and adhesion as compared to the coatings deposited without the duplex treatment.

3:00pm **PP1-2-MoA-5 Influence of Post-Heat Treatment on Structural, Photocatalytic, Dielectric, and Tribological Properties of TiO<sub>2</sub>/Al/TiO<sub>2</sub> Multilayer Thin Films**, *Anand Joshi [anandjoshi@gmail.com]*, *Mahendra Singh Rathore*, *Unnati Joshi*, Parul University, India

The purpose of this study was to evaluate the impact that post-heat treatment has on the structural, physical, photo-catalytic, and dielectric properties of multilayer structures of thin films composed of TiO<sub>2</sub>/Al/TiO<sub>2</sub>. Radiofrequency (RF) magnetron sputtering and direct current (DC) magnetron sputtering were used to deposit a multilayer of titanium dioxide and aluminum on glass and silicon substrates at room temperature. The flow rate of argon gas was kept constant. After that, the films that had been deposited were annealed in air for three hours at temperatures ranging

# Monday Afternoon, May 12, 2025

from 200 degrees Celsius to 500 degrees Celsius. After that, samples that had been deposited and annealed were characterised by employing techniques such as X-ray diffractometer, scanning electron microscopy (SEM), and atomic force microscopy. The purpose of these techniques was to explore the structural and physical properties of the samples that had been deposited and annealed. The technique of energy dispersive spectroscopy was utilised in order to investigate the impact that temperature has on the constituent composition. Experiments were conducted in the presence of ultraviolet (UV) light and sunlight to investigate the catalytic behaviour of samples against MB and RHD dye. Temperature was found to be a significant factor in the improvement of the percentage of dye degradation. Both the unaltered and the annealed samples were subjected to analytical examinations of their dielectric characteristics, AC conductivity, dielectric loss, and tangent loss. Interdiffusion of Al atoms in TiO<sub>2</sub> matrix as a result of annealing demonstrates an improvement in the characteristics and potential usefulness of the material as a catalyst and electrode material for applications involving energy storage. In addition, a pin-on-disc tribometer has been utilised in order to evaluate the tribological characteristics of the coating. An in-depth discussion has been held regarding the potential mechanisms of tweaking the properties, as well as the potential applications of these qualities.

**3:20pm PP1-2-MoA-6 Reactive Magnetron Sputtering to Design 2D Cobalt Nitride - Carbon Nanotube Buckypaper Hybrids: Co-N Phase Diagram Screening and Thin Film Porosity Enhancement, Saraf Khan [sarafumeed.fr@gmail.com],** 3 Rue Mademoiselle 54000 Nancy, France

The decade ahead brings the challenge of eco-friendly generation of hydrogen fuel. Seeking substitutes, transition metal nitrides, far less studied than metal oxide so far, have the potential to serve as platinum free alternatives. This study explores synthesis of flexible, free standing cobalt nitride thin films deposited onto multi-walled carbon nanotube 2D films (buckypapers) to further serve as electrochemical electrodes. The reactive magnetron sputtering technique which allows to control the purity, stoichiometry, crystalline structure of the grown thin films is used to synthesize several cobalt nitrides. These latter are here characterized with complementary techniques to ascertain the nature of the synthesized cobalt nitride. When deposited onto flat silicon substrates, dense cobalt nitride thin films are obtained while disorganized porous nanostructures of Co<sub>3</sub>N are formed on the carbon nanotube surface.

**4:00pm PP1-2-MoA-8 Optimizing Bi Stoichiometry in Bi<sub>0.5</sub>Na<sub>0.5</sub>TiO<sub>3</sub> Thin Films Deposited via Low-Pressure RF Magnetron Sputtering in Ar Plasma, Zikriya Khan [Zikriya.Khan@student.umons.ac.be],** University of Mons (UMONS), Belgium; *Kristiaan Temst*, Catholic University of Leuven, Belgium; *Denis Rémiens*, Polytechnic University of Hauts-de-France; *Stéphanos Konstantinidis*, University of Mons (UMONS), Belgium

Depositing Bismuth-based thin films by the sputtering technique often results in a non-stoichiometric excess of Bi across various materials, including the ferroelectric piezoelectric Bi<sub>0.5</sub>Na<sub>0.5</sub>TiO<sub>3</sub>. This phenomenon is attributed to the lower scattering of heavier sputtered species in the plasma phase. Common mitigation strategies include multi-target sputtering to control Bi flux and promoting Bi re-evaporation at elevated growth temperatures by exploiting its temperature-sensitive sticking coefficient. Herein, we systematically investigate this issue, focusing on BNT thin film deposition without *in-situ* substrate heating and using a mixed-powder target by single-cathode RF Magnetron sputtering in Ar plasma. Compositional analysis of the films via EDX and RBS reveals a 25-30% excess of Bi by sputtering a stoichiometric Bi<sub>0.5</sub>Na<sub>0.5</sub>TiO<sub>3</sub> (BNT50/50) target. Simulations indicate a relatively unhindered transfer of Bi towards the substrate while other species are impeded by the background gas, as shown by the target sputtering combined with species transport using TRIM and SIMTRA codes, respectively. Reducing the sputtering yield of Bi by adjusting the target composition to Bi<sub>0.35</sub>Na<sub>0.5</sub>TiO<sub>2.8</sub> (BNT35/50) eliminates the excess Bi from the BNT films. This study provides a clear insight into the origin of bismuth excess and a route map for its regulation inside the Bi-based thin films deposited via the sputtering technique.

**Keywords:** “Bi<sub>0.5</sub>Na<sub>0.5</sub>TiO<sub>3</sub>”, “Thin Films”, “Bi Excess”, “Magnetron Sputtering”, “Powder Targets”, “Ar Plasma”.

**4:20pm PP1-2-MoA-9 The Effect of an Additional Cooled Graphitic Anode to the Magnetron Sputtering of Al Films, Daniela Shealsey Jacobo Mora [shealseyjacob015@gmail.com],** Stephen Muhl, Marco Antonio Martínez Fuentes, Instituto de Investigaciones en Materiales, Universidad Nacional Autónoma de México

In this work, aluminum (Al) thin films were deposited onto glass substrates using a two-plasma system. A standard 2” MAK DC magnetron sputtering and an additional water-cooled anodic plasma. The second anodic plasma was generated using a graphite electrode placed approximately 5 cm from the magnetron. We found that the anodic plasma generated additional argon ions, which were incorporated in the magnetron discharge. These additional ions changed the characteristic of the magnetron discharge and the deposition of the aluminum atoms. Here we report the dependence of the changes as a function of the position of the anode and the temperature of the graphite electrode. Similarly, we report the changes in the properties of the films, hardness, and wear resistance as a function of the experimental parameters, gas pressure, MS voltage, and the voltage applied to the graphite anode, as well as the deposition rates measured by optical profilometry.

**4:40pm PP1-2-MoA-10 Low Temperature Deposition of Silicon Nitride Thin Films by Reactive RF Diode Sputtering, Rakesh Singh [Rakesh.singh@ferrotec.com],** Ferrotec Inc., USA

Silicon nitride films have drawn increasing attention due to their high demand in various engineering applications. Considering many disadvantages of chemical vapor deposition (CVD) such as high process temperature and hydrogen contamination, reactive RF diode sputtering is an alternative method to produce high quality SiN<sub>x</sub> films. In this work, we report synthesis of SiN<sub>x</sub> films at low temperature by reactive RF diode sputtering.

Target power density, substrate bias, reactive gas (Ar+N<sub>2</sub>) composition, and working pressure are some of the parameters that significantly influence the composition and optical properties of the films. SiN<sub>x</sub> films with variable refractive index (1.9 to 2.2 at 632 nm) were obtained by changing Ar to N<sub>2</sub> ratio in the reactive gas mixture. Target-substrate gap was adjusted to improve the thickness uniformity and achieve 1-Sigma of <1% over 200 mm Si wafer.

**5:00pm PP1-2-MoA-11 Experimental and Simulative Investigation of Crack Growth in TiAlCrN PVD Coatings, Ujjwal Suri [u.suri@iwm.rwth-aachen.de],** Felix Weber, Christoph Broeckmann, Institute of Applied Powder Metallurgy and Ceramics (IAPK) at RWTH Aachen e.V., Germany; *Kirsten Bobzin*, *Christian Kalscheuer*, *Xiaoyang Liu*, RWTH Aachen University, Surface Engineering Institute (IOT), Germany

Hard physical vapor deposition (PVD) coatings are widely used as protective layers on cemented carbide tools due to their exceptional mechanical properties. However, these coatings can be susceptible to damage and cracking. Gaining a deeper understanding of how the coating microstructure influences the cracking behavior is essential. Moreover, most tool wear prediction does not include the effect of the cracking behavior. Thus, crack initiation and propagation under external loads and its contribution to tool wear should be investigated. A precise micromechanical simulation of cracks could enhance the accuracy of tool wear simulations in cutting applications.

This study combines experimental and mesoscale simulation to investigate the cracking behavior of a TiAlCrN PVD coated cemented carbide tool. Initially, nanoindentations coupled with inverse FEM simulations are conducted to determine mechanical properties of coatings, specifically Young’s modulus and parameters for the Ludwik-Hollomon model. These properties are then applied to simulate high-load nanoindentation at a macroscopic scale. Subsequently, scanning electron microscopy (SEM) is applied to characterize the grain morphology. Using this data, a representative finite element model is developed. Numerical simulations of the local crack initiation and growth are performed based on the implemented model in combination with the extended finite element method (XFEM). SEM micrographs taken after indentation are analyzed to study crack behavior, enabling a correlation between experimental results and numerical simulations.

The combined experimental and detailed numerical modelling approach facilitates insights into how microstructural parameters including grain size and orientation influence crack growth in the coating system. This study presents a combined analysis using experimental nanoindentation and a mesoscopic simulation model of the nanoindentation to investigate the crack growth in PVD coated cemented carbide. The correlation of experimental and simulative results allows a detailed study of the



# Monday Afternoon, May 12, 2025

interaction of microstructure and crack growth in PVD coatings. Models comparable to the one here presented may be used in future work for optimization of coated cemented carbide tools.

**5:20pm PP1-2-MoA-12 Determination of Mechanical Properties of PVD Tool Coatings Using Machine Learning**, *Kirsten Bobzin, Christian Kalscheuer, Xiaoyang Liu [liu@iot.rwth-aachen.de]*, Surface Engineering Institute - RWTH Aachen University, Germany

The wear resistance of physical vapor deposition (PVD) coatings is heavily influenced by their elastic and plastic properties. These properties serve as essential inputs for finite element method (FEM) simulations to predict tool wear, including the elastic modulus for the characterization of elastic properties and parameters of the Johnson-Cook model for the description of the plastic behavior. A precise determination of these parameters is required for simulation of tool wear. In this study, machine learning models are developed to directly map load-depth curves from nanoindentations on TiAlSiN and TiAlCrN coatings to parameters of coatings in FEM. An FEM simulation model of nanoindentation is employed to generate a dataset comprising load-depth curves resulting from a wide range of input material properties. Several machine learning models including support vector regression (SVR), multilayer perceptron (MLP), long short-term memory (LSTM) and gated recurrent unit (GRU) are then trained, validated, and compared using this dataset. The input to these models consists of simulated load-depth curves, with the target being parameters required for the definition of the material in commercial FEM softwares. Among these machine learning models, GRU achieves the best prediction performance. Ultimately, GRU is used to predict material parameters of TiAlSiN and TiAlCrN coatings based on experimental load-depth curves. FEM simulations using the GRU-predicted material parameters show excellent alignment with experimental measurements, achieving accurate results in a single iteration without further parameter adjustments. The determined parameters can be directly used as reasonable inputs for further FEM simulations as parts of a Greybox model to predict tool wear during cutting.

## Plasma and Vapor Deposition Processes Room Palm 3-4 - Session PP6-MoA

### Greybox Models for Wear Prediction

**Moderators:** Philipp Immich, IHI Hauser Techno Coating B.V., Netherlands, Prof. Dr. Ludvik Martinu, Polytechnique Montréal, Canada

**1:40pm PP6-MoA-1 Greybox Models for the Qualification of Coated Tools for High-Performance Cutting**, *Kirsten Bobzin [info@iot.rwth-aachen.de], Christian Kalscheuer, Muhammad Tayyab, Xiaoyang Liu*, RWTH Aachen University, Germany

**INVITED**

The real application behaviour of coated cutting tools cannot be satisfactorily described mathematically. The incipient failure, wear progression and remaining service life cannot be predicted. However, there is a solid basic knowledge in machining technology and materials engineering, which is being described more and more fundamentally and atomistically in the form of white box models. This includes numerical simulations, which are becoming increasingly computationally and time intensive as the level of detail increases. However, the highly non-linear interactions of reality can never be fully described due to idealized assumptions. In contrast, black box models of machine learning can model complex correlations with a sufficient database and are capable of learning. However, physical interactions are then often not understood and their robustness in relation to changing boundary conditions remains uncertain.

As a new research approach, the existing deterministic white box models are to be combined with new data-driven black box models in grey box models. The robust but inaccurate predictions from white box models will be converged into a precise target window using data-driven and adaptive black box models. Already existing machine learning algorithms form the solution space for this. The gap that currently exists between stationary material properties before and after use, i.e. the unsteady system behaviour of coated tools during machining, is being researched and closed. This should enable knowledge-based selection and qualification of coated tools for more efficient machining processes in the future.

The large amounts of data collected but largely unused in research are seen as key. On the materials engineering side, the coated tools are initially analysed in their manufacturing state. However, the focus here is much more on time-dependent changes due to thermal, mechanical, and chemical loads during machining. The stress collective in the machining

process is increasingly being monitored in situ in the form of forces, temperatures, images, or noises. The aim is to be able to trace changes in the in-situ measurement data back to the damage progress of the tools. Initially heterogeneous data formats from the machining process and from materials analysis need to be combined. As much real data as possible is systematically recorded, qualified, and correlated. The valid interpretation of the results requires a holistic view of the entire service life and interdisciplinary cooperation.

**2:20pm PP6-MoA-3 A Grey-Box Modell for Predicting Friction Coefficients of Coated Cutting Tools for Improved Wear Modelling**, *Jan Wolf [jan.wolf@ifw.uni-stuttgart.de]*, University of Stuttgart - Institute for Machine Tools, Germany; *Nithin Kumar Bandaru, Martin Dienwiebel*, Karlsruhe Institute of Technology (KIT), Institute for Applied Materials (IAM), Germany; *Hans-Christian Möhring*, University of Stuttgart - Institute for Machine Tools, Germany

Wear of cutting tools is known to affect the surface integrity of the workpiece and contributes significantly to machine downtime. It has been shown that the wear rate increases dramatically once the coating is worn through. Predicting the wear of the coating is therefore a good indicator for the remaining useful life. Although white-box models based on Finite Element Analysis exist and showed good wear prediction capabilities for uncoated tools, transferring this approach to only model wear of coatings is challenging. One of the main factors for precise wear modelling is to use a precise friction model which captures the frictional behavior of the coating and the workpiece material under process conditions in cutting. Based on the design of a custom pin-on disk test setup in a vertical turning machine build for elevated temperatures and sliding velocity for matching the conditions in machining, a friction model is determined for a TiN/AlTiN coated cutting tool. The non-linear friction behavior is then determined via a regression approach by training machine learning algorithms. A custom-made python interface for the seamless incorporation of typical AI libraries and their models is presented for the software DEFORM 2D. The interface of the tool and the chip is discretized due to employed friction windows, for which the determined regression approach predicts the friction coefficient based on the calculated state variables of the FEA. Thus, this work presents a novel Grey-Box approach for locally predicting friction coefficients along the surface of coated cutting tools, which is the basis for an improved wear modelling of cutting tool coatings.

**2:40pm PP6-MoA-4 Coating-Dependant Thermomechanical Loading of Cutting Tools for Greybox Modeling**, *Thomas Bergs, Markus Meurer, Mustapha Abouridouane [m.abouridouane@mti.rwth-aachen.de]*, Manufacturing Technology Institute (MTI) - RWTH Aachen University, Germany; *Kirsten Bobzin, Christian Kalscheuer, Muhammad Tayyab*, Surface Engineering Institute - RWTH Aachen University, Germany

For economically efficient cutting processes, cutting tool life can be extended through physical vapor deposition (PVD) coatings. However, imprecise tool life prediction models limit the cost-effective qualification of PVD coated tools. Analytical or simulation-based whitebox models mostly ignore coating effect on tool wear and cannot fully capture nonlinear interactions in cutting processes due to necessary simplifications of boundary conditions. In contrast, data-driven blackbox models can represent complex correlations but often lack an understanding of physical causality and robustness under variable conditions. To overcome these limitations, greybox models can be developed by coupling whitebox and blackbox models to create a balanced predictive framework. Such models require an inclusive dataset containing information on coating properties, realistic thermomechanical tool loading, process data and tool wear behavior. The current investigation focuses on determination of coating-dependent thermomechanical loading of cutting tools, required for development of greybox models. Monolayer TiAlCrSiN and bilayer TiAlCrSiN/TiAlCrSiON coatings were deposited on cemented carbide substrates and characterized. In order to assess thermomechanical tool loading, analogy tests representing orthogonal cutting were carried out on heat-treated C45 and 42CrMo4 steels. The process forces and tool temperatures were measured by dynamometer and high-speed infrared camera, respectively. Moreover, the heat flow into the tool was determined by placing a pyrometer directly under the rake face of the cutting inserts. The experimental data from coating properties and cutting tests contributed to the extension and validation of finite element chip formation simulation for coated tools. Thermomechanical stress distributions on coated tools with high spatial and temporal resolution were computed using the validated simulation model. The experimental as well as simulative data was combined to understand the effect of coating and workpiece material combinations on the process forces, tool temperatures



# Monday Afternoon, May 12, 2025

as well as the resulting friction and tool wear behavior. The study contributes towards extension of existing numerical whitebox models for consideration of coating as well as determination of more accurate thermomechanical loading on PVD coated tools. The resulting high-resolution spatial and temporal thermomechanical tool loading data can be instrumental to the development of greybox models for tool life prediction.

**3:00pm PP6-MoA-5 Bridging the Gap Between Milling and Tribological Wear Mechanisms: Comparative Analysis of Coated Carbide Tools, Amod Kashyap [amod.kashyap@kit.edu],** Institute for Applied Materials (IAM-ZM), Micro-Tribology Centre ( $\mu$ TC), Karlsruhe Institute of Technology, Germany; *Amirmohammad Jamali*, Institute of Production Science (wbk), Karlsruhe Institute of Technology, Germany; *Johannes Schneider*, Institute for Applied Materials (IAM-ZM), Micro-Tribology Centre ( $\mu$ TC), Karlsruhe Institute of Technology, Germany; *Michael Stueber*, Institute for Applied Materials (IAM-AWP), Karlsruhe Institute of Technology, Germany; *Volker Schulze*, Institute of Production Science (wbk), Karlsruhe Institute of Technology, Germany

Milling tools used in metal manufacturing face severe challenges such as complex wear scenarios, heat generation and dissipation, and vibration, which lead to reduced tool life, poor surface quality, and higher operational costs. To address these issues, advanced coatings are applied to enhance their performance and longevity by reducing wear and friction, enabling higher cutting speeds and improved efficiency, and minimizing the formation of built-up edges. Coatings based on Titanium Nitride (TiN) and Aluminum Titanium Nitride (AlTiN) provide excellent heat resistance and hardness, crucial for maintaining tool integrity under high-temperature conditions.

The wear mechanisms of a milling tool vary depending on cutting parameters, and extensive research has been conducted on tool wear in coated milling tools with large-scale milling machines. Traditionally, researchers have attempted to evaluate coating performance using laboratory-based tribological setups. However, tribological tests do not accurately replicate the actual milling process. In this study, the authors aim to correlate tool wear in milling machines with wear observed in tribological model experiments. Milling tests were conducted with coated cemented carbide tools on C45 steel, and tribological tests involved coated cemented carbide cylinders against C45 discs. In-house TiN and AlTiN model coatings, deposited by pulsed-DC and high-power impulse magnetron sputtering techniques, were applied in these experiments. Tribological test parameters were optimized to replicate similar wear mechanisms on both the milling tools and coated cylinders, allowing for a detailed study of wear development through tribological testing only. Scanning electron and focussed ion beam microscopy including energy dispersive X-ray analysis were employed to analyse oxidation, adhesion, and diffusion wear on the coated carbide tools and cylinders. Additionally, the in-house-developed coatings were also compared with industrial coatings, enabling a comprehensive examination of wear mechanisms across different coatings.

**3:20pm PP6-MoA-6 Prediction of Tool Wear Depending on the Coating Architecture for Coated Cemented Carbide Tools by Machine Learning, Benjamin Bergmann,** Institute of Production Engineering and Machine Tools - Leibniz University Hannover, Germany; *Christian Kalscheuer*, Surface Engineering Institute - RWTH Aachen University, Germany; *Berend Denkena*, Institute of Production Engineering and Machine Tools - Leibniz University Hannover, Germany; *Kirsten Bobzin*, *Xiaoyang Liu*, Surface Engineering Institute - RWTH Aachen University, Germany; **Nico Junge [junge@ifw.uni-hannover.de],** Institute of Production Engineering and Machine Tools - Leibniz University Hannover, Germany

Cutting tools based on cemented carbide are usually coated by physical vapor deposition. In machining operations, the specific characteristics of the process parameters and the machined material determine the different wear behavior. However, the utilization of diverse coating properties enables the targeted enhancement of wear resistance. Furthermore, the coatings are adjusted to the individual substrate. It could be shown, that the interaction between the substrate and the interlayer thickness and coating architecture exhibit a significant influence on the tool wear behavior. Due to the high complexity for predicting the influence of the interlayer on the wear behavior wear models are not available. Therefore, machine learning was used to predict the tool wear based on coating properties, considering the complex interaction between process parameters, tool and material.

In this study PVD coated cutting tools with three different interlayer thicknesses were prepared. This method is used to analyze different

substrate-coating systems while preserving the properties of the functional layer of the tool. The initial coating properties such as residual stress, hardness and thermal conductivity were measured and served as input parameters for the ML- model. Afterward experimental wear investigations in turning different steels and process parameters were conducted. The wear data and the process parameters were also used as the input for the machine learning model. Different machine learning models such as support vector regression (SVR) and multilayer perceptron (MLP) were tested regarding the wear prediction. It can be shown, that the used models can predict the wear form and the size of wear for the turning operation depending on the operating time and the different coating properties, such as the interlayer thickness.

**4:00pm PP6-MoA-8 Greybox Modeling the Run-in and Wear Behavior of Milling Tools Coated with Arc-Evaporated TiAlN Based on Operando, in Situ and Ex Situ Analyses, Wolfgang Tillmann [wolfgang.tillmann@udo.edu],** Finn Rügenapf, Nelson Filipe Lopes Dias, Simon Jaquet, Rafael Garcia Carballo, Dirk Biermann, Nils Denkmann, Jörg Debus, TU Dortmund University, Germany **INVITED**

In modern machine manufacturing, a controlled cutting process is crucial for high workpiece quality and production efficiency. The dynamic stability of milling processes depends, e.g., on the cutting parameter values and the system behavior of the machine tool including the cutting tool. Milling tools are subjected to significantly more wear during dynamically unstable processes. To enhance wear resistance, cathodic arc evaporated TiAlN thin films are widely used. Throughout the cutting process, varying tribological loads alter the transient system behavior of the coated tools, which in turn impacts run-in behavior, tool wear, and lifetime. In this regard, the system behavior under varying dynamic load profiles remains largely unknown during the cutting process, thus complicating efforts to predict dynamic stability and tool wear accurately.

These challenges are addressed by using a greybox model approach designed to characterize the transient system behavior of TiAlN-coated tools. In a greybox model, experimental data of the steady-state and transient system behavior are exploited to reveal the wear initiation and development with respect to the dynamic run-in behavior. The experiments focus on the milling process of normalized C45 steel, utilizing tools coated with arc-evaporated TiAlN thin films. For the input of the greybox model a comprehensive dataset is produced, including *operando* cutting force measurements, *in situ* Raman spectroscopy, and *ex situ* analyses of chemical composition, hardness, and adhesion of the coatings pre- and post-cutting. A supervised machine learning model is used to enhance signal clarity and reliability of *in situ* input data. Furthermore, artificial neural networks with k-means clustering provide correlations between thin film properties, wear behavior and cutting performance. The combination of these AI-driven insights with physical and material-specific causalities allows the greybox model to predict tool wear progression and failure onset of the arc-evaporated TiAlN-coated milling tools.

Initial greybox model approaches demonstrate that the run-in behavior of the coated tools is influenced by the initial droplet distribution of the TiAlN, which in turn is affected by the choice of target material. This underlines the importance of considering the entire process, from coating deposition to tool performance. Additionally, a preliminary clustering of measurement data reveals meaningful patterns related to wear and stability. These first results highlight the potential of greybox models in describing the transient system behavior and predicting the lifetime of TiAlN-coated tools.

**4:40pm PP6-MoA-10 Determination of Residual Stress and Crystallite Size for TiAlN-Coated Milling Tools Using Laser-Spectroscopy-Based Grey-Box Modeling, Nils Denkmann [nils.denkmann@tu-dortmund.de],** Department of Physics, TU Dortmund University, 44227 Dortmund, Germany; *Nelson Filipe Lopes Dias*, *Finn Rügenapf*, Institute of Materials Engineering, TU Dortmund University, 44227 Dortmund, Germany; *Simon Jaquet*, *Rafael Garcia Carballo*, *Dirk Biermann*, Institute of Machining Technology, TU Dortmund University, 44227 Dortmund, Germany; *Wolfgang Tillmann*, Institute of Materials Engineering, TU Dortmund University, 44227 Dortmund, Germany; *Jörg Debus*, Department of Physics, TU Dortmund University, 44227 Dortmund, Germany

TiAlN thin films are widely used in machining processes due to their high hardness and high wear resistance. However, continuous and intermittent thermo-mechanical loads during machining impair the structural properties of the thin film, e.g., the phase composition and the residual stress state. Such an impact alters the wear resistance of the thin film as well as the constitution of the tools, which ultimately leads to a drastic increase in tool wear. For a comprehensive understanding of the wear of coated milling

# Monday Afternoon, May 12, 2025

tools, it is crucial to gain insight into the microscopic structural-chemical properties that determine early-predictively the degradation of the coating.

We use laser scattering spectroscopy combined with AI supported data analysis to determine changes in the residual stress and crystallite size of TiAlN coatings applied to milling tools for C45 steel machining. By utilizing confocal Raman scattering with micrometer spatial resolution, we measure the longitudinal and transversal optical and acoustic lattice vibrations, whose spectral line features grant access to the residual stress and crystallite size of TiAlN.

The  $k$ -means clustered changes in the residual stress and crystallite size  $h$  of TiAlN are correlated for initial and different material removal volumes of the TiAlN-coated tool. In the initial state and after minor material removal, the residual stress changes are given by  $(1.2 \pm 0.6)$  GPa, while  $h$  fluctuates around 50 nm. In case of high material removal, the residual stress switches from compressive to positive tensile stress ranges with decreasing  $h$ . The sign switching in the residual stress is attributed to a temperature-induced spinodal segregation in fcc-TiN and fcc-AlN. This phase transformation appears to be present at  $h$  below about 30 nm. As the wear is significantly lower than for the uncoated reference tool, it can be assumed that the spinodal segregation has a wear-reducing effect.

In addition to that, a possible wear initiation for the TiAlN thin films is determined by the frequency of missing TiAlN Raman scattering signals at local tool surface positions. The  $k$ -means cluster analysis of the scattering spectra shows that with increasing material removal volume a non-specific background is formed in 5 % and 11 % of the cases, respectively.

Raman spectroscopy combined with grey-box modeling reveals possible wear initiations for the TiAlN thin films and outlines that the observed wear mitigation is related to the formation of self-organized nanostructures, so that structural-chemical changes at the tool surface may be used to develop robust and early-predictive criteria for wear.

**5:00pm PP6-MoA-11 Predicting Solid Particle Erosion of Metals: A Machine Learning Approach, Stephen Brown** [[stephen.brown@polymtl.ca](mailto:stephen.brown@polymtl.ca)], Foutse Khomh, Polytechnique Montréal, Canada; Juan Manuel Mendez, MDS Coating Technologies, Canada; Marjorie Cavarroc, Safran Tech, France; Ludvik Martinu, Jolanta Ewa Klemberg-Sapieha, Polytechnique Montréal, Canada

Solid particle erosion (SPE) is a tribological phenomenon in which a surface is impacted by a stream of particles, causing a gradual removal of the material. It is a critical challenge in aerospace, where compressor blades and other components are exposed to harsh particle-laden environments. Despite decades of research, accurately predicting SPE under diverse conditions remains difficult due to the non-linear relationships between erosion rates, material properties, and environmental factors. While several white-box models exist for the prediction of erosion, they rely on the use of empirically determined values that are sensitive to changes in erosion conditions and material properties, and are not easily adaptable to different erosion environments.

Machine learning (ML) offers a powerful alternative for handling variability and extracting insights from diverse datasets. This study compiles a database of over 1,000 erosion tests on metals based on the erosion literature and internal experiments, encompassing material and particle properties, experimental conditions, and article metadata. Using ML models such as XGBoost, Neural Networks, and Random Forests, erosion rates were predicted, achieving mean absolute errors (MAE) of 15-16% for the unseen test data. Model performance was further validated against interlaboratory test results from the ASTM G76 standard, with accurate predictions being made in two of three cases. The influence of different variables on erosion predictions was analyzed using feature importance metrics and partial dependence plots. Key features like particle velocity and impact angle showed expected effects, while the importance of target features such as density and Poisson's ratio was sometimes overstated due to their ability to act as classifiers for outlier materials.

These results demonstrate the potential of data-driven approaches to improve wear modeling by quantitatively predicting erosion rates across a wide range of conditions, while also highlighting the challenges arising from issues such as data sparsity and feature correlation.

**5:20pm PP6-MoA-12 Characterization of AlCrVY(O)N Thin Film Properties and Thermo-Mechanical Load Profiles in Machining AISI 304 Stainless Steel Using Greybox Modelling Approaches, Erik Krumme** [[erik.krumme@tu-dortmund.de](mailto:erik.krumme@tu-dortmund.de)], Institute of Machining Technology (ISF), TU Dortmund University, Germany; Finn Rügenapf, Chair of Materials Technology (LWT), TU Dortmund University, Germany; Kai Donnerbauer, Chair of Materials Test Engineering (WPT), TU Dortmund University, Germany; Jannis Saelzer, Institute of Machining Technology (ISF), TU Dortmund University, Germany; Nelson Filipe Lopes Dias, Chair of Materials Technology (LWT), TU Dortmund University, Germany; Pascal Volke, Andreas Zabel, Institute of Machining Technology (ISF), TU Dortmund University, Germany; Wolfgang Tillmann, Chair of Materials Technology (LWT), TU Dortmund University, Germany; Frank Walther, Chair of Materials Test Engineering (WPT), TU Dortmund University, Germany

The thermo-mechanical load collective prevailing in machining significantly determines the wear of coated carbide tools and therefore also has an influence on the productivity and sustainability of many industrial value chains. The tool wear can be described and predicted by developing greybox models, whereby it is known that the temperatures occurring in the chip formation zone have a greater impact on wear than the mechanical tool loads. AlCrVY(O)N thin films thus show significant promise for reducing tool wear due to lower friction and enhanced thermal stability at elevated temperatures compared to conventional thin films. Based on the complex coupling of friction, temperature and wear, the need for further development of such systems is substantial. To initiate greybox modeling of wear behavior, these thin-film systems were tested in whitebox approaches, i.e. when machining AISI 304 during an orthogonal turning process. As a benchmark, the thin films were compared to TiAlN and AlCrN thin films as well as uncoated cemented carbide tools. The thin film properties of AlCrVY(O)N on the cemented carbide inserts were evaluated and correlated with the cutting performance. The test set-up used, enables a comprehensive examination of the thermo-mechanical load collective concerning the measurement of the process forces and rake face temperatures. A variation of the cutting parameters was carried out to investigate the performance of the thin films under different levels of load. The tool wear identified was evaluated using blackbox approaches. In particular, a neural network for image segmentation was trained and applied to optical micrographs of the used tools. As a result, an automated evaluation of the tools was possible and new criteria for quantifying tool wear were developed. In order to improve the prediction of the transient tool wear behavior in form of cracks in the thin film and cutting edge failures, a further machine learning approach was chosen. For this purpose an autoencoder was developed and trained, which first analyzes the experimentally determined force measurement signals *ex situ* and can subsequently identify process windows of interest with regards to the tool wear behavior. The fundamental investigations show that the applied thin films on the inserts generally have a homogeneous chemical composition and a high hardness around 35 GPa. In the operational tests the temperatures on the rake face were reduced by using the AlCrVY(O)N thin films compared to TiAlN. Despite the low level of wear due to the short cutting time, image segmentation was validated as a suitable method for wear quantification.

## Topical Symposium on Sustainable Surface Engineering Room Town & Country B - Session TS1-2-MoA

### Coatings for Batteries and Hydrogen Applications II

**Moderators: Prof. Chen-Hao Wang**, National Taiwan University of Science and Technology, Taiwan, **Dr. Martin Welters**, KCS Europe GmbH, Germany, **Prof. Fan-Bean Wu**, National United University, Taiwan

**1:40pm TS1-2-MoA-1 The Effect of the Transition Metal Dopant on the Microstructure and Electrochemical Performance of Magnetron Sputtered Electrodes for Solid Oxide Fuel Cells Applications, Justyna Kulczyk-Malecka** [[j.kulczyk-malecka@mmu.ac.uk](mailto:j.kulczyk-malecka@mmu.ac.uk)], Katharina Steier, David Shaw, Kleitos Panagi, Peter Kelly, Manchester Metropolitan University, UK

The electrolytic energy conversion has become one of the main technologies considered to deliver actions on reducing CO<sub>2</sub> emissions in the energy, heavy-duty transportation and industrial processes sectors. The electrolytic cells (fuel cells and electrolysis cells) can be utilised in energy conversion, generation, and storage, which has been demonstrated at scale in many regions around the world already. Solid oxide cells are typically composed of porous ceramic matrix and Ni metal catalyst fuel electrodes, dense ceramic electrolytes, such as YSZ or GDC, and perovskite air

# Monday Afternoon, May 12, 2025

electrodes. These cells operate at relatively high temperatures (typically 600-850°C) and, therefore do not require precious metal group catalysts to drive the reaction forward in both electrolysis (H<sub>2</sub> generation) and fuel cell (energy conversion) modes. Moreover, they are more versatile in terms of required fuel type allowing utilisation of hydrogen as well as alternative fuels, such as methanol, ammonia, or biogas.

In this work, thin (~3 µm) nanostructured cermet anodes consisting of YSZ-Ni and GDC-Ni were doped with transition metals to study their influence on coatings microstructure and electrochemical performance. The anodes were deposited onto commercial YSZ electrolyte support cells using oblique angle pulsed DC reactive magnetron sputtering. The coating microstructure was evaluated using FIB-SEM and TEM and focused on the triple-phase boundary evolution in relation to the amount of the added dopant (0-5 wt.%). The chemical composition of the coatings was assessed using EDX, XPS and XRD analysis. The polarization curves were obtained from SOFC single stack assemblies under hydrogen and air flows for anode and cathode, respectively, at operating temperatures of 850°C to evaluate the electrochemical performance of the deposited films.

**2:00pm TS1-2-MoA-2 Investigation of Ba<sub>0.5</sub>Ce<sub>0.3</sub>Zr<sub>0.18</sub>Y<sub>0.01</sub>Yb<sub>0.01</sub>O<sub>3-δ</sub> / Y<sub>0.2</sub>Ce<sub>0.8</sub>O<sub>2-δ</sub> Composite Coatings for the Electrolyte of Solid Oxide Fuel Cell, Yen-Yu Chen [yychen@mail.npust.edu.tw], Ke-Hsing Wang, National Pingtung University of Science and Technology, Taiwan**

Solid oxide fuel cells (SOFCs) are one of the potential power generation devices for the sources of renewable energy. In this study, the composite coatings consisted of BaCe<sub>0.7</sub>Zr<sub>0.12</sub>Y<sub>0.1</sub>Yb<sub>0.1</sub>O<sub>3-δ</sub> (BCZYYb) and Y<sub>0.2</sub>Ce<sub>0.8</sub>O<sub>2-δ</sub> (YDC) were developed by a colloidal coating process as the electrolyte for SOFC. Both of the powders of BCZYYb and YDC were synthesized by the solid-state reaction methods. The well dispersed suspensions after refined by the planetary ball method were spin coated on the porous NiO/BaZr<sub>0.85</sub>Y<sub>0.15</sub>O<sub>3-δ</sub> (BZY) substrates, which were prepared by a die pressing method after pre-sintering at 1200°C for 1 h. Several properties were analyzed including microstructures, crystallographic phases, and electrical performance. The BCZYYb/YDC composite coatings still showed dual-phases including perovskite-type BCZYYb and fluorite-type YDC after sintered at 1550°C for 24 h. The coating layer shows high density after sintered. And the thickness of the coating layers are around several µm. The composites show ionic conductive behaviors from the temperature between 500~800°C. The details will be reported in the presentation.

**2:20pm TS1-2-MoA-3 Unveiling the ORR Mechanism on Co Single-Atom Catalysts Using Operando Raman Spectroscopy with Catalyst-Coated Membrane (CCM) Methodology, Sun-Tang Chang [suntang925@gmail.com], Yi-Qing Chu, Zih-Jhong Huang, Chen-Hao Wang, National Taiwan University of Science and Technology, Taiwan**

In this study, operando Raman spectroscopy was employed to investigate the mechanism of the oxygen reduction reaction (ORR) on a cobalt single-atom catalyst (Co-SAC). The Co-SAC was synthesized and utilized as a cathode catalyst for an alkaline anion exchange membrane fuel cell (AAEMFC). The results demonstrate excellent ORR activity, with an electron transfer number of 3.96 and  $J_{\text{limit}}$  is 5.5 mAcm<sup>-2</sup>.

X-ray absorption spectroscopy (XAS) revealed that the Co-SAC features a Co-N5 coordination structure, with cobalt in the +3 oxidation state. Furthermore, wavelet transform (WT) analysis confirmed the presence of isolated cobalt single atoms.

To minimize interference from the electrolyte during Raman laser measurements, the catalyst-coated membrane (CCM) method was adopted. This approach effectively prevents direct interaction between the laser and the electrolyte while ensuring efficient OH<sup>-</sup> group transfer to the catalyst. Additionally, in the operando setup, electrochemical impedance spectroscopy (EIS) was integrated with Raman spectroscopy. This combination enabled a detailed observation of the ORR mechanism and the evolution of surface phenomena under different applied biases.

This study represents a significant breakthrough in unveiling the ORR mechanism, particularly for Co-based single-atom catalysts.

**2:40pm TS1-2-MoA-4 Study on Mo<sub>x</sub>N Thin Films Deposited by HiPIMS and RF Sputtering with Heteroatom Doping for Hydrogen Evolution Reaction Catalysts, Hung-I Wu [a8794191@gmail.com], National Yunlin University of Science and Technology, Taiwan; Ying-Hsiang Lin, National United University, Taiwan; Shih-Hung Lin, National Yunlin University of Science and Technology, Taiwan; Fan-Bean Wu, Chi-Yueh Chang, National United University, Taiwan; Thi Xuyen Nguyen, Chia-Ying Su, Ruei-Chi Lin, Jyh-Ming Ting, National Cheng Kung University (NCKU), Taiwan; Wan-Yu Wu, National United University, Taiwan**

In recent years, materials such as transition metal oxides and nitrides have been popular in catalyst research. Compared to scarce noble metals, molybdenum-based materials not only have more abundant resources but also exhibit excellent activity[1], making them highly suitable to replace the costly noble metal catalysts (Ru, Ir, RuO<sub>2</sub>, IrO<sub>2</sub>). Molybdenum nitride (MoN) possesses outstanding corrosion resistance and electronic conductivity[2], allowing it to perform the hydrogen evolution reaction (HER) in acidic media. If different elements like Ti, Co, Ni, and V are doped into Mo<sub>x</sub>N as a substrate, a synergistic effect is expected to further enhance HER performance. Additionally, when attaching catalysts to electrodes, one must consider the uniformity of surface coverage and adhesion on electrodes of various shapes. As is well known, sputtering offers advantages such as uniform coating, easy control of film thickness, and excellent adhesion. Therefore, using this method to prepare catalyst thin films on electrodes is the optimal choice.

In this study, we employed RF sputtering and High Power Impulse Magnetron Sputtering (HiPIMS) techniques to deposit Mo<sub>x</sub>N thin films for comparison. Initially, we deposited Mo<sub>x</sub>N thin films using HiPIMS and found in preliminary results that the HiPIMS-deposited Mo<sub>x</sub>N thin films exhibited an overpotential of 415 mV at η=10 during hydrogen evolution reaction (HER) tests in 0.5M H<sub>2</sub>SO<sub>4</sub>. Energy-dispersive X-ray spectroscopy (EDS) analysis revealed that the Mo and N contents in the Mo<sub>x</sub>N thin films were 60 at.% and 40 at.%, respectively. Grazing-incidence X-ray diffraction (GIXRD) results indicated that the thin films have a face-centered cubic (FCC) structure similar to Mo<sub>3</sub>N<sub>2</sub>. Building on these Mo<sub>x</sub>N results, we will further explore the impact of varying the N/Mo ratio on HER performance. Additionally, we plan to attempt doping other elements into Mo<sub>x</sub>N to observe the changes induced by doping.

**3:00pm TS1-2-MoA-5 Ternary FeCoNi / Graphene Composites as Electrocatalysts for Highly Efficient Hydrogen Evolution Reaction, Yu Tsung Lin [asds881228@gmail.com], Jow Lay Huang, Sheng Chang Wang, Yu Min Shen, National Cheng Kung University (NCKU), Taiwan**

As a consequence of the depletion of fossil fuels, the escalating energy crisis has driven researchers to explore innovative energy. To address this problem, exploring hydrogen energy generation via water splitting emerges as a promising solution. This process involves the hydrogen evolution reaction (HER), a multi-electron transfer process necessitating catalysts to facilitate efficient rates. Despite noble metals have conventionally served this purpose due to their favorable Gibbs free energy, their prohibitive costs pose challenges for widespread adoption and commercialization. In response, our investigation focuses on HER within alkaline electrolytes, aiming to engineer alternative electrocatalysts that are both cost-effective and efficient.

Transition metals from the first row are active centers for the HER due to their 3d orbital, exhibiting excellent activity. Among them, nickel (Ni) and cobalt (Co) shows the most promising potential because the hydrogen adsorption energy of them approaches that of Pt. Furthermore, recent studies have indicated that the incorporation of third transition metals, such as iron (Fe), can further enhance the HER activity. This is attributed to the synergistic effect among the three metals. Additionally, it can be observed that a large number of studies use two-dimensional carbon materials as supports. Graphene, a highly conductive 2D material, serves as an excellent supporting matrix due to its high surface area, facilitating efficient electron transfer during HER. Consequently, we synthesized ternary FeCoNi-LDH/graphene composite by hydrothermal method and measured the HER performance in 1.0 M KOH electrolyte. We used X-ray diffraction (XRD), X-ray photoelectron spectroscopy (XPS), and transmission electron microscope (TEM) to determine the crystal structure and morphology of the composite. The results demonstrate that we successfully synthesized FeCoNi-LDH/graphene. In addition, Linear Sweep Voltammetry (LSV) were employed to confirm the HER performance. The overpotential and Tafel slope is -386.6 mV and 85.8 mV/dec, respectively.

# Monday Afternoon, May 12, 2025

3:20pm **TS1-2-MoA-6 Ti-Cr-N Nanopyramid/Nitrogen-Doped Carbon Quantum Dot/Stainless Steel Mesh as a Flexible Supercapacitor Electrode**, **Rajesh Kumar [rgangwar1997@gmail.com]**, *Bhanu Ranjan, Krishan Kumar, Satyam Shankhdhar, Davinder Kaur*, Indian Institute of Technology Roorkee, India

Nitrogen-doped carbon quantum dots (N-CQDs) incorporated into highly conductive transition metal nitride offer enhanced electrochemical performance, delivering high energy density and outstanding electrochemical stability. The present study reports a high-performance supercapacitor electrode consisting of electrophoretic anchored zero-dimensional N-CQDs with reactively co-sputtered titanium chromium nitride nanopyramids (Ti-Cr-N) thin film on flexible stainless-steel mesh (SSM) substrates. The nanopyramids of N-CQDs/Ti-Cr-N offer remarkable electrochemical performance through  $\text{Li}^+$  storage, ascribed to the abundant electroactive sites and enhanced synergism between the high specific surface area of N-CQDs and higher conductivity of Ti-Cr-N. Subsequently, the N-CQDs/Ti-Cr-N/SSM electrode in 1M  $\text{Li}_2\text{SO}_4$  aqueous electrolyte exhibits an excellent gravimetric capacitance of  $393.8 \text{ F.g}^{-1}$  at a specific current density of  $0.32 \text{ A.g}^{-1}$ . Further, the N-CQDs/Ti-Cr-N/SSM heterostructure outperforms other multi-cationic-based supercapacitors with a maximum energy density of  $41.41 \text{ Wh.kg}^{-1}$  and a superior power density of  $7.0 \text{ kW.kg}^{-1}$ . Impressive electrochemical stability of  $\sim 88.6\%$  is retained by the heterostructure even after 5000 continuous charge-discharge cycles. Insights into charge-storage mechanisms highlight the dominance of surface-limited capacitive and pseudocapacitive kinetics, with fewer contributions from diffusion-controlled faradaic processes. Furthermore, an exemplary mechanical stability of  $\sim 99.98\%$  over 1200 bending cycles demonstrates the N-CQDs/Ti-Cr-N/SSM heterojunction's excellent resilient structural strength, validating the present electrode potential for high-performance flexible supercapacitor application.

4:00pm **TS1-2-MoA-8 Effects of Nb Content on the Water Splitting Performance of FeNiMoWNbx High Entropy Coating Grown by Magnetron Sputtering**, **Naveen Karuppusamy [naveen10111@gmail.com]**, *Ming Chi University of Technology, Taiwan; Bih-Show Lou, Chang Gung University, Taoyuan City, Taiwan; Jyh-Wei Lee, Ming Chi University of Technology, Taiwan*

Hydrogen fuel is an alternative green energy to neutralize the carbon emission and to fulfill the global energy demand. Electrochemical water splitting is a technique to produce hydrogen comprising of both oxygen evolution reaction (OER) and hydrogen evolution reaction (HER), where OER is a bottleneck reaction in water splitting for efficient performance. Thus, it is necessary to prepare a suitable catalyst with an excellent water splitting performance. Though  $\text{RuO}_2$  is a benchmark catalyst for OER performance, scarcity and cost of resources are limited to the use of  $\text{RuO}_2$  in water splitting performance. Transition-metal based electrocatalyst already garners attention due to its excellent redox properties, earth abundant and cost-effective, which makes it suitable for alternative catalyst.

In this study, FeNiMoWNbx high entropy alloy (HEA) coatings with different Nb contents were fabricated on carbon cloth (CC) at high inclined angle using magnetron sputtering technique. The composition of Nb is altered with changing the RF power from 0 to 100 W. Chemical composition of FeNiMoWNbx was analyzed by the field emission electron probe microanalyzer (FE-EPMA). Phase analysis and crystallinity of FeNiMoWNbx were analyzed with glancing angle X-ray diffractometer (GA-XRD). Surface roughness and cross-section morphologies of FeNiMoWNbx films were examined using atomic force microscope (AFM) and field emission scanning electrochemical microscopy (FE-SEM). The OER performance of FeNiMoWNbx films was investigated with the polarization curve obtained in 1 M KOH and 1 M KOH + 3.5 wt.% NaCl aqueous solution. FeNiMoWNbx thin films exhibited a superior OER performance with low overpotential in 1 M KOH and 1 M KOH + 3.5 wt.% NaCl solution. The effects of Nb concentration in FeNiMoWNbx film and the sputtering inclined angle on the kinetics of OER performance was discussed. This work provides the strategy for the fabrication of cost effective FeNiMoWNbx HEA thin film catalyst for efficient water splitting performance.

4:20pm **TS1-2-MoA-9 Pseudocapacitive Storage in Molybdenum Oxynitride Nanostructures Reactively Sputtered on Stainless-Steel Mesh Towards an All-Solid-State Flexible Supercapacitor**, **Bhanu Ranjan [branjana@ph.iitr.ac.in]**, *Davinder Kaur*, Indian Institute of Technology Roorkee, India

Exploiting pseudocapacitance in rationally engineered nanomaterials offers greater energy storage capacities at faster rates. The present research

reports a high-performance Molybdenum Oxynitride (MoON) nanostructured material deposited directly over stainless-steel mesh (SSM) via reactive magnetron sputtering technique for flexible symmetric supercapacitor (FSSC) application. The MoON/SSM flexible electrode manifests remarkable  $\text{Na}^+$ -ion pseudocapacitive kinetics, delivering exceptional  $\sim 881.83 \text{ F.g}^{-1}$  capacitance, thanks to the synergistically coupled interfaces and junctions between nanostructures of  $\text{Mo}_2\text{N}$ ,  $\text{MoO}_2$ , and  $\text{MoO}_3$  co-existing phases, resulting in enhanced specific surface area, increased electroactive sites, improved ionic and electronic conductivity. Employing 3D Bode plots, b-value, and Dunn's analysis, a comprehensive insight into the charge-storage mechanism has been presented, revealing the superiority of surface-controlled capacitive and pseudocapacitive kinetics. Utilizing PVA- $\text{Na}_2\text{SO}_4$  gel electrolyte, the assembled all-solid-state FSSC (MoON/SSM | MoON/SSM) exhibits impressive cell capacitance of  $30.7 \text{ mF.cm}^{-2}$  ( $438.59 \text{ F.g}^{-1}$ ) at  $0.125 \text{ mA.cm}^{-2}$ . Moreover, the FSSC device outputs superior energy density of  $4.26 \text{ } \mu\text{Wh.cm}^{-2}$  ( $60.92 \text{ Wh.kg}^{-1}$ ) and high power density of  $2.5 \text{ mW.cm}^{-2}$  ( $35.71 \text{ kW.kg}^{-1}$ ). The device manifests remarkable flexibility and excellent electrochemical cyclability of  $\sim 91.94\%$  over 10,000 continuous charge-discharge cycles. These intriguing pseudocapacitive performances combined with lightweight, cost-effective, industry-feasible, and environmentally sustainable attributes make the present MoON-based FSSC a potential candidate for energy-storage applications in flexible electronics.

References:

1. Bhanu Ranjan and Davinder Kaur, *Small*, 20 (20), 2307723 (2024). <https://doi.org/10.1002/sml.202307723>
2. Bhanu Ranjan and Davinder Kaur, *ACS Applied Materials & Interfaces*, 16 (12), 14890-14901 (2024). <https://doi.org/10.1021/acsami.4c00067>
3. Bhanu Ranjan and Davinder Kaur, *ACS Applied Energy Materials*, 7 (10), 4513-4527(2024). <https://doi.org/10.1021/acsae.4c00563>
4. Bhanu Ranjan and Davinder Kaur, *Journal of Energy Storage*, 71, 108122. (2023). <https://doi.org/10.1016/j.est.2023.108122>
5. Bhanu Ranjan, Gagan Kumar Sharma, and Davinder Kaur, *Applied Surface Science*, 588, 152925 (2022). <https://doi.org/10.1016/j.apsusc.2022.152925>
6. Bhanu Ranjan, Gagan Kumar Sharma, and Davinder Kaur, *Applied Physics Letters*, 118 (22), 223902 (2021). <https://doi.org/10.1063/5.0048272>
7. Bhanu Ranjan, Gagan Kumar Sharma, Gaurav Malik, Ashwani Kumar, and Davinder Kaur, *Nanotechnology*, 32 (45), 455402 (2021). <https://doi.org/10.1088/1361-6528/ac1bdf>

4:40pm **TS1-2-MoA-10 Applicability of  $\text{MoS}_2$ -aSiC Heterostructure for Durable Supercapacitance and  $\text{NO}_2$  Gas Sensing in Harsh Environment**, **Habeebur Rahman [h\_rahman@ph.iitr.ac.in]**, *Indian Institute of Technology Roorkee (IIT Roorkee), India; Gagan Kumar Sharma, Indian Institute of Technology Roorkee, India; Preetam Singh, CSIR-National Physical Laboratory Delhi, India; Davinder Kaur, Indian Institute of Technology Roorkee, India*

In the present work, the heterostructure of molybdenum disulfide ( $\text{MoS}_2$ ) with amorphous silicon carbide (aSiC) on stainless steel (SS) and Si substrates was fabricated using a DC magnetron sputtering system. This unique heterostructure was examined for energy storage and  $\text{NO}_2$  gas sensing applications suitable for harsh environmental conditions. The 2D  $\text{MoS}_2$  nanostructured with dissolution resistive aSiC supercapacitor electrode delivers 1.5-fold enhancement in the gravimetric capacitance, a voltage window enlargement from 0.8V to 1.8 V, and an excellent stability of more than 4,000 charge-discharge cycles. Further, the high concentration  $\text{NO}_2$  gas sensing performance of the  $\text{MoS}_2$ -aSiC on Si substrate revealed the stable and recoverable response at high operating temperatures. Therefore, loading aSiC with 2D  $\text{MoS}_2$  enables durable electrode material for energy storage and  $\text{NO}_2$  gas sensing applications in adverse conditions. The as-fabricated heterostructure was systematically studied by various material and electrochemical characterizations.

5:00pm **TS1-2-MoA-11 One Step Fabrication of Highly Ordered Binder Free Vanadium Oxide Thin Film Cathode for Next Generation Micro Batteries**, **Ananya Bansal [ananya\_b@ic.iitr.ac.in]**, *Indian Institute of Technology Roorkee, India; Ramesh Chandra, Indian Institute of Technology Roorkee, India*

The increasing demand for microelectronics has significantly driven the advancement of thin film energy storage devices, specifically batteries. Till

# Monday Afternoon, May 12, 2025

now, a range of materials have been investigated for lithium-ion batteries, with vanadium oxide emerging as a promising material. Vanadium oxides are known for multiple oxidation-reduction states during electrochemical reaction, hence, can promote multiple diffusion of Lithium ions resulting in high energy and power density. In this work, binder-free Vanadium oxide ( $V_2O_5$ ) has been synthesized by reactive DC magnetron sputtering on aluminium foil substrate. Vanadium target (99.99% pure) is bombarded with high-energy  $Ar^+$  ions which dislodge atoms from the vanadium surface. These ejected atoms then react with oxygen ions to form highly pure  $V_2O_5$  and deposit onto a substrate, forming a thin film. The deposited layers were analyzed for their structural and surface morphology using XRD and SEM techniques. Highly ordered brick like nanostructures were observed during SEM analysis. X-ray photoelectron spectroscopy measurements were carried out to understand the chemical bonding of the cathode. The surface of vanadium oxide obtained from this binder-free approach helps us to create a high-quality cathode-electrolyte interface with high wettability ( $33.3^\circ$ ). Cyclic voltammetry (CV), galvanostatic charge-discharge (GCD) cycling, and electrochemical impedance measurements were used to investigate the capacity and cycling stability of the  $V_2O_5$  cathode in 1 M lithium hexa-fluoro-phosphate. As a result, it can be interpreted that this binder-free technology can be used to fabricate efficient lithium free cathode for new generation thin film batteries.

5:20pm **TS1-2-MoA-12 Research Coating Conductive Material on  $SiO_x@rGO$  Composite Materials as Anode Material in Lithium-Ion Batteries, Yi-Ling Chen [n56124155@gs.ncku.edu.tw]**, National Cheng Kung University (NCKU), Taiwan

With the advancement of technology, lithium-ion batteries have emerged as a future energy storage technology with the gradual development of electric vehicles. Silicon-based materials, due to their high theoretical capacity, energy density ( $\sim 4200\text{mAh/g}$ ), and natural abundance, are considered as candidates for negative electrode materials in lithium-ion batteries.

In this study, our research team successfully prepared reduced graphene oxide (rGO) using the Hummer method and incorporated commercial  $SiO_x$  micron-sized powder to synthesize  $SiO_x@rGO$  composite material as an anode for lithium-ion batteries. The initial charge capacity was measured at  $1487\text{mAh/g}$ , with a discharge capacity of  $1060\text{mAh/g}$ , yielding an initial coulombic efficiency of 71%. After 40 cycles, the capacity retention remained at 91%. However, there are currently no theoretical studies addressing the lithiation process and lithium ion insertion/extraction mechanisms in  $SiO_x$  materials.

Therefore, in our study, we not only explore the use of  $SiO_x@rGO$  composite material as an anode to improve the theoretical capacity and energy density of lithium-ion batteries but also aim to enhance the electrical conductivity and electrochemical performance of the battery. Conductive materials such as copper, gold, and platinum will be deposited on the prepared  $SiO_x@rGO$  anode material. These conductive coatings will provide additional electrons, creating a driving force for lithium ion diffusion into the anode material during discharge to achieve charge conservation. This process is expected to enhance the capacity and cycling stability of lithium-ion batteries. We will characterize the materials using X-ray diffraction (XRD), scanning electron microscopy (SEM), energy-dispersive spectroscopy (EDS), and transmission electron microscopy (TEM). Furthermore, charge-discharge and cycling performance tests will be conducted on the lithium-ion batteries to investigate the effect of the conductive materials on their performance. Cyclic voltammetry will be employed to observe the electrochemical reactions during charge and discharge cycles.

This study conducts a theoretical analysis of  $SiO_x@rGO$  composite material as an anode for lithium-ion batteries by coating it with conductive materials, aiming to provide valuable reference data for both commercial and academic purposes.

## Surface Engineering - Applied Research and Industrial Applications

### Room Palm 1-2 - Session IA1-TuM

#### Advances in Application Driven Research and Hybrid Systems, Processes and Coatings

**Moderators:** Dr. Vikram Bedekar, Timken Company, USA, Prof. Dr. Hana Barankova, Uppsala University, Sweden

8:00am **IA1-TuM-1 Advancing Correlative Microscopy: In-Situ Integration of AFM-SEM-EDS for Multi-Modal Analysis**, Kerim T. Arat [karat@qdusa.com], William K. Neils, Stefano Spagna, Quantum Design Inc., USA

There is a growing interest in in-situ correlation microscopy, which brings the complementary strengths of different imaging modalities without the inherent complications of sample transfer. These approaches ensure high confidence in correlation accuracy and eliminate the risk of sample contamination and alteration during the sample transfer.

We have developed a correlative microscopy platform based on AFM-SEM [1]. These techniques can map the surface in high resolution, and the trunnion stage, with up to 80° tilt capability, allows monitoring of tip quality and tip-sample interaction [2]. However, these methods fall short in identifying the elemental composition of the sample.

To address this issue, we have extended the capabilities of the correlative platform with an energy-dispersive X-ray spectrometer (EDS). The spectrometer is based on a state-of-the-art silicon drift detector [3], which provides high energy resolution. Its graphene window offers improved transmission performance, especially at the lower energy range, allowing elemental detection down to carbon. The elemental identification algorithm uses a background subtraction method to remove non-characteristic signals and compares the resulting spectra to reference datasets based on the NIST database for standardless quantification [4]. Both hardware and software integration allow the correlation of elemental information with the other imaging modalities that the tool can provide (see the supplementary document), where one can superimpose topography and elemental information.

Integration of the X-ray detector adds a comprehensive analysis capability to AFM-SEM techniques applicable to a diverse range of fields such as materials science, semiconductors and biosciences. With this option, researchers can obtain an in-situ correlation of high-resolution, localized elemental information with high-resolution lateral and vertical topographical information.

[1] A. Alipour et al., *Microscopy Today* 31 (2023), p. 17-22. doi: 10.1093/mictod/qaad083

[2] "FusionScope by Quantum Design," Open a world of easy-to-use correlative microscopy, 2022. <https://fusionscope.com/> (accessed Apr. 27, 2023).

[3] D. E. Newbury and N. W. M. Ritchie, *Journal of Materials Science* 50 (2015), p. 493-518. doi: 10.1007/s10853-014-8685-2

[4] D. E. Newbury and N. W. M. Ritchie, *Scanning Microscopies* 9236 (2014), p. 9236OH. doi: 10.1117/12.2065842

8:20am **IA1-TuM-2 Non-stick Hydrophobic and Superhydrophilic Metallic Coatings: Their PVD Fabrications and Applications**, Jinn P. Chu [jpchu@mail.ntust.edu.tw], National Taiwan University of Science and Technology, Taiwan

The presentation will begin with an introduction to a non-stick, low-friction hydrophobic metallic glass coating and its applications. This amorphous coating, fabricated using PVD techniques, has been successfully applied in various fields, including medical devices. For the superhydrophilic coating, a 316 stainless steel layer is sputtered onto the substrate, resulting in a water contact angle of approximately 10 degrees on the coated surface. This coating also demonstrates antifouling and underwater superoleophobic properties, which are advantageous for use in separation membranes for oil/water emulsions. Furthermore, it has proven highly effective in enhancing electrochemical responses in electrodes used as electrochemical sensors.

8:40am **IA1-TuM-3 Novel CO<sub>2</sub> Laser Direct-Write Energy-Efficient Process for Functional Oxide-Carbon Composite Coatings and Their Energy Applications**, swati Jadhav [swatijadhav1602@gmail.com], Pratibha Jadhav, Ishwari Belle, Anuradha Ambalkar, Supriya Kadam, Satishchandra Ogale, Indian Institute of Science Education and Research, Pune, India

The performance and operational longevity of several energy devices such as Batteries, Fuel Cells, and Electrolysers critically depend on the chemical and physical functionality, micro (nano) porosity, and robustness of the specialized coatings on metal current collectors. A large number of methods are available to obtain such coatings, but these are chemically complex and generally energy intensive. Moreover, several of these methods do not allow concurrent control of porosity and surface chemistry that drive the overall process efficiency, especially in surface catalytic phenomena. In this work we show that CO<sub>2</sub> laser (wavelength 10.6 mm) induced surface processing allows an excellent parametric control on achieving the desired results and that too with a dramatic reduction of energy inputs vis a vis the conventional methods. The key control parameters include laser power density, scanning speed, and coating constitution/thickness. The laser surface processing method is intrinsically direct-write type in scanning mode and as such allows in-plane micro-gradient patterning. We will show and discuss the results of several interesting cases wherein the effectiveness of this approach is demonstrated for composite oxide-carbon coatings obtained by using biomass (or biomass-derived) precursors and functional binary oxide systems. The biomass precursors include furfural alcohol, lemon grass, sugarcane bagasse while the oxide systems include NiO, CuO, TiO<sub>2</sub>. Use of urea and thiourea in the composite is also examined to achieve doping of nitrogen and Sulfur in carbon to enhance its conductivity. The resulting engineered coatings are studied for energy applications such as Anode-free (AF) Li and Na ion batteries, and Electrocatalysis for water splitting applications (oxygen evolution reaction, OER and Hydrogen evolution reaction (HER)). For AF batteries the laser processed coatings render low Li/Na nucleation overpotential, good columbic efficiency and cycling stability of up to 800 cycles limited by Li/Na inventory. In case of water splitting application as well superior properties are realized in terms of overpotential and stability.

9:00am **IA1-TuM-4 PVD Coatings for the Hydrogen economy - Applications, Testing and Production**, Herbert Gabriel [h.gabriel@pvtvacuum.de], PVT Plasma und Vakuum Technik GmbH, Germany

**INVITED**

Green hydrogen could be the fuel of the future. Generated by electrolysers powered by photovoltaics and used in fuel cells could be part of the solution to the human mankind's problems with the climate change.

The harsh environments in electrolysers and fuel cells require components to be coated for corrosion resistance, electrical conductivity and other related properties..

Most of the components are made of stainless steel or titanium, but still need for their performance and long lifetimes up to 100.000 hours coatings with high performance properties.

Depending on the application, whether PEMWE, PEMFC, AEM, SOFCs, SOECs or others, thin coatings made of materials such as C, Ti, Cr, Nb, Au, Pt, Ir, MCO, Al<sub>2</sub>O<sub>3</sub>..... are deposited in the nanometer to a couple of micron range.

Preferred coating processes are magnetron sputtering, respectively HIPIMS, high power impulse magnetron sputtering to deposit highly adherent and dense coatings.

Most components of fuel cells and electrolysers to be coated are thin 2-dimensional structures in high quantity. For this reason high productive so-called in-line systems with vertical orientation are the preferred coating systems for double-sided deposition.

Apart from a number of other QC – tests, adhesion, corrosion and ICR (interface contact resistance) prior and after corrosion testing are essential properties to continually be tested and monitored.

# Tuesday Morning, May 13, 2025

## Surface Engineering - Applied Research and Industrial Applications

### Room Town & Country D - Session IA2-2-TuM

#### Surface Modification of Components in Automotive, Aerospace and Manufacturing Applications II

**Moderators:** Dr. Satish Dixit, Plasma Technology Inc., USA, Dr. Jan-Ole Achenbach, KCS Europe GmbH, Germany, Masaki Okude, Mitsubishi Materials Corporation, Japan

#### 8:00am IA2-2-TuM-1 2D Material-Based Coatings for Superlubricity in Dry Sliding and Rolling Contacts, *Diana Berman [diana.berman@unt.edu]*, University of North Texas, USA

INVITED

Friction and wear-related failures are critical challenges for modern mechanical systems, affecting applications from microelectromechanical devices to automotive assemblies and biomedical implants. The pressing need to reduce these tribological failures has intensified efforts to design advanced coatings and lubrication solutions tailored to withstand extreme operating conditions. This presentation emphasizes our progress in the precise design of 2D material-based coatings, particularly those using graphene, molybdenum disulfide, and MXene, to achieve superlubricity—an ultra-low friction regime that greatly enhances component lifespan and efficiency.

By establishing a fundamental understanding of material interactions at sliding interfaces, we are able to develop coatings that not only improve performance but also contribute to the reliability and sustainability of tribological systems. These engineered coatings are evaluated for their tribological properties under a range of conditions, demonstrating that superlubricity can be achieved at the macroscale, under high contact pressure and shear conditions. We also propose experimental pathways to realize superlubricity in rolling-sliding contact conditions using solid-lubricant coatings, which could open new opportunities for industrial applications requiring highly durable, low-friction surfaces. Overall, this work lays the groundwork for next-generation tribologically optimized coatings, offering promising solutions for critical sectors reliant on advanced friction and wear management.

#### 8:40am IA2-2-TuM-3 Exploring Controlled Plastic Deformation as a Preferable Pre-Treatment for Enhanced Tribo-Mechanical Properties of Fundamental Industrial Materials: Design of Wear Resistant Surfaces/sub-Surfaces, *Daniel Tobota [daniel.tobota@kit.lukasiewicz.gov.pl]*, Puneet Chandran, Łukasiewicz Research Network – Krakow Institute of Technology, Poland; *Łukasz Maj, Jerzy Morgiel*, Institute of Metallurgy and Materials Science of Polish Academy of Sciences, Poland

The need for superior physical, mechanical and tribological properties in modern industrial applications has driven manufacturers to develop advanced materials or provide tailor-made/innovative solutions for utilizing existing high performance materials. Aerospace and automotive industries are known to employ innovative materials like modern steels, titanium alloys, advanced ceramics etc., to meet the exponentially growing demand for ‘sustainable’ materials, taking into account industrial and economic viability. However, an exclusive solution addressing the increased adaptability of these materials is always inadequate owing to the excellent mix of inherent physical and mechanical properties. Although industry favors a ‘one solution’ to all materials/problems approach, it is practically impossible to implement it in real time. In this study, we aim to strategically propose solutions to enhance the tribo-mechanical properties of well-known, critical industrial materials like titanium, ceramics (alumina/Si) and advanced steels (Vancron/Vanadis) - through the synergistic effects of cold working and thermo-chemical processing.

The substrates of all the materials were subjected to simple finishing processes like grinding, turning/milling followed by controlled burnishing and shot peening/micro-blasting. Low temperature gas/plasma nitriding formed the last stage of pre-processing. Detailed tribological studies were carried out on all the samples. The nanoscale characterization of the pre-processed samples and the wear track via SEM/TEM revealed the formation of a thin ‘tribo zone’ with improved tribo-mechanical properties. The nature of tribo zone formed in each material, based on the type of cold working along with thermo chemical treatment will be outlined for all the materials and presented in the conference.

#### Acknowledgments

The support from the National Centre for Research and Development of Poland, Warsaw, Grant no. INNOGLOBO/11/60/CoatTool4.0-2023,

aswellasthe National Science Center, Krakow, Poland, Grant no. SONATA UMO-2020/39/D/ST8/02610 are gratefully acknowledged.

#### 9:00am IA2-2-TuM-4 Liquid Feedstock Thermal Spraying for Advanced Functional Coatings, *Shrikant Joshi [shrikant.joshi@hv.se]*, University West, Sweden

INVITED

Thermal spraying with liquid feedstock offers an exciting opportunity to obtain coatings with characteristics vastly different from those produced using conventional spray-grade powders. The two extensively investigated variants of this technique are Suspension Plasma Spraying (SPS), which utilizes a suspension of fine powders in an appropriate medium, and Solution Precursor Plasma Spraying (SPPS), which involves use of a suitable solution precursor that can form the desired particles *in situ*. The advent of axial injection high power plasma spray systems in recent times has also eliminated concerns regarding low deposition rates/efficiencies associated with liquid feedstock. The 10-100  $\mu\text{m}$  size particles that constitute conventional spray powders lead to individual splats that are nearly two orders of magnitude larger compared to those resulting from the fine (approximately 100 nm - 2  $\mu\text{m}$  in size) particles present in suspensions in SPS or formed *in situ* in SPPS. The distinct characteristics of the resulting coatings are directly attributable to the above very dissimilar ‘building blocks’ responsible for their formation. This talk will discuss the advancements in suspension and solution precursor thermal spraying associated with axial plasma spraying, with specific emphasis on thermal barrier coating (TBC) and environmental barrier coating (EBC) applications. Prospects of liquid feedstock thermal spraying for addressing some other niche applications will be discussed through some illustrative examples. A further extension of deploying solutions and suspensions that involves use of hybrid powder-liquid feedstock combinations for thermal spraying will also be presented. This approach can be used to elegantly deposit coatings with unusual microstructures to develop a wide array of composite coatings. The possibilities unplugged by such hybrid feedstock processing will also be illustrated through case studies.

## Protective and High-temperature Coatings

### Room Town & Country A - Session MA1-1-TuM

#### Coatings to Resist High-temperature Oxidation, Corrosion, and Fouling I

**Moderators:** Dr. Justyna Kulczyk-Malecka, Manchester Metropolitan University, UK, Prof. Francisco Javier Pérez Trujillo, Universidad Complutense de Madrid, Spain

#### 8:00am MA1-1-TuM-1 High Temperature Corrosion Resistant Coatings: Recent Aluminide Developments for Renewable Energy Applications, *Pauline Audigié [audigiep@inta.es]*, *Cristina Lorente, Sergio Rodriguez, Loïc Oger, Alina Agüero*, Instituto Nacional de Técnica Aeroespacial (INTA), Spain

INVITED

Protective coatings are known for many decades as first-rate mitigation methods to hinder high-temperature oxidation and corrosion in several industrial sectors. For many years, INTA has been developing diffusion coatings by spraying Al slurry onto different substrates such as different composition of Fe, Ni, Ti and Mo-based alloys. Recently, new developments have been focused on renewables energies including concentrated solar power (CSP) plants with thermal energy storage systems and hydrogen-fueled combustion systems. For those applications, some components require coatings that are resistant to corrosion/oxidation and mechanical stresses which might also give rise to considerable cost reduction by using lower cost alloys. In particular, new slurry aluminide coatings deposited onto TA6V and Ti6246 Ti-based alloys are being explored for compressor parts of aircraft engines and also onto 310H and 347H austenitic steels for molten nitrate and carbonate resistance in hot storage tanks and tubes in CSP plants. An overview of the global deposition process including surface preparation, deposition methods and thermal treatments will be shown for each generated coating. The coating formation mechanism and their prevailing protection mechanism in their respective corrosive environment will be presented. Furthermore, the loss of the protective oxide former element, Al in this case, by coating-substrate interdiffusion during exposure at high temperature can lead to premature degradation of the coating. Efforts have thus been pursued to reduce interdiffusion in the Ti6246 and 310H coated systems by incorporating Si particles in the slurry. This led to the formation of Si-Al rich diffusion barriers for which the latest progresses and corrosion results in both environments will be presented.

# Tuesday Morning, May 13, 2025

8:40am **MA1-1-TuM-3 Molten Salt Corrosion and Stress Corrosion Cracking Performance of Slurry Aluminate Coated Steels for Thermal Energy Storage**, *Loïc OGER [loge@inta.es]*, *Pauline Audigé*, Instituto Nacional de Técnica Aeroespacial (INTA), Spain

Thermal energy storage systems associated to concentrated solar power (CSP) plants emerged as key technologies to allow consistent energy distribution while reducing electricity cost. However, their wide-range deployment is limited by the cost of the structural materials and by their short lifespan which imposes recurrent and expensive operation and maintenance. This is mainly due to the use of corrosive high-temperature molten salts as heat transfer fluid and to stresses generated by temperature variations. The European project COMETES was thus designed to develop coated materials as cost-effective alternatives suitable in current plants and in more aggressive operating conditions considered for next-gen CSP. The present study focused on molten salt corrosion and stress corrosion cracking (SCC) resistance of:

(1) A slurry aluminate coated P91 martensitic-ferritic steel considered as a promising alternative for current use in Solar Salt (60wt%NaNO<sub>3</sub> – 40wt%KNO<sub>3</sub>) up to 580 °C because of its 3 to 10 times lower cost than the currently used Ni-based materials.

(2) a newly developed coated 347H austenitic steel, capable to withstand higher operating temperatures – 700 °C in the present study – with 32wt%Li<sub>2</sub>CO<sub>3</sub> – 33wt%Na<sub>2</sub>CO<sub>3</sub> – 35wt%K<sub>2</sub>CO<sub>3</sub> carbonate to achieve higher plant efficiency and increase the heat storage duration.

1000 h-hot corrosion study of the uncoated materials in their respective molten salt and temperature showed significant degradation of the substrates with the formation of various alkaline oxides. Tensile tests performed at a strain rate of 10<sup>-3</sup> s<sup>-1</sup> after such exposure showed a relatively low sensitivity of the P91 to SCC while a collapse of the 347H mechanical properties was evidenced. The slurry aluminate coated P91, composed by a homogeneous FeAl outer layer with Kirkendall pores formed in the interdiffusion zone, significantly increased the corrosion resistance when compared with the uncoated P91 in Solar Salt capable to withstand up to 10,000 h at 580 °C. On the 347H, a 3-layers coating developed with several Fe-Al-Cr rich phases in the top layer. Despite the hardness heterogeneity (200 to 1000 HV<sub>0.05</sub>) and the coating evolution along the exposure with the occurrence of phase transformations and Cr<sub>3</sub>Si precipitation, aluminate coated 347H withstood at least 2,500 h in carbonates at 700 °C with the formation of a mixed γ/α-LiAlO<sub>2</sub> top layer. From the mechanical view, both steels were shown to have slightly lower maximal stresses after coating, which was attributed to crack initiation in the latter and then propagation into the substrate. Nonetheless both coatings efficiently increased the SCC resistance of the steels in molten salts.

9:00am **MA1-1-TuM-4 Prediction of the Ageing Behavior of Diffusion Aluminate Coatings Using Machine Learning**, *Vladislav Kolarik [vladislav.kolarik@ict.fraunhofer.de]*, *Maria del Mar Juez Lorenzo*, Fraunhofer Institute for Chemical Technology ICT, Germany; *Pavel Praks, Ranata Praksová*, IT4Innovations National Supercomputing Center, VSB - Technical University of Ostrava, Czechia

Aluminate diffusion coatings provide an effective and cost-efficient solution for protecting steels from high-temperature corrosion in harsh environments. They can be applied as aluminum slurries through various deposition techniques, such as spraying or brushing, followed by heat treatment to create the diffusion layer. Machine learning algorithms show great potential for modeling and predicting the aging behavior of these coatings, while facilitating their optimization and customization. Machine learning relies solely on data and does not require physical models to describe dependencies. This is especially advantageous for systems influenced by multiple parameters, where the extent of each parameter's impact on the system is not well known. Symbolic regression and decision tree-based algorithms, such as XGBoost and Catboost were employed to explore the potential of machine learning in modelling the coating characteristic over time and forecasting the ageing behavior.

Data files for input were created collecting parameters, such as time, temperature, atmosphere, overall coating thickness, thicknesses of the partial layers, number of the partial layers, type of slurry etc. To evaluate the aging process, two key output parameters were modeled based on selected input variables: (1) the ratio of the outer Fe<sub>3</sub>Al layer to the total coating thickness, and (2) the aluminum concentration within the outer Fe<sub>3</sub>Al layer. The first parameter indicates the conditions under which the diffusion coating evolves into a single aluminum-poor layer—this occurs when the ratio equals 1. The aluminum concentration, on the other hand,

reflects how much aluminum remains in the coating, which is essential for forming a protective alumina layer. Decision tree-based algorithms, such as XGBoost, are well-suited for assessing the degree of influence of individual parameters, with time emerging as the most significant factor, followed by the thickness of the aluminum-poor Fe<sub>3</sub>Al layer.

The results demonstrate that machine learning is highly effective for analyzing complex material systems influenced by numerous parameters, where the relationships and significance of these parameters are challenging to capture through traditional physical modeling.

9:20am **MA1-1-TuM-5 AI-Enhanced Correlative Microscopy: A Multi-Modal Approach to Automotive Coating Evaluation**, *Hugues G. Franco-Saint-Cyr [hugues.fsc@thermofisher.com]*, Thermo Fisher Scientific, USA; *Alice Scarpellini, Bartłomiej Winiarski*, Thermo Fisher Scientific, Netherlands; *Roger Maddalena, Rengarajan Pelapur*, Thermo Fisher Scientific, USA

The automotive industry extensively employs zinc-based coatings to enhance corrosion resistance and extend the lifespan of steel components exposed to harsh atmospheric conditions. These protective layers, applied through hot-dip galvanizing and electroplating, prevent oxidation of the underlying steel. The effectiveness of these coatings depends on thorough material quality assessment, adhesion evaluation, and stringent final product control.

Scanning electron microscopy (SEM), along with other advanced analytical characterization techniques, is crucial for detailed evaluation of zinc-based coatings. SEM supports correlative microscopy (CM) workflows, integrating imaging, analytical solutions, and AI-assisted image analysis to provide a multi-modal and multi-dimensional view of the materials under investigation. The site-specific use of Plasma Focused Ion Beam-SEM (PFIB-SEM) cross-sections enables highly targeted analysis, revealing detailed microstructural features and providing comprehensive compositional and crystallographic information.

The Apreo ChemiSEM exemplifies this approach by enabling comprehensive surface and cross-sectional analysis of both coatings and steel substrates. Its correlative capabilities combine imaging, energy dispersive X-ray spectroscopy (EDS) via ChemiSEM Technology, and electron backscatter diffraction (EBSD) with the TruePix detector. Cross-sectional analysis is performed on both metallographically prepared sections and PFIB-prepared cross-sections, providing detailed insights and accelerating the characterization of coating morphology and defect identification.

Integrating imaging with ChemiSEM Technology allows for detailed investigation of surface oxidation, inclusions, and inhibition layers within the coatings. The TruePix detector identifies areas of high dislocation density and other crystalline defects, offering a deeper understanding of material weaknesses that may correlate with reduced adhesion or other issues.

AI-assisted image analysis enhances the characterization process by significantly reducing the time required to interpret complex datasets. Deep learning models integrated into the workflow provide accurate, large-scale analysis of data collected at both micro- and nanoscale levels, enabling validation over millimeter-scale regions. This synergy between advanced microscopy and AI ensures a robust and comprehensive evaluation of zinc-based coatings, linking structure, processing, property, and performance in automotive applications.

9:40am **MA1-1-TuM-6 High-Temperature Corrosion in Contact with Molten Glass Improved by Thermal Spray Coating**, *Michelle Hartbauer [michelle.hartbauer@uni-bayreuth.de]*, University of Bayreuth, Germany; *Thomas Dörflinger*, Neue Materialien Bayreuth GmbH, Germany; *Helge Schumann*, Wiegand-Glashüttenwerke GmbH, Germany; *Gilvan Barroso*, Rauschert Heinersdorf-Pressig GmbH, Germany; *Haneen Daoud*, Neue Materialien Bayreuth GmbH, Germany; *Florian Scherm, Uwe Glatzel*, University of Bayreuth, Germany

Glass manufacturing demands extreme conditions, exposing components to high-temperature corrosion through contact with molten glass at temperatures above 1100 °C. Thermal spray processes have emerged as a valuable solution for creating protective coatings that can significantly enhance material performance in such harsh environments. These coatings improve component longevity by increasing hardness, wear resistance, and corrosion resistance. Known for their performance, ease of application, and cost-effectiveness, thermal spray coatings are widely used across various applications.

To address these challenges, this study employs thermal spray processes to deposit an Al-Ni alloy onto a substrate of lamellar grey cast iron. Al and Ni



# Tuesday Morning, May 13, 2025

wires are applied simultaneously via arc spray process. An electric arc generated between two consumable wires produces intense heat, melting the wire tips. Nitrogen gas then propels the molten material onto the substrate's surface, where it rapidly solidifies to form the protective coating. Heat treatment was then carried out.

To examine the coating's corrosion resistance, samples were immersed in molten glass for up to 48 h and subsequently prepared for analysis using metallographic procedures. Cross-sectional imaging allowed the analysis of the reaction zone between the thermal spray coating and molten glass.

Analyses of microstructure and chemical composition were conducted using SEM and energy-dispersive spectroscopy (EDS) across various stages: after thermal spraying, post-heat treatment, and after glass contact. Additionally, phase identification was carried out using X-ray diffraction (XRD).

Coating thicknesses with 100 - 300  $\mu\text{m}$  were achieved. The differences in composition and heat treatment have a great influence on the microstructure of the thermal sprayed coatings. Differences in elemental distribution, phases formed, and their corresponding properties, particularly hardness, were observed.

10:00am **MA1-1-TuM-7 Microstructural Characterization and Isothermal Oxidation Behavior of a Nanolaminate  $\text{Ti}_2\text{AlC}$  MAX Phase Coating on TiAl 48-2-2**, *Radostaw Swadzba [radoslaw.swadzba@git.lukasiewicz.gov.pl]*, Łukasiewicz Research Network – Uppersilesian Institute of Technology, Poland; *Bogustaw Mendala, Lucjan Swadzba*, Silesian University of Technology, Poland; *Nadine Laska*, German Aerospace Center (DLR), Germany; *Sarra Boubtane*, German Aerospace Center, Germany; *Dariusz Garbicz*, Łukasiewicz Research Network – Poznań Institute of Technology, Poland

This study investigates the application of the Closed Hollow Cathode Physical Vapor Deposition (CHC-PVD) method for depositing  $\text{Ti}_2\text{AlC}$  MAX phase nanolaminate coatings on a TiAl 48-2-2 alloy substrate. During deposition, samples were placed within an 80 mm-diameter, 160 mm-long hollow cathode using a target composition of Ti-25Al-25C (at.%). The resulting coatings, approximately 12  $\mu\text{m}$  thick, exhibited a columnar microstructure. Advanced characterization techniques, including High-Resolution Scanning Transmission Electron Microscopy (STEM) and High-Resolution TEM (HRTEM), were employed to analyze the microstructure of both as-deposited coatings and coatings subjected to isothermal oxidation testing.

The oxidation resistance of the obtained coatings was evaluated using Thermogravimetric Analysis (TGA) at 850 °C for 20 hours in an air atmosphere. Mass change analysis revealed that the parabolic rate constant for the coated material was over five times lower than that of the uncoated substrate. Detailed STEM and HRTEM analyses showed  $\text{Ti}_2\text{AlC}$  nanolaminates within the columnar structures, with basal planes of the  $\text{Ti}_2\text{AlC}$  phase aligned parallel to the growth direction at the core and tilted in sub-columnar regions.

After the isothermal oxidation test it was found that a very thin and continuous alumina oxide scale is formed on the coated TiAl 48-2-2 with a thickness of around 320 nm. HRTEM and FFT (Fast Fourier Transform) imaging were applied to study the phase composition of the oxide scale and showed the presence of a mixture of transition  $\theta\text{-Al}_2\text{O}_3$  and stable  $\alpha\text{-Al}_2\text{O}_3$ .

10:20am **MA1-1-TuM-8 Harnessing  $\text{Ti}_2\text{AlN}$  MAX Phase Based PVD Coatings on Titanium Aluminide Alloys for High Temperature Applications**, *Sarra Boubtane [sarra.boubtanepammouri@dlr.de]*, German Aerospace Center, Germany

Nanolaminate coatings based on MAX phases (where M= Ti, A=Al, and X is nitrogen) exhibit a distinctive combination of ceramic and metallic material properties, offering considerable potential for utilization in high-temperature environments.

It is unfortunate that the application of MAX phases as coating material on various Ti- or Ni-based alloys results in degradation due to interdiffusion processes between the coating and the alloy, which is accompanied by an Al-depletion. A promising strategy involves combining a  $\gamma\text{-TiAl}$  substrate with a MAX phase coating, as the substrate can serve as an Al reservoir, replenishing the coating through outward diffusion of Al. This approach could also enhance the mechanical properties of such coated components compared to other protective but brittle intermetallic coatings on TiAl alloys.

In this study, a  $\text{Ti}_2\text{AlN}$ -MAX phase-based coating was deposited using reactive magnetron sputtering using pure elemental targets of Ti, Al and

nitrogen as a reactive gas. The deposition process was studied using a variety of substrates, including inert  $\text{Al}_2\text{O}_3$  and MgO substrates, as well as an already been used  $\gamma\text{-TiAl}$  alloy. This alloy TiAl48-2-2 (48Ti-48Al-2Nb-2Cr in at.%), supplied by GfE-Gesellschaft für Elektrometallurgie in Nuremberg, Germany, was utilized for all oxidation and interdiffusion experiments. The two-fold rotation ensures homogeneous deposition, with a thickness of 10  $\mu\text{m}$  and near to the requisite stoichiometric composition of the  $\text{Ti}_2\text{AlN}$  MAX phase. Due to the low substrate temperature during deposition, the resulting layer was X-ray amorphous. A post-annealing treatment was performed at 800°C in a high vacuum furnace for one hour for crystallization. Additionally, high-temperature X-ray diffraction (HT-XRD) in a vacuum atmosphere was conducted from room temperature to 1000°C to observe in-situ the phase formation in the  $\text{Ti}_2\text{AlN}$  coating.

Following the production of  $\text{Ti}_2\text{AlN}$  MAX Phase, a series of oxidation tests are conducted to assess the coating's performance. These include isothermal oxidation for 10 hours at 850°C in laboratory air. Hereby, the  $\text{Ti}_2\text{AlN}$  MAX phase based coating develop a thermally grown layer of predominantly alumina, which is suitable as protection in high temperature environments. Below the alumina layer the  $\text{Ti}_2\text{AlN}$  MAX phase as well as the intermetallic Al-rich phase.

Analysis techniques included GD-OES for chemical composition, XRD for phase analysis, and SEM/EDS and TEM for structural evaluation are used.

10:40am **MA1-1-TuM-9 Empowering Pvd for Corrosion Protection: Ti(Al,Mg)Gdn Coatings with Game-Changing Corrosion Performance**, *Holger Hoche [holger\_claus.hoche@tu-darmstadt.de]*, Grafenstraße 2, Germany

Today, PVD technology is not the first choice for surface functionalization under corrosive conditions. The state-of-the-art for corrosion protection involves multilayers of electroplating or chemical corrosion protection layers, followed by a PVD top layer. This negatively affects sustainability and economic factors.

The authors successfully developed PVD-TiMgGdN and TiAlMgGdN coatings, sputtered with powder metallurgical targets in an industrial DC-magnetron PVD unit. With only a 5  $\mu\text{m}$  coating thickness, corrosive mild steel substrates can be protected for at least 1000 hours in the salt spray test against corrosion [1]. By partially substituting magnesium with aluminum, the corrosion properties and manufacturability were further improved. Additionally, TiAlMgGdN coatings exhibit excellent corrosion behavior in alkaline (pH 8.5) and acidic (pH 5) environments.

This improvement is based on the synergistic effects of magnesium and gadolinium: Magnesium lowers the free corrosion potential of the coating, thereby reducing the susceptibility to galvanic corrosion. Gadolinium enhances the hydrophobicity of the surface, affects the conductivity, and supports the formation of stable passivation layers [2].

The influence of Gd, Mg, and Al on the corrosion protection performance will be investigated. Therefore, coatings with different Al/Mg proportions and varying Gd content were produced and compared regarding their microstructural, chemical, physical, and corrosion properties. Corrosion properties were investigated using different corrosion tests. The coating surfaces were also analyzed by nanoindentation measurements and chemical analysis to gather knowledge about the coating stability during corrosive stress.

The key properties influencing the corrosion protection effect of Ti(Al, Mg)Gd will be evaluated. Additionally, the effect of the specific chemical composition on the coating properties will be investigated. Understanding the key properties and their correlation with chemical composition allows for the specific design of functional corrosion-resistant PVD coatings.

[1] T. Ulrich, C. Pusch, H. Hoche, P. Polcik, M. Oechsner, Surface and Coatings Technology 422 (2021) 127496.

[2] H. Hoche, T. Ulrich, P. Kaestner, M. Oechsner, Vakuum in Forschung und Praxis 36, 2 (2024) 40.

## Protective and High-temperature Coatings

### Room Palm 3-4 - Session MA3-1-TuM

#### Hard and Nanostructured Coatings I

**Moderators:** Dr. Rainer Hahn, TU Wien, Institute of Materials Science and Technology, Austria, Dr. Stanislav Haviar, University of West Bohemia, Czechia, Dr. Fan-Yi Ouyang, National Tsing Hua University, Taiwan

8:00am **MA3-1-TuM-1 Hard TiAlTaN Coating by HIPIMS Deposition for Cutting Tools: Experiments, Simulations and Cutting Tests, Emile Haya [emile.haya@unamur.be]**, University of Namur, Belgium; Jérôme Muller, Pavel Moskovin, University of Namur, Innovative Coating Solutions, Belgium; Loris Chavee, University of Namur, Belgium; Szilard Kolozsvari, Plansee Composite Materials GmbH, Germany; Stéphane Lucas, University of Namur, Innovative Coating Solutions, Belgium **INVITED**

The quaternary  $Ti_{1-x-y}Al_xTa_yN$  system has been shown to possess superior thin film properties compared to  $Ti_{1-x}Al_xN$ . In addition to the impact of Ta content, the sputtering technique significantly influences the structural and mechanical characteristics of these films. In this study, high power impulse magnetron sputtering (HiPIMS) was employed to deposit dense, tough, and hard  $Ti_{1-x-y}Al_xTa_yN$  thin films from composite targets, which were then compared to TiAlN thin films. The effects of Ta addition were explored both experimentally and through simulations. VirtualCoater<sup>®</sup> was used to simulate thin film growth and properties, providing insight into the role of Ta in the densification process and the relationship between target composition and film composition. Subsequently, the mechanical, structural, and thermal properties of the films were experimentally examined, highlighting the significant benefits of Ta addition.

The observed enhancements are attributed to: (1) increased hardness due to film densification facilitated by intense Ta bombardment, (2) stabilization of the cubic structure at elevated temperatures, and (3) superior thermal resistance resulting from the formation of a mixed  $(Ti_xAl_yTa_z)$  oxide monolayer, as opposed to the  $Al_2O_3/TiO_2$  bilayer observed in TiAlN-based coatings, as confirmed by XPS depth profiling.

Finally, dry cutting tool tests demonstrated a substantial increase in tool life and improved surface finish of the machined parts.

8:40am **MA3-1-TuM-3 Development and Comparison of AlTiN-Based HiPIMS Coatings for Microtool Machining Applications, Ivan Fernández-Martínez [ivan.fernandez@nano4energy.eu]**, Nano4Energy S.I.N.E, Spain

Currently, the coating of microtools plays a critical role in precision manufacturing, as tool performance and longevity are heavily influenced by the properties and quality of the coating employed. In this context, HiPIMS technology provides hard coatings with a smooth finishing, a low defect density, and homogeneous coverage of 3D intricate parts – an essential advantage when coating tools with diameters smaller than a millimeter – thus representing an ideal choice for these applications.

AlTiN-based coatings doped with silicon (AlTiSiN) and boron (AlTiBN) have been developed to meet the specific demands of micro-tool applications, such as enhanced wear resistance, high thermal stability, and low friction in extreme operating environments. Properties such as hardness, adhesion, and residual stress were tailored and correlated to HiPIMS process parameters. In addition to mechanical properties analysis, tool performance was evaluated through machining tests, selecting Hardened Steel (HRC60) and Ti6AlV4 alloy as case materials. Both the finishing of the machined parts, and the wear suffered by the tool were analyzed.

The results highlight the potential of HiPIMS-deposited AlTiN-based coatings to significantly extend tool life and improve machining quality in precision manufacturing. Furthermore, this study provides insights into the trade-offs between boron and silicon doping, offering practical guidelines for selecting the most appropriate coating for specific micro-tool applications.

Our findings underline the versatility of HiPIMS technology in tailoring thin-film properties for high-performance applications, demonstrating its growing relevance in the field of advanced microtools.

**Keywords:** hard coatings, nitrides, sputtering, HiPIMS.

9:00am **MA3-1-TuM-4 Micro-Fracture Toughness and Durability of HiPIMS-Deposited Hard Coatings used for Micro-Machining of TiAl<sub>6</sub>V<sub>4</sub> Alloys, Arley Garcia [arley.garcia@imdea.org]**, Nano4Energy SL, IMDEA Materiales, Spain; Jose Antonio Santiago, Nano4Energy SL, Spain; Christoph Kirchlechner, Karlsruhe Institute of Technology (KIT), Institute for Applied Materials (IAM), Germany; Pablo Diaz Rodriguez, Nano4Energy SL, Spain; Miguel Monclús, IMDEA Materiales, Spain; Iván Fernández Martínez, Nano4Energy SL, Spain; Alvaro Guzmán, Universidad Politécnica de Madrid, Spain; Subin Lee, Karlsruhe Institute of Technology (KIT), Institute for Applied Materials (IAM), Germany; Jon Molina Aldareguia, Universidad Politécnica de Madrid, Spain

The High-Power Impulse Magnetron Sputtering (HiPIMS) technique enables the deposition of coatings with high hardness, low defect densities, and uniform, conformal coverage over complex 3D geometries, meeting the strict tolerances required in micromachining applications. High-speed machining (HSM) applications demand not only high hardness but also sufficient fracture toughness  $K_{IC}$ , which is critical for maintaining the structural integrity of both bulk and coated engineering components [1]. However, these mechanical properties are often antagonistic, particularly in materials capable of plastic deformation, where high hardness typically correlates with lower fracture toughness [2].

This study aims to systematically evaluate the fracture toughness and machining performance of AlTiN- and TiN-based coatings doped with Si, deposited by HiPIMS using different process parameters. Micro-fracture toughness was assessed on freestanding films using single cantilever bending tests, effectively minimizing residual stress and substrate interactions to obtain precise  $K_{IC}$  values. Crack formation at the cutting edge of a 0.4 mm diameter microdrill was observed using FIB, while the composition of the coatings was determined by GDOES. Additionally, XRD was employed to analyze grain growth texture and peak shifts, enabling the evaluation of biaxial stresses. The AlTiSiN coatings exhibited a hardness of 35 GPa, while TiSiN coatings reached 40 GPa. Fracture toughness ranged from 1.78 MPa·√m to 2.2 MPa·√m, depending on the HiPIMS parameters used. In micromachining tests on the TiAl<sub>6</sub>V<sub>4</sub> alloy, the coatings allowed continuous micro-milling to be extended from 40 minutes to over one hour. These findings link toughness values, stress reduction, and crack formation at the cutting edges with tool durability in machining applications.

[1]. BARTOSIK, M., et al. Fracture toughness of Ti-Si-N thin films. *International Journal of Refractory Metals and Hard Materials*, 2018, vol. 72, p. 78-82.

[2]. HAHN, Rainer, et al. Superlattice effect for enhanced fracture toughness of hard coatings. *Scripta Materialia*, 2016, vol. 124, p. 67-70.

9:20am **MA3-1-TuM-5 Effect of Process Parameters on the Structure and Mechanical Properties of TiZrN Thin Films Prepared by Co-Sputtering HPPMS/UBMS, Chun Lin Yang [a0903271975@gmail.com]**, Jia-Hong Huang, National Tsing Hua University, Taiwan

Transition metal nitrides (TMeNs) are widely used in protective hard coatings for cutting tools due to their superior mechanical and tribological properties, and high thermal stability. Among the TMeNs, TiZrN possesses higher hardness, better thermal stability, and greater corrosion resistance, compared with their counterpart binary TMeNs, and therefore TiZrN becomes a promising hard coating material and attracts attention from both academia and industry. The purposes of this study is to investigate the effects of duty cycle (D-series) and working pressure (P-series) on the structure and mechanical properties of TiZrN thin films. TiZrN coatings were deposited on Si substrate using high-power pulsed magnetron and unbalanced magnetron co-sputtering techniques (HPPMS/UBMS). The dc-UBMS was for sputtering zirconium, while HPPMS was for sputtering titanium. The duty cycle of HPPMS was adjusted from 100% to 5%, and at a duty cycle of 5%, the working pressure was varied from 3 to 10 mTorr. The results of X-ray diffraction (XRD) showed that the film structure varied with the two process parameters. As the duty cycle decreased, the preferred orientation of the TiZrN thin films changed from random to (200), with increasing peak power density finally reaching 0.3 kW/cm<sup>2</sup>, indicating that the increase in energy facilitated the formation of the (200) texture. Residual stress increased with decreasing duty cycle, except in the D5 sample. However, the hardness, resistivity, and roughness of D-series samples remained unaffected by changing duty cycle. With increasing working pressure, the preferred orientation of the TiZrN coatings switched from (200) to (111). The cross-sectional observation of P-series samples by scanning electron microscopy revealed that the microstructure of the coatings changed from dense to a loosely packed columnar structure for the specimen deposited at the highest working pressure of 10 mTorr, where

high roughness, high electrical resistivity, and low residual stress were also measured.

Keywords: TiZrN; high power pulse magnetron sputtering (HPPMS); duty cycle; working pressure

9:40am **MA3-1-TuM-6 Superstoichiometric (Al,Cr)N<sub>x</sub> Coatings with Superior Hardness, Fracture Toughness, and Wear Resistance, Fedor F. KLIMASHIN [fedor.klimashin@empa.ch]**, Empa, Swiss Federal Laboratories for Materials Science and Technology, Switzerland; *Martin Učík*, PLATIT a.s., Czechia; *Martin Matas, David Holec*, Montanuniversität Leoben, Austria; *Martin Beutner*, Otto-von-Guericke-Universität Magdeburg, Germany; *Jan Klusůň, Mojmír Jílek*, PLATIT a.s., Czechia; *Andreas Lümekmann*, PLATIT AG, Switzerland; *Johann Michler, Thomas E. J. Edwards*, Empa, Swiss Federal Laboratories for Materials Science and Technology, Switzerland

Many transition-metal carbides, nitrides, and oxides are inherently non-stoichiometric compounds, characterised by broad homogeneity ranges in their phase diagrams. Deviations from stoichiometry, defined as the ratio of non-metal to metal atoms ( $x$ ), can drastically affect properties. While substoichiometric compounds ( $x < 1$ ) have been widely studied, superstoichiometric compounds ( $x > 1$ ) remain largely unexplored.

Here we present our finding on superstoichiometric (Al,Cr)N<sub>x</sub> coatings sputter-deposited from an Al<sub>60</sub>Cr<sub>40</sub> target at power densities reaching 840 W/cm<sup>2</sup>. Experimental and computational analyses reveal that excess nitrogen predominantly occupies interstitial lattice sites. Upon surpassing a critical concentration ( $x \approx 1.06$ ), grain renucleation rates increase, disrupting columnar growth and altering the preferential orientation from (111) to (220). The coatings exhibit a single-phase, face-centred cubic structure, a dense microstructure, and reduced surface roughness compared to benchmark coatings produced by cathodic arc evaporation.

Remarkably, hardness, fracture toughness, and wear resistance equal or exceed those of the benchmark coatings. Our findings highlight the advantages of superstoichiometric (Al,Cr)N<sub>x</sub> as effective wear-resistant materials for advanced engineering applications, while also suggesting broader implications for the utilisation of superstoichiometric nitrides across various industries.

10:00am **MA3-1-TuM-7 Connecting Phase Stability and Mechanical Properties of Ti–B–N Thin Films, Rebecca Janknecht [rebecca.janknecht@empa.ch]**, Empa, Swiss Federal Laboratories for Materials Science and Technology, Thun, Switzerland; *Tomasz Wójcik*, TU Wien, Austria; *Fedor F. Klimashin*, Empa, Swiss Federal Laboratories for Materials Science and Technology, Thun, Switzerland; *Johann Michler*, EMPA, Switzerland; *Paul H. Mayrhofer, Rainer Hahn*, TU Wien, Austria

Understanding the relationship between thermally induced decomposition in metastable material systems and their mechanical properties is critical for designing thin films with improved wear resistance and thermal stability. Our previous work revealed that achieving improved solubility of B in fcc-TiN requires a deviation from the TiN-TiB tie line toward Ti-rich compounds, facilitated by the formation of vacancies in the non-metal sublattice. This deviation was achieved by non-reactive co-sputtering of a Ti target alongside TiN and TiB<sub>2</sub> targets, allowing full incorporation of 8.9 at.% B into the fcc-TiN lattice. In contrast, co-sputtering TiN and TiB<sub>2</sub> yielded compositions along the TiN-TiB<sub>2</sub> tie line, with excess B forming amorphous grain boundary phases [1]. In this study, we systematically annealed (1) a single-phase fcc-Ti–B–N coating with a composition of Ti<sub>1.08</sub>B<sub>0.18</sub>N<sub>0.74</sub> and (2) a Ti–B–N coating with amorphous B-rich grain boundary phases with a Ti<sub>1.01</sub>B<sub>0.21</sub>N<sub>0.78</sub> stoichiometry. Annealing was performed at 700°C, 800°C, 900°C, 1000°C, 1200°C and 1400°C for 10 minutes. Both coatings retained high hardness of 30±1 GPa up to 1200°C. The results of micro-cantilever bending tests indicate an inverse relationship between fracture toughness ( $K_{IC}$ ) and annealing temperature ( $T_a$ ). The Ti<sub>1.01</sub>B<sub>0.21</sub>N<sub>0.78</sub> coating exhibits a  $K_{IC}$  of  $2.1 \pm 0.1 \text{ MPa}\cdot\text{m}^{0.5}$ , which increases to  $3.8 \pm 0.3 \text{ MPa}\cdot\text{m}^{0.5}$  upon increasing  $T_a$  to 1000°C, but  $K_{IC}$  for the Ti<sub>1.08</sub>B<sub>0.18</sub>N<sub>0.74</sub> sample was observed to decrease from  $2.7 \pm 0.1 \text{ MPa}\cdot\text{m}^{0.5}$  in the as-deposited state to  $2.3 \pm 0.1 \text{ MPa}\cdot\text{m}^{0.5}$  at  $T_a=1000^\circ\text{C}$ . X-ray diffraction (XRD) and transmission electron microscopy (TEM) analyses confirm that  $K_{IC}$  improves only when metastable Ti–B–N decomposes into co-existing thermodynamically more stable fcc-TiN and hcp-TiB<sub>2</sub> phases without the formation of additional hcp-Ti precipitates. These findings highlight the critical influence of compositional and structural control on the thermal and mechanical stability of Ti–B–N thin films, providing new pathways for their use in high-performance applications.

[1] R. Janknecht et al., *A strategy to enhance the B-solubility and mechanical properties of Ti–B–N thin films*, Acta Mater., 271 (2024), Article

119858, 10.1016/j.actamat.2024.119858  
[https://doi.org/10.1016/j.actamat.2024.119858]

10:20am **MA3-1-TuM-8 Effect of Oxygen Content and Thickness on the Property and Structure of Zr(O,N) Thin Film, Chi Feng Hung [rbisme@gapp.nthu.edu.tw]**, Jia Hong Huang, National Tsing Hua University, Taiwan

Transition metal nitrides (TMeNs) have been widely applied as the protective coatings for tools due to their excellent properties. Zirconium nitride (ZrN) coatings, in particular, attract attention for the outstanding mechanical properties, corrosion resistance, and attractive golden color. It has been extensively reported that by adding oxygen in ZrN, the coating becomes Zr(N,O), where the ionic/covalent bond ratios can be tuned by adjusting the nitrogen-to-oxygen (N/O) ratio, and consequently influencing the optical, electrical, and mechanical properties of the coatings. However, most studies of Zr(N,O) coatings are on the effect of phase transition on structure and properties within a wide range of N/O contents, while limited research was conducted with range of oxygen content where Zr(N,O) remains a single phase. The purpose of this study is to explore the effect of oxygen content and film thickness on the structure and properties of single-phase Zr(N,O) films. In this study, the Zr(N,O) coatings were prepared using dc unbalanced magnetron sputtering with different durations and oxygen flow rates. Four different oxygen flow rates were used to control the oxygen content, and the coating thickness was controlled by varying the deposition times. The preferred orientation of the coatings was observed by X-ray diffraction. The results showed that dominant (111) and (200) textures appeared in the specimens with low and medium oxygen contents, respectively; in contrast, the texture of the specimens with high oxygen contents varied from random to (200) with increasing thickness. The hardness and Young's modulus of the coatings were nearly constant for all samples, with no observable trends with respect to thickness or oxygen content. The results revealed that the electrical resistivity increased with increasing oxygen content. The variation of residual stress with increasing oxygen content could be divided into two regimes, where compressive stress dropped sharply when the texture changed from (111) to (200) and then gradually decreased with further increase of oxygen content. The specimens with higher oxygen contents exhibited a significant decrease in electrical resistivity with decreasing thickness, while the specimens with medium oxygen contents showed a less distinct decrease, and the specimens with the lowest oxygen contents showed no change in resistivity with thickness. The residual stress also showed two trends, in which residual stress decreased with thickness for the specimens with the lowest oxygen contents, while residual stress increased with thickness for the other specimens.

10:40am **MA3-1-TuM-9 Effect of Fluence on Zirconium Nitride Coating Irradiated by 5-MeV-Proton, Rou-Syuan Chen [250201chen@gmail.com]**, Department of Engineering and System Science, National Tsing Hua University, Taiwan (ROC); *Kuan-Che Lan*, Institute of Nuclear Engineering and Science, National Tsing Hua University, Taiwan (ROC)

The development of advanced nuclear reactors and small modular reactors (SMR) will require nuclear fuel at a higher enrichment, which can introduce higher fluence of ionizing radiation such as fission products, neutron and proton etc. It will bring a severe challenge for fuel cladding materials. Zirconium nitride (ZrN) thin films are known for their thermal stability, high hardness, low resistivity, and better tribological properties, and they are widely used as hard coatings on deposited on the edge surface of cutting. Previous studies have also shown that ZrN exhibits great resistance to ionizing radiation. However, report about the irradiation damage of ZrN thin film as a function of proton fluence are rare. The objective of this study is to investigate on effect of fluence on ZrN thin film irradiated by 5-MeV-proton. Post irradiation examination of ZrN thin film will be performed to analyze the electronic properties, crystal structure, hardness and young's modulus. The crystal structure and grain size of each sample are characterized by X-ray diffraction (XRD). The electronic resistivity is measured by a four-point probe. The film thickness is examined by scanning electron microscope (SEM). The residual stress is assessed by the laser curvature method (LCM) and average X-ray strain (AXS) method. The surface hardness and young's modulus are measured by nanoindentation (NIP).

# Tuesday Morning, May 13, 2025

## Functional Thin Films and Surfaces

### Room Palm 5-6 - Session MB2-3-TuM

#### Thin Films for Electronic Devices III

**Moderators:** Dr. Jiri Houska, University of West Bohemia, Czechia, Dr. Ufuk Kilic, University of Nebraska - Lincoln, USA

8:00am **MB2-3-TuM-1 Morphological Effects and Impurity Levels on the High-Temperature Electrical Insulation of reactively sputtered AlN, Norma Salvadores Farran [norma.salvadores@tuwien.ac.at]**, Christian Doppler Laboratory for Surface Engineering of high-performance Components, TU Wien, Austria; *Tomasz Wojcik*, Christian Doppler Laboratory for Surface Engineering of high-performance Components, Austria; *Carmen Jerg*, Oerlikon Balzers, Oerlikon Surface Solutions AG, Liechtenstein; *Astrid Gies*, Oerlikon Balzers, Oerlikon Surface Solutions, Liechtenstein; *Jürgen Ramm*, Oerlikon Balzers, Oerlikon Surface Solutions AG, Liechtenstein; *Szilard Kolozsvári*, *Peter Polcik*, Plansee Composite Materials GmbH, Germany; *Jürgen Fleig*, *Tobias Huber*, Institute of Chemical Technologies and Analytics, TU Wien, Austria; *Eleni Ntemou*, *Daniel Primetzhofner*, Department of Physics and Astronomy, Uppsala University, Sweden; *Helmut Riedl*, Christian Doppler Laboratory for Surface Engineering of high-performance Components, TU Wien, Austria

Aluminum nitride-based ceramics are renowned for their insulating properties and high thermal conductivity. Consequently, these materials have been employed for various applications across a range of temperature conditions, with a particular focus on insulating purposes. Nevertheless, as the electrical conductivity is a thermally activated process, the mobility of charge carriers at elevated temperatures presents a significant challenge for insulating thin film materials.

The aim of this study is to explore the effect of morphological features (i.e. grain size or porosities) and impurities on hexagonal structured AlN thin films using different physical vapor deposition techniques. Given the difficulties associated with maintaining process stability during the deposition of insulating coatings, various reactive PVD techniques have been explored, including magnetron sputtering (DCMS), high-power pulsed magnetron sputtering (HIPIMS), and pulsed magnetron sputtering (PMS). All films were grown in an in-house developed magnetron sputter system using 3" Al targets in a mixed Ar/N<sub>2</sub> atmospheres. Phase formation has been examined using X-ray diffractometry (XRD), while the morphology was investigated in detail through scanning and transmission electron microscopy (SEM and TEM). The insulating behaviour of all films grown on metallic substrates was analysed using in-situ impedance spectroscopy across a temperature range from 400°C to 750°C – utilizing differently sized Ti/Pt lithography pads. The concentration of impurities, especially oxygen, was determined through the use of electron-induced X-ray emission spectroscopy (ERDA).

The results of the impedance measurements demonstrated a correlation between the electrical properties of the films and their morphological characteristics. The films grown via HIPIMS exhibited the highest morphological density and the greatest resistance over temperature. The samples deposited via PMS also demonstrated high electrical resistivity, although the values decreased at a certain level. It was not possible to determine the insulating properties of the films grown via DCMS, due to the presence of pinholes in the samples which also signifies a less dense morphology. Moreover, the influence of impurities as O<sub>2</sub> has a significant effect on reducing the electrical resistivity of the films.

8:20am **MB2-3-TuM-2 Pulsed Laser Deposition of Epitaxial Ti<sub>3</sub>AlC<sub>2</sub> MXene Thin Films on Al<sub>2</sub>O<sub>3</sub>(0001) Substrate, Pramod Kumar [pramod.kumar@surrey.ac.uk]**, Indian Institute of Technology Roorkee, India, University of Surrey, UK; *Ananya Bansal*, Indian Institute of Technology Roorkee, India; *Satheesh Krishnamurthy*, University of Surrey, UK; *Ramesh Chandra*, Indian Institute of Technology Roorkee, India

The newly explored two-dimensional transition metal carbides/nitrides, popularly known as MXene, are a new family of 2D materials with diverse applications. The coexistence of both ceramic and metallic nature, giving rise to exceptional mechanical, thermal, electrical, chemical properties and wide range of applications. Although several solution process techniques are there to deposit the MXene on substrate, but there is a need of high-quality epitaxial thin films for the above stated applications. In this work, Ti<sub>3</sub>C<sub>2</sub>T<sub>x</sub> MXene powder was synthesized using acid etching method. Epitaxial thin films were deposited on sapphire substrate (Al<sub>2</sub>O<sub>3</sub>, 0001) for the first time using pulse laser deposition (PLD) with Ti<sub>3</sub>C<sub>2</sub>T<sub>x</sub> pellet as the source. The X-ray diffractometer and morphology studies showed the epitaxial nature of the film with columnar growth. The electrical conductivity of the film

was found to be ~9421 S/cm. Resistance-temperature graph showed semiconductor-like behaviour for all the thickness tested. The thin film was also highly corrosive resistant in nature when tested with standard acidic, alkaline and saline solutions, which makes it ideal for anticorrosive coatings. Moreover, the p-n and n<sup>+</sup>-n devices on silicon substrate also resulted in a high switching ratio compared to other 2D materials. Our results demonstrate the potential of PLD as a novel method for the growth of epitaxial MXene thin films.

**Keywords:** MXene; pulsed laser deposition, epitaxial growth, corrosion resistance, switching diode

8:40am **MB2-3-TuM-3 Sputter Epitaxy of Predicted Dirac Semimetal MgTa<sub>2</sub>N<sub>3</sub>, Julien Baptiste [baptiste.julien@nrel.gov]**, Sage Bauers, National Renewable Energy Laboratory, USA

Ternary nitrides exhibit a wide range of functional properties, including superconductivity, magnetism, thermoelectricity, as well as topological properties. Among these, MgTa<sub>2</sub>N<sub>3</sub> (MTN) has been predicted to be a Dirac semimetal with an interesting potential for topological phases tunability. These unique electronic properties tied to its layered crystal structure. In this work, we synthesized epitaxial MTN thin films using reactive RF sputtering on c-cut sapphire substrates. The as-deposited films exhibit a (111)-oriented disordered rocksalt structure (rs-MTN), with a high-quality epitaxy, confirmed by X-ray diffraction (XRD) and rocking curve analysis. To transform the disordered rocksalt phase into the targeted layered phase (P6<sub>3</sub>/mcm), we annealed the precursor films in NH<sub>3</sub>. This method showed significant promise, successfully inducing the phase transformation at lower temperatures while maintaining film integrity, decent epitaxy and mitigating secondary phase formation. Structural analysis revealed that annealing the epi-film precursor under NH<sub>3</sub> yields to a phase transformation from the (111)-oriented rs-MTN into a c-axis textured layered MTN. Whereas the precursor rocksalt shows weak thermally activated conduction, preliminary electro and magneto-transport measurements on the layered MTN films reveal promising properties for a Dirac semimetal.

9:00am **MB2-3-TuM-4 Stabilization of Cubic or Orthorhombic Structure in Sputtered Tin Sulfide Thin Films for Thermoelectric Applications, Rémy Juliac, David Pilloud, Sylvie Migot, Axel Tahir, Jaafar Ghanbaja, Brigitte Vigolo, Nicolas Stein, Jean-François PIERSON [jean-francois.pierson@univ-lorraine.fr]**, IJL / CNRS / Univ. Lorraine, France

Tin sulfide (SnS) is a p-type semiconducting material with a band gap of approx. 1.3 eV. This compound is a promising material for thermoelectric applications, as an alternative to SnSe with the same crystallographic phase Pbnm but with no critical chemical elements [1]. Indeed SnS may crystallize in various structures, the orthorhombic phase (Hertzenbergite, α-SnS) being the most stable one. Other structures are also reported in the literature, such as the π-SnS one that crystallizes in a cubic structure (P2<sub>1</sub>3) [2].

In the present work, SnS thin films have been deposited using pulsed-DC magnetron sputtering of a tin sulfide target. The effect of the experimental deposition conditions (total pressure and substrate temperature) to the structure, the microstructure, the composition and the functional properties has been studied.

The deposition total pressure strongly influences the structure of SnS thin films. The use of low pressure (0.5 Pa) favors the growth of the metastable cubic phase. A columnar microstructure with stacking faults has been evidenced by high resolution transmission electron microscopy for the films deposited at low pressure. Deposition at high pressure (1.5 Pa) induces the synthesis of the orthorhombic phase, the most stable phase. At intermediate pressure, the films are biphased: cubic + orthorhombic. The electrical properties of the films are strongly influenced by their structure. On one hand, the orthorhombic phase exhibits a high electrical resistivity that strongly decreases the transport properties. On the other hand, the cubic phase shows a low electrical resistivity that improves the film properties.

The cubic structure being a metastable one, this phase is not obtained anymore when the films are deposited on a heated substrate. For temperature lower than 100 °C, the orthorhombic phase is the only one detected by X-ray diffraction and Raman spectroscopy. The film microstructure becomes porous when the SnS films are deposited at a temperature higher than the ambient one. Such a porous microstructure has a negative impact on the electrical properties and therefore the thermoelectric properties.

# Tuesday Morning, May 13, 2025

[1] Tan *et al.*, Thermoelectrics with earth abundant elements: low thermal conductivity and high thermopower in doped SnS, *J. Mater. Chem. A* 2 (2012) 17302

[2] Guc *et al.*, Structural and vibrational properties of  $\alpha$ - and  $\pi$ -SnS polymorphs for photovoltaic applications, *Acta Mater.* 183 (2020) 1

9:20am **MB2-3-TuM-5 Governing Metal-Insulator Transition in Ultra-Thin VO<sub>2</sub> Films by Surface Engineering**, *Andres Hofer [juhofer@ucsd.edu]*, UC San Diego, USA; *Ali Basaran*, ali.basaran@ga.com, USA; *Alexandre Pofelski*, Brookhaven National Laboratory, USA; *Damir Wang*, *Victor Palin*, UC San Diego, USA; *Yimei Zhu*, Brookhaven National Laboratory, USA; *Ivan Schuller*, UC San Diego, USA

The metal-insulator transition (MIT) in vanadium dioxide (VO<sub>2</sub>) thin films is strongly affected by grain size, thickness, and interfacial properties. Typically, the MIT is substantially suppressed for thickness below 50 nm when substrates like sapphire and silicon are used. While some studies have shown that films below 20 nm thickness can be achieved without compromising the integrity of the MIT, complex pre or post-growth processing is required. We show that engineering the substrate surface before the deposition facilitates the direct deposition of ultra-thin 15 nm thick films, exhibiting over four orders of resistance change across the MIT, which is comparable to its bulk counterpart. Our findings indicate that the interface between the thin film and the substrate is crucial to the structural evolution during the initial growth layer. With the appropriate surface preparation, the desired VO<sub>2</sub> MIT transition can be obtained independently of the substrate's crystalline orientation. Furthermore, we propose a novel approach to obtain high-quality MIT in ultra-thin VO<sub>2</sub> films by magnetron sputtering. Unlike traditional film depositions, we incorporate a pre-deposited 1.5 nm thick vanadium oxide buffer layer, thereby eliminating the need of different materials besides vanadium oxide or complex pre- and post-growth processing. We also demonstrate that our unique growth methodology improves the MIT of 25 nm VO<sub>2</sub> thin films on standard silicon substrates. This study reveals a compelling approach for the direct growth of ultrathin VO<sub>2</sub> films exhibiting a high-quality MIT, which is commonly accepted as unattainable on technologically essential substrates such as sapphire and silicon.

9:40am **MB2-3-TuM-6 Probing the Metal-Insulator Transition at YTiO<sub>3</sub>/LaTiO<sub>3</sub> Interfaces via Soft Chemical Synthesis**, *Alexandre Simoes [zirpoll.simoese@unesp.br]*, Rua Souza Oliveira, Brazil

In this study, we present optimized growth conditions for the fabrication of YTO/LTO heterostructured thin films using the polymeric precursor method combined with spin coating. The films were deposited on (100) Pt/TiO<sub>2</sub>/SiO<sub>2</sub>/Si substrates at 850 °C, resulting in films with a mean grain size of approximately 20.0 nm and a surface roughness of 5.50 nm. X-ray diffraction (XRD) analysis reveals that the YTO/LTO heterostructured films, synthesized via the polymeric precursor method, are free of secondary phases and exhibit a highly homogeneous morphology with no evidence of interaction between the sublayers. The piezoelectric and magnetic properties of the YTO/LTO heterostructures are attributed to modifications in the Ti-O-Ti bond lengths and tilting of the oxygen octahedra, which in turn affect the electrons in the *eg* orbitals of the Ti atoms in both layers. This hypothesis is further supported by Rietveld refinement and X-ray photoelectron spectroscopy (XPS) results, which suggest that the magnetic behavior of the films is not only due to the non-integer 3d occupancy of Ti ions at the surface but also the structural distortion of the YTO/LTO interface, influenced by the underlying silicon-coated platinum substrates. The films exhibit a high intrinsic dielectric constant ( $\epsilon_r \approx 70$ ) and a loss tangent ( $\tan \delta$ ) of approximately 0.41 at 1 kHz, indicating structural distortions along the TiO<sub>6</sub> octahedra in the basal plane of the film. A metal-to-insulator transition observed in the heterostructured films supports the idea of a competing mechanism, where strong electron orbital dynamics and multi-orbital electronic correlations govern the switching behavior between SET and RESET states. Additionally, the electrode area and switching cycles influence the film's properties, making it suitable for use as a correlated random access memory (CeRAM). In conclusion, we demonstrate that this simple, low-cost chemical process yields high-quality heterostructured films with promising potential for applications in non-volatile resistive memories.

10:00am **MB2-3-TuM-7 the Influence of Substrate Bias on Properties and Microstructure of High-Density Nanotwinned Ag Thin Films for High Power Device**, *Pinn-Chun Kuo [icanfire93@gmail.com]*, *Fan-Yi Ouyang*, Department of Engineering and System Science, National Tsing Hua University, Hsinchu, Taiwan

In response to the increasing demands for advanced technologies, including autonomous vehicles, self-driving systems, and artificial intelligence computing (AIPC), the concept of 3D-IC has emerged. Advanced packaging techniques that exhibit high reliability, superior properties, and the capacity to endure elevated operating temperatures are necessary to address these demands. The predominant technique employed is Cu-to-Cu direct bonding; however, this method necessitates high-temperature processing (>350°C), during which Cu tends to oxidation, thus requiring a high vacuum environment for execution. In contrast, Ag has demonstrated superior electrical and thermal conductivity, and great oxidation resistance, making it a promising candidate for metal-to-metal direct bonding techniques in atmospheric conditions.

This study successfully fabricated high-density nanotwinned Ag thin films on SiC substrates utilizing magnetron sputtering and investigated the impact of substrate bias on the microstructure and properties of the films. The results show that nanotwinned structures were found on all samples, characterized by a high density of nanotwins with an average twin spacing of 7 nm. The grain size remained relatively consistent as the substrate bias was increased from 0 V to -80 V; however, grain growth was observed when the substrate bias was further increased from -80 V to -120 V. In addition, the samples deposited without bias exhibit a resistivity of 2.17  $\mu\Omega \cdot \text{cm}$  and a hardness of 1.9 GPa, significantly surpassing that of bulk Ag (0.58GPa). When the substrate bias increases to -60 V, the resistivity further decreases to 1.96  $\mu\Omega \cdot \text{cm}$  and hardness reduce to 1.55 GPa. Moreover, a comparative analysis was also conducted on the microstructure and properties of nanotwinned Ag thin films deposited on Si and SiC substrates. The influence of the substrate bias on nanotwin formation of Ag thin films for both substrates is discussed and compared.

Key word : nanotwin, metal-to-metal direct bonding, advanced packaging techniques

10:20am **MB2-3-TuM-8 Electrodeposited Zirconium Titanate Thin Films: Structural, Magnetic, and Dielectric Properties for Spintronic Applications**, *Ifra Saeed [ifrasaeed1998@gmail.com]*, University of Milano Bicocca, Milan, Italy, Pakistan

Zirconium titanate (ZrTiO<sub>4</sub>) thin films have emerged as a cornerstone material in the advancement of spintronic devices, owing to their exceptional structural, magnetic, and dielectric properties [1,2]. This study harnesses a precise electrodeposition technique to fabricate ZrTiO<sub>4</sub> thin films, meticulously varying the molarity of electrolytes from 0.01M to 0.05M. X-ray diffraction (XRD) analysis reveals a transition from amorphous behavior at 0.01M to the formation of phase-pure, orthorhombic ZrTiO<sub>4</sub> at higher molarities, with a notable increase in crystallite size, indicative of enhanced phase stability. Vibrating Sample Magnetometer (VSM) measurements demonstrate a pronounced soft ferromagnetic behavior, with an impressive saturation magnetization peaking at 29 emu/cm<sup>3</sup> at 0.05M. Dielectric studies reveal a significant dielectric constant of 180 at  $\log f=2$  and a minimal tangent loss of 0.02 at 0.05M, showcasing superior dielectric performance. Cole-Cole plots further elucidate the dielectric properties, indicating dominant grain boundary resistance. The comprehensive analysis underscores the potential of ZrTiO<sub>4</sub> thin films as pivotal components in next-generation spintronic devices, offering unparalleled structural integrity, magnetic prowess, and dielectric efficiency [2].

These findings pave the way for the integration of ZrTiO<sub>4</sub> thin films in high-performance, energy-efficient spintronic applications, marking a significant leap forward in material science and device engineering.

## References:

Polliotto, V., Albanese, E., Livraghi, S., Agnoli, S., Pacchioni, G., & Giamello, E., (2020). Structural, electronic & photochemical properties of cerium doped zirconium titanate. *Catalysis today*, 340, 49-57.

Juma, A., Acik, I.O., Oluwabi, A.T., Mere, A., Mikli, V., Danilson, M., & Krunk, M., (2016). Zirconium doped TiO<sub>2</sub> thin films by chemical spray pyrolysis. *Applied surface science*, 387, 539-54.

# Tuesday Morning, May 13, 2025

10:40am **MB2-3-TuM-9 Revolutionizing High-Entropy MEMS with Superior Thermal Stability and Scalability, Li-Hui Tsao [nthu031239@gmail.com]**, National Tsing Hua University, Taiwan

Microelectromechanical Systems (MEMS) are essential in modern technology due to the increasing demand for multi-functional devices and Internet-of-Things (IoT) applications. In typical cases, the piezoelectric layers in MEMS serve as the main component for actuation, sensing, and transduction, which lead zirconate titanate (PZT) is widely used with high piezoelectricity. However, challenges, including poor thermal stability and degradation after long-term usage, have hindered its further development. Thus, it is crucial to introduce new material designs to solve these problems. In this work, a high-entropy material,  $\text{Pb}(\text{Mg}_a\text{Nb}_b\text{Ti}_c\text{Hf}_d\text{Zr}_e)\text{O}_3$  (PMNTHZO), is developed with colossal piezo-response and superior thermal stability. The sluggish diffusion effect diminishes the critical phase transformation and contributes to the robust properties at 523 K. Meanwhile, the integration with an 8-inch silicon substrate further suggests the massive potential for practical usage. In conclusion, this work demonstrates a novel high-entropy material with several intriguing physical properties, paving the way for next-generation electronic devices.

## Plasma and Vapor Deposition Processes Room Town & Country C - Session PP5-TuM

### Microfabrication Techniques with Lasers and Plasmas

**Moderators:** **Dr. Carles Corbella**, National Institute of Standards and Technology (NIST)/ University of Maryland, College Park, USA, **Dr. Valentina Dinca**, National Institute for Laser, Plasma, and Radiation Physics, Romania

8:00am **PP5-TuM-1 Synthesis of 2D Transition Metal Dichalcogenides Using Advanced ALD Cycle Schemes, Ageeth Bol [aabol@umich.edu]**, University of Michigan, Ann Arbor, USA **INVITED**

2D materials have been the focus of intense research in the last decade due to their unique physical properties. This presentation will highlight our recent progress on the large-area synthesis of two-dimensional transition metal chalcogenides for nanoelectronics using advanced plasma-enhanced atomic layer deposition cycle schemes. First, I will show how we can use advanced cycle schemes to deposit wafer-scale polycrystalline  $\text{MoS}_2$  thin films at very low temperatures down to 100 °C. We have identified the critical role of hydrogen during the plasma step in controlling the composition and properties of molybdenum sulfide films. By increasing the  $\text{H}_2/\text{H}_2\text{S}$  ratio or adding an extra hydrogen plasma step to our ALD process, we can deposit pure polycrystalline  $\text{MoS}_2$  films at temperatures as low as 100 °C. To the best of our knowledge, this represents the lowest temperature for crystalline  $\text{MoS}_2$  films prepared by any chemical gas-phase method.[1]

The most dominant methods for preparing  $\text{MoS}_2$  via ALD is to alternately expose a substrate to a metalorganic precursor and a hydrogen sulfide ( $\text{H}_2\text{S}$ ) or a plasma containing  $\text{H}_2\text{S}$ .  $\text{H}_2\text{S}$  is a corrosive, toxic, and flammable gas that is heavier than air, which makes it hazardous and expensive to store, install, and transport. Alternative sulfur precursors in the solid or liquid phase would be beneficial in terms of cost and safety and would require the installation of no additional hardware for most ALD reactors. In the second half of this contribution, the widely researched ALD process using bis(tert-butylimido)bis(dimethylamino)molybdenum(IV) ( $(^t\text{BuN})_2(\text{NMe}_2)_2\text{Mo}$ ) and  $\text{H}_2\text{S}$  plasma is compared to a novel ALD process using  $(^t\text{BuN})_2(\text{NMe}_2)_2\text{Mo}$ , hydrogen plasma, and di-tert-butyl disulfide (TBDS), which is an inexpensive, liquid-phase sulfur precursor.

8:40am **PP5-TuM-3 Nanocalorimetry for Plasma-Assisted Process Metrology in Semiconductor Microfabrication, J. Trey Diulus**, National Institute of Standards and Technology (NIST), USA; **Carles Corbella [carles.corbellaroca@nist.gov]**, National Institute of Standards and Technology (NIST)/ University of Maryland, College Park, USA; **Feng Yi, David LaVan, Berc Kalanyan, Mark McLean**, National Institute of Standards and Technology (NIST), USA; **Lakshmi Ravi Narayan**, National Institute of Standards and Technology (NIST)/ University of Maryland, College Park, USA; **William A. Osborn, James E. Maslar, Andrei Kolmakov**, National Institute of Standards and Technology (NIST), USA

New methods to monitor plasma processes in microelectronics industry, such as deposition, etching, and surface modification, require fine control of plasma parameters, basic plasma-surface interactions, and structural/chemical resolution. These challenges can be solved by implementing nanocalorimeter devices, which usually consist of a 100 nm-thin self-sustained silicon nitride membrane with lithographically defined

metallic structure as a resistive temperature sensor and heater. The lateral sizes of the sensor can range from micrometer to millimeter scales. The small size/thermal mass, functionalization versatility, and low wafer-scale fabrication cost of nanocalorimeters, enable their facile integration into any reactor chamber to meet specific plasma process requirements. Here, we report on pilot tests of NIST-microfabricated nanocalorimeters aimed to detect reactive radicals generated by hydrogen cold plasma at typical conditions for semiconductor manufacturing (75 W RF, 10-30 Pa). The setup consists of a parallel arrangement of one gold-coated active sensor and a second alumina-coated reference sensor. Au layer serves as a catalyst with known hydrogen recombination coefficient. Hence, the difference in heat of recombination reactions is detected comparatively by activated and reference nanocalorimeters. The inert, reference sensor enables discrimination against the incoming UV-vis radiation, and fluxes of ions and electrons, which constitute the major parasitic signals. The setup was successfully tested, and parameters such as sensitivity in radical detection ( $5 \times 10^{20} \text{ m}^{-2}\text{s}^{-1}$ ) and in radical density ( $10^{18} \text{ m}^{-3}$ ), and response time (sub-100 ms), are discussed within the framework of standard plasma diagnostic techniques. In conclusion, fast-scanning nanocalorimetry constitutes a promising platform for plasma process monitoring, whose flexibility enables its possible integration into other optical or electrical metrologies.

9:00am **PP5-TuM-4 Pulsed Laser Deposition for Energy Materials, Thomas Lippert [thomas.lippert@psi.ch]**, Paul Scherrer Institute, Switzerland **INVITED**

One of the material systems which we study are oxynitrides that are applied as photoanodes in photo-electrochemical water splitting. Shortcomings of this material class are a fast decay in activity over the first few electrochemical cycles and a decay on the long term. While the long-term decay is possibly related to a degradation of the material, i.e., a loss of nitrogen, the fast decay is not really understood, and therefore also no approach can be envisioned how to overcome this problem. We studied the fast decay of the material (and first approaches how to prevent this) by using thin films as model system. We could detect a surface modification, i.e., a change in density, by NR in the range of 3 nm, while XAS was utilized to analyze changes in oxidation state (order) for the different elements. A change of oxidation state of the A cation was detected, while the B cation (here for  $\text{LaTiO}_x\text{N}_y$ ), which is normally assumed to be the active site, undergoes local disordering. This surface modification reduces the overall water splitting activity, but we could identify a co-catalyst, which suppresses these modifications. We could also identify critical steps in the water splitting mechanisms, where during surface modifications the formation of  $\text{NO}_x$  competes with the oxygen evolution. Without highly defined, high quality PLD films it would have not been possible to utilize the large facilities, and therefore to identify (mitigate) the origins of activity decay of these oxynitrides for water splitting.

Fundamental understanding material properties and reactions of energy materials can often be very well studied by large facility techniques, e.g., at synchrotrons or neutron sources, as unique information can be obtained in this way. A number of these methods require the application of well-defined samples, controlling crystallinity, roughness to interface quality. These requirements can often be fulfilled by thin films. We apply pulsed laser deposition (PLD) to create these thin films to utilize complementary techniques, ranging from neutron reflectometry (NR) to grazing incidence X-ray absorption spectroscopy (GIXAS).

9:40am **PP5-TuM-6 Honeycomb Structured Pdms Microtopography Modulates In Vitro Cell Behaviour and Bacteria Growth, Valentina Dinca [valentina.dinca@infpr.ro]**, National Institute for Laser, Plasma, and Radiation Physics, Romania

Nowadays, the reduction of complications following breast implant surgery together with the enhancement of implant integration and performance through the modulation of the foreign body response (FBR) still represents a fundamental challenge. Therefore, influencing FBR by tailoring the material's physical characteristics can provide a significant outcome in implantology. While polydimethylsiloxane (PDMS) patterning on 2D substrates is a relatively established and available procedure, micropatterning multiscaled bioactive interfaces on a controlled large area has been more challenging. Therefore, in the present work, novel PDMS-based shell interfaces featuring honeycomb-like wells microtextures were designed and their effectiveness towards creating a pro-healing environment was investigated. The microtextures were achieved through replication on a large-scale using moulds obtained by an innovative laser-based 3D fabrication assisted by a grayscale masks process. By comparison to the smooth substrate, the honeycomb topography altered the fibroblasts' behaviour in terms of adhesion and morphology and reduced

the macrophages' inflammatory response. Additionally, the microstructured surface hindered the macrophage fusion process, and decreased the retention of Gram-positive and Gram-negative microbial strains. Overall, our study presents a novel approach for an attenuated in vitro FBR to silicone through the development of honeycomb like topography of prosthetic interfaces.

10:00am **PP5-TuM-7 Sputtering onto Liquids : From Nanoparticle Suspensions to Functional Polymer Composites**, **Stephanos Konstantinidis** [[stephanos.konstantinidis@umons.ac.be](mailto:stephanos.konstantinidis@umons.ac.be)], France - Emmanuelle Bol, Valentine Jauquet, Jeremy Odent, Anastasiya Sergievskaya, University of Mons, Belgium

Magnetron sputter deposition of metal atoms onto vacuum compatible liquids allows producing colloidal solutions of small metal nanoparticles (NPs) without any additional reducing or stabilizing reagents [1]. This presentation aims at presenting the results during which the process parameters were varied to study how the properties of the as-formed metal NPs are impacted. Parameters such as pressure, sputter power, and sputtering regime, e.g., DC or HiPIMS, were varied as well as the characteristics of the host liquid chemistry and viscosity. To monitor in space and time the behaviour of the NPs inside the liquid, in situ UV-Vis absorption spectrophotometry was implemented [2]. The temperature of the liquid was measured as well.

Our data show that the formation of a cloud of particles underneath the oil surface is usually observed while films form in the case of high viscosity liquids [3]. The effect of sputtering time and power, argon pressure, type of sputtering plasma (dcMS vs HiPIMS) were also studied taking castor oil, a vegetable liquid, as substrate. In this case, few - nm - in - diameter Au-NPs have a higher stability in the oil than Ag-NPs but secondary growth processes take place. Interestingly, HiPIMS promotes the formation of NPs larger than those obtained in dcMS mode [4]. Most recent experiments highlight the possibility of elaborating hydrogel / nanoparticle composites in a two step process by choosing an appropriate polymerizable host liquid [5]. Preliminary measures confirm that the as-obtained Ag-NPs / hydrogel composite can be used to detect mercury cations in aqueous solutions through color change.

Our data highlight that sputtering onto liquid allows for the synthesis of a few nm in diameter NPs but the plasma and liquid parameters matter. Ultimately, by choosing carefully the liquid host, it is possible to elaborate polymer / NP functional composites.

[1] A. Sergievskaya, A. Chauvin, S. Konstantinidis. *Beilstein J. Nanotechnol.* 13 (2022) 10–53.

[2] S. Konstantinidis, F.- E. Bol, G. Savorianakis, P. Umek, P., A. Sergievskaya, *Instr. Sci. Technol.* 52(2), 125–137.  
<https://doi.org/10.1080/10739149.2023.2223627>

[3] A. Sergievskaya, R. Absyl, A. Chauvin, K. Yusenko, J. Vesely, T. Godfroid, S. Konstantinidis, *Phys. Chem. Chem. Phys.* 25 (2023), 2803–2809.

[4] A. Sergievskaya, A. O'Reilly, H. Alem, J. De Winter, D. Cornil, J. Cornil, S. Konstantinidis, *Front. Nanotechnol.* 3 (2021) 57.

[5] V. Jauquet, Master Thesis, University of Mons (June 2023).

10:20am **PP5-TuM-8 Rapid Single Step Atmospheric Pressure Plasma Jet Deposition of a SERS Active Surface**, **Oliver S. J. Hagger** [[oliver.hagger.21@ucl.ac.uk](mailto:oliver.hagger.21@ucl.ac.uk)], M. Emre Sener, University College London, UK; Imran Khan, Defence Science Technology Laboratory, UK; Francis Lockwood Estrin, Ivan P. Parkin, Daren J. Caruana, University College London, UK

This research introduces an innovative approach for the rapid and efficient deposition of silver and gold using atmospheric pressure plasma jets (APPJs) to produce Surface-Enhanced Raman Spectroscopy (SERS) substrates and conductive tracks. Central to this method is the utilisation of plasma, which enables precise and uniform deposition of zerovalent metallic nanoparticles on a variety of substrates, including glass, ceramics, and metallic objects.

The APPJ technique takes advantage of the unique properties of non-thermal plasma, facilitating the reduction of metal ions to zerovalent metals in a single step. The highly energised electrons in the plasma allow intricate redox chemistry to occur. The flexibility of the APPJ method extends to a wide range of materials, including silver, gold, and binary metal mixtures. Furthermore, by mounting an APPJ on a 5-axis manifold enables metallic deposition on topologically complex surfaces, which has significant applications in analytical chemistry and materials science.

SERS substrates can be produced using an APPJ by depositing silver or gold directly onto topologically complex, multi-material surfaces without the

need for post-plasma treatment. The APPJ prints metallic islands with diameters of  $150 \pm 25 \mu\text{m}$  and heights of approximately 370 nm, spaced 500  $\mu\text{m}$  apart, forming the fundamental structure of the SERS substrates. With a production time of only 5 seconds per SERS substrate, our method offers a significantly faster alternative compared to other manufacturing techniques.

Our APPJ SERS substrates have undergone rigorous testing with various analytes, demonstrating performance on par with commercially available products. The substrates exhibit an impressive detection limit of 154 ppb when tested with 4-mercaptobenzoic acid.

Plasma-prepared substrates show significant gains with respect to the economical use of materials and the rapidity of the synthesis of the substrates. We showcase using the atmospheric pressure plasma jet method for synthesis and deposition as an integral part of an analytical device. This approach presents a key advantage for academic and industrial applications.

10:40am **PP5-TuM-9 Synergies Between Laser Technology and Thin Films for Advanced Functionalities**, **Sylvain Le Coultre** [[sylvain.lecoultre@bfh.ch](mailto:sylvain.lecoultre@bfh.ch)], BFH-ALPS, Switzerland

In our ALPS Institute, laser technology and thin-film deposition are combined with the objective to unlock novel functionalities in nanofabrication. As a first example, by leveraging precise and partial laser ablation within multilayer systems, we achieve high-resolution decorative effects with nanometric precision. Laser structuring on thin-film materials enables tuning of material properties, as seen on carbon allotropes. Additionally, laser processing can be employed to generate nanoparticles by ablating a target, which can then be embedded in coatings to form nanocomposites with enhanced mechanical, optical, or catalytic properties. This presentation will explore a few specific applications and case studies that highlight the advantages of integrating laser processing with thin-film technologies.

# Tuesday Morning, May 13, 2025

## Exhibitors Keynote Lecture

Room Town & Country A - Session EX-TuM

## Exhibitors Keynote Lecture

Moderator: Prof. Johanna Rosen, Linköping University, Sweden

11:00am EX-TuM-1 **Surface Engineering and Rocket Science –Surface Engineering Solutions to Protect Spacecrafts and Ground Infrastructure Against Terrestrial and “Extraterrestrial” Harsh Environments**, *Juan Flores Preciado* [[Juan.FloresPreciado@spacex.com](mailto:Juan.FloresPreciado@spacex.com)], SpaceX, USA **INVITED**

Spacecrafts (rockets, probes, satellites) and ground support equipment (launch pads) are constantly exposed to harsh environments. From a corrosive and aggressive climate to high temperature engine plumes. Launch pad infrastructure (particularly materials surfaces), must be protected to maintain mission’s reliability and safety. Satellites and other spacecrafts are exposed to even harsher environments such as: ultrahigh vacuum, atomic oxygen, thermal cycles, radiation and debris impacts.

Understanding how harsh environments affect the properties of materials and the functionality of complex mechanisms is crucial to advance space exploration and return humans to the moon and beyond. In this talk, we will discuss how these environments can be characterize, how they can affect the integrity of structural materials and even modify tribological and corrosion mechanisms. Protective solutions based on surface engineering technologies will be presented and the importance of preparing the next generation of space materials engineers will be highlighted.



# Tuesday Afternoon, May 13, 2025

## Surface Engineering - Applied Research and Industrial Applications

### Room Palm 1-2 - Session IA3-TuA

#### Innovative Surface Engineering for Advanced Cutting and Forming Tool Applications

**Moderators:** Markus Esselbach, Oerlikon Balzer, Liechtenstein, Dr. Christoph Schiffrers, CemeCon AG, Germany

1:40pm **IA3-TuA-1 Natural Rock Star: PVD-Functionalizing of Nature-Derived Materials for Cutting Applications**, *Wolfgang Tillmann, Dominic Graf [dominic.graf@tu-dortmund.de], Nelson Filipe Lopes Dias, TU Dortmund University, Germany; Bernd Breidenstein, Berend Denkena, Benjamin Bergmann, Hilke Petersen, Leibniz Universität Hannover, Germany*  
The manufacturing process of traditional cutting materials such as cemented carbide involves significant energy consumption and costly raw materials that are often linked to environmental harm during extraction. To address these concerns, there is a growing demand for developing sustainable cutting materials. In this context, natural materials are both environmentally friendly and abundant. Natural rocks, in particular, are promising due to their hardness, which typically ranges from 8 to 16 GPa depending on the rock type. The suitability of these natural materials for machining can be enhanced via functionalization of the surface properties by applying a protective thin film using physical vapor deposition (PVD) technology.

Preliminary studies show the suitability of various rock types as cutting material. Cutting inserts are crafted from these natural rocks and subsequently ground. A TiN thin film is deposited onto the various natural rock inserts using a magnetron sputtering process. The resulting TiN thin films crystallize in a cubic structure on all rock types. The obtained hardness values are comparable to TiN thin films grown on tool steel. In contrast to a polished surface, a ground surface of the natural rocks promotes good adhesion of the TiN thin films. To assess the cutting performance and wear characteristics of PVD-coated natural rocks, turning tests are conducted using the aluminum alloy Al7075. The TiN thin film significantly enhances wear resistance, thus extending the service life of the cutting inserts. Additionally, it is observed that the distinct material properties of the natural rocks significantly affect the wear behavior. Rock types with a more homogeneous structure demonstrate improved wear resistance over extended cutting lengths.

To analyze the effect of the substrate on the TiN thin film adhesion three different glass substrates were chosen as surrogates for natural rocks. Glasses are particularly suitable as surrogates because of their similar SiO<sub>2</sub> content. The investigations reveal a strong influence of the stress state on the adhesion, as TiN on window glass shows weaker adhesion due to high compressive residual stresses. The possible adaptation of thin film design strategies developed for glass onto natural rock surfaces is evaluated. The utilization of a PVD-coated natural rock emerges as a promising concept for broadening the spectrum of cutting materials and promoting sustainability in their manufacturing. A tailored adjustment of the grinding process for cutting inserts with an adapted thin film design is anticipated to further elevate the cutting performance of natural rock inserts.

2:00pm **IA3-TuA-2 Properties and Metal Cutting Performance of High Entropy Nitride (HEN) and HEN-MN Coatings**, *Abhijit Roy [abhijit.roy@kennametal.com], Brittany Macshane, Kennametal Inc., 1600 Technology Way, Latrobe, PA 15650, USA; Joern Kohlscheen, Kennametal GmbH, Altweiherstr. 27, 91320 Ebermannstadt, Germany; Dev Banerjee, Kennametal Inc., 1600 Technology Way, Latrobe, PA 15650, USA*

Hard and wear protective coatings are normally deposited on cutting tools to improve their metal cutting performance and lifetime. These coatings, depending on metal cutting conditions and workpiece materials, often require specific properties which are difficult to achieve by conventional (using binary, ternary or quaternary) nitride coatings. High entropy nitride (HEN) coatings, with disordered multi-cations sublattice and ordered anionic sublattice, show many remarkable properties including high thermal stability induced by entropy stabilization, high hardness, and fracture toughness originating from multiple-elemental lattice distortions and impeded dislocations, as well as excellent corrosion resistance caused by sluggish diffusion. Moreover, multilayer and superlattices of HEN containing layers allow an additional degree of design-flexibility to improve fracture toughness and other properties. This work investigated crystalline structure and morphology, residual stresses, adhesion, mechanical properties and metal cutting performance of cathodic arc plasma deposited thin films of HEN and HEN-MN. The HEN target contains five different

elements from groups IV, V and VI of the periodic table and the target for MN contains a single transition metal element. X-ray diffraction results indicate presence of two NaCl type FCC phases for both the single layer HEN and multilayer HEN-MN coatings. The residual compressive stress value of the films does not change much with increase in deposition bias voltages. Nanohardness values of the films were found to be in the range of 32-35 GPa and bulk modulus values of the multilayered HEN-MN coatings were slightly higher than the single layered HEN coatings. No correlation was found between the scratch adhesion or indent adhesion strength and substrate bias voltages. Scanning electron microscopy (SEM) images of the coatings show deposition of dense HEN coatings and formations of nanolayers in case of HEN-MN coatings. The elemental analysis using energy dispersive x-ray (SEM-EDX) indicates formation of nitrogen deficient sub-stoichiometric nitrides for both the single layer HEN and multilayer HEN-MN coatings. Turning tests with coated carbide inserts using IN718 as workpiece material showed promising tool life compared to conventional AlTiN coatings.

2:20pm **IA3-TuA-3 Surface Engineering of AlCrN-Coated Carbide through Laser Texturing for Performance Enhancement**, *Yassmin Seid Ahmed [yassminm66@gmail.com], KFUPM, Saudi Arabia*

Utilization of coating and surface texturing techniques combines to great effect to further enhance the overall performance of carbide surfaces. For these materials, adhesion is most critical in defining the performance of the coating. Poor adhesion and coating quality can lead to eventual failure. With cemented carbide being one of the materials of concern, LST has gained much attention as having superior mean coating adhesion. However, the effects of the combined processes of coating followed by texturing and texturing followed by coating and their interactions remain poorly understood.

This study analyzes micro-structured coated cemented carbide surfaces prepared from varying processes and property conditions while examining their surface characteristics and friction performance. The performance of the substrates, which had undergone surface treatments followed by ball-on-disk tests, was then evaluated and compared. The coated surface sample, where surface texturing was done first and coating applied afterward (AC), showed better microhardness, more refined microstructures, and better wear resistance than the coating surface first, followed by surface texturing (BC). Although the sample coated was found to show superior hardness values across the board, the AC sample displayed more favourable results in other areas. A prime example is that the AC sample was 12% more microhard than the coating sample, although the overall hardness was reduced by 3%, coupled with a reduction in friction force by 8%.

It creates an insightful mark to realize that the order of application of the texturing and coating processes would bear significant relevance in affecting the final performance of the material. This study now stresses that enhanced adhesion and wear resistance were found in the coating substrate wherein the texturing technique was performed first and then coated (AC) as being very consistent in proposing that these combined techniques can make way into producing contributions toward more durable and effective coatings for industrial usages.

2:40pm **IA3-TuA-4 Advanced Cyclic Load Resistance of AlXN Coatings for Metal Forming Applications**, *Simon Evertz [simon.evertz@eifeler-vacotec.com], Stefan A. Glatz, Tobias Oellers, Markus Schenkel, voestalpine eifeler Vacotec GmbH, Germany*

Cyclic loading is critical for the industrial application of PVD coatings, especially in metal forming applications. With the increasing interest in using thin super-high-strength steel sheets for forming bodies/parts with reduced component weight, light-weight design and less fuel consumption could be achieved for example in automotive industry. Consequently, the loads become more demanding on molding dies and therewith protective coatings. These applications require coatings resistant to cyclic mechanical and/or thermal loading and fatigue. The specific structure of voestalpine eifeler's Duplex-VARIANTIC® -1400-plus with its multiple hard material AlXN layers overcomes the very demanding requirements in terms of strength, hot-hardness, and load-bearing capacity in such metal forming applications and outperforms other commercially used hard nitride protective coatings. This property profile makes voestalpine eifeler's Duplex-VARIANTIC® -1400-plus the optimal solution for metal forming high-strength and advanced high-strength steel sheets.

# Tuesday Afternoon, May 13, 2025

## Protective and High-temperature Coatings

### Room Town & Country A - Session MA1-2-TuA

#### Coatings to Resist High-temperature Oxidation, Corrosion, and Fouling II

**Moderators:** Dr. Vladislav Kolarik, Fraunhofer Institute for Chemical Technology ICT, Germany, Dr. Eli Ross, Pratt & Whitney, USA

1:40pm **MA1-2-TuA-1 The Role of Circular Economy in Materials Science: Thermal Spray and Laser Coatings Originated from Abandoned Scrap for Protectiveness of Metallic Alloys at High Temperature, Tomasz Dudziak [tomasz.dudziak@kit.lukasiewicz.gov.pl], Filip Kateusz, Adelajda Polkowska, Lukasiewicz - Krakow Institute of Technology, Poland INVITED**

The role of recycling is growing from year to year, circular economy is a new trend that reach material science and technology. The number of wastes that are recycled globally is enormous and still is growing. To protect natural resources and natural environment the new processes that reduce impact on environment are highly seekable. In material science from years, Fe based scrap was introduced to a fresh melted iron ore to develop new grades, this process is still in use, since iron scrap is widely present. Often the metallic waste is present in the form of low grade steels as C45 or similar where mostly Fe is present with no additional elements. However in advanced steels i.e. stainless steels, many of valuable elements exists, i.e. Cr. The element that is responsible for protective scale formation at high temperatures (up to 800 °C) leading to resistance of the exposed material in aggressive environments. The project: Additive manufacturing and Projected Parts by using Recycled Powder from scraps, with acronym RePoParts shows the answer how to process the waste according to circular economy, recycling process of steel wastes containing at least 12 wt.% Cr to fabricate a fine grain powder for Selective Laser Melting (SLM) process, a powder that helps develop new grades of coatings against wear, high temperature degradation. The work shows the data related to protectiveness of metallic alloys at high temperature when coatings from recycling process is used.

2:20pm **MA1-2-TuA-3 Advanced Chemical Vapor Deposition Technology for High Temperature Applications, Natasa Djordjevic [natasa.djordjevic@ihi-bernex.com], Anne Zhang, Hristo Strakov, IHI Bernex AG, Switzerland**

Recent research explores the potential of Chemical Vapor Infiltration (CVI) and Chemical Vapor Aluminizing (CVA) technologies to produce advanced coating solutions for high temperature applications and materials with enhanced performance at demanding conditions.

CVI is increasingly used for establishing coating solutions for fiber-reinforced composites, enabling deposition of interface layers or infiltration of ceramic matrices with different precursors at elevated temperatures. The technique allows production of materials with greatly enhanced properties such as thermal stability, mechanical strength, oxidation and corrosion resistance.

On the other hand, CVA is a modern advanced process for applying diffusion coatings on metallic-based turbine blades and vanes in the hot section of aero- and land-based turbines against oxidation and corrosion. The CVA process is capable of controlled alloying the coating with additional elements by using metal chlorides and tight control of the coating composition and on this way increasing the life time of such components.

This work will highlight the latest developments of different coating technology solutions for high temperature applications, including improvements in precursor chemistry, reaction kinetics, stoichiometry and process control. Emphasis will be placed on the challenges related to maintaining uniformity and quality of deposition in different geometries and the influence of the coating equipment in order to precise control the parameters.

2:40pm **MA1-2-TuA-4 Magnetron Sputtering of Advanced Multi-Elemental Aluminide Thin Films: Impact of Alloying with Refractory Metals and Cu, Vincet Ott [vincet.ott@kit.edu], Michael Dürrschnabel, Karlsruhe Institute of Technology (KIT), Germany; Tomasz Wojcik, Paul Mayrhofer, Helmut Riedl, TU Wien, Austria; Sven Ulrich, Michael Stüber, Karlsruhe Institute of Technology (KIT), Germany**

Intermetallic phases in the CsCl structure have promising properties for use in highly demanding environments. Major limitations are the synthesis of single-phase materials on one hand and the brittle failure at room temperature on the other hand. The RuAl phase in B2 structure is an outstanding candidate of this material class due to its ductile behavior at

room temperature. A promising route for the synthesis as a thin-film material is offered by nanoscale multilayer coatings from which the targeted phase can be synthesized by a subsequent heat treatment. To further improve the resulting thin films properties and to reduce the Ru content, alloying can help to increase the maximum service temperature, improve ductility and at the same time maintain good oxidation resistance.

To achieve this goal, thermally activated phase formation in nanoscale multilayer precursors is used to obtain single phase multi elemental aluminides with tailored properties. The partial substitution of Ru with the stable oxide forming alloying element Cr or with the Ru affine element Hf, while maintaining the Al content at 50 at%, is aiming at improving the oxidation resistance and mechanical properties. On the other hand, alloying the RuAl-phase with Cu shows the extent to which properties are influenced by the introduction of a ductile material. In-situ HT-XRD is used to observe the phase formation during the heat treatment of single phase (Ru, Me)Al (RM=Cr, Hf, Cu) and the resulting microstructure, characterized by TEM-methods, is linked to their mechanical and oxidative properties.

3:00pm **MA1-2-TuA-5 Oxygen Concentration Governs High-Temperature Oxidation Behavior of (Cr<sub>0.5</sub>Al<sub>0.5</sub>)(O<sub>v</sub>N<sub>1-v</sub>) Thin Films, Pauline Kümmerl [kummerl@mch.rwth-aachen.de], Felix Leinenbach, Janani Ramesh, RWTH Aachen University, Germany; Daniel Primetzhofer, Uppsala University, Sweden; Marcus Hans, Jochen M. Schneider, RWTH Aachen University, Germany**

In (TM,Al)(O,N) (TM = Ti, V) thin films, the addition of oxygen enhances the thermal stability as for the decomposition into the hexagonal and cubic phases mobility on the metal and nonmetal sublattices is required, while for (TM,Al)N decomposition the activation of diffusion on the metal sublattice is sufficient. Little is known about the oxidation resistance of (TM,Al)(O,N) thin films; thus a systematic study of the influence of the O concentration in (Cr,Al)(O,N) on the oxidation resistance and oxide scale formation is presented here.

(Cr<sub>0.5</sub>Al<sub>0.5</sub>)(O<sub>v</sub>N<sub>1-v</sub>) thin films were grown by reactive high power pulsed magnetron sputtering where the O content was systematically varied through adjustment of the O<sub>2</sub> partial pressure leading to compositions of (Cr<sub>0.50</sub>Al<sub>0.50</sub>)<sub>0.49</sub>N<sub>0.51</sub>, (Cr<sub>0.48</sub>Al<sub>0.52</sub>)<sub>0.48</sub>(O<sub>0.15</sub>N<sub>0.85</sub>)<sub>0.52</sub>, and (Cr<sub>0.44</sub>Al<sub>0.56</sub>)<sub>0.46</sub>(O<sub>0.40</sub>N<sub>0.60</sub>)<sub>0.54</sub>. The oxidation behavior was investigated as a function of the O concentration at 1000 °C, 1100 °C, and 1200 °C for up to 16 h.

During oxidation an Al-rich oxide scale is formed. Between the (Cr<sub>0.5</sub>Al<sub>0.5</sub>)(O<sub>v</sub>N<sub>1-v</sub>) thin films and the scale, the formation of an Al-depleted and O-enriched region is observed whereby the geometric extent and the level of porosity were strongly time and temperature dependent. At 1100 °C after 16 hours of oxidation the oxide scale thickness on (Cr<sub>0.48</sub>Al<sub>0.52</sub>)<sub>0.48</sub>(O<sub>0.15</sub>N<sub>0.85</sub>)<sub>0.52</sub> was with 369± 48 nm significantly smaller than the 513± 96 nm and 462± 53 nm thick scale layers measured on (Cr<sub>0.50</sub>Al<sub>0.50</sub>)<sub>0.49</sub>N<sub>0.51</sub> and (Cr<sub>0.44</sub>Al<sub>0.56</sub>)<sub>0.46</sub>(O<sub>0.40</sub>N<sub>0.60</sub>)<sub>0.54</sub>, respectively. Furthermore, chemical environment dependent DFT calculations are performed to determine the species specific energy requirements for vacancy formation and mass transport in an effort to elucidate the time and temperature dependent oxidation behavior.

## Protective and High-temperature Coatings

### Room Town & Country A - Session MA2-1-TuA

#### Thermal and Environmental Barrier Coatings I

**Moderators:** Dr. Sabine Faulhaber, University of California, San Diego, USA, Prof. Fernando Pedraza, La Rochelle University, Laboratory LaSIE, France, Francisco Javier Perez Trujillo, Universidad Complutense de Madrid, Spain, Gustavo García-Martín, REP-Energy Solutions, Spain

4:00pm **MA2-1-TuA-8 Multicomponent Rare Earth Oxide Coatings for Refractory Alloys, Rachel Rosner, Kristyn Ardrey, Will Riffe, Alejandra Salanova, Prasanna Balachandran, Bi-Cheng Zhou, Carolina Tallon, Jonathan Laurer, Jon Ihlefeld, Patrick Hopkins, Sandamal Witharamage, Elizabeth Opila [opila@virginia.edu], University of Virginia, USA INVITED**

Rare earth oxide (RE<sub>2</sub>O<sub>3</sub>) exhibit three crystal structures across the lanthanide series: hexagonal, monoclinic, and cubic, with all showing exceptionally high-melting temperatures (>2100°C) and excellent thermochemical stability. The cubic RE<sub>2</sub>O<sub>3</sub>, dysprosium through lutetium oxides, have isotropic thermal expansion with a reasonable match to Nb, making them suitable high temperature coatings for oxidation-prone refractory alloys. Multicomponent rare-earth oxides (MRO) allow the additional ability to target and optimize thermal expansion, resistance to

# Tuesday Afternoon, May 13, 2025

molten deposits, and especially thermal conductivity, enabling their use as thermal/environmental barrier coatings (T/EBCs) in high-temperature, reactive environments such as turbine engines. Thermal conductivity of MROs has been shown to decrease with mixtures of  $\text{RE}_2\text{O}_3$  with increasing mass and size variation. The larger, lighter, non-cubic lanthanide oxides, lanthanum through terbium oxides, mixed in a majority MRO cubic phase in non-equimolar proportions will precipitate as second phases once their solubility limit in the cubic  $\text{RE}_2\text{O}_3$  is exceeded, enabling further reductions in thermal conductivity. In this work, MRO compositions are systematically varied to aid in achieving targeted thermal conductivity, thermal expansion, and resistance to molten deposits. Powder mixtures were combined, ball milled, and sintered via spark plasma sintering. Room temperature thermal conductivity was measured using the laser-based time domain thermoreflectance method. Thermal expansion was determined by dilatometry or lattice parameter measurements as a function of temperature. Resistance to molten  $\text{CaO-MgO-Al}_2\text{O}_3\text{-SiO}_2$  was quantified after exposure at temperatures of 1300-1500°C for times between 1 and 96h. Here we evaluate whether a single layer MRO will meet all design requirements for a (T/EBC) enabling cost efficient coating synthesis or whether additional coating layers are required to achieve adherent, protective properties for hot section turbine engine component applications.

4:40pm **MA2-1-TuA-10 Characterization of the Environmental Barrier Coatings with Al-containing dopants exposed to Steam Environments**, **Michael Lance** [[lancem@ornl.gov](mailto:lancem@ornl.gov)], **Mackenzie Ridley**, Oak Ridge National Laboratory, USA

SiC ceramic matrix composites (CMCs) are desired for use in combustion environments to achieve higher turbine operating temperatures, although CMCs require environmental barrier coatings (EBCs) for protection from the gas environment. EBC systems are known to primarily fail through coating delamination via growth of a thermally grown oxide (TGO) at the EBC – silicon bond coating interface especially when exposed to steam, which accelerates the TGO growth rate. The TGO undergoes a phase transformation during thermal cycling, which results in stresses that encourages EBC spallation. Yb-silicate EBCs with mullite and yttrium aluminum garnet (YAG) dopant additions were deposited on SiC substrates with a Si intermediate bond coating and exposed to thermal cycling in steam at 1350 °C. The impact of Al dopant additions on the TGO growth rate and the  $\text{SiO}_2$  phase transformation were assessed. Annealing prior to steam exposure was found to significantly change the course of TGO growth with unannealed samples forming an amorphous Si-Al-Y glassy phase at short cycling durations. The composition of the EBC, TGO and Si bond coating were assessed with wavelength dispersive x-ray spectroscopy (WDS) using an electron probe microanalyzer (EPMA). In addition, photo-stimulated luminescence spectroscopy (PSLS) and Raman spectroscopy was used to characterize the composition and stress in the coating phases.

## Protective and High-temperature Coatings Room Palm 3-4 - Session MA3-2-TuA

### Hard and Nanostructured Coatings II

**Moderators:** **Dr. Rainer Hahn**, TU Wien, Institute of Materials Science and Technology, Austria, **Dr. Stanislav Haviar**, University of West Bohemia, Czechia, **Dr. Fan-Yi Ouyang**, National Tsing Hua University, Taiwan

1:40pm **MA3-2-TuA-1 Designing Nanocrystalline Alloys and Compounds: Unraveling Compositional and Microstructural Pathways to Exceptional Properties**, **Rostislav Daniel** [[rostislav.daniel@unileoben.ac.at](mailto:rostislav.daniel@unileoben.ac.at)], **Michal Zitek**, **Tobias Ziegelwanger**, Montanuniversität Leoben, Austria; **Ranming Niu**, The University of Sydney, Australia; **Edoardo Rossi**, **Marco Sebastiani**, Università degli studi Roma Tre, Italy; **Petr Zeman**, **Stanislav Haviar**, University of West Bohemia, NTIS, Czechia; **Jozef Keckes**, Montanuniversität Leoben, Austria

**INVITED**

This talk presents advanced methods in combinatorial synthesis and microstructural design to achieve extraordinary properties in multielement alloys and layered coatings. Using the  $\text{CrCuTiW}$  alloy system as a primary example, we demonstrate how large compositional variations and the limited miscibility between elements lead to diverse self-assembled multicomponent phases, combining solid solutions, nanocomposites, and metallic glasses. These structures exhibit unexpected combinations of hardness and elastic modulus, demonstrating the potential for unique property tailoring.

In a second example, a cross-sectional combinatorial synthesis of nanostructured  $\text{CrMnFeCoNi}$  alloy is employed to address the thermal stability of this metastable alloy. This approach enables an in-depth analysis of segregation kinetics in the primary phase at moderate temperatures (50-450°C) resulting in the formation of a variety of coexisting phases that enhance alloy strength while maintaining ductility and fracture toughness. This approach demonstrates its capability to provide insights into the thermal behavior of complex, metastable microstructures and allows for controlled property enhancement.

Additionally, the talk emphasizes a bio-inspired approach to compositional and microstructural design within a layered Zr-Cu-N system, where antibacterial properties are combined with enhanced fracture toughness and stress resistance. These multifunctional coatings represent a new class of sustainable materials, suitable for both hard and smart coating applications.

Our methodology integrates advanced multi-technique characterization tools, including 2D (XRD, EDX) and 3D (nano-XRD, nanoindentation) mapping capabilities, combined with transmission electron microscopy and atom probe tomography. These techniques facilitate a rapid assessment of processing-structure-property relationships in these novel nanostructured alloys, bridging the gap between theoretical predictions and practical applications. Together, these methodologies provide a pathway to the design of next-generation multifunctional layered architectures, tailored down to the nanoscale, to enable exceptional mechanical and functional properties and robust thermal stability.

2:20pm **MA3-2-TuA-3 Evolution of the Pulsed-DC Powder-Pack Boriding Process: Exploring Low-Temperature Boride Layer Formation**, **J.L. Rosales-Lopez** [[jrosales1401@alumno.ipn.mx](mailto:jrosales1401@alumno.ipn.mx)], **M. Olivares-Luna**, **L.E. Castillo-Vela**, **I.E. Campos-Silva**, Instituto Politécnico Nacional, Mexico

This study rigorously investigates the transformative potential of the Pulsed-DC Powder-Pack Boriding (PDCPB) process to catalyze boride layer formation on AISI H13 steel at remarkably reduced temperatures (600°C, 650°C, and 700°C) under substantial current densities ( $\sim 952\text{mA}\cdot\text{cm}^{-2}$ ) and significantly minimized exposure times of 1800s, 2700s, and 3600s. Enabled by the implementation of a custom high-capacity power supply, this innovation generates the essential electric field to support boriding at unprecedented low temperatures. Traditionally, achieving similar results in AISI H13 required treatments at temperatures exceeding 900°C with exposure times of at least 14400s, underscoring the extraordinary advancement represented by this approach.

Through meticulous microstructural and physicochemical analyses using SEM-EDS and XRD, the study reveals substantial findings: at a mere 600°C, PDCPB successfully produced dense, biphasic  $\text{FeB}+\text{Fe}_2\text{B}$  layers with thicknesses ranging from  $\sim 8\mu\text{m}$  to  $\sim 17\mu\text{m}$ , uniformly distributed across the sample surfaces. Remarkably, and contrary to established reports on borided AISI H13, the substrate retained its  $\alpha$ -phase microstructure without transformation to the  $\alpha'$ -phase, and the interface between the boride layer and substrate remained free of any diffusion zone. This breakthrough not only introduces significant commercial scalability for low-temperature boriding but also opens possibilities for further innovations, potentially achieving effective boriding near the 530°C threshold. The insights presented mark a seminal advancement in boriding technology, with vast implications for industrial applications and the future of materials engineering.

2:40pm **MA3-2-TuA-4 Three-Fold Superstructured HfN/HfAlN Multilayers**, **Marcus Lorentzon** [[marcus.lorentzon@liu.se](mailto:marcus.lorentzon@liu.se)], Linköping University, IFM, Thin Film Physics Division, Sweden; **Rainer Hahn**, TU Wien, Institute of Materials Science and Technology, Austria; **Lars Hultman**, **Justinas Palisaitis**, Linköping University, IFM, Thin Film Physics Division, Sweden; **Johanna Rosen**, Linköping University, IFM, Materials Design Division, Sweden; **Grzegorz Greczynski**, **Jens Birch**, **Naureen Ghafoor**, Linköping University, IFM, Thin Film Physics Division, Sweden

Brittleness and poor fracture toughness are limiting factors for the application of hard protective coatings. To resolve these issues, we explore multilayer superlattice (SL) coating designs based on  $\text{HfN}_{1.33}$  and  $\text{Hf}_{0.76}\text{Al}_{0.24}\text{N}_{1.15}$ . We achieve high-quality single-crystal films and superlattices with superior mechanical characteristics by epitaxial growth on  $\text{MgO}(001)$  substrates using ion-assisted reactive magnetron sputtering at high temperatures.

The structure and properties of monolithic single-crystal  $\text{HfN}_{1.33}$  and  $\text{Hf}_{0.76}\text{Al}_{0.24}\text{N}_{1.15}$  are studied to evaluate the SL-coating performance. Overstoichiometric  $\text{HfN}_y$  exhibits metal-like ductility in micropillar

# Tuesday Afternoon, May 13, 2025

compression tests, with easy dislocation nucleation and movement along multiple {111}<110> slip systems, which results in significant strain hardening and a doubled ultimate strength at 17% strain, compared to the yield point at 2%. The improved ductility is attributed to point defects—vacancies and nitrogen interstitials—forming a checkerboard superstructure of hyper-overstoichiometric and near-pristine domains. In contrast, HfAlN shows improved hardness and yield strength in pillar compression, however, it fails by strain-burst with fractures on the {110}<110> slip system. These properties stem from strain fields, pinning dislocations, which develop between coherent Hf- and Al-rich nanodomains, formed by surface-initiated spinodal decomposition. In addition, the domains similarly self-organize into a checkerboard superstructure.

Thus, by combining overstoichiometric HfN<sub>1.33</sub> and Hf<sub>0.76</sub>Al<sub>0.24</sub>N<sub>1.15</sub> in SL designs with equal layer thicknesses but varying bilayer period of 20 nm, 10 nm, and 6 nm, fascinating three-fold superstructured SLs are created by checkerboard superstructuring in 1) the HfN layers and 2) the HfAlN layers, as well as 3) the multilayer structure itself. While the interfaces provide dislocation pinning to maintain an equally high hardness as Hf<sub>0.76</sub>Al<sub>0.24</sub>N<sub>1.15</sub>, about 20% higher than HfN<sub>1.33</sub>, other multilayer effects and inherent ductility of HfN<sub>1.33</sub> enhance the toughness through coherency strains, crack-tip blunting or deflection. The SLs are analyzed using X-ray diffraction, reciprocal space maps, high-resolution z-contrast scanning transmission electron microscopy, selected area electron diffraction, nanoindentation, and micropillar compression tests. Post-mortem imaging of the pillars reveals the underlying plastic deformation mechanisms. Superlattice effects enhance mechanical performance, combining properties of both materials for coatings with high hardness and improved toughness, ideal for advanced protective applications.

3:00pm **MA3-2-TuA-5 Effects of Different Interlayer Layers on Residual Stress Relief in  $\gamma$ -MoN/Ti and  $\gamma$ -MoN/Mo Thin Films, Ding-Hsuan Yang [dave35116@gmail.com], Jia-Hong Huang, National Tsing Hua University, Taiwan**

Transition metal nitrides have been widely used by their outstanding properties such as wear resistance, high corrosion resistance and excellent mechanical properties.  $\gamma$ -Mo<sub>2</sub>N coating is becoming more popular in terms of high temperature tribological properties, which results from the formation of Magnéli oxide phase. However, residual stress from the deposition of the hard coatings is a common issue that may decrease the adhesion strength and fracture toughness. Adding a metal interlayer is a convenient method to relieve the residual stress of hard coatings. The purpose of this research was to compare the behavior of stress relief by using different metal interlayers, Ti and Mo. In this study, the Ti and Mo interlayers were deposited by DC-unbalanced magnetron sputtering, while the  $\gamma$ -Mo<sub>2</sub>N coatings with Ti and Mo interlayer were deposited using high pulsed power magnetron sputtering on Si (100) substrates. The  $\gamma$ -Mo<sub>2</sub>N layer thickness was maintained at 1000 nm with three different interlayer thicknesses controlled at 50, 100, and 150 nm. The overall residual stress of the bilayer coatings was determined by the laser curvature method ( $\sigma_{LCM}$ ), while individual layer stress was evaluated by the average X-ray strain method ( $\sigma_{AXS}$ ). Contrary to our expectations, the results show that  $\sigma_{LCM}$  values are consistently higher than  $\sigma_{AXS}$ , suggesting that the Ti and Mo interlayer cannot effectively relieve stress through plastic deformation. The Ti interlayer may be partly converted to TiN due to the reaction of N<sub>2</sub> gas or N<sub>2</sub><sup>+</sup> ions with the pre-deposited Ti, and consequently the interlayer cannot be plastic deformed to relieve stress. In contrast, due to the high elastic constant of Mo, the compressive residual stresses in the Mo interlayer is higher than that in  $\gamma$ -Mo<sub>2</sub>N coating, where the stress is higher than the yield strength of Mo metal, indicating that Mo interlayer cannot serve as a buffer layer to relieve residual stress of  $\gamma$ -Mo<sub>2</sub>N coatings.

## Protective and High-temperature Coatings Room Town & Country D - Session MA4-1-TuA

**High Entropy and Other Multi-principal-element Materials I**  
Moderators: Dr. Shih-Hsun Chen, National Yang Ming Chiao Tung University (NYCU), Taiwan, Dr. Pavel Soucek, Masaryk University, Czechia

1:40pm **MA4-1-TuA-1 Phase-Adjustable High-Entropy Alloy Coatings Prepared via Thermal Spray Process, Shih-Hsun Chen [brucechen@nycu.edu.tw], NYCU, Taiwan** INVITED

The alloy design in HEAs has impacts the resultant microstructure, phase structure, and hardness and wear resistance. Careful selection of HEAs

elements is critical depending on the intended application of the alloy. Development of HEAs alloys follows careful selection of elements such as Co, Cr, Ni, Al, Fe, Ti among others. Mechanical properties in HEAs depend on existing phases whether single phase (BCC or FCC) or a mixture of phases and intermetallics or oxides. AlCoCrFeNi alloy has been widely studied and is considered an excellent base for additional strengthening strategies through compositional optimization. In this study, Al<sub>0.5</sub>CoCrFeNi<sub>2</sub>Ti powders were prepared using the gas atomization method, and annealing treatments were performed to characterize the phase transformation behavior, providing essential insights into the effects of thermal energy during the atmospheric plasma spraying process. To further explore these effects, the study examined effects of plasma energy and powder size in the production of Al<sub>0.5</sub>CoCrFeNi<sub>2</sub>Ti coatings. The characterization of both powders and coatings was consolidated to better understand the influence of Ti addition on the Al<sub>0.5</sub>CoCrFeNi<sub>2</sub> HEA system and to assess the performance of its plasma-sprayed coatings.

2:20pm **MA4-1-TuA-3 Three Noble Metals, Three Different Stories: Unraveling the Complex Behavior of Cu, Ag, and Au in CrMnFeCoNi High-Entropy Alloy Thin Films, Salah-eddine benazzouq [salah-eddine.benazzouq@univ-lorraine.fr], Institut Jean Lamour - Université de Lorraine, France; Ekaterina V. Gunina, Svyatoslav Povarov, School of Physics and Engineering, ITMO University, Russian Federation; Jaafar Ghanbaja, Sylvie Migot, Alexandre Nominé, Jean François Pierson, Valentin A. Milichko, Institut Jean Lamour - Université de Lorraine, France**

Advanced electronic devices and sensing technologies demand materials with precisely tunable electrical and optical properties, alongside excellent structural stability. While high-entropy alloys (HEAs) show promise for such applications due to their unique multi-element composition, controlling their functional properties remains challenging. Noble metals (Cu, Ag, Au) were strategically chosen for this study due to their similar electronic configurations and increasing metallic radii ( $r_{Cu}=0.127$  nm,  $r_{Ag}=0.144$  nm,  $r_{Au}=0.147$  nm) compared to the average metallic radius of the Cantor alloy (0.125 nm).

This study unravels the distinct stories of how Cu, Ag, and Au additions transform the structure and properties of CrMnFeCoNi Cantor alloy thin films, revealing behaviors that challenge our initial expectations. Using DC magnetron co-sputtering, we systematically investigated these transformations through comprehensive characterization including X-ray diffraction (XRD), high-resolution transmission electron microscopy (HRTEM), electrical resistivity measurements, and non-linear optical response.

Each noble metal reveals a unique chapter in phase evolution and property modification, far from the expected systematic progression based on atomic size. Copper tells a story of structural preservation, maintaining the fcc structure while systematically reducing nano-twin density, culminating in near-zero TCR (-2.86 ppm/K) at 37 at% Cu. Silver writes a different narrative through unexpected phase separation, creating artistic patterns of nano-precipitates with a characteristic tweed-like microstructure, despite predictions of solid solution formation. Gold presents perhaps the most surprising tale, where HRTEM unveils large grains with intricate twin boundary networks, contrasting sharply with its apparent amorphous nature in XRD analysis and defying expectations based on atomic size considerations.

These distinct structural modifications yield equally diverse functional properties. Cu-modified films demonstrate precise control over electrical behavior while maintaining metallic characteristics, aligning with initial predictions. Ag-modified films combine decreased electrical resistivity with enhanced second harmonic-generation (SHG) response, providing unexpected opportunities for multifunctional properties. Au-modified films exhibit unique optical properties tied to their complex grain structure. These three different stories highlight how noble metals can orchestrate dramatically different transformations in HEA thin films, while comparing their properties with sustainability metrics offers guidance for future technological implementations

2:40pm **MA4-1-TuA-4 Mechanical, Tribological and Corrosion Behavior of CoCrFeNiMn High-Entropy Thin Films, Lin Wu [lin.wu2@mail.mcgill.ca], McGill University, Canada; León Zendejas Medina, McGill University, KTH Royal Institute of Technology, Canada; Richard Chromik, Janine Mauzeroll, McGill University, Canada**

The CoCrFeNiMn (Cantor alloy) thin films deposited under ambient and high temperature conditions have been studied from the aspect of microstructure, mechanical, tribological and corrosion properties. The Cantor films were deposited by pulsed direct current magnetron sputtering

# Tuesday Afternoon, May 13, 2025

on silicon wafers at ambient and 350 °C. An FCC phase appeared in both ambient and high temperature films, with small amounts of an unidentified secondary phase. Using nanoindentation, film hardness (H) and reduced elastic modulus ( $E_r$ ) were measured.

Micro-tribology testing was conducted using a 20  $\mu\text{m}$  radius spherical diamond tip in the dry air atmosphere (RH% value under 4.0%), applying normal loads ranging from 2 to 7 mN. The worn surfaces were characterized by atomic force microscopy. Schiffmann's model was used to evaluate the elastic and plastic components of the friction. The corrosion behaviors of the films were studied by using anodic polarization in 3.5% NaCl, followed by a tribological testing carried out on the corroded surfaces, to address the correlation of corrosion response with the phase composition, mechanical properties and tribological behavior of the films.

3:00pm **MA4-1-TuA-5 Microstructure and Mechanical Properties Evaluation of CoCrNiTiAl Multiple-Principal Element Alloy Thin Films: Effect of TiAl Additions, Pongpak Chiyasak [pongpak.c@ku.th]**, Department of Materials Engineering, Faculty of Engineering, Kasetsart University, Thailand; *Jun-Xing Wang*, Ming Chi University of Technology, Taiwan; *Chia-Lin Li*, Center for Plasma and Thin Film Technologies, Ming Chi University of Technology, Taiwan; *Surapit Posri*, *Thanawat Santawee*, *Worawat Wattanathana*, *Aphichart Rodchanarowan*, Department of Materials Engineering, Faculty of Engineering, Kasetsart University, Thailand; *Jyh-Wei Lee*, Ming Chi University of Technology, Taiwan  
Multiple-principal element alloy thin films have attracted lots of interest from academia due to their optimized properties for both functional and structural applications, for example, high strength, good thermal stability, cost efficiency, and lower stacking fault energy. Several previous studies have shown that adding Ti and Al as alloying elements into CoCrNiTiAl multiple-principal element alloy thin films could further enhance their performance. In general, Ti element can transform the face-centered cubic structure into the amorphous structure, while Al generates body-centered cubic (BCC) structures, promoting higher hardness and wear resistance. However, the effect of the addition of Ti and Al elements into CoCrNiTiAl multiple-principal element alloy thin films is still unexplored.

In this work, the CoCrNiTiAl multiple-principal element alloy thin films with different amounts of Ti and Al contents were fabricated by the co-sputtering of TiAl and CoCrNi targets through a hybrid magnetron sputtering system. The CoCrNi and TiAl target were connected with a high power impulse magnetron sputtering system and a radio frequency power supply, respectively. The power input of the TiAl target was adjusted to achieve multiple-principal element alloy thin films with different TiAl contents. The field-emission (FE) scanning electron microscopy, FE-electron probe microanalyzer, X-ray diffraction, nanoindentation, tribometer, and electrochemical workstation were used to characterize microstructure, chemical composition, phase evolution, hardness, wear resistance, and corrosion behavior of multiple-principal element alloy thin films. The effect of TiAl contents on the microstructure and mechanical properties of CoCrNiTiAl multiple-principal element alloy thin films were discussed in this work.

**Keywords:** multiple-principal element alloy, CoCrNiTiAl, phase transformation, mechanical properties

4:00pm **MA4-1-TuA-8 Effects of Deposition Parameters and Post-Annealing Treatment on the Microstructure and Mechanical Properties of TiZrNbTaMo High Entropy Alloy Films, Chia-Lin Li [chialinli@mail.mcut.edu.tw]**, Center for Plasma and Thin Film Technologies, Ming Chi University of Technology, Taiwan; *Sen-You Hou*, Department of Materials Science and Engineering, National Tsing Hua University, Taiwan; *Bih-Show Lou*, Chemistry Division, Center for General Education, Chang Gung University, Taiwan; *Jyh-Wei Lee*, Department of Materials Engineering, Ming Chi University of Technology, Taiwan; *Po-Yu Chen*, Department of Materials Science and Engineering, National Tsing Hua University, Taiwan

TiZrNbTaMo high-entropy alloys (HEAs) with a body-centered cubic structure are known for their excellent compressive yield strength and significant compressive plasticity, retained even in thin film forms. These properties make them promising for various applications. The deposition parameters significantly influence the density and microstructure of thin films, affecting mechanical properties. In this study, TiZrNbTaMo high-entropy alloy films (HEAFs) were prepared using high power impulse magnetron sputtering (HIPIMS), DC, and RF power sources. The effects of pulse frequency and duty cycle in HIPIMS on their structure and properties were systematically investigated. The microstructure and crystal structure of

TiZrNbTaMo HEAFs were characterized using transmission electron microscopy (TEM) and X-ray diffractometry (XRD), while their mechanical properties were evaluated by nanoindentation. TiZrNbTaMo HEAFs deposited by HIPIMS exhibited increased hardness due to higher peak power density resulting in the coexistence of amorphous and nanocrystalline structures. However, the highest hardness of 5.78 GPa was achieved with RF power source, which was attributed to more nanocrystalline content and stacking faults. To further improve the mechanical properties of HEAs, post-annealing is used to modify the grain size and structure by inducing microstructures such as stacking faults and twins. In this study, the effects of post-annealing at 900 °C on microstructure and mechanical properties were investigated, and detailed features such as grain sizes, annealing twins, and variations in mechanical properties were discussed.

4:20pm **MA4-1-TuA-9 High Entropy Alloys Coatings for Inertial Confinement Fusion Hohlräume, Leonardus Bimo Bayu Aji [bayuaji1@llnl.gov]**, Daniel Goodelman, David Strozzi, Brandon Bocklund, Scott Peters, Alison Engwall, Swanee Shin, Gregory Taylor, Eunjeong Kim, James Merlo, Sergei Kucheyev, Lawrence Livermore National Laboratory, USA

Hohlraums, centimeter-scale sphero-cylindrical heavy-metal cans with wall thickness of 10 - 100  $\mu\text{m}$ , are a key component of an indirect-drive inertial confinement fusion (ICF) target as it determines the x-ray drive that implodes the fuel capsule. A previous study [Jones et al., Phys. Plasmas 14, 056311 (2007)] has demonstrated the feasibility of improving the x-ray drive by using a hohlraum made from a mixture ("cocktail") of elements, instead of a single element hohlraums, such as Au or U traditionally used for ICF. Here, we present our results on developing sputter-deposited heavy-metal high-entropy alloys (HEAs) for hohlraums with improved x-ray drive, high electrical resistivity to support a magnetized ICF, and material properties that are compatible with the ICF target fabrication process.

This work was performed under the auspices of the U.S. DOE by LLNL under Contract DE-AC52-07NA27344 and LDRD project 23-ERD-005.

## Tribology and Mechanics of Coatings and Surfaces Room Palm 5-6 - Session MC2-1-TuA

### Mechanical Properties and Adhesion I

**Moderators:** Carsten Gachot, TU Wien, Austria, Alice Lassnig, Austrian Academy of Sciences, Austria

1:40pm **MC2-1-TuA-1 Nanoscale Interface Engineering for Thin Films on Polymer Substrates, Barbara Putz [barbara.putz@empa.ch]**, EMPA (Swiss Federal Laboratories for Materials Science and Technology), Switzerland  
**INVITED**

Atomic layer deposition (ALD) holds enormous potential to design interfaces, due to the unique way in which a material is built in an atomic layer-by-layer fashion. When combined with other thin film techniques, such as magnetron sputtering (PVD), without breaking vacuum, the layer-by-layer nature of ALD can be harvested to design (sub)nanoscale interface architectures. An interesting area for this combined deposition are metal-polymer interfaces, where thin amorphous interlayers (IL, 5 nm thick) between metal film and polymer substrate favour strong and stable interfaces [1-3]. Until now, interlayer formation is governed by the film/substrate chemistry and deposition method, preventing high interface quality for the majority of material combinations and fabrication routes. Since ultrathin ALD layers uniquely resemble the reported interlayer in structure and chemistry, interlayer formation can, for the first time, be mimicked artificially to clarify the role of these structures in thin film delamination.

Through a combined ALD/PVD setup, we fabricate and study Al thin films (150 nm) with different ALD interlayer thicknesses ( $\text{Al}_2\text{O}_3 + \text{H}$ , 0.12 - 25 nm) on a polyimide substrate. Mechanical properties are measured via uni- and equi-biaxial tensile loading [4] with in-situ X-ray diffraction and electrical resistivity measurements from the evolution of Al film stress, width of the Al diffraction peak and electrical resistivity as a function of IL thickness and applied strain. Adhesion energy between metal film and polymer substrate is calculated using the tensile induced delamination method.

In our study, differences in the system's mechanical behaviour (yield strength, crack onset strain) are found to be driven by the microstructure of the metallic Al layer (film thickness and grain size), while the crack propagation (electrical failure strain) and adhesive performance (buckle

# Tuesday Afternoon, May 13, 2025

density) is dominated by the interface structure. Significant embrittlement and fracture is only observed for thick interlayers ( $\geq 25$  nm).

[1] Putz, B. et al., Adv. Eng. Mater. (2022), 2200951

[2] Putz, B. et al. Surf. Coat. Technol. 332, 368–375 (2017)

[3] S. Oh. Et al., Scripta Materialia 65 (2011) 456–459

**2:20pm MC2-1-TuA-3 Trilayer Fracture and Adhesion Investigated with in-Situ Synchrotron Radiation, Megan J. Cordill [megan.cordill@oeaw.ac.at],** Erich Schmid Institute of Materials Science, Austrian Academy of Sciences, Austria; *Shuhel Altaf Husain*, Université Sorbonne Paris Nord, France; *Claus O.W. Trost*, Erich Schmid Institute of Materials Science, Austrian Academy of Sciences, Austria; *Damien Faurie*, Université Sorbonne Paris Nord, France; *Pierre O. Renault*, University of Poitiers, Pprime Institute, France

Flexible and wearable electronics use multiple metal films on polymer substrates to achieve functionality where the resistance to through thickness fracture and the adhesion to the polymer substrates determines device performance. Commonly, flexible material systems are made of layers ductile metals of copper or aluminum as the conducting layers with more brittle molybdenum and chromium used as interlayers to improve adhesion to the polymer substrate or as protective capping layers. In this work, in-situ uniaxial tensile straining was used to investigate the fracture and delamination behavior of brittle-ductile-brittle trilayers. The method uses uniaxial straining to cause fracture of the film system perpendicular to the tensile loading direction and film delamination parallel to the tensile loading direction, which allows the adhesion energy to be evaluated. Experiments on the differently layered samples, namely Mo-Cu-Cr and Nb-Cu-Mo, were performed with in-situ resistance measurements and X-ray diffraction (XRD). Combined with post-straining confocal laser scanning microscopy, XRD provided the film stress evolution simultaneously in every layer to understand fracture of trilayer systems and how adhesion can be measured using tensile induced delamination. The main aspects presented will be adhesion energy along with the stress evolution under uniaxial tensile loading of the various trilayer architectures. Results indicated that the position of the Mo layer can influence the fracture behavior. It was also observed that only the presence of a brittle layer, rather than the position (interface layer vs. top layer), aids delamination in trilayers. Compared to single layer films of similar thickness, no significant change in the calculated adhesion energy of the same trilayer interfaces was found.

**2:40pm MC2-1-TuA-4 The Model to Explain the Origin of Residual Thin Film Stress, Tong Su [tong\_su@brown.edu], Eric Chason**, Brown University, USA

Residual stress has been a long-standing problem in thin film deposition, and it is critical to the adhesion and physical properties of their applications. In previous works, we have studied the mechanisms and used modeling to explain the stress evolution in the post-coalescence stage (typically 50 nm  $\sim$  400 nm) and steady state ( $>400$  nm or when the stress does not change significantly). The early stage of growth ( $<50$  nm) is not as well studied as the others and yet this state is important to the origin of the thin film stress. Here we present a model to explain the behavior of residual stress in the early stage with the assumption that the deposited particles form hemisphere islands on the substrate. The model is applied to analyze stress measurements of e-beam evaporated Ag and Ni from the wafer curvature measurements. The results suggest that the end of the coalescence stage may not be sufficient to explain the occurrence of the tensile peak in the early state. Rather, the balance between tensile and compressive stress mechanisms as the grain boundary is formed between islands needs to be considered.

**3:00pm MC2-1-TuA-5 Novel Approach for Scratch Analysis of Ductile Metallic Layers on Fragile Substrates, Mohammad Arab Pour Yazdi [mohammad.arab@anton-paar.com], Pavel Sedmak**, Anton Paar TriTec SA, Switzerland; *Parth Katak*, Anton Paar USA; *Jiri Nohava*, Anton Paar TriTec SA, Switzerland

In the electronics and semiconductor industries, there is a growing demand for precise characterization of adhesion properties in soft metallic multilayers on fragile substrates, such as semiconductor wafers and glass. Consequently, nondestructive testing methods have become essential to prevent damage to these sensitive substrates during testing. Conductive metallic layers including gold (Au), platinum (Pt), copper (Cu), and silver (Ag) are critical for microchip pathways; however, their ductility poses challenges for adhesion testing on brittle substrates. Traditional nanoscratch methods, which use sphero-conical indenters, rapidly traverse these soft layers and exert significant stress on the fragile substrates. This

often results in substrate failure rather than yielding valuable insights into the interfacial adhesion of the layers.

In this study, we introduce a novel scratch testing method specifically designed for soft metallic layers or multilayers on fragile substrates. This approach employs a micro wedge blade indenter, rather than the conventional spheroconical indenter, along with a two-axis tilt stage sample holder, enhancing precision and reducing substrate damage to yield more reliable adhesion measurements. This method is particularly suited for ductile metallic coatings deposited via PVD, CVD, and ALD, providing a robust solution for accurately assessing the adhesion properties of soft metallic coatings on sensitive substrates.

**Keywords:** Ductile coatings; Fragile substrates; Adhesion testing; Wedge blade indenter; Nanoscratch testing.

**4:00pm MC2-1-TuA-8 The Comparison in Microstructure and Mechanical Properties of MoN Films Deposited by RFMS and HiPIMS Techniques, Chi-Yueh Chang [w6208asx@gmail.com],** National United University, Taiwan

The MoN films are gathering increasing attentions for their high-performance characteristics, making the production of high-quality MoN films an important research focus. In this study, Mo-N thin films are coated using radio frequency magnetron sputtering, RFMS, and high intensity power impulse magnetron sputtering, HiPIMS, techniques. The input power and Ar/N<sub>2</sub> ratio are adjusted from 150 to 200W and 15/5 to 18/2 sccm/sccm to control the microstructure. The duty cycle of the HiPIMS from 4 to 10% is also manipulated to trigger higher peak power density and current. A columnar structure feature was observed across all thin films. Nevertheless, the phase of the Mo-N changes under different parameters. Through RFMS, as the Ar/N<sub>2</sub> ratio was raised from 15/5 to 18/2 sccm at 150 W input power, a significant evolution of major Mo<sub>2</sub>N to MoN phase was observed. With higher peak current and power density through HiPIMS deposition, a multiple phase feature with decreased grain size of Mo-N phases were discovered. The microhardness, elastic modulus, wear resistance and indentation cracking behavior were investigated. The correlation between microstructure evolution and the mechanical properties were also discussed.

**Keywords:** Refractory Thin film coatings MoN HiPIMS

**4:20pm MC2-1-TuA-9 Quantitative 3D FIB-SEM Characterization of Single Cu Particle Impacts for Cold Spray Applications, Veera Panova [vpanova@mit.edu],** Massachusetts Institute of Technology, USA; *Christopher Schuh*, Northwestern University, USA

Cold spray is a solid-state additive manufacturing process that produces coatings and standalone parts by accelerating micron-sized metallic particles to supersonic velocities. Upon impact, the particles and substrate undergo plastic deformation, surface oxide layers get disrupted, and direct particle-substrate contact is achieved to attain metallurgical bonding. Our recent works take advantage of the Laser-Induced Particle Impact Test (LIPIT) to produce single microparticle impacts under carefully controlled conditions, providing a unit-process understanding of cold spray physics. Each launched particle is well-characterized: its size, morphology, microstructure, velocity, and in-flight behavior are known. We then analyze impact sites using focused ion beam-scanning electron microscopy (FIB-SEM) to study multiple aspects of the impact event: bonding at particle-substrate and particle-particle interfaces, deformation at high strain rates, and microstructural evolution. The major advantage of this approach is that it is tomographic, providing direct 3D observations of the interfaces, as well as quantitative measurements of the bonded area and microstructural changes around the impact site.

This talk will review several observations that 3D tomography of the impact sites reveals about structure development in cold spray. First, we observe generally non-symmetrical bonding at the particle-substrate interface and conclude that bonding takes place top-down; regions experiencing high strain bond first. These insights conform to a model for particle-substrate bonding through oxide-layer rarefaction and provide guidelines for how to optimize processing parameters to produce well-bonded cold spray coatings. Second, our microstructural observations reveal limiting conditions for the development of recrystallization structures. Such information speaks to the development and dissipation of adiabatic heat upon impact.

# Tuesday Afternoon, May 13, 2025

4:40pm **MC2-1-TuA-10 Mechanical Properties and Deformation Mechanisms of Metallic Thin Films Synthesized by Pulsed Laser Deposition**, *Francesco Bignoli, Davide Vacirca, Philippe Djemia*, Laboratoire des Sciences des Procédés et des Matériaux (LSPM) – CNRS, France; *Andrea Li Bassi*, Department of Energy, Politecnico di Milano, Italy; *James Paul Best, Gerhard Dehm*, Max-Planck Institut für Eisenforschung, Germany; **Matteo Ghidelli** [[matteo.ghidelli@lspm.cnrs.fr](mailto:matteo.ghidelli@lspm.cnrs.fr)], Laboratoire des Sciences des Procédés et des Matériaux (LSPM) – CNRS, France

The ongoing trend toward miniaturization in device components across key technologies demands the synthesis of high-performance nanostructured films with exceptional combination mechanical properties such as high yield strength and plasticity which, however, are mutually exclusive. In order to overcome such trade off, it is crucial to control the atomic composition and the microstructure, going beyond currently nanoengineering design approaches for thin films. One main limitation arises from conventional thin film deposition techniques (sputtering) with limited possibility to fabricate novel microstructures such as with ultrafine grains or nanoscale laminates alternating layers of different compositions and phases with intrinsic dimensions on the order of a few nanometers. Such features could induce mechanical size effects, influencing deformation mechanisms and enabling highly tunable and enhanced mechanical properties.

Here, I will show the potential of Pulsed Laser Deposition (PLD) as a novel technique to synthesize advanced metallic thin films, reporting the fabrication of a variety of microstructures with tailored composition and nanoscale features including compact, nanogranular and crystal/glass ultrafine nanolaminates and focusing on the deformation behavior and mechanical properties.

First, I will focus on the on the fabrication of thin film metallic glasses with different composition ZrCu, ZrCuAl (with also O addition) and controlled microstructure, compact and nanogranular [1]. The mechanical characterization with optoacoustic techniques, nanoindentation and *in situ* SEM micropillar compression reports large and tailored mechanical properties, above sputter-deposited counterparts, reaching ultimate yield strength (>4 GPa) and ductility (>15 %) for ZrCuAl/O films. Then, I will show the fabrication of ultrafine glass/crystal (ZrCu/Al) nanolaminates with high and tunable density of interfaces (nanolayer thickness <5 nm), reporting shear bands blocking and homogenous deformation, in combination with large plasticity (> 10%) and yield strength (>3.4 GPa) [2].

Lastly, I will focus on the PLD synthesis of CoCrCuFeNi crystalline high entropy alloys showing unique microstructure and ultrafine grains ( $\approx 10$  nm), triggering Hall-Petch strengthening resulting in high hardness ( $\approx 10.5$  GPa) and yield strength (1.9 GPa) significantly above sputter-deposited counterparts, while retaining large plastic deformability (30%) [3].

[1] M. Ghidelli *et al.*, *Acta Mater.*, 213, 116955, 2021.

[2] F. Bignoli *et al.*, *ACS Appl. Mater. Interfaces*, 16, 27, 35686–96, 2024.

[3] D. Vacirca *et al.*, Submitted to *Acta Mater.*, 2024.

## Topical Symposium on Sustainable Surface Engineering Room Town & Country C - Session TS3-TuA

### Circular Strategies for Surface Engineering

**Moderators:** Dr. Marcus Hans, RWTH Aachen University, Germany, Dr. Nina Schalk, Montanuniversität Leoben, Austria

2:00pm **TS3-TuA-2 Scalable Solar-Thermal Synthesis of High-Yield Flake Graphite and Hydrogen**, *Timothy S. Fisher* [[tsfisher@ucla.edu](mailto:tsfisher@ucla.edu)], University of California Los Angeles, USA

**INVITED**

Current industrial processes for power, fuel, and commodity production are responsible for massive, ongoing CO<sub>2</sub> emissions that adversely affect the stability of Earth's climate with potentially disastrous consequences. Increased use of hydrogen as a fuel and chemical building block promises to reduce CO<sub>2</sub> emissions in critical sectors, but contemporary hydrogen production technologies also involve high greenhouse gas emissions. This talk considers a process in which concentrated radiation from a simulated solar source converts methane and similar hydrocarbons to high-value synthetic flake graphite and hydrogen gas. Methane flows within a photo-thermal reactor through the pores of a thin substrate irradiated by several thousand suns at the focal peak. The methane decomposes primarily into hydrogen while depositing highly graphitic carbon that grows conformally over ligaments in the porous substrate. The direct heating of the porous

substrate serves to capture the solid carbon into a readily captured and useful form while maintaining active deposition site density with persistent self-catalytic activity. The talk will cover topics including solar irradiation profile modeling and measurements, chemical kinetics, gas-phase diagnostics, material characterization, product yields, and solar-to-chemical efficiency.

2:40pm **TS3-TuA-4 Developing Next Generation Sustainable Flexible Food Packaging Materials**, *Peter Kelly* [[peter.kelly@mmu.ac.uk](mailto:peter.kelly@mmu.ac.uk)], Manchester Metropolitan University, UK; *Carolin Struller*, Bobst Manchester Ltd, UK; *Glen West*, Manchester Metropolitan University, UK; *Nick Copeland*, Bobst Manchester Ltd, UK; *Gwyneth Spence*, Manchester Metropolitan University, UK

Flexible food packaging materials are complex surface engineered products that must meet demanding quality criteria yet be produced at very high volume and low cost. Until recently, typical flexible packaging material might consist of an inner heat sealable polyethylene (PE) film, then combinations of adhesives to hold the laminated structure together, inks for printing product details, a topcoat, a barrier layer and finally an outer polymer film, such as polyethylene terephthalate (PET). The barrier layer provides extended shelf life to the food product by preventing moisture and oxygen ingress, which spoils the product over time. Barrier layers can be organic layers (e.g. polyvinylidene chloride (PVdC)) deposited by wet chemical techniques, aluminium foil layers or as in the case here, either aluminium or aluminium oxide ('AlOx') coatings deposited by thermal evaporation techniques. These coatings are deposited at very high rates (line speeds are up to 1000m/min) and over very large areas (up to 4.85m wide x 100km long rolls) in roll-to-roll vacuum systems. Average barrier layer thicknesses are 40-50nm for Al films and 8-15nm for AlOx layers.

As a consequence of the mixed materials used in conventional flexible packaging, most products cannot be recycled and go to landfill or are incinerated. The increasing demand for sustainable packaging products has led Bobst and other companies in the packaging value chain (ranging from raw material producers and converters to brand owners and retailers) to develop new products that meet the criteria of 'recyclable, reusable or compostable'.

This paper describes progress towards mono-material polyolefin-based solutions for fully recyclable polymeric packaging and paper-based products, which are suitable to be processed in the existing paper recycling stream. In both cases, the Bobst oneBARRIER PrimeCycle PE product and the FibreCycle paper-based product provide high barrier performance and meet international recyclable standards. In addition to the development of these products, extensive life cycle analyses (LCAs) have been undertaken on each stage of the manufacturing process to allow accurate and comparable assessments to be made of the environmental impact and sustainability of the product.

3:00pm **TS3-TuA-5 PFAS Free Anti-Stick Coatings for Superior Electrosurgical Performance**, *Noora Manninen* [[noora.manninen@oerlikon.com](mailto:noora.manninen@oerlikon.com)], Oerlikon Surface Solutions, Liechtenstein; *Sanna Tervakangas*, Oerlikon Surface Solutions, Finland; *Klaus Boebel*, Oerlikon Surface Solutions, Liechtenstein

Per- and polyfluoroalkyl substances (PFAS) are a large class of thousands of synthetic chemicals currently used in a wide variety of products (e.g. food packaging, cookware, textiles, medical devices, semiconductor components, batteries, among many others). PFAS contain carbon-fluorine bonds, which are one of the strongest chemical bonds in organic chemistry, meaning they are very attractive in different consumer products as they can resist to degradation. Nevertheless, the degradation resistance also persists once they are disposed. Currently PFAS are increasingly detected as environmental pollutants and some are linked to negative effects on human health, which has led to the current restriction proposal by European Chemical Agency (ECHA).

The restriction on use of PFAS will require the development of new solutions, which must fulfill health and environmental requirements. Medical devices are one of the main fields of use of PFAS, where PTFE based coatings are widely used, among many applications as anti-stick coatings in electrosurgical devices. In the current work existing coating solutions already in use for medical market and approved by regulatory authorities (e.g. FDA) have been tested (e.g. TiN, CrN, DLC, Parylene C) and compared to new coating solutions under research and development. The main goal is to obtain coatings with good anti-stick performance, which ideally can be re-used as multiple use devices, opposed to concept of single-use devices, which are discarded after each surgery generating large amount of waste. In order to fulfill the requirements for multiple use

devices the coatings must stand multiple cleaning and sterilization cycles meaning they must have good corrosion properties as well as good abrasion resistance.

In the present study the coatings are characterized regarding their surface energy given that this surface property is connected with anti-sticking properties, and also functional tests are performed in a test set-up consisting of an electrosurgical unit (ESU) where coatings anti-stick performance is tested against pork liver. Additionally, the corrosion and abrasion resistance of the coatings are evaluated under autoclave and alkaline cleaning conditions and under abrasive cleaning test condition in order to resemble the lifecycle of multiple-use electrosurgical devices.

4:00pm **TS3-TuA-8 Design of Defect Structure in an Epitaxial VN Bilayer Film by Tailoring Nitrogen Concentration and Interfacial Strain, Marcus Hans [hans@mch.rwth-aachen.de], Damian Holzapfel, RWTH Aachen University, Germany; Zhuo Chen, Erich Schmid Institute of Materials Science, Austria; Soheil Karimi Aghda, Michal Fečik, RWTH Aachen University, Germany; Daniel Primetzhofer, Uppsala University, Sweden; Zaoli Zhang, Erich Schmid Institute of Materials Science, Austria; Jochen Schneider, RWTH Aachen University, Germany**

A  $V_{0.48}N_{0.52}/V_{0.54}N_{0.46}(001)$  bilayer has been grown epitaxially on  $MgO(001)$  by reactive high power pulsed magnetron sputtering at a temperature of 400 °C in an industrial-scale deposition system. Based on ion beam analysis, atom probe tomography, X-ray diffraction, high-resolution transmission electron microscopy data as well as *ab initio* calculations, it is demonstrated that the defect structure is affected by the nitrogen concentration and interfacial strain. Strain at the  $MgO/V_{0.48}N_{0.52}$  interface is caused by a lattice parameter mismatch of ~2.3% as predicted by density functional theory. The experimentally determined lattice parameter difference is only ~1.3%, hence, the interfacial strain is partially relaxed by formation of misfit dislocations. Consequently, the dislocation density in  $V_{0.48}N_{0.52}$  is reduced from ~0.20 nm<sup>-2</sup> to ~0.10 nm<sup>-2</sup> within a distance of ~10 nm from the  $MgO/V_{0.48}N_{0.52}$  interface. The dislocation density is reduced to ~0.04 nm<sup>-2</sup> at the  $V_{0.48}N_{0.52}/V_{0.54}N_{0.46}$  interface and < 0.01 nm<sup>-2</sup> in the  $V_{0.54}N_{0.46}$  layer within a distance of ~35 nm from the interface due to strain relaxation. Based on the here presented findings, it is evident that control of the nitrogen concentration and interfacial strain allows for the design of layered architectures with a variation in dislocation density by two orders of magnitude.

4:20pm **TS3-TuA-9 Low Friction Sputtering Coatings, a Sustainable Option to Reduce Energy Consumption and Harmful Lubricant Usage, Albano Cavaleiro [albano.cavaleiro@dem.uc.pt], University of Coimbra, Portugal**  
**INVITED**

From the more than 500 EJ of the World energy consumption, 20% regards losses due to friction in mechanical contacts<sup>1</sup>. The obvious solution to decrease friction, the use of liquid lubricants, rises increasing concerns to the environment due to their harmful impact. Therefore, alternatives that can either provide a decrease of the friction in solid contacts or a reduction/removal of the usage of liquid lubrication, will have a significant and positive impact in both saving of energy and protection of the environment.

Low friction coatings were intensively developed in last decades as solutions for applications where liquid lubrication is restricted (space, food industry, vacuum,...) as well as a tool for removing either the usage of liquid lubrication or the extremely harmful additives of lubricant oils. As friction is a surface phenomenon, the main advantage of low friction coatings is that they can be applied over the currently used materials for mechanical applications without significant changes of the components and devices.

In this talk several examples related with the development and application of sputtering coatings in mechanical applications (moulding, cutting, forming,...) with main objectives of decreasing friction and reducing the harmful impact of oil lubricants, will be presented. The sliding mechanisms, in particular the understanding of tribolayers formation, will be addressed and connected to different concepts which were in the basis of the coatings development.

<sup>1</sup> K. Holmberg, A. Erdemir, Influence of tribology on global energy consumption, costs and emissions, *Friction* 5 (2017) 263–284



## Protective and High-temperature Coatings

### Room Town & Country A - Session MA2-2-WeM

#### Thermal and Environmental Barrier Coatings II

**Moderators:** Prof. Fernando Pedraza, La Rochelle University, Laboratory LaSIE, France, Prof. Francisco Javier Pérez Trujillo, Universidad Complutense de Madrid, Spain

9:00am **MA2-2-WeM-4 Sandphobic Thermal/Environmental Barrier Coatings for Gas Turbine Engines, Andrew Wright [andrew.j.wright6.ctr@army.mil], Clara Mock, DEVCOM Army Research Laboratory, USA; Timothy Sharobem, Oerlikon Metco, USA; Luis Bravo, Anindya Ghoshal, DEVCOM Army Research Laboratory, USA**

Previous published work on similar materials, components, and environments has shown that degradation typically is caused by either erosive damage leading to spalling of the coatings or chemical attack from particulates, such as sand, that leads to cracking and delamination. In this work, controlled isothermal furnace tests were conducted to study the chemical compatibility of T/EBCs in the presence of CMAS. The same coatings were also investigated in a hot particulate ingestion rig (HPIR). This rig mimics conditions found in the hot turbine section of a gas-turbine engine and conducts particulate entrainment in a gas-turbine engine relevant combustor test environment. Here, specimens were subjected to thermal cycling and CMAS impingement at high velocity and high temperature to investigate the survivability of the coatings in a more realistic case study. Finally, the wettability characteristics of CMAS were investigated using high temperature contact angle measurements to examine CMAS effects on various T/EBC chemistries. While coating chemistry is certainly a factor affecting CMAS spreading on the surface, results show that surface roughness is also a significant factor. Results were used to develop and validate novel wettability and full-engine scale models.

9:20am **MA2-2-WeM-5 A New Thermal Barrier Coating with Strong Resistance to Molten Silicate Attack and Fracture, Ying Chen [ying.chen-2@manchester.ac.uk], The University of Manchester, UK**

We report a new thermal barrier coating (TBC) with strong resistance to calcia–magnesia–alumina–silicate (CMAS) attack and fracture. The design is based on a core-shell concept in which each microstructural unit of the coating comprises a tough yttria stabilised zirconia (YSZ) core and a thin, CMAS-resistant shell. The core-shell TBC was realised by synthesising core-shell powder and then translating the core-shell structure from powder to coating by thermal spray. The CMAS resistance test shows that the CMAS penetration depth through the core-shell TBC is an order of magnitude lower than that through the industrial benchmark YSZ TBC. The erosion and micromechanical tests show that the core-shell TBC has lower material loss and higher fracture toughness than the benchmark YSZ TBC, suggesting its stronger fracture resistance at both macro and microscales. The strong CMAS and fracture resistance of the core-shell TBC was rationalised by multiscale compositional and microstructural analysis.

9:40am **MA2-2-WeM-6 Enhanced Oxidation Resistance of Ni substrate by Sputtered Nanotwinned Al<sub>5</sub>SiCo<sub>20</sub>Cr<sub>20</sub>Ni<sub>45</sub>NbMo<sub>4</sub> Medium-Entropy Alloy Thin Films at High Temperatures, Jun-Hui Qiu [junhui-qiu@gapp.nthu.edu.tw], Yi-Chun Yen, Fan-Yi Ouyang, Department of Engineering and System Science, National Tsing Hua University, Taiwan**  
High-entropy alloys exhibit various properties, such as superior thermal stability, oxidation resistance, and corrosion resistance. These characteristics have sparked interest in using HEAs as anti-oxidation protective coatings. The nanotwinned structure within these alloys contributes to their high hardness and thermal stability, while the sluggish diffusion in high entropy alloys helps lower oxidation rates.

In this study, Al<sub>5</sub>SiCo<sub>20</sub>Cr<sub>20</sub>Ni<sub>45</sub>NbMo<sub>4</sub> medium-entropy alloy thin films with a nanotwinned structure were successfully fabricated using magnetron sputtering system on a nickel-metal substrate. Then, the samples were subjected to high-temperature oxidation tests at 600°C, 700°C, and 800°C for 72 hours in dry air using a thermogravimetric analyzer to investigate the high-temperature oxidation behavior of these films and their protective effects against oxidation on nickel substrates. The results demonstrated that the medium-entropy alloy films exhibited strong oxidation resistance, leading to significantly lower oxidation rates and mass gain than pure nickel. The oxidized films had smoother surfaces than bare nickel substrates, with no pores or cracks. Due to grain growth at high temperatures, the (111) texture and nanotwinned structure in the films partially disappeared at 600°C and 700°C, although some twin structures remained. At 800°C, the twin structures were nearly absent, forming larger grains and a more pronounced (200) diffraction peak. After 24 hours of

oxidation at 800°C, chromium oxide particles began to precipitate on the surface, with size and density increasing over time. At 600°C, the oxide layer on the films consisted of an inner aluminum oxide layer and an outer chromium oxide layer, mainly driven by the inward oxygen diffusion. After oxidation at 700°C and 800°C, the oxide layer evolved into a three-layer structure with an inner aluminum oxide layer, a middle chromium oxide layer, and an outer aluminum oxide layer. With prolonged oxidation time, the outer aluminum oxide layer developed an island-like structure with a discontinuous thickness. After extended oxidation at 800°C, form chromium oxide within and on the surface of the aluminum oxide. Additionally, internal oxidation of aluminum occurred inside the film.

## Protective and High-temperature Coatings

### Room Palm 3-4 - Session MA3-3-WeM

#### Hard and Nanostructured Coatings III

**Moderators:** Dr. Rainer Hahn, TU Wien, Institute of Materials Science and Technology, Austria, Dr. Stanislav Haviar, University of West Bohemia, Czechia, Dr. Fan-Yi Ouyang, National Tsing Hua University, Taiwan

8:00am **MA3-3-WeM-1 Controlling Phase Selection, Preferred Orientation, and Van Der Waals or Conventional Epitaxy in Molybdenum Oxide Films, Faezeh Alijan Farzad Lahiji [faezeh.alijan.farzad.lahiji@liu.se], Linköping University, IFM, Sweden; Biplab Paul, PLATIT AG, Switzerland; Ganpati Ramanath, Rensselaer Polytechnic Institute, USA; Arnaud le Febvrier, Per Eklund, Uppsala University, Angstrom Laboratory, Sweden**

Molybdenum oxide MoO<sub>x</sub> films (x = 2, 3) are attractive for a variety of applications, but exclusive phase selection remains challenging due to the presence of multiple polymorphs. To achieve pure van der Waals epitaxy (vdWE), which relies on van der Waals forces for strain-free growth, we explored phase control of molybdenum oxide (MoO<sub>x</sub>), aiming to grow both non-layered monoclinic MoO<sub>2</sub> and layered orthorhombic α-MoO<sub>3</sub>.

By adjusting the oxygen pressure p<sub>O2</sub> during reactive magnetron sputtering, we demonstrate control over phase selection, texture, and epitaxy in MoO<sub>x</sub> films on f-mica and c-sapphire. Our results show non-layered monoclinic MoO<sub>2</sub> formation on both f-mica and c-sapphire at 500 °C for 0.1 ≤ p<sub>O2</sub> ≤ 0.25, outside which the films are amorphous. The result is similar at 400 °C except for layered orthorhombic α-MoO<sub>3</sub> formation at high p<sub>O2</sub> and a greater sensitivity of phase selection to p<sub>O2</sub>. High p<sub>O2</sub> fosters large thin-sheet crystals with texture and/or epitaxy, while low p<sub>O2</sub> results in fine-grained flowery microstructure. Pole figure analyses reveal that the orthorhombic α-MoO<sub>3</sub> films on f-mica exhibit van der Waals epitaxy [1] wherein the out-of-plane *OkO* d-spacings are invariant with film thickness, indicative of negligible interfacial strain. In contrast, α-MoO<sub>3</sub> films on c-sapphire showed *OkO* fiber texture. In the case of MoO<sub>2</sub>, epitaxy occurs on both f-mica and c-sapphire characterized by conventional epitaxy with strong interfacial bonding, promoting strain in the film but enables high crystalline quality and controlled orientation on both substrates [2]. The aforementioned results provide a framework for the controlled synthesis of MoO<sub>x</sub> films with tunable orientation, epitaxy, strain, and microstructure for applications.

[1] E. Ekström, *et al.*, *Materials & Design* 229 (2023) 111 864.

[2] F.A. Lahiji, *et al.*, *Thin Solid Films* (2024) 140566.

8:20am **MA3-3-WeM-2 Comparative Study of the Effect of W and Nb Addition on Microstructure and Properties of Zr-Cu-Based Thin-Film Metallic Glasses, Deepika Thakur [deep0808@kfy.zcu.cz], Michaela Červená, Radomír Čerstvý, Petr Zeman, University of West Bohemia - NTIS, Czechia**

Zr-Cu-based thin-film metallic glasses (TFMGs) have emerged as a promising class of materials due to their exceptional properties such as high glass-forming ability, superior elastic strain limit, enhanced hardness and plasticity. Moreover, these TFMGs offer the potential to be combined with nanocrystalline materials (transition metals or metal nitrides) to create heterogeneous dual-phase nanocomposite structures and thus achieving a better balance of toughness and hardness and/or unlocking new functionalities.

Therefore, this study explores the effect of gradual addition of W (negative mixing enthalpy with Zr but positive with Cu) and Nb (positive mixing enthalpy with both Zr and Cu) on microstructure and properties of Zr-Cu-based TFMGs. Two film series, W-Zr-Cu and Nb-Zr-Cu, were prepared, keeping Zr:Cu as 1:1 and gradually varying the W and Nb content in the respective series. Each deposition was done in Ar using three magnetrons

# Wednesday Morning, May 14, 2025

equipped with Zr and W/Nb targets operated in the dc regime and a Cu target in the HiPIMS regime.

A systematic investigation revealed that W and Nb additions have a significant impact on microstructure and other properties of the films. The films remain amorphous with smooth surfaces (roughness < 2 nm) up to 65 at.% of W or Nb, displaying vein-like features typical of metallic glasses upon fracture. W-Zr-Cu films with 67 at.% W are characterized by a combination of featureless structures (amorphous-like) close to the substrate and thin columns in the upper part of the film. Films with even higher W contents grow in a V-shaped columnar microstructure corresponding to the bcc  $\alpha$ -W crystalline structure. Nb-Zr-Cu films with 70 at.% Nb clearly exhibit a dual-phase structure with thin columns surrounded by vein-like features. Further increase in the Nb content above 70 at.% leads to the formation of a crystalline structure with parallel columns and very small voids. These voids tend to vanish with increasing Nb content. A gradual increase in hardness and reduced Young's modulus is observed with increasing W content for the amorphous W-Zr-Cu films and the crystalline films show an enhancement in hardness of up to 15% compared to films with pure W due to solid solution hardening. In the case of Nb-Zr-Cu films with up to 70 at.% Nb, the hardness remains nearly constant. However, further addition of Nb results in a decreased hardness and this reduction might be attributed to a less dense structure of the films.

Results of ongoing analysis and experiments on W-Zr-Cu and Nb-Zr-Cu films based on ZrCu TFMG will also be presented, providing new insights into the material's phase transitions, mechanical strength, and electrical properties.

**8:40am MA3-3-WeM-3 Tailoring Nanostructure and Functional Properties of Sputter-Deposited Cu-Based Films by Zr Alloying, Mariia Zhadko [zhadko@ntis.zcu.cz], Anna Benediktová, Radomír Čerstvý, Jiří Houška, Jiří Čapek, David Kolenatý, Pavel Baroch, Petr Zeman, University of West Bohemia, Czechia**

Cu and Cu-based films, known for their superior electrical and thermal conductivity, find primary applications in electronic devices and the electrical industry. However, the implementation of various strengthening mechanisms often compromises the conductivity. Therefore, it is crucial to carefully control the structural state and composition of these films to achieve an optimal balance between mechanical strength and conductivity.

In this work, we prepared nanocrystalline Cu-Zr films with a minor Zr content ranging from 0 to 2.7 at.% using non-reactive direct current magnetron co-sputtering of separate Cu and Zr targets in pure Ar at a pressure of  $\sim 0.5$  Pa without substrate bias and external heating. The effects of Zr alloying on the structure, surface, mechanical, and electrical properties were systematically investigated using X-ray diffraction, electron microscopy, atomic force microscopy, indentation, and the four-point probe method. We demonstrate that Zr alloying within the investigated composition range is an effective approach for modifying the structural state and properties of sputter-deposited films, with the most notable changes observed between 0.3 and 1.3 at.% Zr. Beyond this range, only minor changes in the microstructure and mechanical properties are observed, while the solubility, electrical resistivity, and surface roughness continue to rise.

Our systematic investigation shows that during film deposition, a redistribution of Zr atoms occurs between the supersaturated solid solution and grain boundaries resulting in the formation of a complex microstructure along with significant texture weakening and structural refinement. As a result, the alloyed Cu-Zr films exhibit hardness values between 3.2 and 4.2 GPa, exceeding the 2.5 GPa observed in the unalloyed Cu film. This hardness enhancement is attributed to the combined effect of grain boundary strengthening due to the structural refinement and Zr segregation, and solid solution strengthening. An observed increase in electrical resistivity is primarily attributed to electron scattering by Zr atoms dissolved in the Cu lattice and additional scattering at the grain boundaries, especially at Zr contents above 1.5 at.%. However, the as-deposited Cu-Zr films exhibit a combination of hardness and electrical conductivity that is comparable to or better than reported values in the literature. These findings provide a pathway for optimizing structure-property combinations in Cu-Zr films and suggest potential for further enhancement of mechanical and electrical properties through the precipitation hardening mechanism.

**9:00am MA3-3-WeM-4 Influence of Bilayer Periodic Thickness Ratios on the Mechanical Properties and Corrosion Resistance of AlCrNbSiTiN/AlCrN High-Entropy Alloy Nitride Multilayer Thin Films, Shang-Hua Tseng [bnb515032@gmail.com], National Taiwan University of Science and Technology, Taiwan**

High entropy alloy (HEA) nitride thin films have attracted considerable attention from the global industrial and academic communities due to their excellent mechanical properties. HEA multilayer nitride films also exhibit good interfacial stability, outstanding mechanical performance, and superior corrosion resistance. In this study, AlCrNbSiTiN/AlCrN nitride multilayer thin films were deposited using a high power impulse magnetron sputtering (HiPIMS) system with AlCrNbSiTi and AlCr targets in a mixed argon and nitrogen atmosphere. By adjusting the residence time of the substrates in the plasma regions of the AlCrNbSiTi and AlCr targets, multilayered thin films with varied bilayer periodic thicknesses ranging from 6 to 40 nm were fabricated. For the multilayer thin film with 15 nm bilayer period thickness, the thickness ratios of AlCrNbSiTiN and AlCrN single layer were adjusted to evaluate their influence on the hardness and corrosion resistance of films. XRD analysis indicated that all AlCrNbSiTiN/AlCrN multilayer films, as well as single-layer AlCrNbSiTiN and AlCrN films, exhibited a face-centered cubic crystal structure. Notably, the AlCrNbSiTiN/AlCrN multilayer film with a 15 nm bilayer period demonstrated a high hardness of 28 GPa and excellent corrosion resistance in 0.5 M H<sub>2</sub>SO<sub>4</sub> aqueous solution, with a corrosion impedance value of  $1.19 \times 10^6 \Omega \cdot \text{cm}^2$ . The influence of AlCrNbSiTiN to AlCrN thickness ratios on the mechanical properties and corrosion resistance of AlCrNbSiTiN/AlCrN multilayer thin film with 15 nm bilayer period was explored in this work.

**9:20am MA3-3-WeM-5 Impact of Microstructural Characteristics of HVOF-Deposited Cr<sub>3</sub>C<sub>2</sub>-Cermets on Their Performance in Sliding Abrasive Wear, Xinqing Ma [Chin.ma@cwst.com], Peter Ruggiero, Curtiss-Wright Corporate, USA**

Nowadays, Cr<sub>3</sub>C<sub>2</sub>-based cermet hardface coatings manufactured by advanced HVOF processes are well recognized for their corrosion and erosion resistance, particularly at high temperatures. Their lightweight nature and high temperature capability make them an attractive alternative to WC-based alloy coatings and hard Cr plating coatings. The objective of this study is to develop optimal Cr<sub>3</sub>C<sub>2</sub>-NiCr coatings by comparing different feedstock materials, including feedstock with nanocrystalline and/or submicron sized Cr<sub>3</sub>C<sub>2</sub> phases. The focus of the investigation is on understanding the impact of feedstock features such as particle size, morphology, and nanocrystalline carbide sizes, as well as sliding abrasive wear conditions on the coating properties and sliding wear performance. The results of the study indicate that the sliding wear resistance of the Cr<sub>3</sub>C<sub>2</sub>-NiCr coatings is highly influenced by the features of the Cr<sub>3</sub>C<sub>2</sub> carbides. With the special interest of nano-crystalline and or submicron-sized carbides, the presence of nano, submicron and a few microns sized carbides in the coatings was revealed to improve their density, residual stress and hardness, leading to a significant reduction in wear rates under test conditions. Furthermore, the size of the abrasive SiC grit on the counter surface plays a significant role in determining the sliding wear behavior of these coatings. Based on the analysis of the test data, the mechanisms behind the performance of the Cr<sub>3</sub>C<sub>2</sub>-NiCr coatings have been investigated and used to interpret their sliding wear behaviors. This study has identified and recommended optimized materials for improved coating properties based on the key findings and results analyses. These findings and model analyses contribute to the understanding of the relationship between feedstock features, sliding abrasive wear conditions, and the wear rates of HVOF-sprayed Cr<sub>3</sub>C<sub>2</sub>-NiCr coatings. Hence, the optimized manufacture method by advanced HVOF method will meet the on-going need for a robust alternative solution to hard chromium plating (HCP) method.

**9:40am MA3-3-WeM-6 Interface Amorphization Controls Maximum Wear Resistance of Multi-Nanolayer Carbon/WC Coatings, Narguess Nemati [narguess.nemati@gmail.com], Langtoftevej 9, Viby, Denmark**

Multilayer coatings offer significant advantages in protecting materials' surfaces by shielding the underlying materials hierarchically from damage and wear. The layering morphology and structure of multilayer coatings directly affect their wear resistance capacity. Using a systematic set of experiments and molecular dynamic simulations, we studied the effect of layering thickness on the macroscale wear response of DLC/WC multi-nanolayer coatings. Our study revealed the existence of a critical bilayer thickness where maximum scratch hardness and wear resistance can be achieved. Our large-scale molecular dynamics simulations showed that reducing the WC layer thickness to a certain limit increases the scratch

hardness due to the confinement of dislocation motion. However, when the thickness of WC layers falls below 2 nm, the deformation mechanism transitions from the interface-induced dislocation confinement to the interface-mediated amorphization of WC layers, reducing the scratch hardness of the coating. This finding offers a procedure for optimizing the macroscale wear performance of multi-nanolayer coatings.

## Protective and High-temperature Coatings

### Room Town & Country D - Session MA4-2-WeM

#### High Entropy and Other Multi-principal-element Materials II

**Moderators:** Prof. Dr. Jean-François Pierson, IJL - Université de Lorraine, France, Frederic Sanchette, Université de Technologie de Troyes, France

8:00am **MA4-2-WeM-1 Oxidation Resistance of High Entropy Nitride Thin Films Deposited by Magnetron Sputtering**, Djallel Eddine Touaibia, Abdelhakim Bouissil, Sofiane Achache, Mohamed El Garah, Frederic Sanchette [frederic.sanchette@utt.fr], Université de Technologie de Troyes, France **INVITED**

In the last decades, Refractory High Entropy Alloys (RHEAs) thin films have attracted more attention owing to their enhanced mechanical properties and better thermal stability at high temperatures, compared to conventional alloys. TiTaZrHfW-N and TiTaZrHfAl-N RHEAs thin films were deposited by reactive magnetron sputtering technology at different N<sub>2</sub> flow rates. For both systems, nitrogen-free films are amorphous, and the nitrides are columnar, single-phased with an FCC-NaCl type structure. The strong Me-N bonds lead to hardness up to 29 GPa and a Young's modulus up to 257 GPa, for the TiTaZrHfW-N system whereas the highest hardness and Young's modulus for the TiTaZrHfAl-N system are 25.3 GPa and 201.3 GPa respectively. Unlike metallic films, TiTaZrHfW-N and TiTaZrHfAl-N nitride films are thermally stable at 800 °C under vacuum and have a much better oxidation resistance. Nanolayered architectures TiTaZrHfW-N/Si<sub>3</sub>N<sub>4</sub> and TiTaZrHfAl-N/Si<sub>3</sub>N<sub>4</sub> result in a significant improvement of the oxidation resistance at 800 °C due to the formation of amorphous Si-N barrier nanolayers, hindering the oxygen diffusion.

8:40am **MA4-2-WeM-3 Plasmonic Behaviour of Multi-Component Nitride (TiVZrNbTa)<sub>x</sub> Thin Films**, Miguel Piñeiro [miguel.pineiro-sales@univ-lorraine.fr], Institut Jean Lamour - Université de Lorraine, France, Peru; Salah-Eddine Benazzouq, Institut Jean Lamour - Université de Lorraine, France, Morocco; Valentin Milichko, David Pilloud, Thomas Easwarakhanthan, Institut Jean Lamour - Université de Lorraine, France; Frank Mücklich, Saarland University, Germany; Jean-François Pierson, Institut Jean Lamour - Université de Lorraine, France

Although transition metal nitrides such as TiN or ZrN have been widely studied as plasmonic properties, the optical and electrical properties of multi-component nitride thin films are rather lacking in the literature for plasmonic applications, in spite of their well-known mechanical properties [1]. We attempt in this paper to alleviate this drawback by depositing the multi-component nitride (TiVZrNbTa)<sub>x</sub> films on silicon substrates by using reactive magnetron sputtering under different nitrogen flow rates (R<sub>N<sub>2</sub></sub>) and at different working pressures. The X-ray diffractograms of the as-deposited films have shown that they crystallize in a single-phase with a rocksalt-like structure. Moreover, the plasmonic potential of the films was investigated from their dielectric function determined by variable angle spectroscopic ellipsometry. The films prepared at low working pressures exhibit optimal metallic behaviour with the real part of their dielectric function displaying zero-crossover. In contrast, those fabricated at high working pressure show non-metallic behaviour without any zero-crossover and with low absorption in the near-infrared region. In particular, the real part of the dielectric function of the film produced at 0.5 Pa has a notable feature of double epsilon-near-zero (2ENZ) comparable to other transition metal nitrides such as TiN, ZrN and NbN [2-4]. The dielectric function of (TiVZrNbTa)<sub>x</sub> can be tuned by tailoring the deposition parameters such as working pressure to some desired plasmonic application. Specifically, the screened plasma energy (E<sub>ps</sub>) is tuneable from near UV to visible ranges, from 3.4 to 2.1 eV. Their plasmonic performance were evaluated by calculating their intrinsic quality factor for surface plasmon polaritons (SPP). Additionally, the free-carrier density, the scattering time and the electrical resistivity of the films were also determined by means of Drude model for the free charge carrier contribution to the dielectric function [2]. Drude parameters were compared with additional electrical measurements performed by four-probe method.

#### References

- [1] Von Fieandt, K., Pilloud, D., Fritze, S., Osinger, B., Pierson, J. F., & Lewin, E. Vacuum, 2021, 193, 110517.
- [2] Kassavetis, S., Hodroj, A., Metaxa, C., Logothetidis, S., Pierson, J. F., & Patsalas, P. Journal of Applied Physics, 2016, 120(22).
- [3] Guo, Q., Wang, T., Ren, Y., Ran, Y., Gao, C., Lu, H., ... & Wang, Z., Physical Review Materials, 2021, 5(6), 065201.
- [4] Ran, Y., Lu, H., Zhao, S., Guo, Q., Gao, C., Jiang, Z., & Wang, Z., Applied Surface Science, 2021, 537, 147981.

9:00am **MA4-2-WeM-4 Temperature Stability of High Entropy Ceramic Cr-Hf-Mo-Ta-W-N Refractory Metal Coatings**, Pavel Soucek [soucek@physics.muni.cz], Stanislava Debnarova, Matej Fekete, Masaryk University, Czechia; Sarka Zuzjakova, University of West Bohemia, NTIS, Czechia; Shuyao Lin, Technische Universitat Vienna, Austria; Ondrej Jasek, Tatiana Pitonakova, Masaryk University, Czechia; Nikola Koutna, Technische Universitat Vienna, Austria; Petr Zeman, University of West Bohemia, NTIS, Czechia

High entropy alloys (HEAs) are multi-component materials composed of five or more principal elements, with each element's content ranging from 5 to 35 atomic percent. The properties of HEAs arise from four core effects: the high entropy effect, severe lattice distortion, sluggish diffusion, and the cocktail effect. This high entropy concept also extends to ceramics, including oxides, nitrides, borides, and carbides.

In this study, we are examining the temperature stability of high entropy nitrides from the Cr-Hf-Mo-Ta-W-N system. We utilized magnetron co-sputtering of segmented elemental targets for all depositions, which were performed on silicon and sapphire substrates. The first set of depositions was conducted at ambient temperature, while an elevated temperature of 700°C was used for the second set to enhance coating crystallization.

All the deposited coatings exhibited strong diffraction peaks corresponding to a face-centred cubic (fcc) lattice, which is anticipated for the formation of these high entropy ceramics. The coatings were annealed at temperatures of 1000°C, 1200°C, and 1400°C to observe changes in their chemical composition, phase, crystal structure, morphology, and mechanical properties.

We will discuss the significant role of coating adhesion in withstanding annealing, the impact of nitrogen loss on changes in the coating structure, and the influence of the inherent multilayered structure of the coatings on phase emergence and stability. Furthermore, we will identify critical elements that enhance the temperature stability of the coatings and discuss the limits of high entropy stabilization in the studied nitride system.

9:20am **MA4-2-WeM-5 Influence of Si on Structural, Mechanical, and Thermal Properties of High Entropy Carbide Thin Films Based on (Hf, Ta, Ti, V, Zr)**, Muhammad Awais Altaf [muhammad.altaf@tuwien.ac.at], Alexander Kirnbauer, Balint Hajas, TU Wien, Institute of Materials Science and Technology, Austria; Szilard Kolozsvari, Plansee Composite Materials GmbH, Germany; Paul Mayrhofer, TU Wien, Institute of Materials Science and Technology, Austria

In this research work, high-entropy carbide thin films based on (Hf, Ta, Ti, V, Zr) with Si addition were developed by magnetron sputtering to explore the effects of Si on their structural, mechanical, and thermal properties. XRD results indicate that all films have a single-phase face-centered cubic (fcc) structure (Fm-3m, space group number 225). Si addition leads to an increased hardness (30 GPa to 36 GPa) and elastic modulus (396 GPa to 427 GPa). SEM Images of fractured cross-sections show that films containing Si have a higher thickness and less pronounced columnar growth. With the addition of Si, the onset temperature for an exothermic reaction during a thermal treatment increased from 665 °C to 703 °C. All the samples (without and with Si) retained their single-phase fcc structure even when annealed at 900 °C for 10 min in a vacuum. However, their elastic modulus slightly increased (e.g., from 423.34 GPa to 442.21 GPa for the film) while the hardness decreased (e.g., from 33.12 GPa to 29.08 GPa) with 21.72 at% Si in vacuum annealing. In summary, the structural, mechanical, and thermal properties of high-entropy carbide thin films were improved with the addition of Si.

# Wednesday Morning, May 14, 2025

11:00am **MA4-2-WeM-10 The Microstructure, Mechanical Properties and Performance of High-Entropy (AlCrTiMoVN)N Coatings Produced by Cathodic Arc Evaporation**, Qi Yang [qi.yang@nrc-cnrc.gc.ca], National Research Council of Canada; Alex Lothrop, Xiao Huang, Carleton University, Canada

High-entropy (AlCrTiMoVN)N coatings were prepared using cathodic arc evaporation. The target composition was varied to investigate the effect of nickel concentration on the microstructure, mechanical properties and tribological performance of the coatings. All coatings assume a B1 face centered cubic structure, and contain many small droplet and large splat defects; and the amounts of those defects increase with the concentration of Ni. All coatings showed excellent high-temperature phase stability. The hardness and elastic modulus of the coatings reached maximum values at 2% Ni and then, decreased as the Ni content increases. In terms of performance, the coating with 2% Ni had the lowest wear rate while in erosion testing the coating free of Ni had the lowest erosion rates. Overall, the presence of droplets/splats had a significant influence on the tribological performance of the coating.

11:20am **MA4-2-WeM-11 Correlating the Structural and Mechanical Properties of (AlCrNbSiTi)N Thin Films as a Function of Substrate Bias**, Vinay Joru [20enph03@uohyd.ac.in], Sudharshan Phani Pardhasaradhi, Venkata Girish Kotnur, University of Hyderabad, India

This study investigates the relationship between the structural and mechanical properties of (AlCrNbSiTi)N thin films deposited on Si (100) substrates using direct current magnetron sputtering (DCMS), varying the substrate bias from 0 to -200 V. Characterization techniques employed include X-ray diffraction (XRD) and X-ray photoelectron spectroscopy (XPS) for crystal structure analysis, along with field emission scanning electron microscopy (FESEM) and atomic force microscopy (AFM) for microstructural assessment. Mechanical properties were evaluated through nanoindentation. The results indicate that all films exhibit a NaCl-type face-centred cubic (FCC) crystal structure with a predominant (200) orientation. Notably, surface morphology transitioned from granular to triangular facets, eventually leading to a featureless and smooth appearance as substrate bias increased from 0 V to -200 V. The growth morphology shifted from columnar to dense and featureless with increasing bias. Additionally, film thickness decreased from 950 nm to 650 nm due to ion bombardment during growth. Mechanical properties improved significantly, with hardness rising from 18 GPa to 31 GPa and film modulus increasing from 173 GPa to 261 GPa as substrate bias changed from 0 V to -200 V. The ratios  $H/E$  and  $H^3/E^2$  for the film at -200 V were found to be 0.12 and 0.44, respectively, surpassing values reported in existing literature for the (AlCrNbSiTi)N system. This enhancement in mechanical properties will be reported in correlation with their structural characteristics.

**Keywords:** (AlCrNbSiTi)N thin films, substrate bias, growth mechanism, and mechanical properties.

11:40am **MA4-2-WeM-12 Effect of Elemental Concentration on Mechanical and Tribological Properties of (AlNbSiTiZr)N Thin Films**, Tongyue Liang [tongyue.liang@mail.mcgill.ca], Stéphanie Bessette, Raynald Gauvin, Richard Chromik, McGill University, Canada

(AlNbSiTiZr)N thin films were deposited on silicon wafer and steel substrates using pulsed DC magnetron sputtering with four distinct targets (AlSi, Ti, Nb, Zr). The elemental concentration of each constituent was tuned by adjusting the discharge current applied to each target. The thickness of the deposited films was maintained at approximately 1.3  $\mu\text{m}$ . Three different (AlNbSiTiZr)N thin films with slight variations in elemental concentrations were studied to assess the impact of compositional changes on their structure and properties. The films were characterized for surface and cross-sectional morphology, microstructure, roughness, and mechanical properties. A minor increase in the concentrations of Nb and Zr (5 at.% for each) led to a significant improvement in hardness, increasing from  $12.7 \pm 0.7$  GPa to  $20.8 \pm 0.5$  GPa. The tribological properties of the films were studied using a ball-on-plate tribometer under dry air conditions with a load of 0.5 N for 1000 sliding cycles. The results indicate that the wear resistance of the (AlNbSiTiZr)N thin films improved with the increased concentrations of Nb and Zr.

**Tribology and Mechanics of Coatings and Surfaces**  
Room Palm 5-6 - Session MC2-2-WeM

## Mechanical Properties and Adhesion II

**Moderators:** Nagamani Jaya Balila, Indian Institute of Technology Bombay, India, Bo-Shiuan Li, National Sun-Yat Sen University, Taiwan

8:00am **MC2-2-WeM-1 Adhesion, Delamination and Cracking of Thermal Spray Coatings: Understanding Critical Phenomena During Processing and Service**, Sanjay Sampath [sanjay.sampath@stonybrook.edu], Stony Brook University, USA

**INVITED**

The efficacy of coatings in engineering applications rely on their ability to be well bonded to the underlying substrate. Many factors govern this adhesion including deposition materials, substrate materials, substrate attributes, surface chemistry, processing conditions, thickness, build rate, mismatch between the coating and substrate etc. Methods to measure adhesion in present day is largely phenomenological with “go/no-go” agenda. Of importance is that today’s measures of adhesion strength may not be appropriate for coatings which are largely brittle, where cracking is a predominant mode of failure representing a toughness problem rather than strength consideration. Furthermore, even well bonded coatings can delaminate during service where compounding effects of service load can superpose to accentuate the interfacial stresses. Thus, understanding these phenomena is critical. The debonding of the interface is driven by energy dissipation. In situation where bonding is strong, an alternative energy release mechanism is cracking of the coating. When harnessed they provide a pathway to build strain-tolerant vertically cracked coating with implications for novel design and manufacturing of thermo-structural coatings. In many instances, the factors of cracking and delamination compete. This is dependent on adhesion and microstructure. In this presentation, the above attributes are critically discussed through phenomenological and quantitative strategies.

8:40am **MC2-2-WeM-3 A Study on the Surface Morphology and Tribological Behavior of Hydrided Zircaloy**, Jun Xian Lin [linst214200@gmail.com], Kuan-Che Lan, National Tsing Hua University, Taiwan

The integrity of used nuclear fuel claddings is one of the keys to assess the safety margin during interim dry storage. Nuclear fuel claddings made of zirconium alloys have been widely applied in commercial nuclear reactors such as boiling and pressurized water reactors. The accumulation of hydrogen in the form of zirconium hydride which could deteriorate the integrity of used nuclear fuel claddings during interim dry storage is one of critical concerns intrinsically. Besides, existence of hydride in zirconium alloys could weaken the tribological resistance of the cladding materials during the loading and transportation procedures of used fuel prior to a long-term dry storage and hurt the integrity externally. A thorough understanding of about the microstructure and tribological behavior of zirconium alloy with hydrides will improve the reliability of evaluation on the integrity of used fuel cladding during interim dry storage. The objective is to study the influence of zirconium hydride on the tribological resistance. Scratch tests were conducted on as-hydrided Zircaloy-4 plate using a scratch tester to determine the minimum load causing cracks and to analyze the morphology of surface cracks. Additionally, a pin-on-disc test was conducted to assess the wear resistance, followed by SEM analysis over the damaged surface to observe the effect of hydrogen permeation on the tribological behavior of the Zircaloy-4.

9:00am **MC2-2-WeM-4 Effects of Stored Elastic Energy and Stress Gradients on the Tribological Behavior of TiN Coatings on D2 Steel**, I-Sheng Ting [gary820902@yahoo.com.tw], Jia-Hong Huang, National Tsing Hua University, Taiwan

Residual stress is one of the most pivotal issues in protective hard coatings deposited by physical vapor deposition methods. It is generally acknowledged that low residual stress is beneficial for prolonging the lifespan of hard coatings. In our previous studies [1,2], a Ti interlayer was added to alleviate the residual stress of TiZrN coating on D2 steel, thereby improving its wear resistance. An energy-based hypothesis was proposed to explain the enhancement in wear resistance [2], where by lowering the stored elastic energy ( $G_s$ ) in the TiZrN coating, the margin for reaching the fracture toughness ( $G_c$ ) was extended, indicating that the coating could endure more external loading. However, the energy-based perspective neglected the effect of stress gradient that significantly affects the propagation of cracks in coatings. This study aimed to measure the stored elastic energy and energy gradients of TiN coating on D2 steel and evaluate the effect of gradients on the tribological behavior. TiN coatings were

deposited on D2 steel and Si substrates using DC unbalanced magnetron sputtering, where the stress gradient of TiN coating was controlled by adjusting the working pressure during deposition. The average stress of the TiN coating was determined using the average X-ray strain (AXS) combined with nanoindentation methods [3-5], and the stress gradient was acquired by changing the X-ray incident grazing angles. The adhesion and wear resistance of the TiN coatings on D2 steel were respectively evaluated using scratch test and pin-on-disk wear test. Through the adjustment of working pressure during deposition, it is feasible to control the tribological behavior of a hard coating by tuning the distribution of stored elastic energy and stress gradients.

- [1] Y.-W. Lin, J.-H. Huang, W.-J. Cheng, G.-P. Yu, Surf. Coat. Technol., 350 (2018) 745-754.  
[2] Y.-W. Lin, P.-C. Chih, J.-H. Huang, Surf. Coat. Technol., 394 (2020) 125690.  
[3] C.-H. Ma, J.-H. Huang, H. Chen, Thin Solid Films, 418 (2002) 73-78.  
[4] A.-N. Wang, C.-P. Chuang, G.-P. Yu, J.-H. Huang, Surf. Coat. Technol., 262 (2015) 40-47.  
[5] A.-N. Wang, J.-H. Huang, H.-W. Hsiao, G.-P. Yu, H. Chen, Surf. Coat. Technol., 280 (2015) 43-49.

9:20am **MC2-2-WeM-5 Adhesion at the Glass/Metal interface probed by Colored Picosecond Acoustics, Arnaud Devos [arnaud.devos@iemn.fr], IEMN, France**

Glass is a common material already employed in everyday applications, which has gained considerable interest for electronic components, due to its attractive electrical, physical, and chemical properties, as well as its prospects for a cost-efficient solution. Adhesion of thin metal film on glass is especially critical and bonding between glass and metal can broaden the applications of glass in many industrial areas. A large number of methods have been developed to characterize the adhesion of a thin film to a substrate. Acoustic waves and especially ultra-high frequency acoustic waves are also sensitive to adhesion defects as they affect the way acoustic waves are transmitted and reflected at the interface concerned. At a poor interface, acoustic waves are much more reflected than expected and therefore much less transmitted. In this work, we use picosecond acoustics for measuring the metal film thickness and the acoustic transmission coefficient at the interface with a glass substrate. Picosecond acoustics is a ultrafast laser technique that implements a nanoscale pulse-echo technique [1]. A femtosecond optical pulse excites a short acoustic pulse inside the sample and another optical pulse is used to monitor acoustic propagation and reflections. We show that we can take advantage of the laser tunability to improve the measurement of adhesion between metal and glass: by making picosecond acoustic measurements at different wavelengths (spectroscopy), we observe very sensitive changes in the photo-acoustic response which can be used to improve measurement accuracy.

References: [1] A. Devos, Ultrasonics 56, pp. 90-97 (2015) DOI 10.1016/j.ultras.2014.02.009

9:40am **MC2-2-WeM-6 The Mechanical and Tribological Performance of (V,Mo)N Coatings Deposited by Magnetron Sputtering, Yuqun Feng, Jia-Hong Huang [jhuang@ess.nthu.edu.tw], National Tsing Hua University, Taiwan**

The wear resistance of transition metal nitrides (TMeNs) can be enhanced by introducing self-lubricating oxide forming alloy elements, such as V and Mo. However, TMeNs are usually brittle under dynamic loading conditions. (V,Mo)N is a recently developed material for wear-resistant coatings due to its high fracture toughness. The objective of this study was to evaluate the mechanical and tribological properties of single-phase (V,Mo)N coatings. (V,Mo)N coatings with different N/metal ratios were deposited on AISI D2 steel substrates using direct current unbalanced magnetron sputtering (dc-UBMS) and high power pulsed magnetron sputtering (HPPMS). The results showed that the coatings deposited on steel substrates have higher N/metal ratio and (200)-preferred orientation than those on Si substrates. This may be attributed to the higher electrical conductivity of the steel substrate, leading to more intense ion bombardment that delivers more energy in forming N-metal bonding and enhances the channeling effect. The hardness of the coatings increases with decreasing N/metal ratio. Additionally, the coatings deposited by HPPMS on steel substrates have lower residual stress than those by dc-UBMS. This may be due to the stress induced by the power cycle being relieved by plastic deformation of the steel substrate. All (V,Mo)N coatings show a very low wear rate ranging from  $1.1 \times 10^{-7}$  to  $4.0 \times 10^{-7}$  mm<sup>3</sup>N<sup>-1</sup>m<sup>-1</sup> at room temperature. As temperature

increases to 500 °C and above, the wear resistance of the (V,Mo)N coatings significantly decreases, while low friction coefficients are maintained by the formation of self-lubricating V- and Mo-oxides. All coatings remain intact after 150k impact fatigue test, even when the deformation depth is larger than the coating thickness, implying the remarkable toughness of the (V,Mo)N coatings. In contrast, the coatings deposited using dc-UBMS have the worst impact fatigue resistance, which may be related to their lower fracture toughness.

## Tribology and Mechanics of Coatings and Surfaces Room Town & Country C - Session MC3-1-WeM

### Tribology of Coatings and Surfaces for Industrial Applications I

**Moderators: Rainer Cremer, KCS Europe GmbH, Germany, Stephan Tremmel, University of Bayreuth, Germany**

9:00am **MC3-1-WeM-4 Cyclic and Randomized Micro-Impact Tests of Coatings for Erosion Protection: Role of Multilayer Structure in Providing Damage Tolerance, Ben Beake [ben@micromaterials.co.uk], Micro Materials Ltd, UK; Daniel Tobola, Lukaszewicz Research Network, Krakow Institute of Technology, Poland; Lukasz Maj, Institute of Metallurgy and Materials Science of Polish Academy of Sciences, Krakow, Poland; Tomasz Liskiewicz, Manchester Metropolitan University, UK; Puneet Chandran, Lukaszewicz Research Network, Krakow Institute of Technology, Poland**

Coating systems for applications in machining and forming tools, and in applications where they are subject to solid particle erosive wear, are subject to high loads which can result in high wear and premature failure. To aid the design of coating systems to mitigate this with improved surface fatigue resistance, cyclic micro-impact tests have been performed on three hard multilayered coatings (TiN/TiCrN/TiN, TiN/TiCrN/10x(TiN/CrN)/TiN and 25x(Cr/CrN)) deposited by arc evaporation onto hardened tool steel and results compared to a monolayer TiN reference. To more closely replicate the statistical, and apparently stochastic, distribution of multiple impacts that occur in solid particle erosion randomized micro-impact tests were performed where multiple impacts occur with controlled energy at different (chosen) locations on the coating surface. The cyclic and randomized impact tests were both performed using a multi-sensing approach where the depth and dissipated energy were monitored for every impact improving detection of the onset of severe wear. The multilayered TiN-based coatings were more prone to chipping than the monolayer TiN in the cyclic and randomized tests. Although the 25x(Cr/CrN) coating was susceptible to radial cracking and cracking within impact craters this localized cracking relieved the impact-induced stresses and minimized the chipping failure found on the other coatings. SEM and TEM imaging has been used to investigate the impact damage phenomena.

9:20am **MC3-1-WeM-5 Effect of Bias Voltage and Temperature on the Structural and Tribo-Mechanical Properties of Chemically Complex TiSiBn Nanocomposites, Wolfgang Tillmann, Julia Urbanczyk [julia.urbanczyk@tu-dortmund.de], TU Dortmund University, Germany; Alexander Thewes, TU Braunschweig University, Germany; Nelson Filipe Lopes Dias, TU Dortmund University, Germany**

TiSiBn thin films show promising properties for applications at elevated temperatures due to improved thermal stability and oxidation resistance, as well as friction-reducing characteristics. While previous studies investigated mainly the effect of the chemical composition on the thin film properties, it remains unclear how deposition parameters, such as the bias voltage and the heating power, affect the structural and tribo-mechanical properties of TiSiBn. For this reason, the effect of the bias voltage and heating power on magnetron-sputtered TiSiBn nanocomposites with different chemical compositions was analyzed. In the first line of investigation, the bias voltage was varied from -100, -150, and -200 V, and in the second line, the heating power was set to 2, 5, and 8 kW.

The chemical composition remains nearly unaffected by the heating power, while the bias voltage has a slight effect on the quantity of the elements. X-ray diffraction (XRD) analysis revealed a polycrystalline structure with randomly oriented crystallites, characterized by different peak shifts depending on the chemical composition. Identified crystalline phases include TiN, TiC, TiB, and TiB<sub>2</sub>, coexisting with various amorphous phases. Transmission electron microscopy (TEM) images reveal a nanocomposite structure and changes in microstructure, such as crystallite refinement with higher bias voltage or growth, as well as further self-assembly with higher deposition temperatures, depending on the chemical composition and

# Wednesday Morning, May 14, 2025

initial phase structure. An increased bias voltage induces residual stresses while the hardness tends to decrease. With higher heating power, internal stresses are released and the hardness increases up to 41 GPa. To explore the application potential of the TiSiBCN thin films for forming processes of aluminum alloys, the tribological behavior was evaluated against AW-6060 in tribometer tests, highlighting TiSiBCN as a promising protective coating.

9:40am **MC3-1-WeM-6 Lubrication Mechanism of CrAIN+MoWS Coatings in Gear Contacts under Dry Rolling-Sliding Conditions**, *Kirsten Bobzin, Christian Kalscheuer, Max Philip Möbius, Marta Miranda Marti [marti@iot.rwth-aachen.de]*, Surface Engineering Institute - RWTH Aachen University, Germany

The use of liquid lubricants for wear and friction reduction in geared transmissions is well established. However, in applications like the food industry, liquid lubricants are undesirable due to contamination risks. A promising alternative involves applying a wear-resistant CrAIN coating incorporated with solid lubricant components, such as molybdenum, tungsten and sulfur. Previous studies demonstrated the functionality of graded CrAIN+MoWS coatings, analyzing the lubrication mechanism on flat samples using pin-on-disc method. Further studies extended this analysis to gear applications, where the coating reduced friction and wear by 88 % compared to uncoated contacts.

In this study the lubrication mechanism of PVD deposited graded CrAIN+MoWS on gears was analyzed. The coated wheels were tested against uncoated pinions under varying Hertzian pressure at pitch point, with  $p_{H1} = 589 \text{ N/mm}^2$  and  $p_{H2} = 1.723 \text{ N/mm}^2$ , and circumferential speed  $v_{t1} = 2 \text{ m/s}$  and  $v_{t2} = 8,3 \text{ m/s}$ . After tribological testing, the gear tooth surfaces were examined using confocal laser scanning microscopy (CLSM) and energy-dispersive X-ray spectroscopy (EDX) to determine the coating distribution. Raman spectroscopy was employed to analyze the possible formation of the solid lubricant  $\text{MoS}_2$  and  $\text{WS}_2$  phases, as well as other friction-reducing oxides. At lower Hertzian pressures, the triboactive elements on the wheel tooth flank are effectively consumed, leading to a friction reduction compared to uncoated gear contacts. On the wheel tooth faces, the triboactive elements remain present and are identified through Raman spectroscopy as  $\text{MoS}_2$ , which could further contribute to friction reduction. On the corresponding uncoated pinions, traces of Mo, W, and S are detected, confirming the effective transfer mechanism of CrAIN+MoWS coatings in gear contacts at lower Hertzian pressure. At higher Hertzian pressures and high circumferential speeds, traces of  $\text{MoS}_2$  are observed on the wheel tooth face, indicating the coating consumption to reduce friction and demonstrating the effectiveness of the coating under extreme testing conditions, which expand the gear's lifespan compared to uncoated gear contacts.

The results demonstrate the lubrication mechanism of the CrAIN+MoWS coating in gear contact.  $\text{MoS}_2$  is generated at the gear contact, even under low Hertzian pressure, and is efficiently utilized within the contact zone to ensure a friction reduction. At higher speeds, these triboactive elements remain effective, continuing to enhance lubrication and reduce wear within the gear contact when compared to uncoated gears.

11:00am **MC3-1-WeM-10 Wear Protection via Triboactive CrAlMoN Coatings in Chain Drives**, *Kirsten Bobzin, Christian Kalscheuer, Max Philip Möbius [moebius@iot.rwth-aachen.de]*, Surface Engineering Institute - RWTH Aachen University, Germany; *Martin Rank, Oliver Koch*, Institute of Machine Elements, Gears and Tribology - RPTU Kaiserslautern-Landau, Germany

Within chain drives, critical wear occurs between the chain pin and chain bush, leading to chain elongation. This determines the service life of a chain. Hard coatings deposited by physical vapor deposition (PVD), such as CrAIN, can effectively reduce wear. However, coating the inner surfaces of chain bushes presents economic and technological challenges. A promising alternative is the use of triboactive CrAlMoN coatings, which interact with lubricants and their additives to form protective tribofilms. These tribofilms can transfer to uncoated chain bushes, providing essential wear protection.

In this study, three chains were assembled using uncoated, CrAIN and CrAlMoN coated pins. These chains were then tested on a chain drive test bench. All chains were lubricated with grease containing sulfur additives. Analyses of the as-coated chain pins included geometry, surface roughness, coating thickness, coating morphology and compound adhesion. The chains underwent testing under medium load conditions corresponding to a power transmission of  $P_M = 2.3 \text{ kW}$  and high load conditions corresponding to  $P_H = 9.5 \text{ kW}$ . Wear was monitored through periodic measurements of chain elongation to determine wear rates over time. Upon completion of testing, both chain pins and bushes were analyzed for visual appearance

changes, wear volume, surface topography, and remaining coating thickness. Under medium load conditions, CrAlMoN coated chains exhibited slightly higher wear rates compared to reference systems. However, under high load conditions, CrAlMoN coated chains demonstrated the lowest wear rates among all tested configurations. Notably, wear distribution between the chain pin and bush was more uniform in CrAlMoN coated systems compared to others where higher wear predominantly affected uncoated bushes.

This observation suggests that the formation and transfer of protective tribofilms in CrAlMoN systems contribute significantly to enhanced wear resistance under high stress conditions. Analysis after high-load testing revealed that CrAlMoN coated pins retained substantial coating thickness within the wear areas of the pin. The findings indicate that triboactive CrAlMoN coatings hold considerable promise for reducing wear in high-performance chain drives by forming protective tribofilms during tribological operation that can be transferred to uncoated chain bushings.

11:20am **MC3-1-WeM-11 Tribological Contact Formation on PVD-Coated Tools**, *Aljaz Drnovsek [aljaz.drnovsek@ijs.si], Peter Panjan, Matjaž Panjan, Miha Čekada*, Jožef Stefan Institute, Slovenia

INVITED

Tools surface topography changes dramatically after PVD coating deposition. Various topographical imperfections on the coating surface can negatively impact the quality of the coating and, in some cases, cause the failure of the coating. The imperfections in coated forming tools initiated over a decade of research into the phenomena associated with coating surfaces, particularly the growth defects.

I will present results related to the formation of the coating topography and how it depends on factors such as substrate material, ion etching, and deposition processes. The topographical features of the coating significantly influence oxidation, corrosion, and especially the tribological behavior of PVD coatings.

The influence of the coated surface on the formation of a tribological contact has been the focus of several studies, as the contact area between two sliding bodies is not constant with time. Initially, only the asperities which appear as growth defects are in real contact with the counter body. Under load, these asperities can fracture, spall, and produce small particles. The real contact area is increasing sharply before it stabilizes. In terms of friction, we recognize this behavior as the running-in period. The coefficient of friction increases in this period until it reaches a steady state value. It is still poorly understood how this transition from the run-in to the steady state friction occurs and, more importantly, how the growth defects affect the tribological performance. The role of defects in the formation of the tribological contact changes depending on counter body materials and operating temperature. The latter was studied recently. The results indicate that in the case of the TiAIN coating, the highest wear was measured during the room temperature test. Conversely, the wear during the running-in phase and steady-state friction were low at elevated temperatures initially, but as the temperature increased, the wear rate rose, which can be attributed to increased tribological oxidation and fatigue.

The growth defects on the coating surface played a significant role in the friction and wear behavior, as they were a primary source of wear particles and the first spots of oxidation on the coating. The measurements suggest that the running-in phase depends mainly on the asperities density at room temperature tests. In contrast, at high temperatures, they attributed to the formation of a stable tribological oxide layer in the wear track, which elongates the running-in period and protects the coating underneath.

12:00pm **MC3-1-WeM-13 Effect of Transition Metals (Nb, V, and Ta) Doping on the High-Temperature Mechanical and Tribological Properties of CrYN Coatings**, *Gokhan Gulten, Banu YAYLALI, Mustafa YESILYURT, Yasar TOTIK*, Atatürk University, Turkey; *Justyna Kulczyk Malecka, Peter Kelly*, Manchester Metropolitan University, U.K.; *Ihsan EFEGLU [iefeoglu@atauni.edu.tr]*, Atatürk University, Turkey

This study aims to develop a high temperature wear resistant coating for AISI 316L. As a functional coating, CrYN coatings with added niobium, tantalum, and vanadium (a-C:H:Nb/Ta/V) were deposited using a closed-field unbalanced magnetron sputtering (CFUBMS) system. The Taguchi L9 orthogonal array approach was used to test and systematically change a variety of parameters in order to achieve the optimal coating properties. The microstructural properties of the coatings were examined using a scanning electron microscope (SEM), while X-ray diffraction (XRD) and X-ray photoelectron spectroscopy (XPS) analysis were conducted to determine crystallographic and surface chemistry properties, providing a detailed understanding of the coating structure. Nanoindentation tests were performed to determine mechanical properties, yielding precise

# Wednesday Morning, May 14, 2025

measurements of hardness and elasticity. The adhesion of the coatings was measured through scratch tests at varying temperatures (400, 600, and 800 °C) and room temperature. The tribological characteristics of the a-C:H:Nb/Ta/V coatings were assessed using a high-temperature pin-on-disc tribometer, examining their wear resistance and frictional behavior under ambient air and at varying temperatures (400, 600, and 800 °C). These comprehensive analyses reveal the potential of the a-C:H:Nb/Ta/V coatings for applications requiring enhanced surface properties, offering superior tribological performance across different temperature conditions.

## Surface Engineering of Biomaterials, Medical Devices and Regenerative Materials

### Room Palm 1-2 - Session MD2-WeM

#### Surface Response to Biological Environments, Biointerphases, and Regenerative Biomaterials

**Moderators:** **Po-Chun Chen**, National Taipei University of Technology, Taiwan, **Dr. Jean Geringer**, Ecole Nationale Supérieure des Mines, France, **Dr. Hamdy Ibrahim**, University of Tennessee at Chattanooga, USA

8:00am **MD2-WeM-1 Modulating Cell Responses via Surface Engineering**, **Huinan Liu** [[huinanliu@engr.ucr.edu](mailto:huinanliu@engr.ucr.edu)], University of California, Riverside, USA **INVITED**

Engineered surfaces provide promising solutions to meet the clinical needs for medical implants and devices. Bioresorbable implants and devices are designed to degrade harmlessly in the body over time as new tissues grow, which eliminates the need for secondary surgeries and associated complications. Recent researches on biodegradable polymers and metals have demonstrated their potentials for clinical applications, but there are still major challenges yet to be addressed, e.g. (1) controlling their degradation rates and cellular responses to match tissue healing rates, and (2) modulating their bioactivities to promote healing functions of desirable cells while inhibiting bacterial infections. In this presentation, our recent progress on engineering bioresorbable alloys and surfaces to regulate the degradation rates and cell responses will be presented. The relationships between surface microstructure, degradation, and interactions with host cells and pathogenic microorganisms will be discussed.

8:40am **MD2-WeM-3 Nanomaterials and Thin Films: Revolutionizing Bio-Applications for Early Disease Detection**, **Samir Iqbal** [[smiqbal@utrgv.edu](mailto:smiqbal@utrgv.edu)], University of Texas at Rio Grand Valley, USA **INVITED**

Modern nanofabrication techniques have enabled the creation of innovative architectures to interface with living systems, opening new frontiers in biotechnology and medical diagnostics. These development involves nanostructured or nanotextured sensor interfaces made from diverse materials, which exhibit remarkable antibacterial properties, enhanced cell adhesion, and, in some cases, unique interactions with normal and diseased cells. These surfaces hold significant promise for advancing biomedical applications.

Simultaneously, advancements in electronic miniaturization have led to the reproducible fabrication of nanoscale devices capable of interfacing with biological molecules. Leveraging microfluidics and nanoscale features, these devices can detect and identify molecular biomarkers and diseased cells with unprecedented precision. Such systems enable rapid, label-free, and selective chemical analyses from minute sample volumes, offering transformative potential for early diagnostics. Early detection of diseased cells, particularly when present in small numbers, is critical for improving survival rates in conditions such as cancer.

Nanomanufactured frameworks allow the combinatorial measurement of viscoelastic, mechanical, electrical, and chemical properties to transduce molecular and cellular anomalies into meaningful diagnostic signals. This talk will explore the role of nanoscale thin film properties in disease detection, emphasizing the importance of early cancer diagnosis. A comprehensive overview of molecular detection, isolation, and sorting of diseased cells using nanotechnology and microfluidics will also be provided, highlighting the transformative potential of these approaches in modern medicine.

9:20am **MD2-WeM-5 Green Fabrication of Conductive Carbon Thin Film Patterns for Biosensors**, **Ying-Chih Liao** [[liaoy@ntu.edu.tw](mailto:liaoy@ntu.edu.tw)], National Taiwan University, Taiwan **INVITED**

The demand for sustainable and cost-effective materials in biosensing is growing, especially for real-time and portable health monitoring. However, conventional electrode fabrication methods often require multiple

processing steps and use non-renewable materials. This reliance raises environmental concerns and limits scalability. In this study, a green approach is developed to directly transform biodegradable bacterial cellulose (BC) into conductive carbon thin films using CO<sub>2</sub> laser-induced carbonization under ambient conditions for biosensor fabrication. Bacterial cellulose (BC) a biopolymer generated by specific bacteria, features a highly porous, nanoscale fibrous structure along with notable mechanical strength and biocompatibility. These properties make it a highly versatile material for biomedical applications. The laser-induced carbonization process leverages these unique structural features of BC, converting it into a conductive carbon matrix suitable for electrochemical applications. This one-step technique involves the precise application of a CO<sub>2</sub> laser, which locally heats the BC, breaking down organic components and rearranging carbon atoms to create conductive graphitic structures.

This approach integrates essential elements into the BC matrix, enhancing conductivity and sensor functionality without requiring complex post-treatments. The laser-induced carbonized BC electrode offers promising detection capabilities for glucose and lactate, enabling concurrent sensing in phosphate buffer solution (PBS) and demonstrating selectivity, reproducibility, and stability, verified through differential pulse voltammetry (DPV). This streamlined laser carbonization method facilitates electrode fabrication and yields electrodes capable of application in real sweat sample analysis. These characteristics highlight BC-based electrodes as highly promising candidates for portable, cost-effective on-site biosensors for monitoring key biomarkers in sweat, underscoring the potential of laser-induced carbonization in advancing sustainable, high-performance materials for health monitoring technologies.

11:00am **MD2-WeM-10 Functionalized Graphene for Sensor Applications**, **Chi-Hsien Huang** [[chhuang@mail.mcut.edu.tw](mailto:chhuang@mail.mcut.edu.tw)], Ming Chi University of Technology, Taiwan **INVITED**

Graphene (G), a one-atom-thick, two-dimensional material, exhibits great potential as a biosensor transducer due to its high sensitivity to foreign atoms or molecules. However, its inertness limits its application, making functionalized graphene is very crucial for biosensor applications. In this presentation, I will talk about an atomic layered composite of graphene oxide/graphene (GO/G) by functionalizing chemical vapor deposition (CVD)-grown bilayer graphene (BLG) using our developed low damage plasma treatment (LDPT). This process selectively oxidized only the top layer of BLG, leaving the bottom layer intact. The GO top layer provides active sites for stable covalent bonding with biorecognition elements, while the G bottom layer acts as a sensitive transducer. With this GO/G composite, we constructed a solution-gated field effect transistor (SGFET)-based biosensors for miRNA-21, a cancer biomarker and p-tau 217, a Alzheimer's disease biomarker. In addition, laser induced graphene attracts a lot of attention because the preparation is low-cost, easy pattern fast and environment friendly. However, the electrochemical performance of standalone LIG is limited. To address this, the study enhances LIG by synthesizing nickel-iron Prussian blue analogues through co-precipitation and calcination, forming porous NiFe-Oxide, which is subsequently deposited onto the LIG surface via a facile physical deposition method. The porous NiFe-Oxide@LIG electrode material demonstrates excellent electrochemical sensing capabilities due to its high conductivity, improved surface area, enhanced active sites, and superior electrocatalytic performance for detecting the antioxidant propyl gallate (PG).

Keywords: graphene, LIG, sensor, biomarker

References:

1. S. Chinnapaiyan, N. R. Barveen, S.-C. Weng, G.-L. Kuo, Y.-W. Cheng, R. A. Wahyuno, C.-H. Huang\*. *Sensors and Actuators B: Chemical*, 423, 136763, 2025
2. S.-H. Ciou, A.-H. Hsieh, Y.-X. Lin, J.-L. Sei, M. Govindasamy, C.-F. Kuo\*, C.-H. Huang\*. *Biosensors and Bioelectronics*, 228, 115174, 2023.
3. C.-H. Huang\*, W.-T. Huang, T.-T. Huang, S.-H. Ciou, C.-F. Kuo, A.-H. Hsieh, Y.-S. Hsiao, Y.-J. Lee. *ACS Applied Electronic Materials*, 3, 4300-4307, 2021.
4. C.-H. Huang\*, T.-T. Huang, C.-H. Chiang, W.-T. Huang, Y.-T. Lin. *Biosensors and Bioelectronics*, 164, 112320, 2020.



## Plasma and Vapor Deposition Processes

### Room Town & Country B - Session PP2-1-WeM

#### HiPIMS, Pulsed Plasmas and Energetic Deposition I

**Moderators:** Dr. Martin Rudolph, Leibniz Inst. of Surface Eng. (IOM), Germany, Dr. Shimizu Tetsushide, Tokyo Metropolitan University, Japan

8:00am **PP2-1-WeM-1 Energetics and Chemistry of Cathodic Arc Ti-N Plasma: A Combinatorial Investigation Using Experimental Probes and Fluid Mechanical Modelling, Nikolaos Giochalas [nikolaos.giochalas@liu.se]**, Linköping Univ., IFM, Nanostructured Materials Div., Sweden; *Grzegorz Greczynski*, Linköping Univ., IFM, Thin Film Physics Div., Sweden; *Ferenc Tasnadi*, Linköping Univ., IFM, Theoretical Physics Div., Sweden; *Lina Rogström, Magnus Odén*, Linköping Univ., IFM, Nanostructured Materials Div., Sweden

Cathodic Arc Deposition, a commonly used PVD process of growing hard coatings, involves high fluxes of ions and electrons in a dense, expanding plasma. The composition of the arc plasma may vary significantly within the deposition chamber, and the source-to-substrate distance impacts the coating growth conditions. This study investigates the Ti-N plasma generated by a 100 mm, dc-operated arc source at 20 V and 120 A, in an 1 Pa N<sub>2</sub> ambient within a cylindrical, lab-scale HV chamber. A combinatorial approach of experimental probes and finite element fluid mechanical modelling is used to understand the varying plasma composition in terms of ions, neutrals, and radicals, and their corresponding fluxes. The measured and simulated ion species are Ti<sup>1+</sup>, Ti<sup>2+</sup>, Ti<sup>3+</sup>, Ti<sup>4+</sup>, TiN<sup>1+</sup>, TiN<sup>2+</sup>, N<sub>2</sub><sup>1+</sup>, and N<sup>1+</sup>. The dominant ion species in every probed spatial configuration is Ti<sup>2+</sup>, while Ti<sup>1+</sup> follows closely and equalizes the energetic footprint of Ti<sup>2+</sup> when the distance from the source is increased. Atomic Nitrogen ions maintain a significant presence throughout the plasma volume, largely due to a sustained emission from the nitrided Ti-source surface, N<sub>2</sub> dissociation and charge exchange collisions. In general, the plasma density and average charge state follow a decreasing trend for distances larger than 35 cm from the source, where the presence of Ti<sup>3+</sup> and Ti<sup>4+</sup> is suppressed. At the same time, TiN-ions retain their presence, leading to different growth conditions at the substrate, depending on the chosen distance from the source.

8:20am **PP2-1-WeM-2 Exploring the Microstructure and Mechanical Properties of TiZrNbTaMoN Highentropy Alloy Nitride Coating: Effect of Nitrogen Content, Sen-You Hou [housenyou23@gmail.com]**, National Tsing Hua University, Taiwan, China; *Po-Yu Chen*, National Tsing Hua University, Taiwan; *Bih-Show Lou*, Chang Gung University, Taiwan; *Jyh-Wei Lee*, Ming Chi University of Technology, Taiwan

The highpower impulse magnetron sputtering (HiPIMS) generates highdensity plasma through higher instantaneous pulse currents, resulting in thin films with fewer defects, higher density, and denser microstructure. In this work, a combination of HiPIMS and radio frequency power supply system was used to deposit TiZrNbTaMoN highentropy alloy (HEA) thin films with varying nitrogen contents on Si wafer, AISI304 and 420 stainless steel substrates. The cross-sectional morphology, composition, and crystal structure of thin films were analyzed using scanning electron microscopy, electron probe microanalyzer, X-ray diffraction, and transmission electron microscope, respectively. Subsequently, potentiodynamic polarization corrosion tests were conducted on the HEA thin films in 3.5 wt.% NaCl aqueous solution using an electrochemical workstation to evaluate their corrosion resistance. We found that TiZrNbTaMoN HEA nitride coatings exhibited a hardness of up to 29 GPa, along with outstanding corrosion resistance. The effect of nitrogen content on the phase, mechanical properties, and corrosion resistance of TiZrNbTaMoN HEA thin films was discussed in this work. The potential applications for the TiZrNbTaMoN HEA thin films in the machining industries were proposed.

8:40am **PP2-1-WeM-3 Insights into the Carbon HiPIMS Discharge: Ionized Flux Fraction and Ion Energy Distribution, Tetsuhide Shimizu [simizu-tetuhide@tmu.ac.jp]**, Ryo Sakamoto, Erdong Chen, Tokyo Metropolitan University, Japan; *Caroline Hain*, Empa, Swiss Federal Laboratories for Materials Science and Technology, Switzerland; *Peter Klein*, Masaryk University, Czechia; *Daniel Lundin*, Linköping University, Sweden

Magnetron sputtering-based physical vapor deposition (PVD) has gained considerable attention for the synthesis of functional carbon and carbide coatings, such as tetrahedral amorphous carbon (ta-C), due to its scalability, cost-effectiveness, and uniform film deposition capabilities. In this context, enhancing the ionization degree of carbon using high-power impulse magnetron sputtering (HiPIMS) presents a promising opportunity to expand its applicability. Therefore, substantial progress has been made toward increasing carbon ionization in HiPIMS discharge, through techniques such

as adding neon (Ne) gas and employing bipolar pulse schemes. However, the ionization fraction of carbon achieved by HiPIMS remains significantly lower than other techniques, e.g. filtered cathodic vacuum arc (FCVA) and pulsed laser deposition (PLD), presenting significant challenges to its adoption as an alternative approach. Despite these limitations, effectively utilizing the carbon ions generated in HiPIMS discharges requires a detailed quantitative understanding of the ionization fraction, their transport to the substrate, and their role in film growth. In this study, we aim to quantitatively investigate the ionized flux fraction and ion energy distributions in HiPIMS carbon discharges using argon (Ar) as the working gas, correlating these metrics with key process parameters. To achieve this, plasma diagnostics were performed using a magnetically shielded charge selective quartz crystal microbalance (ionmeter), time-of-flight (TOF) mass spectrometry, and time-resolved optical emission spectroscopy, with particular focus on the effects of the peak discharge current density, working gas pressure, and magnetic field. Our results demonstrate that the ionized flux fraction of carbon increases with higher peak current density, lower working pressure, and weaker magnetic fields. The maximum ionized flux fraction of ~12% was observed at a peak current density of 3.1 A/cm<sup>2</sup> under the weakest magnetic field configuration at a working pressure of 0.6 Pa. Furthermore, the ion energy distribution functions (IEDFs) revealed a distinct high-energy tail exceeding 100 eV, a feature not commonly observed in conventional HiPIMS discharges involving metal targets. Using time-resolved optical emission imaging, we also investigated the kinetic mechanisms underlying the acceleration of these high-energy carbon ions. This study highlights the importance of process parameter control in achieving efficient carbon ionization and transport, which is essential for advancing HiPIMS as a viable technique for carbon coating technologies.

9:00am **PP2-1-WeM-4 Reactive Mode Transition in Multi-Pulse HiPIMS Discharge of Vanadium in Ar/O<sub>2</sub> Gas Mixtures, Erdong Chen [chen-erdong@ed.tmu.ac.jp]**, Tetsuhide Shimizu, Tokyo Metropolitan University, Japan; *Caroline Hain*, Empa, Swiss Federal Laboratories for Materials Science and Technology, Thun, Switzerland; *Stephanos Konstantinidis*, University of Mons, Belgium; *Daniel Lundin*, Linköping University, Sweden

Vanadium dioxide (VO<sub>2</sub>) is a thermochromic material that undergoes a metal-insulator transition (MIT) at approximately 68°C, resulting in significant alterations in optical and electrical properties. However, the formation of single-phase VO<sub>2</sub> films is challenging in reactive sputtering due to the wide range of vanadium-oxygen (V-O) stoichiometries [1], leading to a limited process window. Based on the relationship between the oxidation state on the target surface and peak current in reactive high-power impulse magnetron sputtering (R-HiPIMS) systems [2], hysteresis examinations were performed to assess peak current evolution in response to variations in oxygen gas flow, aiming to identify an optimal process window for VO<sub>2</sub> fabrication. An abrupt decline in peak current was observed upon increasing the O<sub>2</sub> gas flow to 1 standard cubic centimeter per minute (sccm), accompanied by a relatively large hysteresis window, which hindered process stabilization and suggested the formation of vanadium pentoxide (V<sub>2</sub>O<sub>5</sub>) on the target surface. To address these challenges, we employed a novel approach utilizing very short, multi-pulse sequences in the R-HiPIMS process. This method eliminated the abrupt drop in peak current and reduced the hysteresis window by 36.6%, facilitating improved control over the VO<sub>2</sub> deposition process. Additionally, multi-pulse HiPIMS (m-HiPIMS) enhanced both the ionization flux fraction and deposition rate while effectively managing arcing phenomena. Further analysis revealed characteristic variations in peak current (I<sub>pk</sub>) as a function of O<sub>2</sub> gas flow, with distinct peak current values and waveforms for each micro-pulse. Pulse on time and the number of micro pulses were also investigated to find a suitable process condition for VO<sub>2</sub> deposition using multi-pulse mode R-HiPIMS. Comprehensive investigations into these micro-pulses were conducted using mass spectrometry to correlate findings with the surface chemistry of the vanadium target. The growth and properties of the deposited films were characterized using X-ray diffraction (XRD) and scanning electron microscopy (SEM). The crystallinity of VO<sub>x</sub> films and their electrical and optical performance were evaluated.

9:20am **PP2-1-WeM-5 HiPIMS goes Ferroelectric: Improving the Remnant Polarization and Leakage in Ferroelectric AlScN for Memory Applications, Federica Messi, Jyotish Patidar, Nathan Rodkey**, Empa, Swiss Federal Laboratories for Materials Science and Technology, Switzerland; *Morgan Trassin*, ETH Zurich, Switzerland; *Sebastian Siol [sebastian.siol@empa.ch]*, Empa, Swiss Federal Laboratories for Materials Science and Technology, Switzerland

The increasing demands of big data and AI necessitate breakthroughs in energy-efficient computing and data storage. Ferroelectric nitrides, such as



# Wednesday Morning, May 14, 2025

aluminum scandium nitride (AlScN), show great potential for non-volatile memory technologies due to their high remnant polarization, temperature stability, and compatibility with current semiconductor manufacturing processes.

The performance of ferroelectric nitrides is directly linked with their structural properties. The remnant polarization can be improved by increasing the c-axis orientation of the film, whereas the leakage current density can be improved by optimizing the microstructure. Point defects however negatively affect the breakdown behavior of the material, which represents a major challenge in the deposition of ferroelectric thin films.

Metal-ion synchronized high-power impulse magnetron sputtering (MIS-HiPIMS) can be used to accelerate film-forming metal ions onto the growing film, resulting in enhanced crystalline quality, improved c-axis texture, and a compact microstructure. Building on our recent successful demonstration of MIS-HiPIMS for piezoelectric thin films [1] we leverage the unique advantages of the technique for the deposition of ferroelectric AlScN with excellent performance.

Through a combinatorial study, we investigate the influence of HiPIMS on the ferroelectric properties of  $Al_{1-x}Sc_xN$  films while correlating these properties with crystallinity and Sc composition. Our optimized deposition process successfully yields  $Al_{1-x}Sc_xN$  films on Si substrates with performance that is otherwise only achieved using epitaxial growth.[2] Compared with previous reports using conventional sputtering the HiPIMS films show significantly enhanced remanent polarization with values of  $> 170 \mu C/cm^2$  while maintaining comparable coercive fields of 5.0 MV/cm. Notably, our findings reveal that the remanent polarization remains stable even with increasing scandium concentrations. At the same time the leakage current densities are among the lowest reported to date.[3] These results can be explained by the excellent c-axis texture enabled by HiPIMS. In the future HiPIMS could enable dense ferroelectric films with low thickness to reduce the switching potential. To our knowledge this is the first report of ferroelectric switching in HiPIMS-deposited nitride thin films. Overall, the results are more than promising and highlight the potential of HiPIMS for the development of defect-sensitive electronic thin films.

[1] Patidar et al. Physical Review Materials 8 (9), 095001, 2024

[2] Deng et al. Journal of the American Ceramic Society, **107**, (3), 2023

[3] Yazawa et al. arXiv preprint arXiv:2407.14037, 2024

9:40am **PP2-1-WeM-6 Controlling Film Growth by Changing the Target Thickness**, **Diederik Depla** [Diederik.Depla@ugent.be], **Farzaneh Ahangarani Farahani**, **Andreas Debrabandere**, Ghent University, Belgium

This paper summarizes a series of experiments demonstrating the significance of energetic species during DC magnetron sputter deposition. The first example focuses on the phase composition of tungsten (W) films, which can consist of a mixture of a-W and b-W crystals. Various mechanisms have been proposed to explain phase selection, including substrate heating due to plasma exposure and residual gas pressure. However, a broad parameter scan rules out these trends and shows that the phase composition can be quantitatively correlated with the flux of reflected neutrals with energies exceeding the displacement energy threshold. To establish this correlation, the phase composition is quantitatively determined using X-ray diffraction (XRD) analysis and combined with test particle Monte Carlo simulations to evaluate the energy of the reflected neutrals. The energy of these neutrals is defined by binary collisions between argon (Ar) and tungsten (W) atoms and the initial energy of the argon ions, which is set by the discharge voltage. Increasing the target thickness results in a lower magnetic field strength and, consequently, a higher discharge voltage. This effect allows the phase composition to be tuned by just adjusting the target thickness. The role of target thickness is further illustrated in a study on the percolation film thickness during the growth of silver (Ag) thin films. In-situ four-point probe resistance measurements are used to investigate the initial nucleation of these films. A power-law correlation between the percolation thickness and the deposition flux is observed, with the correlation exponent adjustable through variations in target thickness. Both studies highlight that reporting only the discharge power during experiments omits essential information critical for other researchers.

F. Ahangarani Farahani, D. Depla. "Phase Composition of Sputter Deposited Tungsten Thin Films." *Surface and Coatings Technology*, vol. 494 (2024) 131447

11:00am **PP2-1-WeM-10 Effect of Nitrogen Content on the Microstructure, Mechanical, and Anti Corrosion Properties of AlCrNbSiTiN High Entropy Alloy Films Fabricated by High Power Impulse Magnetron Sputtering**, **Sheng-Jui Tseng** [pprayray0915@gmail.com], National Taipei University of Technology, Taiwan; **Chia-Lin Li**, Center for Plasma and Thin Film Technologies, Ming Chi University of Technology, Taiwan; **Yung-Chin Yung**, National Taipei University of Technology, Taiwan; **Bih-Show Lou**, Chemistry Division, Center for General Education, Chang Gung University, Taiwan; **Jyh-Wei Lee**, Ming Chi University of Technology, Taiwan

High entropy alloy (HEA) films, especially the HEA nitride coatings, have attracted much attention from industries and researchers due to their unique mechanical properties and corrosion resistance. In this work, the AlCrNbSiTiN HEA coatings were fabricated on Si wafers, AISI 420 and 304 stainless steel plates by high power impulse magnetron sputtering. To investigate the impact of equimolar AlCrNbSiTi target poisoning ratios (ranging from 10 to 90 %) and the nitrogen contents on the phase, microstructure, mechanical, and anti corrosion properties of AlCrNbSiTiN coatings, a plasma emission monitoring (PEM) feedback control system was employed during sputtering. A systematic analysis of the microstructure and mechanical properties was conducted. The chemical compositions of HEA coatings were investigated by a field emission (FE) electron probe microanalyzer. FE-scanning electron microscopy and transmission electron microscopy were used to examine the microstructure of HEA films. Additionally, X-ray diffraction was employed to assess grain size, lattice constants, and crystallinity. A series of mechanical property tests, including hardness, adhesion, wear, and residual stress measurements were performed. The potentiodynamic polarization test of coatings in the 0.5 M H<sub>2</sub>SO<sub>4</sub> aqueous solution was examined. It is anticipated that the AlCrNbSiTi HEA film exhibited an amorphous structure. With increased nitrogen contents and target poisoning ratios, the AlCrNbSiTiN HEA nitride films transformed into a face-centered cubic structure. The HEA nitride films are projected to show enhanced hardness and elastic modulus, primarily due to the formation of a saturated metal nitride phase and solid solution strengthening from multiple elements. Based on the experimental results, the effects of target poisoning and nitrogen contents on the phase, microstructure, mechanical properties, and corrosion resistance of AlCrNbSiTiN coatings were discussed in this study.

11:20am **PP2-1-WeM-11 Effects of High-Power Impulse Plasma Source (HiPIPS) Parameters on the Properties of Aluminum Thin Films Synthesized at Atmospheric Pressure**, **Brianna Hoff** [brianna.hoff@mines.sdsmt.edu], **Forest Thompson**, **Nathan Madden**, **Grant Crawford**, South Dakota School of Mines and Technology, USA

High vacuum is required for conventional physical vapor deposition (PVD) techniques which restricts the application space that benefits from the dimensional stability, functionality, and chemically benign processing afforded by PVD thin films. Motivated by this limitation, a high-power impulse plasma source (HiPIPS) has been developed for surface engineering at atmospheric pressure. HiPIPS technology utilizes high-voltage, low duty cycle DC pulses to generate a plasma discharge between a consumable feedstock (cathode) and a conductive plasma jet nozzle (anode). The plasma is forced out of the nozzle by high flow rates of process gas where it subsequently interacts with a substrate which may be biased to increase the kinetic energy of ionized species. The HiPIPS design enables high plasma density to be achieved while maintaining low average power. In this study, processing-microstructure-property relationships are reported for the HiPIPS deposition of metallic aluminum (Al) films. Argon (Ar) was used as the working gas, and Al thin films were deposited at atmospheric pressure by utilizing Al alloy electrodes. HiPIPS system design variables and plasma discharge characteristics were correlated with the mechanical, compositional, and microstructural properties of the Al films. Film characterization was conducted via adhesion testing, energy dispersive x-ray spectroscopy, transmission electron microscopy, and atomic force microscopy. In this presentation, HiPIPS parameters which lead to desirable film qualities are discussed.

11:40am **PP2-1-WeM-12 Enhancing CrAl Ionization in HiPIMS Using Auxiliary Targets: Insights from Time-Averaged OES**, **Kai-Shawn Tang** [a0966877063@gmail.com], **Ying-Xiang Lin**, **Chih-Yen Lin**, **Yi-Hui Lee**, **Wan-Yu Wu**, National United University, Taiwan

Recently, High-Power Pulsed Magnetron Sputtering (HiPIMS) technology, due to its high ionization rate, has enabled increased ion bombardment during film growth, resulting in dense and smooth films. Previous studies using Bipulse-HiPIMS to deposit Ag-Cu and Ti-Cu films showed that, compared to unipolar mode, Ag-Cu co-sputtering significantly increased the ionization of Ag, while Ti-Cu co-sputtering greatly enhanced the ionization

# Wednesday Morning, May 14, 2025

of Cu. These findings suggest that, in the Bipulse-HiPIMS process, the selection and configuration of targets, as well as the tuning of each target's parameters, are closely related to the ionization rate of plasma species.

CrAlN possesses excellent oxidation resistance; however, ternary metal nitride films are no longer sufficient to meet current demands. Therefore, we further investigated quaternary metal nitride films, doping with elements such as Cr, Ti, and Zr to enhance mechanical properties and oxidation resistance. This study uses Bipulse-HiPIMS co-sputtering, with CrAl as the main target at a fixed power of 1.5 kW and Cr, Ti, and Zr as auxiliary targets. Since Cr has a relatively high second ionization energy (16.49 eV), whereas Ti and Zr have second ionization energies of 13.58 eV and 13.13 eV respectively, Ti and Zr are expected to ionize more readily than Cr. The Bipulse-HiPIMS technique aims to assist the ionization of the less readily ionized material (Cr) by more easily ionized materials. Time-averaged OES was used to measure the effect of different target materials on the plasma spectrum during the process.

The auxiliary target power was increased from 0.2 kW to 0.8 kW, observing plasma conditions on the CrAl target. It was found that plasma intensity was lowest in single-target mode, while the addition of an auxiliary target significantly enhanced plasma intensity. The study showed that as auxiliary target power increased, the intensities of  $\text{Cr}^+$ ,  $\text{Ar}^+$ ,  $\text{N}_2^+$ ,  $\text{N}_2^{2+}$ , and  $\text{Cr}^0$  in the plasma also increased. Next, with the auxiliary target power fixed at 0.5 kW, the auxiliary target's duty cycle was varied from 3% to 15%. Under different duty cycle conditions, it was observed that lower duty cycles led to increased  $\text{Cr}^+$  and  $\text{Al}^+$  intensities, with minimal differences in  $\text{N}_2^+$  and  $\text{N}_2^{2+}$ , while  $\text{Ar}^+$  intensity increased with higher duty cycles. The effect of different auxiliary targets is also demonstrated.

# Wednesday Afternoon, May 14, 2025

## Keynote Lectures

### Room Town & Country A - Session KYL-WeKYL

#### Keynote Lecture II

Moderator: Dr. Peter Kelly, Manchester Metropolitan University, UK

1:00pm KYL-WeKYL-1 **Spatial Atomic Layer Deposition for High Throughput Industrial Production of Lithium-Ion Batteries and Photovoltaic Cells**, *Tommi Kääriäinen [tommi.kaariainen@beneq.com]*, Beneq, USA **INVITED**

Atomic Layer Deposition (ALD) is an enabling thin film technology which found its use in energy applications such as energy storage (Li-ion batteries) and PV applications (TOPCon and perovskite PVs). Thin oxide coating deposited by ALD has been shown to improve battery performance through the introduction of thin film coatings to modify interface surfaces on cathodes, anodes and separators. ALD can help to improve thermal stability, stabilize Solid Electrolyte Interphase (SEI), suppress dendrite growth, inhibit transition metal dissolution, and increase interfacial contact between layers, all of which are current issues facing lithium-ion battery technology. ALD SnO<sub>2</sub> has been a material of choice for electron transport layers (ETL) of perovskite based solar cells and Al<sub>2</sub>O<sub>3</sub> as a passivation layer for TOPCon solar cells.

Spatial ALD (SALD) is an advanced coating technique, which has been studied for more than 10 years for various applications. We will demonstrate how SALD technology can be used to scale-up the throughput of ALD technology used in battery and PV applications.

## Protective and High-temperature Coatings

### Room Town & Country D - Session MA4-3-WeA

#### High Entropy and Other Multi-principal-element Materials III

**Moderators:** Prof. Dr. Jean-François Pierson, IJL - Université de Lorraine, France, Dr. Pavel Soucek, Masaryk University, Czechia

2:00pm **MA4-3-WeA-1 Few-Layered Multi-Transition Metal Chalcogenide Heterostructured Alloy Absorber for High-Performance Photodetector**, **Chia-Ying Su** [[ineowwow1114@gmail.com](mailto:ineowwow1114@gmail.com)], National Cheng Kung University, Taiwan; **I-Hsi Chen**, **Jyh-Ming Ting**, National Cheng Kung University (NCKU), Taiwan

Few-layered MoWSSe alloy with composition spread was synthesized using salt-assisted atmospheric pressure chemical vapor deposition. A heterojunction photodetector device was then made by connecting two electrodes to two areas that across a composition gradient. Basic material characteristics the photodetector performance were examined. We demonstrate that the photodetector exhibits the highest performance under visible light among a wide range of the incident light, with responsivity greater than 10 A/W, detectivity over  $5 \times 10^{10}$  Jones, and external quantum efficiency exceeding 3000%. Even in the near-infrared wavelength range, the device still shows a responsivity greater than 1 A/W, detectivity over  $5 \times 10^9$  Jones, and external quantum efficiency over 150%. The rise time was also less than 5 milliseconds. The outstanding performance of this photodetector device is attributed to the multiple p-n heterojunctions formed within a few-layered composition-gradient MoWSSe alloy, generating an internal electric field that facilitates the separation of photo-generated electron-hole pairs.

2:20pm **MA4-3-WeA-2 Sputter Deposition of Ta-W-Au-Bi High Entropy Alloys for Inertial Confinement Fusion Hohlräume**, **Daniel Goodelman** [[goodelman1@llnl.gov](mailto:goodelman1@llnl.gov)], Lawrence Livermore National Laboratory, USA; **Nikhil Vishnoi**, **Gregory Taylor**, **Eunjeong Kim**, **Alison Engwall-Holmes**, **Swanee Shin**, **David Strozzi**, **Brandon Bocklund**, **Scott Peters**, **Sergei Kucheyev**, **Leonardus Bimo Bayu Aji**, Lawrence Livermore Laboratory, USA  
The hohlraum is a centimeter-scale spherocylindrical canister used as the housing for a hydrogen fuel capsule in an indirect-drive inertial confinement fusion (ICF) target. The hohlraum is a critical component in increasing the ICF energy yield. Our simulations with the radiation hydrodynamics code LASNEX suggest that the fusion yield can be improved by using hohlraums made of Ta-W-Au-Bi high entropy alloys (HEAs). However, the magnetron sputter deposition of these HEAs with low porosity and submicron grains remains a challenge. Here, we examine how tailoring the main deposition process parameters, including the average plasma discharge power, working pressure, substrate bias, target-to-substrate distance, and substrate temperature, can be leveraged to enable the fabrication of Ta-W-Au-Bi films with a dense microstructure and high electrical resistivity, thus providing a promising path forward for the development of next-generation ICF targets.

This work was performed under the auspices of the U.S. DOE by LLNL under Contract DE-AC52-07NA27344 and was supported by the LLNL-LDRD Program under Project No. 23-ERD-005.

2:40pm **MA4-3-WeA-3 ADREnALINE : Accelerated Design of Revolutionary Entropy-Augmented, Lasting and Innovative Nitrides – First Results on Oxidation Resistance of Binary and Ternary Nitrides**, **Ludovic Méreaux**, IRCER, France; **Ederm Menou**, **Thomas Vaubois**, SAFRAN, France; **Cédric Jaoul**, IRCER, France; **Marjorie Cavarroc** [[marjorie.cavarroc@safrangroup.com](mailto:marjorie.cavarroc@safrangroup.com)], SAFRAN, France

Increasing aircraft engine temperature is one method, amongst others, to decarbonize aviation. But at high temperature, e.g., 1200 °C, metallic materials performances are drastically decreased due to the effect of hot corrosion. To limit this impact, metallic materials need to be protected with dedicated coatings with adequate properties, which Entropy-augmented ceramics could feature.

However, the composition space of complex ceramics is very wide, and comparatively very few bibliographical data are available as these specific ceramics have not been widely studied to date. While the use of a data-driven screening tools to identify relevant compositions appears necessary, it is not sufficient as (1) it requires data to be trained on, and (2) final properties should be experimentally assessed.

Due to considered temperatures, coatings based on refractory elements such as Zirconium (Zr), Niobium (Nb), Molybdenum (Mo), Hafnium (Hf); Tantalum (Ta), Tungsten (W), Ruthenium (Ru) or Rhenium (Re), combined

with Carbon (C), Nitrogen (N) or Boron (B), are credible potential candidates [1]. Cheaper and more abundant elements, as Iron (Fe) and Aluminium (Al), could also be considered in the mix to comply with industrial and environmental constraints.

High Entropy Alloys (HEA) (or Complex Concentrated Alloys (CCA) for their multiphase counterparts) are single-phase multielementary alloys showing original combination of properties (chemical resistance, mechanical resistance...) over a wide temperature range. The relatively new paradigm of HEA design, translated into the space of ceramics, offers new opportunities to meet high temperature requirements [2].

Two main challenges have to be overcome: achieving a single solid solution films to guarantee both material and property homogeneity throughout the coatings, and assessing the long term mechanical and environmental stability of the materials.

In this talk, we will highlight our methodology to combine numerical and experimental studies. First results about binary and ternary nitrides will be shown, together with the prospective work to come.

[1] W. G. Fahrenholtz, « A Historical Perspective on Research Related to Ultra-High Temperature Ceramics », in *Ultra-High Temperature Ceramics*, John Wiley & Sons, Ltd, 2014, p. 6–32. doi: 10.1002/9781118700853.ch2

[2] H. Xiang *et al.*, « High-entropy ceramics: Present status, challenges, and a look forward », *J. Adv. Ceram.*, vol. 10, n° 3, p. 385–441, 2021, doi: 10.1007/s40145-021-0477-y

3:00pm **MA4-3-WeA-4 Effect of Substrate Bias on Structural and Mechanical Properties of (MoNbTaW)N Coatings Deposited by Reactive DC Magnetron Sputtering**, **Saikumar Katta** [[saikumar.uoh@gmail.com](mailto:saikumar.uoh@gmail.com)], University of Hyderabad, India

MoNbTaW is well known for its refractory high entropy properties which can maintain the same crystal structure even at very high temperatures without losing its mechanical properties. Nitrides of such (MoNbTaW)N will be a prime focus to get a hard and tough, mechanically stable high temperature withstanding coatings at room temperature.

In this study, (MoNbTaW)N hard coatings were deposited using a DC magnetron sputtering technique at a working pressure of 0.3 Pa by varying substrate bias voltage from 0V to -200V. Optimized deposition parameters, including nitrogen flow and substrate temperature (400°C), were employed to produce dense and homogenous coatings on Silicon (100) substrates. X-Ray diffraction studies revealed that all the deposited films have Face Centered Cubic (FCC) crystal structure. A significant decrease in intensity ratio of principal reflection peak (111) to (200), from 2.39 to 0.84, is observed with increasing bias voltage from 0V to -200V. AFM studies indicated all the films have a fine granular morphology, with a maximum film thickness of 636 nm at 0V, reducing to 550 nm as the bias voltage is increased.

Topological analysis demonstrated that higher bias voltage led to smoother coatings, achieving an RMS roughness of < 2 nm. XPS studies revealed that the covalency due to the increased bonding of p(N)-d(TM) with the increase in bias voltage. Nanoindentation studies confirmed a maximum hardness of  $32 \pm 2$  GPa and a modulus of  $345 \pm 18$  GPa at -200V bias. Additionally, the coatings displayed improved toughness, with the highest H/E value of 0.09 achieved at -200V.

3:20pm **MA4-3-WeA-5 Effect of Substrate Bias Voltage on Microstructure and Mechanical Behaviour of Equimolar VCrCoNi Alloy Thin-films Deposited via Unbalanced Magnetron Sputtering**, **Razie Hanafi** [[r.hanafi@unsw.edu.au](mailto:r.hanafi@unsw.edu.au)], UNSW, Australia; **Yujie Chen**, University of Adelaide, Australia; **Zhifeng Zhou**, City University of Hong Kong; **Zonghan Xie**, University of Adelaide, Australia; **Paul Munroe**, UNSW, Australia  
Equimolar medium-entropy alloy VCrCoNi thin films were deposited on tool steel substrates by way of unbalanced magnetron sputtering, under different substrate bias voltages ranging from -20V to -120V. The deposited films were typically ~5.4 μm thick. Variations in chemical composition as a function of bias voltage were observed, showing fluctuations in the concentrations of V, Ni, and Cr, while Co remained constant. These compositional variations arose from the interaction between the sputtered metal cations and the kinetic energy differences of the adatoms induced by changes in bias voltage. The thin films exhibited strong crystallographic textures and a microstructure characterized by ultrafine (< 5 nm) equiaxed grains. Changes in phase composition were also observed with variations in bias voltage. Hardness values ranged from 11 GPa to 14 GPa, peaking at -100 V bias. Additionally, scratch resistance and wear performance were examined, revealing correlations between microstructural characteristics and tribological behaviour.

# Wednesday Afternoon, May 14, 2025

## Functional Thin Films and Surfaces

### Room Palm 1-2 - Session MB1-WeA

#### Thin Films and Surfaces for Optical Applications

**Moderators:** **Rajiv Pethé**, Vital Chemicals, USA, **Dr. Juan Antonio Zapien**, City University of Hong Kong

2:00pm **MB1-WeA-1 Experimental and Theoretical Insights into UV-Active Chirality in Glancing Angle Deposited Zirconia Nano-Helical Metamaterial Platforms**, **Ufuk Kilic [ufukkilic@unl.edu]**, **Matthew Hilfiker**, University of Nebraska-Lincoln, USA; **Shawn Wimer**, **Raymond Smith**, University of Nebraska - Lincoln, USA; **Christos Argyropoulos**, Pennsylvania State University, USA; **Eva Schubert**, **Mathias Schubert**, University of Nebraska - Lincoln, USA

**INVITED**

Chirality, the property of handedness in molecules or objects that prevents them from being superimposed on their mirror images, is optically manifested as circular dichroism (CD)—the differential absorption of left- and right-handed circularly polarized light. However, chirality found in nature is inherently weak, challenging to spectrally control, and primarily active in the ultraviolet (UV) region of the spectrum [1-3]. Enhancing UV-active chirality, crafting UV-active photonic wave-guide systems and also detecting chiral molecules through metamaterial platforms remains a challenge, as most designs are optimized for the infrared (IR) to visible spectral ranges [3].

In this study, we fabricated ultra-wide bandgap (~5 eV) zirconia (ZrO<sub>2</sub>) thin films using the glancing angle deposition (GLAD) method with electron beam evaporation. When the particle flux was directed at normal incidence (0°), uniform coating of flat ZrO<sub>2</sub> thin films were successfully fabricated. In contrast, directing the flux at an oblique angle (85.5°) with continuous substrate rotation (24 seconds per revolution) yielded spatially coherent, super-lattice nano-helices. Generalized spectroscopic ellipsometry (GSE) technique was used to extract frequency-dependent complex dielectric functions and identify band-to-band transitions spanning the near-IR to vacuum-UV (VUV) spectrum. Strong VUV-active CD responses were experimentally observed in ZrO<sub>2</sub> nano-helical metamaterials using Mueller matrix GSE. Additionally, visualization of both near- and far-field characteristics induced by circularly polarized illumination, along with the theoretical validation of the VUV-active chiroptical response, were investigated using finite element modeling (FEM) based full wave simulations. The systematic FEM calculations also revealed that the chiral properties could be tuned by (i) adjusting the structural parameters of the nano-helices and (ii) incorporating plasmonic subsegments into the helical structure.

Our research outputs suggest that the proposed metamaterial design holds significant potential for applications such as high-power chiro-optic photonic and electronic circuits, quantum information systems, UV-active topological insulators, and chiral sensing technologies.

[1] Kilic, U., *et al.*, *Nat. Commun.* 15, 3757 (2024).

[2] Kilic, U. *et al.*, *Adv. Funct. Mater.* 31.20: 2010329,(2021).

[3] Sarkar, S. *et al.*, *Nano letters* 19.11: 8089-8096,(2019).

2:40pm **MB1-WeA-3 Optical and Electrical Properties of Thermo-chromic W-Doped VO<sub>2</sub> Films Prepared at a Reduced Temperature (350 °C) on Glass Substrates with YSZ Interlayers**, **Sadoon Farrukh [sadoon@kfy.zcu.cz]**, **Jaroslav Vlček**, **Jiří Rezek**, **Radomír Čerstvý**, **Jiří Houška**, **Tomáš Kozák**, University of West Bohemia - NTIS, Czechia

Vanadium dioxide (VO<sub>2</sub>) is an extremely interesting and increasingly investigated coating material due to its reversible first-order transition between a low-temperature monoclinic VO<sub>2</sub>(M1) semiconducting phase and a high-temperature tetragonal VO<sub>2</sub>(R) metallic phase relatively near room temperature (approximately 68 °C for the bulk material). High modulation of the infrared transmittance, and electrical and thermal conductivity makes VO<sub>2</sub>-based films a suitable candidate for numerous applications, such as electronic and optical switches, thermal sensors, smart thermal radiator devices for spacecraft, adaptive thermal camouflage, and energy-saving smart windows with automatically varied solar energy transmittance.

The application potential of these films depends on the ability to achieve not only the VO<sub>2</sub> stoichiometry but also the crystallization of the VO<sub>2</sub>(M1/R) phase under as industry-friendly process conditions as possible, i.e., at a deposition temperature close to 300 °C (usually used temperatures are higher than 450 °C) and without any substrate bias voltage in case of usually used magnetron sputter techniques. Moreover, the transition temperature needs to be reduced down to 25 °C for many applications

(e.g., smart windows). Besides the optical transmittance in the visible range, the characteristics of the semiconductor-metal transition, such as phase-transition amplitude, hysteresis width, and phase-transition sharpness, are of key importance.

The paper deals with crystal structure, optical and electrical properties, and semiconductor-metal transition characteristics of strongly thermo-chromic W-doped VO<sub>2</sub> films with a reduced transition temperature (24-33 °C). They were deposited at a reduced temperature (350 °C) onto glass substrates with two versions of Y-stabilized ZrO<sub>2</sub> (YSZ) interlayers (serving also as a highly optically transparent bottom antireflection layer) possessing different crystal orientations, and onto bare glass and monocrystalline YSZ and Al<sub>2</sub>O<sub>3</sub> substrates for comparison. The W-doped VO<sub>2</sub> films were deposited using a controlled reactive deep oscillation magnetron sputtering (DOMS) of a single V-W (3.0 wt.%) target. The DOMS is a modified version of HiPIMS with packages (macropulses) of short high-power micropulses.

3:00pm **MB1-WeA-4 Enhancing Optical Properties and Photocatalytic Performance with Nanopatterned Anodized Aluminum Oxide on transparent substrate**, **Fu-Gi Zhong [fugi.en12@nycu.edu.tw]**, **Shih-Hsun Chen**, National Yang Ming Chiao Tung University (NYCU), Taiwan

In recent years, the rapid advancement of nanotechnology has driven an increasing demand for high-performance nanostructured materials. Among various fabrication techniques, anodic aluminum oxide (AAO) films have attracted significant attention due to their excellent chemical and thermal stability, transparency, and tunable nanoporous structure. AAO features highly ordered nanopore arrays, making it an ideal template for functional thin films, especially in applications requiring high surface area and aspect ratios. By integrating functional ceramic or semiconductor coatings, materials

deposited on AAO can self-assemble into nanostructures, further enhancing their optical and chemical reactivity and making them highly suitable for applications in sensors, photocatalysis, and other fields requiring heightened sensitivity and resolution.

This study focuses on the fabrication of AAO structures on transparent substrates, followed using Atomic Layer Deposition (ALD) to coat these structures with ZnO thin films, aiming to produce transparent, nanostructured porous films on both sides of the substrate. By integrating ZnO coatings

with AAO structures, we plan to investigate light transmission and surface interaction properties, thereby enhancing optical performance and photocatalytic efficiency and making the films more suitable for high-sensitivity, multifunctional sensor and photocatalytic applications.

3:20pm **MB1-WeA-5 A Comparative Study: The Structural and Optoelectronic Properties of Al- and Ga-Doped ZnO Films Deposited by Atmospheric Pressure Plasma Jet**, **Chih-Yun Chou [f10k45003@ntu.edu.tw]**, National Taiwan University, Taiwan

Aluminum-doped zinc oxide (AZO) and gallium-doped zinc oxide (GZO) are leading transparent conductive oxides (TCOs) for optoelectronic applications, valued for high transparency and conductivity. GZO provides superior carrier mobility and lower resistivity, while AZO is more cost-effective and less toxic. This study compares AZO and GZO films prepared via atmospheric pressure plasma jet (APJ) deposition, allowing for precise parameter control to evaluate Al and Ga's effects on ZnO film properties and their suitability in advanced optoelectronics.

Structural analysis using X-ray diffraction (XRD) and scanning electron microscopy (SEM) reveals both AZO and GZO films exhibit a hexagonal wurtzite structure with a c-axis orientation. The broader full-width at half maximum (FWHM) at (002) peak and higher strain in GZO films suggest more pronounced lattice distortion, likely due to Ga's higher doping efficiency. Further, reducing the working distance, thereby increasing processing temperature, effectively eliminates surface particles in GZO films but not in AZO films. This temperature-driven improvement enhances the mobility of Ga atoms on the substrate surface, leading to a more cohesive and uniform film morphology in GZO.

Optoelectronic properties assessed via UV-Vis spectroscopy and Hall effect measurements indicate that GZO films maintain high visible-range transparency (>80%) compared to AZO films (>70%). In the near-infrared range, GZO transparency decreases significantly (<40% at 1400 nm) due to its higher carrier concentration. Overall, AZO films show lower electronic performance, likely due to complex defect formation and increased impurity scattering, evidenced by higher Urbach energy (E<sub>u</sub>) values (0.28-0.29 eV for AZO films and 0.26 eV for GZO). Decreased APJ working distance enhances carrier mobility, improving the figure of merit at 550 nm

# Wednesday Afternoon, May 14, 2025

for GZO from  $11 \times 10^{-3} \Omega^{-1}$  to  $26.4 \times 10^{-3} \Omega^{-1}$  and for AZO films from  $0.4 \times 10^{-3} \Omega^{-1}$  to  $0.8 \times 10^{-3} \Omega^{-1}$ .

In conclusion, while AZO and GZO films both possess favorable characteristics for TCOs, their electronic behaviors diverge markedly under APPJ processing. Al doping tends to introduce complex defects that limit carrier mobility and concentration, making AZO less suitable where high conductivity is essential. In contrast, GZO films achieve higher carrier concentration and mobility, making them more appropriate for applications where efficient charge transport is critical. The findings also emphasize the significance of the APPJ working distance parameter and underscore the importance of selecting appropriate dopants and understanding defect dynamics to optimize ZnO-based TCO performance.

**3:40pm MB1-WeA-6 Unveiling the Interplay of Structural, Optical, and Hydrophobic Properties of Sputtered Grown PTFE@AlSiN Thin Films,** Raman Devi, Somdatta Singh, Ramesh Chandra [ramesh.chandra@ic.iitr.ac.in], IIT Roorkee, India

Radio frequency (RF) magnetron sputtering technique was used to develop PTFE@AlSiN thin films on glass substrates at temperatures ranging from 250°C to 450°C. Methods like X-ray diffraction (XRD), field emission scanning electron microscopy (FE-SEM), UV-Vis Spectroscopy, water contact angle (CA) measurements, and nanoindentation were used to examine the structural, morphological, optical, hydrophobic, and mechanical properties of PTFE@AlSiN at various substrate temperatures (250°C-450°C). XRD studies showed that the coating deposited with an Ar:N<sub>2</sub> ratio of 20:6 at various substrate temperatures formed a hexagonal phase, demonstrating its polycrystalline nature. A nanocomposite with microstructure has been formed by embedding AlN nanocrystallites in a soft amorphous matrix of Si<sub>3</sub>N<sub>4</sub> provides better mechanical properties. The contact angle measurement method displayed an excellent contact angle of around ~118° (good hydrophobicity). According to optical transparency measurements, all coatings exhibited > 90% transparency in the visible spectrum. The PTFE@AlSiN coated at 450°C had the highest hardness value greater than 25 GPa.

**Keywords:** optical transparency, magnetron sputtering, thin film, hydrophobicity; nanoindentation, hardness

**4:00pm MB1-WeA-7 High-Entropy Oxide Thin Film as Absorber Layer for Near Infrared Photodetectors,** Shao-Chun Chao [sc0705chao@gmail.com], Tai-An Chen, Jyh-Ming Ting, National Cheng Kung University (NCKU), Taiwan  
A novel light-absorbing material of high-entropy oxide (HEO) was synthesized using the sol-gel method. The sol-gel method offers advantages such as low cost, high uniformity, flexible material preparation, and suitability for large-scale production. In this study, a streamlined process was used to produce uniform, controllable nanostructured thin films. By leveraging the properties of HEO, the film properties were adjusted, making it an excellent absorber layer in photodetectors. The HEO material demonstrated an unparalleled ability to absorb a broad spectrum of light, ranging from 300 to 1400 nm. We measured the performance of a photodetector with an Ag/HEO/n-Si structure. Under near-infrared illumination, this photodetector exhibited an impressive high photoresponse, generating a high photocurrent density of approximately 10 mA/cm<sup>2</sup> at an incident light wavelength of 1050 nm, with a peak responsivity of 1.545 A/W, and an external quantum efficiency (EQE) exceeding 182%, surpassing most oxide-based photodetectors reported in the literature. The outstanding performance of this device is attributed to the high concentration of oxygen vacancies in the HEO compound, resulting in significant light absorption and high EQE. Furthermore, this study is the first to use the sol-gel method to prepare HEO thin-film absorber layers, demonstrating the material's excellent potential in the field of photodetectors.

**4:20pm MB1-WeA-8 Effective Ways to Enhance the Performance of N-MoS<sub>2</sub>/P-CuO Heterojunction Based Self-Powered Photodetectors,** Davinder Kaur [davinder.kaur@ph.iitr.ac.in], Indian Institute of Technology Roorkee, India

The present study investigated two effective routes to improve the response time and the detection range for the n-MoS<sub>2</sub>/p-CuO heterostructure (a conventional p-n heterojunction). In the first rectification, an insulating aluminium nitride (AlN) layer was inserted in between the molybdenum disulfide (MoS<sub>2</sub>) and cupric Oxide (CuO) layer, which eventually converted the conventional p-n heterojunction to Semiconductor-Insulator-Semiconductor (SIS) with a superior carrier tunneling mechanism. Interestingly, the fabricated heterostructure exhibits self-powered and broad-range photoresponse. The response time (rise time

and fall time) of the fabricated n-MoS<sub>2</sub>/p-CuO heterojunction decreases from 93.35 ms and 102.68 ms to 11.31 ms and 12.73 ms with the insertion of ultrathin insulating AlN Layer. The higher responsivity and ultrafast photoresponse in n-MoS<sub>2</sub>/AlN/p-CuO (SIS) heterojunction can be ascribed to the carrier tunneling mechanism through the ultrathin-insulating AlN layer. Moreover, the detection range can be enhanced up to the UV region by adding a layer of MoS<sub>2</sub> quantum dots (QDs) on the surface of the MoS<sub>2</sub> layer in the fabricated heterostructure. The fabricated n-MoS<sub>2</sub> QDs/n-MoS<sub>2</sub>/AlN/p-CuO heterostructure shows photoresponse in a broad range from UV to NIR radiations. The obtained results demonstrate the n-MoS<sub>2</sub>/AlN/p-CuO (SIS) heterostructure with the addition of MoS<sub>2</sub> QDs shows excellent potential for next-generation ultrafast optoelectronics applications.

**4:40pm MB1-WeA-9 Influence of SHI irradiation on the Photoluminescence and Dielectric properties of bilayer structured Au/GeO<sub>2</sub> thin films for Optoelectronics applications,** Mahendra Singh Rathore [mahendra.rathore8944@paruluniversity.ac.in], Anand Y. Joshi, Parul University, India; Srinivasa Rao N., MNIT Jaipur, India  
**Abstract**

In the present work, the effects of swift heavy ion beam irradiation on the engineering the physical, optical, photoluminescence and dielectric properties of bilayer structured Au/GeO<sub>2</sub> thin films have been investigated. GeO<sub>2</sub> and Au thin films have been grown onto silicon substrate using electron beam evaporation. Eventually the prepared Au/GeO<sub>2</sub>/Si thin films were irradiated with 100 MeV Ag ions at different ion fluences ranging from  $1 \times 10^{12}$  to  $1 \times 10^{13}$  ions/cm<sup>2</sup>. The pristine and irradiated samples were characterized using XRD, RBS, SEM, AFM, UV-Vis reflectance and photoluminescence Spectroscopy. The dielectric properties, AC conductivity, dielectric and tangent loss were analyzed of the pristine and irradiated samples. The results reveal that the nucleation of Au NCs was observed with increase in fluence. The elemental composition and film thickness observed using RBS measurements. The surface morphology and topography results reveal that the nucleation of particles with increase in ion fluences. Broad PL band observed in visible region which corresponding to the green light emission due to the presence of Au NCs. The CIE curve plotted from the PL data. The oxygen vacancy related defect states as well as surface Plasmon resonance (SPR) induced absorption and subsequent electron injection from Au NPs to conduction band of GeO<sub>2</sub>. The dielectric properties varied with irradiation. The variation in electronic transition of wide band gap GeO<sub>2</sub> NC's by nucleation of gold NP's are considered to practical application in optoelectronics devices such as wavelength detection and optical switching devices and have been discussed in details.

**Keywords:** Au/GeO<sub>2</sub> thin films, ion beam irradiation, XRD, RBS, Photoluminescence, Dielectric properties.

## Tribology and Mechanics of Coatings and Surfaces Room Town & Country C - Session MC3-2-WeA

### Tribology of Coatings and Surfaces for Industrial Applications II

**Moderators:** Osman Levent Eryilmaz, Oak Ridge National Laboratory, USA, Dr. Giovanni Ramirez, Zeiss Industrial Quality Solutions, USA

**2:00pm MC3-2-WeA-1 Effect of Electrical Current Application on the Tribological Properties of Soft and Hard ta-C Coatings on HSS Substrates,** Amir Masoud Khodadadi Behtash [khodada1@uwindsor.ca], University of Windsor, Canada; Woo-Jin Choi, Jongkuk Kim, Korea Institute of Materials Science, Korea (Democratic People's Republic of); Ahmet T. Alpas, University of Windsor, Canada

As electric vehicles (EVs) become more widespread, managing electrical current effects on friction and wear in moving components is crucial for enhancing durability and efficiency. Diamond-like carbon (DLC) coatings, known for their low friction and insulating properties, show potential in these applications. This study investigates the tribological characteristics of two types of tetrahedral amorphous carbon (ta-C) coatings -soft (51 GPa) and hard (69 GPa)- on high-speed steel (HSS) substrates under the electrical current application. The soft ta-C coating was deposited at 150 °C, while the hard ta-C coating was deposited at room temperature with a -100 V substrate bias, both using filtered cathodic vacuum arc (FCVA) with a Ti interlayer deposited by magnetron sputtering. The average surface roughness (R<sub>a</sub>) values were  $17.1 \pm 0.3$  nm for the soft ta-C coating and  $20.3 \pm 0.9$  nm for the hard ta-C coating. Friction and wear resistance were evaluated using a modified ball-on-disk tribometer with an AISI 52100 steel

# Wednesday Afternoon, May 14, 2025

counterface, under electrical currents from 0 to 1500 mA. Under non-electrified conditions, both hard and soft ta-C coatings displayed low wear rates of  $4.5$  and  $5.27 \times 10^{-7} \text{ mm}^3/\text{m}\cdot\text{N}$ , respectively. With applied electrical currents, however, notable differences emerged. The hard ta-C coating demonstrated coefficient of friction (COF) values ranging from 0.11 to 0.44 under electrical currents between 0 and 500 mA. In comparison, the soft ta-C coating exhibited lower COF values, ranging from 0.11 to 0.29, across a broader current range of up to 1500 mA. The wear rate of the hard ta-C coating increased significantly to  $1.6 \times 10^{-5} \text{ mm}^3/\text{m}\cdot\text{N}$  at 300 mA, whereas the soft ta-C coating maintained a much lower wear rate of  $1.05 \times 10^{-6} \text{ mm}^3/\text{m}\cdot\text{N}$  at the same current and reached only  $6.17 \times 10^{-6} \text{ mm}^3/\text{m}\cdot\text{N}$  at 1200 mA. These results indicate that the electrical current carrying tribological performance of ta-C coatings on HSS substrates can be tailored by heat treatment to enhance their response. Raman spectroscopy and electron microscopy are utilized to delineate the mechanisms underlying these structural changes and will be presented at the conference.

**2:20pm MC3-2-WeA-2 Impact of Electrification on the Tribological Performance of Metal Doped a-C Coatings, Miguel Rubira Danelon [migueldanelon@usp.br], Newton Kyoshi Fukumasu, Roberto Martins de Souza, André Paulo Tschiptschin, University of São Paulo, Brazil**

Amorphous carbon (a-C) coatings, composed of  $sp^2$  and  $sp^3$  hybridizations of carbon, may enhance the surface properties of materials. These coatings are commonly used as solid lubricants, improving tribological performance by forming a tribolayer that reduces the coefficient of friction by graphitization. In many systems, a-C coatings offer the potential to lower frictional energy losses and wear, improving efficiency and durability. Specific phenomena are anticipated for electric vehicles (EVs), since, from one side, electric current can affect surface wear in electrified systems by promoting accelerated oxidation or arc formation. On the other hand, electrical current flowing through an a-C coated contact can induce carbon crystallization, benefiting EV engine performance. Pure a-C lacks the conductivity needed for this crystallization effect, which can be improved by doping the a-C with metallic elements. Using copper or nickel as dopants can reduce electrical resistivity and catalyze carbon nanostructure formation, further reducing friction. This study investigates the tribological behavior of metal-doped a-C coatings under electrified ball-on-plane tests. Me:a-C coatings were deposited on glass substrates using pulsed DC balanced magnetron sputtering. Ni and Cu were used as dopants, with different concentrations, to improve electrical conductivity. Tribological tests involved a ball-on-plane setup with a 10 N normal load, 5 mm stroke, and 0.28 Hz frequency, applying 30 V in four current flow modes: current flowing from ball to plane, from plane to ball, no current, and intermittent on-off cycling every minute. The coatings' microstructure and composition were analyzed using Scanning Electron Microscopy with Energy-dispersive X-ray spectroscopy (EDS). Raman spectroscopy was used to evaluate carbon structure, while instrumented indentation tests allowed the characterization of mechanical properties. Results showed that doping a-C is essential to promote a direct response to electrical stimulation. Increasing the metal content of the amorphous-carbon coating increases the conductivity but decreases the wear resistance, due to a higher metal content. In contrast, reducing the metal content leads to insufficient conductivity, hindering the electrical current's effect on carbon graphitization. Current flow promoted friction coefficient variations, which were not influenced by thermal effect, since no significant temperature increase was observed. Instead, COF variations were related to instant changes in current flow during contact. The wear resistance has also been influenced by the current, with different outcomes depending on the current direction.

**2:40pm MC3-2-WeA-3 Graphene-Related Materials: Bridging Fundamental Tribology and Industrial Applications Across Multifarious Environments, Mingi Choi [ds602847@gmail.com], Ji-Woong Jang, Pusan National University, Republic of Korea; Anirudha Sumant, Argonne National Laboratory, USA, India; Ivan Vlasiouk, Oak Ridge National Laboratory, USA, Russian Federation; Jae-Il Kim, Korea Institute of Materials Science, Republic of Korea; Young-Jun Jang, Korea Institute of Material Science, Republic of Korea; Songkil Kim, Pusan National University, Republic of Korea**

Solid lubricants play a crucial role as alternatives to liquid lubricants in extreme environments and as solutions for enhancing mechanical system performance under ambient conditions at the macroscale. Among these, graphene, a representative two-dimensional nanomaterial, has attracted significant attention due to its exceptional nanoscale tribological properties. However, its application as a solid lubricant for macroscale industrial systems remains a challenge. Recent studies have highlighted that tailoring graphene's properties through functionalization, oxidation, can significantly

enhance its performance. This underscores the strong correlation between the tribological behavior of graphene-based materials and their elemental and compositional properties.

In this work, we demonstrate the versatility of graphene-related materials as solid lubricants by engineering their structural and compositional properties. Under ambient conditions, we developed a heterogeneous structure of graphene oxide layered on pristine graphene, achieving over 100 times greater durability (>10 km) compared to pristine graphene (~10 m) while maintaining its low COF. In contrast, under humidity- and oxygen-free environments, pure graphene oxide exhibited a super low coefficient of friction (COF). Remarkably, in an argon environment, the COF approached the superlubric regime (COF < 0.01), while in vacuum, the COF gradually increased to 0.07. By unveiling the intrinsic lubrication mechanisms of graphene oxide in these environments, we highlight the potential of graphene-based materials as solid lubricants for diverse engineering applications, bridging fundamental understanding with industrial relevance.

**3:00pm MC3-2-WeA-4 Evaluation of the Reduced Bearing Wear Through Plasma Nitriding for Use in Wind Turbines, Arthur Cid de Abreu, Rayane Dantas da Cunha, João Freire de Medeiros Neto, Salete Martins Alves [salete.alves@ufrn.br], Federal University of Rio Grande do Norte, Brazil**

In 2023, significant advancements in the wind industry led to a record-breaking achievement: over 100 GW of new onshore wind installations and the second-largest total for offshore wind at 11 GW. This type of energy production has proven profitable for investors as it represents a viable source of green and sustainable energy. The trend indicates an expansion of wind farms in the world over the coming years. However, a significant concern in this sector is the damage caused by operational characteristics, such as dynamic loading and severe operating conditions. These factors can lead to reduced efficiency and increased maintenance costs. To address this, developing surface treatments with high wear resistance and friction reduction capabilities is essential to ensure the longevity and efficiency of mechanical components. The main goal of this research was to extend the service life of wind turbine components through plasma nitriding surface treatments to enhance their wear resistance. The study consisted of carrying out a plasma nitriding process in bearing balls of steel AISI 52100 under different temperatures and treatment times to improve wear resistance. Tribological tests were performed to evaluate the wear resistance of the bearings using a pin-on-disc tribometer with non-conformal contact (ball-disc). The disc rotated at a speed of 500 rpm, with an applied load of 60 N for 30 minutes. Tests were performed both in dry and lubricated conditions. After the tribological tests, the discs and balls were analyzed by optical microscopy and 3D and 2D profilometry analysis to quantify the worn volume. The wear mechanisms and morphology were further examined using scanning electron microscopy and energy-dispersive spectroscopy (EDS). The results indicated that the plasma nitriding treatment applied to the SAE 52100 steel balls significantly improved the surface tribological properties, characterized by a reduction in the friction coefficient and decreased wear on the SAE 1045 steel discs.

**3:20pm MC3-2-WeA-5 Plasma Nitriding of Quartz, Stephen Muhl [smuhl@unam.mx], Instituto de Investigaciones en Materiales, Universidad Nacional Autónoma de México; Julio Cruz, Marco Martinez, Instituto de Investigaciones en Materiales, Universidad Nacional Autónoma de México**

Plasma nitriding is a valuable and well-established technique for surface hardening of metals to improve their mechanical and tribological properties, such as hardness and wear resistance. Typically, plasma nitriding involves the use of a glow discharge of a mixture of nitrogen and hydrogen, where the metal component to be treated is the cathode and the chamber wall is the anode. The low-pressure plasma (15–1500 Pa) produced by the application of a DC potential (0.3–1.0 kV) contains nitrogen ions, which are accelerated towards the cathode and implanted in the surface of the metal. The treatment time, surface concentration of nitrogen, and temperature of the metal component determine the depth and gradient of the nitride layer, but various tens of microns are often formed. The same process cannot directly be used to nitride insulators since such materials cannot be used as a cathode in a DC plasma.

We have developed a variant of the normal plasma nitriding scheme where the discharge is produced by applying an RF potential and the piece to be nitrided is mounted on a magnetron cathode. This is, of course, the same as a RF magnetron sputtering system. Previous studies have shown that the DC voltage bias generated on the surface of an insulating target used in a RF magnetron sputtering cathode depends on the following factors: the relative areas of the anode and cathode, the applied RF power, the gas

pressure and composition, and the degree of matching of the impedance of the electrical supply to the impedance of the plasma. We have measured the DC bias potential and the rate of sputtering of a quartz target mounted on a 2" MAK magnetron cathode in a pure nitrogen gas discharge as a function of the area of the anode, the gas pressure, the applied power, and the degree of matching indicated by the ratio  $RF(\text{Reflected Power}) / RF(\text{Forward Power})$ . Using conditions which produced a minimum sputter etching of the target, we produced three samples nitrided for 60, 90 and 120 min. We present the thickness and composition of the nitride layer measured using XPS and RBS, and the hardness and wear resistance of these layers.

**3:40pm MC3-2-WeA-6 Penetrability: A New Parameter for Wear Estimation of Multilayer Coatings, Muhammad Usman [muusman2-c@my.cityu.edu.hk],** City University of Hong Kong

Many efforts are being made to predict the wear of thin films/coatings through indentation. The 10%-depth-hardness defined by the ISO 14577-4 standard to avoid the substrate effect is commonly used for wear estimation of single-layer coatings. The coating structure varies from layer to layer (top to bottom) in multilayer coatings, and no clear guidelines for hardness measurement are available for them at the time of writing. Moreover, hardness is a system parameter that may change with depth, indenter tip shape and size, micro to nanofilm thickness, and the substrate effect. Therefore, this method may not be adequate for multilayers, multi-scale nanostructured materials, and composites. To address the issue, we hypothesize that for the same material (in our case, various C/C multilayer coatings), there should exist a correlation between the mechanical work done due to wear and the mechanical work done due to indentation. A thorough experimental investigation was conducted using a range of multilayer diamond-like carbon coatings at different loading conditions to verify our hypothesis. The penetrability (newly proposed parameter) correlates with the wear process. The test drive of the method successfully predicted multilayer coatings in terms of wear behavior trends and identified coating designs with comparatively low and high specific wear rates. It is anticipated that with further investigations employing penetrability to thin film wear research, the approach could be used to understand the wear of thin films in a more universal manner.

## Plasma and Vapor Deposition Processes Room Town & Country B - Session PP2-2-WeA

### HiPIMS, Pulsed Plasmas and Energetic Deposition II

**Moderators: Dr. Tetsushide Shimizu,** Tokyo Metropolitan University, Japan, **Dr. Martin Rudolph,** Leibniz Inst. of Surface Eng. (IOM), Germany

**2:00pm PP2-2-WeA-1 Introducing an Ionization Region Model for Reactive High-Power Impulse Magnetron Sputtering, Daniel Lundin [daniel.lundin@liu.se],** Joel Fischer, Linköping University, Sweden; **Martin Rudolph,** Leibniz Institute of Surface Engineering (IOM), Germany; **Jon Tomas Gudmundsson,** University of Iceland

**INVITED**

High-power impulse magnetron sputtering (HiPIMS) is a physical vapor deposition (PVD) technique in which short pulses of high instantaneous power are applied to a magnetron cathode to significantly increase the degree of ionization of the film-forming material. This generally results in an improved coating quality including reduced surface roughness, increased density, and increased coverage on complex 3D geometries. In addition, reactive HiPIMS has also been shown to display a reduced hysteresis behavior compared to reactive DC magnetron sputtering. If we can properly control the internal process parameters, this will likely have a great impact on the way compound coatings are being deposited, since it allows for stable operation in the desired transition zone and consequently a dramatically increased deposition rate, while still preserving other inherent advantages of HiPIMS.

In this work we take the first steps towards a more detailed understanding of the reactive HiPIMS process by introducing a novel reactive ionization region model (R-IRM). The R-IRM is based on the established ionization region model (IRM), which has been extended to incorporate an extensive nitrogen reaction set together with all the additional complexities arising from the addition of a reactive gas. We use the R-IRM to study the internal process parameters of reactive HiPIMS discharges that are difficult to investigate experimentally by applying the model to a set of HiPIMS discharges of Ti in various Ar/N<sub>2</sub> mixtures and with different external process parameters. The temporal evolution of the densities of the different plasma species, their fluxes towards the substrate, as well as the

ionization and back-attraction probabilities obtained from the model give valuable insights into how key properties influencing film growth, such as the material flux composition and charge state of film-forming ions, are affected by the choice of the external process parameters. We furthermore observe, that with the small relative flow rates of N<sub>2</sub> typically needed to obtain stoichiometric coatings, nitrogen only plays a minor role in the plasma chemistry.

**2:40pm PP2-2-WeA-3 Investigation of Surface Bond Structure and Colour Variations in Thin Films Deposited via Aca and Hipims Techniques, Milena Pazzi [milena.pazzi@unimore.it],** Giovanni Bolelli, Università degli Studi di Modena e Reggio Emilia, Italy; **Andreas Fuchs, Daniel Barnholt, Philipp Immich,** Hauzer Technocoating, Netherlands; **Luca Lusvardi,** Università degli Studi di Modena e Reggio Emilia, Italy

Understanding surface bond structures and how they affect material properties is crucial for optimizing the optical and functional qualities of thin films for decorative and functional applications. Specifically, the objective of this research is to investigate the reasons behind color changes and physical property differences among coatings based on metal carbonitrides. We tested samples obtained by High-Power Impulse Magnetron Sputtering (HiPIMS) and Advanced Controlled Arc (ACA), two advanced techniques frequently used to deposit this type of coatings.

In order to investigate both chemical and structural issues, several analytical techniques will be employed. The bonding structures and the chemical composition of the coatings will be characterized by Raman spectroscopy, X-ray diffraction (XRD), and X-ray photoelectron spectroscopy (XPS). By combining high-resolution Scanning Electron Microscopy (SEM) with Energy Dispersive Spectroscopy (EDS), we will be able to thoroughly analyze both surface and cross-sectional morphologies, giving us important insights on the compositional uniformity and microstructural integrity of the films. Additionally, mechanical performance will be studied by nanoindentation to evaluate hardness and scratch tests to assess adhesive strength. The exact color values in the CIE L\* a\* b\* color space are measured using a colorimeter on the samples right after each batch.

By determining the parameters influencing these differences, we seek to improve the knowledge of the process-structure-properties relation in metal carbonitride films. The study's findings are expected to provide useful insights into the customisation of optical and mechanical properties in industrial applications that require precise control over both the appearance and performance of thin films.

**3:00pm PP2-2-WeA-4 On Unipolar and Bipolar Hipims Pulse Configurations to Enhance Energy and Ion Flux to Insulating Substrates, Mina Farahani [farahani@ntis.zcu.cz],** Tomáš Kozák, Jiří Čapek, University of West Bohemia - NTIS, Czechia

High-power impulse magnetron sputtering (HiPIMS) is an advanced technique for thin film deposition, delivering high target power in short pulses to achieve greater ionization than conventional DC magnetron sputtering. Despite this increase in ionization, many ions still have relatively low energy, so substrate biasing is often used to boost energy transfer to the growing film. For insulating substrates, where direct biasing is impossible, bipolar HiPIMS (alternating negative and positive pulses with a floating substrate) offers a partial solution. However, rapid charging of insulated substrates limits energy transfer. This study aims to optimize bipolar HiPIMS pulse configurations to explore the potential enhancement of energy transfer even for insulating substrates.

Experiments were conducted using a magnetron and a Ti target powered by a DC source and driven by a bipolar HiPIMS pulsing unit. Various pulse configurations (unipolar HiPIMS, bipolar HiPIMS, chopped unipolar, and chopped bipolar HiPIMS) were applied under unbalanced magnetic fields (Fig. 1) with the same average power. In-situ ion mass and energy spectroscopy (MS) analyses were carried out, and the total energy flux to a substrate was measured using a passive thermal probe at a floating and ground potential. Moreover, the depositions on insulating substrates or films with various capacitances were simulated by connecting a defined external capacitor between the probe and the ground. Finally, Ti films were deposited on a floating substrate holder for structural analysis.

Unlike standard HiPIMS, bipolar HiPIMS introduces a high-energy peak in the IEDF; with multi-pulse configurations, this peak broadens and the high-energy tail is enhanced. Additionally, time-resolved measurements provide valuable insights, like the evolution of energetic ion flux to the film. Both MS and thermal probe measurements show enhancement of ion and energy fluxes to the substrate for chopped configurations (Fig. 2). Moreover, heat flux varies with capacitance: with a low capacitance, ion acceleration occurs only at the start of each positive pulse before the film



# Wednesday Afternoon, May 14, 2025

surface is fully charged, so the effect on the energy delivered to the film is small. With a high capacitance, ion acceleration is effective throughout the positive pulse regardless of its length, as is the case for a grounded substrate. For medium capacitance, chopping the positive pulse boosts the energy delivered to the film as the substrate discharges during pulse pauses. These effects were also manifested in the structure and stress of the deposited films.

3:20pm **PP2-2-WeA-5 Influences of Target Poisoning on the Phase, Microstructure, and Mechanical Properties of Crmonbtwvc High Entropy Alloy Carbide Thin Films Grown by a Superimposed Highpower Impulse and Medium-Frequency Magnetron Sputtering System, Tse Wei Chen [gagamodo@gmail.com], Chia-Lin Li, Ming Chi University of Technology, Taiwan; Bih Show Lou, Chemistry Division, Center for General Education, Chang Gung University, Taoyuan, Taiwan; Jyh Wei Lee, Ming Chi University of Technology, Taiwan**

Since the high entropy alloy (HEA) materials were proposed by Prof. Yeh in 2004, they have been widely studied due to their outstanding mechanical and physical properties. HEAs refer to alloys consisting of at least five elements, with each element's content not exceeding 35 at.%. This compositional constraint prevents any single element from dominating the material's behavior, resulting in unique characteristics arising from the collective contribution of multiple elements. Compared with traditional binary or ternary alloy carbide coatings, HEA carbide coatings have superior performances, such as high hardness, good wear, and corrosion resistance. In this study, an equimolar CrMoNbTiW target was employed to deposit CrMoNbTiWC carbide thin films on 420 stainless steel, 304 stainless steel, and silicon wafer substrates via different target poisoning ratios by a superimposed highpower impulse magnetron sputtering (HiPIMS-MF) system. During the sputtering process, the CrMoNbTiW target poisoning ratios were controlled from 10% to 90% by the feedback control of acetylene gas flow ratios and the optical emission signal intensity of Cr species using a plasma emission monitoring feedback control system. The film thickness and cross-section morphologies were analyzed using field emission scanning electron microscopy and transmission electron microscopy. The crystal structure of the thin film was evaluated by X-ray diffraction. The chemical composition analysis revealed that the carbon content increased from 20.0 at.% to 88.3 at.% as the target poisoning ratio increased from 10 to 90%. The HEA carbide film exhibited an FCC phase. A maximum hardness of 25.1 GPa was obtained for the HEA carbide film containing 53.0 at.% carbon. The friction coefficient of thin film decreased with increasing carbon contents. The impact of target poisoning ratio and carbon content on the phase, microstructure, and mechanical properties of CrMoNbTiWCHEA carbon thin films were discussed in this work.

3:40pm **PP2-2-WeA-6 Novel Superimposed HiPIMS/RF Sputtering Process on a Single Magnetron, Mark Günter, Melec GmbH, Germany; Caroline Adam [c.adam@physik.uni-kiel.de], Melec GmbH, Kiel University, Germany** Reactive sputtering of dielectric films poses significant challenges, primarily due to target poisoning, which can lead to arcing, hysteresis, and generally lower deposition rates [1]. RF (radio-frequency, 13.56 MHz) is a stable option for arc-free processes, even though the films can be porous and grow at lower rates than in DC or MF (mid-frequency) mode. HiPIMS (high power impulse magnetron sputtering) is known to deposit dense films, however the tendency for arcing is higher due to the high peak voltages [1].

To provide stable deposition conditions, a hybrid sputtering process is investigated where HiPIMS and RF are simultaneously applied to the same cathode. For this purpose, a Melec SPIK3000A HiPIMS generator is connected alongside an RF generator and a conventional matchbox to the magnetron. An additional filter (Aurion Anlagentechnik GmbH) is necessary to avoid RF reflection into the HiPIMS generator. The radio-frequency can be either applied continuously or by superposition in the on or off-time of the HiPIMS pulses. The film deposition experiments are complemented by plasma diagnostics with energy-resolved mass spectrometry [2] and so-called non-conventional diagnostics as the passive thermal probe [3].

The addition of an RF plasma provides pre-ionization for the HiPIMS pulses, yields to a faster HiPIMS current rise and allows to reduce the process pressure. This phenomenon was already investigated for the superposition of HiPIMS with DC [4] or MF [5]. During reactive sputtering of Al<sub>2</sub>O<sub>3</sub> and SiO<sub>2</sub>, the addition of RF substantially mitigates arcing, as evidenced by the resulting films, which show a remarkable decrease in droplet density. The deposition rates of the HiPIMS and RF power add up in the superimposed process achieving a higher overall deposition rate.

Proof of principle for a combination of RF and HiPIMS excitation on one magnetron has been established and opens up a new route for arc-free

deposition of Al<sub>2</sub>O<sub>3</sub> and other oxidic layers. Further investigations will include the influence and optimization of pulse parameters as well as the effect of the ratio between the average HiPIMS and RF power.

- [1] A. Anders, *J. Appl. Phys.* 121, 171101 (2017).
- [2] J. Benedikt et al., *J. Phys. D: Appl. Phys.* 45 (2012) 403001.
- [3] H. Kersten et al., *Thin Solid Films* 377–378 (2000) 585–591.
- [4] P. Vašina et al., *Plasma Sources Sci. Technol.* 16 (2007) 501–510.
- [5] W. Diyatmika et al., *Surf. Coat. Technol.* 352 (2018) 680–689

4:00pm **PP2-2-WeA-7 Towards Ti-Si-C MAX-based coatings via reactive cathodic arc evaporation: Advanced Characterization and Process Optimization, Arno Gitschthaler [arno.gitschthaler@tuwien.ac.at], Rainer Hahn, TU Wien, Institute of Materials Science and Technology, Austria; Jürgen Ramm, Carmen Jerg, Oerlikon Balzers, Oerlikon Surface Solutions AG, Liechtenstein; Szilárd Kolozsvári, Peter Polčík, Plansee Composite Materials GmbH, Germany; Eleni Ntemou, Daniel Primetzhofer, Uppsala University, Sweden; Helmut Riedl, TU Wien, Institute of Materials Science and Technology, Austria**

MAX phases are a unique class of nanolaminated compounds that combine properties of metals and ceramics, offering electrical and thermal conductivity alongside creep, oxidation, and corrosion resistance. Consequently, there is growing interest in synthesizing relatively phase pure MAX phase PVD coatings for a broad range of applications. However, the successful development of MAX-based coatings for next-generation technologies requires a comprehensive understanding of the relationships between the deposition processes, chemical composition and phase formation. Among the various MAX phases, the thin film synthesis of the Ti-Si-C system has been the focus of research for quite some time [1], [2]. Yet, reducing the synthesis temperature to below 650 °C remains a major challenge, as it limits compatibility with metallic substrates and therefore practical use. Regarding this issue, cathodic arc evaporation has great potential due to its elevated ionization degree.

Thus, a variety of Ti-Si-C coatings have been grown by arc evaporating metallic targets (Ti or TiSi) in reactive plasma atmospheres (Ar, SiH<sub>4</sub> & C<sub>2</sub>H<sub>2</sub> or Ar & C<sub>2</sub>H<sub>2</sub>) at 550 °C in an industrial coating plant. To improve adhesion to metallic substrates and to prevent element diffusion between the coating and the substrate, a thin Ti interlayer was applied. The first challenge was the adjustment of the reactive gas flow rates in order to maintain the narrow stoichiometric window during film growth and ensure the formation of Ti-C and Si nanolayers. Final confirmation of the selected deposition approaches was provided by the precise determination of elemental composition using elastic recoil detection analysis (ERDA) and Rutherford backscattering spectrometry (RBS). Subsequently, the focus was on the phase characterization of the Ti-Si-C MAX phases and its most competitive phases (e.g. TiC and Ti<sub>5</sub>Si<sub>3</sub>C) through various laboratory and synchrotron X-ray diffraction (XRD) techniques, such as BBXRD, GIXRD, HT-GIXRD and CSnanoXRD. In particular, the high energy X-rays used for transmission nanodiffraction experiments allowed accurate phase identification and provided valuable insights into preferred growth directions. Overall, it has been successfully demonstrated for the first time that Ti-Si-C MAX-based coatings can be synthesized by reactive CAE at temperatures below 650 °C.

- [1] J.-P. Palmquist et al., "Magnetron sputtered epitaxial single-phase Ti<sub>3</sub>SiC<sub>2</sub> thin films," *Appl. Phys. Lett.*, vol. 81, no. 5, pp. 835–837, Jul. 2002.
- [2] J. Alami et al., "High-power impulse magnetron sputtering of Ti-Si-C thin films from a Ti<sub>3</sub>SiC<sub>2</sub> compound target," *Thin Solid Films*, vol. 515, no. 4, pp. 1731–1736, Dec. 2006.

4:20pm **PP2-2-WeA-8 Influence of Pulse Duration on Plasma Chemistry and Thin Film Growth of Plasmonic Titanium Nitride Deposited by Constant Current Regulated HiPIMS, Ethan Muir [e.muir@shu.ac.uk], Arutiun Ehasarian, Sheffield Hallam University, United Kingdom; Ryan Bower, Imperial College London, UK; Yashodhan Purandare, Sheffield Hallam University, United Kingdom**

Plasmonic materials require very high temperatures to manufacture and are not available by conventional methods, this study develops a low temperature process to satisfy this demand.

Typically, plasmonic Titanium Nitride thin films produced via PVD methods are deposited at temperatures between 600-800 °C. The Titanium Nitride films produced for this study were deposited at room temperature, ensuring they are CMOS-compatible and consequently, reducing the energy consumption of the process. Titanium Nitride thin films are ideal for real-

world applications, due to their high hardness and corrosive resistance, extending the lifetime of components the films are applied to. This study aims to produce films for photocatalytic applications with longer lifetimes than currently produced photocatalytic materials such as nanoparticles.

This study documents the results of an investigation into the effect of pulse duration within constant-current HIPIMS discharges, specifically investigating the effects on plasma chemistry, temporal evolution and on the changes to thin film texture of films produced from these discharges. Pulse durations ranging from 40-200 $\mu$ s were studied. Time-Averaged Optical Emission Spectroscopy (OES) and Time-resolved OES have been conducted on a series of discharges with different pulse durations. The data obtained from the Time-Resolved OES shows three stages that can be used to characterise the generation of the discharge: Gas Rarefaction, Pumping and Steady State. Time-resolved and Time-averaged mass spectrometry studies were also conducted which verify the data obtained via OES. There is proof of an increase in electron temperature within the discharge whilst current and voltage remain constant. Titanium Nitride films were produced from the different discharges studied to investigate the role that pulse duration and plasma chemistry plays on the texture of the produced films via x-ray diffraction (XRD). Bragg-Brentano scans and pole figures show how the crystallographic structure of the film changes with the changing pulse duration and the effects it has on the grain sizes and stress within the film on micro and macro scales. Nanohardness and toughness were measured for each of the produced samples showing how the mechanical properties of the film are affected by the pulse duration. These films optical properties have also been studied using ellipsometry to determine their real and imaginary permittivity, to assess their plasmonic capabilities within the visible spectrum.

**4:40pm PP2-2-WeA-9 Monitoring Vanadium Nitride Thin Film Deposited by Reactive Hipims: From Microstructure to Properties, Julien Neyrat [julien.neyrat@safrangroup.com], Marjorie Cavarroc, Safran, France; Angeline Poulon, CNRS, Université de Bordeaux - ICMCB, France**

Among hard coatings materials, transition metal nitrides proved to be valuable candidates with excellent mechanical properties and both chemical and thermal stabilities. This study proposes to show the interest of Reactive High-Power Impulse Magnetron Sputtering (R-HiPIMS) process to produce Vanadium nitride thin films. Thanks to a high ionization degree of the sputtered metal and to high peak power densities applied to the target during few tens of microseconds pulse, deposited films are dense and homogeneous. The influence of several process parameters (target peak power density, N<sub>2</sub> partial pressure, total gas (Ar + N<sub>2</sub>) pressure and pulse parameters) on film microstructure are reported. The obtained structures were investigated by X-ray diffraction (GIXRD and  $\theta$ -2 $\theta$ ) and both scanning and transmission electron microscopy. Discharge composition and electrical characteristics according to processing parameters were studied by optical emission spectroscopy and Langmuir probe measurements. The VN obtained microstructure depends strongly on processing parameters especially pulse parameters and gas parameters which affect the incoming species energy at the substrate. The VN microstructure formation is discussed with respect to conditions promoting both adatoms mobility on the substrate surface and ionized species into the plasma. Comparison of mechanisms involved during the formation of the microstructure depending on the process parameters is presented as well as characterization of mechanical properties (mechanical and electrical) of deposited layers.

## Plasma and Vapor Deposition Processes Room Palm 3-4 - Session PP3-WeA

### ALD, CVD Coating Technologies

**Moderators: Dr. Hiroki Kondo**, Kyushu University, Japan, **Dr. Frederic Mercier**, University of Grenoble Alpes, France

**2:00pm PP3-WeA-1 Electrical Conductivity as a New Parameter for SAMs-Free Area-Selective Atomic Layer Deposition, from Principles to Photoconversion Devices, David Horwat [david.horwat@univ-lorraine.fr], Institut Jean Lamour/Université de Lorraine, France** **INVITED**

Area-selective atomic layer deposition (AS-ALD) has gained a lot of attention in recent years due to the possibility of achieving accurate patterns in nanoscale features, especially for complex 2D or 3D nanostructures [1], which makes this technique compatible with the continuous downscaling in electronics devices. AS-ALD is usually achieved by deactivation of part of the surface by self-assembly monolayer (SAMs) of

certain molecules [2]. Here we propose a different approach that consists in modulating a property of the substrate to achieve localized growth of different materials, its electrical conductivity. This concept is demonstrated by selective growth of high quality metallic Cu, and semiconducting Cu<sub>2</sub>O or absence of deposition, depending on the value of the electrical conductivity and substrate temperature. We will present our understanding of the process and will highlight some of its potentials. It is for instance possible to interface n and p semiconductors or semiconductors and metals with local control in order to fabricate demonstrator devices [3-5] of potential interest for photoconversion purposes.

1. A. J. M. Mackus, A. A. Bol, and W. M. M. Kessels, *Nanoscale* 6, 10941 (2014).
2. A. Mameli, M. J. M. Merckx, B. Karasulu, F. Roozeboom, W. M. M. Kessels, and A. J. M. Mackus, *ACS Nano* 11, 9303 (2017).
3. C. de Melo et al. *ACS Applied Materials and Interfaces* 10 (2018) 37671-37678
4. C. de Melo et al. *ACS Applied Materials and Interfaces* 10 (2018) 40958-40965
5. C. de Melo et al. *ACS Applied Nano Materials* 2 (2019) 4358-4366

**3:00pm PP3-WeA-4 Selective Generation of Nanoparticles in Plasma-Enhanced CVD and Deposition of Carbon Films with Low Compressive Stress, Kazunori Koga [koga@ed.kyushu-u.ac.jp], Kyushu University, Japan** **INVITED**

The stress of diamond-like carbon (DLC) films has been a significant issue in enhancing the performance of protective coatings used in dry etching masks, automotive parts, and battery electrodes. Traditionally, metal nanoparticles have been incorporated into the films to reduce stress. However, this approach often leads to metal contamination, which deteriorates the performance of semiconductor devices. In this study, inspired by the incorporation of metal nanoparticles, we aimed to alleviate stress by incorporating carbon nanoparticles (CNPs) into DLC films. As a first step, we successfully controlled the size of the nanoparticles using plasma chemical vapor deposition (CVD). Subsequently, we managed to control the amount of CNPs deposited on substrates using capacitively coupled plasma CVD, a technique widely employed for large-area deposition. Transmission electron microscopy (TEM) images revealed that the deposited CNPs could be classified into two size groups: the smaller group with a mean size of approximately 2.9 nm, and the larger group with a mean size of around 16 nm. We successfully controlled the amount of CNPs on the films with discharge duration. We shortened the discharge time to prevent the nanoparticles from piling up on the substrate, resulting in sparse deposition on the film surface. The amount of nanoparticles deposited was expressed as a percentage of nanoparticles per unit area of the film, defined as the coverage (Cp) of CNPs. Based on these results, we fabricated a-C:H/CNP/a-C:H sandwich-like films using the plasma CVD. A mixture of Ar and CH<sub>4</sub> gases was introduced from the top of the chamber at flow rates of 19 sccm and 2.6 sccm, respectively, maintaining a total pressure of 0.3 Torr. These conditions were consistent with those used for CNP deposition. The mass density of the deposited a-C:H films was 1.88 g/cm<sup>3</sup>. We observed that the film stress decreased with increasing Cp, from 1.59 GPa at Cp = 0% to 1.02 GPa at Cp = 8.9%, with a similar value at Cp = 15.9%. This represents a reduction rate of 35.8%. These results indicate that incorporating a small amount of CNPs can effectively reduce film stress. Moreover, we successfully expressed the stress reduction rate in terms of Cp using experimental results for different sandwich film thicknesses.

**4:00pm PP3-WeA-7 Direct ALD Deposition by  $\mu$ DALP™. Precision Coatings for Next Gen Devices, Mira Baraket [mira.baraket@mail.com], ATLANT 3D Nanosystems, Denmark**

Advancements in the microelectronics sector demand the ability to create high-quality films with nanoscale accuracy to pattern complex features on substrates. Area-selective deposition (ASD) meets this demand by enabling the selective formation of films on specific surface regions while preventing deposition elsewhere<sup>1</sup>. Atomic Layer Deposition (ALD), a well-established technique in the semiconductor field has been widely investigated for ASD applications. However, this method often requires initial surface treatments, surface functionalization, or alterations to the process<sup>2</sup>.

ATLANT 3D has introduced an innovative technology named microreactor Direct Atomic Layer Processing -  $\mu$ DALP™, enabling precise localized thin film deposition with accuracy down to a few hundred microns, incorporating all conventional ALD advantages (Fig. 1 (a)). This technology leverages a specialized design of micronozzles to spatially separate precursors and reactants, facilitating rapid film deposition at atmospheric

conditions (Fig. 1(b))<sup>3</sup>. The  $\mu$ DALP™ technology stands out for its vertical atomic monolayer precision, achieving an accuracy of 0.2 nm. It is especially effective for selective patterning across diverse surfaces, including microfluidic channels, optical gratings, and nanostructured interfaces, showcasing its versatility and precision. Moreover, this technology enables fast and cost-effective prototyping of devices, facilitating a level of design creativity and optimization that is challenging by traditional thin film deposition approaches.

ATLANT 3D's technology has been successfully utilized to innovate in fields such as optics and photonics, quantum devices, microelectromechanical systems (MEMS), RF electronics, cutting-edge memory technologies, advanced packaging, and energy storage, showcasing its wide-ranging application potential. In this talk we will explain the significant contributions of our  $\mu$ DALP™ technology to the evolution and expansion of thin-film manufacturing and discuss the wide array of opportunities it presents across different sectors.

**Fig. 1.** (a) Top view of aligned Si trenches (aligned horizontally) coated with a perpendicular line of TiO<sub>2</sub> (low magnification SEM). (b) Microfluidic precursor delivery concept: Schematic view of the delivery nozzle in frontal view (top) and in cross-section (lower panel).

## References

- (1) Parsons, G. N.; Clark, R. D., **2020**, *32* (12), 4920–4953.
- (2) Mackus, A. J. M.; Merx, M. J. M.; Kessels, W. M. M., *Chemistry of Materials* **2018**, *31* (1), 2–12.
- (3) Kundrata, I.; Barr, M. K. S.; Tymek, S.; Döhler, D.; Hudec, B.; Brüner, P.; Vanko, G.; Precner, M.; Yokosawa, T.; Spiecker, E., *Small Methods* **2022**, *6* (5), 2101546.

**4:20pm PP3-WeA-8 Temperature Influence on the Chemical Vapor Deposition of Nitrogen-Doped SiC Polycrystalline Films for Brain-Implantable Devices**, *Michalis Gavalas*, SIMaP, CNRS, University Grenoble Alpes, France; *Konstantinos Zekentes*, Microelectronics Group/IESL-FORTH, University of Crete, Hellas, Greece; *Frederic Mercier* [[frederic.mercier@grenoble-inp.fr](mailto:frederic.mercier@grenoble-inp.fr)], SIMaP, CNRS, University Grenoble Alpes, France

Silicon carbide (SiC) is a wide-gap semiconductor, with high chemical stability, that is proposed as a functional material for biomedical applications [1,2]. Epitaxial and polycrystalline SiC has been proposed for neural recording and stimulation electrode devices [3,4]. Unlike the epitaxial case, polycrystalline 3C-SiC is advantageous as it can grow on various substrates (silicon, silica, diamond, sapphire etc) and at lower temperatures. However, the state of the art for the polycrystalline SiC based neural interfaces is still poor. Dense layers of poly-SiC with low resistivity and low stress combined with the good chemical stability of SiC are required for the fabrication of neural interfaces [3,4]. Towards this aim, polycrystalline nitrogen doped 3C-SiC thin films, are grown on 2 inches Si wafers by low-pressure chemical vapor deposition (LPCVD) technique with the aim to be used as support and active material in microelectronic devices and for neural interfaces. The effect of deposition temperature on the structural, mechanical and electrical properties is investigated. Growth rate is varying from 1  $\mu$ m/h to 14  $\mu$ m/h, along with the deposition temperature. We show that we can control simultaneously the structural and electrical properties of polycrystalline SiC by changing the deposition temperature. Films with resistivity as low as (10.0  $\pm$  0.5) m $\Omega$ -cm, low residual stress of (245  $\pm$  13) MPa and RMS surface roughness of (159  $\pm$  54) nm are achieved. Furthermore, the chemical stability of SiC in physiological fluids is investigated and we show that polycrystalline SiC can be a suitable material for neural interfaces applications.

- [1] Maboudian, R. et al., *J. Vac. Sci. Tech.*, **31**, 5, 2013
- [2] Sadow, S. et al., *Microm.*, **13**(346), 1-21, 2022
- [3] Bernardin, E. et al., *Microm.*, **9**(8), 1-18, 2018
- [4] Diaz-Botia, C. et al., *J. Neural. Eng.*, **14**, 11, 2017

## Topical Symposium on Sustainable Surface Engineering Room Palm 5-6 - Session TS2-WeA

### (Photo)electrocatalysis and Solar/Thermal Conversion

**Moderators:** **Dr. Atasi Dan**, National Institute of Standards and Technology (NIST), USA, **Dr. Arnaud Le Febvrier**, Uppsala University, Sweden, **Prof. Carlos Tavares**, University of Minho, Portugal

**2:00pm TS2-WeA-1 Flexible Thermoelectrics: Transforming Wearables, Space Exploration, and IoT**, *André Pereira* [[ampereira@fc.up.pt](mailto:ampereira@fc.up.pt)], University of Porto, Portugal **INVITED**

Flexible thermoelectric (TE) materials are at the forefront of advancing wearable electronics, space exploration, and the Internet of Things (IoT), offering a sustainable and efficient means of converting thermal gradients into electrical energy. Recent research has explored innovative designs and materials to overcome challenges in flexibility, efficiency, and scalability. A pivotal development is the radial flexible thermoelectric device powered by high-power laser beams, showcasing photo-thermoelectric conversion for wireless energy transfer. This approach provides a transformative solution for applications in space exploration, particularly for powering CubeSats and remote sensing systems.

Advances in hybrid thermoelectric materials have also driven significant progress. Nanostructured Bi<sub>2</sub>Te<sub>3</sub> composites, integrated with polymer matrices like PVA, have demonstrated enhanced thermoelectric performance and printability. Devices fabricated with these materials achieve excellent mechanical flexibility and are well-suited for low-power wearable devices and printed electronics. The optimization of hybrid materials and ink formulations has enabled the realization of scalable, printable thermoelectric generators (TEGs) with customizable geometries.

Furthermore, the development of functional thermoelectric inks has opened avenues for high-throughput manufacturing of flexible  $\mu$ -TEGs. These devices exhibit improved thermoelectric properties, mechanical stability, and adaptability to various substrates, ensuring seamless integration into IoT sensor networks and wearable platforms. The interplay of material innovations, device architecture, and advanced manufacturing techniques underscores the potential of flexible thermoelectrics in addressing global energy challenges while enabling novel functionalities in emerging technologies.

This work highlights the role of multidisciplinary approaches in transforming the capabilities of thermoelectric devices, paving the way for their adoption in dynamic environments and applications demanding autonomy and efficiency.

**Acknowledge:**

This work was financially supported by Fundação para a Ciência e a Tecnologia (FCT)/MEC and FEDER under Program PT2020 through the projects UIDB/04968/2020 and UIDP/04968/2020, and NORTE-01-0145-FEDER022096 from NECL.

**References:**

- M. Almeida “Touch Empowerment: Sistema termoeletrico e-Tattoo autossustentável para mapeamento de temperatura” (2024) – Advanced Science
- Printed Flexible  $\mu$ -Thermoelectric Device Based on Hybrid Bi<sub>2</sub>Te<sub>3</sub>/PVA Composites
- AL Pires, et al. *ACS applied materials & interfaces* **11** (9), 8969-8981
- A Photo-Thermoelectric Twist to Wireless Energy Transfer: Radial Flexible Thermoelectric Device Powered by a High-Power Laser Beam

**2:40pm TS2-WeA-3 Alloy/Phosphate Heterostructure as High-Performance Hydrogen Evolution Reaction Electrocatalyst**, *Yung Hsun Yen* [[N56124210@gs.ncku.edu.tw](mailto:N56124210@gs.ncku.edu.tw)], National Cheng Kung University (NCKU), Taiwan; *Thi Xuyen Nguyen*, National Cheng Kung University (NCKU), Taiwan; *Jyh Ming Ting*, National Cheng Kung University (NCKU), Taiwan

With the rising demand for sustainable energy, the development of efficient electrocatalysts for the hydrogen evolution reaction (HER) has become increasingly important. Also, achieving cost-effective water electrolysis in industrial scale is crucial for large-scale green hydrogen production. In this study, we have investigated metal alloy/phosphate heterostructure HER electrocatalysts. Alloy is first synthesized using a two-step hydrothermal process, followed by thermal annealing. Phosphate is then electro-deposited on the surface of as-prepared alloy. The obtained catalyst demonstrates excellent catalytic activity toward HER with a low overpotential of 28.4 mV at 10 mA cm<sup>-2</sup> and small Tafel slope of 42.1 mV dec<sup>-1</sup>. Under a high current density of 500 mA cm<sup>-2</sup>, the catalyst requires an

# Wednesday Afternoon, May 14, 2025

only ultra-low overpotential of 186.3 mV. Stability tests using AEMWE having the heterostructure OER electrocatalyst are performed under 1 M KOH electrolyte and 1 M KOH + 0.3 M NaCl electrolytes. After 1000-h of test at 500 mA cm<sup>-2</sup>, negligible voltage drops are demonstrated under both electrolyte conditions. The excellent HER performance and cost-effectiveness of the synthesized catalyst is highly desirable for real water splitting for sustainable hydrogen production.

3:00pm **TS2-WeA-4 Ni-Co Based Catalysts for the Upcycling of Polyethylene Terephthalate**, *Ruei Chi Lin [a0979116476@gmail.com]*, National Cheng Kung University (NCKU), Taiwan; *Thi Xuyen Nguyen*, National Cheng Kung University (NCKU), Taiwan; *Jyh Ming Ting*, National Cheng Kung University (NCKU), Taiwan

Plastic waste management represents a critical environmental issue. Electrochemical upcycling of polyethylene terephthalate (PET) waste into high-value chemicals has received great attention recently. However, the development of highly active and selective catalysts remains challenging. In this study, we have developed a noble metal-free Ni-Co based electrocatalyst, synthesized via a hydrothermal method, for ethylene glycol oxidation reaction (EGOR). The EG is derived from PET. With its high surface area and tunable electronic structure, the obtained catalyst exhibits an excellent potential of 1.25 V and 1.31 V at current densities of 10 mA cm<sup>-2</sup> and 100 mA cm<sup>-2</sup>, respectively. PET is effectively transformed into potassium terephthalate with excellent Faradaic efficiency and selectivity under high current density. Meanwhile, zero-gap membrane electrode assembly closed-loop flow reactor has been used to achieve outstanding stability of PET upcycling in PET hydrolysis at 100 mA cm<sup>-2</sup>. This work highlights the excellent potential for electro-reforming PET plastic waste into valuable chemicals with simultaneous reduced-cost hydrogen production.

3:20pm **TS2-WeA-5 Single Atom Ag Bonding between PF3T nanocluster and TiO<sub>2</sub> leads the Ultra-stable Visible-Light-Driven Photocatalytic H<sub>2</sub> Production**, *Tsan-Yao Chen [chencaeser@gmail.com]*, *Fan-Gang Tseng*, National Tsing Hua University, Taiwan; *Jyh-Pin Chou*, National Taiwan University, Taiwan

Atomic Ag cluster bonding is utilized to enhance the interface between PF3T nanoclusters and TiO<sub>2</sub> nanoparticles. At an optimized Ag loading of 0.5 wt% (Ag/TiO<sub>2</sub>), the Ag atoms are uniformly dispersed on the TiO<sub>2</sub> surface, generating a high density of intermediate states within the bandgap. This forms an efficient electron channel between the terthiophene groups of PF3T and TiO<sub>2</sub> in the hybrid composite (denoted as T@Ag0.5-P). The enhanced interface broadens the photon absorption bandwidth and facilitates core-hole splitting by enabling photon-excited electrons (from excitons in PF3T) to inject into the conduction band (CB) of TiO<sub>2</sub>. These features enable a remarkable H<sub>2</sub> production efficiency of 16,580 μmol h<sup>-1</sup> g<sup>-1</sup> and exceptional photocatalytic stability, with no degradation observed under visible light exposure for 96 hours. Compared to the hybrid material without Ag bonding (TiO<sub>2</sub>@PF3T), the H<sub>2</sub> production yield and stability improve by 4.1-fold and 18.2-fold, respectively, representing the best performance among similar materials with comparable component combinations and interfacial reinforcement strategies. This innovative bonding approach opens new opportunities for advancing photocatalytic hydrogen production technologies.

3:40pm **TS2-WeA-6 Transition Metal-Based Electrocatalysts for Sustainable Oxygen Reactions in Green Energy Applications**, *Emma Björk [emma.bjork@liu.se]*, Linköping University, IFM, Sweden

Water splitting and recombination are pivotal processes in the transition toward green, renewable, and fossil-free energy production. These reactions are limited by the kinetics of the oxygen reactions—the Oxygen Evolution Reaction (OER) and the Oxygen Reduction Reaction (ORR)—which creates a significant demand for efficient electrocatalysts. Efforts are focused on developing abundant, cost-effective alternatives to the noble metal catalysts currently in use. In this presentation, the possibility to use transition metal oxides, e.g. Co, Ni, and Mn oxides, as oxygen catalysts will be discussed.

The first part will cover multicomponent films, e.g. CoCrFeNi and MnCrFeNi, as catalytically active, corrosion-resistant coatings. The films were synthesized via magnetron sputtering and subsequently subjected to electrochemical activation through anodization, enhancing their catalytic activity towards both ORR and OER. Anodization also altered the ORR mechanism in CoCrFeNi and MnCrFeNi films, shifting it from a (2+1) electron pathway in as-deposited films to either a 4- or 2-electron pathway in anodized films. These changes are attributed to modifications in active

sites and film structure. Substituting Co with Mn slightly improved OER performance but did not affect the ORR activity significantly.

The films also demonstrated excellent corrosion resistance in alkaline and neutral chloride environments, attributed to the formation of a protective oxide layer. The corrosion performance was influenced by film composition and structure, particularly grain size. For example, lattice distortion in CoCrFeNi enhanced resistance in NaCl, while smaller grain sizes improved the corrosion resistance in KOH.

The second part of the talk focuses on increasing catalytic activity of transition metal oxides by introducing nanoporosity to enhance the number of active sites. Nanoporous materials, which often have specific surface areas exceeding 100 m<sup>2</sup>/g, were synthesized via hydrothermal treatment methods to create nanoporous MO<sub>x</sub> (M = Cr, Fe, Co, Ni, Ce) and NiCo<sub>2</sub>O<sub>4</sub> oxygen electrocatalysts. Optimizing pore size in nanoporous NiO revealed a critical balance between the number of active sites and the diffusion of reactants and products. NiO with a pore size of 3.3 nm achieved the lowest overpotential (335 mV at 10 mA/cm<sup>2</sup>), outperforming a commercial Ir/C catalyst under similar conditions.

The different ORR pathways on the various catalysts enable product selectivity, and we have designed electrochemical cells for an oxygen pump, hydroxyl radical generation, and H<sub>2</sub>O<sub>2</sub> production using nanoporous transition metal oxides, air, water, and KOH.

4:20pm **TS2-WeA-8 Bi-Based Photocatalysts Obtained by Reactive Sputtering for the CO<sub>2</sub> Photoreduction – from Thin Films and Composites to Nanoparticles**, *Angélique Bousquet [angelique.bousquet@uca.fr]*, *Sara Ibrahim*, *Jean-Michel Andanson*, *Pierre Bonnet*, Institut de Chimie de Clermont-Ferrand, France; *Mireille Richard-Plouet*, Institut des Matériaux, France; *Maryline Le Granvalet*, Institut des Matériaux de Nantes, France; *Sébastien Roth*, *Audrey Bonduelle*, Institut Français du Pétrole, Energies Nouvelles, France

To reduce the CO<sub>2</sub> emission into atmosphere is a major issue to mitigate the current climate change. Moreover, be able to photo-convert CO<sub>2</sub> into more valuable species and form clean solar fuels and molecules would be a step forward to the industry decarbonation. Among the photocatalysts investigated to photoreduce CO<sub>2</sub>, Bi-based materials have demonstrated their interest to selectively form CO, a molecular building block which can further be used to obtain methanol, acetic acid, aldehyde and even fuels...

In this study, we investigated the deposition of Bismuth oxyfluoride thin films by reactive radiofrequency magnetron sputtering of a pure Bi target in Ar/O<sub>2</sub>/CF<sub>4</sub> atmosphere. We demonstrated, that it is possible to obtain coatings of various crystallized compounds (Bi<sub>7</sub>O<sub>5</sub>F<sub>11</sub>, BiO<sub>0.5</sub>F<sub>2</sub>, BiF<sub>3</sub>...) depending on the injected flow rates of O<sub>2</sub> and CF<sub>4</sub> reactive gases. More interesting, is the possibility to form composites of these compounds with a controlled content of metallic Bismuth nanodomains by reducing the reactive gas flow rates. Hence, we obtained in one step heterojunctions that presents enhanced photocatalytic activities thanks to potential plasmonic effect. The composition, structure and morphology of these coatings were studied by XRD, Raman spectroscopy, XPS, TEM and SEM. Their optical properties, especially their band gap, were determined from UV-visible spectroscopy and ellipsometry. Experiments of photodegradation of pollutants into water shows that an optimum of metallic content has to be found to enhance the photocatalytic properties of the Bi-based materials<sup>[1]</sup>. The CO<sub>2</sub> photoconversion measurements, performed at IFPEN, on these materials demonstrate a photon conversion efficiency close to the one of TiO<sub>2</sub> P25 from Degussa, but with a high selectivity to form CO (= 90% and 10% of H<sub>2</sub>).

To go further, we now working on nanostructuring of these materials in order to increase the contact surface with CO<sub>2</sub> gas using an original method: the reactive sputtering onto liquid. If this technique was already investigated to form dispersion of metallic nanoparticles into liquid, we succeeded for the first time to use it in reactive mode to obtain dispersion of spherical, well-crystallized oxyfluoride nanoparticles with a mean size ranging from 6 to 8 nm and presenting a photocatalytic response<sup>[2]</sup>. These particles may be dispersed on porous support paving the way of high surface specific area system for CO<sub>2</sub> photoreduction.

[1] S. Ibrahim, et al., 2023, hal-04037069v1.

[2] S. Ibrahim, et al., *Nanoscale*, 15, 2023, 5499 - 5509

# Wednesday Afternoon, May 14, 2025

**Awards Ceremony and Honorary Lecture**  
**Room Town & Country A - Session HL-WeHL**

**Bunshah Award Honorary Lecture**

6:05pm HL-WeHL-2 R.F. Bunshah Award and ICMCTF Lecture Invited Talk,  
*Ludvik Martinu* [[ludvik.martinu@polymtl.ca](mailto:ludvik.martinu@polymtl.ca)]<sup>1</sup>, Polytechnique Montréal,  
Canada **INVITED**

---

<sup>1</sup> R.F. Bunshah Awardee  
Wednesday Afternoon, May 14, 2025

# Thursday Morning, May 15, 2025

## Advanced Characterization, Modelling and Data Science for Coatings and Thin Films

### Room Palm 1-2 - Session CM1-1-ThM

#### Spatially-resolved and in situ Characterization of Thin Films, Coating and Engineered Surfaces I

**Moderators:** Dr. Barbara Putz, Empa Thun, Switzerland, Aparna Saksena, MPI für Eisenforschung GMBH, Germany

8:40am **CM1-1-ThM-3 Analysis of Deuterium by Atom Probe Tomography (Apt) - D in V Films and Fe/V Multi-Layered Films, Ryota Gemma [ryota.gemma@tokai.ac.jp]**, Tokai University, Japan; *Talaat Al-Kassab, Astrid Pundt*, University of Göttingen, Germany **INVITED**

In this presentation, we will present the results of deuterium distribution and quantitative analysis by atom probe tomography (APT) in single-layered V or Fe/V multi-layered films. While V is a hydrogen-absorbing metal, Fe hardly dissolves hydrogen (H). Therefore, in Fe/V multi-layered films, almost all of the H atoms are supposed to be in the V layer, and the H distribution should show a clear contrast at the Fe/V interface. This is also the case for deuterium (D). D has a lower diffusion coefficient than H. Hence, a surface segregation of D during the APT analysis can be suppressed, enabling to visualize original D position in the host metal lattice. Furthermore, D can be distinguished from background hydrogen in the APT analysis chamber. By using a portable chamber to prevent the sample from being exposed to oxygen, we were able to measure the D concentration in V or Fe/V films over a wide concentration range. We compared the D concentration measured by APT with the compared with the results of measurements of the hydrogen concentration dependence of electromotive force (EMF) for similar samples, it was found that the average D concentration in the sample could be correctly evaluated using APT.

9:20am **CM1-1-ThM-5 Improving the Elemental Accuracy and Imaging Precision in Atom Probe Tomography of TiSiN Coatings Using Isotopic Substitution and Peak Decomposition, Saeideh Naghdali, Maximilian Schiester**, Montanuniversität Leoben, Austria; *Marcus Hans, RWTH Aachen University, Germany; Markus Pohler, Christoph Czettl, CERATIZIT Austria GmbH, Austria; Michael Tkadletz, Nina Schalk [nina.schalk@unileoben.ac.at]*, Montanuniversität Leoben, Austria

Owing to its excellent mechanical properties TiSiN is commonly used as hard protective coating in cutting applications. However, the detailed investigation of the microstructure of TiSiN is a challenging task due to its nanocomposite structure, typically consisting of nanocrystalline and amorphous regions. Atom probe tomography would be a valuable method to study the local elemental distribution with high resolution, but peak overlaps of Si and N in the mass spectrum do not allow for an unambiguous differentiation, resulting in poor elemental accuracy and imaging precision. In order to improve both, isotopic substitution of naturally abundant nitrogen with <sup>15</sup>N enriched nitrogen was applied, allowing to disentangle the contribution of Si and N to the mass spectrum. In addition, the bulk composition of TiSiN coatings deposited with naturally abundant nitrogen was corrected by peak decomposition considering the corresponding isotopic abundancies, resulting in an improved elemental accuracy. A spatially resolved approach via voxeling the 3D reconstructed data and subsequent peak decomposition of the individual voxels also allows the improvement of the imaging precision. The results showed, that Si is to some extent incorporated into a Ti<sub>1-x</sub>Si<sub>x</sub>N solid solution, but also Ti is incorporated into the amorphous Si<sub>x</sub>Ti<sub>1-x</sub>N<sub>2</sub> phase fraction.

9:40am **CM1-1-ThM-6 Monitoring Thin Film Battery Electrodes via in-Situ/in-Operando Ellipsometry, Máté Fűredi [mate.furedi@semilab.hu]**, Semilab Semiconductor Physics Laboratory Co. Ltd., Hungary; *Jialin Gu, Adam Lovett*, University College London, UK; *Bálint Fodor, András Marton*, Semilab Semiconductor Physics Laboratory Co. Ltd., Hungary; *Stefan Guldin*, Technical University of Munich, Germany; *Thomas Miller*, University College London, UK

The electrochemical energy storage behavior of nano- and microscale (thin- and thick-film) electrodes displays unique characteristics that provide crucial insights into various charge storage mechanisms, essential for the optimal design of commercial battery applications. Additionally, these films are applicable for constructing microbatteries for miniature electronic devices (such as sensors). Critically, material chemistry, crystallinity, and nanostructure significantly influence active charge transfer mechanisms in these systems, generally classified as electrochemical double layer capacitive, pseudocapacitive, or battery-type behaviors. In lithium-ion batteries specifically, the charge storage mechanism involves the

(de)/intercalation of lithium ions in active electrode materials, such as silicon, graphite, or transition-metal oxides.

By optically monitoring thin-film electrodes under electrochemical charge/discharge, a range of time-resolved structural data can be obtained. This work elaborates on this by integrating operando spectroscopic ellipsometric data acquisition. Ellipsometry, highly sensitive to thin films, offers an advantage by effectively excluding any electrolyte side-reactions from measurement, thus providing accurate, real-time data on the evolving structure of lithiated electrodes across charging states. Additionally, ellipsometry tracks thickness changes, enabling precise monitoring of degradation mechanisms.

This work demonstrates (on the example of transition-metal oxide thin-film electrodes) how ellipsometry can reveal intercalation processes, diffusion limitations, and pseudocapacitive contributions. This is further correlated with the complementing electrochemical data. The considerations of this work are furthermore broadly applicable to other thin-film electrode materials.

10:20am **CM1-1-ThM-8 RBS Study of PiTi and NiTi Multilayer Thin Film for Hydrogen Generation and Water Splitting, Enos Nemukula**, University of Venda, South Africa; *Christopher Mtshali*, iThemba laboratory, South Africa; *Fhulufhelo Nemangwele [nemangwele@univen.ac.za]*, University of Venda, South Africa

In this study, thin film samples of Pd-Ti and Ni-Ti systems were prepared using an electron beam evaporator under a vacuum pressure of 10<sup>-6</sup> torr on Si<100>, borosilicate glass, and pure Ti substrates. The absorption of hydrogen, carbon, and oxygen into the thin films was followed by conducting an in-situ real-time Rutherford backscattering (RBS) investigation. RBS confirmed no spontaneous interdiffusion of atoms between the layers during the deposition. The layers were approximately ~30×10<sup>15</sup> atoms/cm<sup>2</sup> (10 nm), and ~433×10<sup>15</sup> atoms/cm<sup>2</sup> (150 nm) for Pd, and Ti layers in the Pd-Ti system, respectively while Ni layer was ~31×10<sup>15</sup> atoms/cm<sup>2</sup> (10.3 nm). The in-situ real-time RBS was performed by linear temperature ramping from room temperature to a maximum temperature of 600 °C at a constant ramping rate of 7 °C per minute. The results showed an interfacial reaction, indicating an unstable system at higher temperatures. Elastic recoil detection analysis (ERDA) revealed an increase in hydrogen absorption of up to 5 at% from the residual gases inside the scattering chamber at a vacuum of 1×10<sup>-6</sup> mbar. Increased oxygen peaks indicated enhanced absorption of this element from the residual gases inside the scattering chamber. These results suggest that this system has potential applications in hydrogen absorption.

10:40am **CM1-1-ThM-9 Exploring the Benefits of Automated, Redox Reactions in XPS Analysis, James Lallo [james.lallo@thermofisher.com]**, Thermo Fisher Scientific, UK, USA; *Robin Simpson, Paul Mack, Tim Nunney*, Thermo Fisher Scientific, UK

This presentation investigates the benefits of automated, in-situ redox reactions for the purpose of producing well controlled oxide growth on the surface of various sample types. The driving force behind using such a procedure is in the potential for generating a sequence of spectra from a progressively chemically-modified surface to remove ambiguities that can lead to misinterpretation, thus aiding in faster understanding of the unmodified surface. Our study presents XPS results from coupled stepwise oxidation/reduction of surfaces, to aid in resolving such ambiguities across a wide array of materials. We use gas-phase oxidation agents to control the redox states of a specimen, leveraging the logarithmic growth of oxide thickness. This oxidation is implemented using vacuum ultraviolet light (VUV) and the generation of ozone and gas-phase hydroxide free radicals close to the surface of the specimens within the entry-lock of the Thermo Scientific Nexsa surface analysis instrument. This work focusses on the benefits of automating this process to ascertain the potential merits of including it into a standard operating procedure for XPS analysis.

11:00am **CM1-1-ThM-10 Hydrofluoric (HF) Acid Corrosion Study of Corrosion Resistant Alloys Used in Semi-Conductor Etching Process Equipment, Donald Williams [donald.williams@horiba.com]**, Kayvon Savadkouei, Brian Chung, Brad Drake, Patrick Lowery, Andrey Krayev, Eddy Robinson, Horiba Instruments Inc., USA

Corrosion studies require the use of complementary analytical techniques, as each method provides results based on the interaction of the investigated material with a probing medium [1]. Obtaining elemental, molecular, and crystal/grain structure information at different spot sizes and probing depths is crucial, particularly for elements that are challenging to observe simultaneously, such as hydrogen and fluorine.

# Thursday Morning, May 15, 2025

In this study, the dissolution of gaseous phase anhydrous hydrogen fluoride and diffusion of fluorine into various metal superalloys were monitored by analyzing changes in concentration, depth, and diffusion rate using Glow Discharge Optical Emission Spectroscopy (GD-OES). A representative area of ultra-high purity (UHP) 316L (composition compliant with SEMI standard F20) and Inconel® 600 alloys were rapidly sputtered to obtain fast elemental depth profiles with nanometer resolution [2]. Atomic Force Microscopy (AFM) provides complementary data with relevance to corrosion studies, ranging from the subtle effects of surface passivation uniformity on the measured surface potential and conductivity of the material to the simple evolution of the surface topography with progression of corrosion (even in the earliest stages) [3].

The corrosion test samples are representative of alloys used in semiconductor manufacturing equipment, where improved alloy durability and the prevention of leaching of corrosion byproducts is critical. The goal is to understand the prevalent corrosion mechanisms in these common semiconductor alloys in order to find ways to increase equipment longevity and minimize contamination to the semiconductor manufacturing processes.

References:

1. Compendium of Surface & Interface Analysis, Springer
2. Review: What Can Glow Discharge Optical Emission Spectroscopy (GD-OES) Technique Tell Us about Perovskite Solar Cells? Small Methods 2022, 2200633
3. Review: Application of AFM-Based Techniques in Studies of Corrosion and Corrosion Inhibition of Metallic Alloys. Corrosion and Materials Degradation 2020, 1, 345–372; doi:10.3390/cmd1030017

11:20am **CM1-1-ThM-11 Numerical Ellipsometry: Artificial Intelligence Based Real-Time, in Situ Process Control for Absorbing Metal Films Depositing on Known Transparent Substrates, Frank Urban [fk\_urban@yahoo.com], David Barton, Florida International University, USA**

Ellipsometry can provide the optical properties and thickness of a thin film depositing on a known substrate, including transparent substrates, in real time using commercially available *in situ* instrumentation. The desired film parameters are related to visible light reflection measurements through Maxwell's equations, wavelength, and geometry. A number of different methods have been developed for obtaining the desired parameters given a reflection or multiple reflections. One category of methods is iterative least squares curve fitting, frequently the Levenberg-Marquardt method. An emerging method is that of artificial intelligence (AI) employing artificial neural networks. One of the primary advantages of the AI method is speed. It can be a thousand times faster than the pre-existing curve fitting methods. The work here demonstrates the use of such an Artificial Intelligence method to enable real-time, *in situ* monitoring of thin film growth. Examples will be given using a single angle of incidence and three angles of incidence for comparison. Thin absorbing films (up to 45 nm) will be given using a multilayer perceptron configuration consisting of either 4 or 12 input and 4 output neurons with two hidden layers of 80 neurons each. Solutions are performed at each wavelength independently and do not rely on fitting functions. The design, training and use of a number of neural networks will be presented.

## Advanced Characterization, Modelling and Data Science for Coatings and Thin Films

### Room Town & Country C - Session CM2-1-ThM

#### Advanced Mechanical Testing of Surfaces, Thin Films, Coatings and Small Volumes I

Moderators: Matteo Ghidelli, CNRS, France, Dr. David Holec, Montanuniversität Leoben, Austria

8:00am **CM2-1-ThM-1 Nano-Mechanical Characterization and Modeling of Plasticity in Metallic Materials, Takahito Ohmura [ohmura.takahito@nims.go.jp], Kyushu University/NIMS, Japan INVITED**

Plastic deformation behavior is characterized through nano-mechanical testing in a small scale associated with microstructures including inter-phase and grain boundary in metallic materials. Deformation behavior was evaluated for Fe-Si bicrystal with different grain boundary plane with S9{221} and S9{114}1. The resistance to a slip transfer at the grain boundary depends on a combination of crystallographic orientation and dislocation character. Plasticity initiation behavior was characterized for

ferrite-cementite interface with different coherency in a pearlitic steel2). The critical stress for the plasticity initiation is lower for a semi-coherent interface than that for an incoherent one, suggesting a potential reason for the continuous yielding phenomenon in macroscopic stress-strain curve of the steel with semi-coherent interface. Transmission Electron Microscope (TEM) in-situ straining was applied to reveal dislocation-grain boundary interactions. In the case of ultra-fine grain steel, dislocations in grain interior can sink at the grain boundary with no remarkable pile-up3). This behavior indicates a dislocation density dominance for the extra-hardening in the UFG steel. Dislocation-Dislocation interaction was also captured through TEM in-situ straining4). The dislocation reaction forms a stable grain boundary, which could be an elementally step of grain refining during severe plastic deformation. The critical stress for a slip transfer was estimated for  $\Sigma 3$  boundary of pure Al5). The mechanism of the slip transfer can be modeled in a simple dislocation reaction generating a grain boundary dislocation. Deformation mechanisms of plasticity initiation and subsequent behavior were modeled through stochastic analysis based on a pop-in phenomenon on a loading segment obtained from nanoindentation measurement6). The critical stress for the plasticity initiation shows Gaussian like distribution function, indicating a thermally-activated process including a nucleation of shear loop dislocation at defect-free region. In the subsequent stage, the loading curve shows intermittent plasticity, and the probability function for the event magnitude shows power-law type, suggesting a catastrophic phenomenon with a fractal dimension such as dislocation avalanche.

References

1. M. Wakeda, Y.-L. Chang, S. Li, T. Ohmura, Int. J. Plasticity, 145, (2021) 103047.
2. Y. Wang, Y. Tomota, T. Ohmura, W. Gong, S. Harjo, M. Tanaka, Acta Mater., 196, (2020) 565-575.
3. H. Li, S. Gao, Y. Tomota, S. Li, N. Tsuji, T. Ohmura, Acta Mater., 206, (2021) 116621.
4. H. Li, S. Li, N. Tsuji, T. Ohmura, Scripta Mater., 207, (2022) 114275.
5. S. Li, T. Enami, T. Ohmura, S. Tsurekawa, Scripta Mater., 221, (2022) 114953.

8:40am **CM2-1-ThM-3 Accelerating Workflows for High-Throughput Nanoindentation, Eric Hintsala [eric.hintsala@bruker.com], Kevin Schmalbach, Douglas Stauffer, Bruker Nano Surfaces, USA**

Heterogenous microstructures are commonly employed across a wide range of applications as a tool for materials scientist to engineer the bulk properties, which can be seen in composite materials, multi-phase alloys or even surface treatments and coatings. Sometimes, property distributions can also arise due to processing history, with laser-based techniques with micro-scale heat affected zones being of particular interest recently. In most cases these structures are nano- to microscale in size, so to isolate mechanical properties from individual regions high-throughput nanoindentation-based techniques have become increasingly popular.

Two recent advances in nanoindentation mapping are highlighted here. First, the indentation depth controls the finest spacing that can be utilized without affecting the subsequent nearby indentations and thereby defines the resolution of a nanoindentation map. Displacement control is particularly important when mapping samples with highly variable hardness. To address this, recent enhancements for the Hysitron TI 990 TriboIndenter (Bruker, USA) allows for trigger points to be used to switch segments and feedback control all within one test. This enables a high-throughput workflow where translation between positions is followed by approach, surface detection, and a displacement-controlled indent. This mode works with both high load and low load transducers for addressing a large range of depths and spacings.

Secondly, relating the measured mechanical properties to local structure and composition is also essential for materials development. This can be done by switching instruments from the nanoindenter to the SEM, but this is time consuming and generally necessitates use of fiducial markers. To facilitate this process, the Hysitron PI 89 Auto (Bruker, USA) in situ SEM indenter utilizes a rotation-tilt stage to move the sample between 3 distinct positions: Indentation position, top-down SEM and EDS position, and 70° tilted EBSD position. The accompanying software enables the same sample region to be co-located in all 3 positions easily, such that regions of interest from an EBSD or EDS map can be directly targeted for indentation testing.

# Thursday Morning, May 15, 2025

9:00am **CM2-1-ThM-4 Understanding the Fracture Behavior, Interface Characteristics of Micro and Nanocrystalline Diamond Laminates Through Flexural Studies**, *Krishna Sarath Kumar Busi [sarath.busi@tudarmstadt.de]*, Technical University Darmstadt, Germany; *Tim Fuggerer*, University of Erlangen-Nuremberg, Germany; *Sebastian Bruns*, Technical University Darmstadt, Germany; *Timo Fromm*, *Stefan M Rosiwal*, University of Erlangen-Nuremberg, Germany; *Karsten Durst*, Technical University Darmstadt, Germany

Diamond metallic laminates (DML) have been demonstrated to exhibit an improved toughening mechanism by modifying the crack driving force with alternate hard and ductile layers [1]. These laminates were produced from free-standing diamond foils using HFCVD, exhibiting distinct crystalline morphologies microcrystalline (conventional) and nanocrystalline integrated with metallic layers deposited through PVD. A systematic investigation was set up to understand the mechanical behavior, interface characteristics of these multilayer system through macro 3PB and micro cantilever flexural studies. Nanocrystalline diamond foils exhibited better toughness, and their fracture sensitivity was analyzed by recording continuous stiffness change with respect to crack propagation for notched cantilevers using nanoindentation. Significant delamination was observed in nanocrystalline laminate (nDML) exhibiting weak interfacial strength between diamond and metal layers. Suitable analytical laminate models were effectively applied to investigate shear stress distribution, critical cracking events and the extent of delamination. Additionally, A 2D model of FEM with cohesive interactions was designed in same experimental scenarios (3-point bending, micro cantilever bending) to understand the diamond-metal interfacial properties, showed strong alignment with the analytical models and offered valuable insights to optimize the overall design of the laminate.

**Keywords:** Laminates, nanoindentation, toughness, fracture, bending, FEM.

## References:

- [1] Yang Xuan et. al (2021), A simple way to make tough diamond/metal laminate, *Journal of European Ceramic Society* 41 (2021) 5138–5146.
- [2] Timo Fromm et. al (2022), Bioinspired damage tolerant diamond-metal laminates by alternating CVD and PVD processes, *Materials & Design*, Volume 213,2022,110315, ISSN 0264-1275.

9:20am **CM2-1-ThM-5 Deposition of Hierarchical Ti/Ti<sub>2</sub>AlC Metal/MAX Multilayered Nanolaminates and Investigating their Mechanical Properties and Deformation Mechanisms**, *Amruta Vaghela [amrutav@iastate.edu]*, Iowa State University, USA; *Skye Supakul*, Pacific Northwest National Laboratory, USA; *Kevin Jacob*, *Sid Pathak*, Iowa State University, USA

We report the challenges (e.g. the diffusion and formation of MAX phase) with the high temperature synthesis of a hierarchical metal/MAX phase multilayered nanolaminate (MMN) where the interface between metal and MAX phase layers are in direct competition with the internal interfaces within the MAX layers. Using a combinatorial physical vapor deposition (PVD) and atomic layer deposition (ALD) system, we report our first successful deposition of a Ti/Ti<sub>n+1</sub>AlC<sub>n</sub> (n=1 or 2) MMN where thin Al<sub>2</sub>O<sub>3</sub> diffusion barrier layers inhibits interlayer diffusion and enables the multilayered architecture to be retained. The mechanical properties of the MMN system show impressive indentation hardness (12.75±0.33GPa), micro-pillar instability stresses (8.1±0.2GPa), and instability strains (8.3±0.4%) compared to a rule-of-mixtures approximation of the hardness and yield strength of the system. Post compression TEM analysis is also being conducted to gain insight on the deformation mechanisms at play in these hierarchical MMN systems.

9:40am **CM2-1-ThM-6 Effect of Fe Addition on the Structural, Mechanical and Electrical Properties of (ZrCu)<sub>1-x</sub>Fe<sub>x</sub> Thin Film Metallic Glass**, *Evgeniy Boltynjuk [evgeniy.boltynjuk@kit.edu]*, *Yulia Ivanisenko*, KIT, Germany; *Marco Ezequiel*, *Francesco Bignoli*, *Damien Faurie*, *Philippe Djemia*, *Matteo Ghidelli*, CNRS, France; *Horst Hahn*, Oklahoma State University, USA

Thin film metallic glasses (TFMGs) have emerged as a promising class of materials for applications in the field of flexible electronics, owing to their large deformability, metallic-like electrical conductivity, and low or even negative temperature coefficient of resistivity. However, despite these advantages, the properties of TFMGs require improvement to expand their range of applications. In this study, we focus on (ZrCu)<sub>1-x</sub>Fe<sub>x</sub> system, as the properties of the ZrCu system have been investigated across a broad range of compositions, while the addition of Fe can potentially improve its glass forming ability and thermal stability. Specifically, we will discuss experimental results and *ab initio* calculations on the effect of Fe addition

on mechanical and electrical properties, with a focus on clarifying the relationship between these properties and atomic structure and local ordering.

(Zr<sub>34</sub>Cu<sub>66</sub>)<sub>1-x</sub>Fe<sub>x</sub> TFMGs were synthesized by magnetron sputtering varying the Fe content from 0 up to 76 at.%. All obtained samples, up to the highest Fe content (76 at. %), have an amorphous structure, indicating a high glass forming ability. The electrical resistivity shows a monotonic decrease with increasing Fe content, reducing from 192.4 down to 113.8 μΩ × cm. At the same time, tensile tests on polymeric substrate show a reduction in crack onset strain (COS) from ~ 2.2 down to 1.6% in the range of Fe concentrations from 0 to 54 at.%. For higher Fe concentrations COS shows inverse trend, reaching ~ 2.0% at 76 at.% Fe. Thus, TFMG containing 76 at.% of Fe shows COS value comparable to that of the ZrCu, while achieving a 1.7-fold decrease in electrical resistivity.

Transmission electron microscopy and atom probe tomography reveal structural modifications, mapping the evolution of local ordering and atomic arrangements. By correlating our experimental findings with *ab initio* calculations, we establish a clear relationship between the modification of atomic order and performance of (ZrCu)<sub>1-x</sub>Fe<sub>x</sub> TFMGs. This correlation not only enhances our understanding of TFMGs but also provides a solid foundation for their potential applications in flexible electronics, guiding future research in optimizing TFMGs for advanced technological uses.

10:20am **CM2-1-ThM-8 Mechanical Properties of Thin Films Studied using 4D-STEM**, *Christoph Gammer [christoph.gammer@oaw.ac.at]*, Erich Schmid Institute of Materials Science, Austrian Academy of Sciences, Leoben, Austria; *Alice Lassnig*, Montanuniversität Leoben, Leoben, Austria; *Lukas Schretter*, *Simon Fellner*, Erich Schmid Institute of Materials Science, Austrian Academy of Sciences, Leoben, Austria; *Jürgen Eckert*, Montanuniversität Leoben, Leoben, Austria **INVITED**

The mechanical behavior of thin films is highly dependent on their microstructure. Micromechanical testing can be used to study small-scale mechanical properties. Modern thin film systems are becoming increasingly complex and their overall mechanical properties are influenced by strong variations in the local elastic and plastic response. Therefore, to understand their deformation behavior the local nanoscale stress distribution during loading has to be considered. The overall load-displacement curve is not sufficient. Recently, we have demonstrated that 4D-STEM allows to perform strain mapping at the nanometer scale during continuous *in situ* deformation in the TEM. In the present talk we will present recent advances demonstrating how 4D-STEM can be used to understand the deformation mechanisms in single-crystalline, nanocrystalline and amorphous thin films.

11:00am **CM2-1-ThM-10 Investigating the Interplay between Biaxial Multicracking of Nanometric Thin Films and Their Magnetic Properties: A Nuanced Separation of Magnetoelastic and Magnetostatic Effects**, *Hatem Ben Mahmoud*, *Damien Faurie [faurie@univ-paris13.fr]*, Laboratoire des Sciences des Procédés et des Matériaux (LSPM) – CNRS, France; *Pierre-Olivier Renault*, *Pierre Godard*, Institut Prime - CNRS - ENSMA - Université de Poitiers, France; *Dominique Thiaudière*, *Philippe Joly*, *Christian Mocuta*, Soleil Synchrotron, France; *Eloi Haltz*, *Noël Girodon-Boulandet*, *Fatih Zighem*, Laboratoire des Sciences des Procédés et des Matériaux (LSPM) – CNRS, France

The magneto-electronic systems of the future will be designed to adapt to complex geometries. Flexible electronics have seen rapid growth, offering promising applications in areas such as confined environments and flexible displays [1]. These systems rely on polymers, which are lighter and more cost-effective than silicon. Understanding the interplay between mechanical strain and magnetic properties is essential [2]: at low strains, magnetic anisotropy is key, while at higher strains, microscopic damage (e.g., fragmentation and decohesion) becomes critical [3].

However, the relationship between thin film fragmentation and magnetic properties [4], especially under biaxial tension, remains poorly studied. This thesis aims to fill this gap through novel experimental techniques and studies on model systems. We investigated flexible magnetic systems using *in situ* methods, applying significant mechanical strain (up to 10%) while simultaneously probing their magnetic properties. A magneto-optical Kerr effect (MOKE) magnetometer was developed at the DiffAbs beamline of the Soleil synchrotron. Our research focuses on the distribution of stress (before and during cracking) and its impact on the magnetic response, along with the underlying mechanisms.

Two main mechanisms are identified: first, stresses generated during mechanical loading can induce a strong magnetoelastic field that alters the



# Thursday Morning, May 15, 2025

magnetic response; second, magnetostatic fields between fragments separated by cracks can contribute to coercivity during magnetization cycles. However, these effects have yet to be fully quantified. To address this, we studied magnetization cycles under large deformations in Ni80Fe20 films (with negligible magnetoelastic contribution), of varying thickness, with or without W layers of different thicknesses to modify fragment size. We demonstrate that the magnetostatic contribution is closely linked to the aspect ratio (diameter/thickness) of the fragments. This study, compared with research on Co layers, clearly distinguishes between geometric (magnetostatic) effects and stress-induced (magnetoelastic) effects.

[1] D. Makarov, M. Melzer, D. Karnaushenko, O. G. Schmidt, Applied Physics Review 3, 011101 (2016)

[2] F. Zighem & D. Faurie, Journal of Physics: Condensed Matter 33, 233002 (2021)

[3] B. Putz, T.E.J Edwards, E. Huszar, L. Pethö, P. Kreiml, M. J. Cordill, D. Thiaudiere, S. Chiroli, F. Zighem, D. Faurie, P.-O. Renault, J. Michler, Materials & Design 232, 112081 (2023)

[4] H. Ben Mahmoud, D. Faurie, P.O. Renault, F. Zighem, Applied Physics Letters 122, 252401 (2023)

11:20am **CM2-1-ThM-11 Cross-Sectional Nanoindentation Mapping of Sputtered Inconel 725 Films, *Ikponmwosa Iyinbor [iyinbor@usc.edu]***, Mork Family Department of Chemical Engineering and Materials Science, University of Southern California., USA; *Jin Wang*, Institute of Energy Materials and Devices, Microstructure and Properties of Materials (IMD-1), Forschungszentrum Jülich GmbH., Germany; *Ruth Schwaiger*, Institute of Energy Materials and Devices, Microstructure and Properties of Materials (IMD-1), Forschungszentrum Jülich GmbH., Germany; *Andrea Hodge*, Mork Family Department of Chemical Engineering and Materials Science, University of Southern California., USA

Heterogeneous nanostructured materials (HNMs) offer significant potential for overcoming the strength-ductility trade-off observed in conventional homogeneous nanostructured materials. Recently, we have demonstrated the influence of heterogeneous stress distribution on the development of unique nanostructured features in sputtered nanotwinned Inconel 725 thick films after undergoing heat treatment. A gradient microstructure with three distinct nanodomains featuring a nanocrystalline equiaxed region, a nanotwinned region with carbides, and a region featuring abnormal recrystallization wherein abnormally large grains, delta-phase precipitates, and rafted structures were observed. This unique combination of nanodomains is expected to contribute distinct responses to mechanical deformation behavior.

In this work, two different HNMs of 8  $\mu\text{m}$  and 20  $\mu\text{m}$  film thicknesses were synthesized and heat treated. A nanoindentation mapping technique using a Femto-Tool NMT04 in-situ SEM nanoindenter was performed in order to generate high-spatial resolution hardness and elastic modulus property maps. The nanoindentation maps show a good correlation to the observed heterogeneous microstructure, revealing trends that provide an understanding of the local deformation behavior of these HNMs. Understanding the contribution of each nanodomain to the overall deformation behavior of the films enables the optimization of design and fabrication strategies to provide a superior combination of properties.

## Advanced Characterization, Modelling and Data Science for Coatings and Thin Films

### Room Town & Country D - Session CM3-1-ThM

#### Accelerated Thin Film Development: High-throughput Synthesis, Automated Characterization and Data Analysis I

Moderators: **Dr. Davi Marcelo Febba**, NREL, USA, **Dr. Sebastian Siol**, Empa, Switzerland

8:00am **CM3-1-ThM-1 Combinatorial Screening of Quaternary Piezoelectric Nitrides, Enabled by HiPIMS, *Nathan Rodkey [nathan.rodkey@empa.ch]***, Jyotish Patidar, Federica Messi, Sebastian Siol, EMPA (Swiss Federal Laboratories for Materials Science and Technology), Switzerland

Increasing demand for data and the surge of AI technologies is escalating the needs of telecommunication devices. RF filters are a limiting factor in this regard, where improvements in bandwidth and selectivity are needed. Advanced RF filters rely on piezo thin films like AlN, valued for its linear response and strong electromechanical coupling, with Sc doping enhancing its  $d_{33}$  and overall performance. While AlScN is considered state-of-the-art,

many proposed dopants (e.g. B, Y, La) could further improve its properties. High-throughput experiments are instrumental in exploring quaternary or multinary materials, but few studies examine combinatorial screening of piezoelectric materials. This is because piezoelectric materials are difficult to screen effectively, as their device properties strongly depend on the c-axis texture of the film. During combinatorial gradient deposition the shallow deposition angles and static substrate can cause significant grain tilt towards the dominant source, convoluting composition and texture gradients. In high-power impulse magnetron sputtering (HiPIMS), additional energy can be introduced to arriving species by synchronizing a substrate bias to arriving metal ions. This improves the adatom mobility of species, removing grain tilt, and resulting in highly textured films without substrate rotation. In this work, we use AlScN as an example material to demonstrate how HiPIMS enables effective device screening of piezoelectric properties.

Before the use of HiPIMS, DCMS screening is used to assess solubility limits in the quaternary phase space. This is typically done using X-ray diffraction mapping while applying the disappearing phase method. However, in combinatorial screening of materials this method loses effectiveness, as precipitates can be tilted out of the diffraction plane. Consequently, we use the peak shift of the (0001) plane to track discontinuities from Vegard's law and identify precipitation. Despite the larger ionic radius of Y, the combined solubility of Y and Sc increases, reaching a maximum of ~50%. For context, the solubility limit of AlScN is ~40%. Materials libraries were then made using metal-ion synchronized HiPIMS. The libraries are highly textured, with rocking curve FWHMs of  $<2^\circ$ . Following this, the coupling (k) and clamped  $d_{33}$  coefficients of these libraries were mapped, showing their dependence on the combined Sc and Y contents. Importantly,  $d_{33}$  coefficients were mapped using a double beam laser interferometer (DBLI) for improved accuracy.

8:20am **CM3-1-ThM-2 High-Throughput Experiments Informed by High-Throughput Theory Reveal Zintl Phosphides as a New Family of High-Performance Semiconductors, *Sage Bauers [sage.bauers@nrel.gov]***, 15013 Denver West parkway, USA **INVITED**

The discovery of a new structural class of semiconductor is a rare occurrence. For example, in the case of solar absorption, nearly all relevant semiconductors can broadly be described as materials derived from the tetrahedrally-coordinated diamond structure (e.g., Si, III-Vs, II-VIs, chalcopyrites, kesterites). This is part of the reason that new high-performing materials, such as perovskites, which are made up of octahedral bonding motifs, garner so much interest and help generate new materials design concepts. Using high-throughput computational workflows, we recently discovered that several  $AM_2P_2$  ( $A = \text{Ca, Ba, Sr}$  and  $M = \text{Cd, Zn}$ ) compounds possess the requisite intrinsic materials properties for high optoelectronic performance, including solar-spectrum matched band gaps, strong optical absorption, and benign intrinsic defects, leading to long photoexcited carrier lifetimes. This family of compounds, which exhibits a mixed octahedral + tetrahedral bonding motif, has been known for several decades but the optoelectronic properties had been almost entirely unexplored.

Using a combinatorial synthesis approach based on a hybrid PVD/CVD method, we recently prepared the first thin films of Zintl phosphides  $\text{CaZn}_2\text{P}_2$  and  $\text{SrZn}_2\text{P}_2$ . By combinatorial sputtering from metallic targets in the presence of  $\text{PH}_3$  at low temperature, we prepare films across the ternary composition space. Growths at higher temperatures result in much narrower compositional spreads pinned around the  $AM_2P_2$  composition, indicating an adsorption-controlled growth regime can be realized. Mapping measurements including x-ray fluorescence, x-ray diffraction, UV-vis spectroscopy, photoluminescence, and Raman spectroscopy are used to probe the properties of the zintl phosphide films. To establish the photoactivity and semiconducting nature of the  $AM_2P_2$  materials, minority carrier lifetimes and electronic properties were measured via time resolved microwave conductivity, transient absorption, and van der Pauw/Hall effect. To summarize the characterization of  $\text{CaZn}_2\text{P}_2$  as an example, we observe high optical absorption of  $\sim 10^4 \text{ cm}^{-1}$  at the  $\sim 1.95 \text{ eV}$  direct transition, near band edge optical emission, and a photoexcited carrier lifetime of up to 30 ns at a fluence of  $2 \cdot 10^{13} \text{ cm}^{-2}$ . Films are intrinsic, but p-dopable with +1 elements such as Na (A site dopant) or Cu (M site dopant). Such performance metrics are usually not observed in inorganic solar absorber materials until well into their development, highlighting the value of coupling high-throughput theory, high-throughput experiments, and targeted experiments toward new functional materials.

# Thursday Morning, May 15, 2025

9:00am **CM3-1-ThM-4 High-Throughput Nanoindentation Methodology for Combinatorial Thin Film Material Libraries**, *Andre Bohn [bohndama@usc.edu]*, University Of Southern California, USA; *Adie Alwen, Andrea Maria Hodge*, University of Southern California, USA

Combinatorial and high-throughput (CHT) methods offer an accelerated pathway for the discovery and development of novel materials with wide ranging biological, electronic, and structural applications. One common approach to accelerate synthesis is the deposition of large compositionally graded thin film arrays with hundreds of distinct samples, often referred to as thin film material libraries. High-throughput characterization techniques are then employed to quickly assess processing-structure-property relationships, which generates large datasets for machine learning models and screens for promising next-generation materials. For assessing mechanical behavior in these libraries, nanoindentation is particularly suitable due to the ease of automation, minimal sample preparation requirements, and compatibility with thin films. However, despite the widespread use of this technique in CHT research, many inconsistencies between reported methodologies in literature can be identified. This work presents a CuNi alloy library to identify how to improve data reliability while minimizing experimental times and costs. Emphasis is given to optimizing the number of indents per sample and the distribution of samples tested. By improving method standardization, both efficiency and reproducibility of combinatorial studies can be enhanced, thus expanding the value of material libraries to the scientific community.

9:20am **CM3-1-ThM-5 Empowering Manufacturers with Low-Temperature Plasma: A Novel Approach to Real-Time Thin Film Metrology**, *Peter Rudd [peter.rudd@sirenopt.com]*, 8000 Edgewater Dr, USA

Thin films, or micro- and nano-scale materials with unique functional properties, enable many clean energy industries, such as lithium-ion batteries, solar cells, and carbon conversion. Minimal-waste manufacturing of high-performance thin films will be vital for achieving society's net-zero carbon emission goals. Because existing thin film sensors cannot operate within most sections of manufacturing lines, manufacturers often complete hundreds of processing steps before they can test (a small portion of) their products and detect problems. Current thin-film manufacturing thus often yields many low-quality products, or off-spec products that must be discarded.

Sirenopt has developed a real-time low-temperature plasma-based thin film metrology sensor. The sensor is compact, can be integrated within existing manufacturing lines, and can collect multiple thin film property measurements (such as thickness with a precision of 1/10th of a nanometer, density, resistivity, chemical composition, and contaminate identification) in parallel and in real-time, thus allowing for the collection of critical manufacturing data that is otherwise unobtainable. Sirenopt is currently applying the sensor to industrial thin film coating processes such as Lithium-ion battery electrodes, where this flexible sensor can be used to accelerate R&D and process optimization, improve quality control, and enable real-time process control.

9:40am **CM3-1-ThM-6 Streamlining Inorganic Thin-Film Data Management with the High-Throughput Experimental Materials Database (HTEM)**, *Davi Febba, Nicholas Wunder [Nick.Wunder@nrel.gov]*, *Hilary Egan, Max Gallant, Andriy Zakutayev*, National Renewable Energy Laboratory, USA

Artificial intelligence (AI) is ushering in a new era of progress in materials science, where self-driving laboratories and autonomous instruments are performing experimental research that was once the exclusive domain of humans. Central to this paradigm shift is effective data management, as AI-driven laboratories make decisions based on the data they collect. Ensuring that materials science data is Findable, Accessible, Interoperable, and Reusable (FAIR) is crucial for accelerating materials discovery, as it facilitates seamless integration of diverse datasets and enhances collaboration across research teams.

In this presentation, we will discuss NREL's Research Data Infrastructure (RDI) [1], which catalogs experimental data from inorganic thin-film experiments at NREL and underpins the High-Throughput Experimental Materials Database (HTEM-DB) (<https://htem.nrel.gov/>) [2]. The HTEM-DB stores comprehensive information about synthesis conditions, chemical composition, crystal structure, and optoelectronic properties of materials, making the data readily accessible and reusable for the research community.

Will also present recent advancements in the HTEM's extract-transform-load (ETL) pipeline. These advancements not only allow for large-scale AI analysis of X-ray diffraction (XRD) patterns [3] but also enable the containerization of applications and instruments, making the database

more modular and maintainable. Enabled by the recently developed Hybrid Environment Resources and Operations (HERO), these improvements help to lower the barriers to accessing NREL's computational resources, data analysis, and visualization capabilities. By facilitating both AI integration and modular design, HERO empowers scientists to share their research and collaborate with external partners through interactive applications.

[1] Patterns, 2, 100373, 2021

[2] Scientific Data 5, 180053, 2018

[3] PEARC '24, 39, 1-5, 2024

10:20am **CM3-1-ThM-8 A Python-Based Approach to Sputter Deposition Simulations in Combinatorial Materials Science**, *Felix Thelen [felix.thelen@ruhr-uni-bochum.de]*, *Rico Zehl, Jan Lukas Bürgel*, Ruhr University Bochum, Germany; *Diederik Depla*, Ghent University, Belgium; *Alfred Ludwig*, Ruhr University Bochum, Germany

In combinatorial materials science, magnetron sputtering plays a key role for the exploration of future high-performance materials due to its capability to produce well-defined, continuous compositional gradients in form of thin-film libraries. Its scalability from laboratory settings to industrial applications, relatively high deposition rates, and compatibility with a wide range of materials make it an effective choice for combinatorial synthesis [1]. However, achieving precise control over the deposition profile and compositional distribution often requires multiple preliminary experiments to optimize process parameters - an approach that can be time- and resource-intensive.

Aiming to predict those properties, several analytical and numerical simulations were reported in literature over the past decade [2-4]. However, only the magnetron sputter deposition model SIMTRA [4] was made publicly available. Based on the Monte Carlo approach, it allows to simulate the deposition profile of a single magnetron source, while taking into account the dimensions of the components through a graphical user interface.

In order to make this tool more suitable for the application in combinatorial materials science, the command line version of the SIMTRA application was wrapped in a Python environment, enabling the definition of sputter chambers through code and executing the time-consuming Monte Carlo calculations through user defined scripts. This approach also enables parallel simulation of multiple magnetrons by using multi-threading, decreasing simulation times significantly, especially when simulating co-sputtering systems with 5-8 cathodes. The accuracy of SIMTRA and the capabilities of the Python wrapper are demonstrated by comparing the compositions predicted by simulation and measured by energy-dispersive X-ray spectroscopy of seven materials libraries in the system Ni-Pd-Pt-Ru.

References:

[1] Gregoire, J. M., Zhou, L., and Haber, J. A. (2023). 'Combinatorial synthesis for AI-driven materials discovery'. *Nature Synthesis*, vol. 2, no. 6.

[2] Ekpe, S. D., Bezuidenhout, L. W. and Dew, S. K. (2004) 'Deposition rate model for magnetron sputtered particles', *Thin Solid Films*, vol. 474, no. 1.

[3] Bunn, J. K., Metting, C. J. and Hatrick-Simpers, J. (2014) 'A semi-empirical model for titled-gun planar magnetron sputtering accounting for chimney shadowing', *The Journal of The Minerals, Metals & Materials Society*, vol. 67, no. 1.

[4] Mahieu, S., Buyle, G., Depla, D., Heirweigh, S., Ghekiere, P. and De Gryse, R. (2006) 'Monte Carlo simulation of the transport of atoms in DC magnetron sputtering', *Nuclear Instruments and Methods in Physics Research*, vol. 243, no. 2.

10:40am **CM3-1-ThM-9 Discovery and Development of Transition Metal Nitride Semiconductors for Photoelectrochemical Energy Conversion**, *Ian Sharp [sharp@wsi.tum.de]*, Walter Schottky Institut, Technische Universität München, Germany **INVITED**

Transition metal nitride semiconductors are rapidly emerging as a promising class of materials for advanced optoelectronic and energy conversion applications. Compared to oxides, nitrides offer narrower bandgaps, stronger bond covalency, and improved carrier transport properties that make them well suited for harvesting sunlight in photovoltaic and photoelectrochemical systems. Despite this considerable promise, far fewer nitrides than oxides have been experimentally investigated due to their synthetic complexity and a broad range of new compounds remain to be explored. Furthermore, synthesis challenges have led to poorly controlled defect and impurity properties within this class of materials. In this work, we overcome these limitations using reactive co-

# Thursday Morning, May 15, 2025

sputtering to synthesize thin film nitride semiconductors with controlled compositions, exploring both dopants and new compounds in the Ti-Ta-N, Zr-Ta-N, and Hf-Ta-N composition spaces. Starting with orthorhombic Ta<sub>3</sub>N<sub>5</sub>, which stands as the best performing photoanode material within this class, we investigate the critical roles of native and impurity defects on carrier transport and recombination, showing that substitutional Ti and Zr doping with rationally optimized concentrations can be used to improve photoconversion efficiencies. While high Ti contents in Ta<sub>3</sub>N<sub>5</sub> lead to the precipitation of a secondary TiN phase, different behavior is observed for the case of Hf and Zr. In particular, solid solutions with broadly tunable compositions across the Hf-Ta-N-(O) and Zr-Ta-N-(O) composition spaces are investigated, leading to bandgap-tunable compounds that exhibit remarkably large refractive indices suitable for photonics applications. Moreover, deposition of a stoichiometric 1:1 Zr:Ta ratio leads to formation of a new ternary nitride compound, bixbyite-type ZrTa<sub>3</sub>N<sub>5</sub>, that it is a strong visible light absorber, functioning as an active photoanode material. Complementary DFT calculations indicate a direct bandgap that is tunable based on cation site occupancy. Thus, this material offers exciting prospects not only for solar energy conversion but also for optoelectronics applications. Overall, these results highlight the promise of both established and new transition metal nitride semiconductors for solar energy harvesting, as well as the importance of precise composition engineering to tune optoelectronic and charge transport characteristics. Considering the compositional complexities of these compounds, exploration and optimization can be dramatically accelerated through use of gradient sputtering and rapid characterization approaches.

## Protective and High-temperature Coatings Room Palm 5-6 - Session MA5-ThM

### Boron-containing Coatings

**Moderators:** Ms. Anna Hirle, TU Wien, Austria, Dr. Martin Dahlqvist, Linköping University, Sweden

8:00am **MA5-ThM-1 Metal Boride Nanocrystal Inks for Applications in Extreme Environments**, *Loredana Protesescu [l.protesescu@rug.nl]*, RUG, Netherlands **INVITED**

How can boron-rich nanocrystalline films be optimized to meet the stringent mechanical demands of extreme environment applications?

Modern advances in clean energy, hypersonic travel, and nuclear technologies place extraordinary demands on materials' thermal and mechanical durability. High-stakes fields, such as aerospace and space exploration, require materials that withstand extreme conditions, often exceeding 4,000 °C, with substantial mechanical strength and oxidation resistance. Refractory materials like ultra-high temperature ceramics (UHTCs), while promising, are limited by high production costs and challenging synthesis processes. This study seeks to address this challenge by exploring nanoscale metal boride materials—specifically, strontium hexaboride (SrB<sub>6</sub>) nanocrystals (NCs)—as a cost-effective, mechanically robust alternative.

Nanocrystals (NCs) offer unique advantages due to their high surface area, tunable crystallization, and the ability to form films with nanoscale precision, which is critical for enhancing mechanical properties in thin coatings. Here, we investigate the potential of surface-modified SrB<sub>6</sub> NCs, blade-coated onto silicon and sapphire substrates, as a pioneering solution for boron-rich, super-hard thin films. Through ligand modification with BF<sub>4</sub> and BI<sub>3</sub>, these NCs achieve distinct structural formations on different substrates, significantly impacting their mechanical performance.

Our findings demonstrate that SrB<sub>6</sub>-BI<sub>3</sub> films on silicon reach up to 10 GPa hardness and a Young's modulus between 180 and 200 GPa. In comparison, SrB<sub>6</sub>-BF<sub>4</sub> films attain 5 GPa hardness and 170 GPa modulus on silicon, with a notably higher modulus of 300 GPa on sapphire, suggesting enhanced stiffness through substrate optimization. Atomic force microscopy (AFM) revealed crystallization patterns where SrB<sub>6</sub>-BI<sub>3</sub> formed micron-sized crystals on silicon, while SrB<sub>6</sub>-BF<sub>4</sub> created spherical clusters, further affecting mechanical properties.

This study highlights that by optimizing ligand choice, substrate selection, and minimizing defects, boron-rich metal boride nanomaterials can be tailored for demanding applications. These findings position SrB<sub>6</sub> NC-based films as a promising, cost-efficient alternative to conventional super-hard materials like diamond, with potential breakthroughs in extreme environment applications.

8:40am **MA5-ThM-3 Influence of Boriding Treatment on the Tribological Performance of Tool Steel Repaired by Wire and Arc Additive Manufacturing**, *Cesar Resendiz [resendiz.cesar@tec.mx]*, Tecnológico de Monterrey, Mexico

Interest in reconditioning metallic components has grown as a means to reduce industrial waste. Electric arc-based repair methods, including additive manufacturing techniques like Wire and Arc Additive Manufacturing (WAAM), impact microstructure and mechanical properties due to high heat input. Moreover, data on the reliability of components repaired through these methods under demanding tribological conditions remain limited. This study presents a tribological characterization of borided WAAM-repaired tool steel. To simulate tool damage, a groove measuring 6.35 mm in width and 3 mm in depth was created in AISI D2 steel samples using a spherical milling cutter. Material deposition was then manually performed by a certified technician using Gas Tungsten Arc Welding (GTAW) with ER308L wire, chosen for its availability and cost-effectiveness. Samples were subjected to three different conditioning treatments: (a) quenching and tempering followed by welding restoration (QTR treatment), (b) welding restoration followed by quenching and tempering (RQT treatment), and (c) welding restoration followed by boriding treatment (RB treatment). The physico-chemical characteristics of all samples were analyzed through optical microscopy and Raman spectroscopy. Mechanical surface properties were evaluated using instrumented indentation tests, while the adhesion of the boride coating on BT samples was assessed with VDI testing. Wear resistance and coefficient of friction (CoF) in both repaired and unrepaired regions of all sample types were measured using a micro-abrasion machine rig equipped with a load sensor. Wear scars were analyzed through scanning electron microscopy to identify dominant wear mechanisms. The results revealed that wear resistance in the repaired regions of QTR and RQT samples was significantly lower than that in their corresponding unrepaired regions. However, RB-treated samples exhibited consistent mechanical properties and tribological behavior, with improved wear resistance in both the repaired and unrepaired regions compared to QTR and RQT samples.

9:00am **MA5-ThM-4 Impact of Thermo-Chemical Treatments on the Wear Performance of DIN 16MnCr<sub>5</sub> Steel**, *Jose Martínez-Trinidad*, Instituto Politécnico Nacional, Mexico; *Roberto Javier Cruz [rjavierc2100@alumno.ipn.mx]*, Instituto Politécnico Nacional, Mexico; *Ricardo García-León*, Universidad Francisco de Paula Santander Ocaña, Colombia

This study presents new findings related to the evaluation of wear resistance through the linear reciprocating dry sliding method on DIN 16MnCr<sub>5</sub> steel subjected to nitriding, nitriding with post-oxidation, and boriding treatments. The nitriding process was conducted using a cyanide salt bath method at 580 °C for 6 hours, forming a 24 μm iron nitride layer (F3N). Subsequently, a post-oxidation treatment in an oxidizing salt bath at 420 °C for 1 hour was applied, forming an additional F3N layer. Finally, a powder-pack boriding process at 950 °C for 4 hours resulted in a composite layer of FeB-Fe<sub>2</sub>B ~64 μm thickness on the steel surface. Physical, chemical, and mechanical characterizations were performed using XRD, Berkovich nanoindentation, and SEM-EDS techniques. Dry sliding wear tests were conducted using a UMT-2/CETR tribometer under the ASTM G133-05 standard guidelines. Parameters include normal loads of 5, 10, and 20 N, a sliding speed of 30 mm/s, and a distance of 100 m over a 10 cm sliding length with an alumina ball (Al<sub>2</sub>O<sub>3</sub>) as a counterpart. Coefficient of friction (CoF) values and wear tracks were obtained on the surface of the DIN steel samples under different treatments. The wear tracks were further evaluated using SEM-EDS to identify failure mechanisms on the worn surfaces. The tests demonstrated that thermo-chemical treatments improved the wear resistance of DIN 16MnCr<sub>5</sub> steel, reducing material removal volume and wear rate, with boriding treatment showing the best mechanical dry wear resistance results.

9:20am **MA5-ThM-5 Tuning Properties of Diborides by Transition Metal Alloying Deposited by Combination of Magnetron Sputtering and Cathodic ARC Evaporation**, *Daniel Karpinski*, *Andreas Lümekemann [a.luemekemann@platit.com]*, *Pavla Karvankova*, *Christian Krieg*, PLATIT AG, Switzerland; *Hannes Joost*, *Heiko Frank*, GFE-Schmalkalden e.V., Germany; *Pavel Soucek*, *Petr Vasina*, Institute of Physics and Plasma Technology, Masaryk University, Czechia; *Fedor Klimashin*, *Johann Michler*, Empa, Swiss Federal Laboratories for Materials Science and Technology, Switzerland; *Jan Kluson*, PLATIT a.s., Czechia; *Hamid Bolvardi*, PLATIT AG, Switzerland

Titanium diboride is currently the most widespread metal boride (MeB<sub>x</sub>) coating used in industry due to its outstanding properties such as high

# Thursday Morning, May 15, 2025

hardness >40 GPa, high melting point >3000 °C, and low propensity for sticking to soft metals. The main drawbacks of diborides are their generally low oxidation resistance (<800°C for TiB<sub>2</sub>) and brittleness. This study investigates the effect of alloying MeB<sub>x</sub> with transition metal on the structure, mechanical and tribological properties, and oxidation resistance of the coating. The coating deposition was performed in a Platin Pi411 machine with LACS® technology which includes simultaneous magnetron sputtering from a central cylindrical cathode (SCiL®) and a cathodic arc evaporation from cylindrical cathode located in the chamber door (LARC®). Here, the MeB<sub>x</sub> target was sputtered, and cathodic arc evaporation of Ti or Cr target was used for alloying the coating. XRD, HRTEM structure study, nanoindentation and isothermal annealing in air at Ta=600–900°C revealed that by alloying of MeB<sub>x</sub> we can form the nanolaminate microstructure, tune the hardness and modulus, and enhance oxidation resistance of the coating, respectively.

9:40am **MA5-ThM-6 Micromechanical Properties of Ti<sub>1-x</sub>Mo<sub>x</sub>B<sub>2+z</sub> Coatings Deposited by DCMS and HIPIMS**, *Anna Hirle [anna.hirle@tuwien.ac.at]*, Christian Doppler Laboratory for Surface Engineering of High-performance Components, TU Wien, Austria; *Philipp Dörflinger, Rainer Hahn*, Christian Doppler Laboratory for Surface Engineering of High-performance Components, TU Wien, Austria; *Christian Gutschka, Tomasz Wojcik*, Christian Doppler Laboratory for Surface Engineering of High-performance Components, TU Wien, Austria; *Maximilian Podsednik*, Institute of Chemical Technologies and Analytics, TU Wien, Austria; *Szilard Kolozsvári, Peter Polcik*, Plansee Composite Materials GmbH, Germany; *Carmen Jerg*, Oerlikon Surface Solutions AG, Liechtenstein; *Helmut Riedl*, Christian Doppler Laboratory for Surface Engineering of High-performance Components, Austria

A promising strategy for enhancing the limited fracture characteristics of sputtered transition metal diboride (TMB<sub>2</sub>) thin films, including hardness and fracture toughness, is the formation of ternary diborides. Theoretical predictions based on density functional theory (DFT) indicate that Mo alloying in TiB<sub>2+z</sub> may prove beneficial in reducing the inherent brittleness of such diboride coatings. The present study aims to provide experimental investigations of ternary Ti<sub>1-x</sub>Mo<sub>x</sub>B<sub>2+z</sub> coatings prepared by direct current magnetron sputtering (DCMS) and high-power impulse magnetron sputtering (HiPIMS) to validate the predictions and to investigate the influence of different deposition techniques.

A series of coatings was deposited using target compositions of TiB<sub>2</sub>/C 99/1 wt. %, TiB<sub>2</sub>/MoB 95/5 mol %, and TiB<sub>2</sub>/MoB 90/10 mol %, resulting in coating compositions ranging from 0 at. % Mo to 4.7 at. % Mo. A variety of analytical techniques, including transmission electron microscopy (TEM), scanning electron microscopy (SEM), and X-ray diffraction analysis (XRD), were employed to characterize the microstructural properties. The chemical composition was determined by inductively coupled plasma optical emission spectroscopy (ICP-OES). To investigate the micromechanical properties of the ternary Ti<sub>1-x</sub>Mo<sub>x</sub>B<sub>2+z</sub> coatings, including hardness, fracture toughness, and fracture strength, nanoindentation, in-situ cantilever bending tests, and micropillar compression tests were employed.

The present study demonstrates that HiPIMS processes result in a considerable enhancement of hardness, fracture toughness, and fracture strength compared to DCMS. Specifically, the hardness of the HiPIMS coatings was enhanced from 38.8 ± 1.7 GPa to 43.7 ± 1.2 GPa, while the fracture toughness increased by 0.4 MPa√m and the R<sub>p0.2</sub> value rose by approximately 2 GPa. In comparison, the DCMS coatings exhibited a consistent decline in mechanical properties with increasing Mo content. Our findings highlight the significance of the energetics of growth conditions for novel ternary diboride systems.

10:20am **MA5-ThM-8 Effect of Duty Cycle on the Microstructure and Mechanical Properties of Titanium Diboride Thin Films Deposited by High-Power Pulsed Magnetron Sputtering**, *Jian-Fu Tang*, National Kaohsiung University of Science and Technology, Taiwan; *Jian-Fu Tang*, Taiwan; *Ming-Yi Lin [M12188007@o365.mcut.edu.tw]*, Department of Materials Engineering, Ming Chi University of Technology, Taiwan, ROC; *Fu-Sen Yang*, Department of Mechanical Engineering, National Taiwan University of Science and Technology, Taiwan, ROC; *Chi-Lung Chang*, Department of Materials Engineering, Ming Chi University of Technology, Taiwan, ROC

With the rapid advancement of modern technology, the growing development of 5G and artificial intelligence (AI) has led to a substantial increase in demand for printed circuit boards (PCB). Enhancing the performance of cutting tools used in PCB drilling has become essential to meet supply and application needs, especially in the application of non-

ferrous metal materials. Surface treatments aimed at improving tool wear resistance, high-temperature durability, anti-adhesion properties, hardness, and overall lifespan are common strategies in the industry. Titanium diboride (TiB<sub>2</sub>) and titanium diboride-based nitride films, known for their high hardness, excellent wear resistance, high-temperature stability, and thermal conductivity, are ideal coating materials for cutting tools.

This study used high-power impulse magnetron sputtering (HiPIMS) to investigate the microstructure and mechanical properties of TiB<sub>2</sub> films deposited under various duty cycles. Five samples were prepared under identical target power output (3.5 kW) and frequency (200 Hz), using different duty cycle settings: 3%, 5%, 10%, 25%, and DC. The analysis results indicate that the peak power density increases with the duty cycle decrease. Energy dispersive spectroscopy (EDS) analysis also confirmed that the film composition was consistent with the alloy target proportions. Nanoindenter analysis shows that as the duty cycle decreases, the hardness increases significantly, from 28.3 GPa to 43.2 GPa, and the residual stress increases, from -0.21 GPa to -6.18 GPa. This can be attributed to the higher peak power density effect. In addition, all samples showed good adhesion (HF1~HF2), excellent wear resistance (< 8.4 × 10<sup>-7</sup> mm<sup>3</sup>N<sup>-1</sup>m<sup>-1</sup>), and lower friction coefficient (0.39 to 0.55), indicating that TiB<sub>2</sub> films have potential in PCB drilling application.

Keywords: TiB<sub>2</sub>, duty cycle, high power impulse magnetron sputtering, hardness, residual stress

10:40am **MA5-ThM-9 TiB<sub>2</sub>/Hf Superlattices: Exploring Mechanical Strength, Fracture Toughness, and Stress-Strain Behavior**, *Naureen Ghaffoor [naureen.ghaffoor@liu.se]*, *Firat Angay, Marcus Lorentzon*, Linköping University, IFM, Sweden; *Rainer Hahn*, TU Wien, Austria, Sweden; *Michael Meindlhuber*, University of Leoben, Austria; *Lars Hultman, Jens Birch*, Linköping University, IFM, Sweden

We present experimental investigations on iso-structural TiB<sub>2</sub>/Hf superlattices, exploring the impact of layer thickness on hardness, toughness, and fracture resistance. Ab initio calculations, which guided material selection, reveal a basal-plane lattice and shear modulus mismatch of 0.16 Å (5.4%) and 200 GPa between TiB<sub>2</sub> and Hf, hindering dislocation glide at interfaces. Superlattices were deposited with periods ranging from 2 to 10 nm and were characterized by XTEM, XRD, and ERDA for structural and compositional details. High hardness (40 GPa) and structural integrity were achieved at lower Hf thicknesses and higher growth temperatures, with boron diffusion from TiB<sub>2</sub> into Hf forming single-crystal TiB<sub>2</sub> and understoichiometric HfB<sub>2</sub>. No strain buildup or epitaxial breakdown was observed in films with up to 375 periods, attributed to self-diffusion. Pillar compression tests were performed to measure stress-strain curves and determine fracture values of the superlattices. A strong correlation between the metallic Hf layer and ceramic TiB<sub>2</sub> was observed, with fracture stress varying across samples—some exhibited values up to 22 GPa, while others showed localized plasticity. Fracture stress showed minimal dependence on the superlattice period, suggesting that morphology did not significantly influence mechanical behavior, as all coatings exhibited similar column diameters. Plasticity was attributed to localized slip, which was visible in SEM and analyzed in TEM. Boron and oxygen diffusion in Hf layers impedes flow, increasing strength but reducing elongation, consistent with the Hall-Petch effect. The high strength of Hf restricts dislocation motion, particularly in thin superlattices, while TiB<sub>2</sub>'s single-crystal structure eliminates easy fracture paths, enhancing toughness. Assuming similar trends to nitrides, TiB<sub>2</sub>/Hf superlattices are expected to exhibit significantly higher fracture stresses. Based on the Young's moduli of TiB<sub>2</sub> (~400 GPa) and Hf (~80 GPa), a maximum outer fiber strain of 4% in bending would result in ~16 GPa in TiB<sub>2</sub> and ~3.2 GPa in Hf. The Hall-Petch effect further strengthens the material, with flow stress estimates between 4.7–6.7 GPa in tension, while bending primarily affects the outer layers. The difference in Young's moduli between TiB<sub>2</sub> and Hf contributes to high fracture toughness, highlighting TiB<sub>2</sub>/Hf superlattices as promising materials for applications requiring high hardness, toughness, and fracture resistance.

11:00am **MA5-ThM-10 Production of Thin Films of Cubic Boron Nitride with Almost No Residual Stresses by Pulsed Laser Deposition and Laser Stress Relaxation**, *Falko Jahn [falko.jahn@hs-mittweida.de]*, Mittweida University of Applied Sciences, Germany; *Thomas Lampke*, University of Technology Chemnitz, Germany; *Steffen Weissmantel*, Mittweida University of Applied Sciences, Germany

For decades boron nitride has been researched as a coating material due to its outstanding mechanical, thermal and chemical properties. Especially the cubic phase (c-BN) as second hardest material known so far with high thermal and chemical resistance has driven the desire to make this material

# Thursday Morning, May 15, 2025

usable for industrial applications. Pulsed Laser Deposition has been one of the few deposition techniques with deposition rates of several tens nm per minute, high enough for industrial needs [1]. However, like other deposition techniques, PLD produced c-BN-coatings show very high compressive intrinsic stresses which limits the film thickness to a few hundred nm.

We present a method to produce thin films of cubic boron nitride which contain almost no residual stresses. These thin films were deposited using Ion Beam Assisted Pulsed Laser Deposition as sublayers of 100 nm film thickness on silicon substrates. Applying a modified laser stress relaxation technique [2], we were able to reduce the intrinsic compressive stresses in these sublayers from 10 GPa to less than 1 GPa.

Alternating deposition and stress relaxation of such sublayers successively enables film thicknesses relevant for industrial applications, such as wear resistant coatings. One possibility is to stack relaxed pure phase c-BN-sublayers in order to obtain applicable cubic boron nitride coatings. Another possibility is the combination of c-BN-sublayers with hard h-BN-sublayers to form multilayer system with increased mechanical properties. These h-BN-sublayers produced by PLD show indentation hardnesses in the range of 15 – 25 GPa, which allows the whole multilayer system to be superhard with indentation hardness above 40 GPa.

[1] S. Weissmantel, G. Reisse, Pulsed laser deposition of cubic boron nitride films at high growth rates, *Diamond and Related Materials* 10 (2001) 1973–1982. [https://doi.org/10.1016/S0925-9635\(01\)00386-7](https://doi.org/10.1016/S0925-9635(01)00386-7).

[2] S. Weissmantel, G. Reisse, D. Rost, Preparation of superhard amorphous carbon films with low internal stress, *Surface and Coatings Technology* 188-189 (2004) 268–273. <https://doi.org/10.1016/j.surfcoat.2004.08.070>.

11:20am **MA5-ThM-11 Influence of Deposition Parameters on the Microstructure, Mechanical and Anti-Corrosion Characteristics of (Hfvtizrw)B2 High Entropy Alloy Boride Thin Films, Jun-Xing Wang [wangxing1470@gmail.com]**, Ming Chi University of Technology, Taiwan; *Bih-Show Lou*, Chang Gung University, Taoyuan, Taiwan; *Riedl-Tragenreif Helmut*, Technische Universität Wien, Austria; *Jyh-Wei Lee*, Ming Chi University of Technology, Taiwan

In recent years, the exceptional mechanical and physical properties of highentropy alloy (HEA) boride thin films have garnered significant attention, sparking interest among the global industrial community, academia, and researchers. This study selected (HfVTiZrW)<sub>2</sub> HEA boride as the target material to sputter (HfVTiZrW)<sub>2</sub> HEA boride films under different substrate temperatures by high power impulse magnetron sputtering.

The results indicated that as the deposition temperature increases from 200°C to 500°C, the HEA boride films consistently exhibited a hexagonal close-packed (HCP) structure. Composition analysis and bonding energy assessments revealed that all films were metallic diborides. The highest hardness of 38.0 GPa was obtained for the film deposited at 500°C. The wear coefficient of friction was from 0.33 to 0.57. An excellent wear rate of  $2.98 \times 10^{-6}$  mm/N·m was achieved.

Observations from high-resolution transmission electron microscopy revealed that the grain size of the films increased from  $11.39 \pm 0.84$  nm to  $27.25 \pm 3.59$  nm as deposition temperature increased from 200 to 500°C. The corrosion resistance of the HEA boride films in the 0.5 M H<sub>2</sub>SO<sub>4</sub> aqueous solution was 38.89 times greater than that of 304 stainless steel. Furthermore, good oxidation resistance of HEA films in dry air atmosphere below 600°C was observed. In summary, this study demonstrated the (HfVTiZrW)<sub>2</sub> HEA boride films exhibited promising applications as protective coatings for cutting tools and forming dies.

## Functional Thin Films and Surfaces

### Room Palm 3-4 - Session MB3-ThM

#### Low-dimensional Materials and Structures

**Moderators:** Dr. Tomas Kubart, Angstrom, Switzerland, Vladimir Popok, FOM Technologies, Denmark

8:40am **MB3-ThM-3 Conformal Multifunctional Polymeric and Inorganic Aerogel-Like Oxide Thin Films for Optical and Energy Applications by Plasma Technology, Gloria P. Moreno, Triana Czermak, Jose Obrero, Francisco J. Aparicio, Juan Ramón Sánchez-Valencia, Ana Borrás, Angel Barranco [angelbar@icmse.csic.es]**, Institute of Materials Science, CSIC, Spain

INVITED

The Remote Plasma Assisted Vacuum Deposition (RPAVD) process is a versatile methodology for fabricating functional nanocomposites from non-

chemically polymerizable organic functional molecules and functional metal coordination compounds. This approach combines the physicochemical reactions inherent to plasma polymerization processes with the vapor deposition of functional molecules tailored to the specific demands of target applications. The resultant cross-linked polymer films exhibit insolubility and exceptional thermal stability. These films can incorporate a precise concentration of nearly any thermally stable, photo-functional molecule. The method exhibits scalability at the wafer level and complete compatibility with solvent sensitive and delicate substrates. Initially, this process was applied to developing thin optical films and photonic devices, encompassing optical filters, photonic sensing chips, and lasing media. Nevertheless, the film properties can be fine-tuned for various other functional applications, such as creating controlled wetting and ice-retarding surfaces, antimicrobial coatings, and high performance dielectric ultrathin films. We will also showcase very recent results about the encapsulation of nanostructures on surfaces and its role in encapsulating and modifying perovskite solar cells. Additionally, we will present recent results about the development of conformal aerogel-like oxide nanostructures by combining RPAVD and plasma processing of metal-containing plasma polymers. These aerogel-like oxide films have straightforward applications in photonics, omniphobic surfaces, solar cells, and smart coatings.

#### References

- 1.- F.J. Aparicio et al. *Advanced Materials* 2011, 23 (6), 761-765
- 2.- M. Alcaire et al. *ACS Applied Materials Interfaces* 2017, 9, 8948,
- 3.- M. Alcaire *Advanced Functional Materials* 2019, 29, 1903535.
- 4.- J. Idígoras et al. *ACS Applied Mater. Interfaces* 2018, 10, 1801076.
- 5.- J. M. Obrero-Pérez, *Advanced Energy Materials* 2022, 2200812.
- 6.- J.M. Obrero-Pérez *ACS Applied Materials Interfaces* 2024, 16, 39745

9:20am **MB3-ThM-5 Cluster-assembled Computers, Paolo Milani [paolo.milani@mi.infn.it]**, University of Milan, Italy

INVITED

Self-assembled nanoparticle or nanowire networks have recently come under the spotlight as systems able to obtain brain-like data processing performances by exploiting the memristive character and the wiring of the junctions connecting the nanostructured network building blocks [1]. Recently it has been demonstrated that nanostructured Au films, fabricated by the assembling of gold clusters produced in the gas phase, have non-linear and non-local electric conduction properties caused by the extremely high density of grain boundaries and the resulting complex arrangement of nanojunctions [2,3]. Starting from the characterization of this system, it has been proposed and formalized a generalization of the Perceptron model to describe a classification device based on a network of interacting units where the input weights are non-linearly dependent. This model, called “Receptron”, provides substantial advantages compared to the Perceptron as, for example, the solution of non-linearly separable Boolean functions with a single device [4]. Here I will present and discuss the relevant aspects concerning the characterization and implementation of nanostructured networks fabricated by supersonic cluster beam deposition of gold and platinum clusters for neuromorphic computing and data processing applications [5,6].

[1] A Vahl, G Milano, Z Kuncic, SA Brown, P Milani, *J.Phys. D: Appl. Phys.* 57 (50), 503001 (2024)

[2] M. Mirigliano, et al., *Neuromorph. Comp. Eng.* 1, 024007, (2021).

[3] G Nadalini, F Borghi, T Košutová, A Falqui, N Ludwig, P Milani *Scientific Reports* 13 (1), 19713 (2023)

[4] B. Paroli et al., *Neural Networks* 166, 634, (2023)

[5] G Martini, E Tentori, M Mirigliano, DE Galli, P Milani, F Mambretti, *Frontiers in Physics* 12, 1400919 (2024)

[6] S Radice, F Profumo, F Borghi, A Falqui, P Milani, *Advanced Electronic Materials*, 2400434 (2024)

10:20am **MB3-ThM-8 Analysis and 3D Modelling of Percolated Conductive Networks in Nanoparticle-Based Thin Films, Stanislav Haviar [haviar@kfy.zcu.cz]**, University of West Bohemia, Czechia; *Benedikt Prifling*, Ulm University, Germany; *Tomáš Kozák*, *Kalyani Shaji*, University of West Bohemia, Czechia; *Tereza Košutová*, Charles University, Czechia; *Šimon Kos*, University of West Bohemia, Czechia; *Volker Schmidt*, Ulm University, Germany; *Jiří Čapek*, University of West Bohemia, Czechia

Thin films composed of copper oxide nanoparticles (NP) were synthesized using a magnetron-based gas aggregation source (MGA), with nanoparticle

# Thursday Morning, May 15, 2025

sizes controlled by varying the exit orifice diameter. The 3D model of the synthesized NP-based was constructed and assessed.

(i) Comprehensive characterization of the nanoparticle-based thin films was performed using SEM, TEM, SAXS, and XRD to determine particle morphology, size distribution, porosity and others.

(ii) The obtained experimental data served as inputs for generating virtual 3D microstructure models through a data-driven stochastic hard sphere packing algorithm, incorporating factors such as particle size distribution, porosity, and vertical density profiles.

(iii) These virtual structures were refined to account for oxidation-induced swelling and film roughness, enabling the simulation of realistic conductive networks.

(iv) A computational model incorporating a simplified adsorption mechanism was developed to simulate oxygen adsorption effects on surface conductivity, and finite element method (FEM) simulations were conducted to calculate the electrical resistivity of the modelled networks under varying oxygen partial pressures.

(v) The simulated resistivity values were validated against experimental measurements obtained via four-point probe resistivity techniques at 150°C under different oxygen concentrations, demonstrating both qualitative and quantitative agreement.

[1] Haviar, S., Prifling B.; Kozák et al. *Appl. Surf. Sci. Adva.* – submitted – 2024

[2] Shaji, K., Haviar, S., Zeman P. et al. *Surf. Coatings Technol.* 2024, 477

[3] Batková; Kozák, T.; Haviar, S.; et al. *Surf. Coatings Technol.* 2021, 417

[4] Haviar, S.; Čapek, J.; Batková, Š.; et al. *Int. J. Hydrogen Energy* 2018, 43

10:40am **MB3-ThM-9 Tailoring of Nanoparticle Deposition Rate and Film Structure Through Substrate Biasing: Enabling Sputtering-Based Synthesis of Novel Catalyst Materials, Dominik Gutnik** [[dominik.gutnik@unileoben.ac.at](mailto:dominik.gutnik@unileoben.ac.at)], Florian Theodor Knabl,

Montanuniversität Leoben, Austria; Prathamesh Patil, CEST GmbH, Austria; Christine Bandl, Montanuniversität Leoben, Austria; Tijmen Vermeij, Daniele Casari, Empa, Swiss Federal Laboratories for Materials Science and Technology, Thun, Switzerland; Michael Burtscher, Christian Mitterer, Montanuniversität Leoben, Austria; Christian M Pichler, CEST GmbH, Austria; Barbara Putz, Montanuniversität Leoben, Austria

Metallic nanoparticles (NPs) exhibit intriguing properties as a consequence of their spatial confinement and their high surface-to-volume ratio. A topic rising in importance is the utilization of NPs as catalysts for energy conversion and storage. To facilitate more advanced use of NPs, a thorough understanding of their synthesis-structure-property relations is crucial.

In this study, the effect of different substrate biases on the deposition of size-selected Cu NPs, fabricated via Magnetron Sputtering Inert Gas Condensation (MS-IGC) in a so-called Haberland system, is analyzed. NPs nucleate and grow within the aggregation zone (usually pressures of 10 to 100 Pa), collect charge through plasma interactions and are accelerated by adiabatic expansion upon exiting the aggregation zone through an orifice. The charge they collect enables analysis and manipulation of nanoparticles through a Quadrupole Mass Spectrometer (QMS) before deposition on the substrate.

With this approach, Cu NPs with a diameter of 1.8 nm and 8 nm were filtered and accelerated towards the substrate with positive bias voltages of 0, 300 and 1000 V. In-situ QMS data reveals a significant increase of the NP-flux with higher biases, especially for smaller NP-diameters. Furthermore, changes in the morphology of the resulting thin films which were deposited for up to 45 minutes are observed with Scanning Electron Microscopy and changes in surface coverage and porosity are studied with X-ray Photoelectron Spectroscopy and Low-Energy Ion Scattering Spectroscopy.

Our results show that with rising bias voltages, the NP deposition rate estimated through QMS increases by 32% for the 8 nm diameter NPs, and the morphology of the resulting thin film shifts towards more densely packed structures, attributed to the higher energy of the NPs on impact [1]. An alternative method of NP synthesis in the form of hollow cathode sputtering will also be presented as a high throughput technique. With this technique, orders of magnitude higher NP deposition rates with position-dependent morphology can be obtained. These findings could facilitate the deposition of NP-based films with higher efficiency and with tailored morphology, making this technique more attractive for e.g. the synthesis of catalysts.

[1] Knabl, F., Gutnik, D., Patil, P., Bandl, C., Vermeij, T., Pichler, C. M., Putz, B., & Mitterer, C. (2024). Enhancement of copper nanoparticle yield in magnetron sputter inert gas condensation by applying substrate bias voltage and its influence on thin film morphology. *Vacuum*, 230, 113724. <https://doi.org/10.1016/j.vacuum.2024.113724>

11:00am **MB3-ThM-10 Tailoring Microstructure and Composition of Composite CuO/WO<sub>3</sub> Nanoparticle-Based Thin Films for Enhanced H<sub>2</sub> Gas Sensing, Kalyani Shaji [kalyanis@kfy.zcu.cz], Stanislav Haviar, Petr Zeman, Michal Procházka, Radomír Čerstvý, Jiří Čapek**, University of West Bohemia - NTIS, Czechia

The conductometric gas sensors operate by modulating the electrical conductivity of the sensing material through adsorption-desorption reactions between the target gas and the sensor surface. Metal oxide semiconductors (MOS) are conductometric materials highly sensitive to oxidizing and reducing gases. In addition, composite MOS-based materials may further benefit from formed heterojunctions potentially significantly improving the sensitivity. Our focus is to develop advanced hydrogen-gas sensing materials composed of a mixture of p-type CuO and n-type WO<sub>3</sub> nanoparticles (NPs) with optimized microstructure of the film and volumetric ratio of CuO to WO<sub>3</sub> NPs in the film for enhanced H<sub>2</sub> gas sensing.

The NP-based thin films were synthesized using a magnetron-based gas aggregation source in Ar+O<sub>2</sub> gas mixture. First, effect of thermal annealing on the microstructure (i.e., NPs diameter, formed necks, porosity) of the films was studied since gas sensing materials are usually operated at elevated temperatures (up to 400°C). The CuO, WO<sub>3</sub> and their composite (1:1 volumetric ratio) samples were annealed at temperatures in the range 200 - 400°C in synthetic air and subsequently thoroughly investigated using various characterisation techniques such as SEM, XRD, XPS, and Raman spectroscopy. Significant changes in particle size were observed in the case of CuO-based material, while WO<sub>3</sub>-based and composite materials exhibited minor microstructural changes, even at elevated temperatures. Notably, at 400°C, the composite crystallized into a novel phase. Second, the volumetric ratio of CuO to WO<sub>3</sub> NPs in the films was optimized to maximize the response of the material. We demonstrate that a synergetic effect is reached when an optimum number of p-n heterojunctions is established in the material providing enhanced response of the composite film compared to the films formed by single-material NPs.

This study highlights the crucial role of thermal treatment in influencing NP microstructure, offering insights into stabilizing and tuning NP-based thin films for enhanced gas sensing. Additionally, the optimized ratio of CuO and WO<sub>3</sub> NPs within the composite improved H<sub>2</sub> sensing performance by promoting optimal p-n heterojunction formation, demonstrating that precise compositional control can significantly boost the sensitivity of nanostructured systems.

11:20am **MB3-ThM-11 Influence of Pretreatment and Deposition Parameters on Carbon Nanotubes Synthesized Directly on Oxidized Steel Substrates via Pulsed DC PACVD, Manuel C. J. Schachinger [manuel.schachinger@fh-wels.at], Francisco A. Delfin**, University of Applied Sciences Upper Austria; Bernhard Fickl, Bernhard C. Bayer, Vienna University of Technology, Austria; Andreas Karner, Johannes Preiner, Christian Forsich, Daniel Heim, University of Applied Sciences Upper Austria; Bernd Rübiger, Christian Dipolt, Thomas Müller, RÜBIG GmbH & Co KG, Austria

Carbon nanotubes have recently attracted considerable attention due to their distinct qualities such as elevated strength-to-weight ratio, excellent thermal conductivity, high aspect ratio and special electronic and optical properties. However, the widespread use of CNTs is limited by their costly production, partly due to the laborious substrate-catalyst preparation involving expensive transition metals like Ni or Co, which must be sputtered and sintered to form sufficient growth sites on the substrate material. To avoid the costly and time-consuming pretreatment, it was shown that direct growth of carbon nanotubes on steel substrates is possible by application of a simple surface oxidation step prior to the synthesis process. The aim of this work is to optimize the oxidation pretreatment of the steel in a way that specific tailoring of the nanotube properties such as diameter, length and morphology becomes possible. To achieve this, cylindrical EN 1.4301 (AISI 304) steel samples were subjected to an oxidation step in air at atmospheric pressure for 15 s, 3 minutes and 15 minutes at 300, 400 and 500 °C, respectively. Subsequently, the synthesis process was carried out in the PACVD 40/60 system (RÜBIG, Austria) utilizing a unipolar pulsed DC discharge. Power density was varied between 50 and 100 W/m<sup>2</sup>. Ar, H<sub>2</sub> and C<sub>2</sub>H<sub>2</sub> gas concentrations were 67 vol.-% 32 vol.-% and 1 vol.-%, respectively. The pressure was 200 Pa and synthesis time was 1 h. The obtained CNTs as

# Thursday Morning, May 15, 2025

well as the oxidized steel surfaces after pretreatment were then analysed using SEM, EDS, TEM, AFM, XPS and Raman spectroscopy. SEM images showed the formation of a high-density forest of CNTs fully covering the steel surface for substrate-oxidation times greater than 15 s. Tube diameter increased with increasing oxidation times and temperatures from 20 to 200 nm. TEM revealed the formation of bamboo-like CNTs involving a tip growth-mechanism. Raman spectroscopy showed the characteristic D, G and D' peaks, with a large I(D)/I(G) ratio, indicating an elevated degree of disorder. AFM revealed significant RMS roughness and morphology variations of the oxidized steel surfaces dependent upon oxidation time and temperature, which were correlated with the nanotube length and diameter. In summary, it was possible to achieve CNTs with tailored properties only via the variation of the surface oxidation step prior to the synthesis, achieving a cost-effective production process that can easily be adapted to the specific requirements of the applicator.

## Plasma and Vapor Deposition Processes

### Room Town & Country B - Session PP8-1-ThM

#### Commemorative Session for Papken Hovsepian I

**Moderators:** Prof. Arutiun P. Ehasarian, Sheffield Hallam University, UK, Philipp Immich, IHI Hauzer Techno Coating B.V., Netherlands

8:00am **PP8-1-ThM-1 How Industry and Research Are Connected to Accelerate Development**, Philipp Immich [pimmich@hauzer.nl], IHI Hauzer Techno Coating B.V., Netherlands **INVITED**

The relationship between Sheffield Hallam University and Hauzer has been long-standing, beginning with Dieter Münz, former CEO of Hauzer, becoming a professor at Sheffield in 1993. When Papken Hovsepian joined Hallam, the collaboration between become even more intense. Papken played a crucial role in the early discussions for the first EU projects focused on HIPIMS development.

In 2003, Hauzer conducted initial tests with Advanced Energy's power supply and AC Converters, marking the first empirical steps in HIPIMS alongside Papken. The EU INNOVATIAL project, which started in 2004, focused on HIPIMS development in collaboration with Sheffield Hallam University (SHU), which later licensed HIPIMS etching to Hauzer. Hauzer's involvement in significant European projects like Alticut and Nanocoat further strengthened this partnership. The first HIPIMS trials at Hauzer led to groundbreaking research and publications, particularly on superlattice coatings, a major focus of Papken's work.

The collaboration with Papken and later Arutiun Ehasarian (Harry) was instrumental in Hauzer's success, resulting in numerous patents, including HIPIMS Bias and ARC handling. The initial impulse for the ABS conference days in 1995 was triggered by Dieter Münz, later involving strong participation from Papken in the HIPIMS Conference. Papken's motto was always about bringing industry and research together to learn from each other and accelerate developments.

In 2023, Hauzer celebrated its 40th anniversary by hosting the HIPIMS community for the 13th HIPIMS conference in Venlo for the second time since 2008, unfortunately a testament to the enduring relationship with Papken and his contributions.

Papken's legacy is deeply cherished by the Hauzer family, and his impact on the HIPIMS community and beyond will always be remembered. Thank you, Papken, for your invaluable contributions and for being an integral part of our history.

8:40am **PP8-1-ThM-3 Invited Paper**, Ivan Petrov [petrov@illinois.edu], University of Illinois at Urbana-Champaign, USA **INVITED**

9:20am **PP8-1-ThM-5 Invited Paper**, Francisco Javier Perez Trujillo [fjperez@quim.ucm.es], Universidad Complutense de Madrid, Spain **INVITED**

10:20am **PP8-1-ThM-8 Recent Progress in Coating Materials Design: Thermal Stability vs Chemical Stability**, Amir Navidi, Deborah Neuss, Soheil Karimi, Marcus Hans, Materials Chemistry, RWTH Aachen University, Germany; Daniel Primetzhofer, Materials Physics, Dep. of Physics and Astronomy, Uppsala University, Sweden; Jochen M. Schneider [schneider@mch.rwth-aachen.de], Materials Chemistry, RWTH Aachen University, Germany **INVITED**

The roles of chemical, structural and interfacial complexity for the design of thermally stable and chemically stable protective coating materials is discussed. In this talk the thermal stability of nitride thin films of varying chemical complexity is compared. Furthermore, the oxidation behavior of monolithic transition metal diboride based coating systems are compared to coating architectures containing multiple interfaces. The role of thermal stability for the oxidation behaviour of the above mentioned coating systems will be discussed.

11:00am **PP8-1-ThM-10 HiPIMS and Magnetron Sputtered Carbon-Based Nanocomposites**, Sven Ulrich [sven.ulrich@imf.fzk.de], Forschungszentrum Karlsruhe, Germany **INVITED**

Carbon-based nanocomposites with adjustable multifunctional properties are suitable candidates for both tribological applications and energy technologies. Reactive DC magnetron sputtering and HiPIMS are selected as coating processes, using a metallic transition metal target, argon as the working gas and methane as the reactive gas. As shown in plasma diagnostic investigations, in contrast to DC magnetron sputtering, HiPIMS exhibits a high ion content of the film-forming particles and the energy deposited by ion bombardment during film growth can be precisely adjusted. The constitution and microstructure were determined by a combination of several analytical methods: EPMA, ERDA, Raman spectroscopy at four different wavelengths, XRD, TEM and HRTEM were used to determine the composition and correlate it with the mechanical properties. It is shown that by varying the methane reactive gas flow, single-phase transition metal carbide coatings as well as nanocomposites consisting of nanocrystalline transition metal carbide grains in a hydrogenated amorphous carbon network can be produced. Thus, by choosing the optimized process parameters (switching function), multilayers can be produced from these two components.

**Keywords:** HiPIMS, Magnetron sputtering, carbon-based nanocomposites

11:40am **PP8-1-ThM-12 Superlattice Coatings: Unleashing Superior Properties Through Architected Nanolayers**, Paul Mayrhofer [paul.mayrhofer@tuwien.ac.at], TU Wien, Institute of Materials Science and Technology, Austria **INVITED**

Inspired by Helmersson, Hovsepian, and Münz's pioneering work on transition metal nitride superlattices, this concept has been a part of my research since 2003, particularly influenced by Papken Hovsepian's application-driven advancements. Here, we explore how nanolamellar microstructures can simultaneously enhance the hardness and fracture toughness of hard coatings. Superlattices, formed by alternating nanometer-thick layers, present opportunities to engineer mechanical properties superior to their individual constituents.

Careful interface design enables superlattices to achieve exceptional hardness, toughness, and thermal stability, essential for extreme environments. This concept applies effectively to nitrides, carbides, borides, and their mixtures. Mechanisms like dislocation blocking, coherent interface strengthening, and stress modulation contribute to this superior performance. The "epitaxial stabilization effect" further plays a key role, where pseudomorphic forces of the stabilizing layer act on the surface of the other layer during nucleation and growth, causing it to crystallize in its metastable but more similar structure rather than its thermodynamically stable but different structure. As a result, in addition to coherency stresses (due to lattice mismatches) and modulus mismatches, phases as well as stoichiometries that may exhibit higher inherent ductility, according to their decreased G/B ratio and increased Cauchy pressure, become accessible (like shown for superlattices containing MoN<sub>2</sub>, WN<sub>2</sub>, SiN<sub>2</sub>, or AlN layers).

Upon loading, dislocation nucleation and interface-triggered phase transformations dissipate energy, enhancing fracture toughness. For instance, TiN/WN superlattices achieve hardness (36.7±0.8 GPa) and fracture toughness (4.6±0.2 MPa·m<sup>0.5</sup>) with optimized layer thicknesses (λ = 8.1–10.2 nm). This work examines the influence of layer thickness, interface quality, and architecture on mechanical behavior, emphasizing the critical balance between toughness and hardness, alongside high-temperature stability. The findings underscore the potential of superlattice designs for protective coatings, high-performance tools, and structural components under severe thermal and mechanical loads.

# Thursday Morning, May 15, 2025

In memorial of Papken Hosenian.



# Thursday Afternoon, May 15, 2025

## Advanced Characterization, Modelling and Data Science for Coatings and Thin Films

### Room Palm 1-2 - Session CM1-2-ThA

#### Spatially-resolved and in situ Characterization of Thin Films, Coating and Engineered Surfaces II

**Moderators:** Dr. Damien Faurie, Université Sorbonne Paris Nord, France, Dr. Barbara Putz, Empa Thun, Switzerland, Aparna Saksena, MPI für Eisenforschung GmbH, Germany

1:20pm **CM1-2-ThA-1 Crystalline-Amorphous Interface Fracture Explored Across Different Length Scales, Alice Lassnig [alice.lassnig@unileoben.ac.at]**, Montanuniversität Leoben, Austria; Michael Meindlhumer, Montanuniversität Leoben, Austria; Stanislav Zak, Erich Schmid Institute of Materials Science, Austrian Academy of Sciences, Leoben, Austria; Megan Cordill, Christoph Gammer, Austrian Academy of Sciences, Austria; Andrew Minor, Lawrence Berkeley Lab, USA **INVITED**

Interfaces separating bi- and multilayered thin film structures, are susceptible to premature failure due to the challenge of bridging distinct physical properties of adjacent materials. Thus, the reliability of these interfaces significantly influences the overall lifespan of such structures. Consequently, a thorough investigation of their reliability and a comprehensive understanding of the underlying failure mechanisms are essential for enhancing novel material composites and combinations.

In this study, we investigate the fracture behavior of model crystalline-amorphous interfaces, specifically focusing on Cu thin films delaminating from bulk glass substrates and nanocrystalline Cu – amorphous CuZr multilayers. Utilizing advanced characterization techniques, we aim to study the delamination behavior, interface adhesion, and fracture under static and cyclic loading of such structures using advanced experimental techniques spanning both the meso-scale and nanoscale, incorporating in situ transmission electron microscopy for a detailed exploration of these phenomena.

2:00pm **CM1-2-ThA-3 Tailoring Structure and Mechanical Properties of TiZrHfTa Refractory Alloy Thin Films, Gregory Abadias [gregory.abadias@univ-poitiers.fr]**, Hocine Slimani, Institut Pprime - CNRS - ENSMA - Université de Poitiers, France; Pietro Vecchiotti, Politecnico Milano, Italy; Meriadeg Chalopin, Institut Pprime - CNRS - ENSMA - Université de Poitiers, France; Ferenc Tasnádi, Linköping University, IFM, Sweden; Matteo Ghidelli, Philippe Djemia, Laboratoire des Sciences des Procédés et des Matériaux (LSPM) – CNRS, France

Complex concentrated alloys (CCAs), including medium- and high-entropy alloys, offer attractive thermomechanical properties which make them promising candidates for various technologies such as corrosion resistant or radiation tolerant structural materials. Among the various CCAs, alloys with multi-principal refractory elements (RCCA) have drawn significant attention for hydrogen (H) storage applications [1-3] due to their ability to reversibly absorb H in the form of metal hydrides. However, up to now, studies on RCCA for H storage have only focused on bulk materials, with limited attention to thin film counterparts, which could be considered as model materials enabling an easy tailor of composition, phase and microstructural features (grain size, porosity or texture), providing valuable insights on the mechanisms of hydride formation and dissolution in RCCAs.

In this work,  $(\text{TiZrHf})_{100-x}\text{Ta}_x$  thin films, with thickness up to 700 nm and Ta content ranging from 0 to 60 at.%, were synthesized by co-sputtering deposition. The phase composition, crystal structure, morphology and elemental composition was determined using a combination of analytical techniques (XRD, SEM/TEM, EDS), while the intrinsic stress was measured *in situ* during deposition by wafer curvature method. The mechanical properties of the films were assessed by nanoindentation and opto-acoustics (Brillouin light scattering and picosecond laser ultrasonics) methods. By tuning the Ta content, different phases were stabilized in these quaternary alloys, from hcp to bcc and amorphous. These structural changes are accompanied by variation in growth morphology (evolving from nanocolumns to vein-like patterns), stress reduction and a progressive softening of hardness, shear and elastic modulus with increasing Ta content. The experimental findings are discussed and compared with results obtained from atomistic models of random alloys and amorphous phases, using *ab initio* molecular dynamics simulations combined with machine-learned interatomic potentials, as well as relevant data from the existing literature [4].

#### References:

1. Marques, F., Balcerzak, M., et al., *Review and outlook on high-entropy alloys for hydrogen storage*. Energy Environ. Sci. 14, 5191 (2021)
2. Kong, L., Cheng, B., Wan, D., Xue, Y., *A review on BCC-structured high-entropy alloys for hydrogen storage*, Front. Mater. 10, 1135864 (2023)
3. Shahi, R. R., Gupta, A. K., Kumari, P., *Perspectives of high entropy alloys as hydrogen storage materials*, Int. J. Hydrogen Energy 48, 21412 (2023)
4. Huang, S., Li, W., Holmström, E., Vitos, L., *Phase-transition assisted mechanical behavior of TiZrHfTa high-entropy alloys*, Sci. Rep. 8, 12576 (2018)

2:20pm **CM1-2-ThA-4 Exploring Mechanical Properties of Thin Films Through Synchrotron X-Ray Diffraction, Digital Image Correlation and Electrical Resistivity Measurements, Pierre-Olivier Renault [pierre.olivier.renault@univ-poitiers.fr]**, University of Poitiers, France **INVITED**

Mechanical behavior of thin films deposited on polymeric substrates was investigated under in-situ controlled tensile biaxial loading conditions. The study employed synchrotron X-ray diffraction (XRD), digital image correlation (DIC) techniques, and electrical resistivity measurements. The combination of X-ray diffraction and digital image correlation provides classical stress-strain curves.

The three complementary measurement techniques allow for a comprehensive analysis of the deformation characteristics of each component of the thin film. This approach helps to identify and distinguish the various deformation regimes that arise during mechanical loading. Beyond the yield stress, distinct mechanical behaviors are observed in the stress-strain curves, which can be attributed to plasticity and fracture phenomena. These behaviors are identified as characteristic signatures of material failure modes.

Additionally, the experimental setup offers the capability to assess whether deformations are fully transmitted through the interfaces between the thin film and the substrate, providing also insight into the interaction between different layers in a multilayer coating.

After describing the experimental setup, examples of the mechanical behaviors observed in metallic bilayer or trilayer systems and, oxide-metal films deposited on polyimide substrates will be presented. These examples illustrate the range of deformation responses that can arise in such multilayer systems. Differences in the mechanical behavior of films are shown to be influenced by factors such as type of interface or the presence of residual stresses in the as-deposited films, as well as variations in film thickness and grain size. These factors play a key role in determining the overall mechanical performance of the thin film systems.

3:00pm **CM1-2-ThA-6 A Combined X-ray Microdiffraction and Micromechanical Testing Approach for Direct Measurement of Thin Film Elastic Constants, Rainer Hahn [rainer.hahn@tuwien.ac.at]**, CDL-SEC, TU Wien, Austria; Rebecca Janknecht, Empa, Swiss Federal Laboratories for Materials Science and Technology, Thun, Switzerland; Nikola Koutná, Institute of Materials Science and Technology, TU Wien, Austria; Anna Hirle, CDL-SEC, TU Wien, Austria; Anton Davydok, Helmholtz-Zentrum Hereon, Germany; Klaus Boebel, Oerlikon Balzers, Oerlikon Surface Solutions AG, Liechtenstein; Szilárd Kolozsvári, Peter Polcik, Plansee Composite Materials GmbH, Germany; Christina Krywka, Helmholtz-Zentrum Hereon, Germany; Paul H. Mayrhofer, Institute of Materials Science and Technology, TU Wien, Austria; Helmut Riedl, CDL-SEC, TU Wien, Austria

The direct measurement of elastic constants for thin films is not yet a routine procedure and presents a number of significant technical and analytical challenges when compared to the analysis of bulk materials. *Ab initio* density functional theory calculations can provide a theoretical basis for understanding the properties of materials. However, discrepancies between model systems and real-world properties persist, primarily due to a lack of available experimental data for newly emerging material systems. Furthermore, computationally affordable models are typically constrained to defect-free single crystals, thereby excluding microstructural effects that exert a pronounced influence on the material's behavior.

This study addresses this gap by proposing a novel experimental approach to measure direction-dependent elastic constants, combining synchrotron microdiffraction and micropillar compression. The approach was tested on a polycrystalline face-centered cubic TiN thin film, where linear elastic failure prevails. An advanced in-situ testing environment has been established to enable the continuous recording of the load-displacement of the indenter, while simultaneously collecting the material's deformation response to uniform uniaxial compression. This dynamic approach permits

# Thursday Afternoon, May 15, 2025

the evaluation of the orientation-dependent elastic strain components and the macroscopic uniaxial compressive stresses, each over time, thereby enabling a differential analysis to assess the elastic and X-ray elastic constants.

The excellent agreement between experimental and ab initio data serves to corroborate the here-proposed robust method for direct elastic constant measurements, which is of crucial importance for advancements in thin film material testing.

**3:20pm CM1-2-THA-7 Real-Time Particle Detection for Enhanced Coating Deposition Processes, Constant Boris Rieille [constant.rieille@bhf.ch], Sylvain LeCoultre, Berner Fachhochschule BFH, Switzerland**

Industries in photonics, optics, and semiconductors are increasingly challenged by particles emitted during PVD/ALD deposition processes. As device miniaturization advances, stricter requirements on defect size and particles inclusions make effective control essential to ensure product conformity.

Currently, these industries rely on preventive maintenance schedules that do not account for unexpected particle emissions or variations in machine usage. When particles appear, repeated maintenance is required due to the lack of a system to detect or locate their source. Integrating a real-time particles sensor into machines would transform this approach by enabling predictive monitoring, reducing downtime, and improving operational efficiency.

This session will deliver key insights into particle emissions during PVD deposition, explore market trends, and present business cases for the PVD/ALD market.

**4:00pm CM1-2-THA-9 Real-Time Monitoring of Sputter Deposition Process: Application in the Context of Ag-Based Low-Emissive Coatings, Rémi Lazzari [remi.lazzari@insp.jussieu.fr], CNRS/Sorbonne Université, France**

**INVITED**

The challenge of green-house gas reduction pushes towards a better thermal insulation of housing. In this context, glass industry strives to decrease the infra-red radiative transfer across windows while keeping transparency. In the so-called low-E or solar control glazings, the functionality is provided by a complex stack of layers deposited by magnetron sputtering in which the active component is a ~10 nm thick Ag film encapsulated in between ZnO dielectric layers. Because of its noble character, Ag follows intrinsically a Volmer-Weber growth mode and is prone to dewetting upon thermal treatments such as windows tempering. Thus, there is tremendous need of understanding and control of its out-of-equilibrium growth process.

In this context, this presentation will illustrate the interest of combining real-time measurements (UV-vis spectroscopy<sup>1,2</sup>; stress measurement via wafer curvature and digital image correlation<sup>3</sup>; film resistivity) with *in situ* photoemission spectroscopy to have a full overview on the Ag growth mechanism. Among others, the impact of sputtering deposition parameters and of gas additives on stress build-up and relaxation, on film percolation and on Ag chemistry will be discussed<sup>4-6</sup>. The second part of the talk will show the contribution of model experiments in understanding the epitaxy at Ag/ZnO interface<sup>7</sup>, the reactivity<sup>8</sup> and band alignment<sup>9</sup> at metal/ZnO interfaces as seen by *in situ* hard x-ray photoemission and the various contributions to Ag film resistivity<sup>7</sup>.

[1] I. Gozhyk, L. Dai, Q. Héroult, R. Lazzari, and S. Grachev. *J. Phys. D: Appl. Phys.*, 52:095202, 2018.

[2] R. Lazzari, J. Jupille, R. Cavallotti, E. Chernysheva, S. Castilla, M. Messaykeh, Q. Héroult, and E. Meriggio. *ACS Appl. Nano Mater.*, 3:12157–12168, 2020.

[3] S. Grachev, Q. Héroult, J. Wang, M. Balestrieri, H. Montigaud, R. Lazzari, and I. Gozhyk. *Nanotechnology*, 33:185701, 2022.

[4] Q. Héroult, I. Gozhyk, M. Balestrieri, H. Montigaud, S. Grachev, and R. Lazzari. *Acta Mater.*, 221:117385, 2021.

[5] R. Zapata, M. Balestrieri, I. Gozhyk, H. Montigaud, and R. Lazzari. *ACS Appl. Mater. Interfaces*, 15:36951–36965, 2023.

[6] R. Zapata, M. Balestrieri, I. Gozhyk, H. Montigaud, and R. Lazzari. *Appl. Surf. Sci.*, 654:159546, 2024.

[7] F. Corbella, V. Haspot, Y. Zheng, D. Guimard, H. Montigaud, and R. Lazzari. *submitted*, 2024.

[8] E. Chernysheva, Rensmo H. Philippe, B., O. Karis, M. Gorgoi, E. Burov, S. Grachev, M. Montigaud, and R. Lazzari. *Appl. Surf. Sci.*, 680:161409, 2023.

[9] E. Chernysheva, W. Srouf, B. Philippe, B. Baris, S. Chenot, R. F. Duarte, M. Gorgoi, H. Cruguel, H. Rensmo, H. Montigaud, J. Jupille, G. Cabailh, S. Grachev, and R. Lazzari. *Phys. Rev. B*, 97:235430, 2018.

**4:40pm CM1-2-THA-11 A Combination of Real-Time Diagnostics Probing the Impact of N<sub>2</sub> on Ag Thin Film Growth, Michal Kaminski [michal.kaminski@kit.edu], KIT, Germany; Gregory Abadias, David Babonneau, Institute Pprime, France; Alessandro Coati, Yves Garreau, Synchrotron SOLEIL, France; Anny Michel, Institute Pprime, France; Anton Plech, KIT, Germany; Andrea Resta, Synchrotron SOLEIL, France; Karan Solanki, Institute Pprime, France; Alina Vlad, Synchrotron SOLEIL, France; Baerbel Krause, KIT, Germany**

Silver thin films are used in a number of applications (e.g., transparent and conductive electrodes and plasmonic devices) which require a continuous layer with thickness below a few nanometers. However, Ag films grown by magnetron sputtering have the tendency to form 3D-structures on weakly interacting substrates, what prevents their application as transparent and conductive layers. It is reported that the use of gas additives (particularly N<sub>2</sub> [1]) allows for obtaining a continuous layer at earlier deposition stage.

A thorough understanding of the nanoscale mechanisms of thin film formation requires real-time techniques [2]. In particular the widely used *ex situ* diagnostics can provide misleading information, as the structure of the thin film can evolve even under high vacuum conditions. We employ a simultaneous combination of real-time grazing incidence small-angle x-ray scattering (GISAXS), grazing incidence diffraction (GID), and substrate curvature measurements to get information about polycrystalline thin film evolution during growth. In particular, GISAXS reveals changes in nanoscale morphology, GID gives insight into the crystallinity of thin films, and substrate curvature measurements provide information about the average intrinsic stress. With our methodology we can study the interdependence between stress state, thin film structure and morphology, using the quantitative information obtained from the scattering techniques. Since the influence of the substrate curvature can be crucial for grazing incidence condition x-ray techniques, we show that in the curvature regime encountered in our experiment the effect on GISAXS is negligible.

Using the information from all three techniques, we will discuss the impact of nitrogen additive on all growth stages (from initial stages of island nucleation, growth, and coalescence, up to formation of percolated and continuous films), including the relaxation of the film during growth interruptions.

**Acknowledgements:** The work is performed within the frame of the ANR-DFG project IRMA (491224986).

**Literature:**

[1] A. Jamnig et al., *ACS Appl. Nano Mater.* 3, 4728–4738 (2020)

[2] B. Krause et al., *ACS Appl. Mater. Interfaces* 15, 11268–11280 (2023)

## Advanced Characterization, Modelling and Data Science for Coatings and Thin Films

### Room Town & Country C - Session CM2-2-THA

#### Advanced Mechanical Testing of Surfaces, Thin Films, Coatings and Small Volumes II

**Moderators:** Dr. Thomas Edwards, NIMS, Japan, Matteo Ghidelli, CNRS, France

**1:20pm CM2-2-THA-1 Influence of Applied Deformation on Magnetic Properties of Ferromagnetic Ni<sub>60</sub>Fe<sub>40</sub> Thin Films Deposited on Polymeric Substrate, Alejandro Toledano Povedano [alejandro.toledano.povedano@univ-poitiers.fr], Institut Pprime - CNRS - ENSMA - Université de Poitiers, France; Dominique Thiaudière, Synchrotron SOLEIL, France; Pierre Godard, Institut Pprime - CNRS - ENSMA - Université de Poitiers, France; Eloi Haltz, Laboratoire des Sciences des Procédés et des Matériaux (LSPM) - CNRS, France; Damien Faurie, Fatih Zighem, Laboratoire des Sciences des Procédés et des Matériaux (LSPM) - CNRS, France; Anny Michel, Pierre-Olivier Renault, Institut Pprime - CNRS - ENSMA - Université de Poitiers, France**

Metallic ferromagnetic thin films are key components in devices including sensors, data storage, and signal processing systems. With the rise of flexible electronics, understanding the relationship between magnetic properties and mechanical deformations in the low and high strain regimes is critical. These deformations induce homogeneous elastic strains as well as strain heterogeneities due to crystalline defects and cracks, impacting

# Thursday Afternoon, May 15, 2025

the magnetic properties of films through magnetostriction and dipolar interactions. This study focuses on how mechanical strain and controlled crack propagation affect the magnetic properties of thin films on polymer substrates. The research aims to reveal the relationship between controlled microstructural changes (residual stress, film thickness) and magnetic properties, from initial strain to crack onset and subsequent propagation. These insights are critical for developing flexible magnetic devices that maintain performance under mechanical stress. To investigate these effects, a multi-scale approach has been carried out thanks to a unique setup developed at Synchrotron SOLEIL (DiffAbs beamline). It combines four techniques to study, in situ, the crystalline and magnetic properties of the sample subjected to equibiaxial or sequenced uniaxial tensile testing: X-ray diffraction to monitor the local lattice strain, digital image correlation to measure macroscopic distortions, electrical resistivity to reveal the crack onset and Magneto-Optical Kerr Effect to track the evolution of magnetic reversal. Ni60Fe40 thin films with varying thicknesses (20 and 200nm) have been deposited by ion beam sputtering on flexible polymer substrates and characterised under strain with this setup. Deformation tests of Kapton/Mo/Ni60Fe40 systems highlight the important role of the magnetoelastic field, induced by the difference of the in-plane stress components, for multi-cracking dynamics. The study also examined different film thicknesses to determine whether these variations were linked to fragmentation effects or magnetoplasticity. These findings show how crack density (which varies with thickness) influences the material's magneto-mechanical properties. The hysteresis loops initially show a square shape. As applied deformation increases, the loops change and exhibit features typical of a direction that resists magnetization, attributed to the negative magnetostrictive coefficient of Ni60Fe40. Beyond the maximum of the lattice strain, the loops appear to return to a square shape.

1:40pm **CM2-2-ThA-2 The Local Electrical Fingerprint of Deformation and Growth -Induced Defects in Alloys, Hanna Bishara [hbishara@tauex.tau.ac.il], Tel Aviv University, Israel INVITED**

A microstructural defect, whether spontaneously or intentionally induced, impacts the electrical properties of its surroundings. Defects dominate the electrical behavior of materials only when they become sufficiently dense. Therefore, capturing the defect's electrical characteristics is usually performed on a macroscopic scale, leading to averaging over multiple defect's types. This prevents studying the structure-properties relations in defects. This talk provides advanced electrical characterization methods of individual defects on surface and within the volume of bulk and thin film alloys.

The presentation initially introduces an experimental procedure to measure the local electrical resistivity of defect segments - with high sensitivity and spatial resolution *in-situ* scanning electron microscopy (SEM). The studied defects, i.e. pure and segregated grain boundaries (GBs), dislocations, stacking faults, and phase boundaries are either growth-controlled or deformation-induced. The segments are chemically and structurally characterized by electron backscatter diffraction (EBSD), transmission electron microscopy (TEM), energy dispersive spectroscopy (EDS), and atom probe tomography (APT), in addition to molecular dynamics (MD) simulations.

In the context of grain boundaries (GBs), we report that the GB resistivity spans over a spectrum of values, depending on the boundary's excess volume. The resistivity values might increase by an order of magnitude due to segregation effects in metallic systems. However, segregation-influenced complexions are found to boost the electrical conductivity of semi-metallic materials. Additionally, the talk relates to the formation and electrical characterization of near-surface dislocations in brittle Heusler alloys.

Revealing the contribution of different GB types to electrical resistivity would pave the path for predicting the electrical degradation of materials upon controlled mechanical deformation. In addition, it allows a novel defect engineering to optimize the performance of conductors and functional alloys.

2:20pm **CM2-2-ThA-4 On the Effect of Thin Film Residual Stress on the Crack Propagation Resistance of ALD Coated Nano-Ceramics, Edoardo Rossi, Università degli studi Roma tre, Dipartimento di ingegneria Civile, Informatica e delle Tecnologie Aeronautiche., Italy; Marco Sebastiani [seba@uniroma3.it], Università degli studi Roma Tre, Dipartimento di Ingegneria Civile, Informatica e delle Tecnologie Aeronautiche, Italy**

The present work aims at investigating the effects of Atomic Layer Deposition (ALD) coatings on 3D printed ceramic micro-pillars, which were produced by Two-photon polymerization-direct Laser Writing (TPP-DLW). With a uniform 50 nm layer of Al<sub>2</sub>O<sub>3</sub> under varying processing conditions

(Plasma Enhanced-ALD at 200 °C, Thermal ALD at 200 °C, and 350 °C), the study first evaluated how these coatings influenced the retention of fracture toughness through the splitting of glassy carbon (GC) pillars across a spectrum of Relative Humidity levels (below 5% and above 60%). Then, incorporating spatially resolved stress measurements through Focused Ion Beam (FIB) ring-core analysis, the specific interface effects of the coatings on the crack propagation process were investigated. A corresponding investigation of lithographically produced fused quartz micro-pillars treated with the same ALD parameters provided a comparative foundation to gauge the coatings' effectiveness in enhancing the composite fracture toughness.

Additionally, the research detailed how the found residual stresses within the ALD coatings, significantly varying depending on the deposition temperature, are critical for the understanding of crack initiation and propagation mechanisms, suggesting that the observed reduction in fracture toughness, when compared to undefective, uncoated pillars under similar humid conditions, might be attributed to premature crack tip opening.

The research clarified these interplayed dynamics with the coating's stresses through the silica system's response to ALD coatings, significantly improving the baseline crack resistance. Indeed, uncoated silica experience an approximate 134% increase in fracture toughness for a 50 nm deposition at 200 °C, while a 100 nm coating at 300 °C resulted in around a 165% enhancement. This illustrates how interface engineering (deposition temperature and induced stresses from ALD coatings) can fine-tune fracture toughness in 3D TPP micro-ceramics, depending highly on the substrate material and surface defects (likely missing in lithography silica structures).

2:40pm **CM2-2-ThA-5 Micromechanical Testing of Ceramic Coatings for Nuclear Applications up to 1000°C, Dong (Lilly) Liu [dong.liu@eng.ox.ac.uk], University of Oxford, UK INVITED**

Multi-layered ceramic coatings, such as SiC and PyC, have been used to encapsulate spherical nuclear fuel kernels for use in the next generation of nuclear fission reactors. These coatings are typically between 30 μm to 100 μm thick and will subject to harsh environments such as elevated operation temperatures and neutron radiation during service. It is important to acquire local mechanical properties of these individual coating layers as well as the interfacial strength between the coatings for better understanding of their structural integrity and to support performance modelling. In this work, nanoindentation tests were carried out on SiC and PyC coatings over a range of temperatures from ambient to 1000°C with and without *in-situ* SEM imaging. The change of modulus and hardness as a function of temperature will be presented and the challenges associated with the high-temperature tests will be discussed. In addition, micro-cantilever bending method was utilized to evaluate the interfacial strength between the SiC and PyC coatings. During the coating deposition process (chemical vapour deposition), residual stresses were generated in the coatings and affected the local properties. Therefore, the residual stresses in each coating layer were characterised by focussed-ion-beam digital image correlation (FIB-DIC) method on unirradiated and neutron irradiated coatings where the magnitude of residual stresses are further modified due to radiation induced dimensional changes. The local mechanical properties and residual stresses measured are correlated with the coating deposition process, radiation damage and 3D microstructure generated using FIB tomography based on conventional Ga+ FIB and Plasmas FIB.

## Advanced Characterization, Modelling and Data Science for Coatings and Thin Films

Room Town & Country D - Session CM3-2-ThA

### Accelerated Thin Film Development: High-throughput Synthesis, Automated Characterization and Data Analysis II

Moderators: Dr. Davi Marcelo Febba, NREL, USA, Dr. Sebastian Siol, Empa, Switzerland

1:20pm **CM3-2-ThA-1 Feature Selection and High-Throughput Synthesis: Can They Be Used to Predict Adsorption Energies on Multinary Materials?, Hannah-Noa Barad [hannah-noa.barad@biu.ac.il], Bar-Ilan University, Israel INVITED**

Electro-reduction of CO<sub>2</sub> to sustainable fuels and value-added chemicals is one of the most promising paths for closing the anthropogenic CO<sub>2</sub> cycle. The catalyst, the main component of the electrochemical CO<sub>2</sub> reduction reaction (CO<sub>2</sub>RR), is used to reduce CO<sub>2</sub> dissociation activation energy.

Metal and metal oxide catalysts have been studied as catalysts for CO<sub>2</sub>RR, yet selectivity towards desired products remains elusive. To overcome this issue, discovery of new materials with more components (e.g., ternary, or quaternary materials), is paramount. These multinary materials, have the potential to improve the selectivity and activity toward a desired product, due to synergistic effects between the elements. However, the exploration space is enormous and needs to be decreased. An important descriptor for realizing the reaction mechanism leading to a specific product by a given catalyst is the adsorption energy of the reaction intermediates, like \*CO. Yet, adsorption energies on these new and complex materials have not been studied systematically.

Here, we present the development of a machine learning model for the prediction of adsorption energies of materials. Our model is based on a simple description of the adsorption environment by choosing very basic features, and more intricate structural features, like orbital field matrix.<sup>[1]</sup> We also apply the moments theorem for the density of states (DOS)<sup>[2]</sup> to depict our materials in terms of closed paths in their lattices, from which we obtain features relating to the adsorption site. We also use high-throughput synthesis and characterization methods to try and obtain more experimental data points on new multinary materials to enhance our dataset. These methods will support prediction of adsorption energies of multinary materials to discover new highly active and selective CO<sub>2</sub>RR catalysts.

[1] T. Lam Pham, H. Kino, K. Terakura, T. Miyake, K. Tsuda, I. Takigawa, H. Chi Dam, *Sci. Technol. Adv. Mater.* **2017**, *18*, 756.

[2] J. P. Gaspard, F. Cyrot-Lackmann, *J. Phys. C Solid State Phys.* **1973**, *6*, 3077.

2:00pm **CM3-2-ThA-3 Development of Cu, Ni-Co-Doped Bi<sub>2</sub>Te<sub>2.7</sub>Se<sub>0.3</sub> for Thermoelectric Energy Generation Using Pulsed Laser Deposition, *Yakubu Sani Wudil [yaqubswudil@gmail.com]*, King Fahd University of Petroleum and Minerals, Saudi Arabia**

This work reports the preparation of ternary Cu/Ni/Bi<sub>2</sub>Te<sub>2.7</sub>Se<sub>0.3</sub> nanocomposite thin films via pulsed laser deposition. For comparison, pure Bi<sub>2</sub>Te<sub>2.7</sub>Se<sub>0.3</sub> (BTS) and binary Cu/Bi<sub>2</sub>Te<sub>2.7</sub>Se<sub>0.3</sub> and Ni/Bi<sub>2</sub>Te<sub>2.7</sub>Se<sub>0.3</sub> nanocomposites were also synthesized. Morphological characterizations revealed the presence of abundant grains typical of the BTS sample. Energy-dispersive spectroscopy confirmed trace amounts of Cu and Ni within the films, while X-ray photoelectron spectroscopy indicated that both metals were present as unoxidized metallic atoms, free from telluride formation. Structural analyses using X-ray diffraction and Raman spectroscopy showed peaks consistent with the pure BTS structure, suggesting that the dopants were primarily located at the grain boundaries within the BTS matrix. The ternary nanocomposites were prepared using a specialized configuration at three different Cu/Ni concentrations. The highest room temperature thermoelectric figure of merit (ZT) of 0.97 was achieved at the optimal doping concentration (BTS-2Cu/Ni), attributed to a simultaneous increase in power factor (2988 μW/mK<sup>2</sup>) and a decrease in thermal conductivity (0.93 W/mK). The enhanced thermoelectric power factor resulted from the selective filtering of low-energy charge carriers, which improved the Seebeck coefficient. Additionally, the introduction of Cu and Ni into the nanocomposites created abundant grain boundaries that scattered phonons, reducing intrinsic lattice thermal conductivity and thereby enhancing the ZT value.

2:20pm **CM3-2-ThA-4 Autonomous Experiments for Thin Films and Solid Materials, *Taro Hitosugi [hitosugi@g.ecc.u-tokyo.ac.jp]*, The University of Tokyo, Japan** **INVITED**

Integrating machine learning, robotics, and big data analysis into established research methodologies can significantly accelerate materials science research. Many studies have already demonstrated the potential of autonomous (self-driving) experiments in materials science [1, 2]. The rapid advancement of digital technologies is changing the way we conduct research.

Here, we discuss the status and prospects of data- and robot-driven materials research using autonomous experiments. We have developed an autonomous experimental system for thin-film materials. We constructed a system that automates sample handling, thin-film deposition, optimization of growth conditions, and data management. By using Bayesian optimization in conjunction with robots, our approach facilitates high-throughput experiments and generates comprehensive datasets that cover many aspects of materials (X-ray diffraction, Raman spectroscopy, scanning electron microscopy, optical transmittance measurement, electronic conductivity measurement). We tuned the hyperparameter for Bayesian

optimization using the domain knowledge of chemistry; the number of trials to reach the global optimum is reduced.

The system demonstrated the synthesis and optimization of the electrical resistance in Nb-doped TiO<sub>2</sub> thin films [5]. Moreover, this autonomous approach has enabled the discovery of new ionic conductors [6]. We discuss the potential impact of this technology in accelerating materials science research, particularly in solid materials.

[1] Autonomous experimental systems in materials science, N. Ishizuki, R. Shimizu, and T. Hitosugi, *STAM Methods* **3**, 2197519 (2023).

[2] The rise of self-driving labs in chemical and materials sciences, M. Abolhasani and E. Kumacheva, *Nature Synthesis* **2**, 483–492 (2023).

[3] Tuning of Bayesian optimization for materials synthesis: simulation of the one-dimensional case, R. Nakayama, T. Hitosugi *et al.*, *STAM Methods* **2**, 119-128 (2022).

[4] Tuning Bayesian optimization for materials synthesis: simulating two- and three-dimensional cases, H. Xu, R. Nakayama, T. Hitosugi *et al.*, *STAM Methods* **3**, 2210251 (2023).

[5] Autonomous materials synthesis by machine learning and robotics. R. Shimizu, T. Hitosugi *et al.*, *APL Mater.* **8**111110 (2020).

[6] Autonomous exploration of an unexpected electrode material for lithium batteries. S. Kobayashi, R. Shimizu, Y. Ando, T. Hitosugi, *ACS Materials Lett.* **5**, 2711–2717 (2023).

## Tribology and Mechanics of Coatings and Surfaces Room Palm 3-4 - Session MC1-1-ThA

### Friction, Wear, Lubrication Effects, & Modeling I

**Moderators: Pierluigi Bilotto**, TU Wien, Austria, **Michael Chandross**, Sandia National Laboratories, USA

1:20pm **MC1-1-ThA-1 Solid Lubrication in Thin Films: Mechanisms, Materials, and Performance, *Daniel Pözlberger*, Institute of Materials Science and Technology, TU Wien, Austria; *Rainer Hahn, Tomasz Wojcik, Philip Kutrowatz*, Christian Doppler Laboratory for Surface Engineering of High-performance Components, TU Wien, Austria; *Klaus Böbel, Julien Keraudy*, Oerlikon Balzers, Oerlikon Surface Solutions AG, Liechtenstein; *Szilard Kolozsvári, Peter Polcik*, Plansee Composite Materials GmbH, Germany; *Philipp G. Grützmacher, Carsten Gachot*, Institute of Design Engineering and Product Development, Research Unit Tribology, TU Wien, Austria; **Helmut Riedl [helmut.riedl@tuwien.ac.at]**, TU Wien, Institute of Materials Science and Technology, Austria** **INVITED**

Tribological contacts play an essential role in the prevalent and required endeavor for increased sustainability and efficient use of resources. Considering the energy losses related to friction and wear, a huge possibility of saving resources, energy, and CO<sub>2</sub> is often overlooked. Here, solid lubricants are an attractive option, especially for applications pushing their conventional liquid counterparts to their thermal and chemical stability limits – typically at elevated temperatures above 200 °C or under extreme conditions excluding liquids (i.e. space industry, semiconductors, or life science). Therefore, this study examines different solid lubrication concepts in thin film materials, classifying them concerning predominant mechanisms, application ranges, and performance.

As a starting point, carbon-containing thin film materials will be discussed comprising diamond-like carbon (DLC) coatings and non-reactively sputter deposited transition metal (TM) carbide thin films (i.e., HfC, TaC, or WC). Here, advances in PVD growth techniques (i.e., HiPIMS) and their impact on tribological performance are in focus. Furthermore, insights on the limits of carbon as the source for solid lubrication will be given by a set of high-resolution characterization techniques (i.e., HR-TEM, APT, etc.). The second part presents an alternative class of TM dichalcogenide coating materials (compared to MoS<sub>2</sub>) and their in-situ formation. In detail, in an innovative approach, selenium nanopowders are converted in-situ into lubricious 2D selenides on sliding W and Mo films, achieving a coefficient of friction (COF) down to 0.1 in ambient air. This in-situ formation is an exciting concept, especially for extreme environmental conditions. Nevertheless, further advances in solid lubricants are required to overcome the limitations for high-temperature applications (above 450 °C). Here, a concept on B<sub>2</sub>O<sub>3</sub> formation in TM borides (i.e., TiB<sub>2+z</sub> or WB<sub>2+z</sub>) leads to a drastic reduction of COF from 0.6 to 0.2 at 500 °C (and higher temperatures), highlighting the capabilities of boron-containing thin films in high-temperature tribological contacts.

# Thursday Afternoon, May 15, 2025

In summary, the different concepts of solid lubrication in thin film materials emphasize the potential of exploring new materials and the need for an in-depth understanding to push these materials in potential applications.

**2:00pm MC1-1-ThA-3 Study of Transparent Coatings for the Preservation of Colored Titanium Surfaces**, Sarah Marion, Renée Charrière, Mines Saint-Etienne, France; Clotilde Minfray, Ecole Centrale de Lyon - LTDS, France; Laurent Dubost, HEF - IREIS, France; Jenny Faucheu, Mines Saint-Etienne, France; Vincent Fridrici [vincent.fridrici@ec-lyon.fr], Ecole Centrale de Lyon - LTDS, France

Although titanium is not a noble metal, it is increasingly attracting interest from the luxury industry (jewelry, watches, packaging) due to its lightweight, hypoallergenic properties, and especially the wide range of colors it can display when coated with a thin layer of TiO<sub>2</sub>. However, its application in luxury products remains limited because these colors tend to lack durability. Improving the wear resistance of these colored TiO<sub>2</sub> layers, and in particular preserving the original color, is a critical challenge for luxury jewelry.

The interference-based nature of titanium's color makes it highly sensitive to changes in oxide layer thickness, as well as to variations in the oxide layer's chemical composition and internal structure, which can alter its refractive index. Tribological tests conducted on thin titanium oxide layers, using a 100Cr6 steel ball in both dry conditions and with artificial sweat, demonstrated a clear correlation between color changes due to friction and a reduction in oxide layer thickness in both environments.

An experimental study of the wear resistance of several potential protective coatings deposited on oxidized titanium samples is carried out in order to preserve the color of the samples. Three coatings—SiAlON, Si<sub>3</sub>N<sub>4</sub>, and a commercial hydrophobic coating—were examined for their wear resistance in both dry and artificial sweat conditions, as well as for their transparency and surface wettability. The challenge is to have a coating that is not only transparent but also resistant to wear in both dry and sweat-exposed conditions and insensitive to fingerprints.

Thus, the color variation before and after coating, the surface wettability of the coating with water and sebum, as well as its resistance to dry friction and friction in the presence of artificial sweat against a 100Cr6 steel ball, will be analyzed and compared to those of uncoated TiO<sub>2</sub> to assess the performance of the coatings.

**2:20pm MC1-1-ThA-4 Beyond Graphene: A ML-Assisted High-Throughput Molecular Dynamics Framework for Screening 2D Materials for Tribological Applications**, Matteo Valderrama [m.valderrama23@imperial.ac.uk], Daniele Dini, James Ewen, Imperial College London, UK; Nicolas Fillot, INSA de Lyon, France

2D materials, with their unique atomic structures and tunable properties, have shown immense potential for achieving superlubricity (COF < 0.01) in sliding contacts. However, the vast design space of these materials presents a significant challenge in identifying optimal candidates for specific tribological applications. To date, only around ten 2D materials have been extensively studied for their tribological properties. This work explores a framework for applying machine learning (ML) assisted high-throughput molecular dynamics (MD) simulations to accelerate the discovery of high-performance 2D materials for tribological applications. 2D materials exhibit fundamentally different frictional behavior compared to their bulk counterparts, a phenomenon that can be observed at the atomic scale. To study this, our framework will computationally screen the tribological performance of thousands of 2D materials. By streamlining simulation cell generation and optimization, this framework facilitates the processing of tens of thousands of MD simulations. Combined with the recent advancements in GPU-powered simulations, this project could transform high-throughput MD, especially through the hybridization of both the computational approaches (CPU vs. GPU) and the implementation of interatomic potentials. The extracted tribological data will be used to train ML models, such as regressive random forests, LSTMS, and LLMs, to predict the performance of new materials. Our goal is to establish correlations between specific material properties and atomic friction mechanisms, gaining deeper insights into the underlying causes of atomic friction. We anticipate that this project will revolutionize the field of 2D materials by accelerating the design, prototyping, and experimental validation of materials that demonstrate robust superlubricity, making research more accessible and reproducible, and ultimately paving the way for their widespread adoption in various applications. In this presentation, I will delve into the details of our framework, demonstrate its validity, and present preliminary results on predicting friction in 2D materials based on their intrinsic properties.

**2:40pm MC1-1-ThA-5 Modelling Complexities of Tribocorrosion Processes: Evaluation and Validation**, Avirup Sinha [asinha38@uic.edu], University of Illinois at Chicago, USA; Feyzi Hashemi, Flinders University, Australia; Maansi Thapa, Bill Keaty, Yani Sun, University of Illinois at Chicago, USA; Reza Hashemi, Flinders University, Australia; Mathew T. Mathew, University of Illinois at Chicago, USA

Introduction:

Biomedical implants are vital medical devices surgically placed to replace or support damaged tissues and organs. Modular implants, such as hip replacements, improve adaptability for diverse patients but introduce challenges like tribocorrosion—a complex interaction of tribology and corrosion. Tribocorrosion releases debris, ions, and particles into surrounding tissues, causing reactions, systemic toxicity, and infections. Biocompatible materials like Ti6Al4V are commonly used in implants. Although various experimental methods exist to study tribocorrosion, limited mathematical modeling efforts have been undertaken. This study reviews available models to identify those most suitable for implant applications, with two aims: a) validating model efficiency using literature data, and b) conducting experiments to generate data for further validation.

Methodology:

Aim 1: Electrochemical current evolution is a key measure of tribocorrosion. Models like “Olsson and Stemp,” “Feyzi and Hashemi,” and the Uhlig model predict tribocorrosion currents, but their efficiency remains insufficiently tested. Data from M.T. Mathew et al.'s “Tribocorrosion Behaviour of TiCxOy” was selected for its robust dataset, clear graphical representation, and systematic evaluation across varying voltages, ensuring analytical versatility. Aim 2: Fretting-corrosion experiments were conducted using a custom-built tribocorrosion apparatus (Pin-on-flat) to validate models against experimental outcomes. Materials included Ti6Al4V and CoCr bases with a Zr pin. Testing was performed in 0.9% saline at 83N load and ±6mm amplitude at 1Hz frequency.

Results:

Aim 1 demonstrated that Mischler's model outperformed Olsson and Stemp's in predicting experimental data. While Olsson's model worked well at -0.5V, it struggled at +0.5V due to assumptions about voltage-dependent oxide film growth, making it better suited for lower voltage predictions. Aim 2 revealed Feyzi and Hashemi's model best predicted tribocorrosion behavior, though significant variance highlighted the need for refined assumptions. Olsson and Stemp's model showed promise with adjustments to variables like oxide layer thickness, emphasizing its role in tribocorrosion modeling.

Conclusions:

The study concludes that tribocorrosion current is influenced by multiple factors, and model predictions improve with accurate variable inputs. Further research is needed to refine models, including developing experimental procedures to determine assumed variable values (e.g., asperity radius) and creating real-time computational models to compare experimental and predicted results.

**3:00pm MC1-1-ThA-6 Electrification of Ti:MoS<sub>2</sub> Coatings for Tribological Applications**, Newton K. Fukumasu [newton.fukumasu@gmail.com], Institute for Technological Research of Sao Paulo State, Brazil; Miguel R. Danelon, André P. Tschiptschin, Izabel F. Machado, Roberto M. Souza, University of São Paulo, Brazil

Next-generation adaptive coatings for heavy-loaded mechanical transmission systems enhance durability and efficiency by coupling external parameters, such as electrical conditions, with tribological performance, particularly relevant for electric vehicle powertrains and energy generation systems, where controlling friction and wear is crucial for improving operational efficiency. Also, in those systems, stray currents could be used for improving tribological aspects of mechanical systems. Coatings of transition metal dichalcogenides, such as molybdenum disulfide, promote excellent solid lubrication under high contact stresses and pure sliding conditions, but higher wear rates compromise coating durability. Metal-doping MoS<sub>2</sub> coatings allows the optimization of mechanical properties, including hardness and elastic modulus, promoting an amorphous coating structure and engineered coating bandgap. In this work, Ti:MoS<sub>2</sub> coatings were deposited using a pulsed D.C. magnetron sputtering, with doping levels controlled by varying the power applied to Ti target. Tribological tests under electrified reciprocating conditions were conducted with uncoated AISI 52100 balls against Ti:MoS<sub>2</sub> coated glass plates. Ti concentration was varied between 10 at% and 20 at% and electrified tests conditions considered positive, negative, and non-electrified contact with, when

# Thursday Afternoon, May 15, 2025

applied, a constant electric current of 100 mA. Ball movement frequency was set at 0.375 Hz with 4 mm stroke. Results indicated that friction was reduced under electrified conditions, particularly for coatings with lower Ti concentrations. Raman spectroscopy revealed recrystallized MoS<sub>2</sub> inside wear tracks, suggesting tribo-induced structural adaptation. Wider wear tracks and greater surface damage were observed when ball was positively charged. Results suggest that the electric field may promote differential migration of Mo, S, and Ti species, altering the tribofilm composition and morphology formed at the ball surface. This selective adsorption on the ball further enhances the formation of MoS<sub>2</sub>-rich regions, in which tribochemical reactions, enhanced by the electric current, may favor MoS<sub>2</sub> retention and regeneration at lower Ti concentrations, while higher Ti concentrations disrupt the lubricating behavior. The integration of tribology and electrification may lead to enhanced efficiency and durability of critical mechanical systems with selective surface chemistry and adaptive tribological performance.

3:20pm **MC1-1-ThA-7 Nanoscale Wear of Metallic Multilayers - the Effect of Interface**, **Tomas Polcar** [[polcar@fel.cvut.cz](mailto:polcar@fel.cvut.cz)], **Ahmed AlMotasem**, Czech Technical University in Prague, Czech Republic

Extensive large molecular dynamics simulations (MD) were conducted to investigate the impact of different Zr/Nb interface orientations on the friction/wear behavior of Zr/Nb multilayers. The primary cause of plastic deformation of the Nb layer was dislocations and BCC twinning, while Zr layers deformed via dislocations and intrinsic stacking faults. The Zr/Nb exhibited better tribological properties, such as lower COF, higher scratch hardness, and improved wear resistance compared to their single-crystal counterparts. The interface structure was analyzed, and its blocking strength was discussed. Tailoring them to achieve desired properties for specific applications.

The simulations of friction and wear were compared with experimentally obtained nanoscratches on Zr/Nb multilayers with a periodicity of 6 nm prepared by magnetron sputtering. The wear was evaluated by AFM, structure by STEM and XRD. Qualitative agreement with experiments demonstrates predictive power of MD simulations in tribology.

## Plasma and Vapor Deposition Processes Room Town & Country B - Session PP8-2-ThA

### Commemorative Session for Papken Hovsepian II

**Moderators:** Prof. Arutian P. Ehasarian, Sheffield Hallam University, UK, Philipp Immich, IHI Hauzer Techno Coating B.V., Netherlands

1:20pm **PP8-2-ThA-1 PVD Based Solutions for Mankind Through Applied Research**, **Ton Hurkmans** [[ton.hurkmans@ionbond.com](mailto:ton.hurkmans@ionbond.com)], IHI Ionbond Group, Germany **INVITED**

During our Ph.D. studies as well as early work at Bodycote and then later at Ionbond, we had a lot of positive interaction with Prof. Dr. Papken Hovsepian. Our shared passion was a desire to use thin film vacuum coating technology to improve products that are being used by people on a daily basis.

Applied research requires insight on both the technology and the market opportunities. It's basically a reversed engineering from macro-scale back to atomic levels, i.e. to translate desired product properties into coating properties and finding a way to synthesize such coating properties. Sheffield Hallam University and Ionbond have worked on many such examples and during the presentation we will elaborate on some of them.

At Bodycote commercial products were introduced and sold, known under tradenames like Supercote 11 (TiAlCrN), Supercote 30 (TiAlN/VN), and Supercote 55 (CrN/NbN). In parallel we collaborated on multiple EU funded development projects, with names like Newchrome (replacement of electroplating), HIDAM (cutting tools), NitraCote (duplex treatments), ALTICUT (high end machining operations), Colour PVD (PVD coating with post-anodizing), HIPIMS (first EU project on HIPIMS), INNOVATIAL (coatings for jet engines), CORRAL (atomic layers against corrosion), and Monaco (the use of OEM within industry 4.0). There were also joined developments where the manufacturer or end user participated as well.

All the hard work also resulted in joined scientific papers and patents.

2:00pm **PP8-2-ThA-3 Managing Relative Abundance of Ions and Neutrals: A New Plasma Performance Metric in Modern Surface Engineering**, **Ganesh Kamath** [[ganesh.kamath@asm.com](mailto:ganesh.kamath@asm.com)], ASML, USA **INVITED**

Modern engineering components made up of metals/alloys, plastics and glass have to meet very stringent multifunctional quality specifications and

must survive under longer operating conditions. The advent of innovative industrial scale ionized plasma technologies have successfully demonstrated the ability to process those components and fulfill such demands. More specifically, these plasma technologies are being used to produce and control desired amount of ions (Metal<sup>+</sup>/Gas<sup>+</sup>) and neutrals to bombard onto engineering component surfaces to create new multifunctional homogeneous/inhomogeneous nanostructured surface. The metal ions have the most important influence on coating properties and structure. The modification of the surface of the substrate-to-be-coated by metal ion etching is important for improvement of coating adhesion, while assistance of the coating deposition process by metal ion bombardment plays the leading role in formation of nanostructured coatings with unique properties, usually outside of the thermodynamic equilibrium. Thus relative abundance of ions and neutrals are considered as new plasma performance metric in today's advanced surface engineering application.

One of the first technologies which used metal ion bombardment as a tool for improvement of magnetron sputtering coatings was arc-bond sputtering (ABS) technology introduced by W.D. Munz in 1991 and later perfected in the collaborative works by W.D. Munz and P. Hovsepian and their coworkers. In this technology the initial coating sublayer was deposited by cathodic arc followed by magnetron sputtering deposition which dramatically improved adhesion of the magnetron sputtering coating to the substrate. The ABS technology was utilized in large industrial-scale coating machines by Hauzer company. The filtered cathodic arc technology developed in 1980s-1990s allows to get rid of macroparticles and produce 100% ionized metal vapor plasma flow. It was developed to industrial scale applications by Large Area Filtered Arc Deposition (LAFAD) systems. The LAFAD process is capable of deposition the thermodynamically non-equilibrium coatings such as hydrogen-free diamond-like carbon (DLC) coatings and DLC-based nanocomposite coatings, both as a single layer and as nano-multilayers with high adhesion and cohesion properties. The productivity of the LAFAD process allowed its application for deposition of multilayer erosion resistant coatings for turbomachinery with coating thickness >100 µm.

2:40pm **PP8-2-ThA-5 Invited Paper**, **Pawel Ozimek** [[pawel.ozimek@trumpf.com](mailto:pawel.ozimek@trumpf.com)], Trumpf, USA **INVITED**

3:20pm **PP8-2-ThA-7 Carbon Based Surface Solutions – from a Glorious Legacy to Recent Advances**, **Vishal Khetan** [[Vishal.Khetan@oerlikon.com](mailto:Vishal.Khetan@oerlikon.com)], Oerlikon Surface Solution AG, Switzerland **INVITED**

Tribology and Surface Engineering, as enabling technologies, have been continuously advancing global manufacturing sectors in terms of fuel economy (reduced friction and wear), improved productivities and product reliability, functionalisation of machine components, providing alternative manufacturing processes due to environment legislations, and electrification of vehicles, etc. Along with the new generation manufacturing and climate change energy challenges surface engineering will phase in a new era of research and innovation. Carbon based surface solutions using technologies such as physical/chemical vapour deposition (PVD, CVD) deliver new and sustainable pathway in multiple manufacturing industries such as automotive, medical, packaging and aerospace can be addressed and introduced to a broader industry perspective.

While developing new carbon coatings and bringing them to industry as solutions, we always stand on the shoulders of giants like Prof. Papken Hovsepian. His work in the field of thin film technology was an inspiration for many and through this talk we illustrate how his work has channelled beautiful scientific ideas which turn into products serving various industrial application especially in the field of carbon-based surface coatings. Further, in co-relation to his work, we would be discussing scientific background, tribological and industrial relevance various carbon based surface solutions offered by Oerlikon Surface Solutions AG ranging from amorphous hydrogenated carbon to hydrogen free carbon coatings via PACVD, S3p (Scalable pulsed power plasma), Cathodic Arc evaporation and PICVD (Plasma induced chemical vapour deposition) with special focus on new upcoming carbon based solutions such as BALINIT® MAYURA, upcoming nanocrystalline diamond coating using PICVD technology.

4:00pm **PP8-2-ThA-9 Invited Paper**, **Arutian P. Ehasarian** [[a.ehasarian@shu.ac.uk](mailto:a.ehasarian@shu.ac.uk)], Sheffield Hallam University, UK **INVITED**

## Advanced Characterization, Modelling and Data Science for Coatings and Thin Films

Room Golden State Ballroom - Session CM-ThP

## Advanced Characterization, Modelling and Data Science for Coatings and Thin Films Poster Session

**CM-ThP-1 How to Predict the Deposition Rate During Reactive Sputtering Using an One-Volume Reference Resource?, Diederik Depla [Diederik.Depla@ugent.be]**, Ghent University, Belgium

A longstanding challenge in reactive magnetron sputtering is the quantitative prediction of the deposition rate, which is primarily determined by the partial metal sputtering yield from the oxide layer formed on the target surface during poisoning. The first step in addressing this issue is to determine the total sputtering yield of the oxide. This has been accomplished by refining a published semi-empirical model. This model has been applied to fit an extensive set of oxide sputtering yield data from the literature, comprising 65 datasets for 21 different materials. The fitting process establishes a relationship between the surface binding energies of metal and oxygen atoms and the cohesive energy of the oxide. The calculated partial sputtering yield of metal from a poisoned target is then compared with previously published experimental data on the metal sputtering yield during reactive magnetron sputtering. While both yields are linearly correlated, the magnetron-based sputtering yields are approximately eight times lower than the model predictions. This reduction in yield is attributed to the formation of an oxygen-rich surface layer, a hypothesis supported by binary collision approximation Monte Carlo simulations. However, these simulations do not fully capture the mechanism, as a more detailed description of the surface oxygen origin is needed. Despite this limitation, the experimental correlation provides a practical strategy for predicting deposition rates during reactive magnetron sputtering in fully poisoned mode. As demonstrated, the oxide sputtering yield can be calculated using standard data sources, and the empirical correlation between the sputtering yields enables a reliable estimate of the metal partial sputtering yield in poisoned mode, thus allowing for an accurate estimation of the deposition rate.

D. Depla, Note on the low deposition rate during reactive magnetron sputtering, *Vacuum* 228 (2024) 113546

D. Depla, J. Van Bever, Calculation of oxide sputter yields *Vacuum* 222 (2024) 112994

**CM-ThP-2 Deep Insertion Induced Fracture in Soft Solids, MUTHUKUMAR MARIAPPAN [muthukumar.iitk@gmail.com]**, Department of Mechanical Engineering, IISc Bangalore, India

Deep insertion of sharp objects like a needle into soft tissues is a common procedure in the medical domain for delivering drugs, biopsies and other medical interventions. It is inevitable to avoid tissue damage during needle insertion which sometimes leads to catastrophic outcomes. Opacity and inhomogeneity of the tissues make it difficult to observe the underlying damage mechanisms. In this context, it is essential to understand the underlying mechanisms of the formation of various cracks, crack nucleation and crack propagation in soft tissue-mimicking materials during deep penetration to minimise tissue damage. In this talk, we discuss the fracture behaviour of soft tissue-mimicking gels during deep penetration of a sharp needle. For the first time, we observed nearly periodic, stable, and well-controlled 3-D cone cracks inside the soft gel during deep penetration. We show that the stress field around the needle tip is responsible for the symmetry and periodicity of the cone cracks. These results provide a better understanding of the fracture processes in soft and brittle materials and open a promising perspective in needle designs and the control of tissue damages during surgical operations.

**CM-ThP-3 Temperature-Dependent Oxidation Mechanisms of Binary Nitride Compounds: A Molecular Dynamics Approach, Sara Fazeli, MS4ALL, France; Edern Menou, Marjorie Cavarroc [marjorie.cavarroc@safrangroup.com]**, SAFRAN, France; Pascal Brault, MS4ALL / GREMI, France

Binary nitride (XN) compounds represent an important class of advanced ceramic materials, increasingly recognized for their suitability in high-temperature applications such as aerospace components, turbine blades, and protective coatings. Transition metal nitrides such as titanium nitride (TiN) and zirconium nitride (ZrN) are especially noted for their outstanding hardness and resistance to corrosion. In addition, nitrides of non-transition metals, including carbon nitride (CN), silicon nitride (SiN), and boron nitride (BN), function as essential refractory materials due to their high stability

under extreme temperatures and durability in harsh environments. The oxidation behavior of binary nitride materials is often a crucial factor in selecting materials for high-temperature use, as the oxidation resistance of a given XN phase depends on its capacity to form a stable, passivating oxide layer. It is worth noting that a distinct change in the oxidation mechanism is observed at high temperatures, which is attributed to phase transformations in the oxidation products. The insights gained from the oxidation behavior will facilitate the more efficient design and rapid discovery of XN phases that maintain optimal performance in oxidizing environments at elevated temperatures. In this study, we perform ReaxFF and COMB3-molecular dynamics (MD) simulations of the oxidation of binary nitride compounds XN (X = B, C, Si, Ti, and Zr) at four different temperatures (900 K, 1300 K, 1500 K, and 1700 K) to elucidate the mechanism of the oxidation states in the oxide layer.

At the lowest temperature, oxygen chemisorption occurred on the binary compounds without significant surface oxidation. In contrast, at higher temperatures, the amount of O<sub>2</sub> adsorbed increased steadily, particularly for transition metal nitrides. High oxygen coverage at elevated temperatures may lead to structural reconstructions of the surface. This study provides valuable insights into the oxidation mechanisms, helping researchers identify strategies to form stable, protective oxide layers, which enhance corrosion resistance and broaden the industrial applications of high-temperature materials, paving the way for the development of other binary nitride compounds.

**CM-ThP-4 Simulating Mode-I Crack Opening Process in Transition Metal Diborides via Machine-Learning Interatomic Potentials, Shuyao Lin [shuyao.lin@tuwien.ac.at]**, TU Wien, Institute of Materials Science and Technology, Austria; Zhuo Chen, Zaoli Zhang, Erich Schmid Institute of Materials Science, Austrian Academy of Sciences, Leoben, Austria; Lars Hultman, Linköping Univ., IFM, Thin Film Physics Div., Sweden; Paul Mayrhofer, Nikola Koutna, TU Wien, Institute of Materials Science and Technology, Austria; Davide Sangiovanni, Linköping Univ., IFM, Thin Film Physics Div., Sweden

The critical stress-intensity factor  $K_{Ic}$  and fracture strength  $\sigma_f$  define the fracture resistance of brittle ceramics. However, their experimental measurement is challenging and provides limited atomic-scale insight into crack tip behavior. In this work, we overcome these limitations by offering atomic-scale information on crack growth while evaluating fracture toughnesses and fracture strengths via machine-learning-assisted simulations. Transition metal diborides (TMB<sub>2</sub>:s) serve as a case study, with a focus on understanding the Mode-I crack opening response across six distinct orientations within 2 different phases ( $\alpha$  and  $\omega$ ). Molecular statics and dynamics calculations were used to systematically test model sizes and thicknesses, ensuring efficient simulations and accurate extrapolation of macroscale mechanical properties via constitutive scaling laws. By incorporating the phase-dependent and anisotropic mechanical properties of the  $\alpha$ -phase TMB<sub>2</sub>:s, the observed phenomena, as revealed through strain distribution and bond distances, align closely with those well-studied ceramics such as nitrides, offering insights into the fracture mechanisms within realistic deformation environments via atomistic level perspective. Furthermore, while  $\alpha$ - and  $\omega$ -WB<sub>2</sub> exhibits minimal phase dependence in deformation plasticity strength, as supported by both theoretical and experimental results, the fracture strength, as determined through the defective model, demonstrates a significant variation. The results show that the  $K_{Ic}$  varies across different orientations and phases within the group IV, V, and VII TMB<sub>2</sub>:s, correlating with their respective tensile and shear strengths.

**CM-ThP-5 Simulation Study on Color Modulation of Diamond Substrates via Localized Surface Plasmon Resonance Effects Induced by Metal Nanoparticles, Tsung-Jen Wu [d09224004@ntu.edu.tw]**, Sheng-Rong Song, Wen-Shan Chen, National Taiwan University, Taiwan; Wen Lin, National Taipei University of Technology, Taiwan; Shao-Chin Tseng, National Synchrotron Radiation Research Center, Taiwan

This study employs the Finite-Difference Time-Domain method to simulate the Localized Surface Plasmon Resonance effects induced by gold, silver, and copper nanoparticles on diamond substrates, aiming to recreate the rare pink, yellow, and blue hues observed in certain diamonds. The simulation results reveal that gold nanoparticles impart a pinkish hue to the diamond, silver nanoparticles produce a yellow tint, and copper nanoparticles create a blue shade. These color variations are significantly influenced by the size and arrangement of the nanoparticles, with optimized configurations enhancing the color effects in synergy with the diamond's crystalline structure. The findings of this study provide an

innovative and cost-effective approach for the jewelry industry to manufacture colored diamond coatings and serve as a valuable reference for thin-film and coating technologies in applications involving optical components and sensors.

**CM-ThP-6 Correlative XPS & SEM Analysis for NMC and Na-Ion Battery Cathode Material Surface Composition, James Lallo [james.lallo@thermofisher.com]**, Thermo Fisher Scientific, UK, USA; *Nannan Shi, Albert Ge*, Thermo Fisher Scientific, UK, China; *Tim Nunney*, Thermo Fisher Scientific, UK

Advanced energy storage has become increasingly vital in many fields, from transportation, to defence, to everyday connectivity. This has led to a growing market demand and development for lithium-ion battery storage solutions. High-tech products such as smartphones, tablets, drones, and electric vehicles all rely on compact, powerful energy storage, with lithium-ion batteries being an essential component. Lithium battery primarily consist of cathode, anode, electrolyte, and separator materials. In lithium battery material research, how to comprehensively characterize and analyse battery materials, and how to use this characterization information to further improve battery material performance has become the focus of current researchers. This poster uses LiNi<sub>x</sub>Co<sub>y</sub>Mn<sub>(1-x-y)</sub>O<sub>2</sub> (NCM)/LiCoO<sub>2</sub> [NMC] composite cathode and Sodium Ion Fe/Mg cathode materials as examples. We employ a combination of Scanning Electron Microscopy (SEM) and X-ray Photoelectron Spectroscopy (XPS) characterization techniques to conduct a comprehensive analysis of the composite cathode materials. This approach yields rich sample information, helping researchers quickly evaluate and study any battery cathode materials.

The workflow combines scanning electron microscopy (SEM) [Thermo Scientific AXIA Chemisem] and X-ray photoelectron spectroscopy (XPS) [Thermo Scientific Nexsa G2 & ESCALAB QXi] into a correlated process, enabling the same regions of interest to be investigated; providing both high-resolution imaging and surface analysis from the same positions, even when collected using separate tools.

While SEM can easily visualize 2D materials, these layers are typically too thin to be easily characterized with the analytics commonly present on the microscope such as energy dispersive X-ray (EDX) analysis. XPS, meanwhile, cannot easily resolve surface structures at the required resolution, but can clearly detect what material is present at the surface, and quantify any chemical changes that might have occurred. XPS instrumentation typically also incorporates additional analytical techniques, such as an in-situ Raman spectrometer that is coincident with the XPS analysis position, which can be used to obtain further information.

**CM-ThP-7 Optimizing Combinatorial Materials Discovery with Active Learning: A Case Study in the Quaternary System Ni-Pd-Pt-Ru for the Oxygen Evolution Reaction, Felix Thelen [felix.thelen@ruhr-uni-bochum.de]**, *Rico Zehl, Ridha Zerdoumi, Jan Lukas Bürgel, Wolfgang Schuhmann, Alfred Ludwig*, Ruhr University Bochum, Germany

Steering through the multidimensional search space of compositionally complex solid solutions towards desired materials properties makes the use of efficient research methods mandatory [1]. Combinatorial materials science offers rapid fabrication, e.g. magnetron sputtering, and high-throughput characterization methods. Still, improvements to materials exploration cycles are necessary, since combinatorial methods are also suffering from the curse of dimensionality. At the scale of multinary systems, planning follow-up experiments based on already acquired data is economically feasible only through the use of machine learning techniques [2].

In this study, we comprehensively explored the quaternary composition space of Ni-Pd-Pt-Ru for electrocatalytic applications with a streamlined discovery workflow. Enabling a fast synthesis, the fabrication of the materials libraries was performed by magnetron co-sputtering, and all libraries were subsequently characterized by energy-dispersive X-ray spectroscopy and X-ray diffraction. Guiding through the composition space, an active learning algorithm was used in an optimization cycle, which balances exploration and exploitation through the expected improvement acquisition function. The libraries were characterized electrochemically by an automated electrochemical scanning droplet cell setup [3] for the oxygen evolution reaction.

Six materials libraries were enough to find the global activity optimum in the system. The findings of six additional libraries are used to validate the activity trend. Our approach illustrates the potential of ML-driven optimization frameworks in accelerating the identification of promising multinary materials and underscores the value of integrating ML with high-

throughput synthesis and characterization techniques in modern materials science.

References:

- [1] Banko, L., Krysiak, O. A., Pedersen, J. K., Xiao, B., Savan, A., Löffler, T., Baha, S., Rossmesl, J., Schuhmann, W. and Ludwig, A. (2022) 'Unravelling composition-activity-stability trends in high entropy alloy electrocatalysts by using a data-guided combinatorial synthesis strategy and computational modelling', *Advanced Energy Materials*, vol. 12, no. 8.
- [2] Ludwig, A. (2019) 'Discovery of new materials using combinatorial synthesis and high-throughput characterization of thin-film materials libraries combined with computational methods', *npj Computational Materials*, vol. 5, no. 1.
- [3] Sliozberg, K., Schäfer, D., Erichsen, T., Meyer, R., Khare, C., Ludwig, A. and Schuhmann, W. (2015), 'High-throughput screening of thin-film semiconductor material libraries I: system development and case study for Ti-W-O.' *ChemSusChem*, vol. 8, no. 7.

**CM-ThP-8 High-Throughput Aging Studies of Vapor-Deposited Perovskite Thin-Films Using Precise Automated Characterization and Machine Learning-Assisted Analysis, Alexander Wiczorek, Sebastian Siol [sebastian.siol@empa.ch]**, Empa, Swiss Federal Laboratories for Materials Science and Technology, Switzerland

High-throughput experimentation (HTE) is increasingly being employed to accelerate metal halide perovskite (MHP) semiconductor thin-film development.<sup>[1]</sup> As of now, most approaches focus on solution-based deposition methods. To address the need for scalable and fabrication approaches, vapor-based deposition methods are gaining popularity.<sup>[2]</sup> However, durability concerns remain a major obstacle for large-scale deployment.<sup>[3]</sup> This motivates high-throughput stability studies of vapor-deposited MHP thin films. Combinatorial materials science is perfectly suited to address this challenge, specifically for time-consuming degradation studies where parallelization of experiments is key.<sup>[4]</sup> Using vapor deposition techniques, large parameter spaces can be covered on single substrates, whereas automated characterization and data analysis facilitate rapid properties screening.<sup>[5]</sup>

In this work, we present a comprehensive workflow for the aging of thin-film MHPs which includes structural, optical and chemical characterization.<sup>[6]</sup> To mitigate ambient degradation during characterization or transfers, we employ a complete inert-gas workflow. Furthermore, we perform a rapid *in-situ* screening of the transmission and reflectance under accelerated aging conditions. The samples are exposed to 85 °C and 1 kW m<sup>-2</sup> white light bias, probing intrinsic material degradation in an accelerated fashion. With a temperature variation of ±1 °C and light intensity variation of <2% across combinatorial libraries, meaningful combinatorial stability screening is enabled. Automated characterizations of the structural properties yield deep insights into the aging process, extending and validating insights from changes in the optical transmission. We further demonstrate how these data sets can be used to better understand changes in the optical properties for highly scattering thin-films using machine learning assisted analysis. Furthermore, the workflow can be combined with high-throughput surface characterization techniques that our group previously demonstrated as a novel tool for accelerated materials discovery and optimization.

As a case study, we investigate the effect of residual precursors on the stability of two-step deposited MHP thin films grown on vapor-deposited templates. This workflow further allows to screen compositional spaces of libraries grown from completely vapor-based deposition methods.

References:

- [1] Ahmadi et al. *Joule* **2021**, 5, 2797.
- [2] Guesnay et al. *ACS Photonics* **2023**, 10, 3087.
- [3] Siegler et al. *ACS Energy Lett.* **2022**, 7, 1728.
- [4] Sun et al. *Matter* **2021**, 4, 1305.
- [5] Gregoire et al. *Nat. Synth.* **2023**, 2, 493.
- [6] Wiczorek et al. *J. Mater. Chem. A* **2024**, 12, 7025.

**CM-ThP-9 Advanced Depth Profiling of Thin Films Using Angle-Resolved XPS/HAXPES, Jennifer Mann [jmann@phi.com]**, *Norb Biderman, Kateryna Artyushkova*, Physical Electronics, USA

X-ray photoelectron spectroscopy (XPS) is a powerful technique for non-destructive analysis of the chemical composition of thin layers and interfaces. Angle-resolved XPS (AR-XPS) has traditionally been used with Al K $\alpha$  (1486.6 eV) X-ray beams to determine non-destructively determine layer



# Thursday Afternoon, May 15, 2025

thicknesses up to 5-10 nm below the surface. Recent advancements in AR-XPS, including the integration of Cr K $\alpha$  (5414.8 eV) hard X-ray photoelectron spectroscopy (HAXPES), have extended capability to 15-30 nm below the surface.

PHI's *StrataPHI* analysis software has been developed to reconstruct quantitative, non-destructive depth profiles from angle-dependent and single-angle photoelectron spectra. The latest version of *StrataPHI* combines Al K $\alpha$  and Cr K $\alpha$  XPS and HAXPES data within a single depth profile, enhancing the analytical information extracted from various depths.

Modern microelectronics devices contain thin films with different properties and purposes. Chips are often comprised of conducting films that form the interconnect layers as well as dielectric films that provide electrical insulation. In multilayer stacks, buried interfaces and subsurface layers are often beyond the analysis depth of traditional XPS. The information depth enabled by combined XPS and Cr K $\alpha$  HAXPES is particularly useful for analyzing these types of materials.

This poster will discuss the principles behind AR-XPS and HAXPES, the new features of *StrataPHI*, and show some recent applications of the combination of these advanced methods to non-destructively probe thin films relevant to microelectronics.

**CM-ThP-10 Numerical Ellipsometry: Artificial Intelligence Based Real-Time, in Situ Process Control for Virtual Substrates Including Multiple Unknown Layers, Frank Urban [fk\_urban@yahoo.com], 7980 SW 144th St, USA; David Barton, Florida International University, USA**

Ellipsometry can be used to determine the optical properties and thickness of a thin film depositing on a known substrate based on light reflecting from the surface. This approach has the advantage of being able to be used in situ during the growth of the film with commercially available equipment to pass the light in and out of the deposition chamber. Nevertheless, a serious challenge in practice is that the material structure underlying the growing film commonly is composed of multiple layers. In these cases, very accurate knowledge of all of the underlying structure is required in order to obtain accurate results. Another challenge is that the computation takes significant time using pre-existing iterative solution methods such as Levenberg Marquardt. The work here demonstrates the use of an Artificial Intelligence (AI) method suitable for real-time growth in which the underlying structure is complicated. This method is based upon previous development using five separate reflections simultaneously to solve for the underlying reflection coefficients at the same time the film parameters are being determined. The method is sufficiently fast that multiple groups of five measurements can be analyzed during the growth to confirm results and to examine the vertical homogeneity of the film being deposited. Examples will be given using a single angle of incidence. Thin absorbing films (up to 45 nm) will be given using a multilayer perceptron configuration consisting of 10 input neurons and 10 output neurons with two hidden layers of 80 neurons each. Solutions are performed at each wavelength independently and do not rely on fitting functions. The design, training and use of a number of neural networks will be presented.

**CM-ThP-11 A Computational DFT Investigation of  $\gamma$ -CuI as an HTM for Perovskite Solar Cells, Salma Naimi [eng.salma.naimi@gmail.com], Green Energy Park (IRESEN/UM6P), Benguerir, Morocco/ Mohammed V university, Rabat, Morocco**

Perovskite solar cells (PSCs) are recognized for their high efficiency and potential for low-cost production. However, the use of organic Hole Transporting Materials (HTMs) in these cells poses challenges due to their high cost and tendency to degrade the perovskite layer over time, threatening the commercial viability of PSCs.

In this study, we employed first-principles calculations based on Density Functional Theory (DFT), utilizing both the Generalized Gradient Approximation (GGA) and GGA + Hubbard correction, to evaluate the potential of  $\gamma$ -CuI as a cost-effective HTM. Initial investigations involved a comprehensive geometry optimization to ensure structural stability, followed by an analysis of elastic and mechanical properties, which confirmed the material's compatibility with flexible PSCs [1].

The electronic and optical properties of  $\gamma$ -CuI were explored, revealing a low extinction coefficient and high refractive index across the infrared and visible spectra. Notably,  $\gamma$ -CuI demonstrated minimal reflectivity and absorption in key spectral regions, highlighting its potential to reduce optical losses in PSCs [1].

These findings position  $\gamma$ -CuI as a promising and economically viable HTM, offering significant advantages for the next generation of perovskite solar cells.

Reference [1]

S. Naimi, S. Laaloui, E. Mehdi Salmani, K. Belrhiti Alaoui, and H. Ez-Zahraoui, "In-depth analysis of  $\gamma$ -CuI as an HTM for perovskite solar cells: A comprehensive DFT study of structural, elastic, mechanical, charge density, and optoelectronic properties," *Solar Energy*, vol. 276, p. 112680, Jul. 2024, doi: 10.1016/j.solener.2024.112680.

**CM-ThP-12 Role of Gold-Doped ZnO Nanoparticles to Degrade Dr-31 Dye as a Photocatalyst, Manik Rakhra [rakhramanik786@gmail.com], Lovely Professional University, Jalandhar, India**

Water contamination is a significant issue in the modern day, caused by the textile dying business, and it has a detrimental impact on living organisms. We report on the manufacture of gold-doped ZnO nanospheres using a simple heat treatment approach, and the use of ZnO nanoparticles as photocatalysts for the degradation of methyl orange dye. To increase this degrading activity, Au was utilized as a modifier, and their temperature quenching effect was noticed. One of the most efficient electron grabbers in the conduction band is an Au ion. The structural, morphological, optical, electrical, and photocatalytic characteristics of the synthesized nanocatalysts were determined. These nanoparticles have a grain size of 45-75 nm. Photocatalytic activity was investigated using UV-Vis spectra, and a significant absorption peak about 482 nm was discovered. With increasing frequency, the dielectric constant and frequency of the produced nanoparticles drop. The kinetic analysis yields a rate constant of 0.0165 min<sup>-1</sup> for nano-sphere-like particles. At a concentration of 1% Au, the produced nanoparticles degrade the dye completely in 150 minutes when exposed to UV light.

**CM-ThP-13 The Application of Environmentally Friendly and Sustainable Corrosion Inhibitor for Carbon Steel in Petroleum Fields, Omotayo Sanni [tayo.sanni@yahoo.com], University of Pretoria, South Africa; Ren Jianwei, university of pretoria, South Africa**

In industrial sectors that deal with metallic materials, corrosion is a major problem. Steel corrosion causes significant economic losses in the oil and gas industry when oil wells are acidized. One common solution to this problem is the use of organic molecules as corrosion inhibitors. Therefore, the goal of this study was to determine the feasibility of using inexpensive, environmentally friendly, and organic compound from agricultural waste to reduce the rate of corrosion of carbon steel in an acidic environment that contains 1 M HCl. This research aims to investigate the potential use of agricultural waste as an inhibitory agent that can be reused for a variety of applications. Additionally, the extraction process in this work is done using water extraction. The compound was tested as a mitigator for the destruction of carbon steel in a 1 M HCl solution, and its composition was verified using a variety of spectroscopic techniques. Scanning electron microscopy-energy dispersive X-ray analysis (SEM-EDX) was used to investigate the surface of some corroded carbon steel samples in addition to electrochemical potentiodynamic polarization, impedance spectroscopy, and gravimetry studies. The data indicated that the addition of the waste compound inhibits the destruction of carbon steel by lowering the corrosion current density ( $i_{corr}$ ) and the double-layer capacitance ( $C_{dl}$ ). Tafel polarization data confirmed that the studied compound acted as a mixed inhibitor. The values of the cathodic Tafel slope ( $b_c$ ), are found to be near to each other demonstrating that the adsorbed chemicals did not modify the mechanism of hydrogen evolution. The spontaneity of the adsorption process is explained by the negative values of  $\Delta G^{\circ}_{ads}$ .

## Surface Engineering - Applied Research and Industrial Applications

### Room Golden State Ballroom - Session IA-ThP

## Surface Engineering – Applied Research and Industrial Applications Poster Session

**IA-ThP-1 Metallurgical Coating by Laser Metal Deposition of H13 Steel Powder for Die Repairs, Sheila Carvalho [sheila.m.carvalho@ufes.br], Federal University of Espirito Santo, Brazil; Vagner Braga, Bruning Tecnolometal Co., Brazil; Rafael Siqueira, Kahl Ziinyk, Technological Institute of Aeronautics, Brazil; Johan Nuñez, University of Sao Paulo, Colombia; Reginaldo Coelho, University of Sao Paulo, Brazil; Milton Lima, Institute for Advanced Studies, Brazil**

The H13 tool steel is a typical hot-work material that exhibits superior thermal resistance, excellent hardness, and exceptional resistance to high-temperature fatigue and wear. This steel is also characterized by its high

resistance to softening at temperatures below 540 °C and is extensively used to produce hot forging dies, hot extrusion channels, and high-pressure dies for low-melting-point metals such as aluminum and magnesium. Components made of H13 steel wear out over time and must be replaced, generating high costs and considerable environmental impact. One way to mitigate these problems is through repair using metallurgical coatings, which involve machining the worn area of the tool and depositing one or more layers of H13 steel using thermal means, notably with a laser beam. In this study, the microstructural and mechanical properties of H13 powder deposited via laser metal deposition (LMD) on H13 hot-work tool steel substrates were examined before and after heat treatment. Scanning electron microscopy (SEM), energy-dispersive X-ray spectroscopy (EDS), and electron backscatter diffraction (EBSD) were used to analyze the grain distribution, layer development, and carbide incidence. The mechanical properties were evaluated by Vickers hardness indentation tests. An  $\alpha$ -ferrite matrix consisting of  $\alpha'$ -martensite was identified along with a crack-free interface containing Mo- and Cr-rich precipitates between the clad H13 steel and substrate. The EBSD results showed a highly consistent combination between the deposition and substrate, along with a structure consisting of columnar and equiaxial grains resulting from the directional solidification process. Wear resistance tests demonstrated that the H13-deposited region was in a better condition than the substrate because of the presence of martensite and carbides in the matrix, and the average wear decreased from  $3.8 \times 10^{-4} \text{ mm}^3/\text{Nm}$  to  $0.5 \times 10^{-4} \text{ mm}^3/\text{Nm}$  from the substrate to the laser cladding. The measured coefficient of friction for the die-repaired H13 rods did not undergo significant changes after laser cladding, with a COF of  $\sim 0.8$ . The average hardness levels of the substrate and deposition regions were determined to be 213 HV ( $\alpha$ -Fe) and 671 HV ( $\alpha'$ ), respectively. The smooth transition in terms of hardness between the regions also indicates a tendency for lower stress concentrations. The results indicate that metallurgically coated H13 steel could be used to repair hot forming tools that extend the lifetime and decrease the discard of high-value components.

**IA-ThP-2 Effects of Cathodic Current Density on the Growth Mechanism and Corrosion Resistance of Micro-Arc Oxidation Coatings on AZ31 Magnesium Alloy, Shih-Yen Huang [f08525129@g.ntu.edu.tw], Chi-Hua Chiu, Yu-Ren Chu, Yueh-Lien Lee, National Taiwan University, Taiwan**

Despite decades of development, many growth mechanisms and properties of the micro-arc oxidation (MAO) process remain unclear, limiting further advancements in this surface treatment. Numerous studies have identified trends in MAO process parameters under specific conditions; however, altering these conditions often leads to varied results, highlighting the need for in-depth mechanistic studies. In this study, we address aspects of the formation mechanism of MAO under cathodic bias control. Preliminary results show that, while maintaining the electric current at a constant value, varying the cathodic current density significantly affects the microstructure and anti-corrosion properties of MAO coatings on AZ31B Mg alloy. Specifically, when the cathodic current density exceeds the anodic current density, a distinct cross-sectional microstructure develops, leading to a significant decrease in corrosion resistance. These findings demonstrate that the instantaneous cathodic current density critically influences the growth path of MAO coatings, altering their microstructure and, ultimately, their corrosion resistance.

## Protective and High-temperature Coatings Room Golden State Ballroom - Session MA-ThP

### Protective and High-temperature Coatings Poster Session

**MA-ThP-1 High Temperature Fracture Characteristics of Si Containing Ternary and Quaternary Transition Metal Diborides, Anna Hirle [anna.hirle@tuwien.ac.at], Ahmed Bahr, Rainer Hahn, Tomasz Wojcik, Christian Doppler Laboratory for Surface Engineering of High-performance Components, TU Wien, Austria; Szilard Kolozsvári, Peter Polcik, Plansee Composite Materials GmbH, Germany; Jürgen Ramm, Carmen Jerg, Oerlikon Surface Solutions AG, Liechtenstein; Helmut Riedl, Christian Doppler Laboratory for Surface Engineering of High-performance Components, TU Wien, Austria**

To enhance the restricted oxidation resistance of transition metal diboride (TMB) ceramics, alloying with Si and disilicide phases is an effective method, resulting in the formation of highly dense and protective  $\text{SiO}_2$  scales. This phenomenon has been well documented in the context of bulk ceramics [1, 2], and recent studies have also corroborated its occurrence in thin-film TMBs, including  $\text{CrB}_2$ ,  $\text{HfB}_2$ , and  $\text{TiB}_2$  [3, 4]. The incorporation of Si,

$\text{TaSi}_2$  or  $\text{MoSi}_2$  into  $\text{TiB}_2$  results in a significant reduction in oxidation kinetics, while exhibiting only minor effects on the mechanical properties. In the case of quaternary  $\text{TiB}_2$ -based coatings, hardness values of 36 GPa ( $\text{TaSi}_2$ ) and 27 GPa ( $\text{MoSi}_2$ ) have been achieved, in comparison to approximately 38 GPa for the binary system. All of the aforementioned coatings exhibited  $\alpha$ - $\text{AlB}_2$  crystal structure, with a preferred (0001) orientation being a key factor in achieving the highest hardness. Nevertheless, the fracture characteristics of these Si-alloyed TMBs remain largely unexplored.

The objective of the present study is to elucidate the fracture characteristics, particularly  $K_{IC}$ , of these Si-containing TMBs at elevated temperatures up to 850 °C through the application of in-situ micromechanical testing techniques. Accordingly, a series of Ti-TM-Si- $\text{B}_{2+z}$  coatings was deposited via non-reactive DC magnetron sputtering using a variety of composite targets, including  $\text{TiB}_2$ ,  $\text{TiB}_2/\text{TiSi}_2$  (90/10 & 80/20 mol%),  $\text{TiB}_2/\text{TaSi}_2$  (90/10 & 80/20 mol%), and  $\text{TiB}_2/\text{MoSi}_2$  (85/15 & 80/20 mol%). To gain a deeper understanding, additional detailed structural investigations were conducted using X-ray diffraction (XRD), scanning electron microscopy (SEM), transmission electron microscopy (TEM), and elastic recoil detection analysis (ERDA).

In comparison to the binary  $\text{TiB}_{2+z}$  and the quaternary Ti-Ta-Si- $\text{B}_{2+z}$ , the Si and  $\text{MoSi}_2$ -containing coatings exhibited a distinct onset of plastic deformation at approximately 600 °C. This phenomenon can be attributed to the precipitation of silicon-containing phases, which underlines the significance of conducting material testing at temperatures relevant to their intended applications.

[1] GB. Raju, et al., J Am Ceram Soc. 2008;91(10):3320–3327.

[2] GB. Raju, et al., Scr Mater. 2009;61(1):104–107.

[3] T. Glechner, et al., Surf. Coat. Technol. 434 (2022) 128178.

[4] A. Bahr, et al., Materials Research Letters. 11 (2023) 733–741.

**MA-ThP-2 Influence of Si on the Oxidation Behavior of High Entropy Carbide Thin Films Based on (Hf, Ta, Ti, V, Zr)C, Muhammad Awais Altaf [muhammad.altaf@tuwien.ac.at], Alexander Kirnbauer, Balint Hajas, TU Wien, Institute of Materials Science and Technology, Austria; Szilard Kolozsvári, Plansee Composite Materials GmbH, Germany; Paul Mayrhofer, TU Wien, Institute of Materials Science and Technology, Austria**

In the present work, the influence of Si addition on the oxidation behavior of high-entropy carbide thin films based on the system (Hf, Ta, Ti, V, Zr)C is investigated. High-entropy carbides thin films were deposited on sapphire ( $\text{Al}_2\text{O}_3$ ) as well as low-alloy steel substrates using magnetron sputtering. Additionally, powdered free-standing coating materials were also produced. All the as-deposited thin films exhibit a single-phase face-centered cubic (FCC) structure (Fm-3m, space group number 225). During non-isothermal oxidation using DSC-TGA, onset-temperature shifted from 490 °C to 502 °C while mass gain was reduced from 11% to 8.88 % with Si addition. Furthermore, the oxide-peak intensities in the obtained XRD patterns are decreased indicating a smaller fraction of formed oxide phases. All samples were fully oxidized during isothermal oxidation but the samples alloyed with Si show denser and thinner oxide scales compared to the samples without Si.

**MA-ThP-3 Spinodal Decomposition and Nano-precipitate Formation in Ag-modified High-Entropy Alloys, Salah-eddine benrazzouq [salah-eddine.benrazzouq@univ-lorraine.fr], Abdelkrim Redjaimia, Jaafar Ghanbaja, Sylvie Migot, Valentin A. Milichko, Jean-François Pierson, Institut Jean Lamour - Université de Lorraine, France**

Phase separation in multi-component alloys presents both challenges and opportunities for material design. While traditionally viewed as a limitation, controlled phase separation could enable unique microstructural features and enhanced properties. High-entropy alloys (HEAs) have garnered significant attention across various research fields owing to their exceptional properties. This study investigates the distinctive behavior of silver addition to the CrMnFeCoNi Cantor alloy, where silver's higher mixing enthalpy creates an interesting case of spinodal decomposition and nano-precipitate formation.

Using DC magnetron co-sputtering, we synthesized CrMnFeCoNiAg thin films with systematically varied silver content. X-ray diffraction (XRD) patterns reveal distinct non-mixing behavior with the emergence of pronounced peaks corresponding to both silver and Cantor alloy phases. Cross-section bright-field TEM micrograph and SAED patterns revealed a dense structure with Ag precipitates dispersed throughout the 900-nm-thick film. HRTEM micrographs showed a nanoprecipitate morphology with fine-scale linear precipitates, while STEM-HAADF imaging highlighted the

internal structure, revealing characteristic modulated patterns with striations parallel to the basal plane, indicative of spinodal decomposition with cuboidal particles and tweed-like contrast patterns.

The controlled formation of these nano-precipitates and their unique distribution pattern suggests potential for mechanical property enhancement through precipitation strengthening mechanisms. Our findings demonstrate how controlled phase separation can be used to engineer microstructure in HEA thin films. This understanding provides new strategies for designing multi-functional materials through deliberate exploitation of immiscibility effects, advancing our knowledge of phase evolution in complex alloy systems and offering pathways for property optimization in advanced coating applications.

**MA-ThP-4 Influence of Si Content on Cracking Behavior of CrAlSiN Coatings**, Kirsten Bobzin, Christian Kalscheuer, Max Philip Möbius [moebius@iot.rwth-aachen.de], Jessica Borowy, Surface Engineering Institute - RWTH Aachen University, Germany

The increasing demands for workpiece quality and cost-effectiveness in machining processes necessitate a comprehensive consideration of all relevant factors, including cutting parameters, materials, tool coatings, and geometry. Physical Vapor Deposition (PVD) manufactured CrAlSiN nanocomposite coatings, composed of CrAlN grains in a SiN<sub>x</sub> matrix, represent a promising solution for improved tool life of milling tools. The elastic-plastic properties of the coating and the deformation behavior of the material composite thereby can be deliberately influenced by varying the silicon content.

CrAlSiN coatings with silicon contents of  $x_{Si} = 10, 15, 20,$  and  $25$  at.-% in the metal portion were fabricated on cemented carbide WC-Co substrates. The indentation hardness  $H_{IT}$  and indentation modulus  $E_{IT}$  of the coatings were measured through nanoindentation (NI) with a force of  $F_{NI} = 10$  mN, using a Berkovich indenter. Additionally, crack resistance was evaluated using quasi-static high load (HL) nanoindentation tests under forces ranging from  $F_{HL} = 750$  to  $1,750$  mN, with increments of  $\Delta F_{HL} = 250$  mN. A conical diamond indenter was used for the high load nanoindentation tests. The resulting indents were subsequently analyzed using scanning electron microscopy (SEM). The findings reveal that the indentation hardness  $H_{IT}$  remains unchanged at  $H_{IT} = (25.48 \pm 1.59)$  GPa, while the indentation modulus increases with higher silicon content, ranging from  $E_{IT} = (222.64 \pm 10.45)$  GPa for  $x_{Si} = 10$  at.-% up to  $E_{IT} = (239.89 \pm 7.78)$  GPa for  $x_{Si} = 20$  at.-%. After high load nanoindentation all coatings exhibit no cracks at  $F_{HL} = 750$  mN. With  $F_{HL} \geq 1,000$  mN on the other hand cracks can be observed in all coatings. Nevertheless, with rising silicon content, the maximum indentation depth  $h_{max}$  decreases, while the residual indentation depth  $h_0$  remains constant. Furthermore, the proportion of plastic work shows a slight reduction as silicon content  $x_{Si}$  increases. These results indicate that the resistance against plastic deformation of the CrAlSiN coating increases with higher silicon content.

Coatings with high silicon content demonstrate promising resistance against plastic deformation at room temperature, highlighting their potential for further investigation. This initial test qualifies these coatings for additional studies under high-temperature conditions, aiming to enhance their applicability in machining processes. The insights gained from this research could lead to the development of more durable and efficient cutting tools, ultimately improving productivity in industrial applications.

**MA-ThP-5 Relationship between Optical and Electrical Properties and the Microstructure of High Entropy Nitride (TiVZrNbTa)<sub>N<sub>x</sub></sub> Thin Films**, Miguel Piñeiro [miguel.pineiro-sales@univ-lorraine.fr], Institut Jean Lamour - Université de Lorraine, France, Peru; Salah-Eddine Benrazzouq, Institut Jean Lamour - Université de Lorraine, France, Morocco; Alexandre Bouché, Valentin Milichko, David Pilloud, Thomas Easwarakanthan, Institut Jean Lamour - Université de Lorraine, France; Frank Mücklich, Saarland University, Germany; Jean-François Pierson, Institut Jean Lamour - Université de Lorraine, France

In this study, high entropy nitride TiVZrNbTa thin films were prepared by DC reactive magnetron sputtering on silicon substrates at room temperature. The impact of varying nitrogen flow rates on the structural, microstructural, optical and electrical properties were investigated. X-ray diffraction technique revealed that all the deposited films exhibited a polycrystalline structure with fcc phase. However, the pure metallic samples displayed an amorphous structure [1]. Optical properties analysis showed a decrement of the reflectance compared with free-nitrogen sample in the infrared region, as determined by UV-VIS spectroscopy [2]. Hall-effect measurements indicate that the electrical resistivity for all samples

remained within the range between 100 and 300  $\mu\Omega$  cm. Interestingly, samples deposited with applied substrate bias power during the deposition process did not show a significant change in resistivity. This suggests that substrate biasing has minimal effect on the electrical transport properties of the latter films. On the other hand, applying adjustable substrate bias led to a blueshift in the epsilon-near-zero (ENZ) wavelength. Furthermore, X-ray photoelectron spectroscopy (XPS) shows the effect of the nitrogen flow rate on the residual stress [3] and plasmon frequency. The impact of varying nitrogen flow rates on the microstructural properties were further investigated and explained.

## References

- [1] Cemin, F., de Mello, S. R., Figueroa, C. A., & Alvarez, F. Surface and Coatings Technology, 2021, 421, 127357.
- [2] Von Fieandt, K., Pilloud, D., Fritze, S., Osinger, B., Pierson, J. F., & Lewin, E. Vacuum, 2021, 193, 110517.
- [3] Pogrebnyak, A. D., Yakushchenko, I. V., Bagdasaryan, A. A., Bondar, O. V., Krause-Rehberg, R., Abadias, G., ... & Sobol, O. V. Materials Chemistry and Physics, 2014, 147(3), 1079-1091.

## Functional Thin Films and Surfaces Room Golden State Ballroom - Session MB-ThP Functional Thin Films and Surfaces Poster Session

**MB-ThP-1 Two-Dimensional Vacancy Confinement in Anatase TiO<sub>2</sub> Thin Films for Enhanced Photocatalytic Activities**, Junwoo Son [junuson@snu.ac.kr], Seoul National University, Republic of Korea  
Light-driven energy conversion devices call for the atomic-level manipulation of defects associated with electronic states in solids. However, previous approaches to producing oxygen vacancy ( $V_O$ ) as a source of sub-bandgap energy levels have hampered the precise control of distribution and concentration in  $V_O$ .

Here, a new strategy to spatially confine  $V_O$  at the homo-interfaces is presented by exploiting the sequential growth of anatase TiO<sub>2</sub> under dissimilar thermodynamic conditions. Remarkably, metallic behavior with high carrier density and electron mobility is observed after sequential growth of the TiO<sub>2</sub> films under low pressure and temperature (L-TiO<sub>2</sub>) on top of high-quality anatase TiO<sub>2</sub> epitaxial films (H-TiO<sub>2</sub>), despite the insulating properties of L-TiO<sub>2</sub> and H-TiO<sub>2</sub> single layers. Multiple characterizations elucidate that the  $V_O$  layer is geometrically confined within 4 unit cells at the interface, along with low-temperature crystallization of upper L-TiO<sub>2</sub> films; this two-dimensional  $V_{O\text{layer}}$  is responsible for the formation of in-gap state, promoting photocarrier lifetime (~ 300 %) and light absorption. These results suggest a synthetic strategy to locally confine functional defects and emphasize how sub-bandgap energy levels in the confined imperfections influence the kinetics of light-driven catalytic reactions.

This work is performed by the collaboration with Mr. Minwook Yoon, Dr. Yunkyu Park, Ms. Hyeji Sim, Ms. Hee Ryeung Kwon, Dr. Yujeong Lee, Prof. Ho Won Jang, Prof. Si-Young Choi.

**MB-ThP-2 Fabrication of Metal-Based Superhydrophilic and Underwater Superoleophobic Surfaces by Laser Ablation and Magnetron Sputtering**, Adham Al-Akhali [alakhali.adham@gmail.com], Guizhou University, China  
Fabricating underwater superoleophobic surfaces is an advanced technique for controlling undesirable oil and wax adhesion on engineering structures and household appliances. This article presented a facile method based on the combination of laser ablation of stainless steel substrates followed by magnetron sputtering of a metallic tungsten target to fabricate superhydrophilic and underwater superoleophobic surfaces. The results showed that the laser-ablated stainless steel substrate without coatings exhibited hydrophilicity and underwater oleophobicity. However, its transition to superhydrophilicity and underwater superoleophobicity with a 0° water contact angle and higher than 156° underwater oil contact angles occurred after the deposition of a thin tungsten film followed by annealing at 300 °C. In addition, the prepared surface maintained its wetting behavior for more than 4 weeks, even in corrosive aqueous HCl and NaOH solutions. According to the data from SEM and XPS, this distinguished wetting behavior resulted from the presence of the regular microscale texture patterns, abundant hydroxyl content, and low carbon content on the tungsten layer after annealing at 300 °C. Thus, laser ablation combined with magnetron sputtering of tungsten demonstrated effective results in

fabricating superhydrophilic and underwater superoleophobic surfaces that are independent of the initial wetting of the substrates.

**MB-ThP-3 Synthesis and Characterization of Zn Doped CsPbI<sub>3</sub> Perovskite Quantum Dots, Ya-Fen Wu [yfwu@mail.mcut.edu.tw], Hao-Yu Jhai, Ming Chi University of Technology, Taiwan**

The increasing focus on sustainable energy has driven advancements in renewable technologies, with quantum dot solar cells gaining particular interest in photovoltaics for their ability to efficiently convert sunlight into electricity. Early cells used II-VI semiconductors with high crystallinity and luminescence but were limited by toxicity and complex synthesis. In contrast, all-inorganic perovskite quantum dots such as CsPbX<sub>3</sub> (X=Cl, Br, I) have gained prominence due to their excellent photoelectric properties, low cost, and easy to be manufactured. Moreover, compared to organic-inorganic perovskites, all-inorganic perovskites are more stable under high temperature and with extremely high quantum yield. Consequently, they are gradually becoming mainstream in research and development.

Metal ion doping is widely recognized as one of the most effective strategies to enhance the efficiency of perovskite light-emitting devices. In this study, CsPbI<sub>3</sub> all-inorganic perovskite QD thin films were prepared with various concentrations of zinc acetate (0%, 3%, 5%, and 7.5%) added as dopants. Temperature-dependent photoluminescence was carried out from 20 K to 300 K. To investigate the thermal behaviors of peak energy, full width at half maximum, and intensity of the PL spectra measured from our samples, the carrier emission mechanism, electron-phonon scattering, electron-phonon interaction and thermal expansion effect on the band-gap are discussed. As the increasing of the Zn doping concentration from 0% to 7.5%, the PL peaks were shifted from 1.74 eV to 1.73 eV at 20 K. In addition, a noticeable blueshift of emission peaks was observed with increasing temperature for all the samples, which attributed to the effects of lattice thermal expansion and electron-phonon interactions. The PL intensity increases as the Zn doping concentration increases from 0% to 5% and then decreases as the doping concentration is 7.5%. It implies that Zn doping lowers the defect density in QDs by reducing lattice distortion and enhancing crystal quality; but under higher doping concentration, the dopants may not have enough time to move into the right positions of the structure, result in the degradation the thin film quality. Furthermore, the PL intensity decreases with increasing temperature for all the samples; however, the sample with 5% Zn doping concentration exhibited the highest intensity at 300 K. It reveals that the optical properties of CsPbI<sub>3</sub> QD thin films was improved by an appropriately increasing Zn doping.

**MB-ThP-4 Improved Photovoltaic Performance of Si-Based Hybrid Solar Cells via Mo<sub>2</sub>C Bridging in 2D MoS<sub>2</sub> nanosheets @ OD Carbon Colloid Dots, Ta-Cheng Wei [dvt8756713@gmail.com], Chia-Yun Chen, National Cheng Kung University (NCKU), Taiwan; Chih-Chiang Yang, National Yunlin University of Science and Technology, Taiwan**

Recent advances in silicon-based hybrid solar cells, distinguished by high photovoltaic efficiency, low production costs, and strong environmental resilience, position them as promising candidates for solar energy conversion. [1] Solution-processed few-layer MoS<sub>2</sub> sheets enhance solar capture, but improved charge separation is essential, and their moisture sensitivity limits stability by attracting electrons. [2] This study introduces MoS<sub>2</sub>/Mo<sub>2</sub>C/carbon colloid dots (CCDs) heterostructures within a PEDOT:PSS matrix, utilizing Mo<sub>2</sub>C electron-transport channels to facilitate the transfer of photoexcited electrons from MoS<sub>2</sub>. This configuration fosters positive trion formation via interactions with defect-bound excitons on CCD surfaces, reducing recombination rates and enhancing photovoltaic performance. [3, 4] To elucidate carrier transfer mechanisms in these heterostructures, MoS<sub>2</sub>@CCD heterojunctions with Mo<sub>2</sub>C bridging interfaces facilitate efficient electron transfer. Photoluminescence (PL) enhancement factors ( $\beta$ ) were used to characterize trion emissions across HT interfaces compared to intrinsic trion emissions in CCDs, by analyzing three distinct MoS<sub>2</sub>@CCD blends within a PEDOT:PSS matrix, grounded in fundamental transport phenomena. [5] This design achieves a 16.1% efficiency, 1.6 times higher than conventional hybrid solar cells, with outstanding long-term stability, advancing photophysical bound-carrier research in photovoltaics.

[1] T. C. Wei, S. H. Chen, C. Y. Chen, *Mater. Chem. Front.* **2020**, 4, 3302.

[2] G. H. Lee, X. Cui, Y. D. Kim, G. Arefe, X. Zhang, C. H. Lee, F. Ye, K. Watanabe, T. Taniguchi, P. Kim, *ACS Nano.* **2015**, 9, 7019.

[3] T. Kim, S. Fan, S. Lee, M.-K. Joo, Y. H. Lee, *Sci. Rep.* **2020**, 10, 13101.

[4] A. Behranginia, P. Yasaei, A. K. Majee, V. K. Sangwan, F. Long, C. J. Foss, T. Foroozan, S. Fuladi, M. R. Hantehzadeh, R.

Shahbazian-Yassar, *Small.* **2017**, 13, 1604301.

[5] L. Zhang, A. Sharma, Y. Zhu, Y. Zhang, B. Wang, M. Dong, H. T. Nguyen, Z. Wang, B. Wen, Y. Cao, *Adv. Mater.* **2018**, 30, 1803986.

**MB-ThP-5 Top-Emitting QLEDs with a Thin Stabilizing Layer to Prevent Ag Agglomeration, Jaehyung Park [parkja0404@kyonggi.ac.kr], Kangsuk Yun, Jaehwi Choi, Jiwan Kim, Kyonggi University, Republic of Korea**

Colloidal quantum dots (QDs) are semiconductor nanoparticles composed of a core, shell, and organic ligands. They have unique optical and electrical properties due to quantum confinement effects, which enable the bandgap to vary with particle size. This characteristic allows easy modification of emission wavelengths, producing various colors of light. QDs are compatible with solution process and notable for their narrow full-width at half-maximum for the high color purity. Due to these advantages, quantum dot light emitting diodes (QLEDs) that use QDs as light emitting layers are being recognized as a promising next-generation display technology. In the field of AR/VR devices, Organic Light Emitting Diode on Silicon (OLEDoS) has received significant attention recently. This technology uses silicon as a substrate and emits light from the top with micropatterned structure, thus research on top-emitting devices is essential. However, there is still limited research on QLEDs in this area.

In top-emitting quantum dot light emitting diodes (TQLEDs), a transparent metal such as Ag is commonly used as the top electrode due to its high transparency and electrical conductivity. However, the deposition of thin Ag layer to achieve high transparency leads to agglomeration, which prevents the formation of a uniform layer, and results decreased conductivity. In this study, we used 2,2',2''-(1,3,5-Benzinetriyl)-tris(1-phenyl-1-H-benzimidazole) (TPBi) as a stabilizing layer to suppress the agglomeration of Ag in TQLEDs. TPBi has high electron affinity, which makes it effective in interacting with Ag to inhibit agglomeration. Various thickness of TPBi was applied to investigate the change of Ag agglomeration. As a result, the transmittance of transparent top electrode was over 50%, and TQLEDs incorporating TPBi as a stabilizing layer successfully achieved a maximum luminance exceeding 100,000 cd/m<sup>2</sup>. Enhanced top electrode can provide another approach to improve the performance of top-emitting devices.

**MB-ThP-6 A Study of Chlorine Incorporation in Amorphous In-Ga-Zn-O Thin Film Transistors by Soaking in NaCl Solution, GIYOONG CHUNG [qu3xing29@gmail.com], Dae Woong Kim, Yong-Sang Kim, Sungkyunkwan University (SKKU), Republic of Korea**

We investigated the influence of chlorine incorporation on solution-processed amorphous indium-gallium-zinc oxide (a-IGZO) thin-film transistors (TFTs). During TFT fabrication, materials inevitably interact with unintended elements. Notably, chlorine is an essential component in various stages of TFT fabrication, including as a precursor for metal oxide deposition and as a dry etching gas, making exposure to chlorine nearly unavoidable. Therefore, understanding chlorine's role in affecting the electrical and material properties of TFT devices is essential.

In this study, we immersed a-IGZO films in NaCl solution to incorporate chlorine. X-ray photoelectron spectroscopy (XPS) analysis revealed that chlorine formed bonds with metals, increasing both metal-oxygen (M-O) bonds and oxygen vacancies (Vo). Additionally, we observed a degradation in IGZO's electrical performance, attributed to structural bonding changes due to chlorine incorporation. Our initial findings indicated that the electrical properties deteriorated as the NaCl soaking time increased. To verify whether these effects were solely due to water exposure, we also examined the electrical properties of a-IGZO films soaked in deionized water. Compared to the pristine device, the saturation mobility and subthreshold slope of a-IGZO TFTs soaked in water for 1 hour decreased from 0.17 to 0.07 cm<sup>2</sup>/Vs and increased from 0.79 to 1.11 V/decade, respectively. However, when soaked in NaCl solution, these values further degraded to 0.02 cm<sup>2</sup>/Vs and 2.08 V/decade, respectively, confirming that chlorine penetration, rather than water exposure alone, caused the observed degradation. This degradation was associated with an increase in carrier concentration, corresponding with a widening bandgap from 3.46 eV to 4.29 eV. However, XRD analysis showed that soaking in NaCl solution did not alter the film's crystallinity. Furthermore, we examined the impact of chlorine diffusion on IGZO films deposited via the sputtering process. These findings suggest that chlorine exposure during fabrication must be carefully controlled to achieve the desired electrical performance targets for a-IGZO TFTs.

**MB-ThP-7 Electrochemical Insights into All-Solid-State Symmetric Supercapacitors Based on Sputter-Grown  $WSe_2$ , Akshay Tomar [atomar@ic.iitr.ac.in], Somdatta Singh, Ananya Bansal, Prachi Gurawal, Ramesh Chandra, IIT Roorkee, India**

All-solid-state supercapacitors represent a promising advancement in energy storage technology, providing superior energy density, enhanced safety, and a compact design compared to conventional supercapacitors and batteries. Their potential as flexible, bendable, and wearable energy storage solutions have garnered significant interest. The capacitance and energy density of supercapacitors can be improved through the introduction of novel electrode materials or by utilizing electrolytes with high potential windows. In this study, we successfully fabricated a high-quality porous thin film of tungsten diselenide ( $WSe_2$ ) on a flexible graphite substrate using an environmentally friendly DC magnetron sputtering technique, without the need for additives or binders, under optimized conditions. The resulting thin film exhibited a nanoflake morphology with an increased surface area, which provided a greater number of active sites for ion adsorption and desorption, thereby enhancing both capacitance and energy density. The  $WSe_2$ @graphite composite demonstrated a remarkable specific capacitance of 310 F/g at a scan rate of 10 mV/s, with 95% capacitance retention after 5000 charge-discharge cycles in a three-electrode configuration. An all-solid-state flexible symmetric supercapacitor (FSS) device was subsequently constructed, utilizing  $WSe_2$  as both the cathode and anode, separated by a highly flexible 6M KOH/PVA solid-state gel electrolyte. This device achieved a high cell voltage of 1.4 V and an excellent specific capacitance of 38.932 F/g at a scan rate of 50 mV/s. Comprehensive electrochemical performance analyses, including charge-discharge measurements at varying current densities, revealed a specific capacitance of 17 F/g, an energy density of 4.62 mWh/g, and a power density of 3457 mW/g, along with outstanding electrochemical stability of 92% after 5000 cycles at a current density of 5 mA/g. The exceptional electrochemical performance, combined with the flexible characteristics of the  $WSe_2$ @graphite thin-film-based symmetric supercapacitor, positions this device as a promising candidate for the development of next-generation flexible, bendable, and wearable energy storage systems.

**MB-ThP-8 Highly efficient of QLEDs Using  $SnO_2$  Electron Transport Layers Deposited by RF Sputtering, Jaehwi Choi [jksix@kyonggi.ac.kr], Jaehyung Park, Kangsuk Yun, Jiwan Kim, Kyonggi University, Republic of Korea**

Colloidal quantum dots (QDs) are semiconductor nanoparticles with unique optical and electrical properties. By controlling particle size, QDs can exhibit various colors and provide excellent color reproducibility. Due to these advantages, quantum dot light-emitting diodes (QLEDs) using QDs as the emissive layer are studied actively. In QLEDs, the electron transport layer (ETL) is essential for electron transport and charge balance, and optimizing ETL can enhance device stability and efficiency. In general, ZnO nanoparticles (NPs) are commonly used as ETL for their high electron mobility and transmittance. However, ZnO NPs aggregate easily at room temperature, leading to reduce stability. Therefore,  $SnO_2$ , which offers high electron mobility, transmittance, and excellent stability, is gaining attention as an ETL material. Typically, the ETL is deposited via solution processes like spin coating, but this method has challenges such as difficulty in thickness control, poor crystallinity and uniformity of the thin films. In this study, we deposited  $SnO_2$  as the ETL using RF sputtering process for high reproducibility and excellent crystallinity. It is well known that crystallinity of inorganic materials are directly related to their electrical properties. To adjust the physical and chemical properties of  $SnO_2$  thin film, we controlled the substrate temperature and Ar/O<sub>2</sub> ratio during RF sputtering while fabricating inverted devices with the structure of ITO/ $SnO_2$ /QDs/CBP/MoO<sub>3</sub>/Al. As the substrate temperature increased, the crystallinity of sputtered  $SnO_2$  thin film improved, which led to the enhancement of electron mobility and improvement of electrical properties of devices. QLEDs employing the optimized  $SnO_2$  ETL exhibited more than 120,000 cd/m<sup>2</sup> and a current efficiency of 15 cd/A which showed comparative performance with QLEDs using soluble  $SnO_2$  NPs as an ETL. Additionally QLEDs with sputtered ETL showed better stability due to the uniform  $SnO_2$  layer, which is advantage for practical display mass production.

**MB-ThP-9 Optimizing  $Y_2O_3$  Coating for Improving Plasma Resistance in Dry Etching Process, Sunil KIM [sunil725.kim@semes.com], Sunghwan CHO, Ja Myung Gu, Seungpil Chung, Gil Heyun Choi, SEMES Co., Ltd., Republic of Korea**

Plasma-resistant  $Y_2O_3$  coating is essential for extending the durability and replacement cycles of semiconductor components that face intense etching conditions. Plasma etching typically involves both physical ion

bombardment and chemical reactions with surface. To counter these effects, recent advancements in  $Y_2O_3$  coating focus on enhancing etch resistance and film density through physical vapor deposition (PVD) methods. While several studies have aimed to further improve the plasma resistance of PVD  $Y_2O_3$  coatings by increasing hardness, our observations suggest that beyond a certain hardness threshold (>900 HV), the relationship between hardness and plasma resistance became weak. Consequently, this study focuses on the characteristics of residual surface stress as a primary factor influencing plasma resistance. The residual stress in the coating was measured using X-ray diffraction (XRD) equipment and calculated based on the peak shift observed with varying psi angles. Comparing residual stress and plasma resistance in PVD  $Y_2O_3$  coatings manufactured under identical conditions, we found that coatings with tensile surface stress exhibited approximately 25% better plasma etch resistance than those with compressive stress. Although both coatings displayed similar grain size and hardness, the superior plasma-resistant coating demonstrated a tensile surface stress of around 600 MPa, whereas the less resistant sample had a compressive stress of approximately 300 MPa. This enhanced resistance in tensile-stressed coatings can be attributed to channeling effects, where the increased atomic spacing prevents accelerated plasma ions from interacting directly with atoms, allowing them to pass through specific crystallographic directions without obstruction. This study aims to establish a better understanding of the correlation between surface residual stress and plasma etch resistance in PVD  $Y_2O_3$  coatings and to propose new criteria for evaluating such coatings, ultimately contributing to enhanced performance in etching equipment.

**MB-ThP-10 Electrical and Morphological Properties of Alloyed  $Al_2O_3$  Thin Films at High Temperatures, Norma Salvadores Farran [norma.salvadores@tuwien.ac.at], Florentine Scholz, Tomasz Wojcik, Christian Doppler Laboratory for Surface Engineering of high-performance Components, TU Wien, Austria; Carmen Jerg, Astrid Gies, Jürgen Ramm, Oerlikon Balzers, Oerlikon Surface Solutions AG, Liechtenstein; Szilard Kolozsvári, Peter Polcik, Plansee Composite Materials GmbH, Germany; Jürgen Fleig, Tobias Huber, Institute of Chemical Technologies and Analytics, TU Wien, Austria; Balint Hajas, Institute of Materials Science and Technology, TU Wien, Austria; Helmut Riedl, Christian Doppler Laboratory for Surface Engineering of high-performance Components, TU Wien, Austria**

Aluminium oxide ( $Al_2O_3$ ) is a well-known insulating material employed in a wide range of applications, both as structural component as well as in thin film form.  $Al_2O_3$  can be stabilized in several polymorphs, in addition to an amorphous modification. Especially the amorphous state of  $Al_2O_3$  exhibits interesting features, considering the absence of crystalline defects for diffusion of charge carriers paired with the difficulties in stabilizing crystalline  $Al_2O_3$  during physical vapor deposition (PVD). Furthermore, amorphous materials are free of pinholes, which is favourable for a number of applications. Consequently, it is crucial to investigate economically and sustainably viable deposition techniques to grow insulating  $Al_2O_3$  thin films.

Therefore, this study focuses on the effect of alloying elements such as silicon and yttrium-zirconium (YZr) on the thermal stability of amorphous  $Al_2O_3$  based thin film materials up to 1200°C. The amorphous  $Al_2O_3$  thin films have been synthesised via a reactive Modulate Pulse Power (MPP) sputtering processes. In all depositions, an in-house developed sputter system, equipped with a 3" Al target, was used in a mixed Ar/O<sub>2</sub> atmosphere. To this end, two types of targets were employed: an Al-Si target and Al-YZr target. The impact of the deposition parameters on the structure, morphology, and electrical resistivity at high temperatures was investigated using high-resolution characterization methods such as XRD, SEM, HR-TEM or in-situ set-ups for annealing treatments. The insulating behaviour of the coatings was analysed using in-situ impedance spectroscopy across a temperature range. Ti/Pt electrode pads were deposited on the thin films using a lithography process for the purpose of electrical characterization. In addition, the bonding type was investigated via XPS, which was also employed to determine the chemical composition across the thickness of the coating.

**MB-ThP-11 Analysis of Four-Point Bending Test for Nb, Ta, and V-Doped CrN Thin Films Deposited by Closed-Field Unbalanced Magnetron Sputtering, Banu YAYLALI, Gokhan Gulten, Mustafa YESILYURT, Yasar TOTIK, Atatürk University, Turkey; Justyna Kulczyk Malecka, Peter Kelly, Manchester Metropolitan University, U.K.; Ihsan EFEGLU [iefeoglu@atauni.edu.tr], Atatürk University, Turkey**

The increasing expectations and requirements for engineering materials are steadily compelling researchers to evolve and innovate further. Adding

transition metals to coating architectures is becoming increasingly attractive as it improves structural and mechanical properties. In this work, CrYN thin films incorporating transition metals Nb, Ta, and V were deposited on a 316L stainless steel substrate using Closed Field Unbalanced Magnetron Sputtering (CFUBMS) with a DC and pulsed-DC power supply. The microstructural properties of the thin films were analyzed using scanning electron microscopy (SEM), while X-ray diffraction (XRD) and X-ray photoelectron spectroscopy (XPS) provided a comprehensive understanding of the coating structure by providing information on crystallographic and surface chemical properties. Mechanical properties were evaluated using nanoindentation testing, which provided accurate measurements of hardness and elasticity, while scratch testing assessed critical load values. In addition, four-point bending tests were performed at room temperature to characterize the CrYN:Nb/Ta/V transition metal nitrides (TMNs), providing a more comprehensive analysis of the mechanical behavior (flexural strength and elastic modulus) and adhesion properties of the coating. The mechanisms of coating damage (crack formation and density, spalling, flaking, and separated coating particles) were analyzed as a result of four-point bending tests. The Taguchi approach was employed to investigate how deposition parameters—such as target current, duty cycle, and pulse frequency—affect elastic modulus and bending strength. Superior structural (homogeneous and dense film) and mechanical properties (CrYN:Nb/Ta/V high hardness values of 21.4, 18.2, 16.1 GPa, and bending strengths of 707, 711, and 697 MPa, respectively) were obtained. The positive correlation between hardness and bending strength points to an enhancement in the overall durability of the thin film.

**MB-ThP-12 Halide-Treated ZnMgO Nanoparticles for Improving Stability of InP Based Quantum-Dot Light-Emitting Diodes, Kangsuk Yun [riverstone@kyonggi.ac.kr], Jaehyung Park, Jaehwi Choi, Jiwan Kim, Kyonggi University, Republic of Korea**

Quantum dots (QDs) are nanometer-sized semiconductor particles, and Quantum Dot Light Emitting Diodes (QLEDs) are electroluminescent devices that use QDs as an emitting layer. As QD size decreases, the quantum confinement effect enhances the discreteness of energy levels, leading to an increased bandgap. Consequently, by manipulating the size of QDs, it is possible to produce various colors of light and enhance color purity by narrow full width at half maximum. ZnMgO NPs, which are currently used as the electron transport layer (ETL) in QLEDs, are actively researched due to their high electron mobility and chemical stability. However, there are inevitable oxygen vacancies in thin films using ZnMgO NPs, which reduce the performance of QLEDs by exciton quenching. In this study, we used ZnMgO NPs as the ETL to fabricate InP QD-based QLEDs, which consisted of multilayers: ITO/ZnMgO/red InP QDs/CBP/MoO<sub>3</sub>/Al. First, we formed ZnMgO NPs film on ITO glass and passivate halides on ZnMgO NPs to reduce oxygen vacancies. New Zn-halide and Mg-halide peaks were observed in the x-ray photoelectron spectroscopy. Additionally, photoluminescence (PL) measurements showed that halide-treated ZnMgO NPs exhibited a higher PL intensity compared to untreated ZnMgO NPs. These results indicate that the halide treatment effectively reduces oxygen vacancies in ZnMgO NPs, and its effect was verified with the inverted structured QLEDs. The maximum luminance of QLEDs with halide-treated ZnMgO NPs (h-QLEDs) showed 1,134 cd/m<sup>2</sup>, compared to 696 cd/m<sup>2</sup> for the QLEDs with pristine ZnMgO NPs (p-QLEDs). After aging for 48 hours in a nitrogen atmosphere, h-QLEDs showed 1,290 cd/m<sup>2</sup>, but the performance of p-QLEDs decreased dramatically to 64.67 cd/m<sup>2</sup>. The experimental results indicated that the halide-treated ZnMgO NPs enhance the optical properties and stability of QLEDs, which can contribute QDs display commercialization.

**MB-ThP-13 Inkjet Printing of Silver Film on Polydimethylsiloxane for Soft Electronics, Hsuan-Ling Kao [snoopy@mail.cgu.edu.tw], Chang Gung University, Taiwan; Li-Chun Chang, Mingchi University of Technology, Taiwan; Min-Hsuan Lu, Chang Gung University, Taiwan**

As the development of fifth-generation mobile communication technology expands into medical intelligence, the demand for flexible and wearable devices has increased significantly. The flexible polymer substrates are very promising for expansion into millimeter wave band applications. Among these polymers, Polydimethylsiloxane (PDMS) has recently gained much attention for the development of wearable antennas, sensors, and RF switch. PDMS is a transparent and colorless high molecular polymer with biocompatibility. Its mechanical properties are similar to human skin (elastic modulus ~2 MPa) and can be smoothly attached to the surface of object. Therefore, PDMS is like human skin and can be attached to various parts of the human body, making it an electronic skin for biological monitoring. In order to fabricate electronic devices on these flexible plastic

materials, the interconnection using metal layers are essential. However, PDMS is softer than other flexible substrates, and its surface has poor wettability, making it difficult for the metal layer to adhere. Therefore, traditional production methods such as transfer printing or screen printing cannot be used to produce electrodes. Inkjet printing technology is used to deposit metal films on PDMS using non-contact material deposition and digital patterning. The inkjet printing technology can produce highly conductive films at a lower process temperature, without the need for etching steps and the process is simple. In this work, Inkjet-printed silver thin film on PDMS substrate process was established. First, the PDMS surface uses plasma technology to control its energy and time to convert hydrophobicity into hydrophilicity. Then, silver films were printed onto PDMS substrate, followed by curing in an oven to remove excess solvent and material impurities. Multi-pass printing is required to achieve good conductivity and enough thickness. The conditions for plasma treatment of PDMS were examined by water contact angle to optimize surface wettability. The conductivity, thickness and surface morphology of the printed metal film depend on the printing thickness and sintering temperature. The conductivity and surface morphology were measured using the four-probe method and SEM photos. The optimization of inkjet printing process and surface treatment study of inkjet-printed silver film were presented with details. Based on optimal conditions, inkjet-printed silver lines on PDMS substrate were implemented to study the RF performance. The results demonstrate that inkjet printing of metals on PDMS substrates offers the feasibility of soft electronics.

**MB-ThP-14 Magnetoelectric Sensors for Flexible MEMS Applications, Davinder Kaur [davinder.kaur@ph.iitr.ac.in], Indian Institute of Technology Roorkee, India**

**Magnetoelectric Sensors (ME)** have the potential to contribute to sustainable development because of their peculiar features such as lower power requirement, enhance energy efficiency, reduced environmental impact, applications in renewable energy, enable precision agriculture, infrastructure monitoring, health monitoring, optimize waste management, and contribution to overall resource conservation. The present study reports the fabrication of highly flexible, cost-effective, nano-structured magnetic field sensor comprising AlN/Ni-Mn-In ME heterostructure fabricated over magnetostrictive Ni foil. The ultra-low magnetic field up to or less than ~1  $\mu$ T has been easily detected from the fabricated sensor. Further the surface acoustic wave (SAW) delay line-based piezo resonator has been fabricated over highly flexible AlN/Ni-Mn-In/Kapton for flexible MEMS application. The fabricated device resonates at ~1.40 GHz. The effect of the external magnetic field on the resonance frequency (fR) of the device has been investigated and tunability ( $\Delta$ fR/fR) ~9% was observed. The device displays high sensitivity of ~0.94 Hz/nT at room temperature. The alteration in the fR can be attributed to the  $\Delta$ E-effect in the AlN/Ni-Mn-In heterostructure. The flexibility of the fabricated magnetic field sensors has been investigated in terms of the bending cycles and bending angle. The sensor characteristics remain unchanged up to ~2500 bending cycles. The integration of these novel ferromagnetic shape memory alloy (FSMA, i.e., Ni-Mn-In) based flexible piezo-resonator into various systems can enhance efficiency, reduces environmental impact, and contributes significantly to the overarching goal of sustainable development.

**Keywords: Ferromagnetic shape memory alloys, flexible magnetic sensor, lead-free piezoelectric, magnetostrictive effect, surface acoustic waves (SAW).**

**MB-ThP-15 Flexible UV-Vis photodetectors based on NiOx thin film obtained by magnetron r.f. sputtering, Eddue Osuna-Escalante [eddue.osuna@uabc.edu.mx], David Mateos-Anzaldo, Oscar Pérez-Landeros, Roumen Nedev, Ivan Cardoza-Navarro, Esteban Osorio-Urquiza, Mario Curiel-Álvarez, Nicola Nedev, Universidad Autónoma de Baja California, Mexico**

Flexible optoelectronic devices based on transparent substrates are attracting interest for potential applications in wearable sensors, flexible displays and transparent electronic devices. Among various fabrication techniques, magnetron r.f. sputtering stands out for preparation of high-quality films. The principal advantages of this technique are high adhesion, low density of defects, high compatibility with flexible substrates, and control over the deposited material composition.

Flexible photodetectors based on NiO<sub>x</sub> deposited by magnetron r.f. sputtering at room temperature and 50°C, using powers in the range of 40-80W over ITO-PET and ITO-PEN substrates were fabricated. The obtained films were evaluated using ellipsometry to determine their thicknesses and

# Thursday Afternoon, May 15, 2025

optical constants. Thermal evaporation was used to deposit Au as top electrodes.

To assess the performance as photodetectors in the UV-visible spectrum, the fabricated devices were electrical characterized by current-voltage measurements in dark and under the incidence of different light emitting diodes. In addition, the fabricated flexible photodetectors were tested for mechanical and electrical stability after cyclic bending stress.

**MB-ThP-16 Large Area Synthesis of Hexagonal Boron Nitride Layers on SiO<sub>2</sub>/Si Substrates,** *Diego Lundquist Lundquist [dlundquist7949@sdsu.edu], Abinash Bhuyan, Mary Becker, Jennifer Brumley, Sanjay Behura, San Diego State University, USA*  
**Diego Lundquist,** C. Abinash Bhuyan, Mary Becker, Jennifer Brumley, Sanjay K. Behura\*

*Department of Physics, San Diego State University, San Diego, CA 92182, United States*

Hexagonal boron nitride (h-BN) is a two-dimensional material that has recently been the focus of research for hosting single photon emitters at room temperature. Its spin-optical properties make an ideal candidate for quantum technologies. Existing research relies on exfoliated hBN for its application which restricts its scalability for various practical applications. Also, the current synthesis of chemical vapor deposition grown hBN is on catalytic substrates such as Cu, Al, Ni, and Co. As a result, hBN film is transferred onto desired substrates for photonics applications. This study focuses on synthesizing large-scale hBN film on dielectric substrates, which allows for direct characterization of its high optical properties. Through the optimization of a two-zone, low-pressure chemical vapor deposition (LPCVD), hBN grown directly on SiO<sub>2</sub>/Si substrates using the sublimation of ammonia borane complex as precursor and ultra-high pure H<sub>2</sub> as carrier gas. CVD-grown hBN films were characterized to confirm the large-area growth. Typical optical and scanning electron microscopic images reveal the uniform growth of hBN on SiO<sub>2</sub>/Si substrate. Raman spectroscopic measurement reveals the signature peaks at 1368 cm<sup>-1</sup> which corresponding to E<sub>2g</sub> in-plane B-N vibrational modes in hBN.

**MB-ThP-17 Influence of partial pressure of argon/oxygen and temperature on photosensors based on n-Si/NiO<sub>x</sub>,** *Esteban Osorio [esteban.osorio@uabc.edu.mx], Autonomous University of Baja California, Mexico; David Mateos-Anzaldo, Mario Curiel-Alvarez, Eddue Osuna Escalante,, Oscar Perez-Landeros, Ivan Cardoza-Navarro, Roumen Nedev, Benjamin Valdez-Salas, Nicola Nedev, Autonomous University of Baja California, Mexico*

This work reports photosensors based on non-stoichiometric nickel oxide obtained by radio-frequency magnetron sputtering on n-Si substrates in a mixed atmosphere of argon/oxygen. The amount of oxygen was varied from 0-4% of the total atmosphere. Also the deposition temperature was varied in the range of 0-100°C. Corning glass substrates were also used to determine the band gap and transparency of the obtained film. The photosensors were characterized by ellipsometry in a 350 to 1000 nm range. Au (~400nm) deposited by thermal evaporation was used as top and back contact for electrical characterization. Current-voltage measurements were performed in a dark chamber under red, green, blue and UV illumination.

**MB-ThP-18 Topological Insulator, Reduced Graphene Oxide/Silicon Nanowire Arrays for Ultra-Broadband Photodetectors,** *Hsu Hsun-Feng [hfsu@dragon.nchu.edu.tw], Huang Tzu-Yun, National Chung Hsing University, Taiwan*

Topological insulator, such as bismuth telluride (Bi<sub>2</sub>Te<sub>3</sub>), has narrow bulk band gap and has a Dirac-type surface state. Thus, it can absorb middle or long-wavelength infrared light and has low resistivity. Graphene, which is a 2D material, exhibits broadband light adsorption and a rapid response due to its Dirac cone structure. Therefore, graphene is an expected material for broadband photodetectors. Its drawbacks are the properties of a high electron-hole recombination rate and a low photoresponse. However, reduced graphene oxide (rGO) has lower electron-hole recombination rate comparing with graphene due to its functional group and edge defects. Silicon has become very popular for many applications because of the unique advantages of CMOS compatibility and high integrated density. Silicon nanowire (SiNW) array has low reflectivity that can raise light harvesting efficiency. Thus, in this study an ultra-broadband photodetector was fabricated by combining with the Bi<sub>2</sub>Te<sub>3</sub>, rGO and SiNW array.

The silicon substrate is etched using metal-assisted chemical etching to obtain SiNW array. Then, Bi<sub>2</sub>Te<sub>3</sub> was deposited on SiNW array by chemical vapor deposition (CVD). Using photocatalytic reduction to reduce graphene

oxide on a SiNW array to form a thin film. Finally, silver electrodes are deposited on both sides of the specimen to create a device. Optical sensing is performed using 940 nm near-infrared light and 5500 nm mid-infrared light.

The results show that, under suitable process conditions using by CVD, Bi<sub>2</sub>Te<sub>3</sub> and tellurium (Te) precipitates with a size of approximately 500 nm can be formed on the SiNW array. It can reduce the reflectance of the device in the near- to mid-infrared range (1200–2500 nm). For sensing 940 nm near-infrared light, the light is primarily absorbed by the SiNW array, generating electron-hole pairs that increase carrier concentration and produce photocurrent. The rGO coating can reduce the contact resistance between the electrode and the silicon nanowires, enhancing the responsivity and sensitivity of the photodetector. When irradiated with mid-wavelength infrared light at 5500 nm, the Bi<sub>2</sub>Te<sub>3</sub>/SiNW array device also exhibits a rapid response characteristic. The reason is that, upon illumination, electron-hole pairs are generated in the Bi<sub>2</sub>Te<sub>3</sub> particles. Electrons are conducted through the SiNW to the electrodes, producing a photocurrent in the external circuit. Notably, the rGO/Bi<sub>2</sub>Te<sub>3</sub>/SiNW device with a mesh-like rGO film, compared to a fully covered rGO film, demonstrates superior responsivity and faster response times in sensing both 940 nm near-infrared light and 5500 nm mid-infrared light.

**MB-ThP-19 Microstructural Evolution of Co-Sputtered Nanocrystalline Cu-Ag Alloy Thin Films During Annealing Process,** *Yu-Lin Liao [20193eileen@gmail.com], College of Semiconductor Research, National Tsing Hua University, Taiwan; Tsai-Shuan Kuo, Fan-Yi Ouyang, Department of Engineering and System Science, National Tsing Hua University, Taiwan*  
Copper and silver films, known for excellent conductivity, are widely used as conductive layers in semiconductors. In 3D IC technology, direct bonding replaces solder balls to reduce RC delay and power consumption. To understand the potential of copper-silver alloys for direct bonding, it is very important to understand the properties and structure of copper-silver films. In the study, we investigate the microstructural evolution of the two-phase Cu-Ag alloy films during the annealing process with different doping concentrations and annealing temperatures for 1, 24 and 48 hours respectively. Oversaturated fine crystalline Cu-Ag alloy films with doping levels of 20 at.% and 40 at.% of Ag were fabricated using a magnetron sputtering system. The films were then annealed at four temperatures, i.e. 200°C, 250°C, 300°C, and 400°C to understand their thermal stability and property evolution. The results show that Cu concentration on the surface slightly increases with rising annealing temperature after annealing for 1 and 24 hours. But when the annealing temperature increased to 400°C, the rich Ag, instead of Cu, was accumulated to the surface of the films. In addition, Oversaturated solid solution films were annealed at 3 different vacuum levels (1×10<sup>-6</sup> torr, 5×10<sup>-3</sup> torr, and 760 torr). The microstructural and property evolution during annealing and the corresponding mechanism will be discussed in detail.

**MB-ThP-20 Multifunctionality in Frequency Tuning of PMN-PT/Ni-Mn-In Integrated Film Bulk Acoustic Wave Resonator for Flexible MEMS Applications,** *Diksha Arora [diksha@ph.iitr.ac.in], Davinder Kaur, Indian Institute of Technology Roorkee, India*

Flexible and tunable bulk acoustic wave (BAW) resonators are opening new possibilities in flexible MEMS, wireless devices, and wearable magnetic sensors. This work presents a highly adaptable thin-film BAW resonator constructed with a PMN-PT piezoelectric layer positioned between magnetostrictive Ni-Mn-In electrodes on a flexible Ni substrate. This device, operating at a resonance frequency (f<sub>r</sub>) of 5.31 GHz, demonstrates significant tunability via both magnetic and electric fields. A magnetic field of 1200 Oe produces an f<sub>r</sub> shift of approximately 450 MHz, achieving a sensitivity of around 3.75 Hz/nT and an impressive 9.6% tunability. Similarly, a 10 V DC bias yields an f<sub>r</sub> downshift of roughly 360 MHz, with electric field sensitivity and tunability measured at about 36 Hz/μV and 6.8%, respectively. The device's resonance performance aligns with the modified Butterworth-Van Dyke model, and its quality and reliability remain intact through 3,000 bending cycles, underscoring its potential in advanced flexible electronics, tunable MEMS, and magnetic sensors.



## Tribology and Mechanics of Coatings and Surfaces

### Room Golden State Ballroom - Session MC-ThP

#### Tribology and Mechanics of Coatings and Surfaces Poster Session

**MC-ThP-1 Role of Layer Position During Thermo-Mechanical Loading of Trilayers, Megan J. Cordill [megan.cordill@oeaw.ac.at], Claus O.W. Trost, Erich Schmid Institute of Materials Science, Austrian Academy of Sciences, Austria**

Thermo-mechanical loading of thin films on rigid substrates is common method to assess film stresses as a function of temperature. However, these experiments have historically only been performed on single layer films even though multilayers are used in all advanced thin film technology. To illustrate the feasibility of measuring the thermo-mechanically induced stresses of multiple layers simultaneously, different architectures of brittle-ductile-brittle and ductile-brittle-ductile trilayers on silicon were heated with in-situ X-ray diffraction (XRD). The use of XRD provides individual film stress evolution simultaneously to understand delamination mechanisms of the trilayer architecture. The main aspects presented will be the strain evolution under thermo-mechanical loading as a function of layer position. Following Mo and Cu films from next to the substrate, to the middle position, and as the top surface film found that position in the trilayer architecture significantly influences the stress-temperature curve, thus the deformation mechanism due to thermo-mechanical loading.

**MC-ThP-2 The Effect of Surface Built-Up Defect on the Coating Process of Automotive Sheet, JIANFENG HE [13166296136@163.COM], Shanghai Jiao Tong University, China**

At present, facing fierce competition in automotive sheet market, defects prevention has been the most important task during cold rolling production. As a key process of automotive sheet (eg. Outer panel), surface coating plays an important role to improve surface quality and erosion resistance. In order to analyze the effect of built-up defect to coating of automotive sheet surface treatment, 3-dimension morphology of build-up defect is measured. The build-up behavior in coating process is also investigated in this article, which is helpful for defect inspection and judgement.

**MC-ThP-3 Investigation of Wear Resistance of 7075 Aluminum Alloy Modified Through Plasma Electrolytic Oxidation (PEO), Bruna Freitas [bruna.michelledefreitas@gmail.com], Ricardo Torres, Carlos Laurindo, PUCPR - Pontifícia Universidade Católica do Paraná, Brazil; Luciane Santos, Vrije Universiteit Brussel, Belgium; Paulo Soares, PUCPR - Pontifícia Universidade Católica do Paraná, Brazil**

The 7075-aluminum alloy is widely used in the aerospace and automotive industries due to its excellent mechanical properties. However, its relatively lower wear resistance may limit its applications. The PEO surface modification process is a method that can improve the surface properties of the 7075 alloy. Thus, this study evaluates the wear resistance of the 7075 alloys modified by PEO. The Al7075 samples were sanded with #500 and cleaned. The PEO process was carried out using a bipolar power source, with an electrolyte based on sodium phosphate and sodium hydroxide, with 352V, 350V, and 475V and a 1000 Hz frequency for 5, 10, and 20 minutes. The samples were characterized using SEM and EDS techniques, X-ray Diffraction, and wear tests. The results show that the oxide surface formed is homogeneous, porous, and crack-free. The XRD results indicate the presence of Al<sub>2</sub>O<sub>3</sub> phases, and EDS showed that the elements Al and O were predominantly present in all coatings after treatment. The tribological resistance significantly improved compared to the substrate.

**MC-ThP-4 Nanoindentation and Micropillar Compression at Cryogenic Temperatures, Eric Hintsala [eric.hintsala@bruker.com], Kevin Schmalbach, Douglas Stauffer, Bruker Nano Surfaces, USA**

Mechanical reliability at low temperatures is required for environments in energy and aerospace applications. Due to its highly localized measurement capabilities, nanomechanical approaches can be useful for isolating individual regions within a more complex microstructure or component or testing of thin films. In general, both modulus and yield strength gradually increase with decreasing temperature, but more sudden shifts in behavior can also be observed, such as phase transformations or ductile-to-brittle transitions. In situ SEM testing enables visualization of the deformation mechanisms coupled with the measured mechanical properties helping complete the interpretation of the behavior. A low temperature control system has been developed for the Hysitron PI89PicoIndenter (Bruker, USA) for in situ SEM testing that enables continuous temperature control from -

130°C to 50°C. Independent temperature control on the tip and sample to enable proper temperature matching in vacuum and minimizes drift. The temperature dependent mechanical response of two metallic samples, Nitronic 50 and Tungsten, both by nanoindentation and micro-pillar compression.

## Surface Engineering of Biomaterials, Medical Devices and Regenerative Materials

### Room Golden State Ballroom - Session MD-ThP

#### Surface Engineering of Biomaterials, Medical Devices and Regenerative Materials Poster Session

**MD-ThP-1 Electrochemical and Antimicrobial Coating: Increasing the Ionic Charge on Titanium Surfaces as a Preventive Strategy for Titanium Implants, João Pedro dos Santos Silva [jpedrooss85@gmail.com], École des mines de Saint-Étienne, France; Daniela Buenos Ayres de Castro, Mariana Mireski, Catia Sufia Alves Freire de Andrade, Maria Helena Rossy Borges, Universidade Estadual de Campinas, Brazil; Jean Geringer, École des mines de Saint-Étienne, France; Valentim Adelino Ricardo Barão, Universidade Estadual de Campinas, Brazil**

Peri-implant conditions and the electrochemical degradation of titanium (Ti) are critical factors in the failure of biomedical implant treatments. Developing functional surfaces to address these challenges is essential. Cationic coatings have proven to be an effective strategy for reducing biofilm formation and enhancing corrosion resistance. This treatment focuses on increasing the surface charge of implants and provides antimicrobial properties without the use of pharmaceutical agents, making the approach safer, more cost-effective, and sustainable. Thus, this coating was developed in two stages: (1) functionalization with hydroxyl groups (-OH) using plasma electrolytic oxidation (PEO), incorporating bioactive elements and enhancing surface functionalization; (2) silanization with tetraethylorthosilicate (TEOS) or 3-glycidyloxypropyltrimethoxysilane (GPTMS), which bind to alkaline surfaces and promote proton release through chemical reactions. Four groups (untreated Ti, PEO, PEO + TEOS, and PEO + GPTMS) were evaluated for surface characterization, electrochemical performance, and antimicrobial activity. Micrographs showed distinct morphologies in the silanized groups, with the alkalization step generating pores that enhanced topography and roughness. The superhydrophilic affinity created by alkalization evolved into hydrophobic (TEOS) and superhydrophobic (GPTMS) characteristics after silanization. The presence of amine groups, detected by X-ray photoelectron spectroscopy (XPS), indicated an increase in surface charge, confirmed by zeta potential measurements. Positively charged surfaces demonstrated superior electrochemical performance and greater antimicrobial potential against *Streptococcus mitis* biofilm formation (24 h). In conclusion, cationic coatings show promise for implantable devices, offering improved resistance in adverse environments and antimicrobial properties.

**MD-ThP-2 Flexible, Enzyme-Free, and Ultra-Sensitive Cholesterol Sensor Based on In-Situ Etched Ti<sub>3</sub>C<sub>2</sub>T<sub>x</sub> MXene Nanosheets, Sanjeev Kumar [sanjeev.kumar@rgu.ac.in], Jyoti Jaiswal, Rajesh Chakrabaty, Kulsuma Begum, Bitupan Prasad, Rajiv Gandhi University, India**

This work presents an enzyme-free cholesterol sensor based on Ti<sub>3</sub>C<sub>2</sub>T<sub>x</sub> MXene nanosheets, offering a highly sensitive detection platform. The Ti<sub>3</sub>C<sub>2</sub>T<sub>x</sub> MXene nanosheets were synthesized via in-situ LiF/HCl etching, and the sensing electrode was prepared by drop-casting a colloidal solution of the as-synthesized MXene onto a paper substrate. To investigate the quality and properties of the synthesized Ti<sub>3</sub>C<sub>2</sub>T<sub>x</sub> MXene nanosheets, microstructural and compositional studies were conducted utilizing FESEM, XRD, Raman spectroscopy, XPS, and EDS. These characterizations confirmed the successful synthesis of the Ti<sub>3</sub>C<sub>2</sub>T<sub>x</sub> MXene nanosheets. Cyclic voltammetry (CV) and electrochemical impedance spectroscopy (EIS) were performed to analyse the electrochemical behaviour of the Ti<sub>3</sub>C<sub>2</sub>T<sub>x</sub> MXene-based electrode. The responses of the fabricated electrode to different cholesterol concentrations were recorded using CV in phosphate buffer solution, exhibiting robust linear response ( $R^2 \sim 0.99$ ) in the range from 1 to 250 nM. The MXene-based electrode exhibited good sensitivity ( $0.75377 \pm 0.01107$  mF nM<sup>-1</sup>), a low detection limit (0.07 nM), high selectivity, practical reproducibility, and excellent cyclic stability, suggesting its potential for real-time cholesterol monitoring in biomedical and healthcare applications.



**MD-THP-3 Effect of the Thickness of Fibrous Cap and Compositions on the Rupture Behaviour of the Atherosclerosis Plaques, Jiling Feng [j.feng@mmu.ac.uk], Mohamed Abdulsalam, Manchester Metropolitan University, U.K.**

Atherosclerotic plaque rupture is the leading cause of the cardiovascular diseases (CVD) such as coronary arteries disease, stroke and heart attack. Early detection of the plaques which are prone to the rupture, also known as vulnerable plaque, can provide important clinical information to prevent the fatal cardiovascular event. The vulnerable plaques are commonly characterized as the large lipid core and thin fibrous caps with the thickness less than 65  $\mu\text{m}$ . However, evidence showed that plaques with fibrous caps > 65  $\mu\text{m}$  are also susceptible to plaque rupture or erosion and can cause acute myocardial infarction and sudden death<sup>[1]</sup>. The effect of the critical thickness of fibrous cap and compositions of the plaques on the rupture behaviour of the arterial plaques has not been fully investigated. In this study, the artificial plaques with a variety of the compositions (lipid core, calcium and collagen) and with a range of thickness of fibrous cap were fabricated. The mechanical properties of the plaques were tested by using the unconfined compression testing. Meanwhile, the deformation of the arterial plaques samples and rupture behaviours were also recorded by using the high-resolution of camera. The initiation and propagation of the rupture of fibrous cap were analysed using digital image correlation (DIC) software. The experimental results indicated that the thicker the fibrous cap, the stiffer the arterial plaque. This phenomenon was observed in the plaques with large lipid core and calcified plaques. The Young's module for the plaques with large lipid core (Figure 1a) ranges from 0.0235 to 3.7174 MPa which are compatible with the value of plaques in the human carotid arteries which were observed in the clinical findings. The plaques with higher percentage of collagen possess the the greater Young's modules (Figure 1b).

## Reference

[1] Liu, X., He, W., Hong, X. *et al.* New insights into fibrous cap thickness of vulnerable plaques assessed by optical coherence tomography. *BMC Cardiovasc Disord* **22**, 484 (2022).

**MD-THP-4 Effects of Electrical Stimulation with Iridium Oxide Plasma Protein Hybrid Film on Nerve Cells, Po-Chun Chen [cpc@mail.ntut.edu.tw], National Taipei University of Technology, Taiwan**

Iridium oxide (IrOx) is a well-known material for neural stimulation, but its rigidity and lack of bioactivity limit its biomedical application. To address this, an IrOx film incorporating plasma proteins (IrOx-PP) was developed to enhance biocompatibility and promote neuronal growth. The addition of plasma proteins created bioactive sites that improved cell adhesion and differentiation while maintaining the electrochemical properties needed for neural stimulation. The IrOx-PP hybrid films showed significantly higher cell viability and metabolic activity, with electrical stimulation further enhancing cell growth and bioactivity. Neurite length increased significantly under electrical stimulation, with the IrOx-PP hybrid films showing the greatest enhancement. In addition, cells on IrOx-PP hybridfilms expressed higher levels of the neuronal markers, indicating their superior potential for promoting neuronal differentiation and neurite outgrowth compared to pure IrOx films. This result demonstrated that the IrOx-PP hybrid film can potentially serve as a platform for advanced neural interfaces, providing improved tissue integration.

## Plasma and Vapor Deposition Processes

### Room Golden State Ballroom - Session PP-THP

#### Plasma and Vapor Deposition Processes Poster Session

**PP-THP-1 Optimizing Thin Film Deposition with Ion Energy and Flux Measurements in Pulsed Plasmas with Plasma Diagnostics, Angus McCarter [angus.mccarter@impedans.com], Thomas Gilmore, Anshu Verma, Chase House, City Junction Business Park, Ireland**

In the field of metallic coatings and thin film deposition, precise control of deposition processes has become crucial. These processes are heavily dependent on the chemical/physical processes occurring on the substrate surface. Like any other surface in contact with plasma, a sheath usually develops on the substrate which pulls down the ions out of bulk plasma necessary to complete the process on the substrate. Furthermore, external RF/DC/tailored waveform biases are applied to the substrate to modify the ion behaviors. As it can affect the chemical composition, microstructure and the associated electrical properties of the thin films during plasma assisted deposition processes. Therefore, the characterization of only bulk

plasma is not sufficient in providing insights necessary to understand the plasma surface interactions. A high-speed monitoring of the ion energy distribution function and ion flux can lead to enhanced understanding of the plasma surface interactions and improved process performance.

We will highlight the successful measurements done by the Semion RFEA diagnostic under different chamber and bias conditions. Such applications enabling accurate and precise control of deposition process on different materials and various plasma chemistries. It measures the ion energies hitting a surface, the ion flux, negative ions and bias voltage at any position inside a plasma chamber using an array of integrated sensors. On the other hand, the Semion pDC system measures these parameters in real time over an energy range up to 2000 eV (process dependent). It can do sub-microsecond time resolved measurements, for studying pulsed ICPs, or pulsed DC biases, as well as floating and grounded substrate conditions. The Semion Pulsed DC system is the key instrument used to measure the temporal evolution of the ion energy and flux at different times through the pulse period of a pulsed DC plasma process. These measurements are essential for establishing the correlation between the plasma inputs and the ion energy/flux which, in-turn, determines the effectiveness of the surface treatment.

**PP-THP-2 Influence of the Substrate on the Growth of Aluminium Oxide Films by Atomic Layer Deposition for Food Packaging Applications, Hugo Patureau, SIMaP, CNRS, University Grenoble Alpes, France; Thierry Encinas, CMTC, Grenoble INP, University Grenoble Alpes, France; Alexandre Crisci, Frederic Mercier [frederic.mercier@grenoble-inp.fr], SIMaP, CNRS, University Grenoble Alpes, France; Erwan Gicquel, CILKOA, France; Arnaud Mantoux, Elisabeth Blanquet, SIMaP, CNRS, University Grenoble Alpes, France**

With the gradual ban on single use plastics, cellulosic products have emerged as suitable candidates to replace plastics in the packaging industry. Cellulose is biodegradable, recyclable and possesses good mechanical properties. To be viable for packaging, especially in the food industry, cellulose surfaces need to be functionalised to obtain additional properties, such as wettability, oxygen/water barriers and mechanical resistance in humid conditions.

In this context, we have investigated the synthesis of aluminium oxide films by an industrial Atomic Layer Deposition (ALD) process on cellulosic substrates using the precursors trimethylaluminium (TMA) and water. While the reactivity of these precursors on silicon are well established, the same cannot be said of cellulosic substrates due to their complex structure and their affinity with water. In this presentation, a study on the growth of ALD Al<sub>2</sub>O<sub>3</sub> on silicon and cellulose is conducted. X-ray fluorescence (XRF) and Inductively coupled plasma mass spectrometry (ICP-MS) on cellulose is developed and implemented to quantify the amount of aluminium deposited. The saturation curves are established on silicon and cellulose, as well as the effect of the synthesis temperature. A comparison of both substrates is made and specific growth mechanisms of aluminium oxide by ALD on cellulosic substrates is discussed.

**PP-THP-3 Minimizing Secondary Electron Yield in Amorphous Carbon Thin Films: A Study on Power Density, Discharge Modes, and Hydrogen Incorporation, Valentine PETIT [valentine.petit@cern.ch], Yorick Delaup, Alessia Pascali, Pedro Costa Pinto, Marcel Himmerlich, Christos Kouzios, European Organization for Nuclear Research, Switzerland**

Amorphous carbon thin films with low Secondary Electron Yield (SEY) are critical for applications where electron multipacting limits achievable performance. Such films are effective to mitigate electron cloud formation within the vacuum beam lines of particle accelerators such as the Large Hadron Collider and Super Proton Synchrotron at CERN. They are now also being implemented in the new Electron Ion Collider under construction at Brookhaven National Laboratory.

Research over the last decade has highlighted the significant role of hydrogen presence in the plasma discharge during deposition. Hydrogen incorporation in the films has been shown to increase the SEY, posing a key challenge in coating the extensive beam pipes for particle accelerators.

In this study, we examine the effects of power density and discharge mode, i.e. Direct Current (DC) and High-Power Impulse Magnetron Sputtering (HiPIMS), on the SEY of amorphous carbon films. These films were produced by sputtering in an Ar atmosphere with 1.3% D<sub>2</sub> to simulate hydrogen-like impurities typically arising from outgassing in the beam pipes and the deposition system. The D<sub>2</sub> consumption during the coating process was monitored by mass spectrometry and is correlated with the SEY, while X-ray Photoelectron Spectroscopy was used to characterize the films. Our findings indicate that higher deposition powers result in films with reduced

deuterium incorporation and lower SEY. Additionally, for the same average power density, films deposited in HiPIMS mode exhibit lower SEY compared to those deposited in DC mode. The results are discussed in the context of hydrogen incorporation mechanisms in carbon films, with a view toward optimizing coating system design and process parameters

**PP-ThP-4 Accurate Reporting of Time-of-Flight Measurements with Gated Mass Spectrometry, Nathan Rodkey [nathan.rodkey@empa.ch], Jyotish Patidar, Sebastian Siol, EMPA (Swiss Federal Laboratories for Materials Science and Technology), Switzerland**

The quality of high-power impulse magnetron sputtering (HiPIMS) deposited films can often be improved through the effective use of metal-ion synchronization (MIS). However, effective synchronization requires precise measurements of the time-of-flight (ToF) of ions, such that an accelerating bias can be properly synchronized. These measurements are commonly done using time- and energy- resolved mass spectrometry but require calibrations of the transit time of ions inside of the mass spectrometer to accurately report the ToF. The transit time can be calculated by estimating the travel length in varying parts of the spectrometer (e.g. from orifice to detector) and accounting for the interactions of ions with varying electrostatic optics (such as the extractor, energy filter, mass filter, and dynode). The errors associated with these estimations can lead to nonphysical values in a HiPIMS process, such as negative ToFs, or metal ions arriving to the substrate before process gas ions. As a result, many groups emphasize that their calibrations are estimations, or relevant only at sufficiently large time steps. Here we report a practical approach to determine the transit time in the spectrometer experimentally, which was already successfully employed for multiple projects in our group. We use a bipolar HiPIMS power supply to synchronize a gating pulse to the front end of a HiDEN Analytical EQP-300 mass spectrometer. The orifice of the mass-spec (50  $\mu\text{m}$ ) was placed at a 12 cm working distance. ToF was then measured by applying a +70 V bias to repel ions, and a 5  $\mu\text{s}$  gating pulse of -30 V to accept them. To prevent interference of the driven front end (kept at +70 V) with the HiPIMS plasma, a grounded shield is placed in front of the mass-spec head with a 1-2 mm opening. The gate was synchronized to the HiPIMS pulse by providing a trigger signal, and data was collected at 5  $\mu\text{s}$  intervals by adjusting the time delay of this pulse. The time-of-flights of  $\text{Ar}^+$ ,  $\text{N}^+$ ,  $\text{Al}^+$ ,  $\text{Cu}^+$  and  $\text{W}^+$  ions measured in this way are compared to those calculated using mass spectrometry flight tube equations.

**PP-ThP-5 Focused Magnetron Sputtering: A Comprehensive Study of Magnetron Power Effects on AlCrN Coatings Under Industrial Conditions, Martin Ucik [m.ucik@platit.com], Masaryk University, Czechia**  
**Introduction**

Traditional coating methods, such as Cathodic Arc Evaporation (CAE), face challenges due to microscopic defects and other limitations. Focused Magnetic Field Magnetron Sputtering (F-MS) has emerged as a transformative solution, achieving a high ionized metal flux fraction even for large-scale targets [1]. Compared to conventional magnetron sputtering (DCMS), F-MS demonstrates a six-fold increase in power density [2]. This advantage, combined with effective cooling and prolonged duty cycles, establishes F-MS as a groundbreaking technology. Its integration into PLATIT's PVD coating unit, Pi411, represents a significant advancement in hard protective coatings for industrial applications.

## Methods

F-MS operates by moving a reduced-size magnetron longitudinally inside a tubular target ( $\varnothing 110 \times 510$  mm). This design enables high-power sputtering of up to 30 kW and allows the deposition of dense coatings at a growth rate of 2  $\mu\text{m}/\text{h}$  using a 3-fold carousel rotation system.

## Results

Coatings of (Al,Cr)N deposited via F-MS exhibited stoichiometric composition, smooth surfaces, and controlled defect levels. Mechanical property tests, plasma diagnostics, and cutting tests demonstrated strong interrelationships and benefits associated with higher power levels. Notably, cutting tests confirmed the superior performance of (Al,Cr)N coatings compared to state-of-the-art CAE coatings.

## Conclusion

F-MS technology represents a significant breakthrough in the coating industry, addressing the limitations of traditional methods. Its ability to achieve high plasma power densities and a high degree of ionization for large-scale targets holds immense potential to advance industrial coating practices by enhancing efficiency and enabling new applications.

[1] Nillica, J. (2024). On direct-current magnetron sputtering at industrial conditions with high ionization fraction of sputtered species. *Surf. Coat. Technol.*, 487, 131028. <https://doi.org/10.1016/j.surfcoat.2024.131028>

[2] Klimashin, F. (2023). High-power-density sputtering of industrial-scale targets: Case study of (Al,Cr)N. *Mat. & Des.*, 237, 112553. <https://doi.org/10.1016/j.matdes.2023.112553>

**PP-ThP-6 Design and Evaluation of a Laboratory-Scale Thermal ALD Reactor: Case Study with Aluminum Oxide and Zinc Oxide., Jackeline Navarro-Rodriguez [jackeline.navarro@uabc.edu.mx], David Mateos-Anzaldo, Jesus Martinez-Castelo, Rogelio Ramos-Irigoyen, Oscar Perez-Landeros, Mario Curiel-Alvarez, Benjamin Valdez-Salas, UNIVERSIDAD AUTONOMA DE BAJA CALIFORNIA, Mexico; Eduardo Martinez-Guerra, CIMAV-Monterrey, Mexico; Hugo Tiznado-Vázquez, UNAM, Mexico; Nicola Nedev, UNIVERSIDAD AUTONOMA DE BAJA CALIFORNIA, Mexico**

Atomic layer deposition (ALD) is a crucial technique in microelectronics for thin film deposition due to its precise thickness control at the atomic scale, although its sustainability remains a challenge due to its high cost. This work presents the results of a customized, cost-effective and efficient thermal ALD system designed to deposit semiconducting and insulating thin films such as aluminum oxide ( $\text{Al}_2\text{O}_3$ ) and zinc oxide (ZnO) films, using trimethylaluminum (TMA) and diethylzinc (DEZ) as precursors, respectively. The oxidizing agent used was hydrogen peroxide ( $\text{H}_2\text{O}_2$ ).

Thin films of  $\text{Al}_2\text{O}_3$  and ZnO were deposited on silicon and corning glass substrates at a temperature of 200°C. Ellipsometry measurements were carried out to determine the thickness, optical constants, band gap and transparency.

The results obtained indicate the presence of a thin film deposited on silicon with 1160 cycles, with a growth rate of 1  $\text{\AA}/\text{cycle}$  which is equivalent to a thickness of  $\sim 116.4$  nm, as well as a refractive index of 1.76, an extinction coefficient of 0. In addition, the zinc oxide film deposited on corning glass present approximately 80% of transparency in visible region.

The system stands out for its optimized design, easy handling and low cost, which makes it a viable option for academic research and applications in electronics and nanotechnology.

**PP-ThP-7 Energy Flux Diagnostics in High Power Impulse Magnetron Sputtering, Caroline Adam [c.adam@physik.uni-kiel.de], Kiel University, Germany; Holger Kersten, Kiel University, Kiel Nano, Germany**

High power impulse magnetron sputtering (HiPIMS) has shown significant potential for thin film deposition. This potential is evident through the enhancement of film quality, specifically in terms of increased density [1] and adhesion [2] along with the diminished requirement for high substrate temperatures [3]. To achieve the optimal deposition process, it is crucial to develop a comprehensive understanding of the plasma-surface interaction at the substrate. This includes, in particular, analyzing the energy flux (transferred power from the plasma to the surface) and its composition.

The energy flux is investigated by using a passive thermal probe (PTP) [4], a so-called non-conventional diagnostic, measuring the integral energy flux to the substrate. Insights into the composition of the energy flux are gained by applying a bias voltage to the thermal probe [4] and using a novel combination of PTP with a retarding field analyzer (RFA) [5]. This allows to measure simultaneously the ion energy distribution (IED) and to perform energy-resolved energy flux measurements. In addition, the neutral energy flux component can be quantified by repelling all charge carriers by the grid potentials. Since the energy resolution and sensitivity of the RFA is limited, the measurements of the IED are completed by energy-resolved mass spectrometry, both time-averaged and time-resolved [6].

These diagnostics have been applied to compare HiPIMS and DC magnetron sputtering processes with same gas pressure and average power sputtering a planar copper target in argon atmosphere. In total, the mean energy flux to the substrate is lower in HiPIMS operation. Hence, temperature sensitive substrates are better protected. Normalizing the energy flux to the deposition rate, which is lower in HiPIMS as well, gives a higher value for the energy flux per adatom in HiPIMS, which can be attributed to the higher kinetic energy of sputtered particles. The dependence of the energy flux on the excitation mode (DC, HiPIMS), the HiPIMS pulse parameters, as well as on power and pressure is investigated. The advantages and limitations of the diagnostics used are discussed.

[1] J. Alami et al., *J. Vac. Sci. Technol. A* 23 (2005) 278–280.

[2] R. Bandorf et al., *Surf. Coat. Technol.* 290 (2016) 77–81.

[3] E. Wallin et al., *Europhysics Letters* 82 (2008) 36002.

[4] H. Kersten et al., *Thin Solid Films* 377–378 (2000) 585–591.

[5] F. Schlichting and H. Kersten, *EPJ Techniques and Instrumentation* 10 (2023) 19.

[6] J. Benedikt et al., *J. Phys. D: Appl. Phys.* 45 (2012) 403001.

## Topical Symposium on Sustainable Surface Engineering Room Golden State Ballroom - Session TS1-ThP

### Coatings for Batteries and Hydrogen Applications Poster Session

**TS1-ThP-1 Room Temperature DC Sputtered  $V_2O_5$ -Based Flexible Robust and Transparent Electrode Over Polymeric PVA Substrate for Green Supercapacitor Applications, Habeebur Rahman [h\_rahman@ph.iitr.ac.in], Davinder Kaur, Indian Institute of Technology Roorkee, India**

This work presents a flexible, robust, and transparent electrode for green supercapacitor device. For biodegradability, a polymeric polyvinyl alcohol (PVA) substrate was utilized for the supercapacitor electrode development. To ensure a robust electrical connection, partially embedded copper contact was made during the substrate development. The vanadium pentoxide active layer was sputter coated at room temperature for the supercapacitor transparent electrode formation. In particular, the active element was fabricated in two different layers possessing an interface in between that assisted in the current collection. The sputtered components were systematically studied using various materials characterization tools. The two similar electrodes were then assembled with an aqueous  $Na_2SO_4$  electrolyte-soaked glassy fiber separator to form the supercapacitor device. The two electrode mode electrochemical measurements demonstrated a wide 1.3 V voltage window with a remarkable 178.7 F/g specific capacitance at 10 mV/s scan rate. It delivered 9.6 kW/kg power density at 3.5 Wh/kg energy density. It retains the 82 %, and 67.3 % capacitance after 10,000, and 18,000 charging-discharging cycles respectively. Further, the device exhibited negligible performance loss upon bending, twisting, and stretching and showed excellent stability with device-to-device variation. In addition, the biodegradability of the electrode was tested in water and moist soil, which illustrated quick degradation. The transparency of the electrode was determined by UV Vis spectroscopy that demonstrated 70 % transmittance in the visible region. Therefore, the biodegradable PVA substrate, environment-friendly  $Na^+$  ion charge storage, and non-toxic  $V_2O_5$  active layer combined together to procure a green energy storage device. The excellent mechanical flexibility of the device and the transparent nature of the electrode make it suitable for modern-day advanced energy storage technology.

**TS1-ThP-2 Y-doped  $Li_7La_3Zr_2O_{12}$ (Y-LLZO) Based all Solid-State Lithium Ion Battery Prepared by Colloidal Coating Processes, Yen-Yu Chen [yychen@mail.npust.edu.tw], Guang-Yi Yao, National Pingtung University of Science and Technology, Taiwan**

All solid-state lithium ion batteries (ASSLIBs) were widely investigated due to safety issue and higher electrical performance. In this study, Y-doped  $Li_7La_3Zr_2O_{12}$  (Y-LLZO)-based solid electrolyte coatings on the  $LiCoO_2$  (LCO)-based cathode substrate with C/Si anode printed on the coatings were prepared. The Y-LLZO powders were synthesized by a solid-state reaction method. Several properties were analyzed including microstructures by scanning electron microscopy (SEM) and transmission electron microscopy, crystal phases by the X-ray diffraction (XRD) method, electrical performance by electrochemical impedance spectroscopy (EIS) and battery testing system. The Y-LLZO coatings after sintered at 1100°C for 12 h show highly dense configuration on the LCO-based cathode substrate. The thicknesses of the coating layers are around several to ten more micrometers. Only a few of pores can be found in the coating layers. The crystal phases after sintering were including the major LLZO garnet and a rare of  $La_2Zr_2O_7$  phases. The interface between Y-LLZO and LCO grains shows slightly inter-diffusion behavior. The electrical conductivity of Y-LLZO is around  $10^{-4} \sim 10^{-5} S \cdot cm^{-1}$ . The more details will be reported in the presentation.

**TS1-ThP-3 MXene Based Thin Film Nonstructural Composite for Oxygen Evolution Electrocatalysis, Md Zaved Hossain Khan [zaved.khan@just.edu.bd], Romzan Ali, Jashore University, Independent Road, Jashore, Bangladesh**

There is a continuous high demand for an effective electrocatalytic-oxygen evolution reaction (OER) to mitigate energy crises by offering renewable energy sources. Metal oxide and metal carbide are well regarded electrocatalysts for water splitting; however, they produce sluggish reaction

kinetics and further require higher energy to launch OER reaction. The transitional metal carbide MXene coupled with earth abundant metal oxide show good catalytic performance overcoming potential barrier by enhancing reaction kinetics. Therefore, MXene ( $Ti_3C_2T_x$ ) coupled earth-abundant metal oxide nanocomposite ( $Zn_{0.92}Cu_{0.04}Ni_{0.02}O_2$ ) based electrocatalyst for OER is presented in this work for the first time.  $Ti_3C_2T_x$  enhances electroconductivity, offers large surface area, increases the number of active sides of the electrocatalyst and enhances the electrocatalytic performances. A simple hydrothermal method was used for the fabrication of the electrocatalyst  $Zn_{0.92}Cu_{0.04}Ni_{0.02}O_2@MXene$ . The proposed electrocatalyst exhibits an extremely low overpotential of 169.5 mV at  $10 mA \cdot cm^{-2}$  and long-term stability (higher than 10 hours) in an acidic condition in 1M  $H_2SO_4$  solution. This work demonstrates a facile and an effective strategy to boost up the electrocatalytic performance of OER in an acidic medium aiming for the design of efficient and cost effective electrocatalyst.

**TS1-ThP-4 Pseudocapacitive Kinetics in Synergistically Coupled  $MoS_2$ - $Mo_2N$  Nanowires with Enhanced Interfaces towards All-Solid-State Flexible Supercapacitors, Bhanu Ranjan [branjn@ph.iitr.ac.in], Davinder Kaur, Indian Institute of Technology Roorkee, India**

Pseudocapacitive kinetics in rationally engineered nanostructures can deliver higher energy and power densities simultaneously. The present report reveals a high-performance all-solid-state Flexible symmetric supercapacitor (FSSC) based on  $MoS_2$ - $Mo_2N$  nanowires deposited directly on stainless-steel mesh ( $MoS_2$ - $Mo_2N/SSM$ ) employing Direct current (DC) Reactive Magnetron Co-sputtering technology. The abundance of synergistically coupled interfaces and junctions between  $MoS_2$  nanosheets and  $Mo_2N$  nanostructures across the nanocomposites results in greater porosity, increased ionic conductivity, and superior electrical conductivity. Consequently, the FSSC device utilizing Polyvinyl alcohol-sodium sulfate ( $PVA-Na_2SO_4$ ) hydrogel electrolyte renders an outstanding cell capacitance of  $252.09 F \cdot g^{-1}$  ( $44.12 mF \cdot cm^{-2}$ ) at  $0.25 mA \cdot cm^{-2}$  and high rate performance within a wide 1.3 V window. Dunn's and  $b$ -value analysis reveals significant energy storage by surface-controlled capacitive and pseudocapacitive mechanisms. Remarkably, the symmetric device boosts tremendous energy density  $\sim 10.36 \mu Wh \cdot cm^{-2}$  ( $59.17 Wh \cdot kg^{-1}$ ), superb power density  $\sim 6.5 mW \cdot cm^{-2}$  ( $37.14 kW \cdot kg^{-1}$ ), ultrastable long cyclability ( $\sim 93.7\%$  after 10,000 Galvanostatic charge-discharge (GCD) cycles) and impressive mechanical flexibility at  $60^\circ$ ,  $90^\circ$ , and  $120^\circ$  bending angles.

#### References:

1. Bhanu Ranjan and Davinder Kaur, *Small*, 20 (20), 2307723 (2024). <https://doi.org/10.1002/sml.202307723>
2. Bhanu Ranjan and Davinder Kaur, *ACS Applied Materials & Interfaces*, 16 (12), 14890-14901 (2024). <https://doi.org/10.1021/acsami.4c00067>
3. Bhanu Ranjan and Davinder Kaur, *ACS Applied Energy Materials*, 7 (10), 4513-4527 (2024). <https://doi.org/10.1021/acsaem.4c00563>
4. Bhanu Ranjan and Davinder Kaur, *Journal of Energy Storage*, 71, 108122. (2023). <https://doi.org/10.1016/j.est.2023.108122>
5. Bhanu Ranjan, Gagan Kumar Sharma, and Davinder Kaur, *Applied Surface Science*, 588, 152925 (2022). <https://doi.org/10.1016/j.apsusc.2022.152925>
6. Bhanu Ranjan, Gagan Kumar Sharma, and Davinder Kaur, *Applied Physics Letters*, 118 (22), 223902 (2021). <https://doi.org/10.1063/5.0048272>
7. Bhanu Ranjan, Gagan Kumar Sharma, Gaurav Malik, Ashwani Kumar, and Davinder Kaur, *Nanotechnology*, 32 (45), 455402 (2021). <https://doi.org/10.1088/1361-6528/ac1bdf>

**TS1-ThP-5 PVD-Coated Interconnects for Solid Oxide Electrolysers, Giuseppe Sanzone [giuseppe.sanzone@teercoatings.co.uk], Teer Coatings Ltd, UK; Kun Zhang, University of Birmingham, UK; Susan Field, Hailin Sun, Teer Coatings Ltd, UK; Jangwoo Seo, Hyo Ki Hwang, In-sung Lee, E&KOA Co., Republic of Korea; Parnia Navabpour, Teer Coatings Ltd, UK**

Achieving net-zero emissions by 2050 continues to be a significant challenge for the global energy sector. Hydrogen, and specifically green hydrogen can play a key role in decarbonisation, as it has the potential to be used as fuel for power and transportation. Green hydrogen can be produced in several ways using renewable energy sources like solar, wind or nuclear, through high- and low-temperature electrolysis, various thermochemical and photochemical processes. Water electrolysis is the most effective technique which is capturing the market's attention.

# Thursday Afternoon, May 15, 2025

Amongst the electrolyser technologies, solid oxide electrolysers (SOE) are the most energy efficient. However, there are challenges related to their performance, lifetime, durability and cost, along with the scale-up from kW to MW level. The interconnect plays an important role as a current collector and a physical barrier that separates the electrodes between cells. It has to meet technical requirements such as matching thermal expansion coefficient to other (ceramic) layers, high thermal and electrical conductivities, formation of a dense low-resistive oxide layer in redox atmospheres, and high thermomechanical strength at elevated temperatures (600 to 900 °C). The metallic interconnects employed in the SOC stack operated usually suffer high temperature corrosion and Cr-evaporation in the steam-rich environment at high temperature, leading to material failure of interconnects and degradation electrolysis stack. There is a need to control the chromium (VI) diffusion from the metallic interconnects and its poisoning of the air electrode to achieve increased electrolyser durability and performance.

This work presents conducting, protective spinel oxide coatings deposited by PVD method in order to reduce chromium evaporation from the interconnects. These coatings benefit from a dense structure as well as scalability, allowing high performance and making them suitable for commercialisation. The effect of coating thickness and composition on high temperature stability and chromium evaporation rate from ferritic stainless steel has been investigated.

**TS1-ThP-6 Porous BiVO<sub>4</sub> Thin Films Deposited by Radiofrequency Co-Sputtering as Photoanode for H<sub>2</sub> Production by Water Splitting**, *Mathias Goutte, Angélique Bousquet [angelique.bousquet@uca.fr], Eric Tomasella, Institut de Chimie de Clermont-Ferrand, France; Guillaume Monier, Institut Pascal, France; Thierry Sauvage, CEMHTI, France*

H<sub>2</sub> is considered as a potential new fuel which will participate to decarbonate the mobility sector. Unfortunately, this molecule is nowadays mainly formed from fossil gases, and so, does not meet criteria for the sustainable development. Efforts are then engaged to develop new clean H<sub>2</sub> synthesis technologies such as water photo(-electro)lysis. However, this latter method still suffers from low global efficiency because of limited properties of photoanode. Thanks to its band gap in the visible range (near 2.4 eV) and its low valence band, Bismuth vanadate BiVO<sub>4</sub> is one of the most promising candidate for this application.

In this paper, we studied the deposition of BiVO<sub>4</sub> thin films by radiofrequency magnetron co-sputtering of Bi and V targets into Ar/O<sub>2</sub> atmospheres. By tailoring the target powers, we were able to deposit coatings with various V/Bi ratios (determined by Rutherford Backscattering Spectroscopy). Since these as-deposited films are amorphous, thermal post-treatments were used to crystallize them. Interestingly, this treatment leads also to the development of porosity into the films thickness (observed by SEM), which will be beneficial to increase contact surface area with water. After 2 hours at 450°C in air, XRD analysis shows that BiVO<sub>4</sub> in monoclinic phase is mainly formed. This phase could be associated to Bismuth or Vanadium oxides ones for non-stoichiometric films. The XPS also confirms these heterojunctions formation following the shift of binding energy positions. Analysis by ellipsometry and UV-visible spectroscopy shows, that the films exhibit direct band gaps between 2.4 and 2.6 eV, while flat band voltages from -0.05 to -0.13 V (vs RHE) are deduced from the Mott-Schottky technique. Hence, diagram with band positions can be drawn for each thin film, indicating that their valence band positions are convenient for O<sub>2</sub> production. Stoichiometric film, that exhibits the lower valence band, also presents the higher photo-current density of 0.05 mA/cm<sup>2</sup> at 1.3 V vs RHE and this current density remains high under irradiation for more than one hour, while significant drop of 75% has usually been reported for electrodes made from powder.

To go further, Bismuth metallic nanoparticles were added on the top surface of BiVO<sub>4</sub> thin film by sputtering the Bismuth target in pure Argon during very short times. The presence of metallic nanoparticles, thanks to heterojunction and plasmonic effect, highly enhances the measured photocurrent, keeping a good stability in time.

**TS1-ThP-7 HiPIMS Deposition of Ti<sub>x</sub>N Coatings for Oxygen Evolution Reaction Catalysts**, *Yi-Cho Tsai [jesskoghjk@gmail.com], National United University, Taiwan; Ying-Hsiang Lin, National United University, Taiwan; Siang-Yun Li, Thi Xuyen Nguyen, Chia Ying Su, Ruei Chi Lin, Jyh-Ming Ting, National Cheng Kung University, Taiwan; Wan-Yu Wu, National United University, Taiwan*

Electrochemical reactions, particularly hydrogen and oxygen evolution reactions (HER/OER), are crucial for advancing clean energy technologies. However, current OER catalysts primarily rely on noble metals like Ir and Ru,

which are expensive and less durable. Transition metal nitrides (e.g., Ti, Fe, Co, Ni) have gained attention due to their high conductivity and cost-efficiency. TiN, specifically, shows metal-like conductivity ( $3.34 \times 10^{-7} \Omega\text{-cm}$ ), strong resistance to acids/alkalis, oxidation, and chemical inertness, making it ideal for OER. In this study, High Power Impulse Magnetron Sputtering (HiPIMS) was used to deposit Ti<sub>x</sub>N films on Ni foam, chosen for its high porosity (98%) and conductivity, to enhance the active surface area. HiPIMS, with its high plasma density and strong film adhesion, is superior to traditional DC sputtering, particularly for complex substrate structures. The Ti<sub>x</sub>N film with 63.1 at.% Ti content showed an overpotential of 377 mV at 50 mA/cm<sup>2</sup> ( $\eta_{10}$ ), a Tafel slope of 121.4 mV/dec, and a charge transfer resistance (R<sub>ct</sub>) of 3.05  $\Omega$ , outperforming commercial RuO<sub>2</sub> (421 mV). Further optimization of the Ti/N ratio revealed that a film with 52.6 at.% Ti and 47.4 at.% N had the best performance, achieving an overpotential of 333 mV, a Tafel slope of 97.8 mV/dec, and R<sub>ct</sub> of 1.95  $\Omega$ . This demonstrates that a near 1:1 stoichiometric ratio in TiN significantly enhances conductivity and electron transfer, thus improving OER efficiency. Preliminary analyses using EDX, XPS, XRD, TEM, and SEM suggest that adjusting the Ti/N ratio may impact the catalytic activity of the films. Based on the current test results, the optimized Ti<sub>x</sub>N films show promising potential in 1 M KOH electrolyte, indicating their prospective application as cost-effective and durable OER catalysts.

## Topical Symposium on Sustainable Surface Engineering Room Golden State Ballroom - Session TS2-ThP

### (Photo)electrocatalysis and Solar/Thermal Conversion Poster Session

**TS2-ThP-1 Heteroepitaxial Growth of ZnTiN<sub>2</sub> for Optimization of Optoelectronic Properties**, *Mellie Lemon [Mellie.lemon@nrel.gov], John Mangum, National Renewable Energy Laboratory, USA; Anna C. Kundmann, University of California at Davis, USA; Andriy Zakutayev, Ann L. Greenaway, National Renewable Energy Laboratory, USA*

The n-type semiconductor, ZnTiN<sub>2</sub>, has been proposed as a potential photoabsorber in devices for CO<sub>2</sub> reduction. Previous studies of this material focused on the characterization of its properties and optimization of its synthesis. These studies revealed that ZnTiN<sub>2</sub> films exhibit cation-disorder, which reduces the bandgap to ~2eV and that the films form passivating oxide layers under conditions relevant for CO<sub>2</sub>R. Additionally, the crystalline quality and optoelectronic properties of ZnTiN<sub>2</sub> can be improved through heteroepitaxial deposition on sapphire substrates at elevated temperatures and by the addition of ~10 cation % Sn. This study builds on this work to further improve the optoelectronic properties by optimization of the synthesis to reduce unintentional dopants. Removal of defect states in the bandgap reduces the sub-bandgap optical absorption and lengthens photoexcited carrier lifetimes. The films in this study are deposited by reactive RF co-sputtering at elevated temperatures, with optical and electronic measurements and photoelectrochemical experiments used to determine the properties. Characterization of ZnTiN<sub>2</sub> via multiple complementary techniques will lead to fundamental insight into the structure-property relationships of this material and insight into how to improve its efficiency for PEC applications. Future efforts will focus on examining the role of polarity on charge transport in ZnTiN<sub>2</sub> and across its interfaces.

**TS2-ThP-2 Synthesis and Photocatalytic Efficiency of Bismuth-Copper Selenide Chitosan Microspheres for Micropollutant Degradation under Solar Radiation**, *Sayed Suliman Shah [ss.shah@unistra.fr]*, The Molecular Innovation and Applications Laboratory (LIMA), University of Strasbourg, France

Among the top trending environmental concerns, water pollution has got a serious attention these days. Technological advancement in industrial sectors for manufacture of diverse products particularly micropollutants is the principle reason for discharging the wastewater of unit operations. In this context various percussive strategies have been followed among which photocatalysis is considered cheap, ideal and eco-friendly in nature. In this work, an effort has been made to have synthesized an effective catalyst bismuth-copper selenide chitosan microspheres via solvothermal process in order to degrade micropollutants in wastewater under solar radiations. The synthesized catalyst nano composite was fabricated with polyaniline (PANI) being conductive in nature for better photocatalytic efficiency and characterized with FTIR, SEM, EDX and XRD. The photocatalytic nature of

the catalyst was examined by varying different variables namely pollutant concentration, catalyst dose, pH, degradation time and batches.

**TS2-ThP-3 Dual-Metal Doped Perovskite Oxides: High-Performance Fenton-Like Catalysts for Antibiotic Degradation, Thi Xuyen Nguyen [nguyenxuyen1511@gmail.com], Yong Yu, Chia-Ying Su, Jyh-Ming Ting, National Cheng Kung University (NCKU), Taiwan**

Water pollution from organic wastewater has become a significant global concern. The Fenton-like process is an effective and practical method for reducing organic pollutants. In this study, we synthesized a dual-metal of Cu and Mn co-doped in LaFeO<sub>3</sub> perovskite oxide using a simple co-precipitation method. The obtained La(FeCuMn)O<sub>3</sub> achieves a remarkable 90.3% removal rate of high-concentration tetracycline (40 ppm) within 30 min without requiring additional light irradiation. This performance is six times higher than that of pristine LaFeO<sub>3</sub> and surpasses that of single-metal-doped samples (LaFeCuO<sub>3</sub> and LaFeMnO<sub>3</sub>). We found that the oxygen vacancies induced by doping can enhance the pollutant adsorption, while Cu<sup>+</sup> facilitates the regeneration of Fe<sup>2+</sup> and Mn promotes charge redistribution. The synergistic effects of dual-metal co-doping substantially enhance Fenton activity.

**TS2-ThP-4 3D Atmospheric Plasma Beam TiO<sub>2</sub> Lamination of Porous Structures for Manufacturing Electro-Photocatalytic Reactors, Yuri Glukhoy [glukhoy1@aol.com], Nanocoating Plasma Systems Inc, USA; Michael Ryaboy, nanocoating plasma systems inc, USA**

Nanocoating Plasma Systems has developed electro-photocatalytic (EPCO) reactor with matrix's honeycomb structure made from welded together quartz capillaries with ID 0.5 mm and 7 mm long/ Due to such a design component like electric field applied to the matrix can increase the area of disinfection. When exposed to moisture (water vapor) and light, TiO<sub>2</sub> undergoes excitation that produces electron-hole pairs, which in turn react with water molecules to form OH<sup>·</sup> and other reactive species, this reaction is further enhanced by the electric field which not only accelerates the production of hydroxyls but also drives their propagation into the surrounding space. This phenomenon called chain reaction is the process, where the ejected from the matrix and energized by a high voltage hydroxyl radicals collide with water molecules in the room to produce secondary hydroxyl radicals. It is essential for extending the disinfecting effects over larger areas and reducing pathogen concentrations rapidly. NPS have used the focused the RF plasma beam carrying the TiO<sub>2</sub> nanoparticles is commonly employed to provide the 2D nanocoating for different application. However, transition to the TiO<sub>2</sub> lamination of the 3D object like the matrix with the capillaries' holes with a high aspect ratio is complicated by the negative charge passivating the entrance of these holes and rejecting the beam. ionize gases and control plasma behavior at atmospheric pressure. This phenomenon called Debye Plasma Law makes impossible lamination of the matrix. To breach this law NPS has applied the auxiliary RF discharge at the exit of the capillary holes. It generates the hollow discharge inside the hole neutralizing the parasitic charge at the entrance. Therefore, the plasma beam is able to penetrate into the interior of the holes, where the TiO<sub>2</sub> coating is deposited on the inner walls. This technique not only overcomes the challenges of applying uniform coatings to complex geometries (such as the small and intricate capillary structures) but also, taking in account the electrical component, ensures enhancing chain reaction to enlarge the disinfection area. Involving the RF plasma beam helps to solve another problem like a low photo-catalytic activity of the commercial TiO<sub>2</sub> nanoparticles with a bandgap about 3.2 eV limited just by UV that includes just 4% of solar spectrum. Therefore, besides generation the fine plasma beam, the nitrogen plasma discharge provides the N-doping of the TiO<sub>2</sub> nanoparticle generates the fine plasma beam particles reducing the bandgap up to 2.75 eV for absorption of all spectrum of visible spectrum.


# Friday Morning, May 16, 2025

## Tribology and Mechanics of Coatings and Surfaces

### Room Palm 3-4 - Session MC1-2-FrM

#### Friction, Wear, Lubrication Effects, & Modeling II

**Moderators:** Julien Keraudy, Oerlikon Balzers Coating AG, Liechtenstein, Pantcho Stoyanov, Concordia University, Canada

8:00am **MC1-2-FrM-1 Linking Atomic-Scale Surface Structure and Friction via Multiscale Modelling: The Case of Carbon-Based Coatings and Tribofilms**, *Gianpietro Moras [gianpietro.moras@iwm.fraunhofer.de]*, Fraunhofer IWM, MicroTribology Center , Germany **INVITED**

Carbon surfaces play a fundamental role in tribology. There is not only the case of carbon-based coatings, but also the less obvious case of low-friction, carbon-based tribofilms deposited on other materials by liquid or solid lubricants. In all cases, friction in dry and boundary lubrication conditions depends on the atomic structure of the sliding surfaces. A stable chemical passivation of surface dangling bonds is a prerequisite for low friction and wear. However, even subtle changes in surface chemistry can cause the friction coefficient of passivated carbon interfaces to vary significantly. In this talk, I will present the results of multiscale simulation studies that combine quantum mechanics, molecular dynamics and contact mechanics to shed light on the relationships between the chemical structure of carbon surfaces and friction.

I will initially focus on superlubricity (friction coefficient  $< 0.01$ ) with diamond-like carbon coatings and silicon nitride. Stable superlubricity over a wide range of operation conditions has been recently achieved at Fraunhofer IWM in plain-bearing test rigs using glycerol as a lubricant. Hydrodynamic superlubricity with glycerol is possible at high temperature and facilitated by the presence of water. However, the mechanisms responsible for superlubricity in boundary lubrication with glycerol are still under debate. Our simulations reveal a complex mechanochemical process involving the tribochemical decomposition of glycerol molecules at surface asperity contacts, the plastic deformation of the resulting H-, O- or N-containing amorphous carbon tribofilm and the formation of partially aromatic surface regions. These smooth and unreactive surfaces enable superlubricity even when asperity contacts run dry or are separated by nanometric, highly viscous glycerol films.

In the second part of my talk, I will extend the study to the effects of boron and fluorine. Our simulations suggest that hydroxyl groups that normally passivate carbon surfaces in humid environments can be activated by boron and form B-O dative bonds across the tribological interfaces, leading to a mild friction increase. Surface passivation by C-F bonds, instead, is very stable. This is the basis of the exceptional tribological properties of some perfluorinated carbon materials, but also of their accumulation in the environment and in biological systems. Our simulations provide answers to open questions about their friction mechanisms that may be useful in the search for alternatives: Why are perfluorinated carbon surfaces polar and hydrophobic? Why are they more slippery than their hydrogenated analogues? Why is PTFE non-sticky but forms transfer films on PTFE-lubricated steel surfaces?

8:40am **MC1-2-FrM-3 Impact of Gaseous Environments on the Tribological Performance of Steel and Advantages of DLC Coatings**, *Pierre-Francois Cardey [Pierre-Francois.Cardey@cetim.fr]*, Cetim, France **INVITED**

The tribological performance of materials is strongly influenced by the gaseous environment, where composition and pressure alter wear and friction mechanisms. In particular, the energy and transportation industries are paying increasing attention to hydrogen-related issues due to its potentially embrittling effects and impacts on tribological performance. At CETIM, a pin-on-disc tribometer was developed to analyze these interactions under various gaseous atmospheres across a wide range of temperatures and pressures.

This study focuses on two steel grades (high carbon and chromium steel 52100, and austenitic stainless steel 316L), tested in nitrogen, helium, and hydrogen atmospheres, with variations in contact pressure, temperature, and sliding speed. The results highlight how these environments affect the formation of protective oxide layers, which play a key role on friction and wear. The effects of hydrogen are also specifically studied due to its embrittling and reducing properties.

In this context, Diamond-Like Carbon (DLC) coatings emerge as a promising solution, acting both as a barrier to hydrogen diffusion and as a tribological enhancement in harsh gaseous environments. This study provides a comprehensive approach to optimizing material selection and surface

treatments to improve the durability of components exposed to challenging industrial gaseous atmospheres.

9:20am **MC1-2-FrM-5 Study of Microabrasive Wear on TiB<sub>2</sub>/TiB Hard Layer Formed on Ti6Al4V Alloy**, *Marco A Melo-Pérez [mmelop@ipn.mx]*, Av. Instituto politécnico nacional, Mexico; *German A. Rodríguez-Castro, Alfonso Meneses-Amador, Ezequiel A. Gallardo-Hernández, Israel Arzate-Vázquez, José A Nieto-Sosa*, Instituto Politécnico Nacional, Mexico

Micro-abrasion wear resistance of TiB<sub>2</sub>/TiB layers was studied by ball cratering tests formed on Ti<sub>6</sub>Al<sub>4</sub>V by powder-pack boriding. The boriding process was carried out at 1273 K over 5 and 20 h of treatment resulting in the formation of TiB<sub>2</sub>/TiB layer with a maximum thickness of 10  $\mu$ m. The layers' mechanical characterization was carried out using Berkovich instrumented indentation, obtaining hardness greater than 2.5 GPa. The wear coefficient of TiB<sub>2</sub> phase was evaluated by micro-abrasion tests using SiC particles dissolved in deionized water as abrasive slurry. The results demonstrated that the titanium borides have wear coefficients higher than Ti<sub>6</sub>Al<sub>4</sub>V and improve their micro-abrasion wear resistance. Furthermore, a wear-mode map was developed to identify the two and three body abrasion mechanisms and the transition between them modifying the concentration of SiC in the slurry and the magnitude of applied load.

9:40am **MC1-2-FrM-6 Tribology of Protective CrN Coatings in Arctic Environmental Conditions**, *Forest Thompson [forest.thompson@sdsmt.edu]*, *Elyse Jensen, Nathan Madden, Grant Crawford*, South Dakota School of Mines and Technology, USA

The friction and wear behavior of protective CrN coatings has been shown to be highly sensitive to Arctic environmental conditions, such as the combination of cold temperatures ( $< 20$  °C) with low dew points ( $< -30$  °C). To advance the mechanistic understanding of the tribological response of CrN to Arctic environments, the relationships between coating architecture, environmental conditions, coefficient of friction, and wear resistance were investigated. A series of CrN coatings were deposited onto stainless steel substrates with varying adhesion layer compositions (Cr, Ti, CrN) by reactive pulsed DC magnetron sputtering. Microstructural characterization of the as-deposited coatings was conducted via laser scanning confocal microscopy, electron microscopy, energy dispersive x-ray spectroscopy, and x-ray diffraction. Linearly reciprocating sliding wear tests were conducted using a ball-on-flat tribometer. The tribometer was equipped with an active cooling stage and a dry air source to achieve coating surface temperatures and environmental dew points representative of conditions that would be encountered in Arctic service environments. After tribological testing, focused ion beam milling and transmission electron microscopy were utilized to analyze specific sites within wear scars and to characterize wear debris structure. The results from this work contribute to efforts related to the design of protective coatings for extreme environments, such as those encountered at Earth's polar regions.

## Plasma and Vapor Deposition Processes

### Room Palm 1-2 - Session PP4-FrM

#### Deposition Technologies for Carbon-based Coatings

**Moderators:** Dr. Ivan Kolev, IHI Hauser Techno Coating B.V., Netherlands, Dr. Biplab Paul, PLATIT AG, Switzerland

8:20am **PP4-FrM-2 Insights Into Solid Lubrication Processes of DLC Films Thanks to Analytical Tribology**, *Julien Fontaine [julien.fontaine@ec-lyon.fr]*, *Antoine Normant, Jules Galipaud, Frédéric Dubreuil*, LTDS, CNRS / Ecole Centrale de Lyon, France **INVITED**

Diamond-Like Carbon coatings may behave as very good solid lubricants, providing a good combination of tribological environment and coating composition is ensured. For instance, highly hydrogenated amorphous carbon (a-C:H) films may lead to super low friction regime ( $\mu < 0.01$ ) under ultra-high vacuum, at least for a limited time. What are the tribological phenomena that allow for such performance, and what brings an end to this unique regime? To answer such questions, a traditional approach consist in performing some surface analysis after the experiments, inside and outside the wear tracks. These analyses are frequently morphological, structural or chemical, sometimes mechanical. While these informations are paramount for the understanding of the surface degradations during sliding, they don't provide information about the respective roles of these degradation on the evolution of the tribological response of the contact. In this work, we use a high resolution environment-controlled tribometer, based on a six axes force sensor, to probe the tribological response of a steel pin / a-C:H film contact, either by crossing existing wear tracks or by

# Friday Morning, May 16, 2025

shifting the tracks to slide on pristine surfaces. This original approach helps understanding the respective role of surface modifications on the a-C:H coated flat or on the facing steel pin on the achievement of superlow friction. These experiments are combined with more traditional analytical means, like in situ XPS, AES and REELS analyses or ex situ SEM or AFM observations. The growth of a carbon-rich tribofilm on the steel counterpart appears necessary, but not sufficient to reach superlow friction. Changes on the topography and chemistry of the a-C:H film seems also paramount, with a smoothening of the a-C:H asperities and an increase of the  $sp^2$  Carbon content. The respective role of these phenomena on the solid lubrication process of a-C:H film will be discussed.

9:00am **PP4-FrM-4 Diamond Like Carbon (DLC) Ablators for Fusion Energy, Nicolas Vargas [nicolas.vargas@ga.com], Kuo-Chun Chen, Priya Raman, Martin Hoppe, Fred Elsner, General Atomics, USA**

On December 5, 2022, after 4 decades of technical improvements, NIF reached "ignition" for the first time, achieving a 150% energy yield and with it unlocking the promise of unlimited energy supply for human society. This historical achievement was enabled by the many esoteric and ultra-high precision Inertial Confinement Fusion (ICF) components General Atomics manufactures and assembles into complex target assemblies, which are subsequently fielded, on national facilities such as the National Ignition Facility (NIF) at Lawrence Livermore National Laboratory (LLNL). Each target assembly has an ablator capsule at its center. HDC (high-density carbon), a form of nanocrystalline diamond, is the current choice for the ablator in these experiments. However, as NIF laser power scales up, Diamond Like Carbon (DLC) ablators are looking increasingly attractive.

Diamond Like Carbon (DLC) material has captured the interest of the laser fusion community due to its unique properties. DLC's amorphous microstructure, high density, and ability to be doped makes it an attractive choice for ablator material. At General Atomics, we developed a Hollow Cathode Radio Frequency Plasma Assisted Chemical Vapor Deposition (HC-RF PACVD) system to deposit DLC coatings on both flat and spherical substrates.

Our DLC capability, with precisely tuned hydrocarbon and carrier gas compositions, enables the deposition of thick, dense, and smooth Diamond-Like Carbon coatings for experiments in Inertial Fusion Technology. In this presentation, we will provide an overview of our major results to create free-standing DLC capsules, including the fabrication, characterization and post processing techniques.

This work performed under the auspices of General Atomics under Internal Research and Development.

9:20am **PP4-FrM-5 Multifunctional Nanocomposite Coatings: Aerosol Assisted Plasma Deposition, alexis aussonne [alexis.aussonne@lcc-toulouse.fr], LCC, Laplace, France**

Amorphous carbon thin coatings are widely used to protect surfaces due to their high hardness and their chemical resistance<sup>1</sup>. They can be deposited by various PVD methods such as ion beams<sup>2</sup>, magnetron sputtering<sup>3</sup> or by PECVD<sup>4</sup> by injection a gaseous precursor into a plasma. PECVD allow to control the structure of the carbon coating by choosing the precursor. However, the continuous injection of gas does not allow to work with complex precursors such as mixtures, solutions containing reactive molecules or colloidal solutions.

An alternative way to inject the precursor in the plasma chamber would be by directly injecting a liquid as an aerosol in a pulsed manner. This would allow to work with liquids of a much more complex composition and thus reaching interesting coatings. Furthermore, by injecting colloids it is possible to deposit various nanocomposite<sup>5</sup> coating encapsulating various kind of nanoparticles (metallic, oxide, sulfide).

Herein we report the carbon deposition by a low pressure RF plasma with pulsed injection of a pentane aerosol. Carbon layers were characterized by Raman and Infrared spectroscopies. Additionally, colloidal solutions of MoS<sub>2</sub> nanoparticles stabilized in pentane were injected to deposit nanocomposite thin films.

(1) Ito, H.; Yamamoto, K. *Mechanical and Tribological Properties of DLC Films for Sliding Parts*.

(2) Aisenberg, S.; Chabot, R. Ion-Beam Deposition of Thin Films of Diamondlike Carbon. *J Appl Phys* 1971, 42 (7), 2953–2958.

(3) Sanchez, N. A.; Rincon, C. Characterization of Diamond-like Carbon  $\checkmark$  DLC . Thin Films Prepared by r . f . Magnetron Sputtering. 2000, 7–10.

(4) Nobuki Mutsukura, K. Y. Deposition of DLC Films in CH<sub>4</sub>/Ar and CH<sub>4</sub>/Xe r.f. Plasmas. *Diam Relat Mater* 1995.

(5) Carnide, G.; Cacot, L.; Champouret, Y.; Pozsgay, V.; Verdier, T.; Girardeau, A.; Cavarroc, M.; Sarkissian, A.; Mingotaud, A. F.; Vahlas, C.; Kahn, M. L.; Naudé, N.; Stafford, L.; Clergereaux, R. Direct Liquid Reactor-Injector of Nanoparticles: A Safer-by-Design Aerosol Injection for Nanocomposite Thin-Film Deposition Adapted to Various Plasma-Assisted Processes. *Coatings* 2023, 13 (3), 630–648.

9:40am **PP4-FrM-6 Amorphous Carbon Thin Films for Electron Multipacting Mitigation in the Large Hadron Collider Vacuum System, Valentine PETIT [valentine.petit@cern.ch], Pedro Costa Pinto, Mathias Gegg, Christos Kouzios, Giovanni Marinaro, Andrea Rocchi, Guillaume Rosaz, European Organization for Nuclear Research, Switzerland**

In modern particle accelerators with high intensity and positively charged beams, electron multipacting due to the exponential multiplication of electrons in the vacuum beam pipes results in the build-up of so-called electron clouds. In the Large Hadron Collider (LHC) at CERN, electron clouds lead to beam quality degradation, pressure rises and heat loads to the cryogenic sections hosting the superconducting magnets. Electron clouds are recognized as a critical limitation to reach the very high beam intensity required for the High-Luminosity upgrade of the LHC (HL-LHC).

To tackle this phenomenon, several mitigation approaches have been developed in the last decades, including clearing electrodes, confinement of electrons by solenoids or lowering of the Secondary Electron Yield (SEY) of the beam pipe surface, the quantity governing the multiplication of electrons. This last approach has been successfully implemented by coating the beam pipes with amorphous carbon thin films, which exhibit an SEY close to unity.

This contribution presents the development and prototyping phases towards the implementation of a coating technology to deposit amorphous carbon along several kilometers of narrow beam lines in-situ, i.e., without removing the superconducting magnets from their positions in the LHC tunnel, located 100 meters underground. The films are deposited by sputtering, using a tandem of 4 mobile targets, powered in HiPIMS mode, that are displaced along the beamlines. We report on the design of the coating system, on the characterization of the coatings, particularly under electron irradiation at 15 K, and on the optimization of the process parameters, considering the constraints for upscaling the technology to kilometers of vacuum pipes within the geometrical constraints of the LHC cryo-magnets.

10:20am **PP4-FrM-8 With Carbon Coatings towards CO<sub>2</sub> Neutrality - Industrialization in Electrochemical and Tribological Applications, Martin Kopte [kopte.martin@vonardenne.com], VON ARDENNE GmbH, Dresden, Germany** INVITED

To date the global mining of fossil fuels continues to increase. As those resources are an integral part of almost any production value chain the CO<sub>2</sub>-equivalent of products needs to be accounted for in a clean balance sheet in every single production step and all the materials involved. The medium-term self-amortization of the CO<sub>2</sub>-equivalent of "active" products, that e.g. can replace fossil energy sources, is a desirable goal towards CO<sub>2</sub>-neutrality. Whereas "passive" products are required to be fabricated in the most efficient and sustainable manner, to keep the footprint as low as possible.

With PVD methods products can be refined to greatly increase in performance efficiency, self-amortization rate and sustainability. Typically, the additional effort of coating is already justified by the functionalization of the product itself. More and more the coating technologies must withstand a thorough review not only for the sake of cost effectiveness but also in terms of its contribution to the CO<sub>2</sub>-equivalent.

Carbon – inherently a good material choice – comes in wide variety of modifications with adjustable properties (e.g. electrical and mechanical) and hence can not only be used in a wide spectrum of electrochemical and tribological applications and thus targeting the scope of sustainable carbon-dioxide-free energy and energy saving solutions.

Paving the way to CO<sub>2</sub>-efficient industrialization of PVD-carbon coating equipment involves a careful consideration of many variables. This work touches on the challenges when it comes to the best choice of optimized materials, processes, methods etc. for engineering and scaling of competitive and efficient coating tools.

**Bold page numbers indicate presenter**

— A —

Abadias, Gregory: CM1-2-ThA-11, 74; CM1-2-ThA-3, **73**  
 Abdrabo, Merna: MD1-1-MoM-1, 4; MD1-2-MoA-1, **13**  
 Abdulsalam, Mohamed: MD-ThP-3, 89  
 Aboutidouane, Mustapha: PP6-MoA-4, **16**  
 Achache, Sofiane: MA4-2-WeM-1, 43  
 Adalati, Ravikant: MB2-1-MoM-6, 3  
 Adam, Caroline: PP2-2-WeA-6, **57**; PP-ThP-7, **90**  
 Adelino Ricardo Barão, Valentim: MD-ThP-1, 88  
 Agüero, Alina: MA1-1-TuM-1, 23  
 Ahangarani Farahani, Farzaneh: PP2-1-WeM-6, 49  
 Al-Akhali, Adham: MB-ThP-2, **83**  
 Ali, Romzan: TS1-ThP-3, 91  
 Alijan Farzad Lahiji, Faezeh: MA3-3-WeM-1, **41**  
 Al-Kassab, Talaat: CM1-1-ThM-3, 62  
 AlMotasem, Ahmed: MC1-1-ThA-7, 78  
 Altaf Husain, Shuhel: MC2-1-TuA-3, 38  
 Altaf, Muhammad Awais: MA4-2-WeM-5, **43**; MA-ThP-2, **82**  
 Alves Freire de Andrade, Catia Sufia: MD-ThP-1, 88  
 Alwen, Adie: CM3-1-ThM-4, 66  
 Ambalkar, Anuradha: IA1-TuM-3, 22  
 Amin, Abdelrahman: MD1-1-MoM-1, 4; MD1-2-MoA-1, 13  
 Andanson, Jean-Michel: TS2-WeA-8, 60  
 Angay, Firat: MA5-ThM-9, 68  
 Aparicio, Francisco J.: MB3-ThM-3, 69  
 Arab Pour Yazdi, Mohammad: MC2-1-TuA-5, **38**  
 Arat, Kerim T.: IA1-TuM-1, **22**  
 Ardrey, Kristyn: MA2-1-TuA-8, 34  
 Argyropoulos, Christos: MB1-WeA-1, 53  
 Arora, Diksha: MB-ThP-20, **87**  
 Artyushkova, Kateryna: CM-ThP-9, 80  
 Arunachalam Sugumaran, Arunprabhu Sugumaran: KYL-MoKYL-1, 8  
 Arzate-Vázquez, Israel: MC1-2-FrM-5, 94  
 Audigié, Pauline: MA1-1-TuM-1, **23**; MA1-1-TuM-3, 24  
 aussonne, alexis: PP4-FrM-5, **95**  
 — B —  
 Babonneau, David: CM1-2-ThA-11, 74  
 Babu, Swetha S.: PP1-2-MoA-2, 14  
 Bahr, Ahmed: MA-ThP-1, 82  
 Balachandran, Prasanna: MA2-1-TuA-8, 34  
 Bandaru, Nithin Kumar: PP6-MoA-3, 16  
 Bandl, Christine: MB3-ThM-9, 70  
 Banerjee, Dev: IA3-TuA-2, 33  
 Bansal, Ananya: MB2-3-TuM-2, 28; MB-ThP-7, 85; TS1-2-MoA-11, **20**  
 Baptiste, Julien: MB2-3-TuM-3, **28**  
 Barad, Hannah-Noa: CM3-2-ThA-1, **75**  
 Baraket, Mira: PP3-WeA-7, **58**  
 Barnholt, Daniel: IA2-1-MoA-5, 10; PP1-1-MoM-5, 6; PP2-2-WeA-3, 56  
 Baroch, Pavel: MA3-3-WeM-3, 42  
 Barranco, Angel: MB3-ThM-3, **69**  
 Barroso, Gilvan: MA1-1-TuM-6, 24  
 Barton, David: CM1-1-ThM-11, 63; CM-ThP-10, 81  
 Barynova, Kateryna: PP1-2-MoA-2, 14  
 Basaran, Ali: MB2-3-TuM-5, 29  
 Basu, Rahul: CM4-1-MoM-3, **2**  
 Bauers, Sage: CM3-1-ThM-2, **65**; MB2-3-TuM-3, 28  
 Bayer, Bernhard C.: MB3-ThM-11, 70

Bayu Aji, Leonardus Bimo: MA4-1-TuA-9, **37**; MA4-3-WeA-2, 52  
 Beake, Ben: MC3-1-WeM-4, **45**  
 Becker, Mary: MB-ThP-16, 87  
 Begum, Kulsuma: MD-ThP-2, 88  
 Behura, Sanjay: MB-ThP-16, 87  
 Belle, Ishwari: IA1-TuM-3, 22  
 Ben Mahmoud, Hatem: CM2-1-ThM-10, 64  
 Benediktová, Anna: MA3-3-WeM-3, 42  
 benrazzouq, Salah-eddine: MA4-1-TuA-3, **36**; MA-ThP-3, **82**  
 Benrazzouq, Salah-Eddine: MA4-2-WeM-3, 43; MA-ThP-5, 83  
 Bergmann, Benjamin: IA3-TuA-1, 33; PP6-MoA-6, 17  
 Bergs, Thomas: PP6-MoA-4, 16  
 Berman, Diana: IA2-2-TuM-1, **23**  
 Bessette, Stéphanie: MA4-2-WeM-12, 44  
 Best, James Paul: MC2-1-TuA-10, 39  
 Beutner, Martin: MA3-1-TuM-6, 27  
 Bhuyan, Abinash: MB-ThP-16, 87  
 Biderman, Norb: CM-ThP-9, 80  
 Biermann, Dirk: PP6-MoA-10, 17; PP6-MoA-8, 17  
 Bignoli, Francesco: CM2-1-ThM-6, 64; MC2-1-TuA-10, 39  
 Billaud, Yann: MB2-1-MoM-4, 3  
 Birch, Jens: MA3-2-TuA-4, 35; MA5-ThM-9, 68  
 Bishara, Hanna: CM2-2-ThA-2, **75**  
 Björk, Emma: TS2-WeA-6, **60**  
 Blanquet, Elisabeth: IA2-1-MoA-6, 11; PP-ThP-2, 89  
 Böbel, Klaus: MC1-1-ThA-1, 76  
 Bobzin, Kirsten: MA-ThP-4, 83; MC3-1-WeM-10, 46; MC3-1-WeM-6, 46; PP1-2-MoA-11, 15; PP1-2-MoA-12, 16; PP6-MoA-1, **16**; PP6-MoA-4, 16; PP6-MoA-6, 17  
 Bocklund, Brandon: MA4-1-TuA-9, 37; MA4-3-WeA-2, 52  
 Boebel, Klaus: CM1-2-ThA-6, 73; TS3-TuA-5, 39  
 Bohn, Andre: CM3-1-ThM-4, **66**  
 Bol, Ageeth: PP5-TuM-1, **30**  
 Bol, France - Emmanuelle: PP5-TuM-7, 31  
 Bolelli, Giovanni: PP2-2-WeA-3, 56  
 Boltynjuk, Evgeniy: CM2-1-ThM-6, **64**  
 Bolvardi, Hamid: MA5-ThM-5, 67  
 Bonduelle, Audrey: TS2-WeA-8, 60  
 Bonnet, Pierre: TS2-WeA-8, 60  
 Borowy, Jessica: MA-ThP-4, 83  
 Borrás, Ana: MB3-ThM-3, 69  
 Boubtane, Sarra: MA1-1-TuM-7, 25; MA1-1-TuM-8, **25**  
 Bouché, Alexandre: MA-ThP-5, 83  
 Bouissil, Abdelhakim: MA4-2-WeM-1, 43  
 Bousquet, Angélique: TS1-ThP-6, **92**; TS2-WeA-8, **60**  
 Bower, Ryan: KYL-MoKYL-1, 8; PP2-2-WeA-8, 57  
 Bozano, Luisa: CM4-1-MoM-6, 3  
 Braga, Vagner: IA-ThP-1, 81  
 Brault, Pascal: CM-ThP-3, 79  
 Bravo, Luis: MA2-2-WeM-4, 41  
 Breidenstein, Bernd: IA3-TuA-1, 33  
 Brenning, Nils: PP1-2-MoA-2, 14  
 Brito, Alana: IA2-1-MoA-1, 10  
 Broeckmann, Christoph: PP1-2-MoA-11, 15  
 Brown, Stephen: PP6-MoA-11, **18**  
 Brumley, Jennifer: MB-ThP-16, 87  
 Bruns, Sebastian: CM2-1-ThM-4, 64  
 Buenos Ayres de Castro, Daniela: MD-ThP-1, 88  
 Bumgardner, Joel: MD1-1-MoM-4, 4

Burant, Britney: PP1-1-MoM-6, 6  
 Bürgel, Jan Lukas: CM3-1-ThM-8, 66; CM-ThP-7, 80  
 Burtscher, Michael: MB3-ThM-9, 70  
 Busi, Krishna Sarath Kumar: CM2-1-ThM-4, **64**  
 — C —  
 Cai, Ran: IA2-1-MoA-8, **11**  
 Campos-Silva, I.E.: MA3-2-TuA-3, 35  
 Cancellieri, Claudia: CM4-1-MoM-5, 2  
 Čapek, Jiří: MA3-3-WeM-3, 42; MB3-ThM-10, 70; MB3-ThM-8, 69; PP2-2-WeA-4, 56  
 Cardey, Pierre-Francois: MC1-2-FrM-3, **94**  
 Cardoza-Navarro, Ivan: MB-ThP-15, 86; MB-ThP-17, 87  
 Caruana, Daren J.: PP5-TuM-8, 31  
 Carvalho, Sheila: IA2-1-MoA-1, 10; IA-ThP-1, **81**  
 Casari, Daniele: MB3-ThM-9, 70  
 Castillo Lozada, David: CM4-1-MoM-6, **3**  
 Castillo-Vela, L.E.: MA3-2-TuA-3, 35  
 Cavaleiro, Albano: TS3-TuA-9, **40**  
 Cavarroc, Marjorie: CM-ThP-3, **79**; MA4-3-WeA-3, **52**; PP2-2-WeA-9, 58; PP6-MoA-11, 18  
 Čekada, Miha: MC3-1-WeM-11, 46  
 Čerstvý, Radomír: MA3-3-WeM-2, 41; MA3-3-WeM-3, 42; MB1-WeA-3, 53; MB3-ThM-10, 70  
 Červená, Michaela: MA3-3-WeM-2, 41  
 Chakrabraty, Rajesh: MD-ThP-2, 88  
 Chalopin, Meriadeg: CM1-2-ThA-3, 73  
 Chandra, Ramesh: MB1-WeA-6, **54**; MB2-1-MoM-6, 3; MB2-3-TuM-2, 28; MB-ThP-7, 85; TS1-2-MoA-11, 20  
 Chandran, Puneet: IA2-2-TuM-3, 23; MC3-1-WeM-4, 45  
 Chang, Chi-Lung: MA5-ThM-8, 68  
 Chang, Chi-Yueh: MC2-1-TuA-8, **38**; TS1-2-MoA-4, 19  
 Chang, Li-Chun: MB-ThP-13, 86  
 Chang, Sun-Tang: TS1-2-MoA-3, **19**  
 Chao, Shao-Chun: MB1-WeA-7, **54**  
 Charrière, Renée: MC1-1-ThA-3, 77  
 Chason, Eric: MC2-1-TuA-4, 38  
 Chavee, Loris: MA3-1-TuM-1, 26  
 Chávez, Efraín: PP1-1-MoM-7, 6  
 Chen, Chia-Yun: MB-ThP-4, 84  
 Chen, Erdong: PP2-1-WeM-3, 48; PP2-1-WeM-4, **48**  
 Chen, I-Hsi: MA4-3-WeA-1, 52  
 Chen, Kuo-Chun: PP4-FrM-4, 95  
 Chen, Po-Chun: MD-ThP-4, **89**  
 Chen, Po-Yu: MA4-1-TuA-8, 37; PP2-1-WeM-2, 48  
 Chen, Rou-Syuan: MA3-1-TuM-9, **27**  
 Chen, Shih-Hsun: MA4-1-TuA-1, **36**; MB1-WeA-4, 53  
 Chen, Szu-Yuan: TS1-1-MoM-3, 6  
 Chen, Tai-An: MB1-WeA-7, 54  
 Chen, Tsan-Yao: TS2-WeA-5, **60**  
 Chen, Tse Wei: PP2-2-WeA-5, **57**  
 Chen, Wen-Shan: CM-ThP-5, 79  
 Chen, Yen-Kai: IA2-1-MoA-9, 11  
 Chen, Yen-Yu: TS1-2-MoA-2, **19**; TS1-ThP-2, **91**  
 Chen, Yi-Ling: TS1-2-MoA-12, **21**  
 Chen, Ying: MA2-2-WeM-5, **41**  
 Chen, Yong-Song: TS1-1-MoM-5, **7**  
 Chen, Yujie: MA4-3-WeA-5, 52  
 Chen, Zhuo: CM-ThP-4, 79; TS3-TuA-8, 40  
 Cheng, Yu-Lun: TS1-1-MoM-7, 7  
 Chevallier, Pascale: MD1-1-MoM-2, 4  
 Chiang, Chih-Hao: MB2-2-MoA-4, 12



## Author Index

- Chiu, Chi-Hua: IA2-1-MoA-2, **10**; IA-ThP-2, **82**  
Chiyasak, Pongpak: MA4-1-TuA-5, **37**  
CHO, Sunghwan: MB-ThP-9, **85**  
Choi, Gil Heyun: MB-ThP-9, **85**  
Choi, Jaehwi: MB-ThP-12, **86**; MB-ThP-5, **84**;  
MB-ThP-8, **85**  
Choi, Mingi: MC3-2-WeA-3, **55**  
Choi, Woo-Jin: MC3-2-WeA-1, **54**  
Chou, Chih-Yun: MB1-WeA-5, **53**  
Chou, Jyh-Pin: TS2-WeA-5, **60**  
Chromik, Richard: MA4-1-TuA-4, **36**; MA4-2-  
WeM-12, **44**  
Chu, Jinn P.: IA1-TuM-2, **22**  
Chu, Yi-Qing: TS1-2-MoA-3, **19**  
Chu, Yu-Ren: IA2-1-MoA-2, **10**; IA-ThP-2, **82**  
Chung, Brian: CM1-1-ThM-10, **62**  
CHUNG, GIYOONG: MB-ThP-6, **84**  
Chung, Ren-Jei: MD1-1-MoM-5, **5**  
Chung, Seungpil: MB-ThP-9, **85**  
Coati, Alessandro: CM1-2-ThA-11, **74**  
Coelho, Reginaldo: IA-ThP-1, **81**  
Copeland, Nick: TS3-TuA-4, **39**  
Copes, Francesco: MD1-1-MoM-2, **4**  
Corbella, Carles: PP5-TuM-3, **30**  
Cordill, Megan: CM1-2-ThA-1, **73**  
Cordill, Megan J.: MC2-1-TuA-3, **38**; MC-ThP-  
1, **88**  
Costa Pinto, Pedro: PP4-FrM-6, **95**; PP-ThP-3,  
**89**  
Costa, Felipe: IA2-1-MoA-1, **10**  
Coulmy, Nicolas: IA2-1-MoA-6, **11**  
Crawford, Grant: MC1-2-FrM-6, **94**; PP2-1-  
WeM-11, **49**  
Crisci, Alexandre: PP-ThP-2, **89**  
Cruz, Julio: MC3-2-WeA-5, **55**; PP1-1-MoM-7,  
**6**  
Curiel-Alvarez, Mario: MB-ThP-17, **87**; PP-  
ThP-6, **90**  
Curiel-Álvarez, Mario: MB-ThP-15, **86**  
Curtin, William A.: CM4-1-MoM-5, **2**  
Czermak, Triana: MB3-ThM-3, **69**  
Czettel, Christoph: CM1-1-ThM-5, **62**  
— **D** —  
Danelon, Miguel R.: MC1-1-ThA-6, **77**  
Daniel, Rostislav: MA3-2-TuA-1, **35**  
Dantas da Cunha, Rayane: MC3-2-WeA-4, **55**  
Daoud, Haneen: MA1-1-TuM-6, **24**  
Davydok, Anton: CM1-2-ThA-6, **73**  
de Abreu, Arthur Cid: MC3-2-WeA-4, **55**  
De Rose, Guy: CM4-1-MoM-6, **3**  
Debnarova, Stanislava: MA4-2-WeM-4, **43**  
Debrabandere, Andreas: PP2-1-WeM-6, **49**  
Debus, Jörg: PP6-MoA-10, **17**; PP6-MoA-8,  
**17**  
Dehm, Gerhard: MC2-1-TuA-10, **39**  
Delaup, Yorick: PP-ThP-3, **89**  
Delfin, Francisco A.: MB3-ThM-11, **70**  
Denkena, Berend: IA3-TuA-1, **33**; PP6-MoA-6,  
**17**  
Denkmann, Nils: PP6-MoA-10, **17**; PP6-MoA-  
8, **17**  
Depla, Diederik: CM3-1-ThM-8, **66**; CM-ThP-  
1, **79**; PP2-1-WeM-6, **49**  
Devi, Raman: MB1-WeA-6, **54**; MB2-1-MoM-  
6, **3**  
Devos, Arnaud: MC2-2-WeM-5, **45**  
Dey, Poulumi: CM4-2-MoA-4, **9**  
Diaz Rodríguez, Pablo: MA3-1-TuM-4, **26**  
Dienwiebel, Martin: PP6-MoA-3, **16**  
Dinca, Valentina: PP5-TuM-6, **30**  
Dini, Daniele: MC1-1-ThA-4, **77**  
Dipolt, Christian: MB3-ThM-11, **70**  
Diulus, J. Trey: PP5-TuM-3, **30**  
Djemia, Philippe: CM1-2-ThA-3, **73**; CM2-1-  
ThM-6, **64**; MC2-1-TuA-10, **39**  
Djordjevic, Natasa: MA1-2-TuA-3, **34**  
Donnerbauer, Kai: PP6-MoA-12, **18**  
Dörflinger, Philipp: MA5-ThM-6, **68**  
Dörflinger, Thomas: MA1-1-TuM-6, **24**  
dos Santos Silva, João Pedro: MD-ThP-1, **88**  
Dösinger, Christoph: CM4-1-MoM-4, **2**  
Drake, Brad: CM1-1-ThM-10, **62**  
Drnovsek, Aljaz: MC3-1-WeM-11, **46**  
Dubost, Laurent: MC1-1-ThA-3, **77**  
Dubreuil, Frédéric: PP4-FrM-2, **94**  
Dudziak, Tomasz: MA1-2-TuA-1, **34**  
Dürschnabel, Michael: MA1-2-TuA-4, **34**  
Durst, Karsten: CM2-1-ThM-4, **64**  
— **E** —  
Easwarakhanthan, Thomas: MA4-2-WeM-3,  
**43**; MA-ThP-5, **83**  
Eckert, Jürgen: CM2-1-ThM-8, **64**  
Edwards, Thomas E. J.: MA3-1-TuM-6, **27**  
EFOGLU, Ihsan: MB-ThP-11, **85**; MC3-1-  
WeM-13, **46**  
Egan, Hilary: CM3-1-ThM-6, **66**  
Ehiasarian, Arutian P.: PP8-2-ThA-9, **78**  
Ehiasarian, Arutiun: PP2-2-WeA-8, **57**  
Ehiasarian, Arutiun P.: KYL-MoKYL-1, **8**  
Eklund, Per: MA3-3-WeM-1, **41**  
El Garah, Mohamed: MA4-2-WeM-1, **43**  
Elsaadany, Mostafa: MD1-1-MoM-1, **4**; MD1-  
2-MoA-1, **13**  
Elsner, Fred: PP4-FrM-4, **95**  
Encinas, Thierry: PP-ThP-2, **89**  
Engwall, Alison: MA4-1-TuA-9, **37**  
Engwall-Holmes, Alison: MA4-3-WeA-2, **52**  
Evertz, Simon: IA3-TuA-4, **33**  
Ewen, James: MC1-1-ThA-4, **77**  
Ezequiel, Marco: CM2-1-ThM-6, **64**  
— **F** —  
Farahani, Mina: PP2-2-WeA-4, **56**  
Farrukh, Sadoon: MB1-WeA-3, **53**  
Faucheu, Jenny: MC1-1-ThA-3, **77**  
Faurie, Damien: CM2-1-ThM-10, **64**; CM2-1-  
ThM-6, **64**; CM2-2-ThA-1, **74**; MC2-1-TuA-3,  
**38**  
Favuzzi, Ilaria: MD1-2-MoA-4, **13**  
Fazeli, Sara: CM-ThP-3, **79**  
Febba, Davi: CM3-1-ThM-6, **66**  
Fečik, Michal: TS3-TuA-8, **40**  
Fekete, Matej: MA4-2-WeM-4, **43**  
Fellner, Simon: CM2-1-ThM-8, **64**  
Feng, Jiling: MD-ThP-3, **89**  
Feng, Yuqun: MC2-2-WeM-6, **45**  
Fernández Martínez, Iván: MA3-1-TuM-4, **26**  
Fernández-Martínez, Ivan: MA3-1-TuM-3, **26**  
Fickl, Bernhard: MB3-ThM-11, **70**  
Field, Susan: TS1-ThP-5, **91**  
Fillot, Nicolas: MC1-1-ThA-4, **77**  
Fischer, Joel: PP1-2-MoA-2, **14**; PP2-2-WeA-  
1, **56**  
Fisher, Timothy S.: TS3-TuA-2, **39**  
Fleig, Jürgen: MB2-3-TuM-1, **28**; MB-ThP-10,  
**85**  
Flores Preciado, Juan: EX-TuM-1, **32**  
Fodor, Bálint: CM1-1-ThM-6, **62**  
Fontaine, Julien: PP4-FrM-2, **94**  
Forsich, Christian: MB3-ThM-11, **70**  
Francois-Saint-Cyr, Hugues G.: MA1-1-TuM-5,  
**24**  
Frank, Heiko: MA5-ThM-5, **67**  
Fransen, Geert-Jan: IA2-1-MoA-5, **10**  
Freire de Medeiros Neto, João: MC3-2-WeA-  
4, **55**  
Freitas, Bruna: MC-ThP-3, **88**  
Fridrici, Vincent: MC1-1-ThA-3, **77**  
Fromm, Timo: CM2-1-ThM-4, **64**  
Fu, Ming: KYL-MoKYL-1, **8**  
Fuchs, Andreas: IA2-1-MoA-5, **10**; PP2-2-  
WeA-3, **56**  
Fuggerer, Tim: CM2-1-ThM-4, **64**  
Fujiwara, Tomoko: MD1-1-MoM-4, **4**  
Fukumasu, Newton K.: MC1-1-ThA-6, **77**  
Füredi, Máté: CM1-1-ThM-6, **62**  
— **G** —  
Gabriel, Herbert: IA1-TuM-4, **22**  
Gachot, Carsten: MC1-1-ThA-1, **76**  
Galipaud, Jules: PP4-FrM-2, **94**  
Gallant, Max: CM3-1-ThM-6, **66**  
Gallardo-Hernández, Ezequiel A.: MC1-2-  
FrM-5, **94**  
Gammer, Christoph: CM1-2-ThA-1, **73**; CM2-  
1-ThM-8, **64**  
Garbicz, Dariusz: MA1-1-TuM-7, **25**  
García Carballo, Rafael: PP6-MoA-10, **17**;  
PP6-MoA-8, **17**  
García, Arley: MA1-1-TuM-4, **26**  
García-León, Ricardo: MA5-ThM-4, **67**  
Garreau, Yves: CM1-2-ThA-11, **74**  
Gauvin, Raynald: MA4-2-WeM-12, **44**  
Gavalas, Michalis: PP3-WeA-8, **59**  
Ge, Albert: CM-ThP-6, **80**  
Gegg, Mathias: PP4-FrM-6, **95**  
Gemma, Ryota: CM1-1-ThM-3, **62**  
Geringer, Jean: MD-ThP-1, **88**  
Ghafoor, Naureen: MA3-2-TuA-4, **35**; MA5-  
ThM-9, **68**  
Ghanbaja, Jaafar: MA4-1-TuA-3, **36**; MA-ThP-  
3, **82**; MB2-3-TuM-4, **28**  
Ghidelli, Matteo: CM1-2-ThA-3, **73**; CM2-1-  
ThM-6, **64**; MC2-1-TuA-10, **39**  
Ghoshal, Anindya: MA2-2-WeM-4, **41**  
Gicquel, Erwan: PP-ThP-2, **89**  
Gies, Astrid: MB2-3-TuM-1, **28**; MB-ThP-10,  
**85**  
Giffard, Rebecca: PP1-1-MoM-7, **6**  
Gilmore, Thomas: PP-ThP-1, **89**  
Giochallas, Nikolaos: PP2-1-WeM-1, **48**  
Girodon-Boulandet, Noël: CM2-1-ThM-10,  
**64**  
Gitschthaler, Arno: PP2-2-WeA-7, **57**  
Glatz, Stefan A.: IA3-TuA-4, **33**  
Glatzel, Uwe: MA1-1-TuM-6, **24**  
Glukhoy, Yuri: TS2-ThP-4, **93**  
Godard, Pierre: CM2-1-ThM-10, **64**; CM2-2-  
ThA-1, **74**  
Goodelman, Daniel: MA4-1-TuA-9, **37**; MA4-  
3-WeA-2, **52**  
Goutte, Mathias: TS1-ThP-6, **92**  
Graf, Dominic: IA3-TuA-1, **33**  
Greczynski, Grzegorz: MA3-2-TuA-4, **35**; PP2-  
1-WeM-1, **48**  
Greenaway, Ann L.: TS2-ThP-1, **92**  
Grützmacher, Philipp G.: MC1-1-ThA-1, **76**  
Gu, Ja Myung: MB-ThP-9, **85**  
Gu, Jialin: CM1-1-ThM-6, **62**  
Gu, Kevin: CM4-1-MoM-6, **3**  
Gudmundsson, Jon Tomas: PP1-2-MoA-2, **14**;  
PP2-2-WeA-1, **56**  
Guldin, Stefan: CM1-1-ThM-6, **62**  
Gulten, Gokhan: MB-ThP-11, **85**; MC3-1-  
WeM-13, **46**  
Günter, Mark: PP2-2-WeA-6, **57**  
Gurawal, Prachi: MB2-1-MoM-6, **3**; MB-ThP-  
7, **85**  
Gutnik, Dominik: MB3-ThM-9, **70**  
Gutschka, Christian: MA5-ThM-6, **68**  
Guzmán, Alvaro: MA3-1-TuM-4, **26**  
— **H** —  
Hagenmuller, Pascal: IA2-1-MoA-6, **11**  
Hagger, Oliver S. J.: PP5-TuM-8, **31**  
Hahn, Horst: CM2-1-ThM-6, **64**

## Author Index

- Hahn, Rainer: CM1-2-ThA-6, **73**; MA3-1-TuM-7, 27; MA3-2-TuA-4, 35; MA5-ThM-6, 68; MA5-ThM-9, 68; MA-ThP-1, 82; MC1-1-ThA-1, 76; PP2-2-WeA-7, 57
- Hain, Caroline: PP2-1-WeM-3, 48; PP2-1-WeM-4, 48
- Hajas, Balint: MA4-2-WeM-5, 43; MA-ThP-2, 82; MB-ThP-10, 85
- Haltz, Eloi: CM2-1-ThM-10, 64; CM2-2-ThA-1, 74
- Hanafi, Razie: MA4-3-WeA-5, **52**
- Hans, Marcus: CM1-1-ThM-5, 62; MA1-2-TuA-5, 34; PP8-1-ThM-8, 71; TS3-TuA-8, **40**
- Hantova, Kamila: CM4-2-MoA-3, 9
- Hartbauer, Michelle: MA1-1-TuM-6, **24**
- Hashemi, Feyzi: MC1-1-ThA-5, 77
- Hashemi, Reza: MC1-1-ThA-5, 77
- Havir, Stanislav: MA3-2-TuA-1, 35; MB3-ThM-10, 70; MB3-ThM-8, **69**
- Haye, Emile: MA3-1-TuM-1, **26**
- HE, JIANFENG: MC-ThP-2, **88**
- Heim, Daniel: MB3-ThM-11, 70
- Helmut, Riedl-Tragenreif: MA5-ThM-11, 69
- Herody, Jean: IA2-1-MoA-6, 11
- Hilfiker, Matthew: MB1-WeA-1, 53
- Himmerlich, Marcel: PP-ThP-3, 89
- Hintzala, Eric: CM2-1-ThM-3, **63**; MC-ThP-4, **88**
- Hirle, Anna: CM1-2-ThA-6, 73; MA5-ThM-6, **68**; MA-ThP-1, **82**
- Hitosugi, Taro: CM3-2-ThA-4, **76**
- Hoche, Holger: IA2-1-MoA-5, 10; MA1-1-TuM-9, **25**
- Hodge, Andrea: CM2-1-ThM-11, 65
- Hodge, Andrea Maria: CM3-1-ThM-4, 66
- Hofer, Andres: MB2-3-TuM-5, **29**
- Hoff, Brianna: PP2-1-WeM-11, **49**
- Holec, David: CM4-1-MoM-4, **2**; MA3-1-TuM-6, 27
- Holzappel, Damian: TS3-TuA-8, 40
- Hong, Seok Hee: MB2-2-MoA-9, 12
- Hopkins, Patrick: MA2-1-TuA-8, 34
- Hoppe, Martin: PP4-FrM-4, 95
- Horwat, David: PP3-WeA-1, **58**
- Hou, Sen-You: MA4-1-TuA-8, 37; PP2-1-WeM-2, **48**
- Houska, Jiri: CM4-2-MoA-3, **9**
- Houška, Jiří: MA3-3-WeM-3, 42; MB1-WeA-3, 53
- Hovsepian, Papken Eh.: KYL-MoKYL-1, 8
- Hsieh, Hsiang-Yu: CM4-2-MoA-5, 9
- HSU, CHENG HAN: MB2-1-MoM-7, **3**
- Hsun-Feng, Hsu: MB-ThP-18, **87**
- Hu, Yang: CM4-1-MoM-5, **2**
- Huang, Chieh-Fu: TS1-1-MoM-5, 7
- Huang, Chi-Hsien: MD2-WeM-10, **47**
- Huang, Chun-Yuan: MB2-1-MoM-5, **3**
- Huang, Jia Hong: MA3-1-TuM-8, 27
- Huang, Jia-Hong: MA3-1-TuM-5, 26; MA3-2-TuA-5, 36; MC2-2-WeM-4, 44; MC2-2-WeM-6, **45**
- Huang, Jow Lay: TS1-2-MoA-5, 19
- Huang, Shih-Yen: IA2-1-MoA-2, 10; IA-ThP-2, **82**
- Huang, Xiao: MA4-2-WeM-10, 44
- Huang, Zih-Jhong: TS1-2-MoA-3, 19
- Huber, Tobias: MB2-3-TuM-1, 28; MB-ThP-10, 85
- Hultman, Lars: CM4-2-MoA-6, 9; CM-ThP-4, 79; MA3-2-TuA-4, 35; MA5-ThM-9, 68
- Hung, Chi Feng: MA3-1-TuM-8, **27**
- Hurkmans, Ton: PP8-2-ThA-1, **78**
- Hwang, Hyo Ki: TS1-ThP-5, 91
- I —
- Ibrahim, Hamdy: MD1-1-MoM-1, 4; MD1-2-MoA-1, 13
- Ibrahim, Sara: TS2-WeA-8, 60
- Ihlefeld, Jon: MA2-1-TuA-8, 34
- Immich, Philipp: IA2-1-MoA-5, **10**; PP1-1-MoM-3, 5; PP1-1-MoM-5, 6; PP2-2-WeA-3, 56; PP8-1-ThM-1, **71**
- Iqbal, Samir: MD2-WeM-3, **47**
- Ivanisenko, Yulia: CM2-1-ThM-6, 64
- Iyinbor, Ikponmwo: CM2-1-ThM-11, **65**
- J —
- Jacob, Kevin: CM2-1-ThM-5, 64
- Jacobo Mora, Daniela Shealsey: PP1-2-MoA-9, **15**
- jadhav, Pratibha: IA1-TuM-3, 22
- Jadhav, swati: IA1-TuM-3, **22**
- Jaggi, Matthias: IA2-1-MoA-6, 11
- Jahn, Falko: MA5-ThM-10, **68**
- Jaiswal, Jyoti: MD-ThP-2, 88
- Jamali, Amirmohammad: PP6-MoA-5, 17
- Janczak-Rusch, Jolanta: CM4-1-MoM-5, 2
- Jang, Ji-Woong: MC3-2-WeA-3, 55
- Jang, Young-Jun: MC3-2-WeA-3, 55
- Janknecht, Rebecca: CM1-2-ThA-6, 73; MA3-1-TuM-7, **27**
- Janowitz, Julia: IA2-1-MoA-5, 10; PP1-1-MoM-5, 6
- Jaoul, Cédric: MA4-3-WeA-3, 52
- Jaquet, Simon: PP6-MoA-10, 17; PP6-MoA-8, 17
- Jasek, Ondrej: MA4-2-WeM-4, 43
- Jauquet, Valentine: PP5-TuM-7, 31
- Javier Cruz, Roberto: MA5-ThM-4, **67**
- Jennings, J. Amber: MD1-1-MoM-4, 4
- Jensen, Elyse: MC1-2-FrM-6, 94
- Jerg, Carmen: MA5-ThM-6, 68; MA-ThP-1, 82; MB2-3-TuM-1, 28; MB-ThP-10, 85; PP2-2-WeA-7, 57
- Jeurgens, Lars P.H.: CM4-1-MoM-5, 2
- Jhai, Hao-Yu: MB-ThP-3, 84
- Jianwei, Ren: CM-ThP-13, 81
- Jílek, Mojmir: MA3-1-TuM-6, 27
- Joly, Philippe: CM2-1-ThM-10, 64
- Joost, Hannes: MA5-ThM-5, 67
- Joru, Vinay: MA4-2-WeM-11, **44**
- Joshi, Anand: PP1-2-MoA-5, **14**
- Joshi, Anand Y.: MB1-WeA-9, 54
- Joshi, Shrikant: IA2-2-TuM-4, **23**
- Joshi, Unnati: PP1-2-MoA-5, 14
- Juez Lorenzo, Maria del Mar: MA1-1-TuM-4, 24
- Juliac, Rémy: MB2-3-TuM-4, 28
- Junge, Nico: PP6-MoA-6, **17**
- K —
- Kääriäinen, Tommi: KYL-WeKYL-1, **51**
- Kadam, Supriya: IA1-TuM-3, 22
- Kalanyan, Berc: PP5-TuM-3, 30
- Kalscheuer, Christian: MA-ThP-4, 83; MC3-1-WeM-10, 46; MC3-1-WeM-6, 46; PP1-2-MoA-11, 15; PP1-2-MoA-12, 16; PP6-MoA-1, 16; PP6-MoA-4, 16; PP6-MoA-6, 17
- Kamath, Ganesh: PP8-2-ThA-3, **78**
- Kaminski, Michal: CM1-2-ThA-11, **74**
- Kao, Hsuan-Ling: MB-ThP-13, **86**
- Kareem, Adnan: MB2-2-MoA-8, **12**
- Karimi Aghda, Soheil: TS3-TuA-8, 40
- Karimi, Soheil: PP8-1-ThM-8, 71
- Karner, Andreas: MB3-ThM-11, 70
- Karpinski, Daniel: MA5-ThM-5, 67
- Karuppusamy, Naveen: TS1-2-MoA-8, **20**
- Karvankova, Pavla: MA5-ThM-5, 67
- Kashyap, Amod: PP6-MoA-5, **17**
- Kateusz, Filip: MA1-2-TuA-1, 34
- Katta, Saikumar: MA4-3-WeA-4, **52**
- Kaufmann, Kevin: CM4-1-MoM-1, **2**
- Kaun, Chao-Cheng: CM4-2-MoA-8, **10**
- Kaur, Davinder: MB1-WeA-8, **54**; MB2-1-MoM-6, 3; MB2-2-MoA-6, 12; MB-ThP-14, **86**; MB-ThP-20, 87; TS1-2-MoA-10, 20; TS1-2-MoA-6, 20; TS1-2-MoA-9, 20; TS1-ThP-1, 91; TS1-ThP-4, 91
- Kaushendra, Kumar: MB2-2-MoA-6, **12**
- Keaty, Bill: MC1-1-ThA-5, 77
- Keckes, Jozef: MA3-2-TuA-1, 35
- Kelly, Peter: MB-ThP-11, 85; MC3-1-WeM-13, 46; TS1-2-MoA-1, 18; TS3-TuA-4, **39**
- Keraudy, Julien: MC1-1-ThA-1, 76
- Kersten, Holger: PP-ThP-7, 90
- Khan, Imran: PP5-TuM-8, 31
- Khan, Md Zaved Hossain: TS1-ThP-3, **91**
- Khan, Saraf: PP1-2-MoA-6, **15**
- Khan, Zikriya: PP1-2-MoA-8, **15**
- Khetan, Vishal: PP8-2-ThA-7, **78**
- Khodadadi Behtash, Amir Masoud: MC3-2-WeA-1, **54**
- Khomh, Foutse: PP6-MoA-11, 18
- Kikuchi, Hokuto: PP1-1-MoM-1, 5
- Kilic, Ufuk: MB1-WeA-1, **53**
- Kim, Dae Woong: MB-ThP-6, 84
- Kim, Eunjeong: MA4-1-TuA-9, 37; MA4-3-WeA-2, 52
- Kim, Jae-Il: MC3-2-WeA-3, 55
- Kim, Jiwan: MB-ThP-12, 86; MB-ThP-5, 84; MB-ThP-8, 85
- Kim, Jongkuk: MC3-2-WeA-1, 54
- Kim, Nahyun: MB2-2-MoA-9, **12**
- Kim, Songkil: MC3-2-WeA-3, 55
- KIM, Sunil: MB-ThP-9, **85**
- Kim, Tae Geun: MB2-2-MoA-9, 12
- Kim, Yong-Sang: MB-ThP-6, 84
- Kirchlechner, Christoph: MA3-1-TuM-4, 26
- Kirnbauer, Alexander: MA4-2-WeM-5, 43; MA-ThP-2, 82
- Klein, Peter: PP2-1-WeM-3, 48
- Klemberg-Sapieha, Jolanta Ewa: PP6-MoA-11, 18
- Klimashin, Fedor: MA5-ThM-5, 67
- Klimashin, Fedor F.: MA3-1-TuM-7, 27
- KLIMASHIN, Fedor F.: MA3-1-TuM-6, **27**
- Kluson, Jan: MA5-ThM-5, 67
- Klusoň, Jan: MA3-1-TuM-6, 27
- Knabl, Florian Theodor: MB3-ThM-9, 70
- Koch, Oliver: MC3-1-WeM-10, 46
- Koga, Kazunori: PP3-WeA-4, **58**
- Kohlscheen, Joern: IA3-TuA-2, 33
- Kolarik, Vladislav: MA1-1-TuM-4, **24**
- Kolenatý, David: MA3-3-WeM-3, 42
- Kolev, Ivan: IA2-1-MoA-5, 10; PP1-1-MoM-5, **6**
- Kolmakov, Andrei: PP5-TuM-3, 30
- Kolozsvári, Szilárd: MA3-1-TuM-1, 26; MA4-2-WeM-5, 43; MA-ThP-2, 82
- Kolozsvári, Szilárd: MA5-ThM-6, 68; MA-ThP-1, 82; MB2-3-TuM-1, 28; MB-ThP-10, 85; MC1-1-ThA-1, 76; PP1-1-MoM-3, 5
- Kolozsvári, Szilárd: CM1-2-ThA-6, 73; PP2-2-WeA-7, 57
- Konstantinidis, Stephanos: PP2-1-WeM-4, 48; PP5-TuM-7, **31**
- Konstantinidis, Stéphanos: PP1-2-MoA-8, 15
- Kopte, Martin: PP4-FrM-8, **95**
- Kos, Šimon: MB3-ThM-8, 69
- Košutová, Tereza: MB3-ThM-8, 69
- Kotak, Parth: MC2-1-TuA-5, 38
- Kotnur, Venkata Girish: MA4-2-WeM-11, 44
- Koutna, Nikola: CM4-2-MoA-6, 9; CM-ThP-4, 79; MA4-2-WeM-4, 43
- Koutná, Nikola: CM1-2-ThA-6, 73

## Author Index

- Kouzios, Christos: PP4-FrM-6, 95; PP-ThP-3, 89
- Kozák, Tomáš: MB1-WeA-3, 53; MB3-ThM-8, 69; PP2-2-WeA-4, 56
- Krause, Baerbel: CM1-2-ThA-11, 74
- Krayev, Andrey: CM1-1-ThM-10, 62
- Krieg, Christian: MA5-ThM-5, 67
- Krishnamurthy, Satheesh: MB2-3-TuM-2, 28
- Krumme, Erik: PP6-MoA-12, 18
- Krywka, Christina: CM1-2-ThA-6, 73
- Kucheyev, Sergei: MA4-1-TuA-9, 37; MA4-3-WeA-2, 52
- Kulczyk-Malecka, Justyna: TS1-2-MoA-1, 18
- Kumar, Krishan: TS1-2-MoA-6, 20
- Kumar, Pramod: MB2-3-TuM-2, 28
- Kumar, Rajesh: TS1-2-MoA-6, 20
- Kumar, Sanjeev: MD-ThP-2, 88
- Kümmerl, Pauline: MA1-2-TuA-5, 34
- Kundmann, Anna C.: TS2-ThP-1, 92
- Kuo, Ping-Chun: MB2-3-TuM-7, 29
- Kuo, Tsai-Shuan: MB-ThP-19, 87
- Kutrowatz, Philip: MC1-1-ThA-1, 76
- Kyioshi Fukumasu, Newton: MC3-2-WeA-2, 55
- L —
- Lallo, James: CM1-1-ThM-9, 62; CM-ThP-6, 80
- Lampke, Thomas: MA5-ThM-10, 68
- Lan, Kuan-Che: MA3-1-TuM-9, 27; MC2-2-WeM-3, 44
- Lance, Michael: MA2-1-TuA-10, 35
- Laska, Nadine: MA1-1-TuM-7, 25
- Lassnig, Alice: CM1-2-ThA-1, 73; CM2-1-ThM-8, 64
- Laurer, Jonathan: MA2-1-TuA-8, 34
- Laurindo, Carlos: MC-ThP-3, 88
- LaVan, David: PP5-TuM-3, 30
- Lazzari, Rémi: CM1-2-ThA-9, 74
- le Febvrier, Arnaud: MA3-3-WeM-1, 41
- Le Coultre, Sylvain: PP5-TuM-9, 31
- Le Granvalet, Maryline: TS2-WeA-8, 60
- LeCoultre, Sylvain: CM1-2-ThA-7, 74
- Lee, Ho Jin: MB2-2-MoA-9, 12
- Lee, In-sung: TS1-ThP-5, 91
- Lee, Jun Hyeok: MB2-2-MoA-9, 12
- Lee, Jyh Wei: PP1-2-MoA-3, 14; PP2-2-WeA-5, 57
- Lee, Jyh-Wei: MA4-1-TuA-5, 37; MA4-1-TuA-8, 37; MA5-ThM-11, 69; PP2-1-WeM-10, 49; PP2-1-WeM-2, 48; TS1-2-MoA-8, 20
- Lee, Sheng-Wei: TS1-1-MoM-3, 6
- Lee, Subin: MA3-1-TuM-4, 26
- Lee, Yi-Hui: PP2-1-WeM-12, 49
- Lee, Yueh-Lien: IA2-1-MoA-2, 10; IA-ThP-2, 82
- Lefebvre, Pauline: IA2-1-MoA-6, 11
- Leinenbach, Felix: MA1-2-TuA-5, 34
- Lemon, Mellie: TS2-ThP-1, 92
- Lewis, Scott: CM4-1-MoM-6, 3
- Li Bassi, Andrea: MC2-1-TuA-10, 39
- Li, Chia Lin: PP1-2-MoA-3, 14
- Li, Chia-Lin: MA4-1-TuA-5, 37; MA4-1-TuA-8, 37; PP2-1-WeM-10, 49; PP2-2-WeA-5, 57
- Li, Siang-Yun: TS1-ThP-7, 92
- Liang, Huan-Chang: IA2-1-MoA-9, 11
- Liang, Tongyue: MA4-2-WeM-12, 44
- Liao, Ying-Chih: MD2-WeM-5, 47
- Liao, Yu-Lin: MB-ThP-19, 87
- Lima, Milton: IA2-1-MoA-1, 10; IA-ThP-1, 81
- Lin, Chia-Yu: MB2-1-MoM-5, 3
- Lin, Chih-Yen: PP2-1-WeM-12, 49
- Lin, Jianliang: PP1-2-MoA-4, 14
- Lin, Jun Xian: MC2-2-WeM-3, 44
- Lin, Ming-Yi: MA5-ThM-8, 68
- Lin, Pei-Chi: TS1-1-MoM-5, 7
- Lin, Ruei Chi: TS1-ThP-7, 92; TS2-WeA-4, 60
- Lin, Ruei-Chi: TS1-2-MoA-4, 19
- Lin, Shih-Hung: TS1-2-MoA-4, 19
- Lin, Shuyao: CM4-2-MoA-6, 9; CM-ThP-4, 79; MA4-2-WeM-4, 43
- Lin, Wen: CM-ThP-5, 79
- Lin, Ying-Hsiang: TS1-2-MoA-4, 19; TS1-ThP-7, 92
- Lin, Ying-Xiang: PP2-1-WeM-12, 49
- Lin, Yu Tsung: TS1-2-MoA-5, 19
- Lippert, Thomas: PP5-TuM-4, 30
- Liskiewicz, Tomasz: MC3-1-WeM-4, 45
- Liu, Dong (Lilly): CM2-2-ThA-5, 75
- Liu, Huinan: MD2-WeM-1, 47
- Liu, Po-Liang: CM4-2-MoA-5, 9
- Liu, Ting-Yu: MD1-2-MoA-8, 14
- Liu, Xiaoyang: PP1-2-MoA-11, 15; PP1-2-MoA-12, 16; PP6-MoA-1, 16; PP6-MoA-6, 17
- Liyanage, Manura: CM4-1-MoM-5, 2
- Lockwood Estrin, Francis: PP5-TuM-8, 31
- Lopes Dias, Nelson Filipe: IA3-TuA-1, 33; MC3-1-WeM-5, 45; PP6-MoA-10, 17; PP6-MoA-12, 18
- Lopes Dias, Nelson Filipe: PP6-MoA-8, 17
- Lorente, Cristina: MA1-1-TuM-1, 23
- Lorentzon, Marcus: MA3-2-TuA-4, 35; MA5-ThM-9, 68
- Lorenzin, Giacomo: CM4-1-MoM-5, 2
- Lothrop, Alex: MA4-2-WeM-10, 44
- Lou, Bih Show: PP1-2-MoA-3, 14; PP2-2-WeA-5, 57
- Lou, Bih-Show: MA4-1-TuA-8, 37; MA5-ThM-11, 69; PP2-1-WeM-10, 49; PP2-1-WeM-2, 48; TS1-2-MoA-8, 20
- Lovett, Adam: CM1-1-ThM-6, 62
- Lowery, Patrick: CM1-1-ThM-10, 62
- Lu, Min-Hsuan: MB-ThP-13, 86
- Lucas, Stéphane: MA3-1-TuM-1, 26
- Ludwig, Alfred: CM3-1-ThM-8, 66; CM-ThP-7, 80
- Lümkemann, Andreas: MA3-1-TuM-6, 27; MA5-ThM-5, 67
- Lundin, Daniel: PP1-2-MoA-2, 14; PP2-1-WeM-3, 48; PP2-1-WeM-4, 48; PP2-2-WeA-1, 56
- Lundquist, Diego Lundquist: MB-ThP-16, 87
- Lusvardi, Luca: PP2-2-WeA-3, 56
- Lyu, Yezhe Lyu: IA2-1-MoA-8, 11
- M —
- Ma, Xinqing: MA3-3-WeM-5, 42
- Machado, Izabel F.: MC1-1-ThA-6, 77
- Machorro, Roberto: PP1-1-MoM-7, 6
- Mack, Paul: CM1-1-ThM-9, 62
- Macshane, Brittany: IA3-TuA-2, 33
- Maddalena, Roger: MA1-1-TuM-5, 24
- Madden, Nathan: MC1-2-FrM-6, 94; PP2-1-WeM-11, 49
- Maj, Łukasz: IA2-2-TuM-3, 23
- Maj, Luksaz: MC3-1-WeM-4, 45
- Majeed, Abdul Mannan: MB2-1-MoM-3, 3
- Malecka, Justyna Kulczyk: MB-ThP-11, 85; MC3-1-WeM-13, 46
- Malik, Gaurav: MB2-1-MoM-6, 3
- Mangum, John: TS2-ThP-1, 92
- Mann, Jennifer: CM-ThP-9, 80
- Manninen, Noora: TS3-TuA-5, 39
- Mantoux, Arnaud: IA2-1-MoA-6, 11; PP-ThP-2, 89
- Mantovani, Diego: MD1-1-MoM-2, 4
- MARIAPPAN, MUTHUKUMAR: CM-ThP-2, 79
- Marinaro, Giovanni: PP4-FrM-6, 95
- Marion, Sarah: MC1-1-ThA-3, 77
- Martínez Fuentes, Marco Antonio: PP1-2-MoA-9, 15
- Martínez, Marco: MC3-2-WeA-5, 55
- Martínez, Marco: PP1-1-MoM-7, 6
- Martínez-Castelo, Jesus: PP-ThP-6, 90
- Martínez-Guerra, Eduardo: PP-ThP-6, 90
- Martínez-Trinidad, Jose: MA5-ThM-4, 67
- Martins Alves, Salette: MC3-2-WeA-4, 55
- Martins de Souza, Roberto: MC3-2-WeA-2, 55
- Martinu, Ludvik: HL-WeHL-2, 61; PP6-MoA-11, 18
- Marton, András: CM1-1-ThM-6, 62
- Maslar, James E.: PP5-TuM-3, 30
- Matas, Martin: MA3-1-TuM-6, 27
- Mateos-Anzaldo, David: MB-ThP-15, 86; MB-ThP-17, 87; PP-ThP-6, 90
- Mathew, Mathew T.: MC1-1-ThA-5, 77
- Mauzeroll, Janine: MA4-1-TuA-4, 36
- Mayrhofer, Paul: CM4-2-MoA-6, 9; CM-ThP-4, 79; MA1-2-TuA-4, 34; MA4-2-WeM-5, 43; MA-ThP-2, 82; PP8-1-ThM-12, 71
- Mayrhofer, Paul H.: CM1-2-ThA-6, 73; MA3-1-TuM-7, 27
- McCarter, Angus: PP-ThP-1, 89
- McGehee, Thomas: MD1-1-MoM-1, 4; MD1-2-MoA-1, 13
- McLean, Mark: PP5-TuM-3, 30
- McNallan, Mike: MD1-2-MoA-2, 13
- Meduri, Angelo: MD1-2-MoA-4, 13
- Meindlhuber, Michael: CM1-2-ThA-1, 73; MA5-ThM-9, 68
- Melo-Pérez, Marco A: MC1-2-FrM-5, 94
- Mendala, Bogustaw: MA1-1-TuM-7, 25
- Mendez, Juan Manuel: PP6-MoA-11, 18
- Meneses-Amador, Alfonso: MC1-2-FrM-5, 94
- Meng, Shirley: PL-MoM-2, 1
- Menou, Edern: CM-ThP-3, 79; MA4-3-WeA-3, 52
- Mercier, Frederic: PP3-WeA-8, 59; PP-ThP-2, 89
- Méreaux, Ludovic: MA4-3-WeA-3, 52
- Merlo, James: MA4-1-TuA-9, 37
- Messi, Federica: CM3-1-ThM-1, 65; PP2-1-WeM-5, 48
- Meurer, Markus: PP6-MoA-4, 16
- Michel, Anny: CM1-2-ThA-11, 74; CM2-2-ThA-1, 74
- Michler, Johann: MA3-1-TuM-6, 27; MA3-1-TuM-7, 27; MA5-ThM-5, 67
- Migot, Sylvie: MA4-1-TuA-3, 36; MA-ThP-3, 82; MB2-3-TuM-4, 28
- Milani, Paolo: MB3-ThM-5, 69
- Milhet, Xavier: MB2-1-MoM-4, 3
- Milichko, Valentin: MA4-2-WeM-3, 43; MA-ThP-5, 83
- Milichko, Valentin A.: MA4-1-TuA-3, 36; MA-ThP-3, 82
- Miller, Thomas: CM1-1-ThM-6, 62
- Minfray, Clotilde: MC1-1-ThA-3, 77
- Minor, Andrew: CM1-2-ThA-1, 73
- Miranda Marti, Marta: MC3-1-WeM-6, 46
- Mireski, Mariana: MD-ThP-1, 88
- Mitterer, Christian: MB3-ThM-9, 70
- Möbius, Max Philip: MA-ThP-4, 83; MC3-1-WeM-10, 46; MC3-1-WeM-6, 46
- Mock, Clara: MA2-2-WeM-4, 41
- Mocuta, Christian: CM2-1-ThM-10, 64
- Möhring, Hans-Christian: PP6-MoA-3, 16
- Molina Aldareguia, Jon: MA3-1-TuM-4, 26
- Monclús, Miguel: MA3-1-TuM-4, 26
- Monier, Guillaume: TS1-ThP-6, 92
- Moras, Gianpietro: MC1-2-FrM-1, 94
- Moreno, Gloria P.: MB3-ThM-3, 69
- Morgiel, Jerzy: IA2-2-TuM-3, 23
- Moskovin, Pavel: MA3-1-TuM-1, 26
- Mtshali, Christopher: CM1-1-ThM-8, 62

## Author Index

- Mücklich, Frank: MA4-2-WeM-3, 43; MA-ThP-5, 83
- Muhl, Stephen: MC3-2-WeA-5, **55**; PP1-1-MoM-7, 6; PP1-2-MoA-9, 15
- Muir, Ethan: PP2-2-WeA-8, **57**
- Muller, Jérôme: MA3-1-TuM-1, 26
- Müller, Thomas: MB3-ThM-11, 70
- Munroe, Paul: MA4-3-WeA-5, 52
- **N** —
- N., Srinivasa Rao: MB1-WeA-9, 54
- Naghdali, Saeideh: CM1-1-ThM-5, 62
- Naimi, Salma: CM-ThP-11, **81**
- Navabpour, Parnia: TS1-ThP-5, 91
- Navarro, Alyssandra: MD1-1-MoM-1, 4
- Navarro-Rodriguez, Jackeline: PP-ThP-6, **90**
- Navidi, Amir: PP8-1-ThM-8, 71
- Nedev, Nicola: MB-ThP-15, 86; MB-ThP-17, 87; PP-ThP-6, 90
- Nedev, Roumen: MB-ThP-15, 86; MB-ThP-17, 87
- Neils, William K.: IA1-TuM-1, 22
- Neiß, Peter: PP1-1-MoM-1, 5
- Nemangwele, Fhulufhelo: CM1-1-ThM-8, **62**
- Nemati, Narguess: MA3-3-WeM-6, **42**
- Nemukula, Enos: CM1-1-ThM-8, 62
- Neuss, Deborah: PP8-1-ThM-8, 71
- Neyrat, Julien: PP2-2-WeA-9, **58**
- Nguyen, Thi Xuyen: TS1-2-MoA-4, 19; TS1-ThP-7, 92; TS2-ThP-3, **93**; TS2-WeA-3, 59; TS2-WeA-4, 60
- Nie, Xueyuan: IA2-1-MoA-8, 11
- Nieto-Sosa, José A.: MC1-2-FrM-5, 94
- Niu, Ranming: MA3-2-TuA-1, 35
- Nohava, Jiri: MC2-1-TuA-5, 38
- Nominé, Alexandre: MA4-1-TuA-3, 36
- Normant, Antoine: PP4-FrM-2, 94
- Ntemou, Eleni: MB2-3-TuM-1, 28; PP2-2-WeA-7, 57
- Nuñez, Johan: IA-ThP-1, 81
- Nunney, Tim: CM1-1-ThM-9, 62; CM-ThP-6, 80
- **O** —
- Obrero, Jose: MB3-ThM-3, 69
- Odén, Magnus: PP2-1-WeM-1, 48
- Odent, Jeremy: PP5-TuM-7, 31
- Oellers, Tobias: IA3-TuA-4, 33
- Ogale, Satishchandra: IA1-TuM-3, 22
- Oger, Loïc: MA1-1-TuM-1, 23
- OGER, Loïc: MA1-1-TuM-3, **24**
- Ohmura, Takahito: CM2-1-ThM-1, **63**
- Olivares-Luna, M.: MA3-2-TuA-3, 35
- Opila, Elizabeth: MA2-1-TuA-8, **34**
- Osborn, William A.: PP5-TuM-3, 30
- Osorio, Esteban: MB-ThP-17, **87**
- Osorio-Urquiza, Esteban: MB-ThP-15, 86
- Osuna Escalante,, Eddue: MB-ThP-17, 87
- Osuna-Escalante, Eddue: MB-ThP-15, **86**
- Öte, Mehmet: TS1-1-MoM-1, 6
- Ott, Vincent: MA1-2-TuA-4, **34**
- Oulton, Rupert: KYL-MoKYL-1, 8
- Ouyang, Fan-Yi: MA2-2-WeM-6, 41; MB2-3-TuM-7, 29; MB-ThP-19, 87
- Owen, David: KYL-MoKYL-1, 8
- Ozimek, Pawel: PP8-2-ThA-5, **78**
- **P** —
- Palin, Victor: MB2-3-TuM-5, 29
- Palisaitis, Justinas: MA3-2-TuA-4, 35
- Panagi, Kleitos: TS1-2-MoA-1, 18
- Panjan, Matjaž: MC3-1-WeM-11, 46
- Panjan, Peter: MC3-1-WeM-11, 46
- Panova, Veera: MC2-1-TuA-9, **38**
- Pardhasaradhi, Sudharshan Phani: MA4-2-WeM-11, 44
- Park, Jaehyung: MB-ThP-12, 86; MB-ThP-5, **84**; MB-ThP-8, 85
- Parkin, Ivan P.: PP5-TuM-8, 31
- Pascali, Alessia: PP-ThP-3, 89
- Patel, Diya: MD1-1-MoM-1, 4; MD1-2-MoA-1, 13
- Paternoster, Carlo: MD1-1-MoM-2, 4
- Pathak, Sid: CM2-1-ThM-5, 64
- Patidar, Jyotish: CM3-1-ThM-1, 65; PP2-1-WeM-5, 48; PP-ThP-4, 90
- Patil, Prathamesh: MB3-ThM-9, 70
- Patureau, Hugo: PP-ThP-2, 89
- Paul, Biplab: MA3-3-WeM-1, 41
- Paulo Tschiptschin, André: MC3-2-WeA-2, 55
- Pazzi, Milena: PP2-2-WeA-3, **56**
- Pelapur, Rengarajan: MA1-1-TuM-5, 24
- Pereira, André: TS2-WeA-1, **59**
- Perez Trujillo, Francisco Javier: PP8-1-ThM-5, **71**
- Perez-Landeros, Oscar: MB-ThP-17, 87; PP-ThP-6, 90
- Pérez-Landeros, Oscar: MB-ThP-15, 86
- Peters, Scott: MA4-1-TuA-9, 37; MA4-3-WeA-2, 52
- Petersen, Hilke: IA3-TuA-1, 33
- PETIT, Valentine: PP4-FrM-6, **95**; PP-ThP-3, **89**
- Petrov, Ivan: PP8-1-ThM-3, **71**
- Petrov, Peter K.: KYL-MoKYL-1, 8
- Petruhins, Andrejs: PP1-1-MoM-3, 5
- Pichler, Christian M.: MB3-ThM-9, 70
- Pierson, Jean François: MA4-1-TuA-3, 36
- Pierson, Jean-François: MA4-2-WeM-3, 43; MA-ThP-3, 82; MA-ThP-5, 83
- PIERSON, Jean-François: MB2-3-TuM-4, **28**
- Pilloud, David: MA4-2-WeM-3, 43; MA-ThP-5, 83; MB2-3-TuM-4, 28
- Piñeiro, Miguel: MA4-2-WeM-3, **43**; MA-ThP-5, **83**
- Pitonakova, Tatiana: MA4-2-WeM-4, 43
- Plech, Anton: CM1-2-ThA-11, 74
- Podsednik, Maximilian: MA5-ThM-6, 68
- Pofelski, Alexandre: MB2-3-TuM-5, 29
- Pohler, Markus: CM1-1-ThM-5, 62
- Polcar, Tomas: MC1-1-ThA-7, **78**
- Polcik, Peter: CM1-2-ThA-6, 73; IA2-1-MoA-5, 10; MA5-ThM-6, 68; MA-ThP-1, 82; MB2-3-TuM-1, 28; MB-ThP-10, 85; MC1-1-ThA-1, 76; PP1-1-MoM-3, 5; PP2-2-WeA-7, 57
- Polkowska, Adelajda: MA1-2-TuA-1, 34
- Pözlberger, Daniel: MC1-1-ThA-1, 76
- Posri, Surapit: MA4-1-TuA-5, 37
- Poulon, Angeline: PP2-2-WeA-9, 58
- Povarov, Svyatoslav: MA4-1-TuA-3, 36
- Praks, Pavel: MA1-1-TuM-4, 24
- Praková, Ranata: MA1-1-TuM-4, 24
- Prasad, Bitupan: MD-ThP-2, 88
- Preiner, Johannes: MB3-ThM-11, 70
- Prifling, Benedikt: MB3-ThM-8, 69
- Primetzhofer, Daniel: MA1-2-TuA-5, 34; MB2-3-TuM-1, 28; PP2-2-WeA-7, 57; PP8-1-ThM-8, 71; TS3-TuA-8, 40
- Procházka, Michal: MB3-ThM-10, 70
- Protesescu, Loredana: MA5-ThM-1, **67**
- Pundt, Astrid: CM1-1-ThM-3, 62
- Purandare, Yashodhan: PP2-2-WeA-8, 57
- Putz, Barbara: MB3-ThM-9, 70; MC2-1-TuA-1, **37**
- **Q** —
- Qiu, Jun-Hui: MA2-2-WeM-6, **41**
- **R** —
- Raadu, Michael A.: PP1-2-MoA-2, 14
- Radloff, Marius: PP1-1-MoM-1, 5
- Radny, Tobias: PP1-1-MoM-5, 6
- Rahman, Habeebur: TS1-2-MoA-10, **20**; TS1-ThP-1, **91**
- Rakhra, Manik: CM-ThP-12, **81**
- Raman, Priya: PP4-FrM-4, 95
- Ramanath, Ganpati: MA3-3-WeM-1, 41
- Ramesh, Janani: MA1-2-TuA-5, 34
- Ramm, Jürgen: MA-ThP-1, 82; MB2-3-TuM-1, 28; MB-ThP-10, 85; PP2-2-WeA-7, 57
- Ramos-Irigoyen, Rogelio: PP-ThP-6, 90
- Ranjan, Bhanu: TS1-2-MoA-6, 20; TS1-2-MoA-9, **20**; TS1-ThP-4, **91**
- Rank, Martin: MC3-1-WeM-10, 46
- Rathore, Mahendra Singh: MB1-WeA-9, **54**; PP1-2-MoA-5, 14
- Ravi Narayan, Lakshmi: PP5-TuM-3, 30
- Redjaimia, Abdelkrim: MA-ThP-3, 82
- Reichmann, Alexander: CM4-1-MoM-4, 2
- Reiners-Sakic, Amin: CM4-1-MoM-4, 2
- Rémiens, Denis: PP1-2-MoA-8, 15
- Renault, Pierre O.: MC2-1-TuA-3, 38
- Renault, Pierre-Olivier: CM1-2-ThA-4, **73**; CM2-1-ThM-10, 64; CM2-2-ThA-1, 74
- Rennebro, Ewa: IA2-1-MoA-3, **10**
- Resendiz, Cesar: MA5-ThM-3, **67**
- Resta, Andrea: CM1-2-ThA-11, 74
- Rezek, Jiří: MB1-WeA-3, 53
- Richard-Plouet, Mireille: TS2-WeA-8, 60
- Ridley, Mackenzie: MA2-1-TuA-10, 35
- Riedl, Helmut: CM1-2-ThA-6, 73; MA1-2-TuA-4, 34; MA5-ThM-6, 68; MA-ThP-1, 82; MB2-3-TuM-1, 28; MB-ThP-10, 85; MC1-1-ThA-1, **76**; PP2-2-WeA-7, 57
- Rielle, Constant Boris: CM1-2-ThA-7, **74**
- Riffe, Will: MA2-1-TuA-8, 34
- Robinson, Eddy: CM1-1-ThM-10, 62
- Rocchi, Andrea: PP4-FrM-6, 95
- Rodchanarowan, Aphichart: MA4-1-TuA-5, 37
- Rodkey, Nathan: CM3-1-ThM-1, **65**; PP2-1-WeM-5, 48; PP-ThP-4, **90**
- Rodriguez, Sergio: MA1-1-TuM-1, 23
- Rodríguez-Castro, German A.: MC1-2-FrM-5, 94
- Rogström, Lina: PP2-1-WeM-1, 48
- Romaner, Lorenz: CM4-1-MoM-4, 2
- Rosales-Lopez, J.L.: MA3-2-TuA-3, **35**
- Rosaz, Guillaume: PP4-FrM-6, 95
- Rosen, Johanna: MA3-2-TuA-4, 35; PP1-1-MoM-3, 5
- Rosival, Stefan M.: CM2-1-ThM-4, 64
- Rosner, Rachel: MA2-1-TuA-8, 34
- Rossi, Edoardo: CM2-2-ThA-4, 75; MA3-2-TuA-1, 35; MD1-2-MoA-4, 13
- Rossy Borges, Maria Helena: MD-ThP-1, 88
- Roth, Sébastien: TS2-WeA-8, 60
- Roy, Abhijit: IA3-TuA-2, **33**
- Rübig, Bernd: MB3-ThM-11, 70
- Rubira Danelon, Miguel: MC3-2-WeA-2, **55**
- Rudd, Peter: CM3-1-ThM-5, **66**
- Rudolph, Martin: PP1-2-MoA-2, **14**; PP2-2-WeA-1, 56
- Ruggiero, Peter: MA3-3-WeM-5, 42
- Rümenapf, Finn: PP6-MoA-10, 17; PP6-MoA-12, 18; PP6-MoA-8, 17
- Ryabov, Michael: TS2-ThP-4, 93
- **S** —
- Saeed, Ifra: MB2-3-TuM-8, **29**
- Saelzer, Jannis: PP6-MoA-12, 18
- Sakamoto, Ryo: PP2-1-WeM-3, 48
- Salanova, Alejandro: MA2-1-TuA-8, 34
- Salvadores Farran, Norma: MB2-3-TuM-1, **28**; MB-ThP-10, **85**
- Sampath, Sanjay: MC2-2-WeM-1, **44**
- Sanchette, Frederic: MA4-2-WeM-1, **43**
- Sánchez-Valencia, Juan Ramón: MB3-ThM-3, 69
- Sanginés, Roberto: PP1-1-MoM-7, 6

## Author Index

- Sangiovanni, Davide: CM4-2-MoA-6, 9; CM-ThP-4, 79
- Sanni, Omatayo: CM-ThP-13, **81**
- Santawee, Thanawat: MA4-1-TuA-5, 37
- Santiago, Jose Antonio: MA3-1-TuM-4, 26
- Santos, Luciane: MC-ThP-3, 88
- Sanzone, Giuseppe: TS1-ThP-5, **91**
- Sarkissian, Andranik: MD1-1-MoM-2, 4
- Saury, Didier: MB2-1-MoM-4, 3
- Sauvage, Thierry: TS1-ThP-6, 92
- Savadvkouei, Kayvon: CM1-1-ThM-10, 62
- Scarpellini, Alice: MA1-1-TuM-5, 24
- Schachinger, Manuel C. J.: MB3-ThM-11, **70**
- Schäfer, Rolf: PP1-1-MoM-5, 6
- Schalk, Nina: CM1-1-ThM-5, **62**
- Schenkel, Markus: IA3-TuA-4, 33
- Scherer, Axel: CM4-1-MoM-6, 3
- Scherm, Florian: MA1-1-TuM-6, 24
- Schiester, Maximilian: CM1-1-ThM-5, 62
- Schmalbach, Kevin: CM2-1-ThM-3, 63; MC-ThP-4, 88
- Schmidt, Volker: MB3-ThM-8, 69
- Schneider, Jochen: TS3-TuA-8, 40
- Schneider, Jochen M.: MA1-2-TuA-5, 34; PP8-1-ThM-8, **71**
- Schneider, Johannes: PP6-MoA-5, 17
- Schnitzer, Ronald: CM4-1-MoM-4, 2
- Scholz, Florentine: MB-ThP-10, 85
- Schretter, Lukas: CM2-1-ThM-8, 64
- Schubert, Eva: MB1-WeA-1, 53
- Schubert, Mathias: MB1-WeA-1, 53
- Schuh, Christopher: MC2-1-TuA-9, 38
- Schuhmann, Wolfgang: CM-ThP-7, 80
- Schuller, Ivan: MB2-3-TuM-5, 29
- Schulze, Volker: PP6-MoA-5, 17
- Schumann, Helge: MA1-1-TuM-6, 24
- Schütte, Thomas: PP1-1-MoM-1, **5**
- Schwaiger, Ruth: CM2-1-ThM-11, 65
- Sebastiani, Marco: CM2-2-ThA-4, **75**; MA3-2-TuA-1, 35; MD1-2-MoA-4, 13
- Sedmak, Pavel: MC2-1-TuA-5, 38
- Seid Ahmed, Yassmin: IA3-TuA-3, **33**
- Sener, M. Emre: PP5-TuM-8, 31
- Seo, Jangwoo: TS1-ThP-5, 91
- Sergievskaia, Anastasiya: PP5-TuM-7, 31
- Sghuri, Anas: MB2-1-MoM-4, 3
- Shah, Sayed Suliman: TS2-ThP-2, **92**
- Shaji, Kalyani: MB3-ThM-10, **70**; MB3-ThM-8, 69
- Shamshirgar, Ali Saffar: PP1-1-MoM-3, 5
- Shankhdhar, Satyam: TS1-2-MoA-6, 20
- Sharma, Gagan Kumar: TS1-2-MoA-10, 20
- Sharobem, Timothy: MA2-2-WeM-4, 41
- Sharp, Ian: CM3-1-ThM-9, **66**
- Shaw, David: TS1-2-MoA-1, 18
- Shen, Chao-Cheng: CM4-2-MoA-5, 9
- Shen, Yu Min: TS1-2-MoA-5, 19
- Shi, Nannan: CM-ThP-6, 80
- Shimizu, Tetsuhide: PP2-1-WeM-3, **48**; PP2-1-WeM-4, 48
- Shin, Swanee: MA4-1-TuA-9, 37; MA4-3-WeA-2, 52
- Shon-Roy, Estrelita (Lita): PP1-2-MoA-1, **14**
- Shuang, Fei: CM4-2-MoA-4, 9
- Simoës, Alexandre: MB2-3-TuM-6, **29**
- Simpson, Robin: CM1-1-ThM-9, 62
- Singh, Preetam: TS1-2-MoA-10, 20
- Singh, Rakesh: PP1-2-MoA-10, **15**
- Singh, Somdatta: MB1-WeA-6, 54; MB2-1-MoM-6, **3**; MB-ThP-7, 85
- Sinha, Avirup: MC1-1-ThA-5, **77**
- Siol, Sebastian: CM3-1-ThM-1, 65; CM-ThP-8, **80**; PP2-1-WeM-5, **48**; PP-ThP-4, 90
- Siqueira, Rafael: IA2-1-MoA-1, 10; IA-ThP-1, 81
- Slimani, Hocine: CM1-2-ThA-3, 73
- Smith, Raymond: MB1-WeA-1, 53
- Soares, Paulo: MC-ThP-3, 88
- Solanki, Karan: CM1-2-ThA-11, 74
- Son, Junwoo: MB-ThP-1, **83**
- Song, Sheng-Rong: CM-ThP-5, 79
- Soucek, Pavel: MA4-2-WeM-4, **43**; MA5-ThM-5, 67
- Souza, Roberto M.: MC1-1-ThA-6, 77
- Spagna, Stefano: IA1-TuM-1, 22
- Spence, Gwyneth: TS3-TuA-4, 39
- Stauffer, Douglas: CM2-1-ThM-3, 63; MC-ThP-4, 88
- Steier, Katharina: TS1-2-MoA-1, 18
- Stein, Nicolas: MB2-3-TuM-4, 28
- Stigelin, Natalie: MB2-2-MoA-2, **11**
- Strakov, Hristo: MA1-2-TuA-3, 34
- Strozzi, David: MA4-1-TuA-9, 37; MA4-3-WeA-2, 52
- Struller, Carolin: TS3-TuA-4, 39
- Stüber, Michael: MA1-2-TuA-4, 34
- Stueber, Michael: PP6-MoA-5, 17
- Su, Chia Ying: TS1-ThP-7, 92
- Su, Chia-Ying: MA4-3-WeA-1, **52**; TS1-2-MoA-4, 19; TS2-ThP-3, 93
- Su, Tong: MC2-1-TuA-4, **38**
- Sumant, Anirudha: MC3-2-WeA-3, 55
- Sun, Hailin: TS1-ThP-5, 91
- Sun, Yani: MC1-1-ThA-5, 77
- Supakul, Skye: CM2-1-ThM-5, 64
- Suri, Ujjwal: PP1-2-MoA-11, **15**
- Swadźba, Lucjan: MA1-1-TuM-7, 25
- Swadźba, Radostaw: MA1-1-TuM-7, **25**
- T —
- T. Alpas, Ahmet: MC3-2-WeA-1, 54
- Tahir, Axel: MB2-3-TuM-4, 28
- Tallon, Carolina: MA2-1-TuA-8, 34
- Tang, Jian-Fu: MA5-ThM-8, 68
- Tang, Kai-Shawn: PP2-1-WeM-12, **49**
- Tanveer, Tooba: MD1-2-MoA-1, 13
- Tasnadi, Ferenc: PP2-1-WeM-1, 48
- Tasnádi, Ferenc: CM1-2-ThA-3, 73
- Tate, Jeremiah: MD1-1-MoM-4, **4**
- Taylor, Gregory: MA4-1-TuA-9, 37; MA4-3-WeA-2, 52
- Tayyab, Muhammad: PP6-MoA-1, 16; PP6-MoA-4, 16
- Tegelaers, Louis: IA2-1-MoA-5, 10; PP1-1-MoM-5, 6
- Temst, Kristiaan: PP1-2-MoA-8, 15
- Tervakangas, Sanna: TS3-TuA-5, 39
- Thakur, Deepika: MA3-3-WeM-2, **41**
- Thapa, Maansi: MC1-1-ThA-5, 77
- Thelen, Felix: CM3-1-ThM-8, **66**; CM-ThP-7, **80**
- Thewes, Alexander: MC3-1-WeM-5, 45
- Thiaudière, Dominique: CM2-1-ThM-10, 64; CM2-2-ThA-1, 74
- Thomassen, Toby: CM4-1-MoM-6, 3
- Thompson, Forest: MC1-2-FrM-6, **94**; PP2-1-WeM-11, 49
- Tillmann, Wolfgang: IA3-TuA-1, 33; MC3-1-WeM-5, 45; PP6-MoA-10, 17; PP6-MoA-12, 18; PP6-MoA-8, **17**
- Ting, I-Sheng: MC2-2-WeM-4, **44**
- Ting, Jyh Ming: TS2-WeA-3, 59; TS2-WeA-4, 60
- Ting, Jyh-Ming: MA4-3-WeA-1, 52; MB1-WeA-7, 54; TS1-2-MoA-4, 19; TS1-ThP-7, 92; TS2-ThP-3, 93
- Tiznado-Vázquez, Hugo: PP-ThP-6, 90
- Tkabetz, Michael: CM1-1-ThM-5, 62
- Tobola, Daniel: MC3-1-WeM-4, 45
- Toboła, Daniel: IA2-2-TuM-3, **23**
- Toledano Povedano, Alejandro: CM2-2-ThA-1, **74**
- Tomar, Akshay: MB-ThP-7, **85**
- Tomasella, Eric: TS1-ThP-6, 92
- Torres, Ricardo: MC-ThP-3, 88
- TOTIK, Yasar: MB-ThP-11, 85; MC3-1-WeM-13, 46
- Touaibia, Djallel Eddine: MA4-2-WeM-1, 43
- Trassin, Morgan: PP2-1-WeM-5, 48
- Trivedi, Chinmay: IA2-1-MoA-5, 10
- Trost, Claus O.W.: MC2-1-TuA-3, 38; MC-ThP-1, 88
- Tsai, Hsiang Yu: PP1-2-MoA-3, 14
- Tsai, Meng-Lin: MB2-2-MoA-4, 12
- Tsai, Yi-Cho: TS1-ThP-7, **92**
- Tsao, Li-Hui: MB2-3-TuM-9, **30**
- Tschiptschin, André P.: MC1-1-ThA-6, 77
- Tseng, Chung-Jen: TS1-1-MoM-3, 6
- Tseng, Fan-Gang: TS2-WeA-5, 60
- Tseng, Shang-Hua: MA3-3-WeM-4, **42**
- Tseng, Shao-Chin: CM-ThP-5, 79
- Tseng, Sheng-Jui: PP2-1-WeM-10, **49**
- Tului, Mario: MD1-2-MoA-4, 13
- Turlo, Vladyslav: CM4-1-MoM-5, 2; CM4-2-MoA-1, **9**
- Tzu-Yun, Huang: MB-ThP-18, 87
- U —
- Ucik, Martin: PP1-1-MoM-4, 5; PP-ThP-5, **90**
- Učík, Martin: MA3-1-TuM-6, 27
- Ulrich, Sven: MA1-2-TuA-4, 34; PP8-1-ThM-10, **71**
- Ulrich, Thomas: IA2-1-MoA-5, 10
- Urbach, Jan-Peter: PP1-1-MoM-1, 5
- Urban, Frank: CM1-1-ThM-11, **63**; CM-ThP-10, **81**
- Urbanczyk, Julia: MC3-1-WeM-5, **45**
- Usman, Muhammad: MC3-2-WeA-6, **56**
- V —
- V. Gunina, Ekaterina: MA4-1-TuA-3, 36
- Vacirca, Davide: MC2-1-TuA-10, 39
- Vaghela, Amruta: CM2-1-ThM-5, **64**
- Valderrama, Matteo: MC1-1-ThA-4, **77**
- Valdez-Salas, Benjamin: MB-ThP-17, 87; PP-ThP-6, 90
- Vargas, Nicolas: PP4-FrM-4, **95**
- Vasina, Petr: MA5-ThM-5, 67
- Vaubois, Thomas: MA4-3-WeA-3, 52
- Vecchietti, Pietro: CM1-2-ThA-3, 73
- Vercoulen, Huub: IA2-1-MoA-5, 10
- Verma, Anshu: PP-ThP-1, 89
- Vermeij, Tijmen: MB3-ThM-9, 70
- Vigolo, Brigitte: MB2-3-TuM-4, 28
- Vishnoi, Nikhil: MA4-3-WeA-2, 52
- Vlad, Alina: CM1-2-ThA-11, 74
- Vlassioux, Ivan: MC3-2-WeA-3, 55
- Vlček, Jaroslav: MB1-WeA-3, 53
- Volke, Pascal: PP6-MoA-12, 18
- W —
- Wahlström, Jens: IA2-1-MoA-8, 11
- Walther, Frank: PP6-MoA-12, 18
- Wang, Chaur-Jeng: IA2-1-MoA-9, 11
- Wang, Chen-Hao: TS1-2-MoA-3, 19
- Wang, Chih-Liang: TS1-1-MoM-7, **7**
- Wang, Damir: MB2-3-TuM-5, 29
- Wang, Jin: CM2-1-ThM-11, 65
- Wang, Jun-Xing: MA4-1-TuA-5, 37; MA5-ThM-11, **69**
- Wang, Ke-Hsing: TS1-2-MoA-2, 19
- Wang, Ruo-Yao: MB2-2-MoA-4, **12**
- Wang, Sheng Chang: TS1-2-MoA-5, 19
- Wattanathana, Worawat: MA4-1-TuA-5, 37
- Weber, Felix: PP1-2-MoA-11, 15
- Wei, Ta-Cheng: MB-ThP-4, **84**
- Wei, Zixiong: CM4-2-MoA-4, 9
- Weissmantel, Steffen: MA5-ThM-10, 68

## Author Index

- Wen, Tzu-Hsu: MB2-1-MoM-5, 3  
West, Glen: TS3-TuA-4, 39  
Wieczorek, Alexander: CM-ThP-8, 80  
Williams, Bryce: MD1-1-MoM-1, 4  
Williams, Donald: CM1-1-ThM-10, **62**  
Wimer, Shawn: MB1-WeA-1, 53  
Winiarski, Bartłomiej: MA1-1-TuM-5, 24  
Witharamage, Sandamal: MA2-1-TuA-8, 34  
Wojcik, Tomasz: MA1-2-TuA-4, 34; MA5-ThM-6, 68; MA-ThP-1, 82; MB2-3-TuM-1, 28; MB-ThP-10, 85; MC1-1-ThA-1, 76  
Wójcik, Tomasz: MA3-1-TuM-7, 27  
Wolf, Jan: PP6-MoA-3, **16**  
Wolfsperger, Fabian: IA2-1-MoA-6, 11  
Wright, Andrew: MA2-2-WeM-4, **41**  
Wu, Fan-Bean: TS1-2-MoA-4, 19  
Wu, Hung-I: TS1-2-MoA-4, **19**  
Wu, Lin: MA4-1-TuA-4, **36**  
Wu, Tsung-Jen: CM-ThP-5, **79**  
Wu, Wan-Yu: PP2-1-WeM-12, 49; TS1-2-MoA-4, 19; TS1-ThP-7, 92  
Wu, Ya-Fen: MB-ThP-3, **84**  
Wudil, Yakubu Sani: CM3-2-ThA-3, **76**  
Wunder, Nicholas: CM3-1-ThM-6, **66**
- **X** —  
Xie, Zonghan: MA4-3-WeA-5, 52
- **Y** —  
Yang, Chih-Chiang: MB-ThP-4, 84  
Yang, Chun Lin: MA3-1-TuM-5, **26**  
Yang, Ding-Hsuan: MA3-2-TuA-5, **36**  
Yang, Fu-Sen: MA5-ThM-8, 68  
Yang, Qi: MA4-2-WeM-10, **44**  
Yang, Yung Chin: PP1-2-MoA-3, 14  
Yao, Guang-Yi: TS1-ThP-2, 91  
YAYLALI, Banu: MB-ThP-11, 85; MC3-1-WeM-13, 46  
Yen, Yi-Chun: MA2-2-WeM-6, 41  
Yen, Yung Hsun: TS2-WeA-3, **59**  
Yeom, Jeyun: CM4-1-MoM-5, 2  
YESILYURT, Mustafa: MB-ThP-11, 85; MC3-1-WeM-13, 46  
Yi, Feng: PP5-TuM-3, 30  
Yu, Yong: TS2-ThP-3, 93  
Yun, Kangsuk: MB-ThP-12, **86**; MB-ThP-5, 84; MB-ThP-8, 85  
Yung, Yung-Chin: PP2-1-WeM-10, 49
- **Z** —  
Zabel, Andreas: PP6-MoA-12, 18  
Zak, Stanislav: CM1-2-ThA-1, 73  
Zakutayev, Andriy: CM3-1-ThM-6, 66; TS2-ThP-1, 92  
Zehl, Rico: CM3-1-ThM-8, 66; CM-ThP-7, 80  
Zekentes, Konstantinos: PP3-WeA-8, 59  
Zeman, Petr: MA3-2-TuA-1, 35; MA3-3-WeM-2, 41; MA3-3-WeM-3, 42; MA4-2-WeM-4, 43; MB3-ThM-10, 70  
Zendejas Medina, León: MA4-1-TuA-4, 36  
Zerdoumi, Ridha: CM-ThP-7, 80  
Zhadko, Mariia: MA3-3-WeM-3, **42**  
Zhang, Anne: MA1-2-TuA-3, 34  
Zhang, Kun: TS1-ThP-5, 91  
ZHANG, YU ZHEN: MB2-2-MoA-5, **12**  
Zhang, Zaoli: CM-ThP-4, 79; TS3-TuA-8, 40  
Zhirkov, Igor: PP1-1-MoM-3, **5**  
Zhong, Fu-Gi: MB1-WeA-4, **53**  
Zhou, Bi-Cheng: MA2-1-TuA-8, 34  
Zhou, Zhifeng: MA4-3-WeA-5, 52  
Zhu, Yimei: MB2-3-TuM-5, 29  
Ziegelwanger, Tobias: MA3-2-TuA-1, 35  
Zighem, Fatih: CM2-1-ThM-10, 64; CM2-2-ThA-1, 74  
Zilnyk, Kahl: IA-ThP-1, 81  
Zitek, Michal: MA3-2-TuA-1, 35  
Zuzjakova, Sarka: MA4-2-WeM-4, 43